Ricardo Nuno Alves

Molecular and cellular changes in Atlantic halibut (*Hippoglossus hippoglossus*) skin during metamorphosis

Universidade do Algarve
Faculdade de Ciências e Tecnologias
2016

Ricardo Nuno Alves

Molecular and cellular changes in Atlantic halibut (*Hippoglossus hippoglossus*) skin during metamorphosis

Tese para a obtenção do grau de Doutor em Ciências Biológicas

Especialidade em Biologia Molecular

Trabalho efetuado sob a orientação de:

Professora Doutora Deborah M Power

Universidade do Algarve
Faculdade de Ciências e Tecnologias
2016

Molecular and cellular changes in Atlantic halibut (*Hippoglossus hippoglossus*) skin during metamorphosis

Declaração de autoria do trabalho

Declaro ser a autora deste trabalho, que é original e inédito. Autores e trabalhos consultados estão devidamente citados no texto e constam da listagem de referências incluída.

_____

A realização deste trabalho foi possível graças ao financiamento da Fundação para a Ciência e Tecnologia (FCT) através da bolsa de doutoramento SFRH/BD/69209/2010 e ao financiamento do projeto LIFECYCLE (FP7 222719. http://www.lifecycle.gu.se/) através do Centro de Ciências do Mar (CCMAR)

Aos meus pais
(a minha raiz, caule e folhas)
e em especial ao Santiago
(my little treasure)
e à minha avó Céu
(o meu eterno anjo da guarda)

Obrigado por toda a inspiração, luz, força e motivação
ao longo destes anos, o meu Orixá (Òrișà), que me guia sempre:

“Vou dar a volta no mundo
eu vou ver o mundo girar
mas eu só saio daqui
quando o coral negro passar
Essa visão do mundo,
permanece ainda, não modificou,
O Ilê aiyê começa onde termina o ponto de eclosão total...” *In* Crença e Fé

“Oyá TeTê
Oyá TeTê Oyá
Oyá TeTê Oyá
Oyá TeTê” *In* Oyá por Nós

“Tua comida comi,
Tua língua aprendi
Tua música e dança bailei
O teu canto entre tantos
Guardei
Lendas, folclores
Crendices, costumes, comidas
Falares, plantas e bichos lugares” *In* América do Amor

"Mori omon kekere towa dje
Olorio
Mori awon arugbo tô na fé kowi
Mori obinrin to dara
Kpelou onan to dara
Monfe ri inanan, iiyansan, ioshun,
Yemandja” *In* Dara

Eparrei oyá – Oxalá, Ogum, Xangô, Oxossi, Oxum, Nanã, Iansã e Iemanjá

Agradecimentos/Acknowledgments

A minha jornada ao longo dos últimos anos nesta "batalha" chamada de doutoramento culmina hoje com a entrega desta dissertação. Este foi sem dúvida o maior desafio da minha vida até hoje, e tal não seria possível se não tivesse as pessoas mais incríveis à minha volta. Foram muitos altos e baixos, e agora que estou prestes a conquistar mais uma vitória é altura de agradecer todo o apoio, motivação, carinho e atenção que sempre tiveram comigo. Sim é verdade a lista é longa, mas não posso deixar de expressar toda a minha gratidão... Espero um dia poder retribuir por tudo o que fizeram de mim e por mim… Um muito obrigado a todos...

Em primeiro lugar gostaria à professora Deborah Power por me ter acolhido no seu laboratório e no projecto Lifecycle mesmo antes de ter começado a tese de doutoramento, e por ter sempre confiado no meu trabalho e ajudar-me a acreditar que seria possível. Agradeço por todo o incentivo, dedicação, partilha de conhecimentos, mas principalmente por me fazer "pensar" no que é fazer ciência. Sem a sua motivação, talento e empenho eu não teria conseguido concluir este trabalho. Obrigado pelas inúmeras horas de reuniões e foi um privilégio poder aprender consigo tudo o que sei hoje sobre o mundo da biologia molecular e das ciências biológicas em geral.

Gostaria também de agradecer ao professor Adelino Canário por me receber tão bem no seu laboratório. O seu talento e motivação é algo incrível. Obrigado por ser o verdadeiro pilar do CCMAR, pois sem si o Centro não se tinha tornado no que é hoje.

I would like to thank Professor Melody Clark for welcoming me to the British Antarctic Survey and giving the opportunity to do part of my bioinformatics analysis there. I am also grateful to Dr. Michael Thorne for the help during the transcriptome analysis and with all the bioinformatics tools

I also would like to express my gratitude to Dr. Richard Reinhard at the Max Planck Institute for Plant Breeding Research for welcoming me in his group and for sharing his knowledge about NGS techniques. I would like to thank Dr. Mbaye Tine for teaching me everything I know about NGS libraries preparation and to Dr. Kurt Stueber for teaching me how deal with the NGS sequencing data. A special thanks to my Max Planck lab colleagues Christoph Bast, Eva Reucker and Anni Stollberg for all the great moments we shared at the Max Planck facilities.

Um agradecimento muito especial e o mais sincero possível à minha colega e companheira da saga "transcriptome analysis", Ana Gomes. Foste sem dúvida uma peça chave na construção da minha tese, desde as infinitas horas de linhas de comando no Linux, até à preparação do capítulo 2. Obrigado por teres tido tanta paciência para mim ao longo destes últimos anos, pelas inúmeras correcções e críticas sempre construtivas. A tua ajuda nesta fase final foi muito importante. Nunca te vou conseguir agradecer.

Nesta longa jornada quero agradecer a todos os meus colegas do grupo CME (Comparative Molecular Endocrinology). Espero não me esquecer de ninguém pois a lista é grande. Um agradecimento aos que ficaram e aos que já foram embora: João Cardoso, Patrícia Pinto, Rute Martins, Rute Félix, Patrícia Mateus, Rita Costa, Ângela, Elsinha, Xana (matrafas), Lili, Maria, Marlene, Pedro Palma, Vera, Bela, Flávia, Sandrinha, Xaninha, Nadège, Peter, Mar, Pedro Guerreiro, André, Soraia,

Eduarda, Alex, Juan, Sílvia, Zélia, Nádia, Bruno, João Saraiva, Alex e todos os que me possa ter esquecido ☺. A todos, um muito obrigado. Cada um de vocês me ajudou à sua maneira.

Agradecer à minha estrelinha, à minha Dondocs, Patrícia Mateus é pouco para expressar a gratidão que sinto por ti, por essa pessoa que tu és. De colegas passámos a ser grandes amigos e acho que tu foste uma das coisas mais importantes que o PhD me deu. Obrigado pelas inúmeras horas de apoio incondicional. Estarei sempre aqui para ti. Rita Costa, a tua simplicidade, educação, inteligência e especialmente respeito por todos os colegas fez-me aprender muito contigo. Nos últimos anos sempre me ajudaste nos melhores e piores momentos em todas as técnicas e mais algumas. Foste o meu primeiro pilar no grupo e só te tenho agradecer por isso. És sem dúvida uma investigadora guerreira. Tenho muito orgulho em ter tido o privilégio de trabalhar contigo.

João Cardoso, o "velhote", Rute Martins, a "santinha" e Patrícia Pinto, a "rainha do carnaval molecular" foram três companheiros ao longo desta jornada, os meus "papás". Aprendi imenso com vocês e agradeço as inúmeras horas de trabalho que partilhámos juntos. Obrigado por todos os conselhos que sempre me deram. Aprendi mesmo muito com vocês. À Joana (ruculinha) e Carina (nina) pela ajuda preciosa durante a realização dos milhares de cortes histológicos da tiróide dos meus "halibuts" e das centenas de colorações. Espero de certa maneira também ter contribuído para a vossa aprendizagem.

Agradecer aos meus camaradas do mítico grupo "Gang do E4", Odete, Tomé, Sofia, Mahaut, Nadège e ao Professor Pedro Rodrigues e ao Doutor Luís Conceição. Nadège, és hoje uma amiga em que posso afirmar que estiveste disponível durante todo o meu doutoramento, sempre disposta a ajudar. Isto sim é amizade e na realidade qualquer doutorando necessita de alguém assim por perto. O primeiro grupo de investigação onde trabalhei, ajudaram-me a criar forças e defesas para levar este doutoramento a bom porto. Muito obrigado.

I would like to thank my new endocrinologists friends, Kenneth Shang-Chien Lee, Florencia, Marylin and Mariano. Thank you for always be very positive and for sent all the inspiring messages and for give me the hope to finish the thesis. Rafael Nóbrega conhecer-te no CECE em Rennes foi um privilégio para mim. Tens sido também um bom apoio para mim sempre com as tuas mensagens carregadas de positividade.

Recentemente, voltei a perceber o que é trabalhar em grupo, o verdadeiro sentido de uma equipa. Obrigado ao Doutor António Marques, chefe e amigo por me teres aceitado no teu grupo de investigação no IPMA. Agradeço a paciência "imensa" que tens tido ao longo deste último ano e meio, OBRIGADO. Agradeço claro às man@s que tiveram de me aturar e não foi pouco: Ana Luísa (a das bichas), Vera Liane (mana queimada), Carolina (crossfit), Patrícia (mana mãe) e recentemente a Fabíola (Zuca). Mais do que colegas de trabalho, têm sido amigas incansáveis e nunca vou esquecer isso. Realmente sabe muito bem trabalhar com vocês.

Muito mais do que o ambiente da investigação fez com que conseguisse acabar a tese e foram inúmeros os amigos e família que sempre estiveram presentes. Não posso deixar de os citar, pois sinto que este doutoramento também é vosso. Eu tenho a sorte de poder dizer que tenho muitos e sinceros amigos. Sem falar que tenho a melhor família do mundo. Obrigado FARO por teres sido a minha casa durante quase 12 anos. Realmente o Algarve é o melhor sítio para se viver.

Aos meus grandes e bons amigos do grande curso de BMP adquiridos ao longo dos últimos treze anos… O curso acabou mas a amizade ficou...o poder saber que vocês estiveram lá para me

apoiar sempre, mesmo nos maus momentos...Nós somos especiais e sabemos disso. Amigos Para Siempre. O Ano Fantástico. A todos vós, um muito obrigado: Vera Jordão (Verinha), Rui Santos (pGem), João Silva (Ratão), Cátia Cardoso (Pintas), Alexandra Alves (Xaninha), Rita Silva (Ritinha afilhada), Pedro Gomes (King), Tânia Pipa (Pipinha), Mónica Inácio (Moca), Maria João (Trombone Comadre), Ângela Vicente (Titi Ângela), Débora Marujo (Bébé), Ana Vidal (Floreca), Joana Salabert, Céline Madeira (Ti Céline) e Catarina. Verinha foste sem dúvida uma pessoa que tanto me "aturou" nestes últimos anos, sempre com aquele positivismo que é só teu e que irei guardar sempre. Como sabes a minha mudança para Lisboa foi um momento muito crítico para mim, mas com o teu apoio e o do Eurico foi possível, e hoje estou aqui para te dizer como tínhamos combinado: entreguei a tese ☺☺☺. Floreca, tens sido um exemplo para mim. A minha admiração por ti só cresce a cada dia que passa, Thank you. Xaninha, Pintas, pGem, Moquinha, Titi, Trombone, Estralabert, uns perto outros longe mas esta grande equipa deu-me todas as ferramentas para finalizar este trabalho. Xana e Pintas, thank you pelos cafés infinitos.

Muitos outros amigos que a faculdade me deu foram cruciais para eu conseguir ultrapassar todas as dificuldades que enfrentei: Coiso (o meu maninho mais novo), Cumeta e Vera "Mónica", Buézinha, Micas, Gonçalo Raposo, Martinha, Peks, Cíntia, Afonso, Galinha, Regueifa, o meu clã do CDSL (Babali, MaryJane, Nadsky e Catarina), Mariana (a minha eterna caloirinha), Shenaps, CTX e muitos outros. Coiso, obrigado por teres paciência para me aturares. Cumeta/Vera aquela amizade que vou querer guardar para sempre. Obrigado por sempre me fazerem sentir que era capaz de o fazer. As minhas loucas do CDSL que tanto me apoiaram quando regressei da Alemanha e nos últimos anos em Faro. Vivemos muitas aventuras juntos, partilhámos muitas experiências e isso também foi essencial para apresentar o que está escrito nas páginas seguintes. MaryJane (and Padeiro) e Babali obrigado por ajudarem o vosso sonho especialmente nesta fase final de escrita, correcções, sítio para eu dormir em Faro, e muito mais.

Não posso também deixar de agradecer às minhas tias algarvias, as melhores funcionárias da Universidade do Algarve. Aquelas que todos os dias me punham a sorrir, já são da família obrigado Cátia, Tina e Isabel.

Agradecer à minha turminha dos acrobatas (os meus GGCs) Ricardo Martins, João Ferreira, Margarida, Guida, Eugénia, Lino, Joaninha, Cláudio, Rita Vidal, João Vidal por sempre me terem apoiado desde o primeiro minuto que nos conhecemos. Podem se passar anos, mas quando estamos juntos tudo é igual ao que sempre foi. Um agradecimento muito especial ao Ricardo Martins e à Joaninha Baião, foram incansáveis a ouvir aqui o vosso amiguinho e as suas "crises". Tentei sempre seguir os vossos conselhos e hoje sei que esta tese também é vossa. Cada um de vocês à sua maneira...Muito obrigado.

Aos meus grandes amigos de sempre, porque a distância nunca foi motivo para perdermos o contacto, sempre me apoiaram e ajudaram em tudo o que precisei…especialmente nos momentos de tristeza e fraqueza…por estar longe de casa…OBRIGADO Susana, Daniela, Paula, Abílio, Lúcia, Diana Leal, Sandrina e Ana Salgueiro…Vocês são especiais e sabem disso.

Um agradecimento muito especial ao Gonçalo e à minha irmã italiana Dina pela sua preocupação de sempre. E se as vossas visitas ao Algarve me ajudaram? Mas com certeza. Às minhas raízes, Sarita, Janota e Primoca que mesmo ausentes tornaram este processo de escrita muito mais fácil. Obrigado sempre pelas palavras de carinho e amizade. Sarita este último ano foste um pilar

muito grande para mim. Obrigado primo Fábio por teres tido tanta paciência para me aturar enquanto morámos juntos.

Quero também agradecer à minha maltinha da capoeira pelos momentos de Axé que passámos juntos. Momentos estes que sempre me davam energia para voltar para o laboratório. Obrigado Mestre Alexandre Batata e toda a Companhia de Capoeira Contemporânea. Um agradecimento muito especial à minha alma gémea do Axé, Maria, Xuxu do Mar.

Agradeço também ao Andrés Rodrigo por todo o apoio que me deu durante a minha estadia em Colónia. Sem o teu apoio, os meus objectivos durante os três meses que estive na Alemanha nunca teriam sido cumpridos.

Faz ano e meio que me mudei para Lisboa. A adaptação à nova vida não foi fácil e por vezes pensei que nunca iria acabar a tese. Mas os Orixás puseram as pessoas certas no meu caminho, afinal considero-me uma pessoa com sorte. Obrigado Raquel (Xonxonete) e Vanessinha as minhas colegas de casa e amigas que tanto me têm apoiado. O incentivo que me deram para escrever me ajudou a ver esta tese, não como um bicho de 100 cabeças, mas sim como uma meta a atingir. Love you (vá e a salafrária também). Obrigado também, Shorty, e a maltinha da dança aérea em especial às melhores professoras Rose e Lili e à minha real companheira Nádia.

Agradeço à minha grande inspiração, aquela que canta para dançar, aquela que alegra os nossos corações, e que foi a verdadeira banda sonora da escrita desta tese, a Rainha do Axé, minha rainha má, da macumba, de umbanda, Daniela Mercury. Obrigado por ter tornado todo este processo muito mais fácil. Falar de Daniela significa falar de amizade. Ao longo destes 5 anos muitos foram os mercuryanos que passaram na minha vida... Obrigado a cada um de vocês pelo incentivo que sempre me deram: Paulinho, Haialla, Edwin, Dany, Roberth, Gus, Laura, Maico, Márcio, Malu, Alexandra, Eliana Martinez, Eliana, Tânia, Elaine, Sueli, Rebeca, Belissima, Arismar, Fernandes, Emerson, Jorginho, Jai, Leo Luz, Efigênia, Leonildo, Edy, Aline, Pris, Cesário e muitos outros. Um agradecimento muito especial ao "Grupo da Macumbra", meus amigos, meus parceiros, o vosso apoio incondicional nos últimos tempos, marcou muito aqui o mercuryano. Agradeço especialmente à Lêlê (minha irmã confidente, minha alma gémea da música), Mercedes (a eterna dondoca espanhola, sempre com suas palavras carinhosas e o seu ar doce), Xana, Teresa, Paulo, Margarida, Ana Mateus, Sónia, Gé e Maria del Mar. Ser um Trio em Transe, Dance, Ser Felini e Fim...

Tiago,nem sei por onde começar. Qualquer coisa que possa escrever será pouco para expressar a minha gratidão. Conhecer-te foi sem dúvida o melhor presente que Lisboa me deu. Obrigado por estares sempre ao meu lado quando eu preciso, pelas horas de companhia, pelos imensos sushis para acalmar aqui o xonxonito, pelos imensos conselhos, pelos "ralhetes", pelas alegrias, enfim por tudo...Thanks pelas horas passadas a ajudar-me com a formatação da tese. Obrigado por seres especial. E como já dizia alguém que nós conhecemos "Em qualquer lugar por onde andar, no meu coração vou guardar você".

Agradeço especialmente à minha família pois sem vocês, nunca teria conseguido, um obrigado sincero a todos…Pais, Mano, Rita, Avós, Santiago Padrinho, Nelinha, Gonçalo, Daniela, Sofia, Martim, afilhadão Gustavo, Tios Rui e Cesaltina, Carol, Laurinha, Tomás, Tia Elsa, Tia Palmira, Felícia e todos os outros.

Ao meu mano Luís Miguel, porque apesar de ser muito esquecido, é o meu irmão que eu adoro acima de tudo… Somos muito diferentes, mas muito iguais ao mesmo tempo…Obrigado mano por tudo, sei que vais estar sempre aqui para me apoiar.

O maior agradecimento vai para o meu pequeno tesouro, o Santiago. Afilhado mais lindo do mundo, mesmo sem saberes tu foste muito importante para me dar muita força nesta fase final. Cada toque, cada beijinho, cada carinho. O padrinho vai estar sempre aqui para ti. Ao meu outro afilhado Gustavo, uma das pessoas mais importantes da minha vida, já estás tão crescido, mas sempre com esse brilho nos olhos…penso sempre em ti…mesmo estando distante… Rita, sabes que serás sempre a minha cunhadinha. Conhecemo-nos desde que estava a acabar o curso, e sempre tiveste lá para me apoiar e dar na cabeça quando foi preciso.

Ao meu Avô Fernando, a minha maior referência. És umas das pessoas que mais admiro no mundo, pela tua enorme sabedoria, pois tu sabes muito e sempre o que dizer na altura certa. És o meu orgulho…sem dúvida…todos gostavam de ser como tu…Tanto tu como a Avó foram uma ENORME ajuda na minha educação, sem esquecer, os trinta anos da minha existência, aos quais vocês estiveram sempre presentes. Obrigado Avô Manuel pela ajuda ao longo destes anos…

Às minhas maravilhosas Avós Céu e Olga, por serem as "velhotas" mais queridas do mundo, por todos os mimos que me deram ao longo de todos estes anos… Vocês são fantásticas…adoro-vos…e também vos devo muito daquilo que sei hoje… Grande ajuda me vocês me deram e estou mesmo muito grato…SÃO MELHORES AVÓS DO MUNDO. Dedico-te esta tese avó Céu, pois não há agradecimento que pague todo o amor que sentes por mim. Eu devo-te o que sou hoje, e sim "Criar é Amor" e eu hoje entendo o significado destas palavras.

À minha Tia Elsa, a minha verdadeira madrinha, irmã e confidente. Tu és das pessoas mais lutadoras que conheço e serás sempre um exemplo para mim. Precisava de uma enciclopédia para te poder agradecer toda a ajuda preciosa que me deste, e sem esquecer que estás tão longe. És uma pessoa que tenho muito orgulho, e és um exemplo de coragem a seguir. Estás sempre disposta a aturar este sobrinho chato, mas que te adora e tem mesmo muito orgulho em ti… Obrigado pelas inúmeras horas passadas ao telefone, gargalhadas, lágrimas, és uma grande mulher. Já dizia a Daniela, "E cada mulher que se impõe nos liberta"

E por fim mas não menos importante, aos Meus Pais (Céu e Luís) a quem dedico esta tese, por todo o sacrifício que sempre fizeram para me proporcionar a melhor formação possível. Só espero não os ter deixado ficar mal. Sempre foram o meu maior pilar e base para suportar todas as dificuldades… os sorrisos, gargalhadas, as lágrimas… Um obrigado por tudo o que fizeram e fazem por mim, agradeço-vos muito aquilo que sou hoje, vocês são sem dúvida modelos a seguir por qualquer pessoa, são o orgulho de qualquer filho. Sem vocês e sem a vossa ajuda teria sido mesmo impossível vir estudar cá para baixo e crescer da maneira que cresci…MUITO OBRIGADO POR TUDO, vocês são os melhores pais do mundo…espero um dia vos poder retribuir tudo o que fizeram por mim…PAI és o maior homem do mundo, vais ser sempre um grande exemplo para mim…Mãe és a maior e melhor mulher do Mundo, não tenho palavras mesmo… espero nunca vos vir a desiludir…vou fazer por isso…

A Todos, um Muito Obrigado… "É melhor ser alegre que ser triste, alegria é a melhor coisa que existe" *In* Benção do Samba.

Abstract

Metamorphosis in vertebrates is driven by thyroid hormones (THs) and in flatfish consists in the extraordinary transformation of a symmetric pelagic larva into an asymmetric benthic juvenile. The mechanisms underlying how THs can orchestrate the cellular, morphological and functional modifications associated with maturation of juvenile/adult states in flatfish are still unexplored. The Atlantic halibut (*Hippoglossus hippoglossus*) was the target of the present thesis and the molecular basis of THs action was determined in the head, skin and gastrointestinal tract using RNA sequencing. The first objective of the present thesis was to generate reference transcriptomes of these three tissues using 454 pyrosequencing. Transcriptome dynamics during metamorphosis were mapped with SOLiD sequencing of whole larvae and revealed greater than 8,000 differentially expressed (DE) genes significantly up- or down-regulated in comparison with the juvenile stage. The present study contributes substantially to the molecular resources available for this species and will be an important tool for identifying new potential molecular markers for solving problems related to Atlantic halibut production during metamorphosis.

The second part of this thesis was focused in the skin due to its importance as the major barrier between the animal and its external environment and the involvement of THs in skin development during metamorphosis has been described. The present work targets the development of the primary barrier, osmoregulatory capacity and pigmentation development of Atlantic halibut skin. A multivariate approach using bioinformatics, biochemistry and molecular biology techniques allowed the characterization of the asymmetric development of *H. hippoglossus* ocular and abocular skin sides. The asymmetric development of skin is associated with metamorphosis although establishment of its primary barriers and osmoregulatory functional properties occurs early and is independent of metamorphosis. In addition, it was hypothesized that thyroid axis has a central role in the asymmetric pigmentation observed during metamorphosis in ocular and abocular skin sides. The third part consisted in study the cross-talk between the thyroid and cortisol axis and it was observed that both THs and cortisol act synergistically in modulating the changes in skin during halibut metamorphosis.

Keywords: Flatfish, metamorphosis, Thyroid hormones, transcriptome, skin development, asymmetry

Resumo

A metamorfose em vertebrados é um processo pós-embrionário desencadeado pelas hormonas da tiróide (THs) e em peixes-chatos (pleuronectiformes) consiste no processo de transformação da larva pelágica simétrica em juvenil bentónico assimétrico. Durante a metamorfose destes peixes teleósteos ocorre a migração de um dos olhos. No fim do processo metamórfico os olhos ficam no mesmo lado da cabeça e a pigmentação acentua-se apenas no lado ocular. A importância das THs durante a metamorfose nos "peixes-chatos" tem sido demonstrada ao longo dos últimos anos, no entanto, o papel destas hormonas durante as modificações celulares, morfológicas e funcionais associadas à maturação dos peixes juvenis/adultos é pouco claro. Após entrar nas células a partir de transportadores específicos (por exemplo os "monocarboxylate transporters", MCTs) e se ligarem a receptores nucleares (TRs), as THs activam a expressão génica e por sua vez induzem mudanças na estrutura, maturação e função dos tecidos e órgãos. A forma biologicamente activa é a T_3 e é originada nos tecidos periféricos pela conversão da T_4 através da acção de enzimas específicas chamadas de deiodinases, que podem também inactivar as THs. Assim, como as THs actuam na transcrição de genes responsivos, definiu-se que uma das principais hipóteses deste trabalho é que a maturação dos tecidos durante a metamorfose deve ser precedida a modificações significativas no transcriptoma.

O alabote do Atlântico (*Hippoglossus hippoglossus*) foi escolhido como modelo de estudo devido à sua importância para a aquacultura mas principalmente devido ao seu lento desenvolvimento larvar (metamorfose dura aproximadamente 58 dias) e ao tamanho das larvas (aproximadamente 14.50-23.00 mm início e fim da metamorfose). Estas características permitiram não só analisar larvas individuais mas também dissecar tecidos e analisá-los em separado a nível molecular. O primeiro objectivo do presente trabalho foi determinar a base molecular da acção das THs através da sequenciação do transcriptoma por RNAseq de três tecidos (cabeça, pele e trato gastrointestinal – trato GI) durante a metamorfose de *H. hippoglossus* (Capítulo 2). Três diferentes transcriptomas de referência foram gerados utilizando a técnica de pirosequenciação 454 e após a "assembly" foram obtidos 90.676 (cabeça), 65.530 (pele) e 38.426 (tracto GI) contigs. Através de uma abordagem de múltiplos passos de Blast, mais de 57 % dos contigs foram anotados com sucesso, permitindo assim identificar para cada tecido um conjunto de processos biológicos e genes candidatos associados às alterações morfológicas e funcionais durante a metamorfose. Posteriormente, a dinâmica do transcriptoma durante a metamorfose foi avaliada através da sequenciação de larvas individuais (n = 3) de vários estados metamórficos. A abordagem utilizada foi uma sequenciação do tipo SOLiD, e após o mapeamento das sequências "reads" contra o transcriptoma de referencia foi possível detectar mais de 8.000 genes diferencialmente expressos, sobre- ou sub-expressos ao comparar os estados metamórficos com o juvenil. A maioria dos genes diferencialmente expressos não são responsivos às THs. Utilizando uma base de dados "*in house*" foram identificados seis grupos (clusters) diferentes de genes responsivos baseados no seu padrão de expressão durante a metamorfose. A maioria dos 145 genes responsivos às hormonas da tiróide encontram-se sub-expressos quando comparados

com o juvenil após a metamorfose. Estes genes responsivos estão associados a diferentes "gene networks", cascatas de sinalização "signalling cascades" e factores de transcrição que devem liderar as alterações no desenvolvimento e maturação dos tecidos durante a metamorfose.

Durante a análise do transcriptoma foram identificados dois transcriptos diferentes que correspndem à deiodinase 3 (Dio3). A Dio3 é uma enzima que desempenha um papel essencial durante o desenvolvimento dos vertebrados, através do controlo da disponibilidade das THs nos vários tecidos. O segundo objectivo da presente tese foi avaliar qual é o papel destes dois transcriptos *dio3* durante a metamorfose do alabote do Atlântico (Capítulo 3). Análises bioinformáticas permitiram concluir que estes dois transcriptos correspondem a genes duplicados (posteriormente designados de *dio3a* e *dio3b*) e que é comum à maioria dos peixes teleósteos. A expressão destes dois genes na pele foi divergente entre os lados ocular e não-ocular durante a metamorfose. Os resultados obtidos da expressão génica indicaram que o gene *dio3b* pode estar associado à maturação divergente dos dois lados da pele. Larvas expostas ao bloqueador de produção de THs, o MMI, resultou numa sobre-expressão de *dio3b* no lado ocular da pele, sugerindo que as THs geralmente inibem a expressão deste gene durante esta fase do desenvolvimento. Os resultados indicam que a expressão divergente de *dio3* nos lados ocular e não-ocular da pele durante a metamorfose pode contribuir para o desenvolvimento assimétrico em resposta às THs.

A pele nos vertebrados é um órgão multifuncional e corresponde à principal barreira entre o animal e o seu meio ambiente. Durante a metamorfose, a pele do *Hippoglossus hippoglossus* muda de um simples epitélio para um tecido composto estratificado em várias camadas após a metamorfose. A epiderme fica composta por vários tipos de células com diferentes funções e a disponibilidade das THs na pele durante a metamorfose é regulada pela acção coordenada das deiodinases. Por estas razões a pele representa um interessante alvo de estudo para a acção das THs durante a metamorfose. Os capítulos 4 e 5 foram dirigidos à pele em especial às suas funções como barreira primária, osmoregulação e pigmentação, e a sua possível relação com as hormonas da tiróide durante a metamorfose do alabote do Atlântico.

A combinação de técnicas de histologia, histoquímica e electrofisiologia permitiu estudar as funções de barreira e osmorregulação da pele, através da análise ontogénica das células goblet (secreção de mucinas) e dos ionócitos (presença da Na^+,K^+-ATPase) na pele ocular e não-ocular (Capítulo 4). A integridade do epitélio e as propriedades electrofisiológicas foram avaliadas por electrofisiologia na pele no lado ocular. As mucinas neutras são as principais glicoproteínas produzidas pelas células goblet da pele durante a metamorfose, e a sua abundância aumenta durante o processo metamórfico. Nos estágios metamórficos 8 a 9B estas células bem como o número de mucinas é mais abundante no lado ocular da pele. Este aumento e a sua abundância assimétrica entre os dois lados da pele é concomitante com o aumento das THs, sugerindo-se que o seu desenvolvimento encontra-se sob o controlo destas hormonas. Ao contrário das goblet cells (mucinas), o número de ionócitos com imunoreactividade positiva para a Na^+,K^+-ATPase (NKA) decresce ao longo da metamorfose e a distribuição é simétrica entre os dois lados da pele. As alterações

morfológicas observadas têm um efeito demonstrado na função de barreira da pele tal como reflectido pelas propriedades electrofisiológicas do epitélio (resistência transepitelial/potencial e "short circuit current"). No entanto, a maturação das características funcionais ocorreu no estágio 8, antes da maturação completa da pele e do clímax da metamorfose. Estes resultados indicam estudo que há um desenvolvimento assimétrico da pele e que este está associado com a metamorfose. No entanto, o estabelecimento das suas propriedades funcionais ocorre cedo e é independente da metamorfose.

No capítulo 5 foi utilizada uma abordagem molecular para avaliar a resposta assimétrica dos dois lados da pele às THs e sua relação com a pigmentação. Neste estudo, foi avaliada a expressão de genes relacionados com o transporte, metabolismo e acção das THs, e de genes envolvidos na melanogénese e na regulação da pigmentação na pele ocular e não-ocular durante a metamorfose do alabote do Atlântico. Foi também avaliada o possivel "cross-talk" entre os eixos da tiróide e stress durante a maturação da pele e pigmentação. A expressão dos receptores da tiróide e deiodinases (*dio1*, *dio2*, *dio3a*, *dio3b*, *trαa* and *trβ*) foi simétrica entre os lados ocular e não-ocular da pele. No entanto, a expressão dos transportadores das THs (*mct8, mct10*) foi assimétrica nos dois lados da pele durante a metamorfose. Genes envolvidos na melanogénese (*tyrp1, dct*) e regulação da pigmentação (*sox10*) tiveram uma expressão semelhante aos transportadores das THs. Este estudo contribui para uma melhor compreensão das bases moleculares da assimetria na pigmentação observada durante a metamorfose do alabote do Atlântico, e revela um papel central para o eixo da tiróide. A hipótese da existência de um "cross talk" entre o eixo da tiróide e do cortisol durante a metamorfose onde as THs e o cortisol actuam de forma sinergética na modulação das alterações na pele durante a metamorfose do alabote do Atlântico foi demonstrada neste capítulo.

A presente tese permitiu gerar novo conhecimento sobre os efeitos das THs no desenvolvimento dos "peixes chatos" em especial na cabeça, pele e trato gastrointestinal. Esta tese contribuiu também para entender melhor acerca do desenvolvimento assimétrico dos lados ocular e não-ocular da pele e como as THs se encontram envolvida neste processo.

Palavras-chave: peixes-chatos, desenvolvimento, metamorfose, hormonas da tiróide, transcriptoma, pele ocular e não ocular, assimetria

List of tables

List of figures

Chapter 1

Chapter 2

Chapter 3

Chapter 4

Chapter 5

List of abbreviations

3’UTR: 3’ untranslated region

AB: alcian blue

AB1: alcian Blue at pH 1

AB2.5: alcian Blue at pH 2.5

AHDS: Allan-Herndon-Dudley syndrome

ALB: serum albumin

AMPs: antimicrobial peptides

ANOVA: analysis of variance

ARA: arachidonic acid

ASAB: Association of Animal Behaviour

BBB: blood-brain-barrier

BDE209: decabromodiphenyl ether

Blast: basic local alignment search tool

BP: biological process

CC: cellular component

cDNA: complementary DNA

CMZ: ciliary marginal zone

CNS: central nervous system

CRH: corticotrophin releasing hormone

CSF: blood-cerebrospinal fluid barrier

CTBPs: cytosolic thyroid-hormone-binding proteins

D3KO: D3-deficient mice

DAB: diaminobenzidine tetrahydrochloride

DDD: deiodinase dimerization domain

DE: differentially expressed

DIT: diiodotyrosine

DMSO: dimethyl sulfoxide

DPH: days post hatch

DPSF: days post start feeding

DPX: 2-Chlorobenzaldehyde oxime

ECM: extracellular matrix

EDTA: ethylenediamine tetraacetic acid

EF1A1: elongation factor I alpha

ER: endoplasmic reticulum

ESTs: expressed sequence tags

FDR: false discovery rate

G: globular or catalytic domain

GH: growth hormone

GI-tract: gastrointestinal tract

GO: gene ontology

GPs: glycoproteins

H: hinge

HAT: heterodimeric amino acid transporters

HPF: hours post-fertilization

HPI: hypothalamus-pituitary-interrenal axis

HPT: hypothalamo–pituitary–thyroid axis

IHC: immunohistochemistry

IOP: Iapanoic acid

IRD: inner-ring deiodination

ISH: in situ hybridization

JTT: Jones-Taylor-Thornton model

KD: Knock-down

kDa: Kilodalton

KEGG: Kyoto encyclopedia of genes and genomes

KO: KEGG orthology

KO: knockout

L: linker

LRO: lysosomal related organelles

MCT: monocarboxylate transporters

MF: Molecular function

MH: myotome height

MH: Myotome height

MIT: monoiodotyrosine

ML: Maximum Likelihood

MMPs: matrix metalloproteinases

MRC: mitochondria-rich cells

MS222: ethyl 3-aminobenzoate methanesulfonate salt

NCBI: National Center for Biotechnology Information

NJ: Neighbor joining

NKA: Na^+/K^+ ATPase

nTRE: negative TREs

OATPs: organic anion transporting polypeptides

ORD: outer-ring deiodination

ORF: open reading frame

OSN: osteonectin

PAS: Periodic acid–Schiff

PBST: phosphate-buffered saline - Triton X100

PCR: polymerase chain reaction

PD: pars distalis

PPT: parts per thousand

PRL: prolactin

PTU: 6-n-propyl-2-thyouracil

qPCR: Quantitative real-time polymerase chain reaction

RACE: rapid amplification of cDNA ends

REVIGO: Reduce + Visual Gene Ontology

rT_3: 3,3',5'-triiodothyronine

RU486: mifepristone

RXR: retinoid X receptor

SB: Abocular skin side

SCC: short circuit current

SECIS element: SElenoCysteine Insertion Sequence

SEM: standard error of the mean

SH: head skin

SHH: sonic hedgehog

SL: Standard length

SLC: solute carrier

SRA: short read Archive

ST: ocular skin side

T_2: 3,3'-diiodothyronine

T_3: 3', 5, 3 triiodothyronine

T_4: thyroxin

TCT: Tris-λ-carrageenan and 0.5 - Triton X100

TEP: transepithelial potential

TER: transepithelial resistance

TFs: transcription factors

THBP: thyroid hormones binding proteins

THs: Thyroid hormones

TM: transmembrane segment

TMDs: transmembrane domains

TREs: thyroid response elements

TRH: thyrotropin-releasing hormone

TRs: thyroid hormone receptors

TSGD: teleost specific genome duplication

TSH: thyroid stimulating hormone

TTR: transthyretin

TU: thiourea

WMISH: whole mount in situ hybridization

Author's publications

Gomes, A.S., Alves, R.N., Rønnestad, I., Power, D.M., 2015. Orchestrating change: The thyroid hormones and GI-tract development in flatfish metamorphosis. General Comparative Endocrinology. 220, 2-12 - Chapter 1

Alves, R.N. & Gomes, A.S., Stueber, K., Tine, M., Thorne, M.A., Smaradottir, H., Reinhard, R., Clark, M.S., Ronnestad, I., Power, D.M., 2016. The transcriptome of metamorphosing flatfish. BMC Genomics. 17, 413 - Chapter 2

Gomes, A.S. & Alves, R.N., Stueber, K., Thorne, M.A., Smaradottir, H., Reinhard, R., Clark, M.S., Ronnestad, I., Power, D.M., 2014. Transcriptome of the Atlantic halibut (*Hippoglossus hippoglossus*). Marine Genomics. 18 Pt B, 101-3 - Chapter 2

Campinho, M.A., Galay-Burgos, M., Silva, N., Costa, R.A., Alves, R.N., Sweeney, G.E., Power, D.M., 2012a. Molecular and cellular changes in skin and muscle during metamorphosis of Atlantic halibut (*Hippoglossus hippoglossus*) are accompanied by changes in deiodinases expression. Cell and Tissue Research 350, 333-346 - Chapter 2

Alves, R. N., Cardoso, J. C. R., Harvoe, T., Martins, R. S. T., Manchado, M., Norberg, B., Power, D. M., 2016. Duplicate deiodinase 3 genes in teleost fish and their role in skin maturation during flatfish metamorphosis. Submitted to Molecular and Cellular Endocrinology – in revision - Chapter 3

Alves, R. N., Sundell, K. S., Anjos L., Sundh, H., Harboe, T., Birgita, N., Power, D. M., 2016. Structural and Functional Maturation of Skin during Metamorphosis in the Atlantic Halibut (*Hippoglossus hippoglossus*). (under submission to Cell and Tissue Research) - Chapter 4

Alves, R. N., Harboe, T., Birgita, N., Power, D. M., 2016. Asymmetric thyroid hormone responsiveness of ocular and abocular skin associated with changing pigmentation during flatfish metamorphosis (under submission) - Chapter 5

Structure of the thesis

The present thesis is organized in six chapters. **Chapter 1** consists of a general introduction to overview the state of the art and present the general aims of the thesis. Part of this introduction is already published as a review paper about the endocrine basis of flatfish metamorphosis with particular emphasis on gastrointestinal tract development and maturation.

In **Chapter 2**, two different next-generation sequencing technologies (NGS) were used to explore the Atlantic halibut transcriptome during metamorphosis and identify putative thyroid hormones responsive genes. The 454 pyrosequencing platform was used to survey for the first time the metamorphosing tissue specific transcriptomes of the head, skin and gastrointestinal tract. SOLiD technology was then used to map the transcriptional changes in individuals at different stages of metamorphosis. Differentially expressed transcripts during metamorphosis were identified by comparing the transcriptome from the different metamorphic stages with the juvenile. This chapter resulted in two publications: a short technical research paper about the 454 sequencing and a full research paper analyzing and characterizing the changes in the transcriptome that accompany Atlantic halibut metamorphosis.

In **Chapter 3**, we took the advantage of massive dataset from the NGS and explored the role in metamorphosis of two deiodinase 3 (*dio3 a* and *b*) genes, identified for the first time in flatfish. We proposed an evolutionary model for deiodinase 3 genes and demonstrated that *dio3* gene duplicates have a divergent expression pattern in the ocular and blind skin at different stages of metamorphosis. We reveal that THs normally repress *dio3b* expression during metamorphosis. This chapter combines "*in silico*" and molecular biology techniques and has been submitted for peer-review.

Chapters 4 and **5** are independent studies that address the structural and functional maturation of Atlantic halibut skin during metamorphosis with emphasis on ocular and abocular skin, which at metamorphosis acquire a asymmetric colouration. In **Chapter 4** we explore the maturation and characteristics of the skin as a primary barrier and osmoregulatory tissue using histochemical and electrophysiological techniques. In **Chapter 5**, we used a molecular biology approach and experimentation. We blocked TH production with methimazole (MMI) manipulate the hypothalamic-pituitary-interenal axis by administering an agonist of cortisol RU486 and assess how this affects the ontogeny of the thyroid hormones

cascade and pigmentation related genes during metamorphosis in both ocular and abocular skin. We make inference about the possible cross-talk between THs and skin pigmentation. These chapters constitute original work and are in the form of scientific papers, submitted or soon to be submitted for publication. **Chapter 6** consists of a general discussion about the way in which the thesis has contributed to advance the state of the art and future perspectives. For chapters 2 to 5 the co-authors involved in the publications are indicated and the contribution of R Alves to the work presented in each of the chapters is indicated.

Table of contents

Chapter 1

General introduction

Chapter 1

1 - General introduction

1.1. Metamorphosis

Metamorphosis is generally used to describe the "change in form" (Greek; *meta* meaning change and *morphe* meaning form) which occurs between an organism's life cycle stages. The most commonly known examples are the transitions from tadpole to frog and caterpillar to butterfly. However, this event is common to a diverse range of animal taxa (Diogo and Ziermann, 2014; Gilbert et al., 1996; Huang et al., 2013; Nakamura et al., 2011; Rubio et al., 2012; Schreiber and Specker, 2000; Wong et al., 2012), (**Figure 1.1**). McMenamin and Parichy (2013) described this process as "*an irreversible developmental and physiological change that affects multiple traits during postembryonic development and is brought about by one or more systematically acting endocrine mediator, but is independent of sexual maturation, sex-specific modifications, or senescence*". Although the term metamorphosis is most commonly used to refer to the abrupt post-embryonic morphological changes of vertebrate larva/fry/tadpole, etc into a juvenile/adult, a series of events related to tissue-specific modifications and timings associated with changes in biochemistry, physiology, habitat, feeding mode and life history stage also occurs (reviewed in Laudet, 2011; Paris and Laudet, 2008; Power et al., 2008) (**Figure 1.1**). Three main elements are identified as being common in organisms that undergo metamorphosis and include: (1) Ecological transformation (i.e. change in habitat, feeding habits); (2) Extensive transformation and reorganization of the body, involving physiological and biochemical remodelling and (3) Environmental cues that act as a trigger or block metamorphosis (e.g. involvement of endocrine systems in the tissue morphogenesis event).

In the most extensively studied models, the amphibians, the metamorphic process is hormonally driven, in particular by the thyroid hormones (THs), thyroxine (T_4) and 3,5,3'-triiodothyronine (T_3) (Shi et al., 1996). THs control the most dramatic developmental changes, preparing the aquatic larvae for its terrestrial life style and in this process a series of tissues undergo extensive remodelling (Gilbert et al., 1996) (**Figure 1.1**). In anurans, THs are involved in apoptosis of tail muscle fibers during its regression and also in the gradual development of the limbs (Chanoine and Hardy, 2003) and the replacement of the tadpole skin with a more stratified and better adapted skin for a terrestrial lifestyle (Suzuki et al.,

2002; Watanabe et al., 2001). The brain and intestine also undergo a remodelling program in these organisms (Yoshizato, 2007).

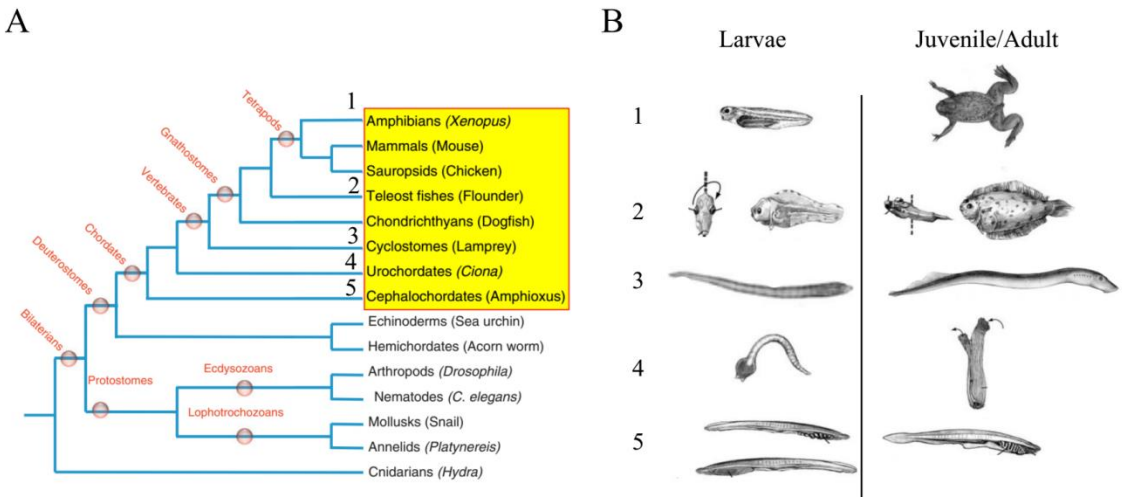

Figure 1.1. Metamorphosis in chordates. (A) A phylogenetic tree resuming the main chordate taxa (yellow box) that are known to undergo metamorphosis and for which the role of THs is established. (B) Examples of chordate models used for studies of metamorphosis. Both larvae and juvenile forms are represented: 1. anuran, *Xenopus laevis*; 2. flatfish, *Paralichthys dentratus*; 3. sea lamprey, *Petromyzon marinus*; 4. urochordate, *Ciona intestinalis* and 5. amphioxus. [Adapted from Paris and Laudet (2009) and Laudet (2011)].

In addition to anurans, metamorphosis also plays a significant role in some fish species resulting in striking changes during the transition from the larva to juvenile stage. The degree and severity of these changes varies between species but it is also a TH driven process. For instance, in zebrafish (*Danio rerio*) THs are essential for the development and differentiation of pelvic and pectoral fins (Brown, 1997). Likewise, in grouper (*Epinephelus coioides*) larvae, THs are required for resorption of the dorsal ray and changes in swimming behaviour and pigmentation (de Jesus et al., 1998). Endogenous T_4 is necessary for the initiation of retinal remodelling and responsible for the ultraviolet-sensitive cone loss during development of rainbow trout retina (Browman and Hawryshyn, 1994). In addition, Witt et al. (2009) suggested the importance of environmental iodide (and therefore the synthesis of THs) in larval metamorphosis and subsequent survival and growth in the aquaculture of the threadfin (*Polydactylus sexfilis*). In striped bass (*Morone saxatilis*), T_3 enhances the development of adult pigmentation suggesting that the melanophores may be regulated by THs (Huang et al., 1998). Although there are a number of examples revealing the role of THs in the morphological changes in several fish species, the most striking example occurs in the pleuronectiformes, or flatfish, (Campinho et al., 2007a; Campinho et al., 2007b; Inui et al.,

1995; Klaren et al., 2008; Manchado et al., 2009; Okada et al., 2003; Tagawa and Aritaki, 2005).

1.1.1. Flatfish metamorphosis

Flatfish undergo dramatic morphologic transformations during early larval development, changing from a pelagic symmetric larva to a benthic asymmetric juvenile, with migration of one eye to join the other eye on the dorsal side of the body and concomitant pigmentation of the skin on this ocular side and resorption of the elongated dorsal fin ray (reviewed by Power et al., 2008). Simultaneously, the development and maturation organs including stomach, skin, otolith structure, erythrocyte/haemoglobin and muscle occurs, and is correlated with the increase in TH levels in several flatfish species, such as Atlantic halibut *Hippoglopssus hippoglossus* (Campinho et al., 2012a; Campinho et al., 2007a; Campinho et al., 2007b; Murray et al., 2006; Ottesen and Strand, 1996; Sæle et al., 2004; Solbakken et al., 1999), Japanese flounder *Paralichthys olivaceus* (Inui and Miwa, 1985; Schreiber, 2001; Sun et al., 2015; Tanaka et al., 1996; Yoo et al., 2000), summer flounder *Paralichthys dentatus* (Keefe and Able, 1993; Martinez and Bolker, 2003; Schreiber and Specker, 1998), turbot *Psetta maxima* (Doldán et al., 2011), winter flounder *Pseudopleuronectes americanus* (Douglas et al., 1999; Murray et al., 2006; Murray et al., 1994), southern flounder *Paralichthys lethostigma* (Schreiber, 2006), Senegalese sole *Solea senegalensis* (Fernández-Díaz et al., 2001; Ribeiro et al., 1999), spotted halibut *Verasper variegatus* (Tagawa and Aritaki, 2005) and half-smooth tongue sole *Cynoglossus semilaevis* (Bao et al., 2011; Zhang et al., 2016) (**Figure 1.2**).

For example, in summer flounder, glycoconjugates (e.g. lectins) and mucous of the stomach, intestine and skin epithelia change during metamorphosis. The changes in lectin histochemistry are associated with the shift in the microbial composition observed during gastroinstestinal tract maturation (Soffientino et al., 2006). In Atlantic halibut, stomach acid production and proteolytic capacity coincides with the metamorphic climax (Gomes et al., 2014b). The pattern of digestive enzyme activities involved during the early stages of *P. olivaceus* is determined by metabolic changes linked to metamorphosis and also to the nutritional condition of larvae (Bolasina et al., 2006). The growth of utricle and sacculus otoliths is evident during the metamorphic process in *P. lethostigma* (Schreiber et al., 2010).

In Senegalese sole, the thyroid gland is already active in the early pre-metamorphic larvae (Klaren et al., 2008). The erythrocytes change in shape from large round cells with a small nucleus in premetamorphic flounder larvae to elliptical cells in the postmetamorphic juvenile and this change is associated with the onset of adult erythropoiesis (Miwa and Inui, 1991). In the Japanese flounder skin, the differentiation of adult melanophores occurs on the ocular side of the skin and starts during metamorphosis (Seikai et al., 1987). Migration of the eye during Atlantic halibut metamorphosis is followed by an increase in the fibroblasts density in the ventral region of the eye (Saele et al., 2006a; Saele et al., 2006b). These examples highlight the importance of THs in a broad range of tissues and reveal them as key regulators of flatfish metamorphosis. Moreover, methimazole (MMI), a well-established inhibitor of the peroxidase enzyme in the thyroid follicle of vertebrates, that interferes with the incorporation of iodine into tyrosyl residues of thyroglobulin and blocks TH production (Campinho et al., 2012b; Fetter et al., 2015; Roy and Mugesh, 2008), inhibits flatfish metamorphosis (Campinho et al., 2015; Schreiber and Specker, 2000; Schreiber et al., 2010).

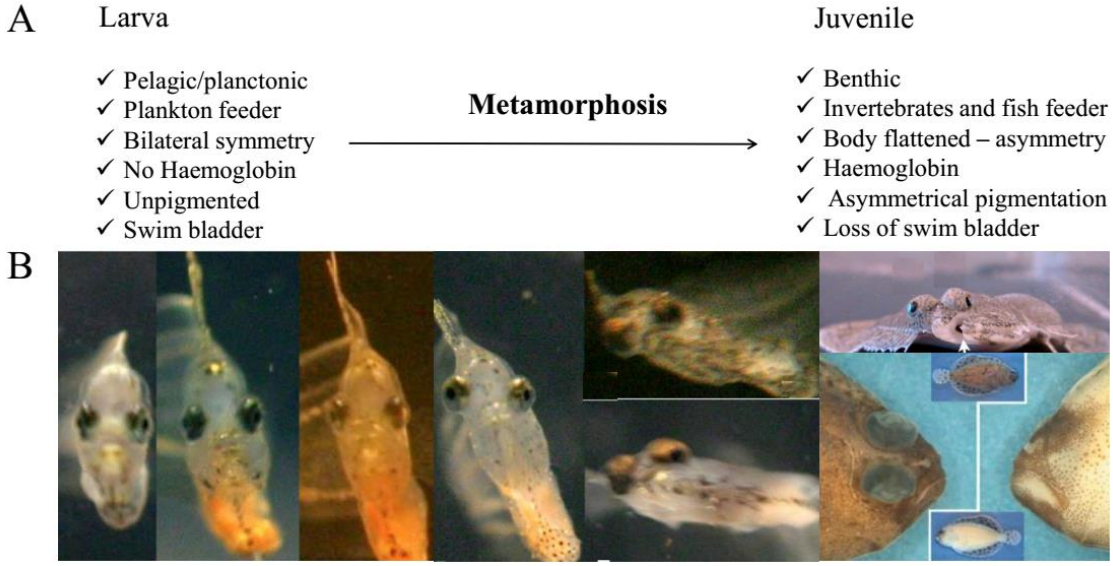

Figure 1.2. Major ecological, external and internal changes associated with flatfish metamorphosis. (A) Description of major changes observed between the pre-metamorphosis larvae and the post-metamorphosis juvenile. (B) Asymmetry generation during the transition from the pelagic symmetrical larva to the benthic asymmetrical juvenile. [Adapted from Tagawa and Aritaki (2005) and Schreiber (2006)].

1.2. The thyroid axis in vertebrates

The hypothalamo–pituitary–thyroid (HPT) axis in vertebrates as well as the mechanism of TH synthesis by thyrocytes, and their central (central nervous system) and peripheral actions are relatively well characterized in vertebrates (**Figure 1.3**). The principal elements of the thyroid axis are already established before the onset of metamorphosis in various flatfish species and a peak in THs coincides with the metamorphic climax (Einarsdóttir et al., 2006; Galay-Burgos et al., 2008; Manchado et al., 2009; Yamano and Miwa, 1998). The thyroid axis players and actions, and their importance during flatfish metamorphosis are described in the following sections.

1.2.1. Thyroid axis and regulation of thyroid hormones production

The thyroid axis shows a high level of conservation within vertebrates. The hypothalamo–pituitary–thyroid axis regulates the production of THs through the stimulatory action of thyroid-stimulating hormone (TSH, thyrotropin-stimulating hormone) produced by the pituitary thyrotrophs in all vertebrates (**Figure 1.3A**) (reviewed in MacKenzie et al., 2009; Szkudlinski et al., 2002). Negative feedback of T_3 and T_4 on the pituitary thyrotrophes regulates TSH beta unit (TSHβ) transcription (Larsen et al., 1997; Manchado et al., 2008; Pradet-Balade et al., 1999; Pradet-Balade et al., 1997). In fish, the identity of the hypothalamic factor that regulates the release of TSH from the thyrotrophs in the pituitary gland still remains to be identified. Although the gene for thyrotropin-releasing hormone (TRH) is present in fish, its function and regulation by plasma THs remains unclear (De Groef et al., 2006). Recently, it was suggested that TRH and/or corticotrophin releasing hormone (CRH, also called CRF) may not be involved in TH production during Senegalese sole metamorphosis (Campinho et al., 2015). The authors hypothesized that Senegalese sole metamorphosis is not dependent on the hypothalamic regulation of the HPT axis, but instead it is the TH metabolism in the thyrotrophs that is the main mechanism of regulation of TSHβ secretion.

1.2.2. Thyroid hormones

Iodine is an essential dietary factor in all vertebrates and its absence has multiple adverse effects on growth and development (Moyano et al., 1996; Zimmermann, 2009; Zimmermann et al., 2013) and in adults leads to goiter (Boyages, 1993). The importance of iodine is linked to its indispensable requirement for the synthesis of the hydrophobic THs, T_4 and T_3 that in vertebrates contain 4 and 3 iodine atoms, respectively (**Figure 1.3C**). THs are the only iodine containing molecules of physiological significance in vertebrates and the number of pathologies associated with their absence gives insight into their functional importance in metabolism, growth, development and reproduction (reviewed by Power et al., 2000). The metamorphic process in flatfish is dependent on T_4 and T_3 (Einarsdóttir et al., 2006; Miwa et al., 1988; Power et al., 2008; Power et al., 2001; Schreiber and Specker, 1998). Two other forms of TH, rT_3 (3,3',5'-triiodothyronine) and T_2 (3,3'-diiodothyronine), are hormone metabolites generated during TH inactivation (**Figure 1.3C**). Little is known about the physiological role of TH metabolites (Hulbert, 2000; Köhrle, 1999) but several non-genomic biological effects have been reported for rT_3 and T_2 (Garcia et al., 2004; Moreno et al., 2008; Senese et al., 2014).

1.2.3. Thyroid gland development and thyroid hormone biosynthesis

The development of the pituitary gland and the proliferation of endocrine cells accompany the increase in TH levels during larval development. In Atlantic halibut, the activation of the thyroid gland occurs in early premetamorphic larvae and this supports the notion that THs play a significant role in the metamorphic process of flatfish (Einarsdóttir et al., 2006). Thyroid follicle activity increases significantly before the metamorphic climax and it is strongly correlated to the appearance of abundant thyrotrophs in the pituitary gland (Einarsdóttir et al., 2006). In fact, when compared to other pituitary endocrine cells such as somatotrophs, lactotrophs and somatolatotrophs, the thyrotrophs are the last endocrine cells to develop, and immunoreactive cells are first detected during pre-metamorphosis (Einarsdóttir et al., 2006). A similar situation occurs in the Senegalese sole and during metamorphosis (12 to 20 dph; days post-hatching), the thyroid follicles increase in both number and size, and at 30 dph they present the same general characteristics as the thyroid in the adult (Delgado et al.,

2006). Complementary studies of Senegalese sole metamorphosis using molecular tools revealed that thyroglobulin (*tg*) transcripts increase significantly at the onset of metamorphosis and decrease after the metamorphic climax (Manchado et al., 2008) and this observations fits well with the importance of thyroglobulin as the precursor of T_4 and T_3 biosynthesis.

THs are produced by the thyroid gland. The basic unit of the thyroid gland is the thyroid follicle which consists of a colloid filled lumen boarded by a monolayer of thyrocytes (**Figure 1.3B**). The most notable difference between the fish thyroid gland and tetrapods is that the follicles are scattered in the loose connective tissue surrounding the ventral aorta in the pharynx instead of aggregated in an encapsulated gland (reviewed in Gorbman et al., 1983). Furthermore, in marine teleosts iodine is unlikely to be a limiting factor, since there is an abundant supply in seawater (Eales and Brown, 1993; Hunn and Fromm, 1966). However, there are occasional reports of goitre in freshwater species although the aetiology is unknown (Leatherland and Farbridge, 1992).

The cellular machinery and biochemical mechanisms for the production and storage of THs have been well characterized in mammals and amphibians (**Figure 3B**). TSH regulates the uptake of iodide by the sodium/iodide symporter (NIS) in thyrocytes and thyroid peroxidase (TPO) oxidizes iodide that is incorporated into tyrosyl groups of the glycoprotein thyroglobulin (TG) in the follicle lumen (Blanton and Specker, 2007; Eales et al., 1999). In the thyroid follicle lumen diiodotyrosine (DIT) and monoiodotyrosine (MIT) are coupled to form T_4 (DIT + DIT) or T_3 (DIT + MIT) (Boas et al., 2006; Degroot and Niepomniszcze, 1977; Eales and Brown, 1993). Gene transcripts encoding proteins involved in the TH biosynthesis in mammals have been identified in the fish thyroid (Pinto et al., 2013) and together with biochemical and immunochemical studies of TH biosynthesis (reviewed by Eales and Brown, 1993) it is suggested that the pathways for TH production in teleosts resembles those of higher vertebrates (**Figure 1.3B**).

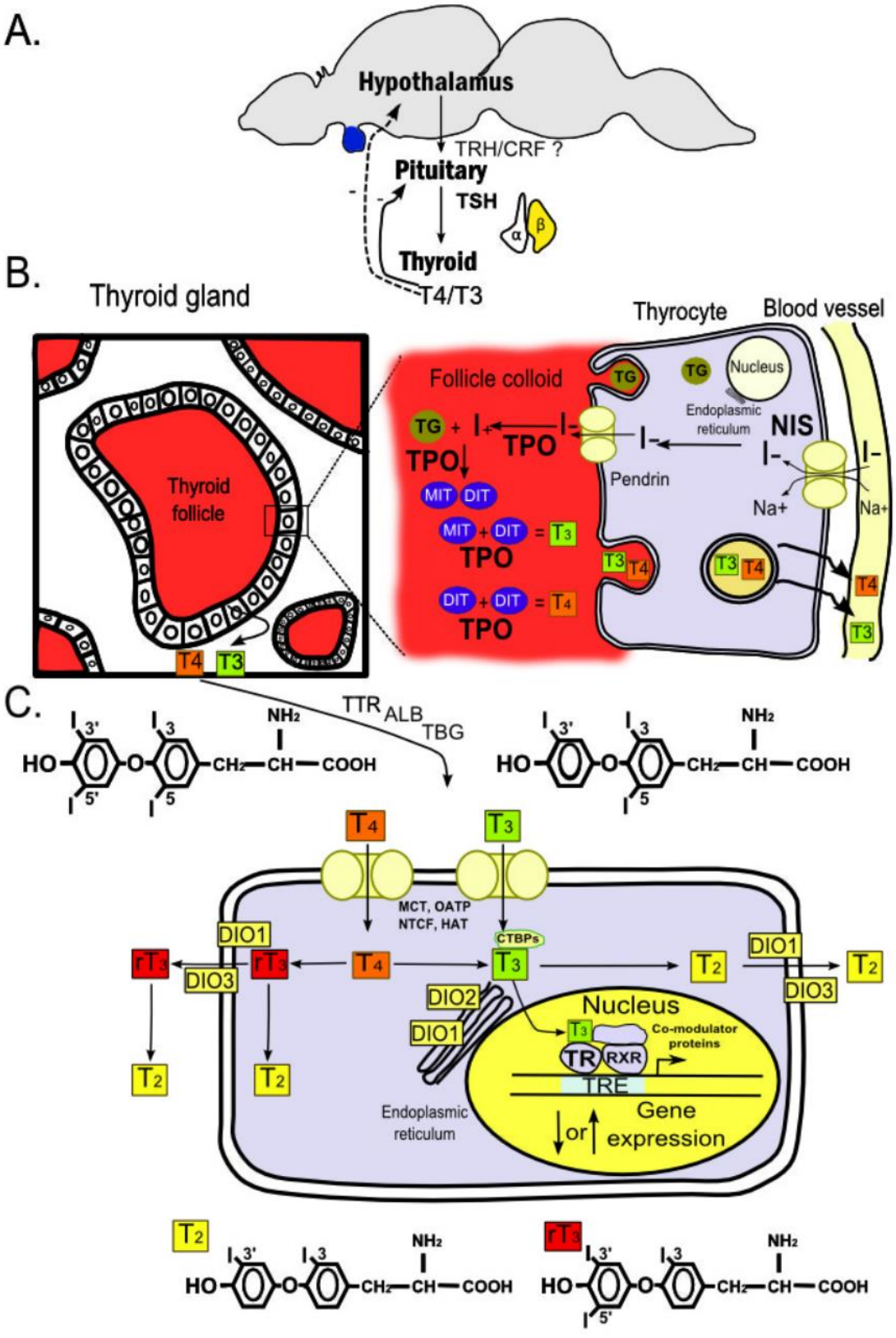
A.
Hypothalamus
TRH/CRF ?
Pituitary
TSH
α
β
Thyroid
T4/T3
B.
Thyroid gland
Thyroid follicle
T4
T3
Thyrocyte
Blood vessel
Follicle colloid
TG
Nucleus
Endoplasmic reticulum
NIS
I-
Pendrin
Na+
TG + I-
TPO
MIT
DIT
MIT + DIT = T3
DIT + DIT = T4
C.
TTR
ALB
TBG
NH2
HO
CH2—CH—COOH
MCT, OATP
NTCF, HAT
DIO1
DIO2
DIO3
rT3
T4
T3
T2
CTBPs
Nucleus
Co-modulator proteins
TR
RXR
TRE
Gene expression
or
Endoplasmic reticulum

Figure 1.3. Schematic representation of the hypothalamo–pituitary–thyroid axis in vertebrates (A), the synthesis of THs by thyrocytes (B), and the mechanism of their central (central nervous system) and peripheral action (C). (A) Thyrotropin-releasing hormone (TRH) is liberated from the hypothalamus and in vertebrates, with the exception of fish and amphibians, stimulates the synthesis and release of thyroid stimulating hormone (TSH) from the thyrotrophs in the pituitary gland (blue). Thyroid-stimulating hormone (TSH) is composed of 2 protein sub-units and the TSH β-subunit confers the hormones thyrocyte specific activity. TSH stimulates TH synthesis and release by the thyrocytes in the thyroid gland. The regulation of TSH synthesis and release from the pituitary thyrotrophs is regulated by negative feedback of THs (solid arrow). The gene for thyrotropin releasing hormone (TRH) has been identified in fish but its function is ambiguous (De Groef et al., 2006). The well-established regulatory feedback of circulating THs on hypothalamic TRH in mammals is represented by a dashed arrow. (B) The functional unit of the thyroid gland is the thyroid follicle that in fish is not encapsulated and the follicles are distributed in the connective tissue surrounding the ventral aorta in the subpharyngeal region. The thyroid follicle consists of a colloid filled lumen surrounded by a monolayer of thyrocytes. Thyroglobulin (TG) is secreted into the lumen by thyrocytes and iodination of tyrosine residues in TG is the starting point for T_4 (thyroxine) and T_3 (3,5,3'-triiodothyronine) biosynthesis. A sodium/iodide symporter (NIS) located in the basal membrane of the thyrocytes ensures iodine uptake from the blood and pendrin located in the thyrocyte apical membrane transports it into the follicle lumen. The iodine is further oxidized to reactive iodinum (I+) by thyroid peroxidase (TPO) and tyrosine residues are coupled to iodine to form mono-(MIT) and diiodotyrosines (DIT), the junction of which generates T_3 or T_4. The thyrocytes endocytose colloid, which is digested to liberate T_4 or T_3 that is then released into the blood. More than 99% of THs present in blood circulate bound to thyroid hormones binding proteins (THBP) that include serum albumin (ALB), transthyretin (TTR) and thyroxine binding globulin (TBG). (C) THs mediate their predominantly genomic effects on peripheral tissues by regulating the transcription of target genes. Less than 10% of the THs enter target cells by passive diffusion (Riley and Eales, 1994) and transporters such as Na+/taurocholate cotransporting polypeptide (NTCP), heterodimeric amino acid transporters (HAT), monocarboxylate transporters (MCT), and organic anion transporting polypeptides (OATPs), located in the plasma membrane are responsible for TH entry in vertebrates. Within the target cell the THs interact with cytosolic thyroid-hormone-binding proteins (CTBPs), such as protein disulfide isomerase and a cytosolic aldehyde dehydrogenase. A group of transmembrane enzymes, the deiodinases DIO1, DIO2 and DIO3 regulate the cellular availability of THs and for the purpose of representation are all shown in the same cell in the scheme although in reality they have a divergent cellular and tissue distribution. DIO1 and DIO3 are generally associated with the inner leaflet of the plasma membrane and DIO2 is associated with the cytosolic side of the endoplasmic reticulum (Bianco and Larsen, 2005). The predominant circulating TH, T_4, is converted into the biologically active form T_3 by DIO1 and DIO2. Inactivation of THs occurs principally through the action of DIO3, which generates the inactive forms, rT_3 (3,3',5'-triiodothyronine) and T_2 (3,3'-diiodothyronine). The TH availability during flatfish metamorphosis is regulated by the coordinated action of DIO2 and DIO3 (Campinho et al., 2012a; Isorna et al., 2009; Itoh et al., 2010). The THs can act via genomic and non-genomic pathways, although the main pathway is genomic and occurs when T_3 binds to the nuclear thyroid hormone receptors (TRs), activating or repressing gene expression. Several TR isoforms exist (TRα and TRβ) and hetero- or homodimers of TRs bind to specific regulatory DNA sequences in target genes known as TH response elements (TREs). TRs also heterodimerize with the retinoid X receptor (RXR). Recruitment of nuclear co-modulator proteins (co-repressors or co-activators) to TR complexes modulates their action on gene transcription in the absence or presence of T_3 (Grimaldi et al., 2013).

1.2.4. Thyroid hormones transport and cellular influx/efflux

Less than 1% of THs circulate in a free form since the majority is bound to TH binding proteins (THBPs). In vertebrates, THBPs include serum albumin (ALB, low-affinity, high binding-capacity), thyroxine-binding globulin (TBG, high affinity, low binding-capacity) and transthyretin (aka. prealbumin, TTR, high-affinity, high binding-capacity) (**Figure 1.3B**), (reviewed in Power et al., 2000). Although the genes encoding for ALB and TTR have been identified in fish, the binding characteristics have only been established for TTR and TBG has not yet been characterized. The functional importance of THBPs during larval fish development, including metamorphosis, remains to be established. In trout (*Onchorynchus mykiss*), high density of lipoproteins in the plasma also make a significant contribution to TH binding activity (Babin, 1992).

Until recently the THs were thought to access the cytoplasm of target cells by passive diffusion. However a shift in the paradigm occurred with the identification of TH membrane transporters: Na^+/taurocholate cotransporting polypeptide (NTCP), heterodimeric amino acid transporters (HAT), monocarboxylate transporters (MCTs) and organic anion transporting polypeptides (OATPs), in mammals (Visser et al., 2011) (**Figure 1.3C**). The way in which TH membrane transporters regulate hormone concentrations is well characterized in mammals, and have given new insights into the mechanism of their regulation and action in vertebrates (Abe et al., 2002; Friesema and Visser, 2002; Merezhinskaya and Fishbein, 2009; van der Deure et al., 2007). In teleosts, a change in TH status (e.g. T_3 or MMI treatment) influences the transcription of several THs transporters (Muzzio et al., 2014). Members of the OATP family are responsible for the transport of various compounds including amphipathic organic compounds, xenobiotics, steroid hormones and THs although with low affinity (Abe et al., 2002; van der Deure et al., 2010). Interestingly, Pizzagalli et al. (2002) and van der Deure et al. (2008) demonstrated that the *oatp1c1* transporter, a member of the subfamily OATP1, is expressed exclusively in the brain and has high specificity for T_4 transport across the blood-brain-barrier (BBB). In addition to OATP1C1, the most well studied transporters is monocarboxylate transporter 8 (MCT8) and monocarboxylate transporter (MCT10) (Friesema et al., 2005; Visser et al., 2010).

1.2.4.1. Monocarboxylate transporters (MCT8 and MCT10)

MCT8 and MCT10 are members of the MCT family and represent a separate clade from other MCT family members (Liu et al., 2008).The primary sequences of the two transporters share a high degree of identity. The two transporters are characterized by 12 putative hydrophobic transmembrane domains (TMDs) and both N- and C- terminal domains are intracellular (Friesema et al., 2008; Friesema et al., 2006) (**Figure 1.4**).

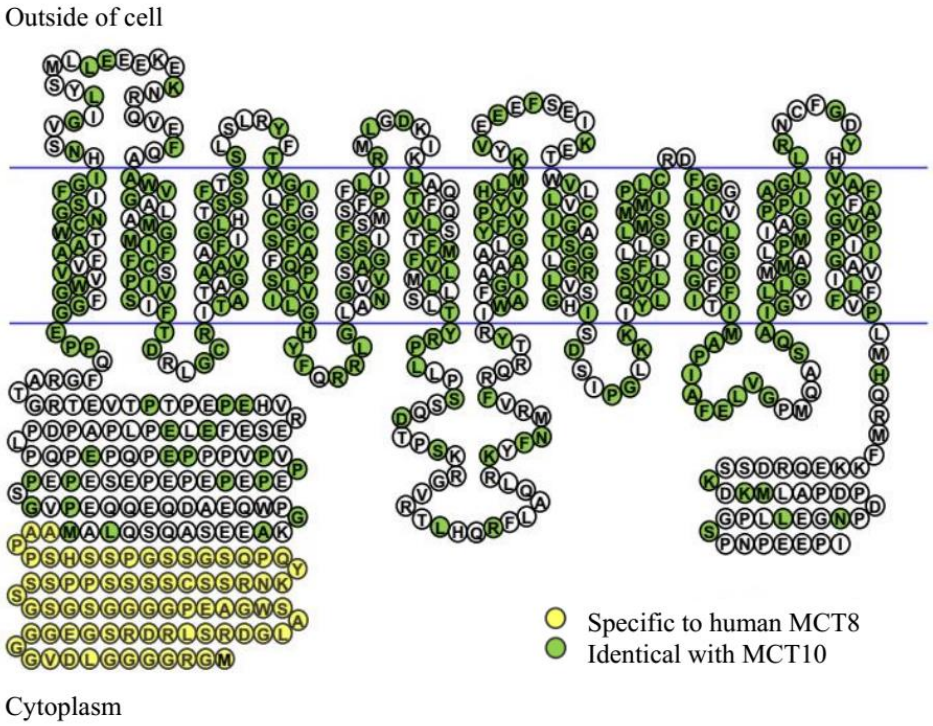

Figure 1.4. Schematic representation of the human MCT8 and MCT10. MCT8 and MCT10 are composed by 12 putative hydrophobic transmembrane domains. Green circles represent the identical amino acids between the two MCTs [Adapted fromKersseboom and Visser, 2011].

MCT8 (also named solute carrier family 16 member 2 or SCL16A2) is a specific transporter for iodothyronines T_4 and T_3 and their inactive metabolites rT_3 and T_2. Lactate, leucine and other aromatic amino acids (e.g. phenylalanine, tyrosine and tryptophan) are not transported by SCL16A2. The ability of MCT8 to exclusively transport THs and facilitate the uptake and mediate the efflux of iodothyronines has been shown for mouse by Friesema et al. (2003; 2006). Additionally, mammalian cells cotransfected with MCT8 and deiodinase reveal a striking increment on intracellular deiodination and an increase in TH intracellular

availability and THs metabolism (Friesema et al., 2006). The biological importance of TH transport by MCT8 is associated with the Allan-Herndon-Dudley syndrome (AHDS), an X-linked developmental disorder caused by mutations or deletion in the *MCT8* gene. Patients diagnosed with AHDS have cognitive impairment and mental retardation with severe developmental delay, neurological damage, spasticity, hypotonia and dystonic movement. TSH levels in patients with AHDS are in the normal range, but high and low levels of serum free T_3 and T_4, respectively, are associated to these mutations (Friesema et al., 2004; Friesema et al., 2005; Friesema et al., 2010; Heuer et al., 2005). MCT8 knockout (KO) mouse strains revealed the same tendency in relation to T_3 and T_4 levels as observed in AHDS patients (Dumitrescu et al., 2004; Schwartz et al., 2005). In mammals, *mct8* is expressed in liver, heart, skeletal muscle, kidney, intestine, brain (neurons and astrocytes of the infundibular and/or paraventricular nuclei), placenta, and thyroid (Alkemade, 2015; Heuer, 2007; Nishimura and Naito, 2008; Schweizer and Kohrle, 2013; reviewed by van der Deure et al., 2010). MCT8 has an important role in TH uptake by neurons and it is involved in TH transport across the blood-cerebrospinal fluid barrier (CSF) and BBB.

MCT10 (also named solute carrier family 16 member 10, or SCL16A10) is generally associated with uptake and efflux of aromatic amino acids, but it is also an active iodothyronine transporter (Friesema et al., 2008; Kim et al., 2001). *Mct10* is expressed in intestine, liver, kidney, skeletal muscle and placenta (Kim et al., 2001; Nishimura and Naito, 2008). MCT10 has higher affinity for T_3 than T_4, and it seems to be a more effective transported of T_3 than MCT8 (Friesema et al., 2008). However, the TH levels in serum and tissues of MCT10 knockout (KO) mice are similar to control mice (Muller et al., 2014). Nonetheless in MCT8/MCT10 KO mice, the thyrotoxic situation in the thyroid gland, liver and kidney is more pronounced than in MCT8 KO mice alone (Müller et al., 2014).

In teleosts, very few studies have target the TH cellular transporters. Arjona et al. (2011a) was the first to characterize the cellular TH uptake by Mct8 in zebrafish. As observed for human and mouse, the zebrafish Mct8 amino acid sequence has 12 predicted hydrophobic transmembrane domains and an intracellular N-terminal PEST domain, which is involved in the proteolytic processing of the precursor protein. In adult zebrafish, *slc16a2* is expressed in the brain, gills, liver, heart, pituitary, gut, kidney and pancreas and it is involved in T_3 uptake (Arjona et al., 2011). In adult fathead minnow (*Pimephales promelas*), *mct8* transcripts are

abundant in the liver and expressed in other tissues including, brain, gills, heart, spleen, digestive tract and muscle, while *mct10* is more abundant in liver and kidney (Muzzio et al., 2014).

The responsiveness of Mct8 and Mct10 to THs was assessed by treating adult fathead minnow male tissues with T_3 and MMI and revealed in brain, the expression of both *mct8* and *mct10* was decreased after T_3 treatment. In the case of liver, only *mct8* expression was down-regulated after T_3 exposure, compared to MMI treated fish (Muzzio et al., 2014). Furthermore, exposure via feeding to decabromodiphenyl ether (BDE 209) up-regulated the *mct8* transcripts in the brain of adult fish (Noyes et al., 2013). Overall the data that exists indicates that in teleosts MCTs have a broad tissue distribution and their expression is responsive to THs and for this reason TH disruptors can also affect their expression.

1.2.4.2. Thyroid hormone transporters and development

Recently, the role of THs transporters during vertebrate's development have started to be uncovered (reviewed by Darras et al., 2015; and Preau et al., 2015). The first evidences of the important role of TH transporters during early development were associated with AHDS, which affects the normal development of the brain in humans (Dumitrescu et al., 2004). In mouse, *Mct8* is present in the forebrain neurons during embryogenesis (stage E14.5) and during early postnatal stages (stage P5-P10), *Mct8* is highly expressed in the cerebellum and neocortex. *In situ* hybridization revealed that *Mct8* has a broad distribution in the brain and is present in the neurons of the cortex, striatum, hypothalamus and hippocampus, the BBB and choroid plexus and in the cerebellar Purkinje cells in early postnatal stages (Heuer et al., 2005). Moreover, MCT8 is also described as a putative candidate factor important in bone development and osteoblast differentiation (Braun et al., 2011; Capelo et al., 2009).

The absence of a functional *Mcto* in MCT8 KO mice is associated with aberrant circulating TH levels but does not induce a phenotype equivalent to that of human AHDS (Trajkovic et al., 2007). Furthermore, during the first seven postnatal days, plasma T_4 levels are similar between MCT8 KO and wild type mice. The overlap of *Mct8* expression with other TH transporters including the *Oatp1c1, Mct10,* L-type amino acid transporter 1 (*Lat1*), and L-type amino acid transporter 2 (*Lat2*) may explain how in mice TH uptake into the brain can occur and compensate for the lack of MCT8 (Braun et al., 2011; Ferrara et al., 2013; Grijota-Martinez et al., 2011). It is suggested that TH transporters in the developing mouse

brain can exhibit their function individually or cooperatively to regulate the uptake and/or efflux of both active and inactive THs amongst the proliferating and maturing brain cells (Darras et al., 2015). In fact, the severe hypothyroid status observed in the mouse MCT8 and OATP1C1 double KO resulted in delayed brain development (Mayerl et al., 2014).

As observed in mammals, TH transporters also regulate the THs availability in the brain of early embryonic stages of chicken (Van Herck et al., 2012). *Mct8* and *oatp1c1* are co-expressed in the blood-cerebrospinal fluid-barrier, and expression in the developing choroid plexus is in accordance with the expression pattern in mammals (Van Herck et al., 2013). In contrast to mammals, LAT1 is considered to be mainly responsible for T3 uptake in the BBB during chicken brain development (Van Herck et al., 2015). MCT10 has a limited role in chicken choroid plexus, since residual or inexistent mRNA expression is detected during development (Van Herck et al., 2015).

In teleosts, the role of TH transporters during development has only been characterized in zebrafish (Arjona et al., 2011a; Campinho et al., 2014; Vatine et al., 2013). Zebrafish *mct8* transcript levels are detected as early as 3 hpf (hours post-fertilization), but the highest expression is detected immediately before hatching (Arjona et al., 2011; Campinho et al., 2014). At 24 hpf *mct8* is most abundant in the forebrain, midbrain, hindbrain, spinal cord, notochord, and eyes, and at hatching (2 dpf) it is limited to the central nervous system and notochord (Campinho et al., 2014; Vatine et al., 2013). *mct10* and *oatp1c1* transcripts are also detected at 2 dpf in liver and trigeminal ganglia (*mct10*) and vascular structures of the brain (*oatp1c*), (Vatine et al., 2013). Using the whole mount *in situ* hybridization (WMISH), Vatine and colleagues (2013) detected *mct8* expression in neurons and oligodendrocytes, but also in blood and lymph vessels of the trunk and in blood vessels surrounding the brain. *mct8* is expressed in the blood vessels close to the BBB (Campinho et al., 2014), but not in choroid plexus, a key difference between zebrafish and mammals (Vatine et al., 2013). The broad distribution of *mct8* transcripts in the central nervous system (CNS) revealed the importance of this transporter during the development of the zebrafish nervous system. Mct8 generated transgenic lines allowed to infer about the role of Mct8 in the uptake of THs in neurons and oligodendrocytes as well as in the involvement in the myelination of neurons. Mct8 knockdown (KD) using morpholinos system in zebrafish revealed the importance of THs in the normal development of the brain, spinal cord, notochord and vascularization (Campinho et al., 2014; de Vrieze et al., 2014; Vatine et al., 2013).

The role of Mct8 and Mct10 during metamorphosis has been suggested by analysis of transcript abundance in *Xenopus tropicalis*, in the major resorbing, growing and remodelling tissues: gills, tail and limb (Connors et al., 2010). In *X. tropicalis*, the temporal expression pattern of *mct8* and *mct10* varies between tissues and is correlated with the timing of their metamorphic changes. For example, Mct10 seems to be the main transporter responsible for the increased TH levels in gills at stages NF 58-61, which corresponds to the stage at which gill death and resorption occurs and coincides with the metamorphic climax of TH concentrations. In the *Xenopus* tail, the most pronounced changes in TH transporter gene expression occurs with an increase of 11-fold in *mct8* during tail regression (Connors et al., 2010). Both *mct8* and *mct10* show robust mRNA expression levels during limb development with significant up-regulation occurring during NF stages 54–56, which corresponds to the timing of limb growth and differentiation. It is also suggested that Mct8 and Mct10 have a role in TH transport into the kidney and liver and therefore influence TH metabolism and excretion after the metamorphic climax. In the brain, only the *mct8* expression patterns change during metamorphosis (2-fold increase between NF64-56 while *mct10* has a constant expression during development (Connors et al., 2010). The authors concluded that changes in cellular TH uptake and efflux are essential for local regulation of nuclear TR-mediated signaling during amphibian metamorphosis. No information exists about the role or importance of Mct8, Mct10 or any other THs transporters during flatfish metamorphosis.

1.2.5. Deiodination: the activation and inactivation of thyroid hormones

1.2.5.1. Iodothyronine deiodinases

The prohormone T_4 is the main product of the thyrocytes and is converted into T_3 through deiodination. The deiodination consists in the removal of specific iodine moieties from the outer or inner benzene ring in the TH and is regulated by specific thioredoxin fold-containing selenoenzymes named deiodinases (DIO), members of the selenocysteine family (Bianco et al., 2002). Three main DIOs exist in vertebrates, DIO1, DIO2 and DIO3 (Bianco and Larsen, 2005) and they regulate the cellular availability of THs in peripheral tissues by intracellular activation or inactivation of T_4 and T_3 (Köhrle, 1999). T_4 is converted by DIO1 and DIO2 into the active form T_3 by outer ring deiodination (ORD). T_3 and T_4 are inactivated

by DIO3 through inner ring deiodination (IRD) that converts them into T_2 and rT_3, respectively (reviewed in Gereben et al., 2008a) (**Figure 1.3C**; detailed in **Figure 1.5**). DIO2 only catalyzes ORD and it is the predominant source of extra-thyroidal T_3 and T_4 is its main substrate. DIO1 can catalyze both ORD and IRD and it converts T_4 into T_3 but reverse T_3 (rT_3) is the preferred substrate. DIO3 is the major physiological inactivator of THs and can inactivate both T_4 and T_3 by IRD producing rT_3 and T_2, respectively. DIO3 has a low K_m and prefers T_3 to T_4 as a substrate (Bianco et al., 2002; Darras et al., 2015; Mol et al., 1997; Salvatore et al., 1995).

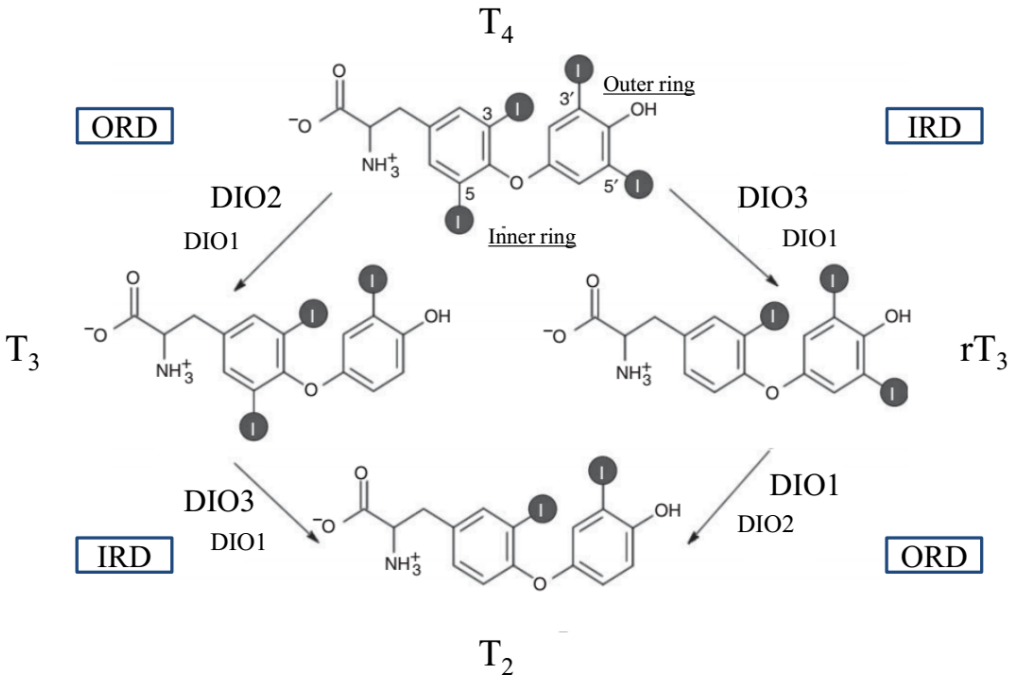

Figure 1.5. Schematic representation of the major reactions catalyzed by the iodothyronine deiodinases in vertebrates. DIO1-DIO3 – deiodinase type 1-3. ORD – outer ring deiodination and IRD – inner ring deiodination [Adapted from Schweizer and Steegborn, 2015].

One characteristic common to all known vertebrate DIOs is the presence of the amino acid selenocysteine (Sec, U), a key residue located in the catalytic center. Sec is encoded by the TGA codon, which usually acts as a stop codon. However, due to the existence in the secondary structure of the DIO mRNAs of a SElenoCysteine Insertion Sequence (SECIS element) in the 3'UTR the TGA encodes Sec (Bianco et al., 2002; Darras and Van Herck, 2012; Isorna et al., 2009; St Germain et al., 1994; Villalobos et al., 2010). The incorporation of the Sec amino acid into the growing polypeptide chain occurs due to the coordination between the conserved *cis*-acting stem-loop RNA structure and special *trans*-acting protein factors that recruit the Sec-charged tRNA (Berry et al., 1991a; Berry et al., 1991b). Two

trans-acting factors are required for the efficient reprogramming of UGA to Sec in eukaryotes, SECIS binding protein 2 (SBP2) and the Sec-specific translation elongation factor (eEFSec). SBP2 binds to the ribosomes and SECIS elements and interacts with eEFSec to recruit Sec-tRNA$^{[Ser]Sec}$, allowing the incorporation of Sec into the nascent, growing polypeptide. Other SECIS-binding proteins identified include ribosomal protein L30, eukaryotic initiation factor 4a3 (eIF4a3) and nucleolin (**Figure 1.6A**) (reviewed by Labunskyy et al., 2014).

In eukaryotes, SECIS elements are composed of two helixes separated by an internal loop, a GA quartet structure, and a bulge or apical loop (**Figure 1.6B**). The GA quartet is located at the basis of helix II and represents the SECIS core, and is composed of four non-Watson-Crick interacting base pairs, including two tandem G.A/A.G base pairs. The GA quartet is essential for SBP2 interaction. Two forms of SECIS elements have been described and form 1 is usually found in the Dio1 sequence and the essential adenosines (AA(R)) (also required for Sec incorporation) are contained in a single open loop. The predicted DIO2 and DIO3 secondary structure generates SECIS form 2 in which the adenosines (AA(R)) are located in a second bulge region, that contains a ministem (bulge) (Gereben et al., 2008a; Labunskyy et al., 2014; Orozco et al., 2002; Orozco et al., 2003) (**Figure 1.6B**).

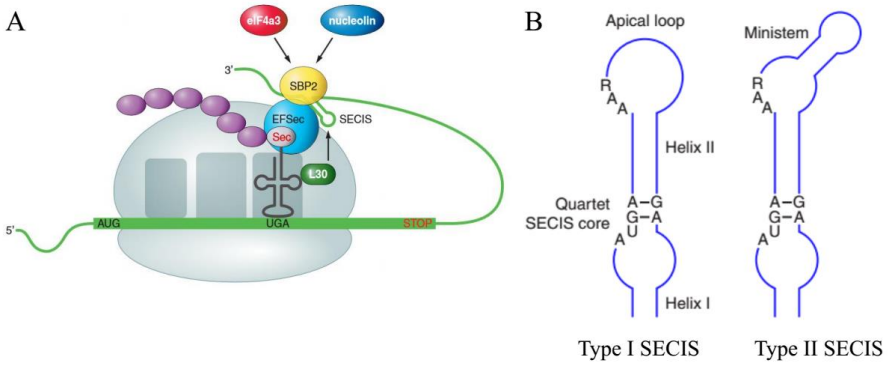

Figure 1.6. Selenocysteine insertion mechanism in vertebrates (A) and the consensus type I and type II SECIS element structure (B). Sec – selenocysteine, SBP2 - SECIS binding protein 2, EFSec - Sec-specific translation elongation factor, L30 - ribosomal protein L30 and eIF4a3 - eukaryotic initiation factor 4a3 [Adapted from Labunskyy et al., 2014].

The three DIOs have a similar protein structure; they are integral membrane proteins (29 – 33 kDa) and act as dimers (generally homodimerization) (Bianco and Larsen, 2005; Bianco et al., 2002). The DIOs have been divided in two distinct structural regions: a

conserved region and a variable region. The variable region is composed by three domains: the single transmembrane segment (TM), hinge (H) and linker (L). The conserved region is the globular or catalytic (G) domain (Callebaut et al. 2003). The TM domain comprises 16 to 40 aa and is located in the N-terminal region (hydrophobic transmembrane region). The TM domain defines the subcellular topology for the three deiodinases: DIO2 is integrated in the endoplasmic reticulum (ER) membrane and its G domain is in contact with the perinuclear cytosol; DIO3 is integrated in the plasma membrane and the G domain is generally extracellular; and DIO1 is in the plasma membrane, but can also be associated to ER and its catalytic G domain is located in the cytosol (**Figure 1.3C**) (Orozco et al., 2012). The G domain contains a 'signature string' composed of nine conserved amino acids (FGS(C/A)(T/S)UP(P/S)F) that are found in DIOs across the vertebrates. The Sec residue is located in the 'signature string'. The G domain also contains the deiodinase dimerization domain (DDD), a well-conserved 16 residues domain located in the C-terminal region, essential for homodimerization (Leonard et al., 2005; Orozco et al., 2012).

Knowledge about the cellular localization and role of DIOs is changing rapidly, and their expression pattern appears to be tissue- and species-specific. Nonetheless, it is generally considered that only one of the DIOs can be expressed by a cell at any given time, although this may vary with age and physiological status and some cells may simultaneously express all deiodinases. The main biochemical properties, expression pattern and substrate preference for vertebrate DIO1-3 is resumed in **Table 1.1**. The ORD and IRD activities have been determined in several fish species including Nile tilapia (*Oreochromis niloticus*), blue tilapia (*Oreochromis aureus*), African catfish (*Clarias gariepinus*), rainbow trout (*Oncorhynchus mykiss*), killifish (*Fundulus heteroclitus*) and turbot (*Scophthalmus maximus*), gilthead seabream (*Sparus aurata*), American plaice (*Hippoglossoides platessoides*), Senegalese sole (*Solea senegalensis*) and common carp (*Cyprinus carpio*), (Adams et al., 2000; Arjona et al., 2011a; Isorna et al., 2009; Klaren et al., 2012; Klaren et al., 2005; Mol et al., 1998; Mol et al., 1997; Sanders et al., 1997; Valverde et al., 1997) in different tissues and has the same activity profile as for mammalian DIOs.

DIO1 acts primarily as a scavenging enzyme and is most important in iodine recycling from inactive forms of THs and is less important for iodothyronines (Schneider et al., 2006). The first DIO identified in fish was Dio1 from Nile tilapia, and it contained the characteristic

domains of functional mammalian DIO1, although they differed since there is a tandem repetition of the SECIS element in the 3'UTR. The tilapia Dio1 recombinant enzyme expressed in COS-1 cells catalyzes both ORD of T_4 and rT_3 and IRD of sulfated T_3 and T_3, but in contrast to mammals, the activity was not inhibited by propylthiouracil (PTU). The resistance of Dio1 to PTU in tilapia has been also observed for other teleost Dio1s (Mol et al., 1998; Orozco et al., 2003). Low levels of *dio1* transcripts are detected in the tilapia liver and its expression is induced by hypothyroid conditions provoked by exposure to MMI, (Van der Geyten et al., 2001). In the kidney from Blue tilapia (*Oreochromis aureus*), the rT_3 ORD activity has similar substrate specificity to mouse liver DIO1, suggesting that in fish, Dio1 may not be the major enzyme responsible for T_3 levels in plasma (Mol et al., 1998; Van der Geyten et al., 2001). In walleye (*Sander vitreus*), besides kidney and liver, *dio1* is also expressed in other tissues including muscle, heart, stomach, spleen, skin and eye; and a non-functional isoform of Dio1 occurs in the liver (Picard-Aitken et al., 2007).

Teleost Dio2 and Dio3 enzyme activities and physical properties are very similar to the higher vertebrates (Mol et al., 1998; Van der Geyten et al., 2005). For example, *O. aureus* liver T_4 ORD and brain and gill T_3 IRD activities have similar substrate specificities and inhibitor sensitivities to mammalian DIO2 and DIO3, respectively (Mol et al., 1997). The high levels of Dio2 activity and the absence or low Dio1 activity in the kidney and liver suggests that Dio2 is the major contributor to T_3 plasma levels (Orozco and Valverde, 2005; Van der Geyten et al., 2005). In striped parrotfish (*Scarus iseri*) and rainbow trout (*Oncorhynchus mykiss*), *dio2* is present in the brain and its expression is regulated by THs (Fines et al., 1999; Johnson and Lema, 2011). Liver is the main source of peripheral T_3 in most teleosts, although walleye *dio2* mRNA expression is observed in brain, eye and gills (Picard-Aitken et al., 2007). Recently, in the Atlantic salmon (*Salmo salar*) two different *dio2* genes arose during the tetraploidization event that occurred in the salmoniform. These duplicate deiodinase 2 (*dio2a* and *dio2b*) genes have distinct expression patterns during smoltification. *Dio2b* is associated with acclimation to the osmotic stress in salmon gills when they enter the sea, while *dio2a* is involved in the changes occurring in the brain and is associated with light-dependent TH regulation (Lorgen et al., 2015). The *dio2* gene including the promotor region is well characterized in killifish and trout (Sambroni et al., 2001; Valverde et al., 2004). In fact, DIO2 is important for local T_3 production in several tissues and also contributes to circulating T_3, especially in fish and amphibians.

The vertebrate *dio3* gene is generally intronless (Hernandez et al., 1999) and, in common with *dio1* and *dio2* contains the selenocysteine-encoding TGA codon and the SECIS element in the 3'UTR (St Germain et al., 1994; Darras and Van Herck, 2012; Bianco et al., 2002; Valverde et al., 1997; Villalobos et al., 2010; Isorna et al., 2009). Two deiodinase 3 paralogs (*dio3a* and *dio3b*) have recently been identified in zebrafish, and their role in embryonic and early larval development stages was recently investigated (Guo et al., 2014; Heijlen et al., 2014). DIO3 amino acid sequences have been well conserved during evolution (Orozco et al., 2012; Darras & Van Herck., 2012) and *in silico dio3* promotor analysis in human and mouse suggests that *dio3* is positively regulated by T_3 (Gereben et al., 2008a) and its tissue expression and activity is widespread. In the walleye (*Sander vitreus*) fish *dio3* is abundant in liver, eye, brain, skin, and gills but is poorly expressed in the heart (Picard-Aitken et al., 2007). In rainbow trout (*Oncorhynchus mykiss*) and in Australian lungfish (*Neoceratodus forsteri*), *dio3* transcripts are also expressed in brain, spleen, liver and kidney (Bres et al., 2006; Sanders et al., 1999; Sutija et al., 2004; Van der Geyten et al., 2005). In other fish species, the expression pattern of *dio3* is similar and functional studies indicate that it is active in different developmental stages and under a range of physiological conditions (Bouzaffour et al., 2010; Dong et al., 2013; Houbrechts et al., 2016; Itoh et al., 2010; Johnson and Lema, 2011; Li et al., 2012; Mol et al., 1997).

DIO3 plays an essential role in maintaining low TH levels in different physiological conditions such as development, metabolism, disease, tissue regeneration and inflammation (reviewed by Darras et al., 2015; Dentice and Salvatore, 2011). *Dio3* mRNA expression decreases in hypothyroidism and increases in hyperthyroidism (Hernandez et al., 2002) and high levels of deiodinase 3 expression are associated with several cardiac disorders (Pol et al., 2010; Wassen et al., 2002). In zebrafish, after fin amputation, *dio3* mRNA expression is induced in the blastema, and an inhibition of Dio3 activity results in the reduction in bastema formation. The local degradation of TH is essential for cell proliferation in the blastema during fin regeneration (Bouzaffour et al., 2010). These authors hypothesized that Dio3 has an important role in fin regeneration by decreasing T_3 concentration in the progenitor cells to allow their proliferation. In addition to the role of DIO3 during several pathophysiological conditions in adult vertebrates, it is also highly expressed in embryonic/fetal vertebrate tissues, and its activity is much higher than that found in adult tissues (Dong et al., 2013;

Galton, 2005; Van der Geyten et al., 2002). Treatment of adult laying hens with MMI (used for treatment of chronic hyperthyroidism) caused a decrease in the adult telencephalon DIO3 activity, but also affected embryonic development (Van Herck et al., 2013).

Table 1.1. Biochemical characteristics and regulation of vertebrate deiodinases (DIO1-DIO3). Data collected from 2004 to 2012. Adapted from St Germain et al., (2009) and Orozco et al., (2012).

Deiodinase characteristic	DIO1			DIO2			DIO3		
Reaction catalyzed	ORD/IRD			ORD			IRD		
Substrate preference	IRD: $T_4S>T_3S>>T_3,T_4$ ORD: $rT_3>rT_3S>T_2S>>T_4$			$T_4>T_3$			$T_3>T_4$		
Km (dithiothreitol as cofactor)	T_4S (IRD): 0.3 μM; rT_3 (ORD): 0.06 μM; T4 (ORD): 2.3 μM			T_4: 1 nM			T_3: 6 nM; T_4: 37 nM		
Selenocystein	Present			Present			Present		
Molecular ma s (kDa)	29			0			332		
Homodemerization	Yes			Yes			Yes		
	Fish	**Amphibians**	**Mammals**	**Fish**	**Amphibia s**	**Mammals**	**Fish**	**Amphibia**	**Mammals**
in tissue distribution	Liver, kidney, gills, brain, gonads	Liver, kidney, brain	Liver, kidney, gut, lungs, pituitary	Liver, retina, brain, gonads	Brain, skin, gut, tail	Pituitary, brain, tanicytes, BAT, adrenals, liver	Liver, skin, gills, brain	Liver, gut, kidney	placenta, skin, brain, uterus
Substrate regulation									
Hyperthyroidism	↓↓mRNA	No effect	↑↑mRNA ↓↓ protein	↓↓ mRNA ↓ protein	↑↑mRNA	↓ mRNA ↓↓ protein	↑ protein	↑↑mRNA	↑↑mRNA
Hypothyroidism	↑↑protein	No data	↓ protein	↑protein	No data	↑protein	No effect	↓ protein	↓ protein

1.2.5.2 Deiodinases and development

Deiodinases have an important role in the peripheral tissue intracellular TH metabolism in adult animals, but they also play an important role during vertebrate development (reviewed by Bianco and Kim, 2006; Darras and Van Herck, 2012; Dentice et al., 2013; Dentice and Salvatore, 2011; Heijlen et al., 2014; Morvan-Dubois et al., 2008; Preau et al., 2015; St Germain et al., 2009; Van Herck et al., 2013). During mouse fetal development, DIO1 is the main deiodinase responsible for TH activation by ORD in the kidney, liver, lung, intestine and eye. The expression of *dio2* is more limited during development and it is the main TH-activating enzyme in brain and in the brown adipose tissue (Galton, 2005). TH availability during brain development is tightly controlled by a dynamic interplay of both *dio2* and *dio3* (Dong et al., 2013; Morvan-Dubois et al., 2006). *DIO2* and *DIO3* are expressed and the respective proteins are active in the cerebral cortex already at 7 to 8 weeks of gestation, and the DIO3 activity at this development stages is higher than in the adult human cerebral cortex (Chan et al., 2002). DIO1 and DIO2 activity tends to increase towards neonatal stages, while DIO3 tends to decrease over the same time frame and is considered to have a protective role during early development (Dentice and Salvatore, 2011). For example, appropriate T_3 signaling is essential during eye development and DIO3 activity in the retina is high in prenatal mice, while little or no DIO1 or DIO2 activity can be detected. In fact, the development of cones, the photoreceptors for daylight, and colour vision requires protection from THs by over-expression of DIO3 (Ng et al., 2010). Similar deiodinases expression patterns are observed in chicken, as during the last week of embryonic development, the majority of tissues express *dio3,* and together with either *dio1* or *dio2,* indicating that each tissue possesses the necessary tools to regulate local thyroid hormone levels independent of plasma levels of T_3 and T_4 (Van der Geyten et al., 2002).

Functional studies using the mouse/mice knock-out (KO) system has provided new insight into the role of deiodinases in development and tissue maturation and differentiation (St Germain et al., 2009; Darras et al., 2015). DIO2 KO mice have low T_3 levels in the postnatal brain, and several TH responsive genes are affected, and abnormal development occurs. For example, DIO2 KO leads to the loss of oxidative capacity and impaired differentiation of brown adipocytes as a consequence of down-regulation of peroxisome proliferator-activated receptor gamma, coactivator 1 alpha (*Ppargc1a*) and uncoupling protein

1 (*Ucp1*), (Hall et al., 2010). Dentice and co-authors observed myotube formation in myoblasts was blocked due to down-regulation of myogenic differentiation 1 (m*yod*) and other essential genes in this process, including myogenin, troponin 1 and myosin, heavy polypeptide 2, skeletal muscle (*myh2*). The DIO2-KO mouse muscle has a phenotype of mild hypothyroidism (Dentice et al., 2010), there is retarded postnatal development of the cochlea, which results in severely impaired auditory function in the adult (Ng et al., 2004) and the bones of adults are brittle, due to increased skeletal mineralization (Bassett et al., 2010). The effects of DIO3-KO in mice are more severe than DIO2-KO and abnormalities include, growth retardation, defects in neural crest migration and in the development of cerebellum, eye and cochlea (Hernandez et al., 2006; St Germain et al., 2009). DIO3-KO in mice significantly affected cerebellar development, which revealed reduced foliation, accelerated disappearance of the external germinal layer and premature expansion of the molecular layer (Peeters et al., 2013). The excessive TH in *dio3* mice morphants is associated with increased apoptotic cell death that causes around 80% of cone loss in the retina (Ng et al., 2010) and highlights the importance of appropriate levels of THs in the development of the visual system. The expression levels of T_3-responsive genes in the CNS of DIO3 deficient mice are higher than normal during neonatal stages and lower than normal later in life (Horn and Heuer, 2010). The maturation of the hypothalamus-pituitary-thyroid axis is severely disturbed in DIO3-KO. Thus, an initial phase of hyperthyroidism gives way in the latter part of the utero and neonatal period to a moderate state of hypothyroidism that persists into adulthood, and is associated with functional abnormalities in the hypothalamus, pituitary gland, and thyroid gland (Hernandez et al., 2007).

In fish, the characterization of deiodinases mRNA expression and the tissues distribution of transcripts is well-studied in zebrafish (reviewed by Heijlen et al. 2014). *Dio1* expression is detected at the start of development (2-cell stages) and its expression increases (~3 fold) between 8 to 75 hpf. ISH revealed a high *dio1* expression in the liver and interrenal tissues up to 10 dpf (Dong et al., 2013; Vatine et al., 2013; Walpita et al., 2007). Dio2 is detected in early development stages but only increases at hatching concomitant with the start of embryonic TH secretion (Darras et al., 2015) and *dio2* is expressed in the retina and the adenohypophysis from 24 hpf onwards and in the spinal cord at 48 hpf (Dong et al., 2013; Thisse et al., 2003). Deiodinase 3 paralogs (*dio3a* and *dio3b*) exist in zebrafish and are expressed from 24 to 72 hpf and encode enzymatically active proteins with high affinity for

THs (Guo et al., 2014). *Dio3b* is more abundant than *dio3a* (Heijlen et al., 2014) and knockdown (KD) delays time of hatching and development of zebrafish. Several abnormalities, including deformities in liver and intestine, muscle contraction, heart function and aberrant swim bladder inflation are identified in *dio3a* and *dio3b* morphants (Bagci et al., 2015). Transcriptome analysis of Dio1 and Dio2-KD revealed a pronounced up-regulation of a large number of transcripts involved in carbohydrate metabolism reflecting a compensatory response to a decreased metabolic rate due to low T_3 levels (Bagci et al., 2015).

Deiodinases act coordinated and locally to regulate the circulating and tissue levels of THs during vertebrate metamorphosis (Brown, 2005; Campinho et al., 2012a; Morvan-Dubois et al., 2008). Transgenic *Xenopus laevis* tadpoles overexpressing *dio3* have delayed tail and gills resorption and severe arrested metamorphosis, and subsequently die (Dentice et al., 2010). Dio3 is also essential for asymmetrical retinal growth in frogs. The increase of circulating THs during metamorphosis allows cell proliferation in the ventral ciliary marginal zone (CMZ) and subsequently formation of ipsilateral projections to the brain. Nevertheless, high levels of *dio3* were observed in the CMZ dorsal cells which prevent the increase of THs in this retinal region and subsequently cell proliferation (Brown, 2005; Marsh-Armstrong et al., 1999). Moreover, the highest Dio2 activity and *dio2* mRNA levels occur in the most profoundly modified tissue, the intestine, skin, tail and limbs from *Rana catesbeiana*. Iapanoic acid (IOP) inhibits Dio2 activity and subsequently delays the metamorphic events in these tissues (Becker et al., 1997). Furthermore, at the metamorphic climax, *dio2* expression increases in response to high circulating THs levels in tissues such as tail (resorption) and intestine (remodelling), while in brain, spinal cord and limb buds the *dio2* decreased, as these tissues stop their proliferation (Cai and Brown, 2004).

In teleosts, deiodinases also has a dynamic spatio-temporal distribution and the intracellular TH concentrations tightly regulate the deiodinases expression pattern during the larval to juvenile transition. During the *Sparus aurata* metamorphosis, only *dio1* and *dio2* increase and peak at the metamorphic climax. This increase in deiodinase mRNA expression matches the change in T_4 levels and both thyroid hormone receptors (Campinho et al., 2010). Using ISH, Itoh and colleagues (2010) mapped the spatial distribution of deiodinase gene expression during *Paralichthys olivaceus* metamorphosis. *Dio1* is restricted to pro-metamorphic and early metamorphic climax stages and is mostly expressed in liver. *Dio2* is

essential expressed in eye but also in tectum and skeletal muscle between pro-metamorphosis and late climax and *dio3* is high at pre- and pro-metamorphic stages in skeletal muscle, gastric gland blastema, spinal cord and eye. Increasing of THs levels during Senegalese sole metamorphosis depends on the coordination between expression and activity of Dio3 and Dio2; while the Dio2 activity increased at mid-late metamorphic stage, both Dio3 activity and expression decreased at this stage (Isorna et al., 2009). These authors observed a positive correlation between *dio3*, thyroid hormone receptor alpha A and THs levels, suggesting that *dio3* is directly responsive to THs during metamorphosis (Isorna et al., 2009). In Atlantic halibut tissue-specific changes in *dio3* expression precede the cell-specific changes in muscle and skin during metamorphosis (Campinho et al., 2012a) and this highlights the importance of local regulation of THs availability to maintain the different phenotypes before, during and after metamorphosis. In contrast to teleosts and amphibians, *dio2* mRNA expression in liver and intestine from sea lamprey (*Petromyzon marinus*) are high prior to and during the early stages of metamorphosis and then decline dramatically to low levels at the metamorphic climax. However, the tissue-specific changes in *dio2* mRNA levels in response to a T_3 and T_4 exposure are consistent with previous observations in other vertebrates (Stilborn et al., 2013).

1.2.6. Thyroid hormones action: thyroid hormones receptors

The most active form of the THs, T_3, brings about its action through classical genomic pathways, and although non-genomic actions have been known to exist for more than 2 decades the mode of action has only recently been explored in detail (Davis et al., 2011). Genomic actions of THs occur when they bind to thyroid hormone receptors (TRs) that act as ligand activated transcription factors that regulate expression of target genes (Cheng et al., 2010) (**Figure 1.3C**). TRs are members of the nuclear receptor superfamily and their structure is composed of several regions containing both DNA and ligand binding domains: the N-terminal A/B domain contains the AF-1 (activation function) site where other transcription factors interact, the C domain composed of two zinc fingers responsible for DNA binding (DBD), the hinge domain D that links the DBD with the ligand binding domain (LBD), the E domain containing the LBD which is involved in ligand binding, dimerisation and transactivation of gene expression and the C-terminus which contains the ligand-dependent AF-2 (Aranda and Pascual, 2001; Yen, 2001; Zhang and Lazar, 2000).

Most vertebrates possess two TRs (TRα and TRβ) that are encoded by two different genes (reviewed by Laudet, 2011); the teleosts have an additional copy of Trα (Trαa, Trαb) as a result of the fish specific whole genome duplication (Galay-Burgos et al., 2008; Kawakami et al., 2008; Takayama et al., 2008; Yamano and Inui, 1995; Yamano and Miwa, 1998) There are some exceptions, such as *Xenopus laevis* that has 2 Trα and 2 Trβ genes as a consequence of the tetraploidization of its genome. Numerous splice variants of the TRs have been identified in vertebrates, although their functional significance still remains to be established. After THs enter a cell they are bound to cytosolic thyroid-hormone-binding proteins (CTBPs) such as protein disulfide isomerase (Denver, 1997) and cytosolic aldehyde dehydrogenase (Yamauchi and Tata, 1994) before interaction with TRs.

In vertebrates TRs bind to specific regulatory DNA sequences of the target genes known as TH response elements (TREs). Typically, TREs are composed of repeats of the half-site sequence AGGTCA. The DR4 type of TREs is the most common form and consists of direct repeats of AGGTCA separated by four nucleotides (Paquette et al., 2011; Umesono et al., 1991; Velasco et al., 2007). Two basic types of responses to THs are described, one using positive TREs and the other using negative TREs (nTRE) (Yen, 2001). In the case of positive TREs, the absence of T_3 allows the interaction between TRs and co-repressor proteins to repress gene expression. Binding of T_3 to TRs releases co-repressor proteins and recruits co-activator proteins and expression of T_3-responsive genes (Buchholz et al., 2006; Oetting and Yen, 2007; Umesono et al., 1991). This mechanism will be discussed in detail in the next section, as it is considered to be the mechanism occurring during amphibian development. The ligand-dependent transcriptional repression of gene expression can also be mediated by nTREs. In this type of gene transcription the role of coactivators and corepressors is not well defined. Although TRs can bind to TREs as monomers or homodimers, they preferentially bind as heterodimers with the retinoid X receptor (RXR) (Lazar et al., 1991; Paquette et al., 2011). A third regulatory mechanism mediated by TRs that does not involve TREs is transcriptional crosstalk in which other transcription factors or signaling pathways are activated (reviewed by Pascual and Aranda, 2013).

1.2.6.1. Thyroid hormones action and role of TR in vertebrate development

TRs play essential roles in vertebrate development. In mammals, TRα is involved in early neurogenesis and both liganded TRs are active in mouse brain before TH is produced by

thyroid gland (Quignodon et al., 2004). In a GFP (green fluorescent protein)-tagged TRα mouse model, the receptor was observed during neurone migration (Wallis et al., 2010). Unlike the ubiquitously expression of *trα* during brain development, *trβ* is mainly found during post-natal stages and its expression is restricted so specific neuronal cells, including granule cells, paraventricular hypothalamic neurons and cerebellar Purkinje cells (Bradley et al., 1989). Nevertheless, KO studies for several TR isoforms in mouse revealed embryonic development was normal but growth was delayed (Flamant and Samarut, 2003; Forrest et al., 2002; Macchia et al., 2001). The ablation of TRα/TRβ in mammals revealed the importance of TRs in skin epidermal proliferation and the inflammatory response (Contreras-Jurado et al., 2011; Garcia-Serrano et al., 2011), myoblasts proliferation in skeletal muscle (Casas et al., 2006), bone mineral deposition and endochondral ossification (O'Shea et al., 2005; O'Shea et al., 2003).

In fish, TRs are expressed in early embryonic stages and their expression increases at hatching until the transition from larvae to juvenile. For example, in zebrafish, the expression of *trα* and *trβ* mRNA is already detected in the zygote and is of maternal origin (Liu et al., 2000). During zebrafish embryogenesis, *trα* is generally more abundant than *trβ*, suggesting Trα is essential for normal embryonic development in contrast to mammals (Essner et al., 1999; Liu et al., 2000). The expression of *trβ* increases dramatically at hatching (Walpita et al., 2007) and the tissue localization of both TRs in zebrafish has been described by Pascual and Aranda (2013). In gilthead sea bream (*Sparus aurata*), expression of both *trα* and *trβ* in combination with *dio1*, *dio2* and T_4 levels increase at the beginning of metamorphosis (20 - 30 dph), peak at metamorphic climax (around 45 dph) and decrease after 90 dph when fish are already in the juvenile stage (Campinho et al., 2010). In Pacific bluefin tuna (*Thunnus orientalis*) and Japanese conger eel (*Conger myriaster*), the highest TR expression occurs in post-flexion stages (Kawakami et al., 2008). TRs have also been identified in several flatfish species, including the Japanese flounder (Trαa, Trαb and Tbβ1 and Trβ2; Yamano & Miwa, 1998), turbot (Trα and Trβ; (TRα and TRβ; Marchand et al., 2004), Atlantic halibut (Trαa, Trαb and Trβ1 and Trβ2; Galay-Burgos et al., 2008), Senegalese sole (Trαa, Trαb and Trβ1 and Trβ2; Manchado et al., 2009; Isorna et al., 2009) and recently in the half-smooth tongue sole (Trα and Trβ; Wang et al., 2014; Zhang et al., 2016). In general, *trα* and *trβ* expression increases during metamorphosis up until climax, but the pattern of expression prior, during and after metamorphosis seems to be species-specific (**Figure 1.7**).

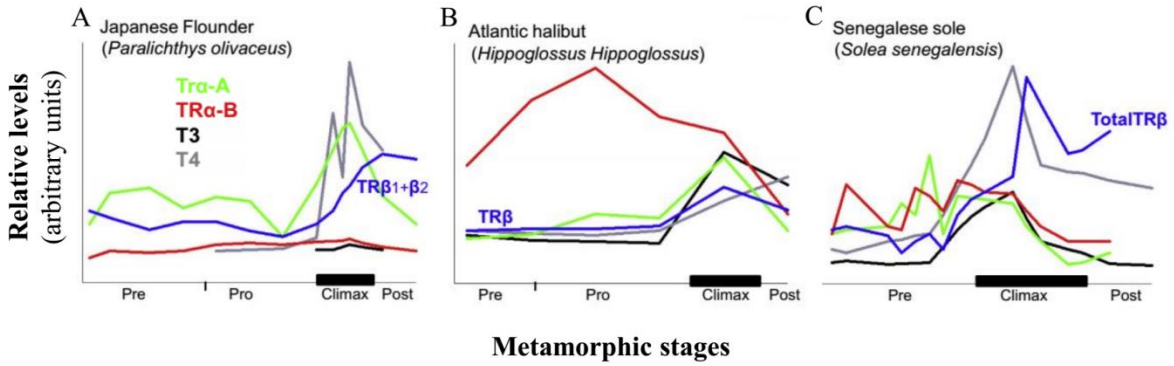

Figure 1.7. Comparison of the developmental profiles of T_3 and T_4 and the receptors (Trαa, Trαb, Trβ), (A) Japanese flounder (*Paralichthys olivaceus*), (B) Atlantic halibut (*Hippoglossus hippoglossus*) and (C) Senegalese sole (*Solea senegalensis*). Metamorphic stages are indicated on the x-axis and the thick black bars indicate the approximate timing of the climax of metamorphosis. The vertical axis represents the relative whole-body levels of T_4 and T_3 or transcripts for trα and *trβ* in arbitrary units. The timing and relative amplitude of change of THs and TRs are based on: (A) Japanese flounder (Miwa et al., 1988; Yamano, 2005; Yamano and Miwa, 1998); (B) Atlantic halibut (Einarsdóttir et al., 2006; Galay-Burgos et al., 2008); and (C) Senegalese sole (Klaren et al., 2008; Manchado et al., 2009).

Yamano and Miwa (1998) were the first to identify TRs in flatfish and suggested that the development of metamorphosing tissues in the Japanese flounder is driven by THs and controlled at the receptors level by the differential expression of TRs. In pre-metamorphic larvae, only *trαa* and *trβ* are detected and *trαa* expression increases rapidly at metamorphic climax and decreases rapidly after the post-metamorphic climax. In contrast, the expression level of *trβ* increases at the metamorphic climax, reaches its peak post-climax, and remains high in the post-metamorphic juveniles (**Figure 1.7A**). In Atlantic halibut, in contrast to Japanese flounder, *trβ* has the most dramatic expression profile during metamorphosis, with a peak occurring during the metamorphic climax (**Figure 1.7B**). In Senegalese sole, the pattern of expression of *trβ* is similar to that observed in Atlantic halibut (**Figure 1.7C**), and treatment with the goitrogen thiorea (TU) induces down-regulation of *trβ* 11 and 15 days after treatment. Additionally, adding exogenous T_4 hormone to the larvae treated with TU, restores the levels of *trβ* to basal levels (Manchado et al., 2009). During metamorphosis, *trαa* in half-smooth tongue sole (*Cynoglossus semilaevis*) has a similar expression pattern to the homologue identified in Japanese flounder, and treatment with MMI induced an up-regulation of *trαA* transcripts six days after exposure (Zhang et al., 2016). These authors consider Trαa as an important mediator for the development of lateral swimming.

Another interesting feature regarding the TRs, is their dual role in vertebrate development especially in metamorphosis where both liganded and unliganded receptors have

an active role (**Figure 1.8**). This TRs duality model has been studied in amphibians and has recently been reviewed (Buchholz, 2015). Briefly, in *Xenopus*, the TR and retinoid X receptor (RXR) bind to the positive TREs and in the absence of T_3 recruit a co-repressor complex. This complex contains several proteins such as the Nuclear receptor CoRepressor (NCoR), Silencing Mediator for RAR and TR (SMRT), and histone deacetylase (HDAC3) (Wen & Shi, 2016) and together they repress the TH responsive genes during the larval period prior to metamorphosis (Buchholz, 2015; Buchholz et al., 2006). This repression is caused by transforming the cromatin to a non-permissive state for transcription due to the histone deacetylation, and prevents premature metamorphosis and ensures adequate tadpole growth. TRα is the predominant TR form during this TH-inducible gene repression larval phase (**Figure 1.8A**) and it represses TH response genes. The repression by unliganded TR of the genes participating in metamorphosis helps to prevent premature metamorphosis and ensure an appropriate period of tadpole growth.

In the presence of T_3, the co-repressor complex is substituted by several co-activator proteins including the steroid receptor coactivator (SRC/p160) and p300 which form a multi-protein complexe and histone acetlytransferase. By acetylation and methylation of the histones, TH responsive genes transcription is induced and this corresponds to the metamorphosis (**Figure 1.8B**). Induction of gene expression is concomitant with the TRβ up-regulation (Tata, 2006). In summary, the TRs are necessary for both preventing premature metamorphosis and also at the appropriate time inducing amphibian metamorphosis, supporting the dual function model of TRs in development (reviewed by Grimaldi et al., 2013; Morvan-Dubois et al., 2008). Studies of transgenic expression of dominant positive TR (fpTR; gene repression, induction of metamorphosis) and dominant negative TR (dnTR; gene repression, induction of metamorphosis) supports that the control of metamorphosis by TH is through TR via genomic action of the hormone and not by the non-genomic action as observed in other cellular and animal contexts (reviewed in Grimaldi et al., 2013).

The findings observed by Galay-Burgos (2008) in Atlantic halibut suggest that the dual role of thyroid receptor during development could be a conserved mechanism across vertebrate. However, interaction of the receptor complex with TREs in TH responsive genes has not yet been studied in fish and such studies would provide insight into cell and tissue responsiveness during metamorphosis. Similarly defining genomic and non-genomic actions of THs during flatfish metamorphosis might give insight into factors underlying the divergent responses of tissue to THs during metamorphosis.

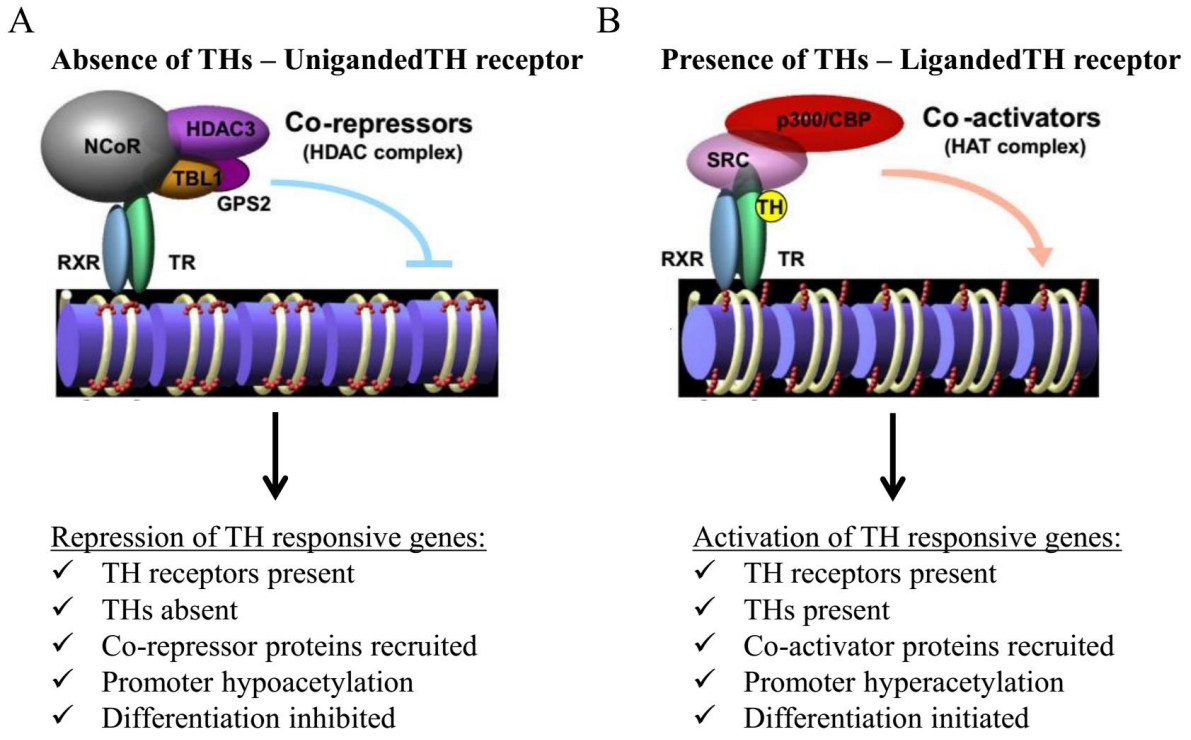

Figure 1.8. Model presenting the basis for the dual function of TRs in gene regulation during metamorphosis. During pre-metamorphosis (**A**) the unliganded TR in the absence of TH forms heterodimers with RXR (retinoid X receptor) and inhibits TH dependent differentiation by binding to gene promoters (TREs) and recruits co-repressors to deacetylate histones and repress gene expression (HDAC complex). NCoR - nuclear co-repressor, HDAC3 - histone deacetylase 3, TBL1 - transducin beta-like protein 1 and GPS2-G protein pathway suppressor 2. As metamorphosis progresses (**B**) the concentration of THs rise and they bind to TRs and initiate TH-dependent development by forming heterodimers with RXR, binding the promoter (TREs), recruiting co-activators to acetylate histones and induce gene expression. SRC - steroid receptor coactivator, p300/CBP – cAMP response element binding protein and HAT-histone acetytransferase [Adapted from Buchholz, 2015].

1.3. Endocrine control of flatfish metamorphosis – summary of THs production, transport, availability and action elements

In the previous sections the importance of the THs axis and their elements during the flatfish metamorphosis was described. **Table 1.2** resumes the molecular data existent for TG, THs, deiodinases, THs transporters and TR during the metamorphic process for some flatfish species. The amount of TG is proposed as a good indicator of thyroid activity during development, but *tg* transcripts are only described and characterized in Senegalese sole and no information exists in other flatfish. TH levels during metamorphosis are described for Atlantic halibut, Senegalese sole, Japanese flounder and summer flounder and in all species they peak at metamorphic climax. The three deiodinases are cloned in Atlantic halibut and Japanese

flounder and in the former species ISH revealed their importance in skin maturation. In the Japanese flounder, ISH was used to characterize the tissue distribution of the three deiodinases and in the Senegalese sole, only DIO2 and DIO3 have been identified and in turbot only DIO2 has been studied. Until the present date, no data exist concerning the THs transporters in flatfish. TRs alpha and beta are described in several flatfish species. Several isoforms including splice variants are reported in the literature for Atlantic halibut, Senegalese sole, Japanese flounder, turbot and in half-smooth tongue sole. Although a number of molecular tools are available to monitor the thyroid axis during metamorphosis of flatfish knowledge concerning the mechanisms of THs production, action, regulation and availability in flatfish is still lacking (**Table 1.2**).

Table 1.2. Molecular information available for genes involved in THs production, transport, availability and action during flatfish metamorphosis. The data is based on results from quantitative real time PCR (qPCR) and *in situ* hybridization for 6 well-studied flatfish species.

	Flatfish species					
TH axis elements	Atlantic halibut (*Hippoglossus hippoglossus*)	Senegalese sole (*Solea senegalensis*)	Japanese flounder (*Paralichthys olivaceus*)	Summer flounder (*Paralichthys dentatus*)	Turbot (*Scophthalmus maximus*)	Half-smooth tongue sole (*Cynoglossus semilaevis*)
TH production (Thyroglobulin - TG)	No study	Manchado et al., 2008 - ↑ during the metamorphic climax	No study	No study	No study	
Thyroid hormones (THs)	Power et al., 2008, Einarsdóttir et al., 2006 T_3 and T_4 – peak at metamorphic climax	Klaren et al., 2008 T_3 and T_4 – peak at metamorphic climax	Miwa et al., 1988 Yamano & Miwa, 1998 T_4 – peak at metamorphic climax and more abundant than T_3	Schreiber & Specker, 1998 T_4 – peak at late metamorphic climax	No study	No study
Deiodinases	Campinho et al., 2012 DIO1, DIO2 and DIO3 identified. During metamorphic climax, *dio3* reached its lowest expression level compared with *dio1* and *dio2*	Isorna et al., 2009 DIO2 and DIO3 identified. *dio2* - ↑ during the metamorphic climax ; *dio3* - ↓ during late metamorphosis	Itoh et al., 2010 Localization of *dio1*, *dio2* and *dio3* by ISH during metamorphosis	No study	Marchand et al., 2004 - *dio2* - ↑ before and after the period of T_4 surge Mol et al., (1997)[1]	No study
THs transporters	No study	No study	No study	No study	No study	No study
THs receptors	Galay-Burgos et al., 2008 TrαA, TrαB, TRβ (two splice variants). *trβ* - ↑ during the metamorphic climax.	Isorna et al., 2009 Manchado et al., 2009 TrαA, TrαB, TRβ (two splice variants). *trβ* - ↑ during the metamorphic climax.	Yamano & Miwa, 1998 TrαA, TrαB, TRβ (two splice variants). *trαa* and *trβ* - ↑ during the metamorphic climax. *trαa* increased rapidly during metamorphosis	No study	Marchand et al., 2004. Northerblot – Trα and TRβ. *trβ* expression level is very low compared to *trα*	Wang et al., 2014 Zhang et al., 2016 TRαA and TRβ - Both ↑ during the metamorphic climax.

1 – ORD and IRD activity, no molecular data

1.3.1. Other endocrine factor involved in flatfish metamorphosis

In Atlantic halibut and other flatfish there is evidence that the pituitary is fully developed and active before the onset of metamorphosis indicating that in addition to the TH axis other endocrine axis are active and so could play a role (Einarsdóttir et al., 2006; Miwa and Inui, 1987). For example, the growth hormone (GH)/Insulin-like growth factor I (IGF-I) axis that promotes growth and regulates metabolism in larval stages of teleosts is active (Björnsson et al., 2002; Yousefian and Shirzad, 2011). In the case of the flatfishes, Atlantic halibut and common sole (*Solea solea*), GH receptor (*ghr*) mRNA expression and *igf-I* body content peaks prior to the metamorphic climax (Ferraresso et al., 2013; Hildahl et al., 2007) and the distribution and abundance of *igf-I* expressing cells in the remodelling craniofacial region of the Atlantic halibut changes during metamorphosis (Hildahl et al., 2008).

A further example, is the hypothalamus-pituitary-interrenal axis (HPI) where cortisol concentrations vary in a similar way to THs during flatfish metamorphosis and this has been taken as evidence for its involvement in metamorphosis (de Jesus et al., 1991). Evidence supporting a direct role for cortisol in tissue remodelling during metamorphosis is scant but it is reported to enhance the effect *in vitro* of THs on dorsal fin ray resorption in the Japanese flounder (de Jesus et al., 1990). Such evidence of synergy between cortisol and thyroid hormone during metamorphosis has also been described in amphibians (Bonett et al., 2010; Denver, 2009). More recent studies suggest a requirement for cortisol in acquisition of salinity tolerance in larval stages of Japanese founder and summer flounder (Hiroi et al., 1997; Veillette et al., 2007) but this ontogenetic process does not appear to be specifically linked with metamorphosis. There is considerable scope for studies looking at the effects of other endocrine factors during metamorphosis and their potential interaction with THs. The mechanisms underlying the possible interaction between the HPT (THs) and HPI (cortisol) axes are unclear and the studies describing this possible interaction in fish are scarce. In adult fish the cross-talk between the HPT and HPI axes can occur at the central level and for example, in common carp (*Cyprinus carpio*) CRH instead of TRH controls the activity of the thyroid. Because of its corticotropic and putative thyrotropic activity, CRH may be important in the central cross-talk between the HPT and HPI axis (Geven et al., 2007). This is further supported by the observation that T_4 can inhibit the HPI axis via CRHBP in the preoptic area (Geven et al., 2009). In adult common carp, cortisol and ACTH stimulate the release of T4 from renal tissues (Geven et al., 2009) and the expression and activity of deiodinases is

modified in response to cortisol exposure in sea bream (*Sparus aurata*) and trout (*Oncorhynchus mykiss*) (Arjona et al., 2011b; Todd and Eales, 2002). In Nile tilapia (*Oreochromis niloticus*) dexamethasone (DEX) and handling stress cause a decrease in circulating T_3 levels by causing changes in deiodinases expression, especially up-regulation of *dio3* in the liver and gills (Walpita et al., 2007).

Recently, both TREs (thyroid response elements) and GREs (glucocorticoid response elements) were identified in *trβ* and both THs and cortisol modulate the expression of this receptor. T_2 and T_3 down-regulate the expression of long and short *trβ* and cortisol up-regulates the expression of *trβ* (Hernandez-Puga et al., 2016; Orozco et al., 2014). In addition, T_2 represses *trβ* expression and impairs its up-regulation by cortisol possibly through a trans-repression mechanism (Hernandez-Puga et al., 2016). RU486 is a selective glucocorticoid receptor (GC) blocker and in teleosts increases the levels of circulating cortisol (reviewed by Mommsen et al., 1999) by inhibiting the negative feedback effects of cortisol on the pituitary and increasing ACTH release which enhances the cortisol production (Marshall et al., 2005; McCormick et al., 2008; Scott et al., 2005).

1.4. Local mechanisms of morphogenetic changes: THs gene responsiveness during metamorphosis

In the most extensively studied models, the amphibians, THs control the most dramatic development changes, preparing the aquatic larvae for a terrestrial life style, and several tissues of the body undergoes extensive remodelling and respond differentially to TH stimulation (Gilbert, 2000).THs are involved in the control of apoptosis of the muscle fibres of the tail during its regression and progressive limb development (Chanoine and Hardy, 2003). THs are also responsible for the onset and control of the replacement of the tadpole larval skin with a skin more stratified and better adapted to a terrestrial lifestyle (Suzuki et al., 2002; Watanabe et al., 2002). The brain and intestine also suffer remodelling in amphibians (Yoshizato, 2007).

Several studies have been performed to understand the action of THs on gene expression. For example, in the brain of Mexican Axolotl approximately 300 genes are differentially expressed (fold change > 1.5) after T_4 treatment in the rearing water, where some of the up-regulated genes are related to neurological processes such as Ras-like protein

family member 11A, oxerin receptor type 2, MAP kinase-activated protein kinase 3, adenosine receptor A1, Interleukin enhancer-binding factor 2 and, neuroligin-4 (Huggins et al., 2012). In earlier *Xenopus laevis* development, several matrix metalloproteinases (MMPs) have distinct spatial and temporal expression indicative of distinct functions. For example, stromelysin 3 (*st3*) responds directly to THs and facilitates apoptotic tissue resorption/remodelling. Matrix metalloproteinases collagenase 3 (*mmp13*) and collagenase 4 (*mmp18*) respond indirectly to THs and appear to be crucial for the degradation of connective tissue during development (Damjanovski et al., 2000; Das et al., 2009) indicating the importance of protein degradation and extracellular matrix remodelling during early metamorphosis. In *Xenopus laevis* the gene regulation programs in brain and limb are similar, and the most up-regulated genes after treatment with T_3 are components of the cell cycle, transcription, translation and RNA and DNA metabolism. Nonetheless, in the tail, a different program response was observed. For example, the major part of the enzymes involved in glycolytic and tricarboxylic acid pathways are down-regulated in tail during the metamorphic climax, but up-regulated in brain and limb (Das et al., 2006).

In addition to the microarray based examples described above, proteomic techniques are being used to evaluate this essential role of THs in anurans metamorphosis. For example, in the tail of *Xenopus laevis* tadpoles undergoing precocious metamorphosis, several T_3-responsive proteins that include a number of tubulin isoforms were up-regulated (Helbing et al. 2003) and the identification of transcripts that coding for enzymes involved in the MAPK signaling cascade (such as Ras, Raf, MAPKK, MPK1, and MAPK phosphatase) suggests posttranslational events are important during T_3-induced apoptosis (Helbing et al., 2003).

Using immunohistochemistry and *in situ* hybridization techniques, Mukhi et al., (2010) described the "gene switching" controlled by THs during the different remodelling events in *X. laevis* metamorphosis. In contrast, to the intestinal epithelium and exocrine pancreas that dedifferentiate to a progenitor state and then redifferentiate to the adult cell type, in other tissues and cell types like fibroblasts, skin and liver a "shut off" mechanism is observed in tadpole genes, and activation of frog genes occur without DNA replication (Mukhi et al., 2010).

In flatfish, there have been a few molecular studies of metamorphosis but the underlying mechanisms remain unexplored. For example, otoliths growth and mineralization occurs during metamorphosis and are induced by THs (Schreiber et al., 2010). Several genes involved in teleost otolith development including otolith matrix protein, alpha-tectorin,

otogelin and otopetrin 2 are up-regulated during metamorphosis and following 72 h of exogenous treatment with T_3, indicating they are TH responsive. The question if asymmetric expression between developing otoliths on the left and right sides and their contribution to the lateralized posture during metamorphosis remains to be addressed (Wang et al., 2011). During metamorphosis, the migration of the left or right eye to produce either dextral (both eyes in the right side) or sinistral (both eyes in the left side) forms changes the bilateral symmetry of flounder. The nodal-lefty-pitx2 (NLP) pathway is involved in this morphogenic process. The paired-like homeodomain transcription factor 2 (*pitx2*) is asymmetrically re-expressed in the left habenula of pre-metamorphic *V. variegatus* and *P. olivaceus* larvae, and this re-expression appears to initiate eye migration (Suzuki et al., 2009). Another gene recognized as relevant for Japanese flounder metamorphosis is the splicing factor arginine/serine rich-3 (*sfrs3*). *In situ* hybridization revealed an up-regulation of *sfrs3* only in the head region during the metamorphic climax, mainly in the proliferative tissues proposed to push eye migration (Bao et al., 2005). In fact, the failure of the eye to migrate constitutes one of the main issues associated with abnormal metamorphosis (Okada et al., 2001; Okada et al., 2003; Saele et al., 2006a) and has major negative consequences for aquaculture.

A series of other genes, responsive to THs during flatfish metamorphosis have been identified. For example, the keratins, generally used as a marker for epidermal development and differentiation, are down-regulated at metamorphic climax in Atlantic halibut (Campinho et al., 2007b) and Senegalese sole (Infante et al., 2007). These genes are an example of negative gene regulation by the THs, suggesting their role in the skin remodelling processes that occur during flatfish metamorphosis (Campinho et al., 2007b). Another example of negative gene regulation by THs during metamorphosis is the heat shock protein 90 (*hsp90aa*) (Manchado et al., 2008c). Five eukaryotic translation elongation factor 1 genes were identified in *S. senegalensis* that are differentially expressed during larval development. Nonetheless, only one gene was up-regulated by THs, suggesting it has a role in regulation of translation during sole metamorphosis (Infante et al., 2008). Similar observations were reported in turbot (Marchand et al., 2004) and glyceraldehyde-3-phosphate dehydrogenase 1 (*gapdh-1*) is up-regulated during the metamorphic climax and has been linked to the high energetic demand of metamorphosis (Manchado et al., 2007).

The gastrointestinal tract (GI-tract) of flatfish undergoes an extraordinary post-embryonic development that includes rapid and extensive remodelling, to prepare it for the shift from a pelagic to a benthic habitat and the associated change in feeding behavior (Luizi

et al., 1999; Pittman et al., 1990). Stomach development in flatfish species is a TH-driven event (Huang et al., 1998; Miwa et al., 1992). During metamorphic climax of Atlantic halibut the stomach volume grows more than 11-fold (Gomes et al., 2014b), simultaneous with the increase in T_3 and T_4 (Galay-Burgos et al., 2008). The initiation of gastric glands development starts just prior to metamorphosis, and pepsinogen mRNA levels increase significantly in postmetamorphic stages of Atlantic halibut as well as in Japanese winter (*Pseudopleuronectes americanus*) and summer flounder (Douglas et al., 1999; Huang et al., 1998; Miwa et al., 1992; Murray et al., 2006). The gastric proton pump (H+/K+-ATPase) a and b subunits and pepsinogen are specific gene markers for stomach organogenesis and functional development, and their absence has been linked to the absence of a stomach in some vertebrate species (Castro et al., 2013; Ordoñez et al., 2008). Pepsinogen and gastric proton pump transcript expression is correlated in several teleost species (Darias et al., 2005; Douglas et al., 1999; Gao et al., 2013; Gawlicka et al., 2000; Gomes et al., 2014b)and pepsinogen transcript abundance is correlated with pepsin activity (Douglas et al., 1999). These genes are used as indicators for the onset of the proteolytic gastric function of the stomach. In Atlantic halibut, the increased mRNA expression of gastric proton pump subunits and pepsinogen occur simultaneous with the increase in acidic capacity of the stomach (Gomes et al., 2014b) during the climax of metamorphosis, in synchrony with stomach development.

1.5. Structure, function and morphogenesis of the piscine skin

As observed for the GI-tract, flatfish skin also undergoes an extensive remodelling process during metamorphosis and it evolves from a thin epithelium in pre-metamorphic larvae to highly stratified epidermis in the juvenile (Campinho et al., 2007b). The skin in vertebrates is a multifunctional organ and corresponds to the major barrier between the animal and its external environment (Madison, 2003; Proksch et al., 2008) making its maturation during metamorphosis important. Fish skin is generally composed by three layers: epidermis, dermis and hypodermis (Le Guellec et al., 2004) (**Figure 1.9**). The epidermis varies in thickness, epidermal layer number and specialized cell types according to species, age and body region location. In contrast to terrestrial vertebrates, the epidermis is nonkeratinized and consists entirely of live cells (**Figure 1.9**) and is organized into three strata, *stratum*

superfeciale, *stratum spinosum* and *stratum basale.* This *stratum basale* contains the basal cells and the basement membrane which contains the undifferentiated epidermal progenitor cells. These progenitor cells are induced to proliferate in the *stratum spinosum*. Two different types of glandular cells exist in the skin, namely, goblet cells and club cells (Elliott, 2011; Rakers et al., 2010). **Table 1.3** shows the different cell types existent in teleost epidermis and their key functions. The basement membrane consists in a layer of filamentous proteins and separates the epidermis from the dermis.

The dermis is divided into the *stratum laxum* and *stratum compactum*, and is separated from the hypodermal adipogenic tissue by yet another endothelial layer, called the dermal endothelium. It is composed of a collagenous matrix which contains fibroblasts, nerves, pigment cells and scales. Scleroblasts are the scale-building cells, and are located in the scale pockets (**Table 1.3**, **Figure 1.9A**) (Esteben, 2012; Rakers et al., 2010). **Figure 1.9B** shows the main similarities and differences between mammalian and fish skin, including the distribution of the cells involved in the innate immune system.

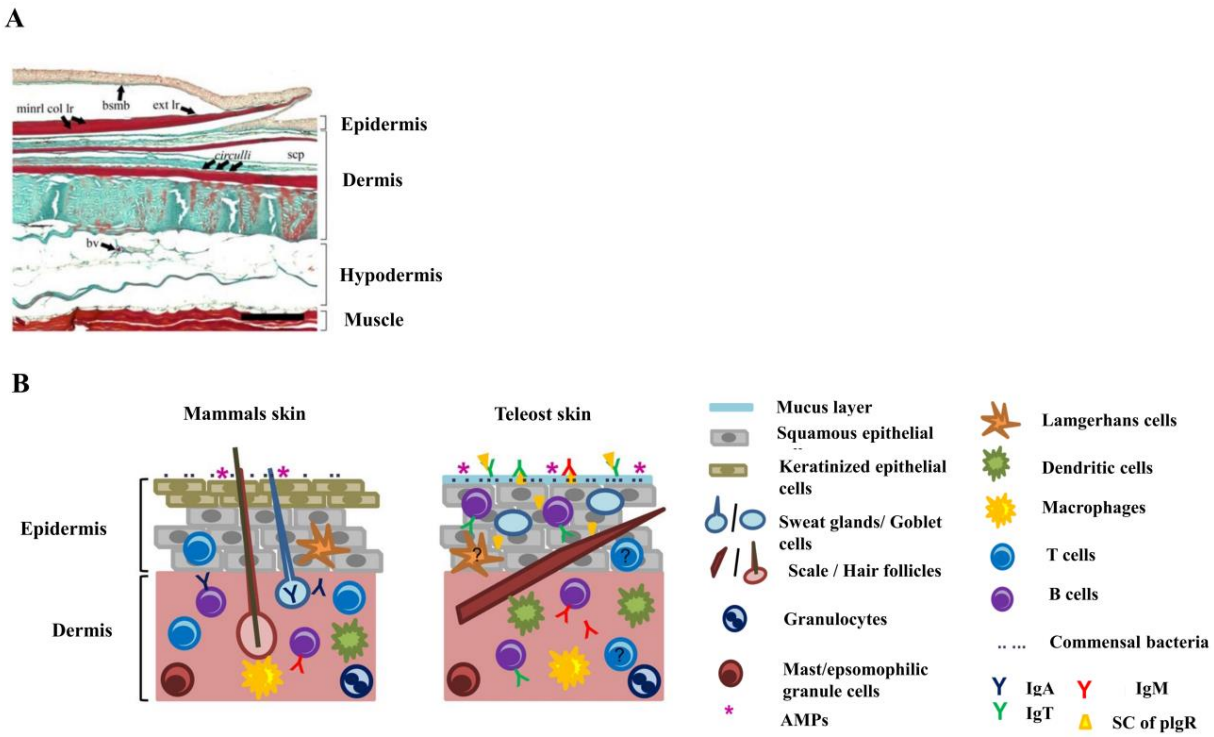

Figure 1.9. The skin of the teleost fish and comparison with mammals. (A) Transverse section of sea bream skin stained with Masson's Trichrome showing the three main skin layers**.** The different layers that compose the integument are identified as well as some typical structures of the elasmoid scale and the superimposed collagen layers. bv: blood vessel, bsmb: basement membrane, ext lr: external layer, minrl col lr: mineralized collagen layers, scp: scale pocket. Scale bar: 200 µm (Costa, 2009). (**B)** Schematic representation of the similarities and differences between teleost fish and mammalians skin. In the epidermis, different cell types and numbers of layers, as well as the presence of keratin or mucus (and mucus-producing cells) are represented. Similarities in the cellular components of the innate immune

system (Langerhans cells, dendritic cells, macrophages, granulocytes and mast cells) are represented in both teleost and mammalian skin. Differences in the localization of B and T cells, the isotype of immunoglobulins and the presence of the secretory component (SC) of the polymeric immunoglobulin receptor (pIgR) are represented as well. Finally, the presence of commensal bacteria and antimicrobial peptides (AMPs) is shown in the outer mucosal surface or over the keratin layer. Elements that are suspected to be present in a tissue but have not been studied so far are marked as unknown (?) (Gomez et al., 2013).

Table 1.3. Cell types in teleost skin identified by different histological methods.
From Rakers et al., (2010).

Cell type	Location	Key function	Equivalente in human skin
Mucous globet cells	Epidermis	Secretion, protection	Cornified envelopes
Club cells (alarm cell)		Alarm system/pheromonal function ?	-
Epithelial cells		Stability, gas exchange, protein source	Keraninocytes
Basal (epithelial) cells		Attachment to dermis, drive differentiation	Basal epithelial cells
Chemosensory cells		Sense of water current, dissolved chemical substances	-
Merkel cells		Hormonal action	Merkel cells
Fibroblast	Dermis	Maintain the structural integrity of connective tissues, structural framework, wound healing	Fibroblast
Melanophore		Protection against UV-radiation, coloration, colour change, infection defense	Melanophore
Iridophore		Light reflection	-
Xantophore		Coloration	-
Blood vessel		Blood transport, supply	Blood vessel
Nerves		Innervation	Nerves
Scales		Protection, decrease of water flow resistance, calcium source, mechanical properties	Hair, teeth
Fat cell (adipocytes)	Hypodermis	Storage, isolation, movability of the skin relative to the musculature	Fat cells

Besides its importance as a barrier, the skin in fish is metabolically active and several functions have been identified in this organ. For example, skin is involved in the camouflage strategies, by retarding detection and/or recognition by a visual predator and includes including background matching, disruptive coloration and masquerade (Allen et al., 2015; Stevens and Merilaita, 2009). For instance, the skin has been shown to play a critical structural role in fish locomotion by regulating wave propagation (Long et al., 1996), and has inherent hydrodynamics properties that are crucial for swimming efficiency. The curvature stiffening capacity of the skin is likely to play a significant biological role in fish swimming and in resistance against puncture loads that result from predator attacks (Vernerey and Barthelat, 2014). Fish skin is also involved in temperature regulation, as epithelial cells from cold-water fish species contain antifreeze proteins (Hobbs and Fletcher, 2008). An active

electro location for orientation in the dark is caused by the lateral line system which can measure distances (von der Emde et al., 1998). In addition, skin is under endocrine control of hormones and neuropeptides, which play multiple roles in the fish (**Table 1.4**, reviewed by Rakers et al., 2010).

Table 1.4. Endocrine regulation of fish skin by hormones. Examples of hormones with an effect in teleost skin. Adapted from Rakers et al., (2010).

Hormone	Classification	Produced by	Key function in fish skin
Melanin-concentrating hormone (MCH)	Peptide hormone	Pituitary gland	Lightens skin colour by stimulating aggregation of melanosomes
Melanocyte-stimulating hormone (MSH)			Antagonistic effect to MCH, causes dispersion of melanosomes
Prolactin			Affects thickening of epidermis, increases number of goblet cells, important
Gonadotropins			Decrease number of goblet cells in marine teleosts
Thyrotropin-releasing hormone (TRH)	Neuropeptide		TRH stimulates growth hormone, and prolactin release, stimulator of alpha-MSH release
Seratonin	Peptide hormone	Club cells/Merkel cells	Involved in pathogen defence, stimulates exocrine glands to secrete amine messengers
Thyroid hormones	Thyroid hormones	Thyroid gland	Essential for the embryonic and postembryonic development, important hormones for metamorphosis in flatfish and also other finfish
Corticosteroids	Steroid hormone	Adrenal cortex	Cortisol influences hydromineral balance, energy metabolism and immune function, corticosterol and growth hormone have stimulatory effects on epithelial cell secretion but do not affect goblet cells
Epinephrine/Norepinephrine	Catecholamines	Adrenal glands	Epinephrine more common and may control chloride cells in fish by lowering cAMP-levels
Melatonin, noradrenaline	Steroid hormone	Gonad, testes	Increase the skin transparency, effect of decoloration in combination with prolactin, show positive effects on both, transparency and coloration
Testosterone			Increases epidermal thickness, 11-ketotestosterone decreases number of superficial goblet cells
Estrogens			No direct effects on skin known, but high concentrations of oestrogens or derivatives in water

Regulation of skin morphogenesis/homeostasis in terrestrial vertebrates is better described than in fish skin. Wnt signaling is the main pathway involved in the functional

control of the differentiated vertebrate skin cells (Katoh and Katoh, 2007; MacDonald et al., 2009). Collagens such as collagen type I *(col1a1*, *col1a2*) and type V (*col5a2*) are important components from the extracellular matrix (ECM) (Shoulders and Raines, 2009). These ECM fibrous structural proteins in combination with other essential proteins such as growth factors, chemokines, adhesion molecules and proteoglycans act as key signals for tissue differentiation, development and morphogenesis in mammals (Daley et al., 2008; Daley and Yamada, 2013; Hubmacher and Apte, 2013; Watt and Fujiwara, 2011) and several are also implicated in skin from fish (Le Guellec et al., 2004) and amphibians (Page et al., 2008; Suzuki et al., 2009). Moreover, other genes are involved in synthesis and remodelling of the ECM during tetrapods organogenesis, including the extracellular matrix protein FRAS1 (*fras1*), epithelial discoidin domain-containing receptor 1 (*ddr1*), junction plakoglobin (*jup*) and desmoplakin (*dsp*).

For example, the *fras1* gene encodes for an extracellular matrix protein involved in the regulation of epidermal and basement membrane adhesion and organogenesis during development (McGregor et al., 2003; Short et al., 2007). In mammals, it has been demonstrated that *p63* is a key transcription factor involved in skin morphogenesis that induces expression of the *fras1*, required for basement membrane integrity (Koster et al., 2007). Interestingly, Gautier and co-authors (2008) demonstrated a low expression of fras genes (including *fras1*) in the developing epidermis from zebrafish fins suggesting that the role of this protein in humans and mice skin development has recently evolved. Ddr1, belongs to the subfamily of tyrosine kinase receptors and its transcripts are expressed in a number of different cell types (Vogel et al., 2006). It has been shown that these non-integrin-type receptors regulate cell adhesion, proliferation and ECM remodelling during tissue morphogenesis by acting by transduction signaling and collagen sensor (Olaso et al., 2011; Vogel, 1999).

1.5.1. Barrier function and mucous production

Fish like all other vertebrates are constantly exposed to microorganisms, some of which are pathogenic, and the production by skin of mucous acts as the first line of defense against infection (Alvarez-Pellitero, 2008; Aranishi, 1999; Cole et al., 1997; Gomez et al., 2013; Subramanian et al., 2007; Subramanian et al., 2008; Tsutsui et al., 2011; van der Marel et al., 2010) (**Figure 1.9B**). Recently, the skin transcriptome from Mud Loach was sequenced

and the immune system was the main KEGG orthology (KO) category described and included chemokine signaling pathway, natural killer cell mediated cytotoxicity, Toll-like receptor and T-cell receptors signaling pathways and hematopoietic cell lineage (Long et al., 2013).

Mucous in fish also acts in osmotic and ionic regulation, excretion, respiration, and communication (Shephard, 1994). The mucous is produced by the goblet cells (Harris and Hunt, 1975), unicellular exocrine glands generally localized in the middle to outer layer of epidermis (Elliott, 2011). The predominant components of the mucous layer are the high molecular weight, large, abundant and filamentous glycoproteins, called mucins. Mucins are long polypeptide chains, which can contains one or more tandem repeat protein domains and extensive sites of O-glycosylation (Cone, 1999; Perez-Vilar and Hill, 1999), which makes them difficult to characterize (Moniaux et al., 2001; Rose and Voynow, 2006). More than twenty mucin genes have been identified in vertebrates that belong to two structurally distinct families: the membrane-bound forms, and the large secreted gel forming. Several recent studies have characterized mucin genes in the sea bream (*Sparus aurata*) (Pérez-Sánchez et al., 2013) and salmon (*Salmo salar*) skin (Micallef et al., 2012). The localization of mucous cells in the epidermis of fish have been studied using conventional histochemical techniques to detect both neutral and acidic glycoproteins (GPs). **Figure 1.10** indicates histochemical methods used to evaluate and detect the presence of glycoproteins (GP) in mucous producing cells. The histological results for different fish species are also represented.

A

Histochemical methodologies	GPs identified
PAS	GPs with oxidizable vicinal diols and or glycogen (magenta)
AB2.5	GPs with carboxyl groups and/or GP with O-sulphate esters (blue)
AB1.0	GP with O-sulphate esters (blue)
AM/KOH/AB2.5	GPs with carboxyl groups (blue)
HID	GP with O-sulphate ester (purplish brown)
AB2.5/PAS	GPs with oxidizable vicinal diols (magenta), GPs with carboxyl groups and/or GP with O-sulphate esters (blue)
HID/AB2.5/PAS	GPs with oxidizable vicinal diols (magenta), GPs with carboxyl groups (blue), GP with O-sulphate esters (purplish brown, black), GPs with oxidizable vicinal diols and/or GPs with carboxyl groups (purple, blue), GPs with oxidizable vicinal diols and/or GP with O-sulphate esters (purplish brown with blue tinge)

B

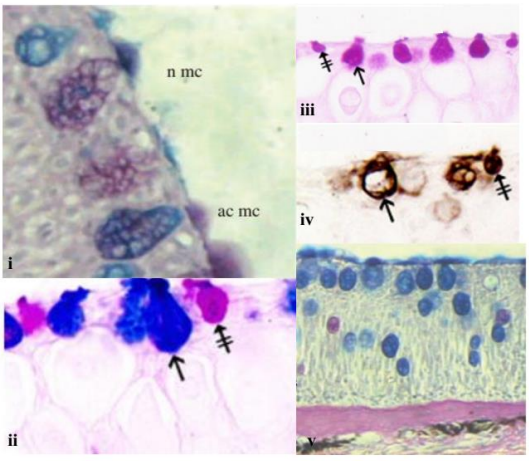

Figure 1.10. Examples of histochemical methods to detect glycoproteins (GPs) in the goblet cells from the epidermis (A). Mucous producing cells observed in the epidermis from several fish (B). (i) The epidermis from *D. labrax* stained with alcian blue and subsequently with Periodic acid–Schiff (PAS) to reveal both acid mucous cells (ac mc, blue) and neutral mucous cells (n mc, magenta) or (v) only with alcian blue; (ii) the epidermis from *L. rohita* stained with alcian blue and subsequently with PAS to reveal both acid mucous cells (arrows) and neutral mucous cells (barred arrows), (iii) with PAS to reveal neutral mucous cells, and (iv) with HID to reveal with acid mucous cells [Adapted from Kalogiannie et al., (2011) and Rai et al., (2012)].

The mucins in the mucous cells of fish epidermis are diverse between species and body regions and also physiological conditions. The mucous secretion at the surface of the skin plays an important role in the maintenance of the structural and functional integrity of skin, as well as its adaptation to its habitat (Jeong, 2008).

During development, the mucus cells in the epidermis of early life stages of plaice (*Pleuronectes platessa*) only contain neutral mucins (Roberts et al., 1973) and the scarce mucous cells in the epidermis of yolk-sac larvae of Atlantic halibut only react with PAS (Ottensen and Olafsen, 1997). In the finfish *Cyprinus carpio*, the number of mucus cells, in the buccal cavity containing acid mucins increased during larval development (El-Gamal, 2009). In Atlantic halibut, a shift from predominantly neutral to a mixture of neutral and acidic sulphated mucins occurred during ontogeny, suggesting that these changes are related to the transition from a pelagic to a benthic habitat (Ottensen and Olafsen, 1997). A similar situation was also observed in the flatfish brill *Scophthalmus rhombus* in tissues such as oesophagus, gills and intestine (Hachero-Cruzado et al., 2009), and during the larval development of Senegalese sole (*Solea senegalensis*) in both epidermis and gills (Sarasquete et al., 1998). Surprisingly, little and contradictory information exists about the ontogeny of mucus cells during flatfish metamorphosis.

1.5.2. Osmoregulation

In addition to the importance of the teleost skin as a barrier and first defense line against pathogens, this integument is also involved in osmoregulation, mainly during the first life-cycle stages, from hatching to juvenile (Varsamos et al., 2002). Ionocytes (chloride cells or mitochondria-rich cells) are the main cells responsible for ion exchange (Pisam, 1991; Wilson and Laurent, 2002). In the basolateral side of ionocytes, Na^+/K^+ ATPase (NKA) is very abundant and drives the excretion of monovalent ions against an electrochemical gradient (Marshall, 2002), and immunohistochemistry (IHC) to detect this enzyme has been used to identify ionocytes (Einarsdottir et al., 2011; Hiroi et al., 1998; Katoh et al., 2000). The existence of ionocytes has been described in several teleosts during development and a high density is found in the lateral skin of *Pleicoglossus altivelis* larvae (Hwang, 1989). In Mozambique tilapia (*Oreochromis mossambicus*) the number of skin ionocytes decreases

after hatching, due to the progressive development of the gills and increase in the number of ionocytes in this tissue (Yanagie et al., 2009). In the late larval stages and juvenile sea bass the highest number of ionocytes is associated with the fins and the lateral line (Diaz, 2003; Varsamos et al., 2002). In most teleost species, the ontogeny of ionocytes is associated with a shift from extra-branchial to branchial ion regulation (reviewed by Varsamos et al., 2005). This was clearly shown in a study that identified and mapped five Na+/K+ ATPase α subunit isoforms during the ontogeny of the Senegalese sole. The Na+/K+ ATPase α 1a (*atp1a1a*) transcripts decreased in the gastrointestinal tract (GI-tract) and increased in the gills and skin between 1 and 3 days post hatch (dph) in larva maintained in 36 ppt (parts per thousand) seawater but this shift was delayed when the larvae were maintained at lower salinity (20 ppt) (Armesto et al., 2014).

1.5.3. Pigmentation

Fish possess exuberant skin pigmentation and this is due to the multitude of dermal and epidermal pigment cells or chromatophores that absorb (melanophores, xantophores, erythrophores and cyanophores) and reflect light (leucophores and iridophores). The melanophores are equivalent to mammal melanocytes and only produce eumelanin with brown-black coloration (Fujii, 2000; Hubbard et al., 2010; Parichy, 2003; Sugimoto, 2002). Such diversity of pigment cells associated with a series of cellular, physiological, environmental and genetic factors, makes fish skin pigmentation a complex biological process (Colihueque, 2000; Kelsh, 2004; Kondo et al., 2009; Parichy, 2006).

1.5.3.1. Genetic basis of pigment cells: melanophore differentiation and melanin synthesis

The genetic basis of pigmentation has been studied in several teleost species including, zebrafish, fugu, goldfish and also in flatfish species (Fukamachi et al., 2004; Klovins and Schioth, 2005; Parichy and Johnson, 2001; Yamada et al., 2010). In most vertebrates, melanophores, the pigment producing cells of the epidermis and dermis, produce a specialized member of the lysosomal related organelles (LRO) family known as melanosome. The melanosomes contain the battery of regulatory mechanisms including the key melanogenic enzymes necessary to orchestrate melanogenesis, which occurs inside the melanosome. The master regulator of melanogenesis, microphtalmia-associated transcription factor (MITF), can

regulate the action of the melanogenic enzymes TYR (tyrosinase), DCT (L-dopachrome tautomerase) and TYRP1 (tyrosinase-related protein 1) that are responsible for the synthesis of melanin (**Figure 1.11**) (Lin and Fisher, 2007; Schallreuter et al., 2008; Yamaguchi et al., 2007).

Several hormonal factors are involved in regulating melanogenesis, such as α-melanocyte stimulating hormone (α-MSH), ß-endorphin, endothelins, catecholamines, cKit ligand estrogens, androgens, vitamin D, melatonin, agouti proteins and their receptors (Slominski et al., 2004). In fish, the main positive regulator is the α-MSH and melanocortin receptor 1 (Mc1r) and agouti signaling protein (Asip) the main melanogenesis negative regulator. The role of Mc1r in the pigmentation pattern during development has recently been reported in zebrafish and cavefish (Gross et al., 2009; Richardson et al., 2008), (**Figure 1.11**). In contrast, the Asip, a paracrine signaling protein antagonizes Mc1r, and causes melanocytes to switch from producing eumelanin to pheomelanin (Guillot et al., 2012). *Asip* mRNA is highly expressed in the ventral skin but scarcely in dorsal skin, showing the involvement of α-MSH and ASIP in the differentiation of a dorsal–ventral pigment pattern in fish (Hunt and Thody, 1995). Moreover, in medaka Asip blocks the melanin dispersion induced by the α-MSH scale melanophores by acting as a competitive antagonist at MC1R (Cerda-Reverter et al., 2005).

Transgenic zebrafish which overexpressed *asip* have a marked reduction in the number of melanophores within the dark stripes and an increased number of iridophores, leading to a severe disruption of the stripe pattern characteristic in this species (Cerda-Reverter et al., 2011). Other genes are involved in regulation of fish skin pigmentation. Slc24a5 (sodium/potassium/calcium exchanger) is a calcium melanosomal transporter and is crucial for proper melanin synthesis and is inhibited by Asip. PAX3 (paired box protein Pax-3) is a key upstream transcription factor in the cascade that can promote or inhibit melanogenesis through transcriptional regulation and cKit is necessary for melanophores differentiation and is responsible for the activation of Tyr. PAX3 also modulate the expression of the two other melanogenic enzymes TRYP1 and DCT. HSP70 (heat shock 70 kDa protein) is a negative regulator of CASP3 (caspase 3), which negatively regulates MITF (reviewed by Darias et al., 2013a). Genes involved in the regulation of melanogenesis and pigment cell development in fish are frequently duplicated (e.g. transcription factors, MITF-*mitfa* and *mitfb*, SOX10 – *sox10a* and *sox10b* and cell surface receptors, KIT - *kita* and *kitb*), (Braasch et al., 2009). The genes for the melanogenesis enzymes, *tyr* and *tyrp1*, have been

retained in duplicate in some teleost lineages (e.g. stickleback and medaka) but *Dct* is a single copy gene in all lineages analysed so far (Braasch et al., 2009; Braasch et al., 2007).

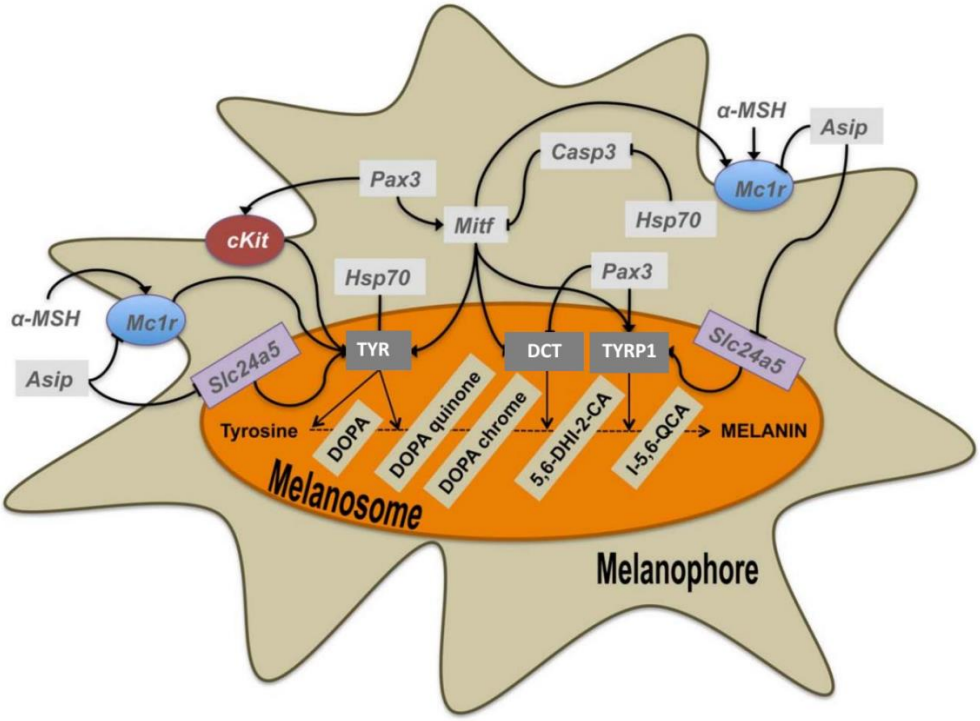

Figure 1.11. Melanophore structure and molecular action of the melanogenic proteins within melanophores. MIFT regulates the expression of TYR, DCT and TYRP1 that are responsible for the synthesis of melanin. MC1R, located to the melanophore membrane, is activated by α-MSH and promotes the activation of TYR. ASIP inhibits the action of MC1R. Several genes have been identified that are involved in direct or indirect regulation of melanogenesis such as PAX3, cKit, SLC24A5, HSP70 and CASP3 [Adapted from Darias et al., 2013a].

1.5.3.2. Pigmentation in flatfish during development and pigment abnormalities: relationship with THs

The asymmetric pigmentation observed in the body of post-metamorphic flatfish is a specific feature of these species. Until the onset of metamorphosis, flatfish larvae are bilaterally symmetric (Seikai, 1992), but in contrast to other teleosts, only the upper (ocular or skin top) side of the body becomes pigmented, whereas the lower side (abocular, blind or skin bottom) that rests on the sea bottom remains without pigmentation (reviewed in Power et al. (2008) and McMenamin and Parichy (2013)). The body pigmentation pattern of flatfish is also formed by various classes of neural crest-derived pigment cells (Burton, 2010). Larval-type melanophores appeared on both sides of the body before metamorphosis (Bolker and Hill, 2000; Hamre et al., 2007; Matsumoto and Seikai, 1992). Large sized larval type

melanophores appear sporadically and bilaterally close on ventral and dorsal skin, and small sized adult type melanophores appear only on the ocular side at the latest stages of metamorphosis. Adult type melanophores are thought to differentiate from melanoblasts or their precursors during metamorphosis (Matsumoto and Seikai, 1992; Yoshikawa et al., 2013). Additionally, after metamorphosis the main chromatophores on the abocular side of flatfish are the iridophores, whereas on the ocular side both melanophores and iridophores are present (Burton, 2010). On the ocular side, iridophores form patches but are dispersed on the abocular side (Matsumoto and Seikai, 1992; Nakamura et al., 2010). This distribution pattern of iridophores is important to define the specific coloration of flatfishes. Furthermore, xanthophores increase on the ocular side during metamorphosis and contribute to the asymmetric pigment pattern (Matsumoto and Seikai, 1992; Nakamura et al., 2010).

Recently, in Senegalese sole metamorphosis the morphological ontogeny of skin pigmentation and its association with a set of key pigmentation related genes was reported (Darias et al., 2013a). Three different biological processes act cooperatively during the pigmentation development including tissue remodelling (involving apoptosis), cellular differentiation of chromatophores and pigment production. These authors showed that the different stages of pigmentation development coincided with the progress of metamorphosis. In the pre-metamorphosis, low expression was observed for the apoptosis marker (*casp 3*) and genes related to melanogenesis (*tyr* and *tyrp1*), but high expression of melanophore differentiating genes (*pax3*, *mc1r*). During the metamorphosis a high expression of *casp3* (apoptosis and tissue remodelling), melanophore differentiating and melanogenic genes (*tyr*, *tyrp1*) was evident. After metamorphosis, low expression of all analyzed genes was observed, especially those associated to the melanophores differentiation (**Figure 1.12**) (Darias et al., 2013a). Since the study was carried out on whole larval pools it was not possible to detect the differences that account for the divergent development of ocular and abocular skin.

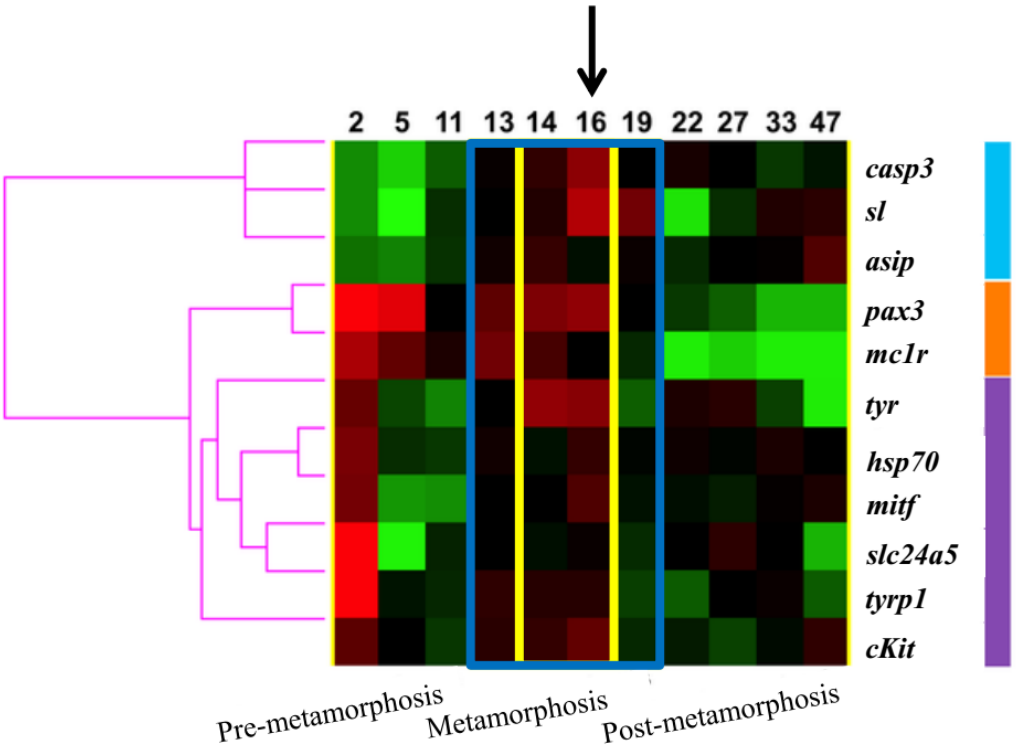

Figure 1.12. Clustering of the pigmentation related genes expression during the larval development of Senegalese sole. Columns represent the mean data values for each sampling point (dph) and rows represent single genes. Expression level of each gene is represented relative to its median abundance across the different stages and is depicted by a color scale: green, black, and red indicating low, medium, and high relative expression levels, respectively. Colored bars to the right margin indicate the three main gene clusters: blue shows genes highly expressed during metamorphosis stage, orange corresponds to genes highly expressed during pre- and metamorphosis and violet to genes highly expressed at 2 dph and at metamorphosis. The three main stages of the larval development are indicated at the bottom of the figure. Note that the expression of all genes was high during the metamorphosis phase (blue square), most of genes displaying a shift in their level of expression before and/or after that period. The climax of pigmentation development at the molecular level was observed between 14 and 16 dph (yellow). Changes in gene expression profiles coincided with morphological changes in pigmentation, showing that the climax of metamorphosis was achieved at 16 dph (arrow) and the end of metamorphosis at 19 dph. The transition from the larval to the adult pattern of skin pigmentation could be clearly observed from 22 dph onwards. [adapted from Darias et al., 2013a].

Abnormal pigmentation reflects perturbations in the mechanisms that control normal pigmentation development, and is an important issue in flatfish aquaculture. Abnormal pigmentation includes hypomelanosis (pseudoalbinism) and hypermelanosis (ambicoloration), (reviewed in Power et al., 2008). Pseudoalbinism is characterized by presence of white areas (partial or total unpigmented) on the ocular side. In contrast, the blind side may display hypermelanosis in the form of dark spots (partial or total pigmented) known as ambicoloration of the skin (Isojima et al., 2013b; Isojima et al., 2013a; Nakamura et al., 2010; Venizelos and Benetti, 1999). Recently, it was demonstrated the role of Asip1 in turbot

pseudoalbinism. This gene is more expressed in ventral region than in the dorsal region. Moreover, expression within the unpigmented patches in the dorsal skin of the pseudoalbin fish was higher than in the pigmented dorsal regions, but similar to those levels observed in the ventral skin (Guillot et al., 2012). In another study, pseudoalbinism was induced by feeding larvae Artemia enriched with high levels of arachidonic acid (ARA). Melanogenesis in the pseudoalbin larvae was repressed probably due to the roles of *asip1* and *slc24a5* genes on the down-regulation of *tyrp1* expression, leading to defects in melanin production. Moreover, gene expression data supports the involvement of *pax3*, *mitf* and *asip1* genes in the developmental disruption of the new post-metamorphic populations of chromatophores including melanophores, xanthophores and iridophores (Darias et al., 2013b).

The involvement of thyroid hormones in abnormal pigmentation during flatfish metamorphosis has been reported in Japanese flounder and spotted halibut. In both species, albinism was induced by adding T_4 to the rearing water at an early stage of metamorphosis (Tagawa & Aritaki., 2005; Yoo et al., 2000). Yoo et al., (2000) suggested three possible mechanisms to explain the action of THs on albinism in Japanese flounder: (1) TYR expression is inhibited by THs, stopping the production of melanin; (2) melanophore apoptosis is induced by THs; and (3) TH exposure accelerates metamorphosis and that this impedes nerve fibers from reaching their target synapses with chromatophores. Tagawa & Aritaki (2005) suggested that THs induce abocular characteristics, and timely differential responsiveness to THs between the ocular and abocular side is essential for development of pigmentation asymmetry. The latter is supported by studies in zebrafish in which the absence of T_3 by knocking down (KD) *dio2* had a negative effect on pigmentation. Furthermore, the *Dio2* KD had down-regulated tyrosinase suggesting THs directly affect pigment formation in addition to other developmental effects (Walpita et al., 2010; Walpita et al., 2009). The relationship between THs (production, transport, availability and action) and pigment (melanogenesis, melanophores differentiation) related genes in the skin and more specifically the ocular and abocular skin during metamorphosis is essential to understand how asymmetric pigmentation develops .

1.5.4. Skin responsiveness to THs

Multiple biological processes and molecular features of skin remodelling in amphibians including the apoptosis of larval cell types, resorption and regeneration of the extracellular matrix and proliferation and differentiation of adult cell types are well described. Suzuki et al., (2009) using a microarray and quantitative real-time PCR analysis described the global gene expression changes in *X. laevis* during 7 days after treatment with 5 nM of T_3. The treatment induced differentially gene expression in 401 transcripts, and functionally grouped genes showed different temporal expression profiles. The genes related to transcription and proteolysis were the first up-regulated genes after T_3 exposure including the *trβ*, *th/bzip* and *bteb,* playing an important role in all gene cascades in *X. laevis* metamorphosis. Genes involved in defense response (such as caerulin) appears only after 5 days of the treatment. These genes are specific of granular glands of the adult skin and are involved in defense against bacterial infections (Suzuki et al., 2009). The adult and larval type keratins were significantly activated and inactivated, respectively (Suzuki et al., 2009; Watanabe et al., 2001). Page et al. identified modifications in abundance (1,000 times fold change) of several keratins transcripts after exposure of salamanders (*Ambystoma mexicanum*) to T_4. These alterations in keratins expression are concomitant with the morphological remodelling of epithelial tissue (Page et al., 2007).

Several molecular markers involved in the axolotl skin remodelling process were identified and correlated with specific expression in adult and larval cells after inducing metamorphosis with 50 nM of T4 (Page et al., 2009; Page et al., 2008). Uromodulin (Umod) is a protection/barrier protein expressed only in the apical cell layer, where the expression decreases significantly being a larval specific gene. Keratin 6 (Krt6) was also down-regulate evidencing the loss of apical cells from the skin during the metamorphosis (Page et al., 2007). Moreover, the expression of keratin 14 (Krt14) is specific from the granular layer of the epidermis and is up-regulated in metamorphosed salamander. The genes Umod, Krt6 and calmodulin 2 (Calm2) were used as markers for larval cell types, and Krt14 was used to identify adult cell types. Another ~90 genes were differentially expressed in response to T_4 treatment (Page et al. 2008).

In contrast, relatively few studies of the change in skin and the importance of the THs exist for flatfish during metamorphosis. In Atlantic halibut down-regulation of both halibut larval keratin 1 and collagen 1α1 and the concomitant disappearance of the keratin bundles in

the cytoplasm of larval cells were observed during the metamorphic climax (Campinho et al., 2007b). These changes are correlated with the expression of Dio2 and Dio3 in basal and supra-basal skin cells (Campinho et al., 2012a) revealing the importance of THs in the maturation of the skin. Nevertheless, questions relating to the possible asymmetric responsiveness to the THs of both ocular and abocular sides of skin to the THs remains to be resolve.

1.6. Atlantic halibut (*Hippoglossus hippoglossus*): aquaculture production

The Atlantic halibut (*Hippoglossus hippoglosus*) is a cold-water flatfish, belongs to the Pleuronectidae family and is the largest extant flatfish. *H. hippoglossus* is distributed throughout the northern part of the North Atlantic Ocean and in parts of the Arctic Ocean (www.fishbase.org, accessed February 2015). This species is distinguishable from other right-eyed flatfishes due its large mouth, which opens as far back as the anterior half of its lower eye, its concave caudal fin, and the distinctive arched lateral line (**Figure 1.13**). Generally, the adult fish is more or less uniformly brown or olive and the blind side is usually white, though in some cases, it may be partially brown (reviewed in Daniels and Watanabe, 2010).

Atlantic halibut is traditionally a highly valued food fish, but due to overfishing and subsequent stock collapses it has become scarce. The fishery was quickly depleted and has not been of economic importance since the 1940's. Annual catches after 1953 have been less than 100 metric tons on an average (reviewed in Daniels and Watanabe, 2010). Nowadays, it is listed as an endangered species (Sobel, 1996) and most fisheries are closed, although there is commonly by-catch mortality through demersal fishing gear (FAO, 2012). The combination of high demand and low abundance demonstrated the interest of the aquaculture industry and resulted in an emerging aquaculture production, initiated by Norway and Iceland in the mid 1980's (FAO, 2012). Actually, production of Atlantic halibut is common in Norway, Iceland, Scotland and Canada (Daniels and Watanabe, 2010).

The industry still has major problems in obtaining high-quality juveniles and abnormal pigmentation (pseudoalbinism) and impaired eye migration were the first problems detected during the production (Harboe et al., 2009). Recently, pseudoalbinism problem can be reduced by enrichment of Artemia with lipid emulsions to feeding heterotrophic algae rich in essential fatty acids. However, impaired eye migration and ambicolouration of juveniles are still major problems (Hamre et al., 2007).

Figure 1.13. Atlantic halibut (*Hippoglossus hippoglossus*) from aquaculture. Atlantic halibut is a right-eyed flatfish species with a large mouth, which opens as far back as the anterior half of its lower eye. It has a concave caudal fin and a distinctive arched lateral line.
(https://www.leroyseafood.com/en/Business/Products/ Products/Farmed-Atlantic-Halibut).

There are multiple advantages of using the Atlantic halibut for studies of tissues development and morphogenesis during metamorphosis: i) slow larval development (metamorphosis occurring over approx. 58 days) allows for collection of well-defined developmental stages; ii) larvae are transparent until the pigmentation starts to intensify during metamorphosis which facilitates individual based physiological studies where the transparent larvae permits *in vivo* observations of both structures and function; iii) its large size (approximately 14.50 - 23.00 mm start and end of metamorphosis) compared to other flatfish such as sole (approximately 5.60 - 9.00 mm start and end of metamorphosis), and flounder facilitates analysis of individuals instead of pools of larvae for molecular analysis. A disadvantage of the species is the extreme sensitivity of early larval stages, which limits experimental manipulation.

The development of a well-define staging scheme for *H. hippoglossus* represented a crucial step for comparisons between and within experiments. Moreover, it facilitates studies of the ontogeny of organ and tissue systems during development and allows the identification of discrete changes in morphology or molecular patterns during key developmental stages in metamorphosis (Power et al., 2008). *H. hippoglossus* can be grouped according to their external morphology and this permits identification of a sequence of distinct larval stages before, during and after metamorphosis. Recently, Saele et al., (2004) established a detailed staging scheme from first feeding through metamorphosis to settlement (**Figure 1.14**). Several parameters were used to define the development stages and include external morphology, skeletal development, degree of ossification and asymmetry which show a

strong correlation with myotome height (MH), (Saele et al., 2004). These authors define the principal development stages: 5 - pre-metamorphosis, 6-7 – prometamorphosis, 8 - proclimax metamorphosis, 9 - climax metamorphosis and 10 - post-metamorphosis juvenile.

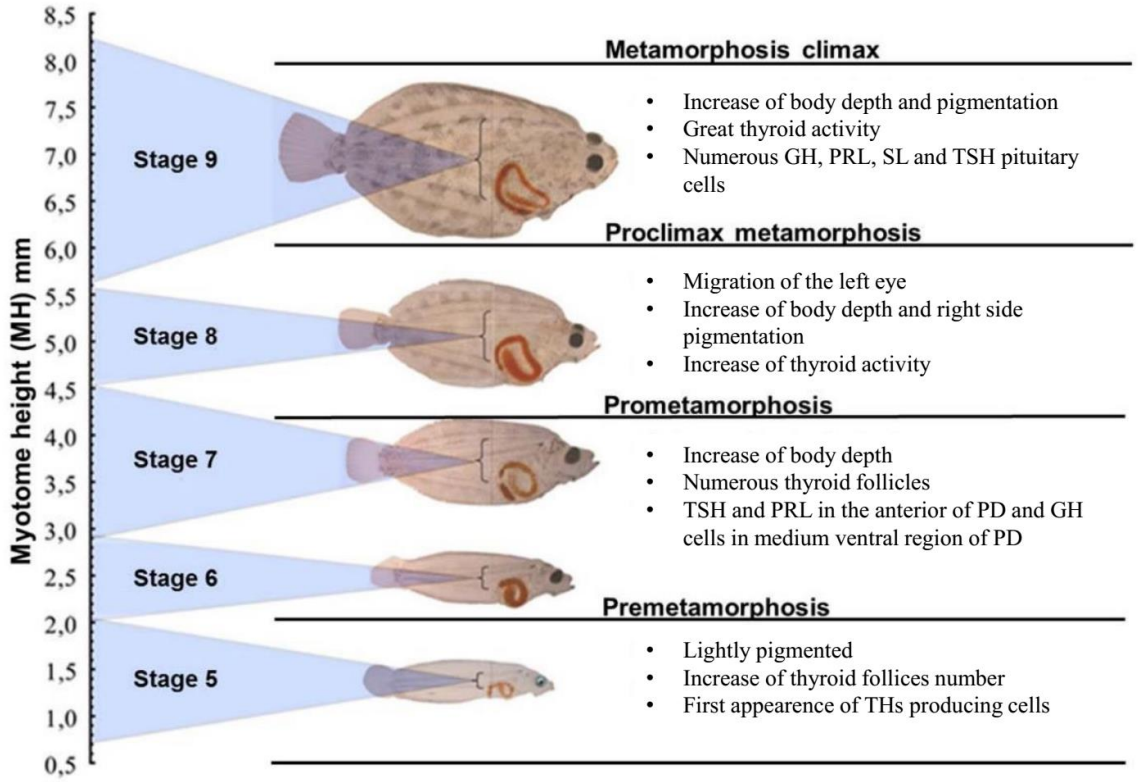

Figure 1.14*:* Myotome height (MH) size (in mm) ranges from stages 5 to 9. Schemes of the Atlantic halibut larvae are representative of the midrange of each stage. Major morphological changes are described for each developmental stage including a summary of the main endocrine cells produced by the pituitary gland during ontogeny. GH, growth hormone; PRL, prolactin; SL, somatolactin, TSH, thyroid stimulating hormone, PD pars distalis [Adapted from Saele et al., (2004) and Einarsdóttir et al., (2006)].

During the stages 5 to 7, halibut larvae are bilaterally symmetrical and transparent, but with pigmented eyes. The transition to asymmetry starts during stage 8, in which larvae are still pelagic, but have a relatively large size and frequently have started to tilt to one side. Stage 9 corresponds to the metamorphic climax and the eye migration is advanced and reaches the midline, giving the larvae an asymmetric appearance. The asymmetric skin pigment patterns emerge and the larvae rest occasionally on the bottom of the tank. In the post-metamorphic juvenile stage 10, the eye migration is complete and animals adopt a demersal lifestyle and settles on the bottom (Saele et al., 2004).

Chapter 1

Knowledge about the mechanisms underlying the global molecular and cellular changes during Atlantic halibut development has being improving due to the development of genomics and transcriptomics technologies. Douglas et al. (2007; 2008) generated cDNA libraries from different *H. hippoglossus* adult tissues and larval stages. ESTs specific for adult tissues and early mouth-opening stages were isolated from cDNA libraries but data from the larvae undergoing metamorphosis is limited. In general, the analysis of the first largescale transcriptome information was enriched in GO terms associated with catalytic activity, binding, transport, metabolism, signal transduction, nucleic acid processes and response to stimuli. The first halibut EST survey identified genes involved in the immune system, signal transduction and transcription factor activity. The scarcity of molecular data for Atlantic halibut especially during metamorphosis at the start of this thesis was perceived as a bottleneck for research into this flatfish species. For this reason, one target of the thesis was the large scale analysis of tissues specific transcriptional changes in responsive tissue in order to identify molecular changes underpinning tissue specific maturation.

1.7. Objectives

The aim of the present PhD thesis was to characterize the mechanisms underlying the molecular and cellular changes which occur in the skin, including pigmentation, during flatfish metamorphosis. The Atlantic halibut was chosen for the study due to its relatively slow larval development, large larval size which facilitates analysis, well-defined developmental scheme and its importance as a high value aquaculture species with an embargo on wild captures due to its highlight endangered status. The PhD thesis was integrated in Lifecyle, an European community project. The skin was one of the target organs due to its multifunctional role and its known responsiveness to THs. In addition, questions about the relationship between the skin TH responsiveness and the asymmetry observed in pigmentation between ocular and abocular (blind) skin after metamorphosis are still unclear and unexplored. A preliminary investigation of the cross-talk between the HPT and the HPI axes in the regulation of metamorphosis is also performed.

For this purpose, the following goals were proposed:

1) Generate for the first time in a non-model flatfish species a reference transcriptome of three major tissues (skin, head and gastrointestinal tract) during metamorphosis. For each tissue, establish enriched or specific transcripts and networks involved in tissue maturation, and identify putative TH responsive genes. Compare the transcriptome at several metamorphic stages with the juvenile to identify differentially expressed transcripts in different metamorphic stages during metamorphosis. Contribute with substantial molecular resources for the community of scientists working on Atlantic halibut and teleost fish in general. Identify new potential molecular markers associated with metamorphosis that may be of use to solve problems related to Atlantic halibut production (Chapter 2).

2) Verify if the two deiodinase 3 (*dio3*) genes identified during the transcriptome sequencing have divergent functions in ocular and abocular skin during metamorphosis, as it has been demonstrated that the availability of thyroid hormones in the skin during metamorphosis is modulated by the coordinated action of the deiodinases. Establish an evolutionary model for *dio3* genes and evaluate how these

two genes are expressed during metamorphosis particularly in the skin. To establish responsiveness of *dio3* to THs, perform *in silico* promoter analysis and manipulation of THs *in vivo* using a well-characterized inhibitor of thyroid peroxidase that disrupts TH production, methimazol (MMI) (Chapter 3).

3) Explore the detailed development of the primary barrier and osmoregulatory functions of Atlantic halibut skin and examine the relative importance of the ocular and abocular skin. Combine histological and histochemical techniques to reveal the developmental changes in the skins morphology and structure and measure barrier and osmoregulatory functions in different metamorphic stages using electrophysiology (Chapter 4).

4) Establish how genes involved in melanogenesis and regulation of pigmentation are expressed in ocular and abocular skin during metamorphosis and how development of pigmentation is correlated to metamorphosis. Study ontogeny of candidate genes for fish skin pigmentation using quantitative real-time PCR. Establish a possible relationship between the THs and pigmentation related genes (Chapter 5).

5) Analyze the responsiveness to THs of both ocular and abocular skin during metamorphosis. Analyze the molecular ontogeny of genes involved in TH transport, metabolism and action in ocular and abocular skin by quantitative real-time PCR (Chapter 5).

6) Investigate if both the HPT and HPI axes are involved in flatfish metamorphosis and particularly in skin pigmentation. Manipulate THs and cortisol *in vivo* using the inhibitor of TH production (MMI) and the glucocorticoid receptor antagonist, mifepristone (RU486), which blocks cortisol action in teleosts. The effect of MMI and RU486 on the larval phenotype during metamorphosis and the molecular ontogeny of genes involved in the thyoid axis and pigmentation in the ocular and abocular skin sides will be analysed (Chapter 5)

References

Adams, B.A., Cyr, D.G., Eales, J.G., 2000. Thyroid hormone deiodination in tissues of American plaice, *Hippoglossoides platessoides*: characterization and short-term responses to polychlorinated biphenyls (PCBs) 77 and 126. Comparative biochemistry and physiology. Toxicology and pharmacology : CBP 127, 367-378.

Alkemade, A., 2015. Thyroid hormone and the developing hypothalamus. Frontiers in neuroanatomy 9, 15.

Allen, J.J., Akkaynak, D., Sugden, A.U., Hanlon, R.T., 2015. Adaptive body patterning, three-dimensional skin morphology and camouflage measures of the slender filefish *Monacanthus tuckeri* on a Caribbean coral reef. Biological Journal of the Linnean Society 116, 377–396.

Alvarez-Pellitero, P., 2008. Fish immunity and parasite infections: from innate immunity to immunoprophylactic prospects. Veterinary immunology and immunopathology 126, 171-198.

Aranda, A., Pascual, A., 2001. Nuclear hormone receptors and gene expression. Physiological reviews 81, 1269-1304.

Aranishi, F., 1999. Purification and Characterization of Serum Serpin from Carp (*Cyprinus carpio*). Marine biotechnology 1, 81-88.

Arjona, F.J., de Vrieze, E., Visser, T.J., Flik, G., Klaren, P.H., 2011a. Identification and functional characterization of zebrafish solute carrier Slc16a2 (Mct8) as a thyroid hormone membrane transporter. Endocrinology 152, 5065-5073.

Arjona, F.J., Vargas-Chacoff, L., Martin Del Rio, M.P., Flik, G., Mancera, J.M., Klaren, P.H., 2011b. Effects of cortisol and thyroid hormone on peripheral outer ring deiodination and osmoregulatory parameters in the Senegalese sole (*Solea senegalensis*). The Journal of endocrinology 208, 323-330.

Armesto, P., Campinho, M.A., Rodriguez-Rua, A., Cousin, X., Power, D.M., Manchado, M., Infante, C., 2014. Molecular characterization and transcriptional regulation of the Na +/K+ ATPase alpha subunit isoforms during development and salinity challenge in a teleost fish, the Senegalese sole (*Solea senegalensis*). Comparative biochemistry and physiology. Part B, Biochemistry & Molecular biology 175, 23-38.

Babin, P.J., 1992. Binding of thyroxine and 3,5,3'-triiodothyronine to trout plasma lipoproteins. The American journal of physiology 262, E712-720.

Bagci, E., Heijlen, M., Vergauwen, L., Hagenaars, A., Houbrechts, A.M., Esguerra, C.V., Blust, R., Darras, V.M., Knapen, D., 2015. Deiodinase knockdown during early zebrafish development affects growth, development, energy metabolism, motility and phototransduction. PLoS One 10, e0123285.

Bao, B., Yang, G., Liu, Z., Li, S., Wang, Z., Ren, D., 2005. Isolation of SFRS3 gene and its differential expression during metamorphosis involving eye migration of Japanese flounder *Paralichthys olivaceus*. Biochimica et Biophysica Acta 1725, 64-70.

Bao, B., Ke, Z., Xing, J., Peatman, E., Liu, Z., Xie, C., Xu, B., Gai, J., Gong, X., Yang, G., Jiang, Y., Tang, W., Ren, D., 2011. Proliferating cells in suborbital tissue drive eye migration in flatfish. Developmental Biology 351, 200-207.

Bassett, J.H., Boyde, A., Howell, P.G., Bassett, R.H., Galliford, T.M., Archanco, M., Evans, H., Lawson, M.A., Croucher, P., St Germain, D.L., Galton, V.A., Williams, G.R., 2010. Optimal bone strength and mineralization requires the type 2 iodothyronine deiodinase in osteoblasts. Proceedings of the National Academy of Sciences of the United States of America 107, 7604-7609.

Becker, K.B., Stephens, K.C., Davey, J.C., Schneider, M.J., Galton, V.A., 1997. The type 2 and type 3 iodothyronine deiodinases play important roles in coordinating development in *Rana catesbeiana* tadpoles. Endocrinology 138, 2989-2997.

Berry, M.J., Kieffer, J.D., Harney, J.W., Larsen, P.R., 1991a. Selenocysteine confers the biochemical properties characteristic of the type I iodothyronine deiodinase. The Journal of biological chemistry 266, 14155-14158.

Berry, M.J., Kieffer, J.D., Larsen, P.R., 1991b. Evidence that cysteine, not selenocysteine, is in the catalytic site of type II iodothyronine deiodinase. Endocrinology 129, 550-552.

Bianco, A.C., Salvatore, D., Gereben, B., Berry, M.J., Larsen, P.R., 2002. Biochemistry, cellular and molecular biology, and physiological roles of the iodothyronine selenodeiodinases. Endocrine Reviews 23, 38-89.

Bianco, A.C., Larsen, P.R., 2005. Cellular and structural biology of the deiodinases. Thyroid : official journal of the American Thyroid Association 15, 777-786.

Bianco, A.C., Kim, B.W., 2006. Deiodinases: implications of the local control of thyroid hormone action. Journal of Clinical Investigation 116, 2571-2579.

Björnsson, B., Johansson, V., Benedet, S., Einarsdottir, I., Hildahl, J., Agustsson, T., Jönsson, E., 2002. Growth Hormone Endocrinology of Salmonids: Regulatory Mechanisms and Mode of Action. Fish Physiology and Biochemistry 27, 227-242.

Blanton, M.L., Specker, J.L., 2007. The hypothalamic-pituitary-thyroid (HPT) axis in fish and its role in fish development and reproduction. Critical Reviews in Toxicology 37, 97-115.

Boas, M., Feldt-Rasmussen, U., Skakkebæk, N.E., Main, K.M., 2006. Environmental chemicals and thyroid function. European Journal of Endocrinology 154, 599-611.

Bolasina, S., Péresz, A., Yamashita, Y., 2006. Digestive enzymes activity during ontogenetic development and effect of starvation in Japanese flounder, *Paralichthys olivaceus*. Aquaculture 253, 503-515.

Bolker, J.A., Hill, C.L., 2000. Pigmentation development in hatchery-reared flatfishes. Journal of Fish Biology 56.

Bonett, R.M., Hoopfer, E.D., Denver, R.J., 2010. Molecular mechanisms of corticosteroid synergy with thyroid hormone during tadpole metamorphosis. General and Comparative Endocrinology 168, 209-219.

Bouzaffour, M., Rampon, C., Ramauge, M., Courtin, F., Vriz, S., 2010. Implication of type 3 deiodinase induction in zebrafish fin regeneration. General and Comparative Endocrinology 168, 88-94.

Boyages, S.C., 1993. Clinical review 49: Iodine deficiency disorders. The Journal of Clinical Endocrinology and Metabolism 77, 587-591.

Braasch, I., Schartl, M., Volff, J.N., 2007. Evolution of pigment synthesis pathways by gene and genome duplication in fish. BMC Evolutionary Biology 7, 74.

Braasch, I., Brunet, F., Volff, J.N., Schartl, M., 2009. Pigmentation pathway evolution after whole-genome duplication in fish. Genome Biology and Evolution 1, 479-493.

Bradley, D.J., Young, W.S., 3rd, Weinberger, C., 1989. Differential expression of alpha and beta thyroid hormone receptor genes in rat brain and pituitary. Proceedings of the National Academy of Sciences of the United States of America 86, 7250-7254.

Braun, D., Kinne, A., Brauer, A.U., Sapin, R., Klein, M.O., Kohrle, J., Wirth, E.K., Schweizer, U., 2011. Developmental and cell type-specific expression of thyroid hormone transporters in the mouse brain and in primary brain cells. Glia 59, 463-471.

Bres, O., Plohman, J.C., Eales, J.G., 2006. A cDNA for a putative type III deiodinase in the trout (*Oncorhynchus mykiss*): influence of holding conditions and thyroid hormone treatment on its hepatic expression. General and Comparative Endocrinology 145, 92-100.

Browman, H.I., Hawryshyn, C.W., 1994. The developmental trajectory of ultraviolet photosensitivity in rainbow trout is altered by thyroxine. Vision Research 34, 1397-1406.

Brown, S.B., MacLatchy, D.L., Hara, T.J., Eales, J.G., 1991. Effects of cortisol on aspects of 3,5,3'-triiodo-L-thyronine metabolism in rainbow trout (*Oncorhynchus mykiss*). General and Comparative Endocrinology 81, 207-216.

Brown, D.D., 1997. The role of thyroid hormone in zebrafish and axolotl development. Proceedings of the National Academy of Sciences of the United States of America 94, 13011-13016.

Brown, D.D., 2005. The role of deiodinases in amphibian metamorphosis. Thyroid : official journal of the American Thyroid Association 15, 815-821.

Buchholz, D.R., Paul, B.D., Fu, L., Shi, Y.-B., 2006. Molecular and developmental analyses of thyroid hormone receptor function in *Xenopus laevis*, the African clawed frog. General and Comparative Endocrinology 145, 1-19.

Buchholz, D.R., 2015. More similar than you think: Frog metamorphosis as a model of human perinatal endocrinology. Developmental Biology 408, 188-195.

Burton, D., 2010. Flatfish (Pleuronectiformes) chromatic biology. Reviews in Fish Biology and Fisheries 20, 31-46.

Cai, L., Brown, D.D., 2004. Expression of type II iodothyronine deiodinase marks the time that a tissue responds to thyroid hormone-induced metamorphosis in *Xenopus laevis*. Developmental biology 266, 87-95.

Campinho, M.A., Silva, N., Sweeney, G.E., Power, D.M., 2007b. Molecular, cellular and histological changes in skin from a larval to an adult phenotype during bony fish metamorphosis. Cell and Tissue Research 327, 267-284.

Campinho, M.A., Silva, N., Nowell, M.A., Llewellyn, L., Sweeney, G.E., Power, D.M., 2007a. Troponin T isoform expression is modulated during Atlantic halibut metamorphosis. BMC Development Biology 7, 71.

Campinho, M.A., Galay-Burgos, M., Sweeney, G.E., Power, D.M., 2010. Coordination of deiodinase and thyroid hormone receptor expression during the larval to juvenile transition in sea bream (*Sparus aurata*, Linnaeus). General and Comparative Endocrinology 165, 181-194.

Campinho, M.A., Galay-Burgos, M., Silva, N., Costa, R.A., Alves, R.N., Sweeney, G.E., Power, D.M., 2012a. Molecular and cellular changes in skin and muscle during metamorphosis of Atlantic halibut (*Hippoglossus hippoglossus*) are accompanied by changes in deiodinases expression. Cell and Tissue Research 350, 333-346.

Campinho, M.A., Morgado, I., Pinto, P.I., Silva, N., Power, D.M., 2012b. The goitrogenic efficiency of thioamides in a marine teleost, sea bream (*Sparus auratus*). General and Comparative Endocrinology 179, 369-375.

Campinho, M.A., Saraiva, J., Florindo, C., Power, D.M., 2014. Maternal thyroid hormones are essential for neural development in zebrafish. Molecular Endocrinology 28, 1136-1149.

Campinho, M.A., Silva, N., Roman-Padilla, J., Ponce, M., Manchado, M., Power, D.M., 2015. Flatfish metamorphosis: a hypothalamic independent process? Molecular and Cellular Endocrinology 404, 16-25.

Capelo, L.P., Beber, E.H., Fonseca, T.L., Gouveia, C.H., 2009. The monocarboxylate transporter 8 and L-type amino acid transporters 1 and 2 are expressed in mouse

skeletons and in osteoblastic MC3T3-E1 cells. Thyroid : official journal of the American Thyroid Association 19, 171-180.

Casas, F., Busson, M., Grandemange, S., Seyer, P., Carazo, A., Pessemesse, L., Wrutniak-Cabello, C., Cabello, G., 2006. Characterization of a novel thyroid hormone receptor alpha variant involved in the regulation of myoblast differentiation. Molecular Endocrinology 20, 749-763.

Castro, L.F.C., Gonçalves, O., Mazan, S., Tay, B.-H., Venkatesh, B., Wilson, J.M., 2013. Recurrent gene loss correlates with the evolution of stomach phenotypes in gnathostome history. Proceedings of the Royal Society B: Biological Sciences 281.

Cerda-Reverter, J.M., Agulleiro, M.J., R, R.G., Sanchez, E., Ceinos, R., Rotllant, J., 2011. Fish melanocortin system. European Journal of Pharmacology 660, 53-60.

Cerda-Reverter, J.M., Haitina, T., Schioth, H.B., Peter, R.E., 2005. Gene structure of the goldfish agouti-signaling protein: a putative role in the dorsal-ventral pigment pattern of fish. Endocrinology 146, 1597-1610.

Chan, S., Kachilele, S., McCabe, C.J., Tannahill, L.A., Boelaert, K., Gittoes, N.J., Visser, T.J., Franklyn, J.A., Kilby, M.D., 2002. Early expression of thyroid hormone deiodinases and receptors in human fetal cerebral cortex. Developmental Brain Research 138, 109-116.

Chanoine, C., Hardy, S., 2003. *Xenopus* muscle development: from primary to secondary myogenesis. Developmental dynamics : an official publication of the American Association of Anatomists 226, 12-23.

Cheng, S.Y., Leonard, J.L., Davis, P.J., 2010. Molecular aspects of thyroid hormone actions. Endocrine Reviews 31, 139-170.

Cole, A.M., Weis, P., Diamond, G., 1997. Isolation and characterization of pleurocidin, an antimicrobial peptide in the skin secretions of winter flounder. The Journal of Biological Chemistry 272, 12008-12013.

Colihueque, N., 2000. Genetics of salmonid skin pigmentation: clues and prospects for improving the external appearance of farmed salmonids. Reviews in Fish Biology and Fisheries 20.

Cone, R., 1999. Mucus, in: P.L. Ogra, Mestecky, L., Lamm, M. E., Strober, W., Bienestock, J., and McGhee, J. R. Eds (Ed.), Mucosal Immunology. Academic Press, London, UK, 43-64.

Connors, K.A., Korte, J.J., Anderson, G.W., Degitz, S.J., 2010. Characterization of thyroid hormone transporter expression during tissue-specific metamorphic events in *Xenopus tropicalis*. General and Comparative Endocrinology 168, 149-159.

Contreras-Jurado, C., Garcia-Serrano, L., Gomez-Ferreria, M., Costa, C., Paramio, J.M., Aranda, A., 2011. The thyroid hormone receptors as modulators of skin proliferation and inflammation. The Journal of Biological Chemistry 286, 24079-24088.

Daley, W.P., Peters, S.B., Larsen, M., 2008. Extracellular matrix dynamics in development and regenerative medicine. Journal of Cell Science 121, 255-264.

Daley, W.P., Yamada, K.M., 2013. ECM-modulated cellular dynamics as a driving force for tissue morphogenesis. Current Opinion in Genetics & Development 23, 408-414.

Damjanovski, S., Puzianowska-Kuznicka, M., Ishuzuya-Oka, A., Shi, Y.B., 2000. Differential regulation of three thyroid hormone-responsive matrix metalloproteinase genes implicates distinct functions during frog embryogenesis. FASEB journal: official publication of the Federation of American Societies for Experimental Biology 14, 503-510.

Daniels, H.V., Watanabe, W.O., 2010. Practical Flatfish Culture and Stock Enhancement, First ed, John Wiley & Sons.

Darias, M.J., Murray, H.M., Martínez-Rodríguez, G., Cárdenas, S., Yúfera, M., 2005. Gene expression of pepsinogen during the larval development of red porgy (*Pagrus pagrus*). Aquaculture 248, 245-252.

Darias, M.J., Andree, K.B., Boglino, A., Fernandez, I., Estevez, A., Gisbert, E., 2013a. Coordinated regulation of chromatophore differentiation and melanogenesis during the ontogeny of skin pigmentation of *Solea senegalensis* (Kaup, 1858). PloS one 8, e63005.

Darias, M.J., Andree, K.B., Boglino, A., Rotllant, J., Cerda-Reverter, J.M., Estevez, A., Gisbert, E., 2013b. Morphological and molecular characterization of dietary-induced pseudo-albinism during post-embryonic development of *Solea senegalensis* (Kaup, 1858). PloS one 8, e68844.

Darras, V.M., Van Herck, S.L., 2012. Iodothyronine deiodinase structure and function: from ascidians to humans. The Journal of Endocrinology 215, 189-206.

Darras, V.M., Houbrechts, A.M., Van Herck, S.L., 2015. Intracellular thyroid hormone metabolism as a local regulator of nuclear thyroid hormone receptor-mediated impact on vertebrate development. Biochimica et Biophysica Acta 1849, 130-141.

Das, B., Cai, L., Carter, M.G., Piao, Y.L., Sharov, A.A., Ko, M.S., Brown, D.D., 2006. Gene expression changes at metamorphosis induced by thyroid hormone in *Xenopus laevis* tadpoles. Devevelopment Biology 291, 342-355.

Das, B., Heimeier, R.A., Buchholz, D.R., Shi, Y.B., 2009. Identification of direct thyroid hormone response genes reveals the earliest gene regulation programs during frog metamorphosis. The Journal of Biological Chemistry 284, 34167-34178.

Davis, P.J., Lin, H.Y., Mousa, S.A., Luidens, M.K., Hercbergs, A.A., Wehling, M., Davis, F.B., 2011. Overlapping nongenomic and genomic actions of thyroid hormone and steroids. Steroids 76, 829-833.

De Groef, B., Van der Geyten, S., Darras, V.M., Kühn, E.R., 2006. Role of corticotropin-releasing hormone as a thyrotropin-releasing factor in non-mammalian vertebrates. General and Comparative Endocrinology 146, 62-68.

de Jesus, E.G., Hirano, T., Inui, Y., 1991. Changes in cortisol and thyroid hormone concentrations during early development and metamorphosis in the Japanese flounder, *Paralichthys olivaceus*. General and Comparative Endocrinology 82, 369-376.

de Jesus, E.G., Inui, Y., Hirano, T., 1990. Cortisol enhances the stimulating action of thyroid hormones on dorsal fin-ray resorption of flounder larvae in vitro. General and Comparative Endocrinology 79, 167-173.

de Jesus, E.G., Toledo, J.D., Simpas, M.S., 1998. Thyroid hormones promote early metamorphosis in grouper (*Epinephelus coioides*) larvae. General and Comparative Endocrinology 112, 10-16.

de Vrieze, E., van de Wiel, S.M., Zethof, J., Flik, G., Klaren, P.H., Arjona, F.J., 2014. Knockdown of monocarboxylate transporter 8 (mct8) disturbs brain development and locomotion in zebrafish. Endocrinology 155, 2320-2330.

Degroot, L.J., Niepomniszcze, H., 1977. Biosynthesis of thyroid hormone: Basic and clinical aspects. Metabolism 26, 665-718.

Delgado, J.B.O., M., R.N., P., P.-F., Sarasquete, S., 2006. Thyroid gland development in Senegalese sole (*Solea senegalensis* Kaup 1858) during early life stages: A histochemical and immunohistochemical approach. Aquaculture 260, 346-356.

Dentice, M., Marsili, A., Ambrosio, R., Guardiola, O., Sibilio, A., Paik, J.H., Minchiotti, G., DePinho, R.A., Fenzi, G., Larsen, P.R., Salvatore, D., 2010. The FoxO3/type 2 deiodinase pathway is required for normal mouse myogenesis and muscle regeneration. The Journal of Clinical Investigation 120, 4021-4030.

Dentice, M., Marsili, A., Zavacki, A., Larsen, P.R., Salvatore, D., 2013. The deiodinases and the control of intracellular thyroid hormone signaling during cellular differentiation. Biochimica et Biophysica Acta 1830, 3937-3945.

Dentice, M., Salvatore, D., 2011. Deiodinases: the balance of thyroid hormone: local impact of thyroid hormone inactivation. The Journal of Endocrinology 209, 273-282.

Denver, R.J., 1997. Environmental stress as a developmental cue: corticotropin-releasing hormone is a proximate mediator of adaptive phenotypic plasticity in amphibian metamorphosis. Hormones and Behavior 31, 169-179.

Denver, R.J., 2009. Stress hormones mediate environment-genotype interactions during amphibian development. General and Comparative Endocrinology 164, 20-31.

Diaz, J.P., Prié-Granié, M., Kentouri, M., Varsamos, S., Connes, R., 2003. Development of the lateral line system in the sea bass. Journal of Fish Biology 62, 24-40.

Diogo, R., Ziermann, J.M., 2014. Development, metamorphosis, morphology, and diversity: The evolution of chordate muscles and the origin of vertebrates. Developmental dynamics : an official publication of the American Association of Anatomists.

Doldán, M.J., Cid, P., Mantilla, L., de Miguel Villegas, E., 2011. Development of the olfactory system in turbot (*Psetta maxima* L.). Journal of Chemical Neuroanatomy 41, 148-157.

Dong, W., Macaulay, L.J., Kwok, K.W., Hinton, D.E., Stapleton, H.M., 2013. Using whole mount in situ hybridization to examine thyroid hormone deiodinase expression in embryonic and larval zebrafish: a tool for examining OH-BDE toxicity to early life stages. Aquatic toxicology 132-133, 190-199.

Douglas, S.E., Gawlicka, A., Mandla, S., Gallant, J.W., 1999. Ontogeny of the stomach in winter flounder: characterization and expression of the pepsinogen and proton pump genes and determination of pepsin activity. Journal of Fish Biology 55, 897-915.

Douglas, S.E., Knickle, L.C., Kimball, J., Reith, M.E., 2007. Comprehensive EST analysis of Atlantic halibut (*Hippoglossus hippoglossus*), a commercially relevant aquaculture species. BMC Genomics 8, 144.

Douglas, S.E., Knickle, L.C., Williams, J., Flight, R.M., Reith, M.E., 2008. A first generation Atlantic halibut *Hippoglossus hippoglossus* (L.) microarray: application to developmental studies. Journal of Fish Biology 72, 2391-2406.

Dumitrescu, A.M., Liao, X.H., Best, T.B., Brockmann, K., Refetoff, S., 2004. A novel syndrome combining thyroid and neurological abnormalities is associated with mutations in a monocarboxylate transporter gene. American journal of human genetics 74, 168-175.

Eales, J.G., Brown, S.B., 1993. Measurement and regulation of thyroidal status in teleost fish. Reviews in Fish Biology and Fisheries 3, 299-347.

Eales, J.G., Brown, S.B., Cyr, D.G., Adams, B.A., Finnson, K.R., 1999. Deiodination as an index of chemical disruption of thyroid hormone homeostasis and thyroidal status in fish, in: D.S. Henshel, M.C. Black, M.C. Harrass (Eds.), Environmental Toxicology and Risk Assessment: Standardization of Biomarkers for Endocrine Disruption and Environmental Assessment. American Society for Testing and Materials, West Conshohocken, PA, 136-164.

Einarsdóttir, I., Silva, N., Power, D., Smáradóttir, H., Björnsson, B., 2006. Thyroid and pituitary gland development from hatching through metamorphosis of a teleost flatfish, the Atlantic halibut. Anatomy and Embryology 211, 47-60.

Einarsdottir, I.E., Power, D.M., Jonsson, E., Bjornsson, B.T., 2011. Occurrence of ghrelin-producing cells, the ghrelin receptor and Na+,K + -ATPase in tissues of Atlantic halibut (*Hippoglossus hippoglossus*) during early development. Cell and Tissue Research 344, 481-498.

El-Gamal, A.E.E., 2009. Effect of Temperature on Hatching and Larval Development and Mucin Secretion in Common Carp, *Cyprinus carpio* (Linnaeus, 1758) Global Veterinaria 3, 80-90.

Elliott, D.G., 2011. Functional Morphology of the Integumentary System in Fishes, in: A.P. Farrell (Ed.), Encyclopedia of Fish Physiology: From Gene to Environment. Academic Press, pp. 476-488.

Essner, J.J., Johnson, R.G., Hackett, P.B., Jr., 1999. Overexpression of thyroid hormone receptor alpha 1 during zebrafish embryogenesis disrupts hindbrain patterning and implicates retinoic acid receptors in the control of hox gene expression. Differentiation 65, 1-11.

Esteben, M.A., 2012. An Overview of the Immunological Defenses in Fish Skin. International Scholarly Research Network, ISRN Immunology, 1-29.

FAO, 2012. Fishery and Aquaculture Statistics, Rome.

Fernández-Díaz, C., Yúfera, M., Cañavate, J.P., Moyano, F.J., Alarcón, F.J., Díaz, M., 2001. Growth and physiological changes during metamorphosis of Senegalese sole reared in the laboratory. Journal of Fish Biology 58, 1086-1097.

Ferrara, A.M., Liao, X.H., Gil-Ibanez, P., Marcinkowski, T., Bernal, J., Weiss, R.E., Dumitrescu, A.M., Refetoff, S., 2013. Changes in thyroid status during perinatal development of MCT8-deficient male mice. Endocrinology 154, 2533-2541.

Ferraresso, S., Bonaldo, A., Parma, L., Cinotti, S., Massi, P., Bargelloni, L., Gatta, P.P., 2013. Exploring the larval transcriptome of the common sole (*Solea solea* L.). BMC Genomics 14, 315.

Fetter, E., Baldauf, L., Da Fonte, D.F., Ortmann, J., Scholz, S., 2015. Comparative analysis of goitrogenic effects of phenylthiourea and methimazole in zebrafish embryos. Reproductive toxicology 57, 10-20.

Fines, G.A., Plohman, J., Eales, J.G., 1999. Effect of experimental 3,5,3'-triiodothyronine hyperthyroidism on thyroid hormone deiodination in brain regions and liver of rainbow trout, *Oncorhynchus mykiss*. Canadian Journal of Zoology 77, 1185-1191.

Flamant, F., Samarut, J., 2003. Thyroid hormone receptors: lessons from knockout and knock-in mutant mice. Trends in Endocrinology and Metabolism: TEM 14, 85-90.

Forrest, D., Reh, T.A., Rusch, A., 2002. Neurodevelopmental control by thyroid hormone receptors. Current Opinion in Neurobiology 12, 49-56.

Friesema, E.C., Ganguly, S., Abdalla, A., Manning Fox, J.E., Halestrap, A.P., Visser, T.J., 2003. Identification of monocarboxylate transporter 8 as a specific thyroid hormone transporter. The Journal of Biological Chemistry 278, 40128-40135.

Friesema, E.C., Grueters, A., Biebermann, H., Krude, H., von Moers, A., Reeser, M., Barrett, T.G., Mancilla, E.E., Svensson, J., Kester, M.H., Kuiper, G.G., Balkassmi, S., Uitterlinden, A.G., Koehrle, J., Rodien, P., Halestrap, A.P., Visser, T.J., 2004. Association between mutations in a thyroid hormone transporter and severe X-linked psychomotor retardation. Lancet 364, 1435-1437.

Friesema, E.C., Jansen, J., Jachtenberg, J.W., Visser, W.E., Kester, M.H., Visser, T.J., 2008. Effective cellular uptake and efflux of thyroid hormone by human monocarboxylate transporter 10. Molecular Endocrinology 22, 1357-1369.

Friesema, E.C., Jansen, J., Visser, T.J., 2005. Thyroid hormone transporters. Biochemical Society Transactions 33, 228-232.

Friesema, E.C., Kuiper, G.G., Jansen, J., Visser, T.J., Kester, M.H., 2006. Thyroid hormone transport by the human monocarboxylate transporter 8 and its rate-limiting role in intracellular metabolism. Molecular Endocrinology 20, 2761-2772.

Friesema, E.C., Visser, W.E., Visser, T.J., 2010. Genetics and phenomics of thyroid hormone transport by MCT8. Molecular and Cellular Endocrinology 322, 107-113.

Fujii, R., 2000. The regulation of motile activity in fish chromatophores. Pigment cell research / sponsored by the European Society for Pigment Cell Research and the International Pigment Cell Society 13, 300-319.

Fukamachi, S., Sugimoto, M., Mitani, H., Shima, A., 2004. Somatolactin selectively regulates proliferation and morphogenesis of neural-crest derived pigment cells in medaka. Proceedings of the National Academy of Sciences of the United States of America 101, 10661-10666.

Galay-Burgos, M., Power, D.M., Llewellyn, L., Sweeney, G.E., 2008. Thyroid hormone receptor expression during metamorphosis of Atlantic halibut (*Hippoglossus hippoglossus*). Molecular and Cellular Endocrinology 281, 56-63.

Galton, V.A., 2005. The roles of the iodothyronine deiodinases in mammalian development. Thyroid : official journal of the American Thyroid Association 15, 823-834.

Gao, C., Yang, R.B., Hu, W.B., Wang, J., 2013. Ontogeny of the stomach in yellow catfish (*Pelteobagrus fulvidraco*): detection and quantifictation of pepsinogen and H+/K+ -ATPase gene expression. Journal of Animal Physiology and Animal Nutrition 97, 20-26.

Garcia-Serrano, L., Gomez-Ferreria, M.A., Contreras-Jurado, C., Segrelles, C., Paramio, J.M., Aranda, A., 2011. The thyroid hormone receptors modulate the skin response to retinoids. PLoS One 6, e23825.

Garcia, G.C., Jeziorski, M.C., Valverde, R.C., Orozco, A., 2004. Effects of iodothyronines on the hepatic outer-ring deiodinating pathway in killifish. General and Comparative Endocrinology 135, 201-209.

Gautier, P., Naranjo-Golborne, C., Taylor, M.S., Jackson, I.J., Smyth, I., 2008. Expression of the fras1/frem gene family during zebrafish development and fin morphogenesis. Developmental dynamics : an official publication of the American Association of Anatomists 237, 3295-3304.

Gawlicka, A., Parent, B., Horn, M.H., Ross, N., Opstad, I., Torrissen, O.J., 2000. Activity of digestive enzymes in yolk-sac larvae of Atlantic halibut (*Hippoglossus hippoglossus*): indication of readiness for first feeding. Aquaculture 184, 303-314.

Gereben, B., Zavacki, A.M., Ribich, S., Kim, B.W., Huang, S.A., Simonides, W.S., Zeold, A., Bianco, A.C., 2008a. Cellular and molecular basis of deiodinase-regulated thyroid hormone signaling. Endocrine Reviews 29, 898-938.

Geven, E.J., Flik, G., Klaren, P.H., 2009. Central and peripheral integration of interrenal and thyroid axes signals in common carp (*Cyprinus carpio* L.). The Journal of Endocrinology 200, 117-123.

Geven, E.J., Nguyen, N.K., van den Boogaart, M., Spanings, F.A., Flik, G., Klaren, P.H., 2007. Comparative thyroidology: thyroid gland location and iodothyronine dynamics in Mozambique tilapia (*Oreochromis mossambicus* Peters) and common carp (*Cyprinus carpio* L.). Journal of Experimental Biology 210, 4005-4015.

Gilbert, L.I., Tata, J.R., Atkinson, B.G., 1996. Metamorphosis: postembryonic reprogramming of gene expression in amphibian and insect cells. Academic Press.

Gilbert, S.F., 2000. Early development and axis formation in amphibians, in: S.F. Gilbert (Ed.), Developmental biology, 6th ed. Sinauer Associates.

Gomes, A.S., Kamisaka, Y., Harboe, T., Power, D.M., Ronnestad, I., 2014b. Functional modifications associated with gastrointestinal tract organogenesis during metamorphosis in Atlantic halibut (*Hippoglossus hippoglossus*). BMC Development Biology 14, 11.

Gomez, D., Sunyer, J.O., Salinas, I., 2013. The mucosal immune system of fish: the evolution of tolerating commensals while fighting pathogens. Fish & shellfish immunology 35, 1729-1739.

Gorbman, A., Dickhoff, W.W., Vigna, S.R., Clark, N.B., Ralph, C.L., 1983. The Thyroid Gland. In: Gorbman, A., Dickhoff, W.W., Vigna, S.R., Clark, N.B., Ralph, C.L. (Eds.), Comparative Endocrinology. John Wiley and Sons Inc., New York, pp. 185–275.

Grijota-Martinez, C., Samarut, E., Scanlan, T.S., Morte, B., Bernal, J., 2011. In vivo activity of the thyroid hormone receptor beta- and alpha-selective agonists GC-24 and CO23 on rat liver, heart, and brain. Endocrinology 152, 1136-1142.

Grimaldi, A., Buisine, N., Miller, T., Shi, Y.B., Sachs, L.M., 2013. Mechanisms of thyroid hormone receptor action during development: lessons from amphibian studies. Biochimica et Biophysica Acta 1830, 3882-3892.

Gross, J.B., Borowsky, R., Tabin, C.J., 2009. A novel role for Mc1r in the parallel evolution of depigmentation in independent populations of the cavefish *Astyanax mexicanus*. PLoS Genetics 5, e1000326.

Guillot, R., Ceinos, R.M., Cal, R., Rotllant, J., Cerda-Reverter, J.M., 2012. Transient ectopic overexpression of agouti-signalling protein 1 (asip1) induces pigment anomalies in flatfish. PloS One 7, e48526.

Guo, C., Chen, X., Song, H., Maynard, M.A., Zhou, Y., Lobanov, A.V., Gladyshev, V.N., Ganis, J.J., Wiley, D., Jugo, R.H., Lee, N.Y., Castroneves, L.A., Zon, L.I., Scanlan, T.S., Feldman, H.A., Huang, S.A., 2014. Intrinsic expression of a multiexon type 3 deiodinase gene controls zebrafish embryo size. Endocrinology 155, 4069-4080.

Hachero-Cruzado, I., Ortiz-Delgado, J.B., Borrega, B., Herrera, M., Navas, J.I., Sarasquete, C., 2009. Larval organogenesis of flatfish brill *Scophthalmus rhombus* L: Histological and histochemical aspects. Aquaculture 286, 138-149.

Hall, J.A., Ribich, S., Christoffolete, M.A., Simovic, G., Correa-Medina, M., Patti, M.E., Bianco, A.C., 2010. Absence of thyroid hormone activation during development underlies a permanent defect in adaptive thermogenesis. Endocrinology 151, 4573-4582.

Hamre, K., Holen, E., Moren, M., 2007. Pigmentation and eye migration in Atlantic halibut (*Hippoglossus hippoglossus* L.) larvae: new findings and hypotheses. Aquaculture Nutrition 13, 65-80.

Harboe, T., Mangor-Jensen, A., Moren, M., Hamre, K., Rønnestad, I., 2009. Control of light condition affects the feeding regime and enables successful eye migration in Atlantic halibut juveniles. Aquaculture 290, 250-255.

Harris, J.E., Hunt, S., 1975. The fine structure of the epidermis of two species of salmonid fish, the Atlantic salmon (*Salmo salar* L.). and the brown trout (*Salmo trutta* L.). Cell and Tissue Research 163, 535-543.

Heijlen, M., Houbrechts, A.M., Bagci, E., Van Herck, S.L., Kersseboom, S., Esguerra, C.V., Blust, R., Visser, T.J., Knapen, D., Darras, V.M., 2014. Knockdown of type 3 iodothyronine deiodinase severely perturbs both embryonic and early larval development in zebrafish. Endocrinology 155, 1547-1559.

Helbing, C.C., Werry, K., Crump, D., Domanski, D., Veldhoen, N., Bailey, C.M., 2003. Expression Profiles of Novel Thyroid Hormone-Responsive Genes and Proteins in the Tail of *Xenopus laevis* Tadpoles Undergoing Precocious Metamorphosis. Molecular Endocrinology 17, 1395-1409.

Hernandez-Puga, G., Navarrete-Ramirez, P., Mendoza, A., Olvera, A., Villalobos, P., Orozco, A., 2016. 3,5-Diiodothyronine-mediated transrepression of the thyroid hormone receptor beta gene in tilapia. Insights on cross-talk between the thyroid hormone and cortisol signaling pathways. Molecular and Cellular Endocrinology 425, 103-110.

Hernandez, A., Fiering, S., Martinez, E., Galton, V.A., St Germain, D., 2002. The gene locus encoding iodothyronine deiodinase type 3 (Dio3) is imprinted in the fetus and expresses antisense transcripts. Endocrinology 143, 4483-4486.

Hernandez, A., Lyon, G.J., Schneider, M.J., St Germain, D.L., 1999. Isolation and characterization of the mouse gene for the type 3 iodothyronine deiodinase. Endocrinology 140, 124-130.

Hernandez, A., Martinez, M.E., Fiering, S., Galvon, V.A., St Germain, D., 2006. Type 3 deiodinase is critical for the maturation and function of the thyroid axis. The Journal of Clinical Investigation 116, 476-484.

Hernandez, A., Martinez, M.E., Liao, X.H., Van Sande, J., Refetoff, S., Galton, V.A., St Germain, D.L., 2007. Type 3 deiodinase deficiency results in functional abnormalities at multiple levels of the thyroid axis. Endocrinology 148, 5680-5687.

Heuer, H., 2007. The importance of thyroid hormone transporters for brain development and function. Best practice & research. Clinical endocrinology & metabolism 21, 265-276.

Heuer, H., Maier, M.K., Iden, S., Mittag, J., Friesema, E.C., Visser, T.J., Bauer, K., 2005. The monocarboxylate transporter 8 linked to human psychomotor retardation is highly expressed in thyroid hormone-sensitive neuron populations. Endocrinology 146, 1701-1706.

Hildahl, J., Power, D.M., Bjornsson, B.T., Einarsdottir, I.E., 2008. Involvement of growth hormone-insulin-like growth factor I system in cranial remodelling during halibut metamorphosis as indicated by tissue- and stage-specific receptor gene expression and the presence of growth hormone receptor protein. Cell and Tissue Research 332, 211-225.

Hildahl, J., Sweeney, G., Galay-Burgos, M., Einarsdottir, I.E., Bjornsson, B.T., 2007. Cloning of Atlantic halibut growth hormone receptor genes and quantitative gene expression during metamorphosis. General and Comparative Endocrinology 151, 143-152.

Hiroi, J., Kaneko, T., Seikai, T., Tanaka, M., 1998. Developmental Sequence of Chloride Cells in the Body Skin and Gills of Japanese Flounder (*Paralichthys olivaceus*) Larvae. Zoological Science 15, 455-460.

Hobbs, R.S., Fletcher, G.L., 2008. Tissue specific expression of antifreeze protein and growth hormone transgenes driven by the ocean pout (*Macrozoarces americanus*) antifreeze protein OP5a gene promoter in Atlantic salmon (*Salmo salar*). Transgenic Research 17, 33-45.

Horn, S., Heuer, H., 2010. Thyroid hormone action during brain development: more questions than answers. Molecular and Cellular Endocrinology 315, 19-26.

Houbrechts, A.M., Vergauwen, L., Bagci, E., Van Houcke, J., Heijlen, M., Kulemeka, B., Hyde, D.R., Knapen, D., Darras, V.M., 2016. Deiodinase knockdown affects zebrafish eye development at the level of gene expression, morphology and function. Molecular and Cellular Endocrinology 424, 81-93.

Huang, J.H., Lozano, J., Belles, X., 2013. Broad-complex functions in postembryonic development of the cockroach *Blattella germanica* shed new light on the evolution of insect metamorphosis. Biochimica et Biophysica Acta 1830, 2178-2187.

Huang, L., Schreiber, A.M., Soffientino, B., Bengtson, D.A., Specker, J.L., 1998. Metamorphosis of summer flounder (*Paralichthys dentatus*): thyroid status and the timing of gastric gland formation. The Journal of Experimental Zoology A 280, 413-420.

Hubbard, J.K., Uy, J.A., Hauber, M.E., Hoekstra, H.E., Safran, R.J., 2010. Vertebrate pigmentation: from underlying genes to adaptive function. Trends in Genetics 26, 231-239.

Hubmacher, D., Apte, S.S., 2013. The biology of the extracellular matrix: novel insights. Current Opinion in Rheumatology 25, 65-70.

Huggins, P., Johnson, C.K., Schoergendorfer, A., Putta, S., Bathke, A.C., Stromberg, A.J., Voss, S.R., 2012. Identification of differentially expressed thyroid hormone responsive genes from the brain of the Mexican Axolotl (*Ambystoma mexicanum*). Comparative biochemistry and physiology. Toxicology & Pharmacology : CBP 155, 128-135.

Hulbert, A.J., 2000. Thyroid hormones and their effects: a new perspective. Biological reviews of the Cambridge Philosophical Society 75, 519-631.

Hunn, J.B., Fromm, P.O., 1966. In vivo Uptake of Radioiodide by Rainbow Trout. Journal (Water Pollution Control Federation) 38, 1981-1985.

Hunt, G., Thody, A.J., 1995. Agouti protein can act independently of melanocyte-stimulating hormone to inhibit melanogenesis. The Journal of Endocrinology 147, R1-4.

Hwang, P.P., 1989. Distribution of chloride cells in teleost larvae. Journal of Morphology 200, 1-8.

Infante, C., Asensio, E., Canavate, J.P., Manchado, M., 2008. Molecular characterization and expression analysis of five different elongation factor 1 alpha genes in the flatfish Senegalese sole (*Solea senegalensis* Kaup): differential gene expression and thyroid hormones dependence during metamorphosis. BMC Molecular Biology 9, 19.

Infante, C., Manchado, M., Asensio, E., Canavate, J., 2007. Molecular characterization, gene expression and dependence on thyroid hormones of two type I keratin genes (sseKer1

and sseKer2) in the flatfish Senegalese sole (*Solea senegalensis* Kaup). BMC Developmental Biology 7, 118.

Inui, Y., Miwa, S., 1985. Thyroid hormone induces metamorphosis of flounder larvae. General and Comparative Endocrinology 60, 450-454.

Inui, Y., Yamano, K., Miwa, S., 1995. The role of thyroid hormone in tissue development in metamorphosing flounder. Aquaculture 135, 87-98.

Isojima, T., Makino, N., Takakusagi, M., Tagawa, M., 2013b. Progression of staining-type hypermelanosis on the blind side in normally metamorphosed juveniles and pigmentation progression in pseudoalbino juveniles of the Japanese flounder *Paralichthys olivaceus* using individual identification. Fish Sciences 79, 787–797.

Isojima, T., Tsuji, H., Masuda, T., Tagawa, M., 2013a. Formation process of staining-type hypermelanosis in Japanese flounder juveniles revealed by examination of chromatophores and scales. Fish Sciences 97.

Isorna, E., Obregon, M.J., Calvo, R.M., Vazquez, R., Pendon, C., Falcon, J., Munoz-Cueto, J.A., 2009. Iodothyronine deiodinases and thyroid hormone receptors regulation during flatfish (*Solea senegalensis*) metamorphosis. Journal of experimental zoology. Part B, Molecular and Developmental Evolution 312B, 231-246.

Itoh, K., Watanabe, K., Wu, X., Suzuki, T., 2010. Three members of the iodothyronine deiodinase family, dio1, dio2 and dio3, are expressed in spatially and temporally specific patterns during metamorphosis of the flounder, *Paralichthys olivaceus*. Zoology Sciences 27, 574-580.

Jeong, G.M., 2008. A study on the epidermal structure and mucosubstance histochemistry of spotty belly, devil stinger, stone fish, cubed Snailfish, and Japanese bluefish. Animal Cells and Systems, 85-91.

Johnson, K.M., Lema, S.C., 2011. Tissue-specific thyroid hormone regulation of gene transcripts encoding iodothyronine deiodinases and thyroid hormone receptors in striped parrotfish (*Scarus iseri*). General and Comparative Endocrinology 172, 505-517.

Kalogianni, E., Alexis, M., Tsangaris, C., Abraham, M., Wendelaar Bonga, S.E., Iger, Y., van Ham, E.H., Stoumboudi, M.T., 2011. Cellular responses in the skin of the gilthead sea bream Sparus aurata L. and the sea bass *Dicentrarchus labrax* (L.) exposed to high ammonia. Journal of Fish Biology 78, 1152-1169.

Katoh, F., Shimizu, A., Uchida, K., Kaneko, T., 2000. Shift of Chloride Cell Distribution during Early Life Stages in Seawater-Adapted Killifish, Fundulus heteroclitus. Zoological science 17, 11-18.

Katoh, M., Katoh, M., 2007. WNT signaling pathway and stem cell signaling network. Clinical cancer research : an official journal of the American Association for Cancer Research 13, 4042-4045.

Kawakami, Y., Nozaki, J., Seoka, M., Kumai, H., Ohta, H., 2008. Characterization of thyroid hormones and thyroid hormone receptors during the early development of Pacific bluefin tuna (*Thunnus orientalis*). General and Comparative Endocrinology 155, 597-606.

Keefe, M., Able, K.W., 1993. Patterns of metamorphosis in summer flounder, *Paralichthys dentatus*. Journal of Fish Biology 42, 713-728.

Kelsh, R.N., 2004. Genetics and evolution of pigment patterns in fish. Pigment cell research / sponsored by the European Society for Pigment Cell Research and the International Pigment Cell Society 17, 326-336.

Kersseboom, S., Visser, T.J., 2011. MCT8: from gene to disease and therapeutic approach. Annales d'endocrinologie 72, 77-81.

Kim, D.K., Kanai, Y., Chairoungdua, A., Matsuo, H., Cha, S.H., Endou, H., 2001. Expression cloning of a Na+-independent aromatic amino acid transporter with structural similarity to H+/monocarboxylate transporters. The Journal of Biological Chemistry 276, 17221-17228.

Klaren, P.H., Geven, E.J., Nagelkerke, A., Flik, G., 2012. Kinetics and thiol requirements of iodothyronine 5'-deiodination are tissue-specific in common carp (*Cyprinus carpio* L.). Biochemistry and Molecular Biology of Comparative Biochemistry and Physiology 161, 275-282.

Klaren, P.H., Haasdijk, R., Metz, J.R., Nitsch, L.M., Darras, V.M., Van der Geyten, S., Flik, G., 2005. Characterization of an iodothyronine 5'-deiodinase in gilthead seabream (*Sparus auratus*) that is inhibited by dithiothreitol. Endocrinology 146, 5621-5630.

Klaren, P.H.M., Wunderink, Y.S., Yúfera, M., Mancera, J.M., Flik, G., 2008. The thyroid gland and thyroid hormones in Senegalese sole (*Solea senegalensis*) during early development and metamorphosis. General and Comparative Endocrinology 155, 686-694.

Klovins, J., Schioth, H.B., 2005. Agouti-related proteins (AGRPs) and agouti-signaling peptide (ASIP) in fish and chicken. Annals of the New York Academy of Sciences 1040, 363-367.

Köhrle, J., 1999. Local activation and inactivation of thyroid hormones: the deiodinase family. Molecular and Cellular Endocrinology 151, 103-119.

Kondo, S., Iwashita, M., Yamaguchi, M., 2009. How animals get their skin patterns: fish pigment pattern as a live Turing wave. The International Journal of Developmental Biology 53, 851-856.

Koster, M.I., Dai, D., Marinari, B., Sano, Y., Costanzo, A., Karin, M., Roop, D.R., 2007. p63 induces key target genes required for epidermal morphogenesis. Proceedings of the National Academy of Sciences of the United States of America 104, 3255-3260.

Labunskyy, V.M., Hatfield, D.L., Gladyshev, V.N., 2014. Selenoproteins: molecular pathways and physiological roles. Physiological Reviews 94, 739-777.

Larsen, D.A., Dickey, J.T., Dickhoff, W.W., 1997. Quantification of Salmon α- and Thyrotropin (TSH) β-Subunit Messenger RNA by an RNase Protection Assay: Regulation by Thyroid Hormones. General and Comparative Endocrinology 107, 98-108.

Laudet, V., 2011. The Origins and Evolution of Vertebrate Metamorphosis. Current Biology 21, R726-R737.

Lazar, M.A., Berrodin, T.J., Harding, H.P., 1991. Differential DNA binding by monomeric, homodimeric, and potentially heteromeric forms of the thyroid hormone receptor. Molecular and Cellular Biology 11, 5005-5015.

Le Guellec, D., Morvan-Dubois, G., Sire, J.Y., 2004. Skin development in bony fish with particular emphasis on collagen deposition in the dermis of the zebrafish (*Danio rerio*). The International Journal of Developmental Biology 48, 217-231.

Leatherland, J.F., Farbridge, K.J., 1992. Chronic fasting reduces the response of the thyroid to growth hormone and TSH, and alters the growth hormone-related changes in hepatic 5′-monodeiodinase activity in rainbow trout, *Oncorhynchus mykiss*. General and Comparative Endocrinology 87, 342-353.

Leonard, J.L., Simpson, G., Leonard, D.M., 2005. Characterization of the protein dimerization domain responsible for assembly of functional selenodeiodinases. The Journal of Biological Chemistry 280, 11093-11100.

Li, N., Jiang, Y., Shan, Z., Teng, W., 2012. Prolonged high iodine intake is associated with inhibition of type 2 deiodinase activity in pituitary and elevation of serum thyrotropin levels. The British Journal of Nutrition 107, 674-682.

Lin, J.Y., Fisher, D.E., 2007. Melanocyte biology and skin pigmentation. Nature 445, 843-850.

Liu, Q., Dou, S., Wang, G., Li, Z., Feng, Y., 2008. Evolution and functional divergence of monocarboxylate transporter genes in vertebrates. Gene 423, 14-22.

Liu, Y.-W., Lo, L.-J., Chan, W.-K., 2000. Temporal expression and T3 induction of thyroid hormone receptors α1 and β1 during early embryonic and larval development in zebrafish, *Danio rerio*. Molecular and Cellular Endocrinology 159, 187-195.

Long, J., Hale, M., McHenry, M., Westneat, M., 1996. Functions of fish skin: flexural stiffness and steady swimming of longnose gar, *Lepisosteus osseus*. The Journal of Experimental Biology 199, 2139-2151.

Long, Y., Li, Q., Zhou, B., Song, G., Li, T., Cui, Z., 2013. De novo assembly of mud loach (*Misgurnus anguillicaudatus*) skin transcriptome to identify putative genes involved in immunity and epidermal mucus secretion. PloS One 8, e56998.

Lorgen, M., Casadei, E., Krol, E., Douglas, A., Birnie, M.J., Ebbesson, L.O., Nilsen, T.O., Jordan, W.C., Jorgensen, E.H., Dardente, H., Hazlerigg, D.G., Martin, S.A., 2015. Functional divergence of type 2 deiodinase paralogs in the Atlantic salmon. Current Biology : CB 25, 936-941.

Luizi, F.S., Gara, B., Shields, R.J., Bromage, N.R., 1999. Further description of the development of the digestive organs in Atlantic halibut (*Hippoglossus hippoglossus*) larvae, with notes on differential absorption of copepod and Artemia prey. Aquaculture 176, 101-116.

Macchia, P.E., Takeuchi, Y., Kawai, T., Cua, K., Gauthier, K., Chassande, O., Seo, H., Hayashi, Y., Samarut, J., Murata, Y., Weiss, R.E., Refetoff, S., 2001. Increased sensitivity to thyroid hormone in mice with complete deficiency of thyroid hormone receptor alpha. Proceedings of the National Academy of Sciences of the United States of America 98, 349-354.

MacDonald, B.T., Tamai, K., He, X., 2009. Wnt/beta-catenin signaling: components, mechanisms, and diseases. Developmental Cell 17, 9-26.

MacKenzie, D.S., Jones, R.A., Miller, T.C., 2009. Thyrotropin in teleost fish. General and Comparative Endocrinology 161, 83-89.

Madison, K.C., 2003. Barrier function of the skin: "la raison d'etre" of the epidermis. The Journal of Investigative Dermatology 121, 231-241.

Manchado, M., Infante, C., Asensio, E., Canavate, J.P., 2007. Differential gene expression and dependence on thyroid hormones of two glyceraldehyde-3-phosphate dehydrogenases in the flatfish Senegalese sole (*Solea senegalensis* Kaup). Gene 400, 1-8.

Manchado, M., Infante, C., Asensio, E., Planas, J.V., Cañavate, J.P., 2008. Thyroid hormones down-regulate thyrotropin β subunit and thyroglobulin during metamorphosis in the flatfish Senegalese sole (*Solea senegalensis* Kaup). General and Comparative Endocrinology 155, 447-455.

Manchado, M., Infante, C., Rebordinos, L., Cañavate, J.P., 2009. Molecular characterization, gene expression and transcriptional regulation of thyroid hormone receptors in Senegalese sole. General and Comparative Endocrinology 160, 139-147.

Manchado, M., Salas-Leiton, E., Infante, C., Ponce, M., Asensio, E., Crespo, A., Zuasti, E., Canavate, J.P., 2008c. Molecular characterization, gene expression and transcriptional regulation of cytosolic HSP90 genes in the flatfish Senegalese sole (*Solea senegalensis* Kaup). Gene 416, 77-84.

Marchand, O., Duffraisse, M., Triqueneaux, G., Safi, R., Laudet, V., 2004. Molecular cloning and developmental expression patterns of thyroid hormone receptors and T3 target genes in the turbot (*Scophtalmus maximus*) during post-embryonic development. General and Comparative Endocrinology 135, 345-357.

Marsh-Armstrong, N., Huang, H., Remo, B.F., Liu, T.T., Brown, D.D., 1999. Asymmetric growth and development of the *Xenopus laevis* retina during metamorphosis is controlled by type III deiodinase. Neuron 24, 871-878.

Marshall, W.S., 2002. $Na^{(+)}$, $Cl^{(-)}$, $Ca^{(2+)}$ and $Zn^{(2+)}$ transport by fish gills: retrospective review and prospective synthesis. The Journal of Experimental Zoology 293, 264-283.

Marshall, W.S., Cozzi, R.R., Pelis, R.M., McCormick, S.D., 2005. Cortisol receptor blockade and seawater adaptation in the euryhaline teleost *Fundulus heteroclitus*. Journal of experimental zoology. Part A, Comparative experimental biology 303, 132-142.

Martinez, G.M., Bolker, J.A., 2003. Embryonic and larval staging of summer flounder (*Paralichthys dentatus*). Journal of Morphology 255, 162-176.

Matsumoto, J., Seikai, T., 1992. Asymmetric pigmentation and pigment disorders in pleuronectiformes (flounders). Pigment cell research / sponsored by the European Society for Pigment Cell Research and the International Pigment Cell Society Suppl 2, 275-282.

Mayerl, S., Muller, J., Bauer, R., Richert, S., Kassmann, C.M., Darras, V.M., Buder, K., Boelen, A., Visser, T.J., Heuer, H., 2014. Transporters MCT8 and OATP1C1 maintain murine brain thyroid hormone homeostasis. The Journal of Clinical Investigation 124, 1987-1999.

McCormick, S.D., Regish, A., O'Dea, M.F., Shrimpton, J.M., 2008. Are we missing a mineralocorticoid in teleost fish? Effects of cortisol, deoxycorticosterone and aldosterone on osmoregulation, gill Na^+,K^+-ATPase activity and isoform mRNA levels in Atlantic salmon. General and Comparative Endocrinology 157, 35-40.

McGregor, L., Makela, V., Darling, S.M., Vrontou, S., Chalepakis, G., Roberts, C., Smart, N., Rutland, P., Prescott, N., Hopkins, J., Bentley, E., Shaw, A., Roberts, E., Mueller, R., Jadeja, S., Philip, N., Nelson, J., Francannet, C., Perez-Aytes, A., Megarbane, A., Kerr, B., Wainwright, B., Woolf, A.S., Winter, R.M., Scambler, P.J., 2003. Fraser syndrome and mouse blebbed phenotype caused by mutations in FRAS1/Fras1 encoding a putative extracellular matrix protein. Nature genetics 34, 203-208.

McMenamin, S.K., Parichy, D.M., 2013a. Chapter Five – Metamorphosis in Teleosts, in: S. Yun-Bo (Ed.), Current Topics in Developmental Biology. Academic Press, 127-165.

Micallef, G., Bickerdike, R., Reiff, C., Fernandes, J.M., Bowman, A.S., Martin, S.A., 2012. Exploring the transcriptome of Atlantic salmon (*Salmo salar*) skin, a major defense organ. Marine Biotechnology 14, 559-569.

Miwa, S., Tagawa, M., Inui, Y., Hirano, T., 1988. Thyroxine surge in metamorphosing flounder larvae. General and Comparative Endocrinology 70, 158-163.

Miwa, S., Inui, Y., 1991. Thyroid hormone stimulates the shift of erythrocyte populations during metamorphosis of the flounder. Journal of Experimental Zoology 259, 222-228.

Miwa, S., Yamano, K., Inui, Y., 1992. Thyroid hormone stimulates gastric development in flounder larvae during metamorphosis. Journal of Experimental Zoology 261, 424-430.

Mol, K.A., Van Der Geyten, S., Darras, V.M., Visser, T.J., Kuhn, E.R., 1997. Characterization of iodothyronine outer ring and inner ring deiodinase activities in the blue tilapia, *Oreochromis aureus*. Endocrinology 138, 1787-1793.

Mol, K.A., Geyten, V., Burel, C., Kühn, E.R., Boujard, T., Darras, V.M., 1998. Comparative study of iodothyronine outer ring and inner ring deiodinase activities in five teleostean fishes. Fish Physiology and Biochemistry 18, 253-266.

Mommsen, T.P., Vijayan, M.M., Moon, T.W., 1999. Cortisol in teleosts: dynamics, mechanism of action, and metabolic regulation. Reviews in Fish Biology and Fisheries 9.

Moniaux, N., Escande, F., Porchet, N., Aubert, J.P., Batra, S.K., 2001. Structural organization and classification of the human mucin genes. Frontiers in Bioscience : A Journal and Virtual Library 6, D1192-1206.

Moreno, M., de Lange, P., Lombardi, A., Silvestri, E., Lanni, A., Goglia, F., 2008. Metabolic effects of thyroid hormone derivatives. Thyroid : official journal of the American Thyroid Association 18, 239-253.

Morvan-Dubois, G., Demeneix, B.A., Sachs, L.M., 2008. *Xenopus laevis* as a model for studying thyroid hormone signalling: from development to metamorphosis. Molecular and Cellular Endocrinology 293, 71-79.

Moyano, F.J., Díaz, M., Alarcón, F.J., Sarasquete, M.C., 1996. Characterization of digestive enzyme activity during larval development of gilthead seabream (*Sparus aurata*). Fish Physiology and Biochemistry 15, 121-130.

Mukhi, S., Cai, L., Brown, D.D., 2010. Gene switching at *Xenopus laevis* metamorphosis. Developmental Biology 338, 117-126.

Muller, J., Mayerl, S., Visser, T.J., Darras, V.M., Boelen, A., Frappart, L., Mariotta, L., Verrey, F., Heuer, H., 2014. Tissue-specific alterations in thyroid hormone homeostasis in combined Mct10 and Mct8 deficiency. Endocrinology 155, 315-325.

Murray, H.M., Gallant, J.W., Johnson, S.C., Douglas, S.E., 2006. Cloning and expression analysis of three digestive enzymes from Atlantic halibut (*Hippoglossus hippoglossus*) during early development: Predicting gastrointestinal functionality. Aquaculture 252, 394-408.

Murray, H.M., Wright, G.M., Goff, G.P., 1994. A comparative histological and histochemical study of the stomach from three species of pleuronectid, the Atlantic halibut, *Hippoglossus hippoglossus*, the yellowtail flounder, *Pleuronectes ferruginea*, and the winter flounder, *Pleuronectes americanus*. Canadian Journal of Zoology 72, 1199-1210.

Muzzio, A.M., Noyes, P.D., Stapleton, H.M., Lema, S.C., 2014. Tissue distribution and thyroid hormone effects on mRNA abundance for membrane transporters Mct8, Mct10, and organic anion-transporting polypeptides (Oatps) in a teleost fish. Comparative Biochemistry and Physiology. Part A, Molecular & Integrative Physiology 167, 77-89.

Nakamura, M., Ohki, S., Suzuki, A., Sakai, K., 2011. Coral Larvae under Ocean Acidification: Survival, Metabolism, and Metamorphosis. PLoS One 6, e14521.

Nakamura, M., Seikai, T., Aritaki, M., Masuda, R., Tanaka, M., Tagawa, M., 2010. Dual appearance of xanthophores, and ontogenetic changes in other pigment cells during early development of Japanese flounder *Paralichthys olivaceus*. Fish Sciences 76.

Ng, L., Goodyear, R.J., Woods, C.A., Schneider, M.J., Diamond, E., Richardson, G.P., Kelley, M.W., Germain, D.L., Galton, V.A., Forrest, D., 2004. Hearing loss and retarded cochlear development in mice lacking type 2 iodothyronine deiodinase. Proceedings of the National Academy of Sciences of the United States of America 101, 3474-3479.

Ng, L., Lyubarsky, A., Nikonov, S.S., Ma, M., Srinivas, M., Kefas, B., St Germain, D.L., Hernandez, A., Pugh, E.N., Jr., Forrest, D., 2010. Type 3 deiodinase, a thyroid-hormone-inactivating enzyme, controls survival and maturation of cone photoreceptors. The Journal of neuroscience : the official journal of the Society for Neuroscience 30, 3347-3357.

Nishimura, M., Naito, S., 2008. Tissue-specific mRNA expression profiles of human solute carrier transporter superfamilies. Drug Metabolism and Pharmacokinetics 23, 22-44.

Noyes, P.D., Lema, S.C., Macaulay, L.J., Douglas, N.K., Stapleton, H.M., 2013. Low level exposure to the flame retardant BDE-209 reduces thyroid hormone levels and disrupts thyroid signaling in fathead minnows. Environmental Science and Technology 47, 10012-10021.

O'Shea, P.J., Bassett, J.H., Sriskantharajah, S., Ying, H., Cheng, S.Y., Williams, G.R., 2005. Contrasting skeletal phenotypes in mice with an identical mutation targeted to thyroid hormone receptor alpha1 or beta. Molecular Endocrinology 19, 3045-3059.

O'Shea, P.J., Harvey, C.B., Suzuki, H., Kaneshige, M., Kaneshige, K., Cheng, S.Y., Williams, G.R., 2003. A thyrotoxic skeletal phenotype of advanced bone formation in mice with resistance to thyroid hormone. Molecular Endocrinology 17, 1410-1424.

Oetting, A., Yen, P.M., 2007. New insights into thyroid hormone action. Best Practice & Research Clinical Endocrinology and Metabolism 21, 193-208.

Okada, N., Takagi, Y., Seikai, T., Tanaka, M., Tagawa, M., 2001. Asymmetrical development of bones and soft tissues during eye migration of metamorphosing Japanese flounder, *Paralichthys olivaceus*. Cell Tissue Research 304, 59-66.

Okada, N., Takagi, Y., Tanaka, M., Tagawa, M., 2003. Fine structure of soft and hard tissues involved in eye migration in metamorphosing Japanese flounder (*Paralichthys*

olivaceus). The Anatomical Record Part A: Discoveries in Molecular, Cellular, and Evolutionary Biology 273A, 663-668.

Okada, N., Morita, T., Tanaka, M., Tagawa, M., 2005. Thyroid hormone deficiency in abnormal larvae of the Japanese flounder *Paralichthys olivaceus*, Fisheries Science 71, 107-114.

Olaso, E., Lin, H.C., Wang, L.H., Friedman, S.L., 2011. Impaired dermal wound healing in discoidin domain receptor 2-deficient mice associated with defective extracellular matrix remodelling. Fibrogenesis & Tissue Repair 4-5.

Ordoñez, G., Hillier, L., Warren, W., Grützner, F., López-Otín, C., Puente, X., 2008. Loss of genes implicated in gastric function during platypus evolution. Genome Biology 9, 1-11.

Orozco, A., Jeziorski, M.C., Linser, P.J., Greenberg, R.M., Valverde, R.C., 2002. Cloning of the gene and complete cDNA encoding a type 2 deiodinase from *Fundulus heteroclitus*. General and Comparative Endocrinology 128, 162-167.

Orozco, A., Navarrete-Ramirez, P., Olvera, A., Garcia, G.C., 2014. 3,5-Diiodothyronine (T2) is on a role. A new hormone in search of recognition. General and Comparative Endocrinology 203, 174-180.

Orozco, A., Valverde, R.C., 2005. Thyroid hormone deiodination in fish. Thyroid : official journal of the American Thyroid Association 15, 799-813.

Orozco, A., Valverde, R.C., Olvera, A., Garcia, G.C., 2012. Iodothyronine deiodinases: a functional and evolutionary perspective. The Journal of Endocrinology 215, 207-219.

Orozco, A., Villalobos, P., Jeziorski, M.C., Valverde, R.C., 2003. The liver of *Fundulus heteroclitus* expresses deiodinase type 1 mRNA. General and Comparative Endocrinology 130, 84-91.

Ottensen, O.H., Olafsen, J.A., 1997. Ontogenetic development and composition of the mucous cells and the occurrence of saccular cells in the epidermis of Atlantic halibut. Journal of Fish Biology 50, 620–633.

Ottesen, O.H., Strand, H.K., 1996. Growth, development, and skin abnormalities of halibut (*Hippoglossus hippoglossus* L) juveniles kept on different bottom substrates. Aquaculture 146, 17-25.

Page, R.B., Monaghan, J.R., Samuels, A.K., Smith, J.J., Beachy, C.K., Voss, S.R., 2007. Microarray analysis identifies keratin loci as sensitive biomarkers for thyroid hormone disruption in the salamander *Ambystoma mexicanum*. Comparative biochemistry and physiology. Toxicology and Pharmacology : CBP 145, 15-27.

Page, R.B., Monaghan, J.R., Walker, J.A., Voss, S.R., 2009. A model of transcriptional and morphological changes during thyroid hormone-induced metamorphosis of the axolotl. General and Comparative Endocrinology 162, 219-232.

Page, R.B., Voss, S.R., Samuels, A.K., Smith, J.J., Putta, S., Beachy, C.K., 2008. Effect of thyroid hormone concentration on the transcriptional response underlying induced metamorphosis in the Mexican axolotl (*Ambystoma*). BMC Genomics 9, 78.

Paquette, M.A., Dong, H., Gagne, R., Williams, A., Malowany, M., Wade, M.G., Yauk, C.L., 2011. Thyroid hormone-regulated gene expression in juvenile mouse liver: identification of thyroid response elements using microarray profiling and in silico analyses. BMC Genomics 12, 634.

Parichy, D.M., 2003. Pigment patterns: fish in stripes and spots. Current biology : CB 13, R947-950.

Parichy, D.M., 2006. Evolution of danio pigment pattern development. Heredity 97, 200-210.

Parichy, D.M., Johnson, S.L., 2001. Zebrafish hybrids suggest genetic mechanisms for pigment pattern diversification in Danio. Development Genes and Evolution 211, 319-328.

Paris, M., Laudet, V., 2008. The history of a developmental stage: metamorphosis in chordates. Genesis 46, 657-672.

Pascual, A., Aranda, A., 2013. Thyroid hormone receptors, cell growth and differentiation. Biochimica et Biophysica Acta (BBA) - General Subjects 1830, 3908-3916.

Peeters, R.P., Hernandez, A., Ng, L., Ma, M., Sharlin, D.S., Pandey, M., Simonds, W.F., St Germain, D.L., Forrest, D., 2013. Cerebellar abnormalities in mice lacking type 3 deiodinase and partial reversal of phenotype by deletion of thyroid hormone receptor alpha1. Endocrinology 154, 550-561.

Pérez-Sánchez, J., Estensoro, I., Redondo, M.J., Calduch-Giner, J.A., Kaushik, S., Sitja-Bobadilla, A., 2013. Mucins as diagnostic and prognostic biomarkers in a fish-parasite model: transcriptional and functional analysis. PloS One 8, e65457.

Perez-Vilar, J., Hill, R.L., 1999. The structure and assembly of secreted mucins. The Journal of Biological Chemistry 274, 31751-31754.

Picard-Aitken, M., Fournier, H., Pariseau, R., Marcogliese, D.J., Cyr, D.G., 2007. Thyroid disruption in walleye (*Sander vitreus*) exposed to environmental contaminants: cloning and use of iodothyronine deiodinases as molecular biomarkers. Aquatic Toxicology 83, 200-211.

Pinto, P.I.S., Guerreiro, E.M., Power, D.M., 2013. Triclosan interferes with the thyroid axis in the zebrafish (*Danio rerio*). Toxicology Research 2, 60-69.

Pisam, M., Rambourg, A., 1991. Mitochondria-rich cells in the gill epithelium of teleost fishes: an ultrastructural approach. International Review of Cytology 130, 191-232.

Pittman, K., Skiftesvik, A.B., Berg, L., 1990. Morphological and behavioural development of halibut, *Hippoglossus hippoglossus* (L.) larvae. Journal of Fish Biology 37, 455-472.

Pol, C.J., Muller, A., Simonides, W.S., 2010. Cardiomyocyte-specific inactivation of thyroid hormone in pathologic ventricular hypertrophy: an adaptative response or part of the problem? Heart Failure Reviews 15, 133-142.

Power, D.M., Einarsdóttir, I.E., Pittman, K., Sweeney, G.E., Hildahl, J., Campinho, M.A., Silva, N., Sæle, Ø., Galay-Burgos, M., Sweeney, G.E., Smáradóttir, H., Björnsson, B.T., 2008. The Molecular and Endocrine Basis of Flatfish Metamorphosis. Reviews in Fisheries Science 16, 95-111.

Power, D.M., Elias, N.P., Richardson, S.J., Mendes, J., Soares, C.M., Santos, C.R., 2000. Evolution of the thyroid hormone-binding protein, transthyretin. General and Comparative Endocrinology 119, 241-255.

Power, D.M., Llewellyn, L., Faustino, M., Nowell, M.A., Björnsson, B.T., Einarsdottir, I.E., Canario, A.V.M., Sweeney, G.E., 2001. Thyroid hormones in growth and development of fish. Comparative Biochemistry and Physiology Part C: Toxicology & Pharmacology 130, 447-459.

Pradet-Balade, B., Burel, C., Dufour, S., Boujard, T., Kaushik, S.J., Quérat, B., Boeuf, G., 1999. Thyroid hormones down-regulate thyrotropin β mRNA level in vivo in the turbot (*Psetta maxima*). Fish Physiology and Biochemistry 20, 193-199.

Pradet-Balade, B., Schmitz, M., Salmon, C., Dufour, S., Quérat, B., 1997. Down-Regulation of TSH Subunit mRNA Levels by Thyroid Hormones in the European Eel. General and Comparative Endocrinology 108, 191-198.

Preau, L., Fini, J.B., Morvan-Dubois, G., Demeneix, B., 2015. Thyroid hormone signaling during early neurogenesis and its significance as a vulnerable window for endocrine disruption. Biochimica and Biophysica Acta 1849, 112-121.

Proksch, E., Brandner, J.M., Jensen, J.M., 2008. The skin: an indispensable barrier. Experimental Dermatology 17, 1063-1072.

Quignodon, L., Legrand, C., Allioli, N., Guadano-Ferraz, A., Bernal, J., Samarut, J., Flamant, F., 2004. Thyroid hormone signaling is highly heterogeneous during pre- and postnatal brain development. Journal of Molecular Endocrinology 33, 467-476.

Rai, A.K., Srivastava, N., Kumari, U., Mittal, S., Mittal, A.K., 2012. Histochemical analysis of glycoproteins in the secretory cells in the epidermis of the head skin of Indian Major Carp, *Labeo rohita*. Tissue & Cell 44, 409-417.

Rakers, S., Gebert, M., Uppalapati, S., Meyer, W., Maderson, P., Sell, A.F., Kruse, C., Paus, R., 2010. 'Fish matters': the relevance of fish skin biology to investigative dermatology. Experimental Dermatology 19, 313-324.

Ribeiro, L., Sarasquete, C., Dinis, M.T., 1999. Histological and histochemical development of the digestive system of *Solea senegalensis* (Kaup, 1858) larvae. Aquaculture 171, 293-308.

Richardson, J., Lundegaard, P.R., Reynolds, N.L., Dorin, J.R., Porteous, D.J., Jackson, I.J., Patton, E.E., 2008. mc1r Pathway regulation of zebrafish melanosome dispersion. Zebrafish 5, 289-295.

Roberts, R.J., Bell, M., Young, H., 1973. Studies on the skin of plaice (*Pleuronectes platessa* L.). II. The development of larval plaice skin. Journal of Fish Biology 5, 103-108.

Rose, M.C., Voynow, J.A., 2006. Respiratory tract mucin genes and mucin glycoproteins in health and disease. Physiological reviews 86, 245-278.

Roy, G., Mugesh, G., 2008. Selenium analogues of antithyroid drugs - recent developments. Chemistry & Biodiversity 5, 414-439.

Rubio, M., de Horna, A., Belles, X., 2012. MicroRNAs in metamorphic and non-metamorphic transitions in hemimetabolan insect metamorphosis. BMC Genomics 13, 386.

Sæle, Ø., Solbakken, J.S., Watanabe, K., Hamre, K., Power, D., Pittman, K., 2004. Staging of Atlantic halibut (*Hippoglossus hippoglossus* L.) from first feeding through metamorphosis, including cranial ossification independent of eye migration. Aquaculture 239, 445-465.

Saele, O., Silva, N., Pittman, K., 2006a. Post-embryonic remodelling of neurocranial elements: a comparative study of normal versus abnormal eye migration in a flatfish, the Atlantic halibut. Journal of Anatomy 209, 31-41.

Saele, O., Smaradottir, H., Pittman, K., 2006b. Twisted story of eye migration in flatfish. Journal of Morphology 267, 730-738.

Salvatore, D., Low, S.C., Berry, M., Maia, A.L., Harney, J.W., Croteau, W., St Germain, D.L., Larsen, P.R., 1995. Type 3 lodothyronine deiodinase: cloning, in vitro expression, and functional analysis of the placental selenoenzyme. The Journal of Clinical Investigation 96, 2421-2430.

Sambroni, E., Gutieres, S., Cauty, C., Guiguen, Y., Breton, B., Lareyre, J.J., 2001. Type II iodothyronine deiodinase is preferentially expressed in rainbow trout (*Oncorhynchus mykiss*) liver and gonads. Molecular Reproduction and Development 60, 338-350.

Sanders, J.P., Van der Geyten, S., Kaptein, E., Darras, V.M., Kuhn, E.R., Leonard, J.L., Visser, T.J., 1997. Characterization of a propylthiouracil-insensitive type I iodothyronine deiodinase. Endocrinology 138, 5153-5160.

Sanders, J.P., Van der Geyten, S., Kaptein, E., Darras, V.M., Kuhn, E.R., Leonard, J.L., Visser, T.J., 1999. Cloning and characterization of type III iodothyronine deiodinase from the fish *Oreochromis niloticus*. Endocrinology 140, 3666-3673.

Sarasquete, C., Gonzalez de Canales, M.L., Arellano, J., Munoz Cueto, J.A., Ribeiro, L., Dinis, M.T., 1998. Histochemical study of skin and gills of Senegal sole, *Solea senegalensis* larvae and adults. Histology and Histopathology 13, 727-735.

Schallreuter, K.U., Kothari, S., Chavan, B., Spencer, J.D., 2008. Regulation of melanogenesis--controversies and new concepts. Experimental Dermatology 17, 395-404.

Schneider, M.J., Fiering, S.N., Thai, B., Wu, S.Y., St Germain, E., Parlow, A.F., St Germain, D.L., Galton, V.A., 2006. Targeted disruption of the type 1 selenodeiodinase gene (Dio1) results in marked changes in thyroid hormone economy in mice. Endocrinology 147, 580-589.

Schreiber, A.M., 2001. Metamorphosis and early larval development of the flatfishes (Pleuronectiformes): an osmoregulatory perspective. Comparative Biochemistry and Physiology. Part B, Biochemistry and Molecular Biology 129, 587-595.

Schreiber, A.M., 2006. Asymmetric craniofacial remodelling and lateralized behavior in larval flatfish. The Journal of Experimental Biology 209, 610-621.

Schreiber, A.M., Specker, J.L., 1998. Metamorphosis in the summer flounder (*Paralichthys dentatus*): stage-specific developmental response to altered thyroid status. General and Comparative Endocrinology 111, 156-166.

Schreiber, A.M., Specker, J.L., 2000. Metamorphosis in the Summer Flounder, *Paralichthys dentatus*: Thyroidal Status Influences Gill Mitochondria-Rich Cells. General and Comparative Endocrinology 117, 238-250.

Schreiber, A.M., Wang, X., Tan, Y., Sievers, Q., Sievers, B., Lee, M., Burrall, K., 2010. Thyroid hormone mediates otolith growth and development during flatfish metamorphosis. General and Comparative Endocrinology 169, 130-137.

Schwartz, C.E., May, M.M., Carpenter, N.J., Rogers, R.C., Martin, J., Bialer, M.G., Ward, J., Sanabria, J., Marsa, S., Lewis, J.A., Echeverri, R., Lubs, H.A., Voeller, K., Simensen, R.J., Stevenson, R.E., 2005. Allan-Herndon-Dudley syndrome and the monocarboxylate transporter 8 (MCT8) gene. American Journal of Human Genetics 77, 41-53.

Schweizer, U., Kohrle, J., 2013. Function of thyroid hormone transporters in the central nervous system. Biochim Biophys Acta 1830, 3965-3973.

Schweizer, U., Steegborn, C., 2015. New insights into the structure and mechanism of iodothyronine deiodinases. Journal of Molecular Endocrinology 55, R37-R52.

Scott, G.R., Keir, K.R., Schulte, P.M., 2005. Effects of spironolactone and RU486 on gene expression and cell proliferation after freshwater transfer in the euryhaline killifish. Journal of Comparative Physiology. B, Biochemical, Systemic, and Environmental Physiology 175, 499-510.

Seikai, T., 1992. Process of Pigment Cell Differentiation in Skin on the Left and Right Sides of the Japanese Flounder, *Paralichthys olivaceus*, during Metamorphosis. Japanese Journal of Ichthyology 39, 85-92.

Seikai, T., Matsumoto, J., Shimozaki, M., Oikawa, A., Akiyama, T., 1987. An association of melanophores appearing at metamorphosis as vehicles of asymmetric skin color formation with pigment anomalies developed under hatchery conditions in the Japanese flounder, *Paralichthys olivaceus*. Pigment cell research / sponsored by the European Society for Pigment Cell Research and the International Pigment Cell Society 1, 143-151.

Senese, R., Cioffi, F., de Lange, P., Goglia, F., Lanni, A., 2014. Thyroid: biological actions of 'nonclassical' thyroid hormones. The Journal of Endocrinology 221, R1-12.

Shephard, K.L., 1994. Functions for fish mucus. Reviews in Fish Biology and Fisheries 4, 401-429.

Shi, Y.B., Wong, J., Puzianowska-Kuznicka, M., Stolow, M.A., 1996. Tadpole competence and tissue-specific temporal regulation of amphibian metamorphosis: roles of thyroid hormone and its receptors. BioEssays : news and reviews in molecular, cellular and developmental biology 18, 391-399.

Short, K., Wiradjaja, F., Smyth, I., 2007. Let's stick together: the role of the Fras1 and Frem proteins in epidermal adhesion. International Union of Biochemistry and Molecular Biology life 59, 427-435.

Shoulders, M.D., Raines, R.T., 2009. Collagen structure and stability. Annual Review of Biochemistry 78, 929-958.

Slominski, A., Tobin, D.J., Shibahara, S., Wortsman, J., 2004. Melanin pigmentation in mammalian skin and its hormonal regulation. Physiological Reviews 84, 1155-1228.

Sobel, J., 1996. *Hippoglossus hippoglossus*. IUCN Red List. International Union for the Conservation of Nature and Natural Resources. Retrieved 2016-06-22.

Soffientino, B., Spivack, A.J., Smith, D.C., Roggenstein, E.B., D'Hondt, S., 2006. A versatile and sensitive tritium-based radioassay for measuring hydrogenase activity in aquatic sediments. Journal of Microbiological Methods 66, 136-146.

Solbakken, J., Norberg, B., Watanabe, K., Pittman, K., 1999. Thyroxine as a Mediator of Metamorphosis of Atlantic Halibut, *Hippoglossus Hippoglossus*. Environmental Biology of Fishes 56, 53-65.

St Germain, D.L., Galton, V.A., Hernandez, A., 2009. Minireview: Defining the roles of the iodothyronine deiodinases: current concepts and challenges. Endocrinology 150, 1097-1107.

St Germain, D.L., Schwartzman, R.A., Croteau, W., Kanamori, A., Wang, Z., Brown, D.D., Galton, V.A., 1994. A thyroid hormone-regulated gene in *Xenopus laevis* encodes a

type III iodothyronine 5-deiodinase. Proceedings of the National Academy of Sciences of the United States of America 91, 7767-7771.

Stevens, M., Merilaita, S., 2009. Animal camouflage: current issues and new perspectives. Philosophical transactions of the Royal Society of London. Series B, Biological Sciences 364, 423-427.

Stilborn, S.S., Manzon, L.A., Schauenberg, J.D., Manzon, R.G., 2013. Thyroid hormone deiodinase type 2 mRNA levels in sea lamprey (*Petromyzon marinus*) are regulated during metamorphosis and in response to a thyroid challenge. General and Comparative Endocrinol 183, 63-68.

Subramanian, S., MacKinnon, S.L., Ross, N.W., 2007. A comparative study on innate immune parameters in the epidermal mucus of various fish species. Comparative Biochemistry and Physiology. Part B, Biochemistry and Molecular Biology 148, 256-263.

Subramanian, S., Ross, N.W., MacKinnon, S.L., 2008. Comparison of antimicrobial activity in the epidermal mucus extracts of fish. Comparative Biochemistry and Physiology. Part B, Biochemistry and Molecular Biology 150, 85-92.

Sugimoto, M., 2002. Morphological color changes in fish: regulation of pigment cell density and morphology. Microscopy Research and Technique 58, 496-503.

Sun, M., Wei, F., Li, H., Xu, J., Chen, X., Gong, X., Tian, Y., Chen, S., Bao, B., 2015. Distortion of frontal bones results from cell apoptosis by the mechanical force from the up-migrating eye during metamorphosis in *Paralichthys olivaceus*. Mechanisms of Development 136, 87-98.

Sutija, M., Longhurst, T.J., Joss, J.M., 2004. Deiodinase type III in the Australian lungfish, *Neoceratodus forsteri*. General and Comparative Endocrinology 136, 152-161.

Suzuki, K.-i., Machiyama, F., Nishino, S., Watanabe, Y., Kashiwagi, K., Kashiwagi, A., Yoshizato, K., 2009. Molecular features of thyroid hormone-regulated skin remodelling in *Xenopus laevis* during metamorphosis. Development, Growth and Differentiation 51, 411-427.

Suzuki, K., Utoh, R., Kotani, K., Obara, M., Yoshizato, K., 2002. Lineage of anuran epidermal basal cells and their differentiation potential in relation to metamorphic skin remodelling. Development, Growth and Differentiation 44, 225-238.

Szkudlinski, M.W., Fremont, V., Ronin, C., Weintraub, B.D., 2002. Thyroid-stimulating hormone and thyroid-stimulating hormone receptor structure-function relationships. Physiological Reviews 82, 473-502.

Tagawa, M., Aritaki, M., 2005. Production of symmetrical flatfish by controlling the timing of thyroid hormone treatment in spotted halibut *Verasper variegatus*. General and Comparative Endocrinology 141, 184-189.

Takayama, S., Hostick, U., Haendel, M., Eisen, J., Darimont, B., 2008. An F-domain introduced by alternative splicing regulates activity of the zebrafish thyroid hormone receptor alpha. General and Comparative Endocrinology 155, 176-189.

Tanaka, M., Kawai, S., Seikai, T., Burke, J.S., 1996. Development of the digestive organ system in Japanese flounder in relation to metamorphosis and settlement. Marine and Freshwater Behaviour and Physiology 28, 19-31.

Tata, J.R., 2006. Amphibian metamorphosis as a model for the developmental actions of thyroid hormone. Molecular and Cellular Endocrinology 246, 10-20.

Thisse, C., Degrave, A., Kryukov, G.V., Gladyshev, V.N., Obrecht-Pflumio, S., Krol, A., Thisse, B., Lescure, A., 2003. Spatial and temporal expression patterns of selenoprotein genes during embryogenesis in zebrafish. Gene Expression Patterns 3, 525-532.

Todd, K.J., Eales, J.G., 2002. The effect of handling and blood removal on plasma levels and hepatic deiodination of thyroid hormones in adult male and female rainbow trout, *Oncorhynchus mykiss*. Canadian Journal of Zoology 80, 372-375.

Trajkovic, M., Visser, T.J., Mittag, J., Horn, S., Lukas, J., Darras, V.M., Raivich, G., Bauer, K., Heuer, H., 2007. Abnormal thyroid hormone metabolism in mice lacking the monocarboxylate transporter 8. The Journal of Clinical Investigation 117, 627-635.

Tsutsui, S., Komatsu, Y., Sugiura, T., Araki, K., Nakamura, O., 2011. A unique epidermal mucus lectin identified from catfish (*Silurus asotus*): first evidence of intelectin in fish skin slime. Journal of Biochemistry 150, 501-514.

Umesono, K., Murakami, K.K., Thompson, C.C., Evans, R.M., 1991. Direct repeats as selective response elements for the thyroid hormone, retinoic acid, and vitamin D3 receptors. Cell 65, 1255-1266.

Valverde, C., Croteau, W., Lafleur, G.J., Jr., Orozco, A., Germain, D.L., 1997. Cloning and expression of a 5'-iodothyronine deiodinase from the liver of *Fundulus heteroclitus*. Endocrinology 138, 642-648.

Valverde, C., Orozco, A., Becerra, A., Jeziorski, M.C., Villalobos, P., Solis, J.C., 2004. Halometabolites and cellular dehalogenase systems: an evolutionary perspective. International Review of Cytology 234, 143-199.

van der Deure, W.M., Peeters, R.P., Visser, T.J., 2010. Molecular aspects of thyroid hormone transporters, including MCT8, MCT10, and OATPs, and the effects of genetic variation in these transporters. Journal of Molecular Endocrinology 44, 1-11.

Van der Geyten, S., Byamungu, N., Reyns, G.E., Kuhn, E.R., Darras, V.M., 2005. Iodothyronine deiodinases and the control of plasma and tissue thyroid hormone levels in hyperthyroid tilapia (*Oreochromis niloticus*). The Journal of Endocrinology 184, 467-479.

Van der Geyten, S., Toguyeni, A., Baroiller, J.F., Fauconneau, B., Fostier, A., Sanders, J.P., Visser, T.J., Kuhn, E.R., Darras, V.M., 2001. Hypothyroidism induces type I iodothyronine deiodinase expression in tilapia liver. General and Comparative Endocrinology 124, 333-342.

Van der Geyten, S., Van den Eynde, I., Segers, I.B., Kuhn, E.R., Darras, V.M., 2002. Differential expression of iodothyronine deiodinases in chicken tissues during the last week of embryonic development. General and Comparative Endocrinology 128, 65-73.

van der Marel, M., Caspari, N., Neuhaus, H., Meyer, W., Enss, M.L., Steinhagen, D., 2010. Changes in skin mucus of common carp, *Cyprinus carpio* L., after exposure to water with a high bacterial load. Journal of Fish Diseases 33, 431-439.

Van Herck, S.L., Delbaere, J., Bourgeois, N.M.A., McAllan, B.M., Richardson, S.J., Darras, V.M., 2015. Expression of thyroid hormone transporters and deiodinases at the brain barriers in the embryonic chicken: Insights into the regulation of thyroid hormone availability during neurodevelopment. General and Comparative Endocrinology 214, 30-39.

Van Herck, S.L., Geysens, S., Delbaere, J., Darras, V.M., 2013. Regulators of thyroid hormone availability and action in embryonic chicken brain development. General and Comparative Endocrinology 190, 96-104.

Van Herck, S.L., Geysens, S., Delbaere, J., Tylzanowski, P., Darras, V.M., 2012. Expression profile and thyroid hormone responsiveness of transporters and deiodinases in early embryonic chicken brain development. Molecular and Cellular Endocrinology 349, 289-297.

Varsamos, S., Diaz, J.P., Charmantier, G., Blasco, C., Connes, R., Flik, G., 2002. Location and morphology of chloride cells during the post-embryonic development of the european sea bass, *Dicentrarchus labrax.* Anatomy and Embryology 205, 203-213.

Varsamos, S., Nebel, C., Charmantier, G., 2005. Ontogeny of osmoregulation in postembryonic fish: a review. Comparative Biochemistry and Physiology. Part A, Molecular and Integrative Physiology 141, 401-429.

Vatine, G.D., Zada, D., Lerer-Goldshtein, T., Tovin, A., Malkinson, G., Yaniv, K., Appelbaum, L., 2013. Zebrafish as a model for monocarboxyl transporter 8-deficiency. The Journal of Biological Chemistry 288, 169-180.

Velasco, L.F.R., Togashi, M., Walfish, P.G., Pessanha, R.P., Moura, F.N., Barra, G.B., Nguyen, P., Rebong, R., Yuan, C., Simeoni, L.A., Ribeiro, R.C.J., Baxter, J.D., Webb, P., Neves, F.A.R., 2007. Thyroid Hormone Response Element Organization Dictates the Composition of Active Receptor. Journal of Biological Chemistry 282, 12458-12466.

Venizelos, A., Benetti, D.D., 1999. Pigment abnormalities in flatfish. Aquaculture 176, 181-188.

Vernerey, F.J., Barthelat, F., 2014. Skin and scales of teleost fish: Simple structure but high performance and multiple functions. Journal of the Mechanics and Physics of Solids 68, 66-76.

Villalobos, P., Orozco, A., Valverde, R.C., 2010. Molecular cloning and characterization of a type 3 iodothyronine deiodinase in the pine snake *Pituophis deppei*. General and Comparative Endocrinology 169, 167-173.

Visser, W.E., Friesema, E.C., Visser, T.J., 2011. Minireview: thyroid hormone transporters: the knowns and the unknowns. Molecular Endocrinology 25, 1-14.

Visser, W.E., Wong, W.S., van Mullem, A.A., Friesema, E.C., Geyer, J., Visser, T.J., 2010. Study of the transport of thyroid hormone by transporters of the SLC10 family. Molecular and Cellular Endocrinology 315, 138-145.

Vogel, W., 1999. Discoidin domain receptors: structural relations and functional implications. FASEB journal : official publication of the Federation of American Societies for Experimental Biology 13 Suppl, S77-82.

Vogel, W.F., Abdulhussein, R., Ford, C.E., 2006. Sensing extracellular matrix: an update on discoidin domain receptor function. Cellular Signalling 18, 1108-1116.

von der Emde, G., Schwarz, S., Gomez, L., Budelli, R., Grant, K., 1998. Electric fish measure distance in the dark. Nature 395, 890-894.

Wallis, K., Dudazy, S., van Hogerlinden, M., Nordstrom, K., Mittag, J., Vennstrom, B., 2010. The thyroid hormone receptor alpha1 protein is expressed in embryonic postmitotic neurons and persists in most adult neurons. Molecular Endocrinology 24, 1904-1916.

Walpita, C.N., Van der Geyten, S., Rurangwa, E., Darras, V.M., 2007. The effect of 3,5,3'-triiodothyronine supplementation on zebrafish (Danio rerio) embryonic development and expression of iodothyronine deiodinases and thyroid hormone receptors. General and Comparative Endocrinology 152, 206-214.

Walpita, C.N., Crawford, A.D., Janssens, E.D., Van der Geyten, S., Darras, V.M., 2009. Type 2 iodothyronine deiodinase is essential for thyroid hormone-dependent embryonic development and pigmentation in zebrafish. Endocrinology 150, 530-539.

Walpita, C.N., Crawford, A.D., Darras, V.M., 2010. Combined antisense knockdown of type 1 and type 2 iodothyronine deiodinases disrupts embryonic development in zebrafish (*Danio rerio*). General and Comparative Endocrinology 166, 134-141.

Wang, W., Yi, Q., Ma, L., Zhou, X., Zhao, H., Wang, X., Qi, J., Yu, H., Wang, Z., Zhang, Q., 2014. Sequencing and characterization of the transcriptome of half-smooth tongue sole (*Cynoglossus semilaevis*). BMC Genomics 15, 470.

Wang, X., Tan, Y., Sievers, Q., Sievers, B., Lee, M., Burrall, K., Schreiber, A.M., 2011. Thyroid hormone-responsive genes mediate otolith growth and development during

flatfish metamorphosis. Comparative Biochemistry and Physiology Part A: Molecular & Integrative Physiology 158, 163-168.

Wassen, F.W., Schiel, A.E., Kuiper, G.G., Kaptein, E., Bakker, O., Visser, T.J., Simonides, W.S., 2002. Induction of thyroid hormone-degrading deiodinase in cardiac hypertrophy and failure. Endocrinology 143, 2812-2815.

Watanabe, Y., Kobayashi, H., Suzuki, K., Kotani, K., Yoshizato, K., 2001. New epidermal keratin genes from *Xenopus laevis*: hormonal and regional regulation of their expression during anuran skin metamorphosis. Biochimica et Biophysica Acta 1517, 339-350.

Watanabe, Y., Tanaka, R., Kobayashi, H., Utoh, R., Suzuki, K., Obara, M., Yoshizato, K., 2002. Metamorphosis-dependent transcriptional regulation of xak-c, a novel *Xenopus* type I keratin gene. Developmental dynamics : an official publication of the American Association of Anatomists 225, 561-570.

Watt, F.M., Fujiwara, H., 2011. Cell-extracellular matrix interactions in normal and diseased skin. Cold Spring Harbor Perspectives in Biology 3.

Wilson, J.M., Laurent, P., 2002. Fish gill morphology: inside out. The Journal of Experimental Zoology 293, 192-213.

Witt, E.M., Laidley, C.H., Liu, K.K.M., Hirano, T., Grau, E.G., 2009. Correlation between environmental iodide concentrations and larval growth, survival, and whole body concentrations of thyroid hormones and cortisol in Pacific threadfin (*Polydactylus sexfilis*). Aquaculture 16, 357-364.

Wong, Y.H., Wang, H., Ravasi, T., Qian, P.-Y., 2012. Involvement of Wnt Signaling Pathways in the Metamorphosis of the Bryozoan *Bugula neritina*. PLoS One 7, e33323.

Yamada, T., Okauchi, M., Araki, K., 2010. Origin of adult-type pigment cells forming the asymmetric pigment pattern, in Japanese flounder (Paralichthys olivaceus). Developmental dynamics : an official publication of the American Association of Anatomists 239, 3147-3162.

Yamaguchi, Y., Brenner, M., Hearing, V.J., 2007. The regulation of skin pigmentation. The Journal of Biological Chemistry 282, 27557-27561.

Yamano, K., Inui, Y., 1995. cDNA Cloning of Thyroid Hormone Receptor β for the Japanese Flounder. General and Comparative Endocrinology 99, 197-203.

Yamano, K., Miwa, S., 1998. Differential gene expression of thyroid hormone receptor alpha and beta in fish development. General and Comparative Endocrinology 109, 75-85.

Yamauchi, K., Tata, J.R., 1994. Purification and characterization of a cytosolic thyroid-hormone-binding protein (CTBP) in Xenopus liver. European Journal of Biochemistry FEBS 225, 1105-1112.

Yanagie, R., Lee, K.M., Watanabe, S., Kaneko, T., 2009. Ontogenic change in tissue osmolality and developmental sequence of mitochondria-rich cells in Mozambique tilapia developing in freshwater. Comparative Biochemistry and Physiology. Part A, Molecular and Integrative Physiology 154, 263-269.

Yen, P.M., 2001. Physiological and molecular basis of thyroid hormone action. Physiological Reviews 81, 1097-1142.

Yoo, J.H., Takeuchi, T., Tagawa, M., Seikai, T., 2000. Effect of Thyroid Hormones on the Stage-specific Pigmentation of the Japanese Flounder *Paralichthys olivaceus*. Zoological Science 17, 1101-1106.

Yoshikawa, N., Matsuda, T., Takahashi, A., Tagawa, M., 2013. Developmental changes in melanophores and their asymmetrical responsiveness to melanin-concentrating hormone during metamorphosis in barfin flounder (*Verasper moseri*). General and Comparative Endocrinology 194, 118-123.

Yoshizato, K., 2007. Molecular mechanism and evolutional significance of epithelial-mesenchymal interactions in the body- and tail-dependent metamorphic transformation of anuran larval skin. International Review of Cytology 260, 213-260.

Yousefian, M., Shirzad, E., 2011. The review of the effect of growth hormone on immune system, metabolism and osmoregulation of fish. Australian Journal of Basic and Applied Sciences 5, 467-475.

Zhang, J., Lazar, M.A., 2000. The mechanism of action of thyroid hormones. Annual review of physiology 62, 439-466.

Zhang, W.T., Liu, K., Xiang, J.S., Zhang, L.Y., Liu, W.J., Dong, Z.D., Li, Y.Z., Li, H.L., Chen, S.L., Wang, N., 2016. Molecular cloning, expression of, and regulation by thyroid-hormone receptor alpha A in the half-smooth tongue sole *Cynoglossus semilaevis* during metamorphosis. Journal Fish Biology 88, 1693-1707.

Zimmermann, M.B., 2009. Iodine Deficiency. Endocrine Reviews 30, 376-408.

Zimmermann, M.B., Aeberli, I., Andersson, M., Assey, V., Yorg, J.A.J., Jooste, P., Jukić, T., Kartono, D., Kusić, Z., Pretell, E., San Luis, T.O.L., Untoro, J., Timmer, A., 2013. Thyroglobulin Is a Sensitive Measure of Both Deficient and Excess Iodine Intakes in Children and Indicates No Adverse Effects on Thyroid Function in the UIC Range of 100–299 μg/L: A UNICEF/ICCIDD Study Group Report. The Journal of Clinical Endocrinology and Metabolism 98, 1271-1280.

Chapter 2

The transcriptome of metamorphosing halibut

Chapter 2

Abstract

Flatfish metamorphosis denotes the extraordinary transformation of a symmetric pelagic larva into an asymmetric benthic juvenile. Metamorphosis in vertebrates is driven by thyroid hormones (THs), but how they orchestrate the cellular, morphological and functional modifications associated with maturation to juvenile/adult states in flatfish is an enigma. Since THs act via thyroid receptors that are ligand activated transcription factors, we hypothesized that the maturation of tissues during metamorphosis should be preceded by significant modifications in the transcriptome. Targeting the unique metamorphosis of flatfish and taking advantage of the large size of Atlantic halibut (*Hippoglossus hippoglossus*) larvae, we determined the molecular basis of TH action using RNA sequencing.

De novo assembly of sequences for larval head, skin and gastrointestinal tract (GI-tract) yielded 90,676, 65,530 and 38,426 contigs, respectively. More than 57% of the assembled sequences were successfully annotated using a multi-step Blast approach. A unique set of biological processes and candidate genes were identified specifically associated with changes in morphology and function of the head, skin and GI-tract. Transcriptome dynamics during metamorphosis were mapped with SOLiD sequencing of whole larvae and revealed greater than 8,000 differentially expressed (DE) genes significantly ($p < 0.05$) up- or down-regulated in comparison with the juvenile stage. Candidate transcripts quantified by SOLiD and qPCR analysis were significantly ($r = 0.843$; $p < 0.05$) correlated. The majority (98%) of DE genes during metamorphosis were not TH-responsive. TH-responsive transcripts clustered into 6 groups based on their expression pattern during metamorphosis and the majority of the 145 DE TH-responsive genes were down-regulated.

A transcriptome resource has been generated for metamorphosing Atlantic halibut and over 8,000 DE transcripts per stage were identified. Unique sets of biological processes and candidate genes were associated with changes in the head, skin and GI-tract during metamorphosis. A small proportion of DE transcripts were TH-responsive, suggesting that they trigger gene networks, signalling cascades and transcription factors, leading to the overt changes in tissue occurring during metamorphosis.

Keywords: Development, Flatfish, RNA sequencing, Thyroid hormone responsive, Tissue-remodelling, Transcriptome

Chapter 2

2.1. Introduction

Metamorphosis describes the "change in form" associated with the transition between life cycle stages in a wide range of animal taxa (Brown and Cai, 2007; Gilbert et al., 1996; Huang et al., 2013; Nakamura et al., 2011; Power et al., 2008; Rubio et al., 2012; Schreiber and Specker, 2000; Wong et al., 2012). This transition can be accompanied by modifications in morphology, physiology, behavior, habitat and feeding mode. The endocrine system and in particular the thyroid hormones (THs), thyroxin (T_4) and triiodothyronine (T_3), play a central role in vertebrate metamorphosis acting as transcription factors (TFs) when they bind to their receptors. In amphibian metamorphosis, it is well established that THs directly or indirectly stimulate apoptosis and resorption of larval tissue and also promote growth, differentiation and remodelling of tissues that are crucial for the adult life form (Brown and Cai, 2007). For instance, THs are involved in the control of muscle fibre apoptosis in the amphibian tail during its regression and also promote development of the limbs (Brown et al., 2005). In amphibians the change in feeding habit from herbivore to carnivore during the transition from tadpole to frog is associated with TH driven remodelling of the intestine that changes from a long coiled tube into a complex differentiated organ (Ishizuya-Oka and Shi, 2007; Ishizuya-Oka and Ueda, 1996; Schreiber et al., 2009). Similarly, THs modulate the change in the amphibian integument from a simple to a stratified structure that is better adapted to terrestrial life (Suzuki et al., 2009).

Teleost fish also undergo a TH driven metamorphosis that marks the larval to juvenile transition (McMenamin and Parichy, 2013; Power et al., 2001). However, the term is more generally applied to the profound modifications associated with the change from bilateral symmetry to asymmetry during the larval-juvenile transition of flatfish (pleuronectiformes) (Inui et al., 1995; Klaren et al., 2008; Manchado et al., 2009; Okada et al., 2003; Power et al., 2008; Tagawa and Aritaki, 2005). In flatfish metamorphosis the external morphology is dramatically transformed and they change from symmetric pelagic larvae to asymmetric benthic juveniles with both eyes on the upper, ocular side of the head (reviewed in Power et al., 2008). The external transformation in flatfish morphology is accompanied by a plethora of changes in the structure and function of tissues and organs. Chemical disruption of the thyroid axis using thiourea or methimazole (MMI) delays or stops stomach development in the

Japanese flounder (*Paralichthys olivaceus*) (Miwa et al., 1992) and otolith mineralization in the Southern flounder (*Paralichthys lethostigma*) (Schreiber et al., 2010). The importance of THs during metamorphosis is further emphasized in other flatfish species where they have been shown to be important for the maturation of the muscle, stomach and skin (Campinho et al., 2012; Campinho et al., 2007a; Campinho et al., 2007b; Gomes et al., 2014a; Yamano et al., 1991; Yamano et al., 1994; Zambonino et al., 2008).

Flatfish have a high economic value and include species such as the Atlantic halibut (*Hippoglossus hippoglossus*), common sole (*Solea solea*), Senegalese sole (*S. Senegalesis*), turbot (*Scophthalmus maximus*) and the half-smooth tongue sole (*Cynoglossus semilaevis*). Overfishing and high consumer demand for flatfish has made them an interesting target for aquaculture production and a better understanding of metamorphosis is of direct relevance for their efficient and successful production. Specific problems linked to failures during metamorphosis include feeding difficulties, reduced growth rate, arrested metamorphosis, abnormal pigmentation (albinism, ambicoloration or mosaicism), failed migration of the eye and skeletal deformities (reviewed in Power et al., 2008). Control of hatchery production requires an understanding of fish biology but also a comprehension of the mediators of metamorphosis, such as the THs and potentially other endocrine factors. Although there are numerous studies of flatfish metamorphosis, the endocrine and molecular basis of the tissue-specific modifications and the timing of the cascade of events that lead to metamorphosis are still largely unknown. Moreover, experiments that have blocked the thyroid axis during metamorphosis with drugs such as MMI do not significantly modify larval viability suggesting thyroid dependent (Coady et al., 2010; Crane et al., 2006; Liu and Chan, 2002; Schreiber et al., 2010) and independent processes underpin this event. A complex task now lies ahead in establishing which developmental processes during metamorphosis are fully TH dependent and which genetic pathways and endocrine systems cross-talk with THs. Furthermore, it remains to be established how profoundly different processes such as skin maturation, eye migration and craniofacial remodelling or gastrointestinal tract (GI-tract) development can be regulated by the same endocrine factors.

One of the challenges of studying metamorphosis in fish larvae is their relatively small dimension, which means pools of larvae rather than individuals or tissues have generally been

used which significantly reduces the resolution of such studies. The advantage of the biggest of flatfish, the Atlantic halibut, is the large size of the larvae and their slow metamorphosis (occurring over approx. 58 days), which means it is possible to analyze individuals or individual tissues. This is advantageous as pools of larvae contain a mixture of tissues and frequently contain individuals at different developmental stages making resolution of tissue specific changes in transcripts and proteins during metamorphosis difficult or impossible.

The working hypothesis of the present study is that since THs exert their action by binding to thyroid receptors that are ligand activated TFs the overt change in flatfish during metamorphosis will be preceded by significant modifications in the transcriptome of responsive tissues. For this reason, large scale analysis of tissue-specific transcriptional changes in responsive tissue should provide insight into the underlying molecular changes of tissue specific maturation. A 454 pyrosequencing approach was used to survey the tissue specific transcriptomes in the skin, GI-tract and head of metamorphosing Atlantic halibut and to also generate a reference transcriptome. SOLiD technology was then used to map the transcriptional changes in individuals (n = 3/stage) at different stages of metamorphosis. Differentially expressed (DE) transcripts during metamorphosis were identified by comparing the transcriptome at metamorphic stages (stage 7, 8 and 9 (Sæle et al., 2004)) with juvenile (benthic) stages. Subsequently, genes of the thyroid axis, TH-responsive transcripts and candidate genes that underpin remodelling and maturation of tissues during metamorphosis were identified and analyzed by quantitative PCR (qPCR).

2.2. Material and methods

2.2.1. Sampling

The samples of Atlantic halibut larvae for sequencing were donated by a commercial producer (Fiskeldi Eyjafjarðar Ltd., Iceland) in December 2009. Samples were collected from a standard commercial production cycle (Galay-Burgos et al., 2008) undergoing normal metamorphosis by a qualified member of staff and were killed humanely. The samples for analysis were collected using established husbandry procedures and were obtained in the

context of routine larval sampling protocols used by the commercial producer to verify the health, welfare and quality of the larvae. The legislation and measures implemented by the commercial producer complied with Directive 98/58/EC (protection of animals kept for farming) and production and sampling conditions were optimized to avoid unnecessary pain, suffering or injury and to maximize larval survival. The study was authorized in accordance with Portuguese legislation for the use of laboratory animals under a Group-1 license from the Direcção-Geral de Veterinária, Ministério da Agricultura, do Desenvolvimento Rural e das Pescas.

After collection the Atlantic halibut larvae (n = 6 per developmental stage) were photographed and staged using myotome height (MH) and standard length (SL) (Sæle et al., 2004). A further subdivision of stage 9 (9A, 9B, 9C) was made to account for differences in eye migration. Individual larvae were collected into RNAlater (Life Technologies, Carlsbad, USA), gently agitated for 24h at 4 °C and then transferred to -20 ºC for long term storage.

2.2.2. Transcriptome sequencing

Larvae (stage 5 to 9A-C, n = 6 per stage) were dissected into skin, GI-tract and head. Stage 5 larvae were divided into head and body only. Total RNA was extracted from all tissues and whole individuals (n = 5 per stage) using a Maxwell®16 System (Promega, Madison, USA) following the manufacturer's instructions. RNA integrity and concentration was verified with an Agilent 2100 Bioanalyzer (Agilent Technologies, Santa Clara, USA) and only samples with RIN values equal to, or above 8 were used. The 454 (GS FLX, Roche Life Sciences, Branford, USA) and SOLiD (AB 5500xl Genetic Analyser system, Applied Biosystems, USA) sequencing was performed at the Max Planck Genome Centre (Cologne, Germany).

2.2.2.1. 454 sequencing

cDNA libraries of the Atlantic halibut skin, GI-tract and head were prepared from pools of 6 samples per stage to obtain 5 µg of total RNA. Ribosomal RNA was depleted using RiboMinusTM Eukaryote Kit (Life Technologies, Carlsbad, USA) and following the manufacturer's instructions. A cDNA Rapid Library Preparation Kit (Roche Life Sciences,

USA) was used to construct sixteen cDNA libraries; head from stage 5 and head, skin and GI-tract from stages 7, 8 and 9A, 9B and 9C. Each library had a unique barcode and was amplified by emulsion PCR and sequenced on a GS-FLX platform (Roche Life Sciences, USA) following the manufacturers recommendations. The sequencing assigned quality scores are available at the NCBI Short Read Archive (SRA; Accession number: SRP044664).

2.2.2.2. SOLiD mRNA sequencing

SOLiD sequencing was carried out on cDNA libraries constructed using SOLiDTM Total RNA-Seq Kit (Applied Biosystems, CA). Ribosomal RNA was depleted from total RNA of whole individual Atlantic halibut extracted as described above. Sixteen cDNA libraries were prepared from individual larvae and included three stage 7, three stage 8, three stage 9A, three stage 9B and two stage 9C libraries from whole individual Atlantic halibut. For the non-metamorphic samples, stage 5 and juvenile, a pool of RNA from 3 individuals was used to prepare the libraries due to sequencing space constraints and cost. Each library had a unique barcode and cDNA was purified to eliminate contaminants, amplified by emulsion PCR and sequenced on a SOLiD AB 5500xl Genetic Analyser platform (Applied Biosystems, USA). The sequencing assigned quality scores are available at the NCBI SRA (Accession number: SRP073364).

2.2.3. Assembly and annotation

2.2.3.1. 454 sequence reads

Raw sequence reads (.sff format) from the sixteen libraries were extracted and quality clipped and sequencing adapters, primers and poly-A tails were removed. Only sequences above 100bp were retained for assembly and food source contamination was removed by screening against Artemia species available in NCBI (38,287 sequences at 04.2012) and *H. hippoglossus* mitochondrial RNA (27 sequences at 04.2012) was removed using BLASTn (settings: score > 100; e-value <1e-25). After quality filtering and removal of potential contaminants, approximately 70% of the initial reads from skin (1,200,186) and head (1,556,954) and 43% from GI-tract (888,165) were kept for assembly. As the number of reads

obtained from the stage-specific tissue libraries was highly variable and did not yield robust stage specific comparisons they were combined to produce 3 tissue-specific assemblies. The filtered reads were assembled into contigs using MIRA V3 (http://sourceforge.net/projects/mira-assembler/files/) with the command: mira project= xyx –job = denovo, est, accurate, 454 –DI: trt =/dev/slim, where xyx represent the file extracted from the *sff files of each library (Chevreux et al., 1999). All singletons were discarded. Files containing the reads have been submitted to the National Center for Biotechnology Information Short Read Archive (Accession number: SRP044664; (Gomes et al., 2014b)). Validation of library assemblies was performed by Blastx sequence similarity searching (Altschul et al. 1997) against all the available ESTs for Atlantic halibut (21,018 sequences at 07.2014) and by manual annotation of 1% of randomly chosen contigs from each individual assembly using BLASTx against the Reference Protein database (refseq_protein; NCBI) for vertebrate species.

Annotation of putative function was performed using a multi-step stringent local blast approach adapted from Yúfera et al. (2012a) (Additional file 2.1). Sequences were first compared against NCBI *Danio rerio* non-redundant protein database (db) (Blastx; e-value < 1e-20), then against Swissprot (Blastx; e-value < 1e-10) and finally against the non-redundant bony fish protein database (Blastx; e-value < 1e-10). All remaining contigs were then subject to a final Blast search against all the available ESTs for bonyfish (1,191,154 sequences at 2012).

2.2.3.2. Functional annotation of 454 tissue transcriptomes

Functional annotation of the assembled 454 tissue transcriptomes was performed using the Blast2GO program v.2.6.0 (Conesa et al., 2005; Götz et al., 2008). Annotated sequences were mapped to gene ontology (GO) terms using the following settings: annotation cut-off: 55; minimum GO weight: 5; and e-value: 1e-06. To augment the GO annotation, ANNEX analyses that gives manually curated univocal relationships between GO terms were also used (http://www.goat.no; (Myhre et al., 2006)). Enrichment of GO terms between different tissues was established using a Fisher's exact test and applying a False Discovery Rate (FDR) adjusted p-value of 0.05. Metabolic KEGG pathway analysis was performed based on the

Enzyme Code (EC) obtained for each GO term during the functional annotation step. Each EC was mapped to the corresponding metabolic pathway. The unique and specific tissue GO terms resulting from the 454 tissue transcriptome was analysed with REVIGO (http://revigo.irb.hr/, (Supek et al., 2011)), which uses a simple clustering algorithm that relies on semantic similarity measures to find representative subsets of GO terms.

2.2.3.3. SOLiD sequence reads

A backbone assembly was created using Newbler and CAP3 (with default parameters) combining all the 454 reads from the different tissues and stages together with the 21,018 ESTs available in public databases (July 2014) to produce 37,073 contigs. The contigs are available at http://ramadda.nerc-bas.ac.uk/repository in the folder: NERC-BAS datasets/Genomics/Transcriptomes/Hippoglossus_hippoglossus. This was then used as the reference for mapping the SOLiD sequences. The paired reads obtained for halibut samples were as follows: 9,532,993 for the pooled stage 5 sample; 11,277,613, 10,533,234 and 9,765,750 for the three stage 7 larvae; 9,658,624, 6,121,383 and 9,518,793 for the 3 stage 8 larvae; 107,948,772, 6,509,721 and 6,343,735 for the 3 stage 9A larvae; 11,101,201, 10,357,984 and 5,282,230 for the three stage 9B larvae; 12,950,027 and 9,195,626 for the two stage 9C larvae and 11,744,701 for the pooled juvenile sample. The reads were mapped to the Atlantic halibut contigs with Maq (Li et al., 2008), using default parameters.

Expression analysis was carried out using pairwise comparisons rather than a factorial design. SOLiD sequences that failed to map to contigs were excluded from the analysis. Normalisation was carried out by dividing counts by library size. Differential expression was established using two approaches to increase stringency: a two-fold expression level difference, and the use of a linear model in Bayseq (Hardcastle and Kelly, 2010), with a Benjamini-Hochberg adjustment for multiple testing (Benjamini and Hochberg, 1995) with a cut-off set at 0.05. For the linear model, a proxy replication for mapping variance consisted of the separate mappings of the paired end reads to the contigs. Only mappings in which both paired end reads mapped to the same contig were used to generate expression levels and calculate significance of expression. The probable identity of the genes to which SOLiD reads mapped was established by sequence similarity searches using Blast (Altschul et al., 1997),

http://blast.ncbi.nlm.nih.gov/Blast.cgi) against the GenBank non redundant database (Benson et al., 2013) with a threshold score of < 1e-10.

2.2.4. Identification of tissue-specific and TH-responsive genes

Candidate genes underlying the tissue specific changes (454 transcriptomes and SOLiD analysis) that accompany metamorphosis, were identified by comparing the annotated contigs against 4 in-house databases of genes (setting: e-value ≤ 1e-20), identified using the QuickGO (http://www.ebi.ac.uk/QuickGO/) database and through literature searches. Databases included: 1) database enriched with skin-specific genes, eg. pigmentation, skin development and morphogenesis (141 sequences; Additional file 2.2); 2) a GI-tract-specific database enriched with genes involved in development, morphogenesis and acid secretion (179 sequences; Additional file 2.3); 3) genes involved in TH signalling and metabolism and genes involved in thyroid gland development (62 sequences; Additional file 2.4); 4) TH-responsive genes (189 sequences; Additional file 2.5).

SOLiD whole larval transcriptome data was used to identify transcripts with differential expression in three individuals per stage by carrying out pairwise comparisons. Two strategies were used for pairwise comparisons: i) pairwise comparisons between metamorphic stages (7, 8, 9A, 9B, 9C) or ii) pairwise comparisons between metamorphic stages (7, 8, 9A, 9B, 9C) and premetamorphic stage 5 larvae or juveniles. Since pairwise comparisons between metamorphic stages (7, 8, 9A, 9B and 9C) yielded very few differential transcripts only the results of the comparison against stage 5 or juveniles was analyzed in detail.

2.2.5. Quantitative real-time RT-PCR (qPCR)

A set of 16 transcripts was assessed by qPCR, using a subsample of the RNA extracted from whole larvae used for SOLiD transcriptome sequencing. Correlation analysis was carried out between transcripts with differential expression in SOLiD analysis (n = 5) and their expression determined by qPCR. The selected transcripts included genes with a constant expression in all developmental stages, transcripts with modified expression during

development and genes involved in the TH cascade (Additional file 2.6). Specific primers for the target genes were designed based on the cDNA contig sequences (Additional file 2.6) using Beacon Design and Primer Premier 5.0 software (Premier Biosoft Int., Palo Alto, CA). The reference gene transcripts used to normalize the cDNA used for the PCR reactions were elongation factor I alpha (*ef1a1*) and 40S ribosomal protein S4 (*rps4*) (Additional file 2.6).

For cDNA synthesis total RNA (10 µg) was first treated with Turbo DNA-Free kit (Ambion, Life Technologies, Carlsbad, USA) to remove contaminating genomic DNA. cDNA synthesis was performed with 500 ng of DNAse treated total RNA, 200 ng of random hexamers (GE Healthcare, Amersham, UK), 100 U of RevertAid M-MuLV Reverse Transcriptase (Fermentas, St Leon-Rot, Germany), 8 U of Ribolock RNase inhibitor (Fermentas, St Leon-Rot, Germany), and 0.5 mM dNTP's. qPCR reactions were performed in duplicate using SsoFast™ EvaGreen® Supermix (Bio-Rad, Marnes La Coquette, France) chemistry in a StepOnePlus™ Real-Time PCR System (Applied Biosystems, Foster City, USA). The qPCR cycling conditions were: 30 sec at 95 ºC; 45 cycles of 5 sec at 95 ºC and 10 sec at the optimal temperature for primer pairs (Additional file 2.4). A final melting curve over a range of 60-95 ºC was performed for all reactions. Standard curves relating initial template quantity to amplification cycle were generated from the target gene cloned in pGEM®-T Easy (Promega, Madison, USA) using a 10-fold stepwise serial dilution series (initial concentration, 10^8 copies amplicon/µl).

The qPCR efficiency for primer pairs ranged from 85% and 100% with an $R2 \geq 0.99$ (Additional file 2.6). The geometric mean of the reference genes *rps4* and *efiai* was used to normalize the qPCR data. Statistical analysis of the relative gene expression between stages was analyzed by one-way, ANOVA using SigmaPlot v10.0 (Systat Software, Inc., CA, USA) after checking for homogeneity. Tukey's post-hoc test was used for pair wise multiple comparisons. The expression of transcripts in the halibut stages analyzed is presented as the mean ± standard error of the mean (SEM). Pearson correlation analysis was used to compare the qPCR relative gene expression levels and SOLiD differential count analysis. For correlation analysis six genes from SOLiD analysis with either a constant (*rpl7* and *fau*) or variable expression (*gloα1*, *cpa2*, *apoai*, and *krt1i2*) during metamorphosis were selected. Statistical significance was established at $p < 0.05$.

2.3. Results

2.3.1. 454 transcriptome sequencing

2.3.1.1. Transcriptome annotation

In spite of stringent quality control of the RNA used for 454 library construction, the number of reads resulting from the stage-specific libraries for skin, GI-tract and head of Atlantic halibut post-embryonic larvae at different metamorphic stages was highly variable. A total of 134 Mbp were produced for the tissue assemblies using MIRA V3 (http://sourceforge.net/projects/mira-assembler/files/) and they assembled into 65,530, 38,426 and 90,676, contigs for skin, GI-tract, and head, respectively. The contigs from the skin, GI-tract and head tissue assemblies were submitted to an iterative stringent four-step local Blast approach (Additional file 2.1). The tissue assemblies were successfully annotated and for the GI-tract library 60% of the initial contigs had a good Blast match after the first 3 annotation steps and 57% of the contigs were annotated for the skin and head libraries (**Table 2.1**). Most of the contigs were successfully annotated in the first step of Blastx against the zebrafish refseq protein db.

Table 2.1. Summary of the Blast results used for annotation of the head, skin and GI-tract assembly.

	Skin	GI-tract	Head
Total number of contigs	65,530	38,426	90,676
Blastx refseq protein zebrafish	27,312	12,845	42,040
Blastx vertebrate swissprot db	3,560	1,141	5,209
Blastx protein bony fish db	6,791	9,166	4,559
Percentage of contigs with annotation	57%	60%	57%
Additional blast matches to non-annotated ESTs (%)	11,418 (17%)	12,354 (32%)	14,460 (13%)
Percentage of contigs with no database match	26%	8%	30%

2.3.1.2. Gene Ontology and KEGG analysis

The active transcriptome in each tissue analyzed was assumed to be equivalent to the number of contigs identified (**Figure 2.1A**). Comparative analyses between the

transcriptomes revealed that 2,541, 2,261 and 8,359 transcripts were unique to the skin, GI-tract and head assembly, respectively. In addition, 4,099 transcripts were common between the three tissues. The head and skin, head and GI-tract and GI-tract and skin shared a further 4,464, 955 and 506 transcripts, respectively (**Figure 2.1A**).

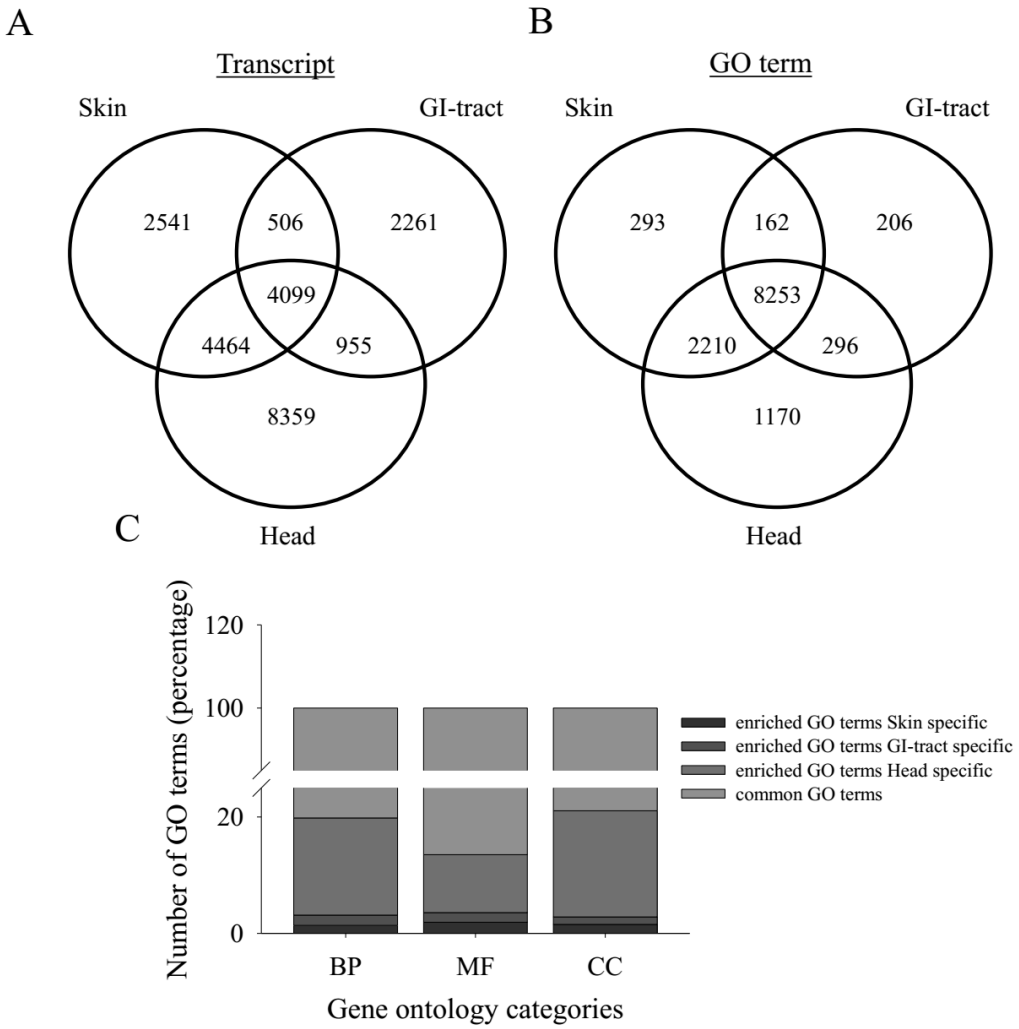

Figure 2.1. Atlantic halibut skin, gastrointestinal tract and head transcriptome annotation. A - Venn diagram of common and unique tissue transcripts (using the transcript name); B - Venn diagram representing the common and specific tissue gene ontology (GO) terms (using the unique GO terms); C - Diagram representing the relative abundance of shared and tissue specific enriched GO terms by GO category (using the over/under-represented GO terms from the Fisher's exact test).

The complete functional (GO) annotation for the skin, GI-tract and head transcriptomes (Additional files 2.7, 2.8 and 2.9, respectively) assigned a total of 12,577 different GO terms to the three tissue assemblies. Comparisons of the assigned GO terms for the skin, GI-tract and head transcriptome assemblies revealed 8,253 common GO terms and

293 identified only in the skin, 206 only in the GI-tract and 1,170 only in the head (**Figure 2.1B**). The most abundant GO terms (level 2) for biological process (BP), molecular function (MF) and cellular component (CC) showed no major differences between skin, GI-tract and head (Additional file 2.10). Cellular process (17%), metabolic process (16%) and biological regulation (10%) were the most representative GO terms in the category biological processes. Other key biological processes linked to development (7%), localization (6%), signaling (5%), cell proliferation (3%) and death (3%) were also found (Additional file 2.10).

For molecular function, the most abundant GO terms (level 2) in the skin and head transcriptomes were binding, catalytic activity and structural molecule activity (Additional file 2.10). For the GI-tract transcriptome, binding and nucleic acid binding transcription factor activity were the most frequent MF GO terms. The exception was the GI-tract for which GO terms specific for DNA binding transcription factor activity (~20%) were more highly represented, when compared to the other tissues (Additional file 2.10). Within the cellular component category, the most represented GO terms in the three tissues transcriptomes were cell, organelle, macromolecule complex and membrane (Additional file 2.10).

Fisher's exact tests were applied to detect significantly over/under-represented GO terms resulting from analysis of the tissue-specific transcriptomes (FDR<0.05). Comparison of the overall GO enrichment for the tissue specific transcriptome revealed that the highest enrichment was associated with the BP category (approx. 60-73%), followed by the MF category (16-31%). Of the 2,316 enriched GO terms identified for the tissue transcriptomes, 8.2 % (190), 9.2 % (214) and 82.6 % (1,912) were from skin, GI-tract, and head, respectively. **Figure 2.1C** shows the representative enriched GO terms for each tissue assembly for BP, MF, and CC gene ontology categories. The halibut head transcriptome had the highest enrichment of BP GO terms (1,395) and they corresponded to 16.7% of the overall GO terms for this tissue, followed by the GI-tract (148 GO terms) and the skin (114 GO terms) (**Figure 2.1C**). Similarly, MF GO terms were most enriched in the head (303 GO terms and 9.9% of overall enriched terms) relative to the skin (58 GO terms) and the GI-tract (51 GO terms).

In the skin transcriptome, GO terms related to the muscle system, development and morphogenetic processes, including epidermis development, appendage morphogenesis, and

transcripts involved in cellular response to hormone stimulus were overrepresented along with immune development and pigmentation (Additional file 2.11). Significant GO categories in the GI-tract that were overrepresented included digestion, proteolysis and lipid metabolism such as the cholesterol metabolic process and triglyceride mobilization (Additional file 2.12). In the head transcriptome, significantly overrepresented GO terms included development of the nervous system, spinal cord and otoliths, cartilage and endochondral bone. In addition, head-specific GO terms, such as pituitary gland development and thyroid hormone metabolic processes were also significantly overrepresented (Additional file 2.13).

REVIGO clustering of enriched Biological Process GO terms for the skin transcriptome identified phosphocreatine metabolism and response to lipopolysaccharides and biotic stimulus. In REVIGO clustering of enriched BP GO terms in the GI-tract transcriptome identified digestion, cell proliferation, rRNA transcription, lipid storage and immune system and response (e.g. foam cell differentiation, positive regulation of macrophage derived foam cell differentiation, low density lipoprotein particle remodelling, lipoproteins transport). In the head, transcriptome REVIGO clustering of enriched BP GO categories identified nervous system development (e.g. glutamate receptor and neuropeptide signaling pathways, proliferation and apoptosis of neural precursor cells, regulation of synaptic plasticity and synaptic vesicle transport), blood vessel morphogenesis, and immune and defense response (T cell activation).

More than 125 metabolic pathways were identified via KEGG mapping comprising ~1,250 different enzyme codes and more than 9,000 of the Atlantic halibut contigs matched an enzyme code (EC) (Additional file 2.14). Overall, there was considerable similarity in the metabolic pathway enrichment between the three tissues but this was unsurprising since many of the pathways were linked to cellular metabolism. Of note was the lower representation of sphingolipids, inositol lipid and phospholipid pathways in the GI-tract. The GI-tract, a soft tissue, had a notable reduction compared to the skin and head of metabolic pathways involved in chondrogenic matrix generation but had an increase in starch and sucrose metabolic pathways relative to the head (Additional file 2.14).

2.3.1.3. Tissue development/morphogenesis – identification of putative tissue-specific genes

Blast of the skin transcriptome against the *in-house* skin-specific database that contained genes characteristic of skin in other vertebrates identified 33 transcripts for skin development and morphogenesis and 40 for pigmentation (**Table 2.2**). Abundant transcripts included the collagens (*col1a1*, *col1a2*), genes involved in pigmentation, melanocyte differentiation and melanosome transport (e.g. apoptosis regulator bax, dedicator of cytokinesis 7, dopachrome tautomerase, lysosomal-trafficking regulator), (**Table 2.2**). Several signal transduction pathways were identified in the skin transcriptome including Notch (>70 transcripts), Wnt (>100 transcripts) and Sonic Hedgehog (Shh) (>30 transcripts) (Additional file 2.7).

Table 2.2. Genes in vertebrate skin development and pigmentation identified in the Atlantic halibut skin transcriptome.

Contig ID	Protein name	Acronym	Accession no.	Species	E-value	Biological role
lcst_c59341	Transcription factor ap-2 alpha (activating enhancer binding protein 2 alpha)	*Tfap2c*	A2APA8	*Mus musculus*	3E-38	*Skin development*
lcst_c6882	Epithelial discoidin domain-containing receptor 1	*Ddr1*	B0V2H8	*Mus musculus*	2E-71	
lcst_c52199	Adenomatosis polyposis coli, isoform CRA_a	*Apc*	B2RUG9	*Mus musculus*	8E-28	
lcst_c5213	T-cell factor-4 variant L	*TCF7L2*	E2GH26	*Homo sapiens*	1E-39	
lcst_c348	Desmoplakin	*Dsp*	E9Q557	*Mus musculus*	0	
lcst_c611	Collagen, type V. Alpha 2	*Col5a2*	F1LQ00	*Rattus norvegicus*	1E-124	
lcst_rep_c10540	Keratin, type I cytoskeletal 9	*Krt9*	F1M7K4	*Rattus norvegicus*	2E-59	
lcst_c88	Sratifin (14-3-3 protein sigma)	*Sfn*	O70456	*Mus musculus*	4E-74	
lcst_c38806	Steryl-sulfatase	*Sts*	P15589	*Rattus norvegicus*	2E-61	
lcst_c1342	Gap junction beta-3 protein	*Gjb3*	P28231	*Mus musculus*	2E-56	
lcst_c5669	Macrophage migration inhibitory factor	*Mif*	P30904	*Rattus norvegicus*	3E-30	
lcst_c7497	Cellular tumor antigen p53	*Trp63*	Q569E5	*Mus musculus*	8E-48	
lcst_c26088	Transcription factor 15	*Tcf15*	Q60756	*Mus musculus*	4E-31	
lcst_c32091	Copper-transporting atpase 1	*Atp7a*	Q64430	*Mus musculus*	8E-47	
lcst_c62343	Calcium release channel (Ryanodine receptor 1)	*crc1, ryr1*	Q6LAA3	*Sus scrofa*	3E-26	
lcst_c54854	Lethal(2) giant larvae protein homolog 2	*llgl2*	Q7SZE3	*Danio rerio*	8E-58	
lcst_c28836	Extracellular matrix protein FRAS1	*Fras1*	Q80T14	*Mus musculus*	1E-70	
lcst_c6455	Alanine-trna ligase, cytoplasmic	*Aars*	Q8BGQ7	*Mus musculus*	0	
lcst_c50366	Nerve growth factor receptor (TNFR superfamily, member 16)	*Ngfr*	Q8CFT3	*Mus musculus*	7E-34	
lcst_c1016	Delta(24)-sterol reductase	*Dhcr24*	Q8VCH6	*Mus musculus*	0	
lcst_c60747	Long-chain fatty acid transport protein 4	*Slc27a4*	Q91VE0	*Mus musculus*	2E-121	
lcst_c28754	Platelet-derived growth factor subunit A	*Pdgfa*	Q99L56	*Mus musculus*	1E-29	
lcst_c4164	Collagen, type I, alpha 2	*Col1a2*	Q91VL4	*Mus musculus*	9E-91	

lcst_c27614	B-cell lymphoma/leukemia 11B	*Bcl11b*	Q99PV8	*Mus musculus*	2E-58	
lcst_rep_c10461	Junction plakoglobin	*jup*	Q9PVF7	*Danio rerio*	4E-180	
lcst_c57261	Suppressor of fused homolog	*Sufu*	Q9Z0P7	*Mus musculus*	3E-64	
lcst_c27807	Serum response factor	*Srf*	Q9JM73	*Mus musculus*	9E-58	*Skin morphogenesis*
lcst_c6845	Collagen, type I, alpha 1	*Col1a1*	Q99LL6	*Mus musculus*	1E-117	
lcst_c4164	Collagen, type I, alpha 2	*Col1a2*	Q91VL4	*Mus musculus*	9E-91	
lcst_c25461	Fibroblast growth factor receptor 1-A	*fgfr1a*	Q90Z00	*Danio rerio*	6E-112	
lcst_c7432	Transformation related protein 63	*Trp63*	Q5CZX0	*Mus musculus*	2E-131	
lcst_c34953	v-erb-b2 erythroblastic leukemia viral oncogene homolog 3b	*erbb3b*	F1Q4T5	*Danio rerio*	2E-83	*Developmental pigmentation*
lcst_c23922	ATPase, H+ transporting, V0 subunit B	*atp6v0b*	F1QYM3	*Danio rerio*	1E-82	
lcst_c4704	Melanocyte protein pmel-like	*pmela*	Q4VW61	*Danio rerio*	1E-56	
lcst_c40663	Macrophage colony-stimulating factor 1 receptor	*csf1r*	Q9I8N6	*Danio rerio*	1E-40	
lcst_c24693	Vacuolar protein sorting-associated protein 18 homolog	*vps18*	P59015	*Danio rerio*	5E-139	*Endosome to pigment granule transport*
lcst_c52806	Mediator of RNA polymerase II transcription subunit 12	*med12*	Q2QCI8	*Danio rerio*	3E-122	*Iridophore differentiation*
lcst_c7916	Forkhead box D3	*foxd3*	Q502Q4	*Danio rerio*	2E-107	
lcst_c467	Rab escort protein 1	*chm*	Q6RFG0	*Danio rerio*	1E-114	
lcst_c8298	Mindbomb E3 ubiquitin protein ligase 2	*mib2*	A0AR23	*Danio rerio*	1E-138	*Melanosome differentiation*
lcst_c2918	Transcription factor Sox-10	*sox10*	A4IIJ8	*Xenopus tropicalis*	1E-49	
lcst_rep_c15027	Mindbomb E3 ubiquitin protein ligase 1	*mib1*	B3DGQ0	*Danio rerio*	9E-66	
lcst_c31755	Transient receptor potential cation channel, subfamily M, member 7	*trpm7*	B3DK48	*Danio rerio*	5E-82	
lcst_c8173	Glutamine-fructose-6-phosphate transaminase 1	*gfpt1*	Q3S344	*Danio rerio*	2E-117	
lcst_c8009	vacuolar protein sorting-associated protein 11 homolog	*vps11*	Q4G0A0	*Danio rerio*	1E-135	
lcst_c31151	RNA polymerase-associated protein LEO1	*leo1*	Q6NYV9	*Danio rerio*	1E-50	
lcst_c366	Histone deacetylase	*hdac1*	Q8JIY7	*Danio rerio*	0	
lcst_c1665	Transcription factor AP2 alpha 2	*tfap2a*	Q8UVE5	*Danio rerio*	3E-55	
lcst_c24989	Microphthalmia-associated transcription factor a	*mitfa*	Q9PWC2	*Danio rerio*	5E-24	
lcst_rep_c15543	Presenilin-1	*psen1*	Q9W6T7	*Danio rerio*	2E-62	

lcst_c2922	Adaptor-related protein complex AP-1, mu subunit 1	*Ap1m1*	Q3UG16	*Mus musculus*	1E-81	*Melanosome organization*
lcst_c31194	Tyrosinase related protein	*tyrp1*	Q6DGE4	*Danio rerio*	1E-84	
lcst_c60613	ras-related protein rab-8a	*rab8a*	A4FVK4	*Danio rerio*	8E-99	*Melanosome transport*
lcst_c1994	Inositol-pentakisphosphate 2-kinase	*ippk*	Q4JL91	*Danio rerio*	2E-33	
lcst_c2227	RAB11a, member RAS oncogene family	*rab11a*	Q5U3E1	*Danio rerio*	7E-75	
lcst_c43921	Tetratricopeptide repeat protein 8	*ttc8*	Q6P5I7	*Danio rerio*	8E-66	
lcst_rep_c10145	Chaperonin containing TCP1, subunit 2 (Beta)	*cct2*	Q6PBW6	*Danio rerio*	0	
lcst_c6090	Synembryn-B	*ric8b*	Q6DRJ9	*Danio rerio*	3E-77	*Pigment cell development*
lcst_c1817	Cadherin-2	*cdh2*	Q90275	*Danio rerio*	0	
lcst_c2222	N-ethylmaleimide-sensitive factor	*nsfa*	Q7ZU50	*Danio rerio*	0	*Pigment granule localization*
lcst_c31478	Dedicator of cytokinesis protein 7	*Dock7*	A2A9M4	*Mus musculus*	9E-84	*Pigmentation*
lcst_c30539	Dopachrome tautomerase	*dct*	A3KDL7	*Sus scrofa*	1E-36	
lcst_c2174	RNA polymerase-associated protein Ctr9 homolog	*ctr9*	A3KDM3	*Danio rerio*	0	
lcst_c307	Phosphoribosylglycinamide formyltransferase	*gart*	Q9I9E6	*Danio rerio*	0	
lcst_c45538	Lysosomal-trafficking regulator	*Lyst*	Q9Z2X9	*Rattus norvegicus*	6E-86	
lcst_c2408	Apoptosis regulator BAX	*Bax*	Q07813	*Mus musculus*	6E-34	*Positive regulation of developmental pigmentation*
lcst_c8805	A disintegrin and metalloproteinase with thrombospondin motifs 9	*Adamts9*	E9PYV8	*Mus musculus*	4E-67	*Positive regulation of melanocyte differentiation*
lcst_c546	Ras-related protein ralb-A	*ralb-a*	Q9YH09	*Xenopus laevis*	3E-65	*Regulation of developmental pigmentation*
lcst_c6473	Guanine nucleotide binding protein, alpha 11	*Gna11*	Q3UPA1	*Mus musculus*	1E-131	*Regulation of melanocyte differentiation*
lcst_c4062	Beta-adrenergic receptor kinase 2	*Adrbk2*	P26819	*Rattus norvegicus*	6E-144	*Rhodopsin metabolic process*

Transcripts identified in the Atlantic halibut skin transcriptome that are involved in vertebrate skin development / morphogenesis and pigmentation. The contig ID of the skin transcriptome assembly, Protein name, acronym, accession number (no.), organism and e-value are shown for each protein and they are grouped by biological function (when identified).

When the GI-tract transcriptome was compared with the *in-house* GI-tract specific database, 72 genes were identified. Identified gene transcripts included those with sequence similarity to signal transduction pathways, such as Sonic Hedgehog (Shh), Wnt and bone morphogenic protein (Bmp), as well as genes involved in gastric function (**Table 2.3,** Additional file 2.8).

The head transcriptome contained genes involved in thyroid gland development and thyroid hormone physiology, such as enzymes involved in the activation or inactivation of THs (*dio1*, *dio2*, *dio3*), TH receptors (*trαb* and *trb*), thyroid hormones transporters (*mct8*, *mct10*) and other nuclear receptors (**Table 2.4**). The pigmentation genes identified in head were coincident with those found in skin. Signalling pathways associated with development were well represented and included in the head transcriptome: i) the Wnt receptor signalling pathway (including casein kinases, low-density lipoprotein receptor related proteins, frizzled-related proteins, spontins, wnt11, wnt7, wnt8, wnt9); ii) the transforming growth factor beta (TGFβ) receptor signalling pathway (including activins, bone morphogenetic proteins, collagens, latent-transforming growth factor beta-binding proteins and tgf-beta receptors); iii) the Notch signalling pathway; iv) the Hippo signalling cascade, and v) the Hedgehog signalling pathway (Additional file 2.9).

Table 2.3. Genes of the vertebrate digestive system identified in the Atlantic halibut GI-tract transcriptome.

Contig ID	Protein name	Acronym	Accession no.	Organism	E-value	Biological role
lcgut_c14148	Adenosine deaminase	*Ada*	Q4FK28	*Mus musculus*	1E-41	*Embryonic digestive tract development*
lcgut_c24687	Protein kinase domain-containing protein, cytoplasmic	*Pkdcc*	Q5RJI4	*Mus musculus*	2E-46	
lcgut_c25681	Transforming growth factor beta receptor type 3 isoform b precursor	*tgfbr3*	Q90998	*Gallus gallus*	4E-36	
lcgut_c26069	Sal-like protein 1	*Sall1*	Q6P5E3	*Mus musculus*	1E-67	
lcgut_c31048	Forkhead box protein F1	*foxf1*	Q28BS5	*Xenopus tropicalis*	1E-55	
lcgut_c34421	Proprotein convertase subtilisin/kexin type 5	*Pcsk5*	Q04592	*Mus musculus*	1E-152	
lcgut_c17559	Ribosomal protein S6 kinase	*rps6ka3a*	Q7ZVH8	*Danio rerio*	5E-75	*Digestive tract development*
lcgut_c33030	TGF-beta receptor type-2	*Tgfbr2*	P38438	*Rattus norvegicus*	9E-40	
lcgut_c35109	G2/mitotic-specific cyclin-B1	*Ccnb1*	P24860	*Mus musculus*	7E-43	
lcgut_c901	Cytochrome P450 family 1 subfamily a polypeptide 1	*Cyp1a1*	Q05A20	*Mus musculus*	3E-156	
lcgut_c17435	Retinoid X nuclear receptor alpha	*NR2B1*	F1D8Q5	*Homo sapiens*	1E-76	*Midgut development*
lcgut_c186	Retinal dehydrogenase 1	*Aldh1a1*	P24549	*Mus musculus*	2E-179	
lcgut_c24118	Ornithine transcarbamylase, isoform CRA_a	*Otc*	Q543H3	*Mus musculus*	3E-72	
lcgut_c2518	Arginase-2, mitochondrial	*Arg2*	O08691	*Mus musculus*	2E-56	
lcgut_c2565	Proto-oncogene tyrosine-protein kinase receptor Ret	*RET*	P07949	*Homo sapiens*	3E-35	
lcgut_rep_c3756	Hydroxymethylglutaryl-coa synthase, mitochondrial	*HMGCS2*	P54869	*Mus musculus*	5E-171	
lcgut_c25668	Homeobox protein Nkx-3.2	*Nkx3-2*	P97503	*Mus musculus*	6E-35	*Intestinal epithelial cell development*
lcgut_c374	GATA-binding protein 6	*gata6*	ENSDARP00000051997	*Danio rerio*	0	

lcgut_c981	Protein-tyrosine kinase 6	*Ptk6*	Q64434	*Mus musculus*	9E-64	
lcgut_rep_c3687	Anterior gradient protein 2 homolog	*agr2*	Q5RZ65	*Danio rerio*	7E-66	
lcgut_rep_c15924	Polypyrimidine tract binding protein 1a	*ptbp1a*	Q503D3	*Danio rerio*	7E-112	*Intestinal epithelial structure maintenance*
lcgut_c2805	Heart and neural crest derivatives expressed transcript 2	*hand2*	Q5XJD8	*Danio rerio*	7E-49	*Determination of intestine left/right asymmetry*
lcgut_c17287	Platelet-derived growth factor receptor alpha	*Pdgfra*	P26618	*Mus musculus*	4E-86	*Embryonic digestive tract morphogenesis*
lcgut_c2545	Sonic hedgehog protein A	*shha*	Q92008	*Danio rerio*	2E-41	
lcgut_c30553	DNA-binding protein inhibitor ID-2	*id2*	Q6PBD7	*Xenopus tropicalis*	8E-44	
lcgut_c32097	GATA binding protein 4	*gata4*	ENSDARP00000090333	*Danio rerio*	2E-42	
lcgut_c37022	Transcription factor 21	*tcf21*	Q32PV5	*Danio rerio*	4E-69	
lcgut_c17569	Hepatocyte nuclear factor 1-beta-A	*hnf1ba*	A1L1N5	*Danio rerio*	5E-66	*Digestive tract morphogenesis*
lcgut_c19328	Caudal type homeobox 1	*CDX1*	ENSP00000367043	*Homo sapiens*	3E-31	
lcgut_c20926	Mib protein	*Mib*	B3DGQ0	*Danio rerio*	8E-45	
lcgut_c22447	Ephrin type-B receptor 3	*Ephb3*	P54754	*Mus musculus*	1E-39	
lcgut_c22825	Probable rna-binding protein 19	*rbm19*	Q6DRI6	*Danio rerio*	3E-32	
lcgut_c25556	Vang-like 2 (Van gogh, Drosophila), isoform CRA_b	*Vangl2*	D3YY75	*Mus musculus*	4E-38	
lcgut_c26	Claudin 15 like	*cldn15a*	Q7T2E7	*Danio rerio*	3E-82	
lcgut_c27711	Secreted frizzled-related protein 1	*Sfrp1*	Q8C4U3	*Mus musculus*	1E-49	
lcgut_c38245	Protein kinase C iota type	*prkci*	Q90XF2	*Danio rerio*	2E-87	

lcgut_c14247	Beta-1,3-galactosyl-O-glycosyl-glycoprotein beta-1,6-N-acetylglucosaminyltransferase 3	*Gcnt3*	Q5JCT0	*Mus musculus*	2E-57	*Intestinal absorption*
lcgut_c14318	2-acylglycerol O-acyltransferase 2	*Mogat2*	Q80W94	*Mus musculus*	8E-73	
lcgut_c425	Sodium/glucose cotransporter 1	*Slc5a1*	F6XY79	*Mus musculus*	6E-142	
lcgut_rep_c3628	Fatty acid binding protein 2, intestinal	*Fabp2*	Q53YP5	*Mus musculus*	9E-47	
lcgut_rep_c38188	Fatty acid binding protein 1, liver	*Fabp1*	Q3V2F7	*Mus musculus*	9E-35	
lcgut_c2583	ATP-binding cassette sub-family G member 5	*Abcg5*	Q99PE8	*Mus musculus*	6E-168	*Intestinal cholesterol absorption*
lcgut_c280	Niemann-Pick C1-like protein 1	*Npc1l1*	Q6T3U4	*Mus musculus*	6E-140	
lcgut_c30941	Caveolin	*cav1*	Q6YLH9	*Danio rerio*	3E-65	
lcgut_c3243	Pancreatic triacylglycerol lipase	*Pnlip*	Q6P8U6	*Mus musculus*	6E-99	
lcgut_c34406	Sterol O-acyltransferase 2	*SOAT2*	O75908	*Homo sapiens*	1E-89	
lcgut_c508	ATP-binding cassette sub-family G member 8	*Abcg8*	Q9DBM0	*Mus musculus*	0	
lcgut_rep_c3552	Pancreatic lipase	*pl*	D4P6H2	*Sus scrofa*	4E-83	
lcgut_rep_c3840	Annexin	*anxa2b*	Q6DHD8	*Danio rerio*	2E-133	
lcgut_c20773	Cholecystokinin receptor type A	*Cckar*	O08786	*Mus musculus*	1E-47	*Gastric acid secretion/Regulation*
lcgut_c14119	Pepsinogen A form iib precursor	*pep2b*	AAD56284	*Pseudopleuronectes americanus*	0	
lcgut_c1099	Bone morphogenetic protein 2a	*bmp2a*	ENSDARP00000013686	*Danio rerio*	3E-35	
lcgut_c17255	Histamine N-methyltransferase	*hnmt*	ENSORLP00000025386	*Oryzias latipes*	1E-87	
lcgut_c17921	MAD homolog 9	*smad9*	ENSDARP00000031108	*Danio rerio*	1E-85	
lcgut_c20823	Histamine receptor H2	*hrh2*	ENSORLP00000004946	*Oryzias latipes*	2E-24	

lcgut_c22281	Epidermal growth factor receptor a	*egfra*	ENSDARP00000125265	*Danio rerio*	4E-42
lcgut_c25854	SRY-box containing gene 2	*sox2*	ENSDARP00000095266	*Danio rerio*	2E-21
lcgut_c28926	Forkhead box A1 (HNF3?)	*foxa1*	ENSDARP00000002213	*Danio rerio*	7E-44
lcgut_rep_c6868	Protein wntmber 5a	*wnt5a*	F1Q8M2	*Danio rerio*	5E-26

List of candidate genes in the Atlantic halibut GI-tract transcriptome assembly that are involved in vertebrate digestive system development and morphogenesis. The contig ID of the GI-tract transcriptome assembly, protein name, acronym, accession number (no.), organism and e-value are shown for each protein and they are grouped by biological function (when identified).

Table 2.4. Genes involved in the TH axis identified in the Atlantic halibut head, skin and GI-tract transcriptomes.

Protein name	Acronym	Accession no.	Organism	Head	Skin	GI-tract	Biological role
Thyrotropin-releasing hormone	*trh*	ACI68323	*Salmo salar*	lchead_c49703			*Hormone-mediated signalling pathway*
Bteb1 protein	*Klf9*	Q8CEC4	*Mus musculus*	lchead_c5876	lcst_c61990		*Cellular response to thyroid hormone stimulus*
Cathepsin B	*Ctsb*	P10605	*Mus musculus*	lchead_rep_c17340		lcgut_c971	
Cathepsin S	*Ctss*	Q3UD32	*Mus musculus*	lchead_c2408	lcst_c25054		
GAS2-like protein 1	*Gas2l1*	Q8JZP9	*Mus musculus*	lchead_c63583			
Mediator of RNA polymerase II transcription subunit 1	*Med1*	Q925J9	*Mus musculus*	lchead_c54375	lcst_c53801		
Rhombotin-2	*Lmo2*	A2BHP2	*Mus musculus*	lchead_rep_c19211			
Tyrosine-protein kinase receptor	*Kit*	Q63116	*Rattus norvegicus*	lchead_c88982		lcgut_c981	
GATA binding protein 3	*gata 3*	Q0ZHH4	*Sus scrofa*	lchead_c10759			*Positive regulation of thyroid hormone generation*
Serine protease hepsin	*Hpn*	O35453	*Mus musculus*	lchead_c1056	lcst_c55583		
Fibroblast growth factor 10	*Fgf10*	O35565	*Mus musculus*	lchead_c59444			*Thyroid gland development*
Forkhead box E3	*foxe3*	B0UXI3	*Danio rerio*	lchead_c14669	lcst_c7916		
Heart and neural crest derivatives expressed transcript 2	*hand2*	Q5XJD8	*Danio rerio*	lchead_c14402			
Hematopoietically-expressed homeobox protein hhex	*hhex*	Q9IAV3	*Danio rerio*	lchead_c76036			
Homeobox protein Nkx2.1a	*nkx2.1a*	Q9I8L7	*Danio rerio*	lchead_rep_c28603			
MAD homolog 3	*Smad3*	A2CG44	*Mus musculus*	lchead_c8437	lcst_c2973	lcgut_c21904	

NK2 homeobox 1	*Nkx2-1*	Q6PFE0	*Mus musculus*	lchead_rep_c45357			
Sonic hedgehog protein	*Shh*	Q62226	*Mus musculus*	lchead_c10675		lcgut_c2545	
T-cell acute lymphocytic leukemia protein 1 homolog	*tal1*	O93507	*Danio rerio*	lchead_c1186			
Thyroglobulin	*Tg*	O08710	*Mus musculus*	lchead_c4966			
Transcription factor gata5	*gata5*	Q9W6U0	*Danio rerio*	lchead_c49264			
Transforming growth factor beta-2	*Tgfb2*	P27090	*Mus musculus*	lchead_rep_c18013	lcst_c97		
Vascular endothelial growth factor A-A	*vegfaa*	O73682	*Danio rerio*	lchead_rep_c38578			
Vascular endothelial growth factor receptor kdr-like	*kdrl*	Q8AXB3	*Danio rerio*	lchead_c15716			
Aldehyde dehydrogenase family 1 member A3	*Aldh1a3*	G3UWP3	*Mus musculus*	lchead_rep_c51532			*Thyroid hormone binding*
Cathepsin H	*ctsh*	B2D1T2	*Sus scrofa*	lchead_rep_c18375	lcst_c35788		
Retinaldehyde dehydrogenase 3	*Aldh6*	Q9DD46	*Gallus gallus*	lchead_c4855	lcst_c276		
Estrogen receptor alpha	-	Q2PUG8	*Hippoglossus hippoglossus*	lchead_c11863			*Thyroid hormone receptor activity*
Farnesoid X activated receptor	-	Q8SPF5	*Oryctolagus cuniculus*	lchead_c38827			
Nuclear receptor subfamily 1, group D, member 4	*nr1d4a*	B8A510	*Danio rerio*	lchead_c5000	lcst_c4716		
Nuclear receptor subfamily 1, group D, member 1	*nr1d1*	Q503Y6	*Danio rerio*	lchead_c56865		lcgut_c766	
Nuclear receptor subfamily 2, group E, member 3	*nr2e3*	A0FCT3	*Xenopus tropicalis*	lchead_rep_c19272	lcst_c50411		
Nuclear receptor subfamily 1, group H, member 4	*nr1h4*	Q6DGW7	*Danio rerio*	lchead_c38092			
Orphan nuclear receptor BXR-beta	*nr1i2*	Q9DF24	*Xenopus laevis*	lchead_c53830			

Orphan nuclear receptor HZF-2	*Nr1d2*	Q62702	*Rattus norvegicus*	lchead_c13737			
Rev-erbgamma-B	*Nr1d4b*	Q1L683	*Danio rerio*	lchead_c801			
Thyroid hormone receptor alpha B	*trαb*	B7XBZ0	*Solea senegalensis*	lchead_c73126	lcst_c51070		
Thyroid hormone receptor beta	*trβ*	A8R655	*Solea senegalensis*	lchead_c15487	lcst_c29077		
Monocarboxylate transporter 10	*mct10*	NP_001073497	*Danio rerio*	lchead_c4262	lcst_c309		*Thyroid hormone transmembrane transporter activity*
Solute carrier organic anion transporter family member 1A5	*Slco1a5*	E0CX25	*Mus musculus*	lchead_c60364			
Solute carrier organic anion transporter family member 4A1	*Slco4a1*	Q8K078	*Mus musculus*	lchead_c13235			
Thyroxine-binding globulin	*Serpina7*	P35577	*Rattus norvegicus*	lchead_c2058			
Monocarboxylate transporter 8	*mct8*	NP_001245159	*Danio rerio*	lchead_c13478	lcst_c54175	lcgut_c2689	
Canalicular multispecific organic anion transporter 1	*Abcc2*	Q63120	*Rattus norvegicus*	lchead_c7363		lcgut_c1215	
Paired box protein Pax-8	*PAX8*	Q06710	*Homo sapiens*	lchead_c53444			*Thyroid-stimulating hormone receptor activity*
Thyroid stimulating hormone receptor	*tshr*	F1Q981	*Danio rerio*	lchead_c79782			
Iodothyronine deiodinase type I	*dio1*	B1B569	*Takifugu rubripes*	lchead_c4984	lcst_c3609	lcgut_c27346	*Thyroxine 5-deiodinase activity*
Iodothyronine deiodinase type II	*dio2*	B3Y056	*Oryzias latipes*	lchead_c13614			
Iodothyronine deiodinase type III	*dio3*	B1B572	*Takifugu rubripes*	lchead_c39730	lcst_c58807		

List of candidate genes identified in the Atlantic halibut head transcriptome with a role in thyroid gland development and thyroid hormone (TH) synthesis, transport and activity. Protein name, symbol, accession number (no.) and organism are shown for each gene product and they are grouped by biological function (when associated). Contig ID from the head, GI-tract and skin transcriptome assembly is given.

2.3.1.4. Identification of thyroid hormone responsive genes

Overall, 135 putative TH-responsive genes were identified in the skin, GI-tract and head transcriptome, which included TFs, genes involved in DNA replication, cell proliferation, cell growth and differentiation and collagen synthesis and degradation (**Figure 2.2**). The skin transcriptome contained 113 putative TH-responsive genes that mainly corresponded to structural proteins, proteases, actins, transmembrane proteins, and several membrane transport proteins of the solute carrier group (**Figure 2.2**). The GI-tract transcriptome contained 62 putative TH-responsive genes and included genes involved in DNA replication, cell cycle and metabolic pathways (**Figure 2.2**). The head transcriptome was enriched with 99 putative TH-responsive genes of which 11 were specific to the head transcriptome and included TFs, DNA replication and ion binding proteins (**Figure 2.2**).

Figure 2.2. Putative thyroid hormone (TH) responsive genes identified in the Atlantic halibut transcriptomes. Heat map of putative thyroid hormone (TH) responsive genes identified in the transcriptomes of skin, GI-tract and head of metamorphosing Atlantic halibut. The acronyms of TH-responsive genes are indicated and full names are given in Additional file 2.4.

2.3.2. SOLiD transcriptome comparison between metamorphic stage transitions

2.3.2.1. Identification of differentially expressed transcripts during metamorphosis

Pairwise comparisons of whole larvae transcriptomes between metamorphic stages generated a very low number of DE genes (Additional file 2.15f-j). For the premetamorphic stage 5, 4,155 transcripts were DE when the transcriptome was compared with the transcriptome for the juvenile stage. In contrast, more than 8,000 transcripts were DE when the transcriptome of whole larvae of each metamorphic stage was compared with the transcriptome of whole juveniles. The majority of the 8,000 DE transcripts per stage were up-regulated in the juvenile stage relative to the metamorphic stages (**Figure 2.3**) and 3,336 of the DE transcripts were common between the metamorphic stages (7, 8, 9A, 9B and 9C). The number of DE transcripts specific to each stage was 403, 365, 1,214, 446 and 362 for stages 7, 8, 9A, 9B and 9C, respectively. The number of DE transcripts common between stages 7 and 8 was 5,999, between stages 8 and 9A was 5,638, between stages 9A and 9B was 5,272 and between 9B and 9C was 5,972.

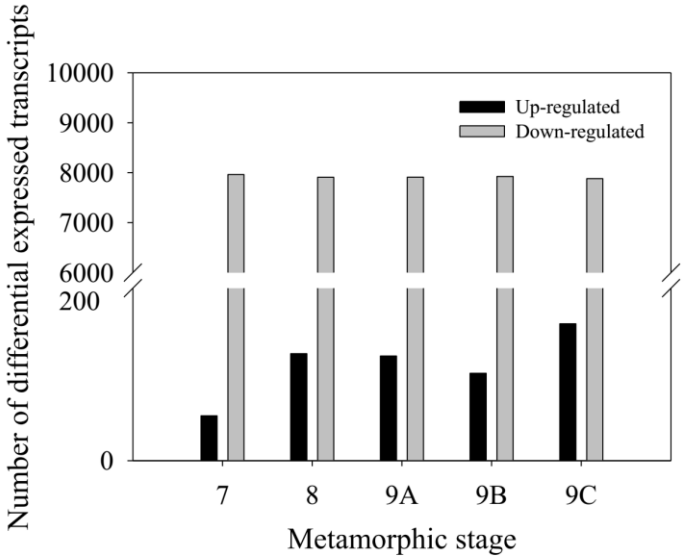

Figure 2.3. Differentially expressed transcripts between Atlantic halibut metamorphic stages and juveniles. Graphical representation of the relative number of DE transcripts (up- and down-regulated) identified when pro-metamorphic (stage 7), proclimax-metamorphic (stage 8) and metamorphic climax (9A, 9B and 9C) Atlantic halibut are compared with the juvenile post-metamorphic stage.

2.3.2.2. Expression of thyroid related transcripts during metamorphosis

TH-responsive transcripts DE with SOLiD transcriptional profiling were identified by filtering all differential transcripts using the "in house" database. Overall, 145 putative TH-responsive transcripts were DE (log2 of the fold change of juvenile versus all metamorphic stages), (**Figure 2.4**, detailed information regarding transcripts in Additional files 2.16 and 2.17). The majority of the putative TH-responsive transcripts were down-regulated in the metamorphic stages relative to the juvenile (**Figure 2.4A**). The exception was stages 7 and 8 that had 10 and 2 up-regulated putative TH-responsive transcripts, respectively (Additional file 2.16). Comparison of the putative TH-responsive genes in each stage revealed 41 that were common. Stage 8 had the greatest number of putative TH-responsive transcripts (119), followed by stage 9B (101), stage 9A (98), stage 9C (96) and then stage 7 (85) (**Figure 2.4C**). Enriched reactomes of TH-responsive transcripts during metamorphosis included cellular response to stress, the cell cycle, DNA repair, DNA replication, apoptosis, metabolism, and signal transduction (Additional file 2.18).

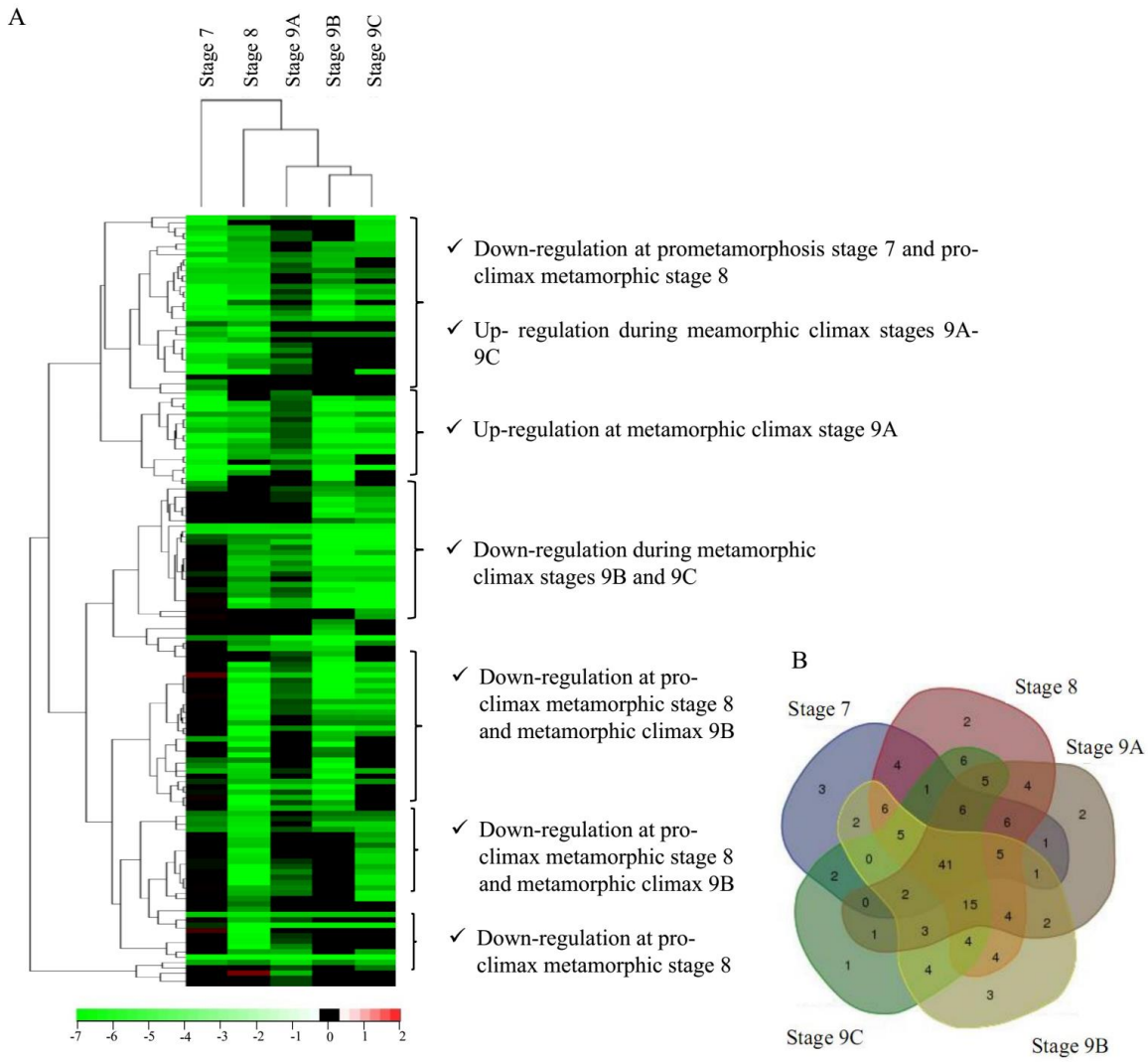

Figure 2.4. Putative TH-responsive transcripts with differential expression between Atlantic halibut metamorphic stages and juveniles. Clustering of the putative thyroid hormone (TH) responsive transcripts with differential expression between metamorphic stages and juveniles of Atlantic halibut. A - Heat map of the DE TH-responsive transcripts clustered by expression pattern. Transcript expression is represented as log2 of fold change for metamorphic stages versus juveniles; B - Venn diagram revealing the number of DE TH-responsive transcripts that are shared between stages or that have a stage specific expression.

2.3.3. Up-regulation of TH axis related genes during metamorphic climax

Transcripts that were not DE in SOLiD analysis (presumably due to methodological limitations) but that are involved in the thyroid axis, such as, TH production (thyroglobulin - *tg*), transport (monocarboxylated transporter 8 - *mct8*, monocarboxylated transporter 10 - *mct10*), metabolism (deiodinase 1 - *dio1*, deiodinase 2 - *dio2*, deiodinase 3 - *dio3*) and action (thyroid hormone receptor alpha A - *trαa*, thyroid hormone receptor alpha B - *trαb*, thyroid

hormone receptor beta - *trβ*) were analyzed by qPCR using the same samples used for SOLiD analysis (**Figure 2.5,** Additional file 2.19). Tg transcript levels were lower in the pre-metamorphic stage (stage 5), significantly ($p < 0.05$) higher during metamorphosis, and then decreased significantly ($p < 0.05$) in the post-metamorphic stage (Additional file 2.19). TRs had a variable expression during metamorphosis and the relative transcript abundance was *trβ* > *trαb* > *trαa* (**Figure 2.5A**). The transcript abundance of all the TRs increased significantly ($p < 0.05$) during metamorphosis. *trαa* transcript abundance was significantly higher at metamorphic climax (stages 9B and 9C) relative to stages 5, 6 and 7 and *trαb* transcript abundance was also significantly ($p < 0.05$) higher at metamorphic climax (stage 9A) compared to premetamorphic stage 7. The transcript abundance of *trβ* throughout metamorphosis (stages, 8, 9A, 9B and 9C) was significantly ($p < 0.05$) higher than during pre-metamorphosis (stages 5 and 7). The transcript abundance of the three TRs was significantly ($p < 0.05$) lower in juveniles relative to metamorphic climax (9C), (**Figure 2.5A,** Additional file 2.19). The relative gene expression of *mct10* was higher than that of *mct8* throughout metamorphosis, although it did not change significantly at any stage (**Figure 2.5B,** Additional file 2.19). *mct8* gene expression increased significantly ($p < 0.05$) in stage 9A and 9B relative to stage 8. In juveniles, *mct8* mRNA expression levels were significantly ($p < 0.05$) lower than in metamorphic stages. The gene expression profile of the three deiodinases (*dio1*, *dio2* and *dio3*) during metamorphosis was similar, and all were significantly ($p < 0.05$) up-regulated during metamorphosis (stage 9A-9C) compared to pre-metamorphic (stage 7 and 8) and juvenile stages (**Figure 2.5B,** Additional file 2.19).

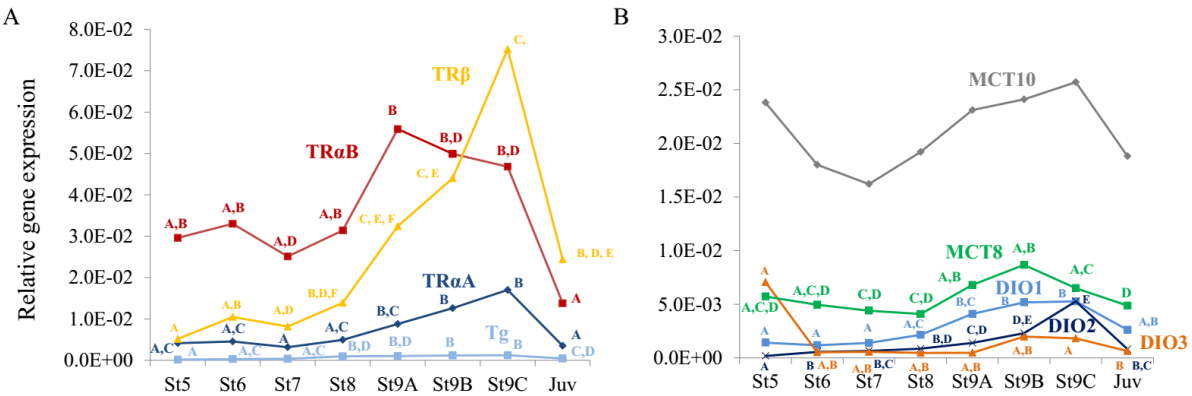

Figure 2.5. Expression pattern of transcripts involved in the TH cascade during halibut metamorphosis. Schematic representation of the relative gene expression by qPCR of **(A)** thyroid hormones action **(***trαa, trαb, trβ*) and production (*tg*); and **(B)** thyroid hormones transport (*mct8*, *mct10*) and regulation of the cellular availability of THs (*dio1*, *dio2*, *dio3*) during Atlantic halibut metamorphosis. Results are presented as relative gene expression (arbitrary units). For detailed information and significance between stages for each transcript, please see Additional file 2.19.

2.3.4. Confirmation of differentially expressed transcripts in SOLiD by qPCR

Six transcripts from SOLiD analysis of metamorphosing Atlantic halibut were also analyzed by qPCR (Additional file 2.20) and had a concordant expression pattern (**Figure 2.6**). Transcripts with unchanged transcript abundance during metamorphosis in SOLiD: ribosomal protein L7 (*rpl7*) and 40S ribosomal protein S30 (*fau*) were not significantly different in qPCR. Transcripts, alpha-globin 1 (*gloα1*), carboxypeptidase A2 (*cpa2*), apolipoprotein AI (*apoai*) and type I keratin isofom 2 (*krt1i2*), significantly modified in SOLiD analysis were also significantly ($p < 0.05$) modified in the qPCR results during metamorphosis. A high and significant positive correlation (r = 0.843; $p = 1.07 \times 10^{-7}$) was obtained when results of SOLiD analysis for six genes (*gloα1*, *cpa2*, *apoai*, *krt1i2*, *rpl7*, *fau*) were compared with qPCR expression levels (relative to the geometric mean of 40S ribosomal protein S4 and Elongation factor 1 alpha - *rps4*/*efiai*) for metamorphic stages 5 - 9C (**Figure 2.6A**). A lower, but significant positive correlation (r = 0.576; $p = 1.23 \times 10^{-4}$) was obtained when the juvenile post-metamorphic stage was included in the correlation analysis between SOLiD and qPCR data (**Figure 2.6B**).

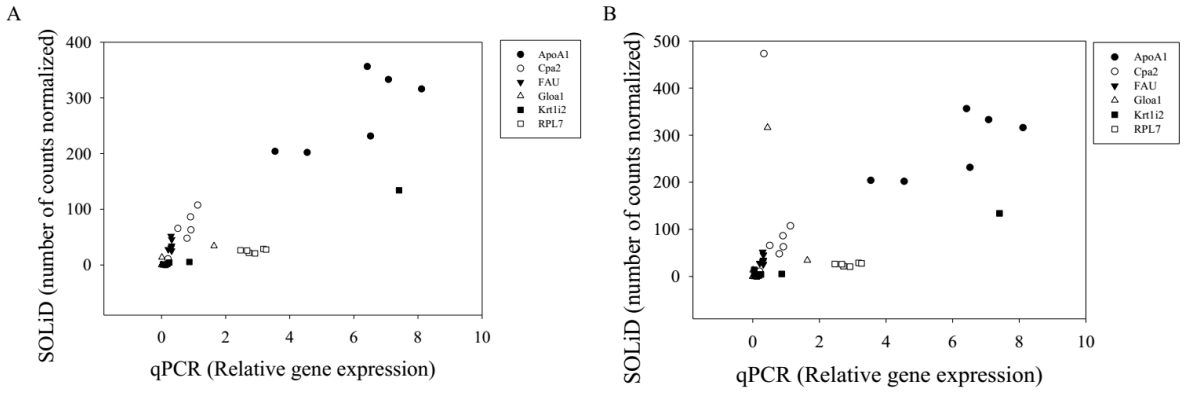

Figure 2.6. Correlation analysis between SOLiD and qPCR expression analysis. Correlation analyses between SOLiD and qPCR expression of transcripts with a constant expression and transcripts with a modified expression during Atlantic halibut metamorphosis. Comparison of normalized counts (SOLiD data) and relative gene expression profile (qPCR data) of six genes: apolipoprotein A-I (*apoai*), carboxypeptidase A2 (*cpa2*), 40S ribosomal protein S30 (*fau*), alpha-globin 1 (*gloα1*), type I keratin isoform 2 (*krt1i2*) and ribosomal protein L7 (*rpl7*). Different genes are represented by a specific symbol in the graph. Panel A - Pearson Product Moment Correlation using metamorphic stages 5 to 9C ($r = 0.843$; $p = 1.07 \times 10^{-7}$). Panel B - A Pearson Product Moment Correlation using metamorphic stages 5 to juvenile ($r = 0.576$; $p = 1.23 \times 10^{-4}$).

2.4. Discussion

Changes during flatfish metamorphosis are not limited to modifications in external morphology but include many structural and functional modifications. The role of TRs as ligand activated TFs means that a significant part of the action of THs on tissues is associated with tissue specific modifications in the transcriptome. In the present study, the large size of Atlantic halibut was utilized to establish for the first time in flatfish specific transcriptomes for larval skin, GI-tract and head during metamorphosis using 454 sequencing. SOLiD sequencing of individual larvae (n = 3/stage) and stage specific comparisons (e.g. 7 vs 8; 8 vs 9A, 9A vs 9B and 9B vs 9C) revealed a very low number of DE transcripts and no sudden or dramatic change between any particular stage. In contrast, pairwise comparisons of the juvenile transcriptome with stage specific transcriptomes revealed a high number of DE transcripts (> 8,000/stage), with the majority highly up-regulated in the juvenile stage.

Comparisons of the approximately 8,000 differential transcripts per stage generated a stage specific molecular fingerprint. The large majority of DE transcripts (approx. 98%) were not classified as TH-responsive and presumably represented transcripts underlying ontogenetic changes and belonging to gene networks that lead to the overt changes that accompany metamorphosis. The latter probably explains why blocking TH action with MMI during flatfish metamorphosis is not lethal and only modifies the development of some specific tissues (Schreiber et al., 2010). In line with this observation THs maintain neoteny in only some of the tissues in salamanders (Callery and Elinson, 2000; Rosenkilde and Ussing, 1996; Vlaeminck-Guillem et al., 2006). The link between TH-responsive pathways and the numerous other gene networks that change during metamorphosis was not established in the present study, but in future studies will be explored. The majority of the putative DE TH-

responsive genes clustered in specific metamorphic stages rather than over the duration of metamorphosis. The response of the majority of putative TH-responsive transcripts was none synchronous with the peak in whole body TH levels, previously reported to occur at stage 9 and 10 for Atlantic halibut (Galay-Burgos et al., 2008). The non-synchronous tissue specific response of putative TH-responsive genes during metamorphosis suggests the chronology of tissue responsiveness during metamorphosis may vary, presumably as a result of differences in cellular responsiveness to THs. Such a phenomenon was reported in a recent study of GI-tract development in the Atlantic halibut (Gomes et al., 2014a).

2.4.1. Metamorphosis-specific tissue transcriptome

Next-generation pyrosequencing 454 technology has been used to characterize the transcriptome from several flatfish species. In turbot (*Scophthalmus maximus*) the study focused on immune related transcripts (Pereiro et al., 2012), in the common sole a pooled larval and adult liver and GI-tract transcriptome was established (Ferraresso et al., 2013) and in Senegalese sole and common sole reference transcriptomes were derived by sequencing several tissue from juveniles and adults (Benzekri et al., 2014). An oligo-array study of common sole development from larva to juvenile revealed a large variety of biological processes occurred during development and that some genes of the thyroid axis were associated with the initiation of metamorphosis (Ferraresso et al., 2013).

To our knowledge, ours is the first next generation sequencing study analyzing individual tissues and larvae of a metamorphosing flatfish. More than 400,000 sequences per specific-tissue were obtained after filtering to remove poor quality sequences and contaminating transcripts (e.g. prey in the GI-tract Artemia sp., etc). This data substantially increases available molecular resources for Atlantic halibut (Douglas et al., 2007; Mommens et al., 2010). MIRA3 assembly of the tissue transcriptomes (head: 1,186,541; skin: 830,524 and GI-tract: 418,303) generated 90,676; 65,530 and 38,426 contigs for head, skin and GI-tract, respectively, which was similar to previous studies using the same sequencing strategy (Yúfera et al., 2012b), but higher than the gene content of the genome of model teleost species e.g. 19,388 for *Takifugu rubripes* and 31,953 for *Danio rerio* (www.ensembly.org). Technical issues, read length and the heuristic nature of the assembly methods, no doubt

explain the relatively high transcript number as was previously observed in a liver transcriptome study of *Zoarces viviparus* (Kristiansson et al., 2009). Transcript annotation levels in Atlantic halibut were similar to previous 454 studies in turbot, seabream, European eel and silver carp (Coppe et al., 2010; Fu and He, 2012; Pereiro et al., 2012; Yúfera et al., 2012b); the contribution of alternative splicing to the high number of assembled transcripts was not established in the study.

2.4.2. Candidate biological processes and pathways during metamorphosis

Knowledge about the mechanisms underlying the global molecular and cellular changes during fish development, including functional gene annotation during metamorphosis, has significantly increased in the last decade due to genomics and transcriptomics technologies. Previous studies using microarrays, expressed sequence tags (ESTs) and candidate genes in Atlantic halibut identified genes involved in muscle, skin, immune system, signal transduction and transcription factor activity in adult and larvae, but information about larvae undergoing metamorphosis is limited (Campinho et al., 2012; Campinho et al., 2007a; Douglas et al., 2007; Galay-Burgos et al., 2006). Studies in Solea senegalensis focusing more on metamorphosis generated 10,000 ESTs (Cerda et al., 2008) that are enriched in transcripts involved in the reorganization of somatic tissues, such as, ribosomal proteins, elongation factors and cytoskeletal proteins. The global gene ontology of the individual tissue transcriptomes characterized in the present study, are far more detailed than previous EST studies, but where there is coincident sequence data the results are similar. The GO results of metamorphosing Atlantic halibut is similar to results for other developing teleosts (larval, juvenile and adult) (Salem et al., 2010; Yúfera et al., 2012b), but also between sexes (male and female), whole fish (Zhang et al., 2011) and fish under diverse challenges (e.g. viral challenge) (Pereiro et al., 2012), suggesting maintenance of tissue, organ and organism function involves an overwhelming number of common genes that emerge irrespective of the experimental situation. To overcome this problem in the present study we applied a Fisher's exact test to identify significantly over/under-represented GO terms for the tissue-specific transcriptomes of metamorphosing Atlantic halibut. The 454 transcriptome approach gave insight into tissue specific molecular changes and allied to SOLiD analysis of

several individuals / stage revealed core TH-responsive genes responsible for the timing of stage specific responses of individual tissues.

The metamorphosing Atlantic halibut skin transcriptome: is enriched in GO terms related to epidermis and connective tissue development, appendage morphogenesis and pigmentation, which is concordant with the morphological modifications observed (Roosterman et al., 2006; Zouboulis, 2000). Genes involved in vertebrate skin development and morphogenesis are also enriched and include components of the extracellular matrix [ECM, collagen type I (*col1a1*, *col1a2*) and type V (*col5a2*) (Le Guellec et al., 2004; Shoulders and Raines, 2009], ECM remodelling [discoidin domain receptor 1 (*ddr1*) (Olaso et al., 2011; Vogel et al., 2006)] and ECM degradation [stromelysin-3 (*mmp11*), collagenase 3 (*mmp13*), matrix metallopeptidase 2 (*mmp2*) and metalloproteinase inhibitor 3]. Several of the enriched ECM proteins in skin are responsive to THs (Brunelli et al., 2015; Ishizuya-Oka, 2011; Page et al., 2009; Page et al., 2008; Suzuki et al., 2009) and in SOLiD analysis their DE pattern in stages is asynchronous presumably because of their association with opposing biological processes. The TH-responsive proteins together with the detected TH-independent growth factors, chemokines, adhesion molecules and proteoglycans have previously been identified in relation to tissue differentiation, development and morphogenesis in vertebrate skin (Le Guellec et al., 2004; Page et al., 2008; Suzuki et al., 2009; Watt and Fujiwara, 2011).

MMP genes identified for the first time in Atlantic halibut skin may be associated with larval-type cell apoptosis during ECM degradation as previously reported in *Xenopus*. For example, collagenase 3 (*mmp13*) has an important role in *Xenopus* body skin remodelling during metamorphosis (Suzuki et al., 2009) and this transcript is present in the halibut larval skin transcriptome and is DE in SOLiD analysis of several individuals / stage with a significant reduction post-metamorphosis. Pathways involved in “focal adhesion” and “tight junction” are also DE in pools of pre-metamorphic *Solea solea* (Ferraresso et al., 2013). The enriched transcripts identified during Atlantic halibut metamorphosis that contribute to pigmentation are of practical interest as abnormal pigmentation can have a significant impact on commercial production of flatfish (Darias et al., 2013; Ottesen and Strand, 1996; Power et al., 2008; Tagawa and Aritaki, 2005).

The GI-tract in metamorphosing Atlantic halibut: undergoes extensive remodelling to prepare it for the shift in habitat and diet of the juvenile (Gomes et al., 2014a; Gomes et al., 2015; Luizi et al., 1999). SOLiD analysis revealed DE of digestive enzymes, such as trypsin, chymotrypsin and phospholipase A2 during Atlantic halibut metamorphosis, as previously reported in other fish species (Ozkizilcik et al., 1996; Zambonino Infante and Cahu, 1999; Zambonino et al., 2008). Our enriched GO results for GI-tract development in Atlantic halibut are similar to that reported in *Xenopus*, in which GO terms related to digestion are "shut down" at metamorphic climax, but increase again at the end of metamorphosis (Heimeier et al., 2010). The results of the present study corroborate those of a detailed study of GI-tract development in Atlantic halibut that linked up-regulation of pepsinogen and H^+/K^+-ATPase α and β subunit with acquisition of a functional proteolytic stomach in early juveniles (Gomes et al., 2014a). However our results diverge from those of an earlier Atlantic halibut microarray study in which genes involved in digestion are more abundant in larvae entering metamorphosis (2008), and this may be a consequence of differences in staging, sample composition (pools of larvae were used in previous studies) and the more comprehensive results possible with NGS.

The head transcriptome: The enrichment in the head transcriptome of bone related genes ties in with experiments in *Paralichthys lethostigma* in which the development and growth of both sacculus and utricle otoliths are TH dependent during metamorphosis (Schreiber et al., 2010). Alpha-tectorin, otolin and plasma membrane calcium ATPase are also enriched in the Atlantic halibut head transcriptome and a previous candidate gene study suggested they are TH-responsive during flatfish metamorphosis (Wang et al., 2011). Several TFs specific for thyroid gland development, such as homeobox protein NK2.1, hematopoietically expressed homeobox (*hhex*) and *pax8* are enriched in the Atlantic halibut head transcriptome (Fernandez et al., 2015), and suggests that modification of the thyroid tissue is essential for successful metamorphosis (Klaren et al., 2008) and disruption of this process may explain failed metamorphosis in some cases.

Enriched pathways in metamorphosing Atlantic halibut: revealed as expected that the essential signaling pathways that trigger tissue development and cell proliferation and differentiation (e.g. Notch, Sonic hedgehog, Wnt, BMP) (Botchkarev and Sharov, 2004;

Ingham and McMahon, 2001; Janicke et al., 2007; Logan and Nusse, 2004; Paridaen and Huttner, 2014; Pascual and Aranda, 2013), are well represented in all three tissue transcriptomes. This fact lends support to the idea that in Atlantic halibut it is probably not remodelling that gives rise to juvenile tissue but rather de novo tissue development during metamorphosis, as has been demonstrated in *Xenopus* (Huggins et al., 2012; Ishizuya-Oka et al., 2009; Sun et al., 2013). Several of the signaling pathways are regulated by THs and specific studies will be required to establish their precise mode of action and the tissue specific consequences of their up-regulation.

The majority of DE genes detected by SOLiD analysis of several individual halibut larvae per stage: during metamorphosis are not directly TH-responsive, suggesting that many of the TH effects may be indirect. Cross-referencing of putative TH-responsive genes in whole larvae with the tissue specific transcriptomes provides insight into core tissue changes during metamorphosis. The down-regulation of transcripts linked to the MAPK signalling cascade (*c-raf, kras* and *c-jun*) during metamorphosis suggests the coordination of TH actions may be via modulation of signalling pathways as has been suggested in *Xenopus* (Veldhoen et al., 2002). Similarly, modification in TFs may be another way in which THs bring about an indirect effect. Thus fos-related antigen-2 (*fosl2* or *fra-2*), *sox4, tfpa2, tgfb, hmg1, cebpd, gtf2h, nfix* and *gtf2f* that are all TH-responsive (Buchholz et al., 2006; Das et al., 2009; Furlow and Kanamori, 2002; Yúfera et al., 2012a) peaked at metamorphic climax (stage 9A/9B). This is also reminiscent of what occurs during *Xenopus laevis* metamorphosis where TFs have a central role in tissue specific TH-induced programs (Buchholz et al., 2007; Das et al., 2006; Helbing et al., 2003).

The reliability of the results of SOLiD DE analysis is generally confirmed by comparison to the results of previous candidate gene studies in fish and amphibians. For example, osteonectin (SPARC), that plays an essential role in tissue morphogenesis (Brekken and Sage, 2001; Tremble et al., 1993; Yan et al., 2003) is strongly down-regulated in stage 7 (log2 fold change, -6.4) but its abundance increases at metamorphic climax stage 9A (log2 fold change, -1.6) and this is reminiscent of what occurs in the flatfish *Scophthalmus maximus* (Torres-Nunez et al., 2015). DE ECM transcripts (alpha2 Collagen type 1 and fibronectin) during Atlantic halibut metamorphosis linked with epidermal outgrowth (Matsumoto and

Sugimoto, 2007; Plow et al., 2000) are also modified in amphibian metamorphosis (Helbing et al., 2003). The stage specific fingerprint of DE TH-responsive and nonresponsive genes generated by SOLiD analysis of several individuals per stage during Atlantic halibut metamorphosis is a rich resource for future studies of the metamorphic process and its evolution (Ishizuya-Oka, 2011). Furthermore, although in general metamorphosis is comparable between fish and amphibians their divergent evolution, biology and physiology (Marchand et al., 2004) makes flatfish specific data for this process a priority.

2.4.3. Confirmation of the TH axis role in Atlantic halibut metamorphosis

In flatfish, initiation of metamorphosis is associated with a surge in T_4 and T_3, which increases up until the metamorphic climax and decreases in post-climax stages (Einarsdóttir et al., 2006; Galay-Burgos et al., 2008; Klaren et al., 2008; Miwa et al., 1988; Schreiber and Specker, 1998; Yamano, 2005). The failure to detect by NGS analysis DE genes of the thyroid axis in the present and previous studies of flatfish metamorphosis may be a result of: i) their generally low tissue abundance, which is further aggravated by, ii) the dilution effect caused by using mRNA from whole larvae (or pools of larvae) rather than discrete tissue and iii) the asynchronous temporal expression pattern in different tissues. Nonetheless, *tg* transcript abundance detected by qPCR in the present study mirrored the TH profiles in metamorphosing Atlantic halibut (Galay-Burgos et al., 2008) and is reminiscent of what occurs in Senegalese sole (Manchado et al., 2008). Unsurprisingly, transcription of deiodinases (*dio1*, *dio2*, *dio3*), that encode selenoproteins that activate and inactivate THs (Brown and Cai, 2007; Cai and Brown, 2004; Campinho et al., 2010; Darras et al., 2015; Nakajima et al., 2005; Van der Geyten et al., 2002) changed during metamorphosis. The results for DIO expression agreed with previous studies of metamorphosis in the Atlantic halibut (Campinho et al., 2012) and Senegalese sole (Isorna et al., 2009). A limitation of the present study is the impossibility of mapping the spatial and temporal pattern of deiodinase mRNA localization, which is known to be tightly controlled in flounder metamorphosis (Itoh et al., 2010). The spatial distribution of deiodinases probably contributes to the asynchronous pattern of DE genes during metamorphosis.

In the Atlantic halibut qPCR revealed that the recently identified TH transmembrane transporters (members of the solute carrier (Slc) proteins (Friesema et al., 2005; Schweizer and Köhrle, 2013; Visser et al., 2011)), *mct8* and *mct10*, that regulate TH availability in peripheral tissues, are expressed in metamorphosing Atlantic halibut. However, only mct8, a specific TH transporter (Arjona et al., 2011; Campinho et al., 2014; Vatine et al., 2013), is significantly up-regulated during the metamorphic climax (stages 9A and 9B) and significantly decreases in post-metamorphic juveniles. The results in Atlantic halibut suggest that in common with metamorphosis in the amphibian (*Xenopus tropicalis*) the tissue distribution and abundance of Slc proteins is one of the factors explaining the differential tissue responsiveness to THs (Connors et al., 2010; Geysens et al., 2012; Taylor and Ritchie, 2007; Van Herck et al., 2015; Van Herck et al., 2013).

In the Atlantic halibut, TRs had a variable expression pattern during metamorphosis as observed in other flatfish species (Galay-Burgos et al., 2008; Manchado et al., 2009; Marchand et al., 2004; Yamano and Miwa, 1998) and this is intriguing when placed in the context of the duality model of TR actions during vertebrate development (Buchholz, 2015). In this model, TRα is the predominant TR form during the *Xenopus* larval phase and is associated with repression of TH-inducible genes. Repression of TH-responsive genes occurs when TR and retinoid X receptor (RXR) bind to thyroid response elements (T_3RE) and in the absence of T_3 recruit a co-repressor complex (e.g. Nuclear receptor CoRepressor (*NCoR*), Silencing Mediator for RAR and TR (*SMRT*), and other proteins). At metamorphosis the presence of T_3 leads to substitution of the co-repressor complex by co-activator proteins and TH-responsive gene transcription is induced. This event is concomitant with TRβ up-regulation (reviewed by Grimaldi et al., (2013) and Morvan-Dubois et al., (2008)). In Atlantic halibut, our results suggest a dual TR activity model may also exist as *trαb* is the main TR form expressed in premetamorphic stages, while *trβ* is more abundant at the metamorphic climax. In addition, SOLiD analysis reveals DE of co-activator and repressor elements (*ncor*, *hdac1*, *prmt1*) of TRs during metamorphosis.

In summary, although significant changes in transcripts of the thyroid axis are not detected using SOLiD transcriptome analysis, the temporal expression pattern of *DIO*, TH transporters and TRs varied dramatically between larvae at different stages confirming the

importance of the TH axis in Atlantic halibut metamorphosis (Einarsdóttir et al., 2006). In metamorphosing frogs changes in DIOs, TH transporters and TRs are correlated with the timing of tissue specific changes during metamorphosis (Connors et al., 2010; Darras et al., 2015; Grimaldi et al., 2013; Morvan-Dubois et al., 2008; Pascual and Aranda, 2013; Schreiber et al., 2009). The results of our study and those on frog highlight the importance of analysing individuals and tissues rather than pools of individuals if flatfish metamorphosis is to be understood.

2.5. Conclusions

We report for the first time the tissues specific (skin, GI-tract and head) transcriptomes during metamorphosis of a flatfish species *Hippoglossus hippoglossus* with a high economic value. The study contributes substantially to the molecular resources available for this species and will be an important tool for identifying new potential molecular markers for solving problems related to Atlantic halibut production during metamorphosis. The Atlantic halibut skin transcriptome is a powerful resource for studying the asymmetric pigmentation pattern, as well as the putative cross-talk with the THs axis. Questions relating to the possible asymmetric responsiveness to the THs of both ocular and abocular (blind) sides of skin during metamorphosis remain to be resolved.

The candidate TH-responsive genes identified in the transcriptomes generated will be the subject of future studies to assess tissues responsiveness, and how it is correlated with temporal changes in elements of TH signaling and metabolism during flatfish metamorphosis. Further studies will be essential to identify the tissue specific mechanisms underlying the timing and programming of the developmental events occurring during metamorphosis. The involvement of THs in a late developmental event, metamorphosis, highlights an emerging research area: the regulatory role of hormones in early development.

Availability of data and material

The 454 sequences for Atlantic halibut obtained in this study are available at the NCBI SRA under the accession number: SRP044664 and the consensus sequences of the contigs are

available at http://ramadda.nerc-bas.ac.uk/repository in the folder: NERC-BAS datasets/Genomics/Transcriptomes/Hippoglossus_hippoglossus. All SOLiD sequence data were submitted to the NCBI SRA with the accession number: **SRP073364**.

Acknowledgements

This research study was funded by the European Community FP7 project LIFECYCLE (FP7 222719, http://www.lifecycle.gu.se/, 17.08.2012). Ricardo N. Alves was funded by FCT (SFRH / BD/69209/2010). MSC and MAST were funded under the British Antarctic Survey Polar Sciences for Planet Earth programme. The authors thank F. Zimmermann for help with R scripts and comments.

References

Altschul, S.F., Madden, T.L., Schäffer, A.A., Zhang, J., Zhang, Z., Miller, W., Lipman, D.J., 1997. Gapped BLAST and PSI-BLAST: a new generation of protein database search programs. Nucleic Acids Research 25, 3389-3402.

Arjona, F.J., de Vrieze, E., Visser, T.J., Flik, G., Klaren, P.H.M., 2011. Identification and Functional Characterization of Zebrafish Solute Carrier Slc16a2 (Mct8) as a Thyroid Hormone Membrane Transporter. Endocrinology 152, 5065-5073.

Benjamini, Y., Hochberg, Y., 1995. Controlling the False Discovery Rate: A Practical and Powerful Approach to Multiple Testing. Journal of the Royal Statistical Society: Series B (Statistical Methodology) 57, 289-300.

Benson, D.A., Cavanaugh, M., Clark, K., Karsch-Mizrachi, I., Lipman, D.J., Ostell, J., Sayers, E.W., 2013. GenBank. Nucleic Acids Research 41, D36-42.

Benzekri, H., Armesto, P., Cousin, X., Rovira, M., Crespo, D., Merlo, M., Mazurais, D., Bautista, R., Guerrero-Fernandez, D., Fernandez-Pozo, N., Ponce, M., Infante, C., Zambonino, J., Nidelet, S., Gut, M., Rebordinos, L., Planas, J., Begout, M.-L., Claros, M., Manchado, M., 2014. De novo assembly, characterization and functional annotation of Senegalese sole (*Solea senegalensis*) and common sole (*Solea solea*) transcriptomes: integration in a database and design of a microarray. BMC Genomics 15, 952.

Botchkarev, V.A., Sharov, A.A., 2004. BMP signaling in the control of skin development and hair follicle growth. Differentiation 72, 512-526.

Brekken, R.A., Sage, E.H., 2001. SPARC, a matricellular protein: at the crossroads of cell-matrix communication. Matrix Biology 19, 816-827.

Brown, D.D., Cai, L., 2007. Amphibian metamorphosis. Dev. Biol 306, 20-33.

Brown, D.D., Cai, L., Das, B., Marsh-Armstrong, N., Schreiber, A.M., Juste, R., 2005. Thyroid hormone controls multiple independent programs required for limb development in *Xenopus laevis* metamorphosis. Proceedings of the National Academy of Sciences USA 102, 12455-12458.

Brunelli, E., Bernabò, I., Coscarelli, F., La Russa, D., Tripepi, S., 2015. Remodelling of the skin during metamorphosis in the Italian newt (*Lissotriton italicus*) (Amphibia, Urodela): localization pattern of keratins, stromelysin-3 (MMP-11), and pan-cadherin. Zoomorphology 134, 135-147.

Buchholz, D.R., 2015. More similar than you think: Frog metamorphosis as a model of human perinatal endocrinology. Development Biology 408, 188-195.

Buchholz, D.R., Paul, B.D., Fu, L., Shi, Y.-B., 2006. Molecular and developmental analyses of thyroid hormone receptor function in *Xenopus laevis*, the African clawed frog. General and Comparative Endocrinology 145, 1-19.

Buchholz, D.R., Heimeier, R.A., Das, B., Washington, T., Shi, Y.-B., 2007. Pairing morphology with gene expression in thyroid hormone-induced intestinal remodelling and identification of a core set of TH-induced genes across tadpole tissues. Development Biology 303, 576-590.

Cai, L., Brown, D.D., 2004. Expression of type II iodothyronine deiodinase marks the time that a tissue responds to thyroid hormone-induced metamorphosis in *Xenopus laevis*. Development Biology 266, 87-95.

Callery, E.M., Elinson, R.P., 2000. Thyroid hormone-dependent metamorphosis in a direct developing frog. Proceedings of the National Academy of Sciences USA 97, 2615-2620.

Campinho, M.A., Silva, N., Nowell, M.A., Llewellyn, L., Sweeney, G.E., Power, D.M., 2007a. Troponin T isoform expression is modulated during Atlantic halibut metamorphosis. BMC Development Biology 7, 71.

Campinho, M.A., Silva, N., Sweeney, G.E., Power, D.M., 2007b. Molecular, cellular and histological changes in skin from a larval to an adult phenotype during bony fish metamorphosis. Cell Tissue Research 327, 267-284.

Campinho, M.A., Galay-Burgos, M., Sweeney, G.E., Power, D.M., 2010. Coordination of deiodinase and thyroid hormone receptor expression during the larval to juvenile transition in sea bream (*Sparus aurata*, Linnaeus). General and Comparative Endocrinology 165, 181-194.

Campinho, M.A., Galay-Burgos, M., Silva, N., Costa, R.N., Alves, R.N., Sweeney, G.E., Power, D.M., 2012. Molecular and cellular changes in skin and muscle during metamorphosis of Atlantic halibut (*Hippoglossus hippoglossus*) are accompanied by changes in deiodinases expression. Cell Tissue Research 350, 333-346.

Campinho, M.A., Saraiva, J., Florindo, C., Power, D.M., 2014. Maternal Thyroid Hormones Are Essential for Neural Development in Zebrafish. Molecular Endocrinology 28, 1136-1149.

Cerda, J., Mercade, J., Lozano, J.J., Manchado, M., Tingaud-Sequeira, A., Astola, A., Infante, C., Halm, S., Vinas, J., Castellana, B., Asensio, E., Canavate, P., Martinez-Rodriguez, G., Piferrer, F., Planas, J.V., Prat, F., Yufera, M., Durany, O., Subirada, F., Rosell, E., Maes, T., 2008. Genomic resources for a commercial flatfish, the Senegalese sole (*Solea senegalensis*): EST sequencing, oligo microarray design, and development of the Soleamold bioinformatic platform. BMC Genomics 9, 508.

Chevreux, B., Wetter, T., Suhai, S., 1999. Genome sequence assembly using trace signals and additional sequence information, Computer science and biology: proceedings of the German conference on bioinformatics (GCB). Citeseer, 45-56.

Coady, K., Marino, T., Thomas, J., Currie, R., Hancock, G., Crofoot, J., McNalley, L., McFadden, L., Geter, D., Klecka, G., 2010. Evaluation of the amphibian metamorphosis assay: exposure to the goitrogen methimazole and the endogenous thyroid hormone L-thyroxine. Environmental Toxicology and Chemistry 29, 869-880.

Conesa, A., Götz, S., García-Gómez, J.M., Terol, J., Talón, M., Robles, M., 2005. Blast2GO: a universal tool for annotation, visualization and analysis in functional genomics research. Bioinformatics 21, 3674-3676.

Connors, K.A., Korte, J.J., Anderson, G.W., Degitz, S.J., 2010. Characterization of thyroid hormone transporter expression during tissue-specific metamorphic events in *Xenopus tropicalis*. General and Comparative Endocrinology 168, 149-159.

Coppe, A., Pujolar, J.M., Maes, G.E., Larsen, P.F., Hansen, M.M., Bernatchez, L., Zane, L., Bortoluzzi, S., 2010. Sequencing, de novo annotation and analysis of the first *Anguilla anguilla* transcriptome: EeelBase opens new perspectives for the study of the critically endangered European eel. BMC Genomics 11, 635.

Crane, H.M., Pickford, D.B., Hutchinson, T.H., Brown, J.A., 2006. The Effects of Methimazole on Development of the Fathead Minnow, *Pimephales promelas*, from Embryo to Adult. Toxicology Science 93, 278-285.

Darias, M.J., Andree, K.B., Boglino, A., Fernández, I., Estévez, A., Gisbert, E., 2013. Coordinated Regulation of Chromatophore Differentiation and Melanogenesis during the Ontogeny of Skin Pigmentation of *Solea senegalensis* (Kaup, 1858). PLoS One 8, e63005.

Darras, V.M., Houbrechts, A.M., Van Herck, S.L.J., 2015. Intracellular thyroid hormone metabolism as a local regulator of nuclear thyroid hormone receptor-mediated impact on vertebrate development. Biochimica et Biophysica Acta 1849, 130-141.

Das, B., Cai, L., Carter, M.G., Piao, Y.L., Sharov, A.A., Ko, M.S., Brown, D.D., 2006. Gene expression changes at metamorphosis induced by thyroid hormone in *Xenopus laevis* tadpoles. Development Biology 291, 342-355.

Das, B., Heimeier, R.A., Buchholz, D.R., Shi, Y.B., 2009. Identification of direct thyroid hormone response genes reveals the earliest gene regulation programs during frog metamorphosis. Journal of Biological Chemistry 284, 34167-34178.

Douglas, S.E., Knickle, L.C., Kimball, J., Reith, M.E., 2007. Comprehensive EST analysis of Atlantic halibut (*Hippoglossus hippoglossus*), a commercially relevant aquaculture species. BMC Genomics 8, 144.

Douglas, S.E., Knickle, L.C., Williams, J., Flight, R.M., Reith, M.E., 2008. A first generation Atlantic halibut *Hippoglossus hippoglossus* (L.) microarray: application to developmental studies. Journal of Fish Biology 72, 2391-2406.

Einarsdóttir, I., Silva, N., Power, D., Sámaradóttir, H., Björnsson, B., 2006. Thyroid and pituitary gland development from hatching through metamorphosis of a teleost flatfish, the Atlantic halibut. Anatomy and embryology 211, 47-60.

Fernandez, L.P., Lopez-Marquez, A., Santisteban, P., 2015. Thyroid transcription factors in development, differentiation and disease. Nature Reviews Endocrinology 11, 29-42.

Ferraresso, S., Bonaldo, A., Parma, L., Cinotti, S., Massi, P., Bargelloni, L., Gatta, P.P., 2013. Exploring the larval transcriptome of the common sole (*Solea solea* L.). BMC Genomics 14, 315.

Friesema, E.C., Jansen, J., Milici, C., Visser, T.J., 2005. Thyroid hormone transporters. Vitamins and hormones 70, 137-167.

Fu, B., He, S., 2012. Transcriptome Analysis of Silver Carp (*Hypophthalmichthys molitrix*) by Paired-End RNA Sequencing. DNA Research 19, 131-142.

Furlow, J.D., Kanamori, A., 2002. The transcription factor basic transcription element-binding protein 1 is a direct thyroid hormone response gene in the frog *Xenopus laevis*. Endocrinology 143, 3295-3305.

Galay-Burgos, M., Llewellyn, L., Bjornsson, B.T., Pittman, K., Power, D.M., Smaradottir, H., Sweeney, G.E., 2006. Isolation of subtractive clones enriched in sequences that show differential expression during metamorphosis of Atlantic halibut (*Hippoglossus hippoglossus*). GenBank. 2006 [http://www.ncbi.nlm.nih.gov/nucest/?term=LIBEST_020648].

Galay-Burgos, M., Power, D.M., Llewellyn, L., Sweeney, G.E., 2008. Thyroid hormone receptor expression during metamorphosis of Atlantic halibut (*Hippoglossus hippoglossus*). Mol. Cell. Endocrinol 281, 56-63.

Geysens, S., Ferran, J.L., Van Herck, S.L.J., Tylzanowski, P., Puelles, L., Darras, V.M., 2012. Dynamic mRNA distribution pattern of thyroid hormone transporters and deiodinases during early embryonic chicken brain development. Neuroscience 221, 69-85.

Gilbert, L.I., Tata, J.R., Atkinson, B.G., 1996. Metamorphosis: postembryonic reprogramming of gene expression in amphibian and insect cells. Academic Press.

Gomes, A., Kamisaka, Y., Harboe, T., Power, D., Ronnestad, I., 2014a. Functional modifications associated with gastrointestinal tract organogenesis during metamorphosis in Atlantic halibut (*Hippoglossus hippoglossus*). BMC Development Biology 14, 11.

Gomes, A.S., Alves, R.N., Stueber, K., Thorne, M.A.S., Sráradóttir, H., Reinhard, R., Clark, M.S., Rønnestad, I., Power, D.M., 2014b. Transcriptome of the Atlantic halibut (*Hippoglossus hippoglossus*). Marine Genomics 18, Part B, 101-103.

Gomes, A.S., Alves, R.N., Rønnestad, I., Power, D.M., 2015. Orchestrating change: The thyroid hormones and GI-tract development in flatfish metamorphosis. General and Comparative Endocrinology 220, 2-12.

Götz, S., García-Gómez, J.M., Terol, J., Williams, T.D., Nagaraj, S.H., Nueda, M.J., Robles, M., Talón, M., Dopazo, J., Conesa, A., 2008. High-throughput functional annotation and data mining with the Blast2GO suite. Nucleic Acids Research 6, 3420-3435.

Grimaldi, A.G., Buisine, N., Bilesimo, P., Sachs, L.M., 2013. High-throughput sequencing will metamorphose the analysis of thyroid hormone receptor function during amphibian development. Current Topic Development Biology 103, 277-303.

Hardcastle, T., Kelly, K., 2010. baySeq: Empirical Bayesian methods for identifying differential expression in sequence count data. BMC Bioinformatics 11, 422.

Heimeier, R., Das, B., Buchholz, D., Fiorentino, M., Shi, Y.-B., 2010. Studies on *Xenopus laevis* intestine reveal biological pathways underlying vertebrate gut adaptation from embryo to adult. Genome Biology 11, R55.

Helbing, C.C., Werry, K., Crump, D., Domanski, D., Veldhoen, N., Bailey, C.M., 2003. Expression Profiles of Novel Thyroid Hormone-Responsive Genes and Proteins in the Tail of *Xenopus laevis* Tadpoles Undergoing Precocious Metamorphosis. Molecular Endocrinology 17, 1395-1409.

Huang, J.H., Lozano, J., Belles, X., 2013. Broad-complex functions in postembryonic development of the cockroach *Blattella germanica* shed new light on the evolution of insect metamorphosis. Biochimica et Biophysica Acta 1830, 2178-2187.

Huggins, P., Johnson, C.K., Schoergendorfer, A., Putta, S., Bathke, A.C., Stromberg, A.J., Voss, S.R., 2012. Identification of differentially expressed thyroid hormone responsive genes from the brain of the Mexican Axolotl (*Ambystoma mexicanum*). Comparative Biochemistry and Physiology C Toxicology Pharmacology 155, 128-135.

Ingham, P.W., McMahon, A.P., 2001. Hedgehog signaling in animal development: paradigms and principles. Genes and Development 15, 3059-3087.

Inui, Y., Yamano, K., Miwa, S., 1995. The role of thyroid hormone in tissue development in metamorphosing flounder. Aquaculture 135, 87-98.

Ishizuya-Oka, A., 2011. Amphibian organ remodelling during metamorphosis: insight into thyroid hormone-induced apoptosis. Development Growth Differentiation 53, 202-212.

Ishizuya-Oka, A., Shi, Y.B., 2007. Regulation of adult intestinal epithelial stem cell development by thyroid hormone during *Xenopus laevis* metamorphosis. Developmental Dynamics 236, 3358-3368.

Ishizuya-Oka, A., Hasebe, T., Buchholz, D.R., Kajita, M., Fu, L., Shi, Y.B., 2009. Origin of the adult intestinal stem cells induced by thyroid hormone in *Xenopus laevis*. The Federation of American Societies for Experimental Biology Journal. 23, 2568-2575.

Ishizuya-Oka, A., Ueda, S., 1996. Apoptosis and cell proliferation in the *Xenopus* small intestine during metamorphosis. Cell Tissue Research 286, 467-476.

Isorna, E., Obregon, M.J., Calvo, R.M., Vazquez, R., Pendon, C., Falcon, J., Munoz-Cueto, J.A., 2009. Iodothyronine deiodinases and thyroid hormone receptors regulation during flatfish (*Solea senegalensis*) metamorphosis. Journal of Experimental Zoology Part B Molecular and Developmental Evolution 312b, 231-246.

Itoh, K., Watanabe, K., Wu, X., Suzuki, T., 2010. Three Members of the Iodothyronine Deiodinase Family, dio1, dio2 and dio3, are Expressed in Spatially and Temporally Specific Patterns During Metamorphosis of the Flounder, *Paralichthys olivaceus*. Zoology Science 27, 574-580.

Janicke, M., Carney, T.J., Hammerschmidt, M., 2007. Foxi3 transcription factors and Notch signaling control the formation of skin ionocytes from epidermal precursors of the zebrafish embryo. Development Biology 307, 258-271.

Klaren, P.H.M., Wunderink, Y.S., Yúfera, M., Mancera, J.M., Flik, G., 2008. The thyroid gland and thyroid hormones in Senegalese sole (*Solea senegalensis*) during early development and metamorphosis. General and Comparative Endocrinology 155, 686-694.

Kristiansson, E., Asker, N., Forlin, L., Larsson, D.G., 2009. Characterization of the *Zoarces viviparus* liver transcriptome using massively parallel pyrosequencing. BMC Genomics 10, 345.

Le Guellec, D., Morvan-Dubois, G., Sire, J.Y., 2004. Skin development in bony fish with particular emphasis on collagen deposition in the dermis of the zebrafish (*Danio rerio*). The International Journal of Developmental Biology 48, 217-231.

Li, H., Ruan, J., Durbin, R., 2008. Mapping short DNA sequencing reads and calling variants using mapping quality scores. Genome Research 18, 1851-1858.

Liu, Y.W., Chan, W.K., 2002. Thyroid hormones are important for embryonic to larval transitory phase in zebrafish. Differentiation 70, 36-45.

Logan, C.Y., Nusse, R., 2004. The Wnt signaling pathway in development and disease. Annual Review of Cell and Developmental Biology 20, 781-810.

Luizi, F.S., Gara, B., Shields, R.J., Bromage, N.R., 1999. Further description of the development of the digestive organs in Atlantic halibut (*Hippoglossus hippoglossus)* larvae, with notes on differential absorption of copepod and Artemia prey. Aquaculture 176, 101-116.

Manchado, M., Infante, C., Asensio, E., Planas, J.V., Cañavate, J.P., 2008. Thyroid hormones down-regulate thyrotropin β subunit and thyroglobulin during metamorphosis in the flatfish Senegalese sole (*Solea senegalensis* Kaup). General and Comparative Endocrinology 155, 447-455.

Manchado, M., Infante, C., Rebordinos, L., Cañavate, J.P., 2009. Molecular characterization, gene expression and transcriptional regulation of thyroid hormone receptors in Senegalese sole. General and Comparative Endocrinology 160, 139-147.

Marchand, O., Duffraisse, M., Triqueneaux, G., Safi, R., Laudet, V., 2004. Molecular cloning and developmental expression patterns of thyroid hormone receptors and T_3 target genes in the turbot (*Scophtalmus maximus*) during post-embryonic development. General and Comparative Endocrinology 135, 345-357.

Matsumoto, R., Sugimoto, M., 2007. Dermal matrix proteins initiate re-epithelialization but are not sufficient for coordinated epidermal outgrowth in a new fish skin culture model. Cell Tissue Research 327, 249-265.

McMenamin, S.K., Parichy, D.M., 2013. Chapter Five - Metamorphosis in Teleosts, in: S. Yun-Bo (Ed.), Curr. Top. Dev. Biol. Academic Press, 127-165.

Miwa, S., Tagawa, M., Inui, Y., Hirano, T., 1988. Thyroxine surge in metamorphosing flounder larvae. General and Comparative Endocrinology 70, 158-163.

Miwa, S., Yamano, K., Inui, Y., 1992. Thyroid hormone stimulates gastric development in flounder larvae during metamorphosis. Journal of Experimental Zoology 261, 424-430.

Mommens, M., Fernandes, J., Bizuayehu, T., Bolla, S., Johnston, I., Babiak, I., 2010. Maternal gene expression in Atlantic halibut (*Hippoglossus hippoglossus* L.) and its relation to egg quality. BMC Research Notes 3, 1-11.

Morvan-Dubois, G., Demeneix, B.A., Sachs, L.M., 2008. *Xenopus laevis* as a model for studying thyroid hormone signalling: From development to metamorphosis. Molecular and Cellular Endocrinology 293, 71-79.

Myhre, S., Tveit, H., Mollestad, T., Laegreid, A., 2006. Additional gene ontology structure for improved biological reasoning. Bioinformatics 22, 2020-2027.

Nakajima, K., Fujimoto, K., Yaoita, Y., 2005. Programmed cell death during amphibian metamorphosis. Seminars in Cell & Developmental Biology 16, 271-280.

Nakamura, M., Ohki, S., Suzuki, A., Sakai, K., 2011. Coral Larvae under Ocean Acidification: Survival, Metabolism, and Metamorphosis. PLoS One. 6, e14521.

Okada, N., Takagi, Y., Tanaka, M., Tagawa, M., 2003. Fine structure of soft and hard tissues involved in eye migration in metamorphosing Japanese flounder (*Paralichthys olivaceus*). The Anatomical Record. Part A, Discoveries in Molecular, Cellular, and Evolutionary Biology 273A, 663-668.

Olaso, E., Lin, H.C., Wang, L.H., Friedman, S.L., 2011. Impaired dermal wound healing in discoidin domain receptor 2-deficient mice associated with defective extracellular matrix remodelling. Fibrogenesis and Tissue Repair 4, 5.

Ottesen, O.H., Strand, H.K., 1996. Growth, development, and skin abnormalities of halibut (*Hippoglossus hippoglossus* L) juveniles kept on different bottom substrates. Aquaculture 146, 17-25.

Ozkizilcik, S., Chu, F.-L.E., Place, A.R., 1996. Ontogenetic changes of lipolytic enzymes in striped bass (*Morone saxatilis*). Comparative Biochemistry and Physiology Part B: Biochemistry and Molecular Biology113, 631-637.

Page, R.B., Voss, S.R., Samuels, A.K., Smith, J.J., Putta, S., Beachy, C.K., 2008. Effect of thyroid hormone concentration on the transcriptional response underlying induced metamorphosis in the Mexican axolotl (Ambystoma). BMC Genomics. 9, 78.

Page, R.B., Monaghan, J.R., Walker, J.A., Voss, S.R., 2009. A model of transcriptional and morphological changes during thyroid hormone-induced metamorphosis of the axolotl. General and Comparative Endocrinology 162, 219-232.

Paridaen, J.T., Huttner, W.B., 2014. Neurogenesis during development of the vertebrate central nervous system. EMBO Report 15, 351-364.

Pascual, A., Aranda, A., 2013. Thyroid hormone receptors, cell growth and differentiation. Biochimica et Biophysica Acta 1830, 3908-3916.

Pereiro, P., Balseiro, P., Romero, A., Dios, S., Forn-Cuni, G., Fuste, B., Planas, J.V., Beltran, S., Novoa, B., Figueras, A., 2012. High-Throughput Sequence Analysis of Turbot (*Scophthalmus maximus*) Transcriptome Using 454-Pyrosequencing for the Discovery of Antiviral Immune Genes. PLoS One 7, e35369.

Plow, E.F., Haas, T.A., Zhang, L., Loftus, J., Smith, J.W., 2000. Ligand binding to integrins. The Journal of Biological Chemistry 275, 21785-21788.

Power, D.M., Einarsdóttir, I.E., Pittman, K., Sweeney, G.E., Hildahl, J., Campinho, M.A., Silva, N., Sæle, Ø., Galay-Burgos, M., Smáradóttir, H., Björnsson, B.T., 2008. The Molecular and Endocrine Basis of Flatfish Metamorphosis. Reviews in Fisheries Science 16, 95-111.

Power, D.M., Llewellyn, L., Faustino, M., Nowell, M.A., Björnsson, B.T., Einarsdottir, I.E., Canario, A.V.M., Sweeney, G.E., 2001. Thyroid hormones in growth and development of fish. Comparative Biochemistry and Physiology - Part C: Toxicology and Pharmacology 130, 447-459.

Roosterman, D., Goerge, T., Schneider, S.W., Bunnett, N.W., Steinhoff, M., 2006. Neuronal control of skin function: the skin as a neuroimmunoendocrine organ. Physiolgy Reviews 86, 1309-1379.

Rosenkilde, P., Ussing, A.P., 1996. What mechanisms control neoteny and regulate induced metamorphosis in urodeles? The International Journal of Developmental Biology 40, 665-673.

Rubio, M., de Horna, A., Belles, X., 2012. MicroRNAs in metamorphic and non-metamorphic transitions in hemimetabolan insect metamorphosis. BMC Genomics 13, 386.

Sæle, Ø., Solbakken, J.S., Watanabe, K., Hamre, K., Power, D., Pittman, K., 2004. Staging of Atlantic halibut (*Hippoglossus hippoglossus* L.) from first feeding through metamorphosis, including cranial ossification independent of eye migration. Aquaculture 239, 445-465.

Salem, M., Rexroad, C.E., 3rd, Wang, J., Thorgaard, G.H., Yao, J., 2010. Characterization of the rainbow trout transcriptome using Sanger and 454-pyrosequencing approaches. BMC Genomics 11, 564.

Schreiber, A.M., Mukhi, S., Brown, D.D., 2009. Cell–cell interactions during remodelling of the intestine at metamorphosis in *Xenopus laevis*. Developmental Biology 331, 89-98.

Schreiber, A.M., Specker, J.L., 1998. Metamorphosis in the summer flounder (*Paralichthys dentatus*): stage-specific developmental response to altered thyroid status. General and Comparative Endocrinology 111, 156-166.

Schreiber, A.M., Specker, J.L., 2000. Metamorphosis in the Summer Flounder, *Paralichthys dentatus*: Thyroidal Status Influences Gill Mitochondria-Rich Cells. General and Comparative Endocrinology 117, 238-250.

Schreiber, A.M., Wang, X., Tan, Y., Sievers, Q., Sievers, B., Lee, M., Burrall, K., 2010. Thyroid hormone mediates otolith growth and development during flatfish metamorphosis. General and Comparative Endocrinology 169, 130-137.

Schweizer, U., Köhrle, J., 2013. Function of thyroid hormone transporters in the central nervous system. Biochimica et Biophysica Acta 1830, 3965-3973.

Searcy, B.T., Beckstrom-Sternberg, S.M., Beckstrom-Sternberg, J.S., Stafford, P., Schwendiman, A.L., Soto-Pena, J., Owen, M.C., Ramirez, C., Phillips, J., Veldhoen, N., Helbing, C.C., Propper, C.R., 2012. Thyroid hormone-dependent development in *Xenopus laevis*: a sensitive screen of thyroid hormone signaling disruption by municipal wastewater treatment plant effluent. General and Comparative Endocrinology 176, 481-492.

Shoulders, M.D., Raines, R.T., 2009. Collagen structure and stability. Annual Review of Biochemistry 78, 929-958.

Sun, G., Heimeier, R.A., Fu, L., Hasebe, T., Das, B., Ishizuya-Oka, A., Shi, Y.-B., 2013. Expression Profiling of Intestinal Tissues Implicates Tissue-Specific Genes and Pathways Essential for Thyroid Hormone-Induced Adult Stem Cell Development. Endocrinology 154, 4396-4407.

Supek, F., Bošnjak, M., Škunca, N., Šmuc, T., 2011. REVIGO Summarizes and Visualizes Long Lists of Gene Ontology Terms. PLoS One 6, e21800.

Suzuki, K.-i., Machiyama, F., Nishino, S., Watanabe, Y., Kashiwagi, K., Kashiwagi, A., Yoshizato, K., 2009. Molecular features of thyroid hormone-regulated skin remodelling in *Xenopus laevis* during metamorphosis. Development and Growth Differentiation 51, 411-427.

Tagawa, M., Aritaki, M., 2005. Production of symmetrical flatfish by controlling the timing of thyroid hormone treatment in spotted halibut *Verasper variegatus*. General and Comparative Endocrinology 141, 184-189.

Taylor, P.M., Ritchie, J.W.A., 2007. Tissue uptake of thyroid hormone by amino acid transporters. Best Practice & Research Clinical Endocrinology & Metabolism 21, 237-251.

Torres-Nunez, E., Suarez-Bregua, P., Cal, L., Cal, R., Cerda-Reverter, J.M., Rotllant, J., 2015. Molecular cloning and characterization of the matricellular protein Sparc/osteonectin in flatfish, *Scophthalmus maximus*, and its developmental stage-dependent transcriptional regulation during metamorphosis. Gene 568, 129-139.

Tremble, P.M., Lane, T.F., Sage, E.H., Werb, Z., 1993. SPARC, a secreted protein associated with morphogenesis and tissue remodelling, induces expression of metalloproteinases in fibroblasts through a novel extracellular matrix-dependent pathway. Journal of Cell Biology 121, 1433-1444.

Van der Geyten, S., Van den Eynde, I., Segers, I.B., Kühn, E.R., Darras, V.M., 2002. Differential expression of iodothyronine deiodinases in chicken tissues during the last week of embryonic development. General and Comparative Endocrinology 128, 65-73.

Van Herck, S.L.J., Delbaere, J., Bourgeois, N.M.A., McAllan, B.M., Richardson, S.J., Darras, V.M., 2015. Expression of thyroid hormone transporters and deiodinases at the brain barriers in the embryonic chicken: Insights into the regulation of thyroid hormone availability during neurodevelopment. General and Comparative Endocrinology 214, 30-39.

Van Herck, S.L.J., Geysens, S., Delbaere, J., Darras, V.M., 2013. Regulators of thyroid hormone availability and action in embryonic chicken brain development. General and Comparative Endocrinology 190, 96-104.

Vatine, G.D., Zada, D., Lerer-Goldshtein, T., Tovin, A., Malkinson, G., Yaniv, K., Appelbaum, L., 2013. Zebrafish as a model for monocarboxyl transporter 8-deficiency. The Journal of Biological Chemistry 288, 169-180.

Veldhoen, N., Crump, D., Werry, K., Helbing, C.C., 2002. Distinctive gene profiles occur at key points during natural metamorphosis in the *Xenopus laevis* tadpole tail. Developmental Dynamics 225, 457-468.

Visser, W.E., Friesema, E.C., Visser, T.J., 2011. Minireview: thyroid hormone transporters: the knowns and the unknowns. Molecular Endocrinology 25, 1-14.

Vlaeminck-Guillem, V., Safi, R., Guillem, P., Leteurtre, E., Duterque-Coquillaud, M., Laudet, V., 2006. Thyroid hormone receptor expression in the obligatory paedomorphic salamander *Necturus maculosus*. The International Journal of Developmental Biology 50, 553-560.

Vogel, W.F., Abdulhussein, R., Ford, C.E., 2006. Sensing extracellular matrix: An update on discoidin domain receptor function. Cellular Signalling 18, 1108-1116.

Wang, X., Tan, Y., Sievers, Q., Sievers, B., Lee, M., Burrall, K., Schreiber, A.M., 2011. Thyroid hormone-responsive genes mediate otolith growth and development during flatfish metamorphosis. Comparative Biochemistry and Physiology Part A: Molecular & Integrative Physiology 158, 163-168.

Watt, F.M., Fujiwara, H., 2011. Cell-extracellular matrix interactions in normal and diseased skin. Cold Spring Harbor perspectives in biology. 3.

Wong, Y.H., Wang, H., Ravasi, T., Qian, P.-Y., 2012. Involvement of Wnt Signaling Pathways in the Metamorphosis of the Bryozoan *Bugula neritina*. PLoS One. 7, e33323.

Yamano, K., 2005. The Role of Thyroid Hormone in Fish Development with Reference to Aquaculture 39, 161-168.

Yamano, K., Miwa, S., 1998. Differential gene expression of thyroid hormone receptor alpha and beta in fish development. General and Comparative Endocrinology 109, 75-85.

Yamano, K., Miwa, S., Obinata, T., Inui, Y., 1991. Thyroid hormone regulates developmental changes in muscle during flounder metamorphosis. General and Comparative Endocrinology 81, 464-472.

Yamano, K., Takano-Ohmuro, H., Obinata, T., Inui, Y., 1994. Effect of Thyroid Hormone on Developmental Transition of Myosin Light Chains during Flounder Metamorphosis. General and Comparative Endocrinology 93, 321-326.

Yan, Q., Blake, D., Clark, J.I., Sage, E.H., 2003. Expression of the matricellular protein SPARC in murine lens: SPARC is necessary for the structural integrity of the capsular basement membraneJournal of Histochemistry and Cytochemistry 51, 503-511.

Yúfera, M., Halm, S., Beltran, S., Fuste, B., Planas, J.V., Martinez-Rodriguez, G., 2012a. Transcriptomic characterization of the larval stage in gilthead seabream (*Sparus aurata*) by 454 pyrosequencing. Marine Biotechnology 14, 423-435.

Yúfera, M., Moyano, F.J., Astola, A., Pousão-Ferreira, P., Martínez-Rodríguez, G., 2012b. Acidic Digestion in a Teleost: Postprandial and Circadian Pattern of Gastric pH, Pepsin Activity, and Pepsinogen and Proton Pump mRNAs Expression. PLoS One 7, e33687.

Zambonino Infante, J.L., Cahu, C.L., 1999. High dietary lipid levels enhance digestive tract maturation and improve *Dicentrarchus labrax* larval development. Journal of Nutrition 129, 1195-1200.

Zambonino, J.-L., Gisbert, E., Sarasquete, C., Navarro, I., Gutiérrez, J., Cahu, C., 2008. Ontogeny and physiology of the digestive system of marine fish larvae, in: J. Cyrino, D. Bureau, B. Kapoor (Eds.), Feeding and Digestive Functions of Fishes. Oxford & IBH Publishing Co. Pvt. Ltd, Enfield, NH, 281-348.

Zhang, Z., Wang, Y., Wang, S., Liu, J., Warren, W., Mitreva, M., Walter, R.B., 2011. Transcriptome Analysis of Female and Male *Xiphophorus maculatus* Jp 163 A. PLoS One. 6, e18379.

Zouboulis, C.C., 2000. Human skin: an independent peripheral endocrine organ. Hormone Research 54, 230-242.

Additional Files

Additional file 2.1. Scheme of the data processing pipeline for *de novo* transcriptome assembly, annotation and Gene Ontology analysis of Atlantic halibut skin, GI-tract and head transcriptomes.

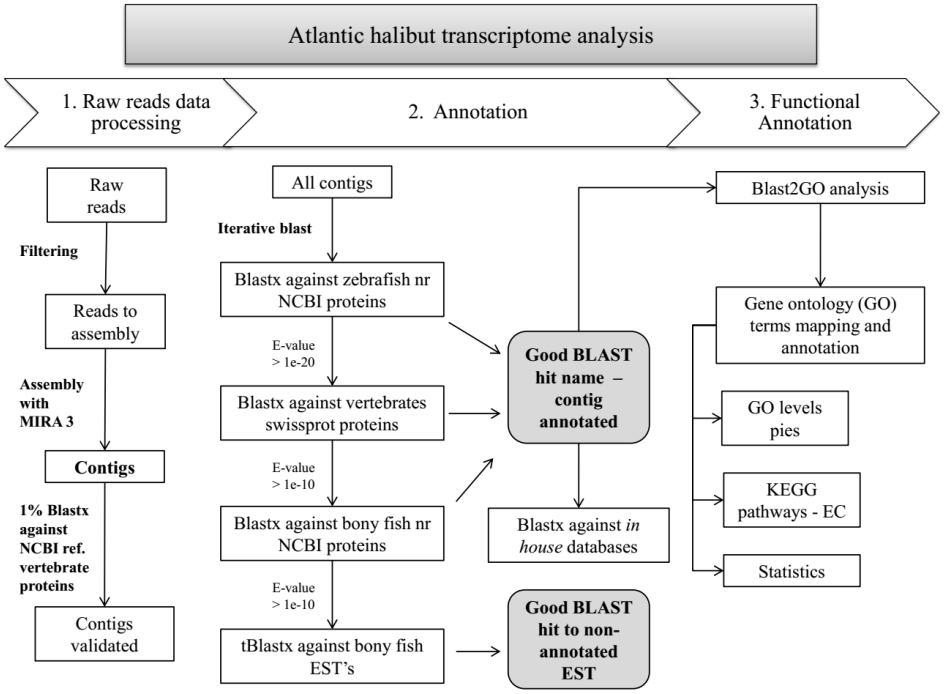

Additional file 2.2. In-house skin-specific database enriched with candidate genes involved in vertebrate skin development, morphogenesis and pigmentation. Protein name, Symbol, Accession number (no.), Organism and Biological role are shown. Please see the Additional file 16 in https://bmcgenomics.biomedcentral.com/articles/10.1186/s12864-016-2699-x#Bib1

Additional file 2.3. In house GI-tract-specific database enriched with genes involved in GI-tract development, morphogenesis and acid secretion. Protein name, Symbol, Accession number (no.), Organism and Biological role (when associated) are shown. Please see the Additional file 17 in https://bmcgenomics.biomedcentral.com/articles/10.1186/s12864-016-2699-x#Bib1

Additional file 2.4. In-house database of candidate genes involved in thyroid gland development / thyroid hormone (TH) metabolism and signaling, including transcripts with a relevant role in TH synthesis, transport and activity. Protein name, Symbol, Accession number (no.), Organism and Biological role are shown. Please see the Additional file 18 in https://bmcgenomics.biomedcentral.com/articles/10.1186/s12864-016-2699-x#Bib1

Additional file 2.5. In-house database of candidate genes involved in TH signaling/metabolism identified in *Xenopus laevis* in previously published literature (Das et al., 2006; Das et al., 2009; Helbing et al., 2003; Searcy et al., 2012). Protein name, Symbol, Accession number (no.), Organism and References are shown. Please see the Additional file 19 in https://bmcgenomics.biomedcentral.com/articles/10.1186/s12864-016-2699-x#Bib1

Additional file 2.6. Specific primers used for qPCR gene expression analysis. Gene symbol, name and function are shown. The annealing temperature (Ta ºC), amplicon length (bp), R^2 and qPCR efficiency (%) are indicated for each primer pair.

Gene symbol	Gene name	Function	Relevance	Primer sequence(5'→3')	Annealing temperature (Ta)	Amplicon length	R^2	PCR efficiency
ef1a1	Elongation factor 1 alpha	Protein synthesis	Genes used as reference	F: AAGAGGACCATCGAGAAGTT R: GTCTCAAACTTCCACAGAGC	60ºC	140	0.99	85%
rps4	40S ribosomal protein S4	Structural component of the small 40S ribosomal subunit		F: CAAGTTTGATACTGCCAACCTGTG R: GGAGAGCCTGGTAGCGAAGC	60ºC	172	0.99	90%
rpl7	Ribosomal protein L7	Structural component of the small 60S ribosomal subunit	Genes without modification during development	F: TTCTCGGTGGACGCAATGG R: GCCAGCATCTTCTTTGACACG	60ºC	120	0.99	100%
fau	40S ribosomal protein S30	Structural component of the small 40S ribosomal subunit		F: TTGAGGTGACCGGACAGGAAAC R: CACAGGATGCCAGGGAGGAATCA	60ºC	135	0.99	89%
gloα1	Alpha-globin 1	Oxygen-transporting protein	Genes with modification during development:	F: CCCACTGGAAGGACCTGAGC R: CACAGCATACTCAACTCCACCC	62ºC	83	0.99	100%
cpa2	Carboxypeptidase A2	Pancreatic carboxypeptidase activity	putative THs responsive	F: CCTAAGAGTCAATGTGCGGTCG R: GGAGCGTGGCACTCGGATG	62ºC	136	0.99	92%
apoai	Apolipoprotein AI	Major protein component of high density lipoprotein (HDL) in plasma		F: GCTGACTTCCGTGCCTCTG R: TATCTGCTGAGTGCTTGGTATG	62ºC	193	0.99	97%
krt1i2	Type I keratin isofom 2	Major structural proteins in epithelial cells		F: GCTGGAGGCGGCTTCAAC R: CCTCGGGTTTGGTCTTGCTC	62ºC	181	0.99	100%
mct8	Monocarboxylate transporter 8	Transport of iodo-thyronines (T_3 and T_4)	Genes involved in THs production, availability and metabolism	F: TTCGGCTGGCTGGTGGTGCTC R: CGTCTGGGTCTGCGTGCTCCTTC	60ºC	115	0.99	90%
mct10	Monocarboxylate transporter 10	Aromatic amino acid transporter. Can transport THs		F: GCTCCGAGAACGATGACGAC R: GTGAAGACGCTGACGATGG	60ºC	100	0.99	94%
dio1	Deiodinase 1	Activation and inactivation of THs by deiodination		F: CCAAAAACTCCTCGTCTATGTCT R: CTTGGTGAGGCTTGGTGAAATAA	60ºC	108	0.99	90%
dio2	Deiodinase 2	Major role in activation of THs by deiodination		F: TGGACGCATACAAGCAGGTG R: TGGCACATTGGTCACATTACTG	60ºC	106	0.99	99%
dio3	Deiodinase 3	Major role in inactivation of THs by deiodination		F: ACTCCAGATAGATAGATTGTGTC R: TAAACAAACCTTTTTTTCCTGAA	60ºC	178	0.99	95%
tg	Thyroglobulin	Production of THs		F: CCAGCAACAAGAAGACATCCC R: CGGACAGTGAGGAGCAGAG	62ºC	151	0.99	95%
trαa	Thyroid receptor alpha A	THs receptor activity		F: GAATCGGGAGAAGAGGAAGCG R: GACCCTGACCGATATCATCCGA	62ºC	179	0.99	100%
trαb	Thyroid receptor alpha B			F: TCCAGAGCCCACCGGCGCC R: GGGGAGGCCGATTTTGTCT	62ºC	129	0.99	99%
trβ	Thyroid receptor beta			F: CAAGCGTCCATGGCAAATACAC R: CAAAGTCCACCACTCGGGTT	62ºC	106	0.99	100%

Additional file 2.7. Annotation of the skin transcriptome. Contig ID, transcript name, number of GOs and their description and enzymatic codes are shown for each contig. Please see the Additional file 2 in https://bmcgenomics.biomedcentral.com/articles/10.1186/s12864-016-2699-x#Bib1

Additional file 2.8. Annotation of the GI-tract transcriptome. Contig ID, transcript name, number of GOs and their description and enzymatic codes are shown for each contig. Please see the Additional file 3 in https://bmcgenomics.biomedcentral.com/articles/10.1186/s12864-016-2699-x#Bib1

Additional file 2.9. Annotation of the head transcriptome. Contig ID, transcript name, number of GOs and their description and enzymatic codes are shown for each contig. Please see the Additional file 4 in https://bmcgenomics.biomedcentral.com/articles/10.1186/s12864-016-2699-x#Bib1

Additional file 2.10. Schematic representation of the functional annotation obtained after analysis of the transcriptomes for skin, GI-tract and head. The GO terms (level 2) used for classification were biological process (BP), molecular function (MF) and cellular component (CC).

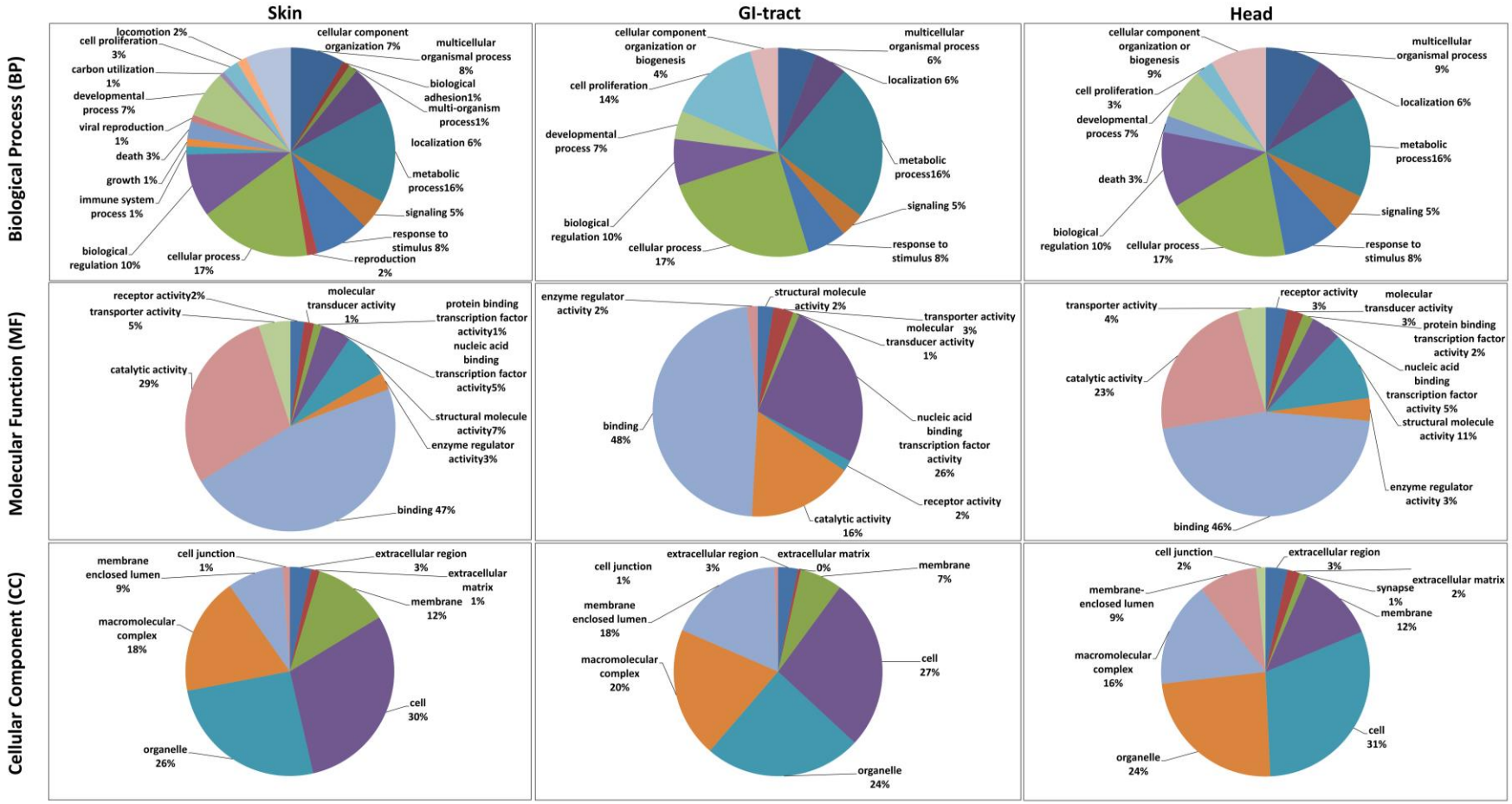

Additional file 2.11. Significantly overrepresented Biological Process GO terms identified for the skin transcriptome (FDR<0.05).

Overrepresented in relation to head			**Overrepresented in relation to GI tract**		
GO term ID	***GO term description***	***FDR***	***GO term ID***	***GO term description***	***FDR***
GO:0003012	Muscle system process	0	GO:3012	Muscle system process	0
GO:0006936	Muscle contraction	0	GO:3008	System process	0
GO:0006941	Striated muscle contraction	2.68E-308	GO:6941	Striated muscle contraction	0
GO:0006096	Glycolysis	1.27E-265	GO:6936	Muscle contraction	0
GO:0006094	Gluconeogenesis	3.24E-265	GO:71842	Cellular component organization at cellular level	0
GO:0019319	Hexose biosynthetic process	6.81E-262	GO:71841	Cellular component organization or biogenesis at cellular level	0
GO:0046364	Monosaccharide biosynthetic process	2.01E-257	GO:71840	Cellular component organization or biogenesis	0
GO:0006007	Glucose catabolic process	2.07E-253	GO:7275	Multicellular organismal development	0
GO:0019320	Hexose catabolic process	6.52E-250	GO:65007	Biological regulation	0
GO:0046365	Monosaccharide catabolic process	3.57E-248	GO:32502	Developmental process	0
GO:0006006	Glucose metabolic process	1.60E-232	GO:32501	Multicellular organismal process	0
GO:0006754	ATP biosynthetic process	8.51E-228	GO:48856	Anatomical structure development	0
GO:0016051	Carbohydrate biosynthetic process	8.90E-224	GO:50896	Response to stimulus	0
GO:0016052	Carbohydrate catabolic process	1.36E-222	GO:50794	Regulation of cellular process	0
GO:0019318	Hexose metabolic process	6.30E-217	GO:50789	Regulation of biological process	0
GO:0009201	Ribonucleoside triphosphate biosynthetic process	6.85E-216	GO:9653	Anatomical structure morphogenesis	0
GO:0009145	Purine nucleoside triphosphate biosynthetic process	1.08E-215	GO:9056	Catabolic process	0
GO:0009206	Purine ribonucleoside triphosphate biosynthetic process	1.08E-215	GO:16043	Cellular component organization	0
GO:0009142	Nucleoside triphosphate biosynthetic process	9.10E-214	GO:6807	Nitrogen compound metabolic process	0
GO:0005996	Monosaccharide metabolic process	9.48E-211	GO:6725	Cellular aromatic compound metabolic process	0
GO:0009152	Purine ribonucleotide biosynthetic process	3.95E-209	GO:71704	Organic substance metabolic process	0
GO:0009260	Ribonucleotide biosynthetic process	1.13E-204	GO:6139	Nucleobase-containing compound metabolic process	0
GO:0001757	Somite specification	5.78E-195	GO:44260	Cellular macromolecule metabolic process	0
GO:0007379	Segment specification	1.05E-187	GO:44238	Primary metabolic process	0
GO:0015976	Carbon utilization	8.34E-180	GO:9058	Biosynthetic process	0

GO:0019438	Aromatic compound biosynthetic process	1.60E-178
GO:0006164	Purine nucleotide biosynthetic process	2.20E-175
GO:0031448	Positive regulation of fast-twitch skeletal muscle fiber contraction	6.35E-175
GO:0031446	Regulation of fast-twitch skeletal muscle fiber contraction	6.35E-175
GO:0014724	Regulation of twitch skeletal muscle contraction	6.35E-175
GO:0009165	Nucleotide biosynthetic process	1.03E-174
GO:0018130	Heterocycle biosynthetic process	1.28E-173
GO:0090407	Organophosphate biosynthetic process	2.63E-172
GO:0072522	Purine-containing compound biosynthetic process	1.35E-170
GO:0031443	Fast-twitch skeletal muscle fiber contraction	4.07E-170
GO:0034654	Nucleobase-containing compound biosynthetic process	1.68E-168
GO:0045988	Negative regulation of striated muscle contraction	9.15E-167
GO:0014819	Regulation of skeletal muscle contraction	1.85E-165
GO:0045989	Positive regulation of striated muscle contraction	1.98E-159
GO:0045932	Negative regulation of muscle contraction	1.98E-159
GO:0031100	Organ regeneration	0.006
GO:0048729	Tissue morphogenesis	0.022

GO:34641	Cellular nitrogen compound metabolic process	0
GO:46483	Heterocycle metabolic process	0
GO:6950	Response to stress	3.51E-289
GO:55086	Nucleobase-containing small molecule metabolic process	1.70E-285
GO:9117	Nucleotide metabolic process	9.75E-278
GO:6753	Nucleoside phosphate metabolic process	2.95E-274
GO:6096	Glycolysis	1.02E-263
GO:72521	Purine-containing compound metabolic process	8.60E-257
GO:6796	Phosphate-containing compound metabolic process	2.71E-256
GO:6793	Phosphorus metabolic process	2.71E-256
GO:44281	Small molecule metabolic process	2.19E-255
GO:8152	Metabolic process	1.98E-254
GO:9205	Purine ribonucleoside triphosphate metabolic process	1.27E-253
GO:9144	Purine nucleoside triphosphate metabolic process	3.74E-252
GO:9199	Ribonucleoside triphosphate metabolic process	1.32E-251
GO:50881	Musculoskeletal movement	6.57E-156
GO:8544	Epidermis development	1.10E-25
GO:61448	Connective tissue development	1,44E-23
GO:35107	Appendage morphogenesis	5.59E-22
GO:2520	Immune system development	5.27E-05
GO:72331	Signal transduction by p53 class mediator	0.0061
GO:14033	Neural crest cell differentiation	0.0062
GO:43589	Skin morphogenesis	1.41E-02
GO:43588	Skin development	1.71E-02
GO:2764	Immune response-regulating signaling pathway	0.0239
GO:2757	Immune response-activating signal transduction	0.0249
GO:2684	Positive regulation of immune system process	0.0273

	GO:48066	Developmental pigmentation	0.0297
	GO:9725	Response to hormone stimulus	4.26E-70
	GO:48545	Response to steroid hormone stimulus	2.19E-58
	GO:43434	Response to peptide hormone stimulus	4.98E-26
	GO:30518	Intracellular steroid hormone receptor signaling pathway	0.0014
	GO:71375	Cellular response to peptide hormone stimulus	0.0164
	GO:71383	Cellular response to steroid hormone stimulus	0.0216

Additional file 2.12. Selected significantly overrepresented Biological Process GO terms in the GI tract transcriptome (FDR<0.05).

Overrepresented in relation to head			**Overrepresented in relation to skin**		
GO term ID	***GO term description***	***FDR***	***GO term ID***	***GO term description***	***FDR***
GO:0032774	RNA biosynthetic process	0	GO:32774	RNA biosynthetic process	0
GO:0006351	Transcription, DNA-dependent	0	GO:6351	Transcription, DNA-dependent	0
GO:0009303	Rrna transcription	0	GO:90304	Nucleic acid metabolic process	0
GO:0008283	Cell proliferation	0	GO:44249	Cellular biosynthetic process	0
GO:0007586	Digestion	2.26E-238	GO:9303	Rrna transcription	0
GO:0010884	Positive regulation of lipid storage	5.38E-18	GO:43170	Macromolecule metabolic process	0
GO:0042157	Lipoprotein metabolic process	3.94E-15	GO:9059	Macromolecule biosynthetic process	0
GO:0034374	Low-density lipoprotein particle remodelling	2.49E-13	GO:16070	RNA metabolic process	0
GO:0010744	Positive regulation of macrophage derived foam cell differentiation	7.59E-11	GO:34645	Cellular macromolecule biosynthetic process	0
GO:0010886	Positive regulation of cholesterol storage	1.15E-10	GO:8283	Cell proliferation	0
GO:0010883	Regulation of lipid storage	1.52E-10	GO:10467	Gene expression	0
GO:0097006	Regulation of plasma lipoprotein particle levels	1.46E-09	GO:7586	Digestion	8.26E-161
GO:0019915	Lipid storage	1.92E-07	GO:6508	Proteolysis	2.26E-47
GO:0010885	Regulation of cholesterol storage	3.32E-07	GO:42632	Cholesterol homeostasis	1.53E-18
GO:0071827	Plasma lipoprotein particle organization	5.61E-07	GO:55092	Sterol homeostasis	3.20E-18
GO:0071825	Protein-lipid complex subunit organization	5.61E-07	GO:8203	Cholesterol metabolic process	4.55E-13
GO:0034369	Plasma lipoprotein particle remodelling	7.89E-07	GO:16125	Sterol metabolic process	1.21E-11
GO:0034368	Protein-lipid complex remodelling	7.89E-07	GO:42157	Lipoprotein metabolic process	2.48E-11
GO:0034367	Macromolecular complex remodelling	7.89E-07	GO:10884	Positive regulation of lipid storage	3.74E-09
GO:0042632	Cholesterol homeostasis	1.64E-06	GO:55088	Lipid homeostasis	1.75E-07
GO:0055092	Sterol homeostasis	1.64E-06	GO:34374	Low-density lipoprotein particle remodelling	9.13E-07
GO:0006642	Triglyceride mobilization	1.90E-06	GO:97006	Regulation of plasma lipoprotein particle levels	2.12E-06
GO:0010878	Cholesterol storage	4.59E-06	GO:10883	Regulation of lipid storage	3.27E-06
GO:0010743	Regulation of macrophage derived foam cell differentiation	6.75E-06	GO:10743	Regulation of macrophage derived foam cell differentiation	4.25E-05
GO:0042159	Lipoprotein catabolic process	2.48E-04	GO:71827	Plasma lipoprotein particle organization	1.58E-04

GO:0090077	Foam cell differentiation	6.03E-04	GO:71825	Protein-lipid complex subunit organization	1.58E-04
GO:0010742	Macrophage derived foam cell differentiation	6.03E-04	GO:90077	Foam cell differentiation	1.91E-04
GO:0019464	Glycine decarboxylation via glycine cleavage system	0.0054	GO:10742	Macrophage derived foam cell differentiation	1.91E-04
GO:0032309	Icosanoid secretion	0.0057	GO:10744	Positive regulation of macrophage derived foam cell differentiation	2.09E-04
GO:0006857	Oligopeptide transport	0.0061	GO:10886	Positive regulation of cholesterol storage	3.92E-04
GO:0006546	Glycine catabolic process	0.0061	GO:10885	Regulation of cholesterol storage	8.13E-04
GO:0061302	Smooth muscle cell-matrix adhesion	0.0065	GO:35814	Negative regulation of renal sodium excretion	0.0016
GO:0009071	Serine family amino acid catabolic process	0.0068	GO:71436	Sodium ion export	0.0023
GO:2000404	Regulation of T cell migration	0.0068	GO:19915	Lipid storage	3.25E-03
GO:0046464	Acylglycerol catabolic process	7.04E-03	GO:51443	Positive regulation of ubiquitin-protein ligase activity	0.0033
GO:0046461	Neutral lipid catabolic process	7.04E-03	GO:19370	Leukotriene biosynthetic process	0.0045
GO:0016125	Sterol metabolic process	7.78E-03	GO:6030	Chitin metabolic process	0.0056
GO:0006956	Complement activation	0.0081	GO:51437	Positive regulation of ubiquitin-protein ligase activity involved in mitotic cell cycle	0.0060
GO:0055089	Fatty acid homeostasis	0.0081	GO:51351	Positive regulation of ligase activity	0.0060
GO:0015889	Cobalamin transport	0.0086	GO:6637	Acyl-coa metabolic process	0.0063

Additional file 2.13. Selected significantly overrepresented Biological Process GO terms in the head transcriptome (FDR<0.05).

Overrepresented in relation to skin			**Overrepresented in relation to GI tract**		
GO term ID	***GO term description***	***FDR***	***GO term ID***	***GO term description***	***FDR***
GO:0043170	Macromolecule metabolic process	1.43E-118	GO:0080090	Regulation of primary metabolic process	0
GO:0044260	Cellular macromolecule metabolic process	7.41E-112	GO:0071842	Cellular component organization at cellular level	0
GO:0050794	Regulation of cellular process	2.07E-97	GO:0071841	Cellular component organization or biogenesis at cellular level	0
GO:0019538	Protein metabolic process	2.78E-94	GO:0071840	Cellular component organization or biogenesis	0
GO:0044267	Cellular protein metabolic process	4.16E-90	GO:0006807	Nitrogen compound metabolic process	0
GO:0009059	Macromolecule biosynthetic process	2.04E-82	GO:0007275	Multicellular organismal development	0
GO:0034645	Cellular macromolecule biosynthetic process	3.98E-81	GO:0019222	Regulation of metabolic process	0
GO:0006412	Translation	3.93E-79	GO:0060255	Regulation of macromolecule metabolic process	0
GO:0010467	Gene expression	5.45E-76	GO:0006725	Cellular aromatic compound metabolic process	0
GO:0031323	Regulation of cellular metabolic process	3.47E-75	GO:0071704	Organic substance metabolic process	0
GO:0080090	Regulation of primary metabolic process	2.01E-71	GO:0065007	Biological regulation	0
GO:0007166	Cell surface receptor signaling pathway	2.17E-71	GO:0007154	Cell communication	0
GO:0023052	Signaling	1.94E-68	GO:0006412	Translation	0
GO:0031326	Regulation of cellular biosynthetic process	6.65E-68	GO:0051716	Cellular response to stimulus	0
GO:0019222	Regulation of metabolic process	3.70E-67	GO:0032502	Developmental process	0
GO:0007154	Cell communication	5.28E-67	GO:0032501	Multicellular organismal process	0
GO:0022613	Ribonucleoprotein complex biogenesis	2.17E-66	GO:0048856	Anatomical structure development	0
GO:0009889	Regulation of biosynthetic process	2.26E-66	GO:0090304	Nucleic acid metabolic process	0
GO:0071843	Cellular component biogenesis at cellular level	8.55E-66	GO:0006139	Nucleobase-containing compound metabolic process	0
GO:0008104	Protein localization	1.18E-63	GO:0048731	System development	0
GO:0010556	Regulation of macromolecule biosynthetic process	1.20E-63	GO:0044267	Cellular protein metabolic process	0
GO:0042254	Ribosome biogenesis	2.44E-63	GO:0044260	Cellular macromolecule metabolic process	0
GO:0051716	Cellular response to stimulus	1.26E-62	GO:0044249	Cellular biosynthetic process	0
GO:0007399	Nervous system development	1.11E-61	GO:0044238	Primary metabolic process	0
GO:2000112	Regulation of cellular macromolecule biosynthetic process	1.42E-61	GO:0050896	Response to stimulus	0

GO:0009987	Cellular process	7.34E-56	GO:0050794	Regulation of cellular process	0
GO:0007165	Signal transduction	8.58E-55	GO:0050789	Regulation of biological process	0
GO:0050789	Regulation of biological process	1.65E-54	GO:0044085	Cellular component biogenesis	0
GO:0065007	Biological regulation	4.08E-53	GO:0051179	Localization	0
GO:0048522	Positive regulation of cellular process	1.25E-52	GO:0009653	Anatomical structure morphogenesis	0
GO:0010468	Regulation of gene expression	3.99E-52	GO:0031323	Regulation of cellular metabolic process	0
GO:0060255	Regulation of macromolecule metabolic process	1.38E-51	GO:0043170	Macromolecule metabolic process	0
GO:0045184	Establishment of protein localization	1.15E-50	GO:0009059	Macromolecule biosynthetic process	0
GO:0033036	Macromolecule localization	1.83E-50	GO:0009058	Biosynthetic process	0
GO:0022008	Neurogenesis	4.90E-50	GO:0016070	RNA metabolic process	0
GO:0070727	Cellular macromolecule localization	9.63E-50	GO:0016043	Cellular component organization	0
GO:0048699	Generation of neurons	1.36E-49	GO:0034645	Cellular macromolecule biosynthetic process	0
GO:0050877	Neurological system process	2.01E-49	GO:0034641	Cellular nitrogen compound metabolic process	0
GO:0034613	Cellular protein localization	5.57E-49	GO:0023052	Signaling	0
GO:0015031	Protein transport	4.20E-48	GO:0046483	Heterocycle metabolic process	0
GO:0048666	Neuron development	5.89E-40	GO:0022008	Neurogenesis	6.69E-144
GO:0031175	Neuron projection development	5.03E-36	GO:0048699	Generation of neurons	9.78E-139
GO:0044281	Small molecule metabolic process	6.64E-24	GO:0048583	Regulation of response to stimulus	2.49E-136
GO:0019637	Organophosphate metabolic process	6.55E-18	GO:0030182	Neuron differentiation	3.85E-130
GO:0001501	Skeletal system development	1.57E-17	GO:0048666	Neuron development	1.66E-114
GO:0007417	Central nervous system development	1.38E-11	GO:0031175	Neuron projection development	7.70E-111
GO:0006950	Response to stress	4.78E-10	GO:0048812	Neuron projection morphogenesis	1.56E-97
GO:0009056	Catabolic process	3.13E-08	GO:0007409	Axonogenesis	7.72E-86
GO:0007420	Brain development	5.71E-06	GO:0007411	Axon guidance	2.66E-67
GO:0030900	Forebrain development	0.0001	GO:0051216	Cartilage development	1.67E-54
GO:0048840	Otolith development	0.0010	GO:0007420	Brain development	2.08E-51
GO:0046879	Hormone secretion	0.0013	GO:0002520	Immune system development	1.70E-41
GO:0009914	Hormone transport	0.0014	GO:0007268	Synaptic transmission	2.87E-34

GO:0021578	Hindbrain maturation	0.0023
GO:0048856	Anatomical structure development	0.0028
GO:0042445	Hormone metabolic process	0.0028
GO:0008152	Metabolic process	3.97E-03
GO:0021575	Hindbrain morphogenesis	0.005
GO:0048170	Positive regulation of long-term neuronal synaptic plasticity	0.005
GO:0035284	Brain segmentation	0.005
GO:0023041	Neuronal signal transduction	0.008
GO:0021983	Pituitary gland development	0.008
GO:0032870	Cellular response to hormone stimulus	0.012
GO:0070167	Regulation of biomineral tissue development	0.013
GO:0045161	Neuronal ion channel clustering	0.018
GO:0021846	Cell proliferation in forebrain	0.020
GO:0021533	Cell differentiation in hindbrain	0.029
GO:0097150	Neuronal stem cell maintenance	0.029
GO:0030072	Peptide hormone secretion	0.030
GO:0042403	Thyroid hormone metabolic process	0.044
GO:0010033	Response to organic substance	0.046

GO:0060350	Endochondral bone morphogenesis	3.02E-34
GO:0060537	Muscle tissue development	2.33E-32
GO:0042246	Tissue regeneration	2.34E-32
GO:0060348	Bone development	7.72E-32
GO:0060349	Bone morphogenesis	9.30E-32
GO:0030900	Forebrain development	1.05E-25
GO:0030099	Myeloid cell differentiation	1.55E-25
GO:0010975	Regulation of neuron projection development	3.59E-24
GO:0001649	Osteoblast differentiation	5.68E-23
GO:0060828	Regulation of canonical Wnt receptor signaling pathway	8.48E-23
GO:0060322	Head development	2.45E-19
GO:0060351	Cartilage development involved in endochondral bone morphogenesis	1.13E-17
GO:0060323	Head morphogenesis	2.72E-17
GO:0001764	Neuron migration	9.86E-10
GO:0021537	Telencephalon development	2.57E-07
GO:0006836	Neurotransmitter transport	2.86E-05
GO:0016358	Dendrite development	6.01E-05
GO:0009755	Hormone-mediated signaling pathway	0.0070
GO:0032400	Melanosome localization	0,0082
GO:0021697	Cerebellar cortex formation	0.0086
GO:0030878	Thyroid gland development	0.012
GO:0021510	Spinal cord development	2,60E-02
GO:0048545	Response to steroid hormone stimulus	2.63E-12
GO:0009725	Response to hormone stimulus	5.30E-10
GO:0009914	Hormone transport	7.58E-05
GO:0043434	Response to peptide hormone stimulus	7,35E-03

Additional file 2.14. List of the most representative metabolic pathways in the skin, GI-tract and head transcriptomes using KEGG analysis.

	Number of enzyme codes (EC)		
KEGG pathway	**Skin**	**GI-tract**	**Head**
Purine metabolism	56	51	58
Amino sugar and nucleotide sugar metabolism	31	31	35
Pyrimidine metabolism	36	33	34
Arginine and proline metabolism	35	30	32
Glycerophospholipid metabolism	30	26*	29
Glycine, serine and threonine metabolism	32	29	29
Glycolysis / Gluconeogenesis	28	27	26
Alanine, aspartate and glutamate metabolism	23	18	25
Cysteine and methionine metabolism	24	20	25
Inositol phosphate metabolism	22	20*	24
Pyruvate metabolism	24	23	24
Aminoacyl-tRNA biosynthesis	22	22	23
Valine, leucine and isoleucine degradation	22	20	22
Phosphatidylinositol signaling system	20	18*	20
Sphingolipid metabolism	19	17*	20
Citrate cycle (TCA cycle)	19	18	19
Glutathione metabolism	19	18	19
Starch and sucrose metabolism	23	24	19★
Drug metabolism - other enzymes	18	18	18
Glycosaminoglycan biosynthesis - chondroitin sulfate	10	4▲	11
Glycosaminoglycan biosynthesis - heparan sulfate	8	4▲	10
Steroid biosynthesis	13	12	13
Steroid degradation	3	3	3
Steroid hormone biosynthesis	18	15*	18

* - indicates lipid related metabolic pathways substantially modified between tissues
▲ - indicates metabolic pathways involved in chondrogenic matrix generation substantially different between tissues
★ - indicates starch and sucrose metabolism is substantially different between tissues

Additional file 2.15. The list of the top most significantly up-regulated genes between premetamorphic stage 5 and the Juvenile stage determined using a linear model in Bayseq with a Benjamin-Hochberg adjustment for multiple testing analysis with a cut-off set at 0.05 (FDR < 0.05). Contig name, Gene name, Accession number (no.), Organism and E-value are shown for each gene.

Additional file 2.15a. List of top most significantly upregulated genes between premetamorphic stage 5 and juvenile stage as determined by a linear model in Bayseq with a Benjamin-Hochberg adjustment for multiple testing analysis with a cut-off set at 0.05 (FDR<0.05). Contig name, Gene name, Accession number (no.), Organism and E-value are shown for each gene.

Upregulated genes in premetamorphic stage 5 compared to juvenile

Contig ID	*Gene name*	*Accession no.*	*Organism*	*E-value*
Contig07799	Putative uncharacterized protein ART2-like	XP_004616260.1	*Sorex araneus*	3E-27
Contig1693	Ribosomal protein S23	AEJ84339.1	*Capra hircus*	8E-30
Contig26083	Hypothetical protein BOS_1871	DAA32622.1	*Bos taurus*	3E-30
Contig26869	Hypothetical protein LOC100559304	XP_003230372.1	*Anolis carolinensis*	6E-21
Contig04456	TOM1-like protein 2	CBN81216.1	*Dicentrarchus labrax*	0
Contig14322	CD59 glycoprotein-like	XP_003460314.1	*Oreochromis niloticus*	2E-43
Contig1667	Vinculin	CBN81495.1	*Dicentrarchus labrax*	0
Contig20143	Collagen alpha-1(I) chain-like	XP_003460741.1	*Cavia porcellus*	2E-31
Contig1362	Rrna promoter binding protein-like	XP_002724111.1	*Oryctolagus cuniculus*	9E-27
Contig16982	Ryanodine receptor 1-like	XP_004560674.1	*Maylandia zebra*	3E-73
Contig17221	Latrophilin-2	XP_002663750.2	*Danio rerio*	2E-67
Contig18157	Neutral ceramidase-like	XP_003961257.1	*Takifugu rubripes*	1E-82
Contig13137	Dedicator of cytokinesis protein 7 isoform X6	XP_005468811.1	*Oreochromis niloticus*	2E-157
Contig1230	Unnamed protein product	BAE33391.1	*Mus musculus*	5E-26
Contig18278	Unnamed protein product	BAE43022.1	*Mus musculus*	6E-40
Contig25150	Translation initiation factor IF-2-like	XP_004450492.1	*Dasypus novemcinctus*	4E-20
Contig1002	Keratin 1	ABC88386.1	*Hippoglossus hippoglossus*	2E-43

Upregulated genes in juvenile compared to premetamorphic stage 5				
Contig1352	Actin alpha skeletal muscle	ACM41845.1	*Epinephelus coioides*	1E-114
Contig1091	AF500273_1 fast skeletal muscle alpha-actin	AAM21702.2	*Gadus morhua*	5E-72
Contig1395	Tetraspanin-12-like	XP_003448856.1	*Oreochromis niloticus*	2E-93
Contig355	Protein-glutamine gamma-glutamyltransferase 5-like	XP_003448488.1	*Oreochromis niloticus*	0
Contig1315	Sarcoplasmic/endoplasmic reticulum calcium atpase 1	P70083.2	*Makaira nigricans*	0
Contig1500	Ribosomal protein, large, P0	NP_001080134.1	*Xenopus laevis*	6E-50
Contig1214	Nucleoside diphosphate kinase A-like	XP_003442598.1	*Oreochromis niloticus*	4E-75
Contig796	Myosin light chain 2, isoform B	CAD32552.1	*Hippoglossus hippoglossus*	2E-86
Contig1162	Cytochrome oxidase subunit I	CAO79645.1	*Hippoglossus hippoglossus*	1E-112
Contig20504	Type-4 ice-structuring protein	Q8JI37.1	*Paralichthys olivaceus*	3E-40
Contig995	Myosin heavy chain	ADG29145.1	*Epinephelus coioides*	1E-136
Contig595	Transcription factor E2F4-like	XP_003447142.1	*Oreochromis niloticus*	1E-106
Contig1137	Heat shock protein 70	NP_001098385.1	*Oryzias latipes*	0
Contig28671	Trypsinogen Flou2	AAY23358.1	*Hippoglossus hippoglossus*	5E-43
Contig18804	Apolipoprotein E	ACF21982.1	*Oplegnathus fasciatus*	8E-87
Contig1000	Parvalbumin	BAF98925.1	*Paralichthys olivaceus*	1E-42
Contig15768	Ribosomal protein L18a	BAF98666.1	*Solea senegalensis*	1E-98
Contig1625	Putative 14 kda apolipoprotein	CAH57705.1	*Platichthys flesus*	3E-58
Contig04453	Trypsinogen 2 precursor	AAC32752.1	*Pseudopleuronectes americanus*	9E-32
Contig25330	Sarcoendoplasmic reticulum calcium atpase	ABG90496.1	*Silurus lanzhouensis*	2E-28
Contig411	Elongation factor 1 alpha isoform 2	BAF64485.1	*Solea senegalensis*	0
Contig29	Alpha-actinin-3-like isoform 1	XP_003447595.1	*Oreochromis niloticus*	0
Contig1056	Sarcoplasmic/endoplasmic reticulum calcium atpase 1-like isoform X1	XP_003454037.1	*Oreochromis niloticus*	0
Contig24482	Actin, gamma-enteric smooth muscle-like isoform 1	XP_003201904.1	*Meleagris gallopavo*	2E-26
Contig1671	Apolipoprotein AI precursor	CAH59609.1	*Platichthys flesus*	1E-102
Contig1001	60S ribosomal protein L21-like	XP_005797910.1	*Xiphophorus maculatus*	3E-104

Contig539	Unnamed protein product	CAG02349.1	*Tetraodon nigroviridis*	1E-126
Contig05820	Fish-egg lectin	BAL61198.1	*Oplegnathus fasciatus*	2E-83
Contig25352	Alpha-cardiac actin	AAA37165.1	*Mus musculus*	1E-22
Contig25161	Alpha-actin	AAX18244.1	*Acipenser transmontanus*	1E-48
Contig13800	Myosin light chain 1, skeletal muscle isoform-like isoform X1	XP_003445346.1	*Oreochromis niloticus*	8E-77
Contig1172	Ribosomal protein L6	AEH76599.1	*Epinephelus bruneus*	2E-56
Contig72	Eukaryotic initiation factor 4A-I isoform X1	XP_003458967.1	*Oreochromis niloticus*	0
Contig26602	Parvalbumin	AAY27426.1	*Paralichthys olivaceus*	7E-17
Contig06809	Heat shock protein 90 beta	AAP20179.1	*Pagrus major*	1E-117
Contig1356	Beta actin	ACZ63697.1	*Hippoglossus hippoglossus*	4E-74
Contig615	Carboxypeptidase B	BAC53789.1	*Paralichthys olivaceus*	1E-146
Contig20859	60S ribosomal protein L3-like	XP_004071207.1	*Oryzias latipes*	2E-123
Contig772	AP-3 complex subunit mu-2	XP_003448631.1	*Oreochromis niloticus*	0
Contig21912	Chymotrypsinogen 1	BAL14136.1	*Thunnus orientalis*	5E-87
Contig1030	Elongation factor 1 alpha	ACE82251.1	*Hippoglossus hippoglossus*	1E-151
Contig1360	Sarcoplasmic/endoplasmic reticulum calcium atpase 1-like	XP_003458779.1	*Oreochromis niloticus*	1E-18
Contig1385	60S ribosomal protein	AEB31272.1	*Epinephelus bruneus*	2E-83
Contig1592	40S ribosomal protein S26	ABU98965.1	*Hippoglossus hippoglossus*	3E-45
Contig834	Keratin, type I cytoskeletal 18-like	XP_003449152.1	*Oreochromis niloticus*	5E-27
Contig25154	Chymotrypsinogen 2	BAL14137.1	*Thunnus orientalis*	2E-43
Contig979	40S ribosomal protein Sa	AAP20147.1	*Pagrus major*	5E-74
Contig399	Rho guanine nucleotide exchange factor 6-like	XP_003445205.1	*Oreochromis niloticus*	0
Contig1572	Receptor for activated protein kinase C	AAT35603.1	*Paralichthys olivaceus*	1E-74
Contig17281	60S ribosomal protein L19	ACO09605.1	*Osmerus mordax*	6E-65
Contig520	Collagen alpha-1(I) chain-like	XP_003453458.1	*Oreochromis niloticus*	9E-71

Additional file 2.15b. List of top most significantly upregulated genes between metamorphic proclimax stage 8 and premetamorphic stage 5 as determined by a linear model in Bayseq with a Benjamin-Hochberg adjustment for multiple testing analysis with a cut-off set at 0.05 (FDR<0.05). Contig name, Gene name, Accession number (no.), Organism and E-value are shown for each gene.

Upregulated genes in metamorphic proclimax stage 8 compared to premetamorphic stage 5

Contig ID	*Gene name*	*Accession no.*	*Organism*	*E-value*
Contig04550	Lactate dehydrogenase-A	AAP44524.1	*Chromis caudalis*	1E-166
Contig347	Carboxypeptidase A2	BAC53787.1	*Paralichthys olivaceus*	0
Contig405	Secretory carrier-associated membrane protein 3-like	XP_003969342.1	*Takifugu rubripes*	3E-83
Contig28608	Beta-enolase	ADG29136.1	*Epinephelus coioides*	1E-27
Contig11326	Phospholipase A2	BAA23737.1	*Pagrus major*	1E-69
Contig179	Lumican-like	XP_003444990.1	*Oreochromis niloticus*	1E-155
Contig10151	Chymotrypsinogen	ADG29171.1	*Epinephelus coioides*	3E-82
Contig1249	Glyceraldehyde-3-phosphate dehydrogenase	ABY19518.1	*Paralichthys olivaceus*	2E-19
Contig28338	Parvalbumin I	1206380A	*Electrophorus sp.*	7E-12
Contig06996	Inositol monophosphatase 1-like isoform X1	XP_003439317.1	*Oreochromis niloticus*	1E-135
Contig16531	Gelsolin-like	XP_003437831.1	*Oreochromis niloticus*	5E-74
Contig1276	Trypsinogen	AEM91638.1	*Channa argus*	5E-48
Contig04519	Myc box-dependent-interacting protein 1-like	XP_003446611.1	*Oreochromis niloticus*	3E-36
Contig1607	Chymotrypsinogen 1	BAA82365.1	*Paralichthys olivaceus*	6E-22
Contig22951	Apolipoprotein B-100-like	XP_003446425.1	*Oreochromis niloticus*	9E-52
Contig06549	Keratin, type I cytoskeletal 18	CBN80920.1	*Dicentrarchus labrax*	1E-154
Contig03409	Hypothetical protein LOC100330916	XP_002660725.2	*Danio rerio*	1E-135
Contig1422	Fructose-bisphosphate aldolase A	NP_001167391.1	*Salmo salar*	2E-18
Contig1087	Phosphoglycerate mutase 2-like	XP_003444406.1	*Oreochromis niloticus*	1E-66
Contig708	Adenine nucleotide translocator s254	NP_001037840.1	*Takifugu rubripes*	1E-68
Contig12118	Elastase-like serine protease	ACG50688.1	*Paralichthys olivaceus*	1E-141
Contig553	15-hydroxyprostaglandin dehydrogenase [NAD(+)]-like	XP_003451463.1	*Oreochromis niloticus*	3E-73
Contig13429	Latisemin-like	XP_003971902.1	*Takifugu rubripes*	5E-132

Contig03682	Heparin cofactor II	ACC86113.1	*Paralichthys olivaceus*	0
Contig12730	Cytochrome c oxidase subunit VIIa-related protein, mitochondrial	CBN81583.1	*Dicentrarchus labrax*	5E-49
Contig00337	NAD(P) transhydrogenase, mitochondrial-like isoform X1	XP_003456827.1	*Oreochromis niloticus*	0
Contig02752	Cytosolic phospholipase A2 zeta-like	XP_003446488.1	*Oreochromis niloticus*	0
Contig06935	Inosine-uridine preferring nucleoside hydrolase-like	XP_003977955.1	*Takifugu rubripes*	0
Contig03255	Protein disulfide-isomerase-like	XP_003456032.1	*Oreochromis niloticus*	0
Contig08871	Cytolysin Src-1-like	XP_003442214.1	*Oreochromis niloticus*	1E-74
Contig05635	Alpha-2-HS-glycoprotein-like	XP_004078952.1	*Oryzias latipes*	2E-111
Contig14518	Uncharacterized protein LOC100709362	XP_003454247.1	*Oreochromis niloticus*	3E-27
Contig15586	Diazepam-binding inhibitor	AEK25827.1	*Micropterus salmoides*	2E-31
Contig149	GTP-binding protein PTD004	ACO09273.1	*Osmerus mordax*	0
Upregulated genes in premetamorphic stage 5 compared to metamorphic proclimax stage 8				
Contig05607	Type I keratin isoform 2	BAF56914.1	*Solea senegalensis*	1E-145
Contig06282	Keratin, type I cytoskeletal 13-like	XP_003453825.1	*Oreochromis niloticus*	1E-144

Additional file 2.15c. List of top most significantly upregulated genes between metamorphic climax stage 9A and premetamorphic stage 5 as determined by a linear model in Bayseq with a Benjamin-Hochberg adjustment for multiple testing analysis with a cut-off set at 0.05 (FDR<0.05). Contig name, Gene name, Accession number (no.), Organism and E-value are shown for each gene.

Upregulated genes in metamorphic climax stage 9A compared to premetamorphic stage 5				
Contig ID	***Gene name***	***Accession no.***	***Organism***	***E-value***
Contig10151	Chymotrypsinogen	ADG29171.1	*Epinephelus coioides*	3E-82
Contig06996	Inositol monophosphatase 1-like isoform X1	XP_003439317.1	*Oreochromis niloticus*	1E-135
Contig1276	Trypsinogen	AEM91638.1	*Channa argus*	5E-48
Contig1422	Fructose-bisphosphate aldolase A	NP_001167391.1	*Salmo salar*	2E-18
Contig12118	Elastase-like serine protease	ACG50688.1	*Paralichthys olivaceus*	1E-141
Contig1087	Phosphoglycerate mutase 2-like	XP_003444406.1	*Oreochromis niloticus*	1E-66
Contig03409	Hypothetical protein LOC100330916	XP_002660725.2	*Danio rerio*	1E-135
Contig708	Adenine nucleotide translocator s254	NP_001037840.1	*Takifugu rubripes*	1E-68
Contig28671	Trypsinogen Flou2	AAY23358.1	*Hippoglossus hippoglossus*	5E-43
Contig553	15-hydroxyprostaglandin dehydrogenase [NAD(+)]-like	XP_003451463.1	*Oreochromis niloticus*	3E-73
Contig06935	Inosine-uridine preferring nucleoside hydrolase-like	XP_003977955.1	*Takifugu rubripes*	0
Contig05820	Fish-egg lectin	BAL61198.1	*Oplegnathus fasciatus*	2E-83
Contig00337	NAD(P) transhydrogenase, mitochondrial-like isoform X1	XP_003456827.1	*Oreochromis niloticus*	0
Contig02752	Cytosolic phospholipase A2 zeta-like	XP_003446488.1	*Oreochromis niloticus*	0
Contig03255	Protein disulfide-isomerase-like	XP_003456032.1	*Oreochromis niloticus*	0
Contig05635	Alpha-2-HS-glycoprotein-like	XP_004078952.1	*Oryzias latipes*	2E-111
Contig08871	Cytolysin Src-1-like	XP_003442214.1	*Oreochromis niloticus*	1E-74
Upregulated genes in premetamorphic stage 5 compared to metamorphic climax stage 9A				
Contig05607	Type I keratin isoform 2	BAF56914.1	*Solea senegalensis*	1E-145
Contig06282	Keratin, type I cytoskeletal 13-like	XP_003453825.1	*Oreochromis niloticus*	1E-144
Contig01282	Uncharacterized protein LOC100691699 isoform X2	XP_005449125.1	*Oreochromis niloticus*	0
Contig00195	Fibrocystin-L	XP_003447322.1	*Oreochromis niloticus*	0
Contig923	Alpha-amylase	ABJ97444.1	*Xiphister atropurpureus*	1E-148

Contig03232	Macrophage mannose receptor 1-like	XP_003437865.1	*Oreochromis niloticus*	3E-77
Contig09466	Zinc finger protein 628-like isoform X5	XP_005455430.1	*Oreochromis niloticus*	8E-112
Contig17770	Ankyrin repeat and KH domain-containing protein 1 isoform X1	XP_003445913.1	*Oreochromis niloticus*	8E-76
Contig08520	UDP-glucose:glycoprotein glucosyltransferase 2	XP_003447406.1	*Oreochromis niloticus*	0
Contig06464	SH2 domain-containing protein 5-like	XP_004069380.1	*Oryzias latipes*	0
Contig12963	Hypothetical protein LOC100696747	XP_003455026.1	*Oreochromis niloticus*	6E-47
Contig03281	Synaptotagmin-11-like	XP_003451315.1	*Oreochromis niloticus*	0
Contig01305	Chromobox protein homolog 2-like	XP_003442539.1	*Oreochromis niloticus*	1E-113
lchead_c16028	Contactin-associated protein-like 2	XP_003456781.1	*Oreochromis niloticus*	1E-149
Contig05135	Tenascin-X-like	XP_003459083.1	*Oreochromis niloticus*	0
Contig09575	Myotubularin-related protein 7-like	XP_003455820.1	*Oreochromis niloticus*	1E-115
Contig03314	Cyclin-T2-like	XP_003443331.1	*Oreochromis niloticus*	9E-17
Contig06850	Cryptochrome-1-like	XP_003452063.1	*Oreochromis niloticus*	0
Contig17960	Low-density lipoprotein receptor-related protein 1-like	XP_003963209.1	*Takifugu rubripes*	2E-107
Contig07286	Phosphorylated CTD-interacting factor 1	XP_003457750.1	*Oreochromis niloticus*	1E-106
Contig02198	Semaphorin-7A-like	XP_003450354.1	*Oreochromis niloticus*	1E-127
Contig02216	Uncharacterized protein LOC100693968 isoform X1	XP_003446915.1	*Oreochromis niloticus*	0
Contig06214	Neural cell adhesion molecule L1-like isoform X1	XP_003448281.1	*Oreochromis niloticus*	1E-174
Contig07338	Protein phosphatase Slingshot homolog 2-like isoform X2	XP_005462386.1	*Oreochromis niloticus*	9E-116
Contig132	Glutamate decarboxylase 2-like	XP_003439331.1	*Oreochromis niloticus*	0
Contig05591	RNA-binding protein 10-like	XP_003448331.1	*Oreochromis niloticus*	1E-173
Contig13972	Hypothetical protein LOC100695447	XP_003459280.1	*Oreochromis niloticus*	5E-66
Contig07598	Phosphoenolpyruvate carboxykinase	AAX21768.2	*Acanthopagrus schlegelii*	0
Contig02885	Microtubule-associated protein 1B-like	XP_005454597.1	*Oreochromis niloticus*	0
Contig1744	Cap-specific mrna (nucleoside-2'-O-)-methyltransferase 1-like	XP_003449946.1	*Oreochromis niloticus*	1E-169
Contig08589	Oxysterol-binding protein-related protein 8 isoform X1	XP_003449817.1	*Oreochromis niloticus*	1E-166
Contig03144	Neuroplastin-like isoform X2	XP_005450939.1	*Oreochromis niloticus*	1E-130

lchead_c7007	Uncharacterized protein c20orf194-like	XP_003447892.1	*Oreochromis niloticus*	4E-57
Contig05034	Sentrin-specific protease 6-like isoform X3	XP_005452489.1	*Oreochromis niloticus*	0
Contig07800	Phosphatidylinositol 4-kinase type 2-beta-like	XP_003448041.1	*Oreochromis niloticus*	0
Contig09966	Oxysterol-binding protein-related protein 1-like	XP_003977651.1	*Takifugu rubripes*	0
Contig23771	Laminin subunit beta-1-like	XP_003448148.1	*Oreochromis niloticus*	4E-69
Contig23056	Pleckstrin homology-like domain family B member 2	XP_003446815.1	*Oreochromis niloticus*	2E-40
Contig10466	NEDD8-activating enzyme E1 regulatory subunit-like isoformx1	XP_003445754.1	*Oreochromis niloticus*	1E-117
Contig17157	Transmembrane protein 134	ACQ58040.1	*Anoplopoma fimbria*	4E-86
Contig16346	Transformation/transcription domain-associated protein	XP_001919276.3	*Danio rerio*	3E-83
Contig07774	Protein FAM91A1-like	XP_003444196.1	*Oreochromis niloticus*	2E-97
Contig17788	Nuclear receptor ROR-beta-like	XP_003451344.1	*Oreochromis niloticus*	7E-13
Contig21166	RNA-binding protein Musashi homolog 1-like isoformx3	XP_003441610.1	*Oreochromis niloticus*	4E-82
Contig09528	CUGBP Elav-like family member 3-like isoform 1	XP_003450950.1	*Oreochromis niloticus*	1E-121
Contig15911	Zinc finger protein ubi-d4-like isoform X1	XP_003444769.1	*Oreochromis niloticus*	6E-75
Contig08795	Inositol 1,4,5-trisphosphate receptor type 3-like	XP_003220443.1	*Anolis carolinensis*	1E-170
Contig23670	C2 domain-containing protein 5-like isoform X1	XP_003440632.2	*Oreochromis niloticus*	2E-79
Contig31354	Fmvia	AAD52005.1	*Morone saxatilis*	2E-26
Contig13284	CAD protein-like	XP_003456748.1	*Oreochromis niloticus*	1E-146
Contig14221	Teneurin-4-like isoform 1	XP_003450204.1	*Oreochromis niloticus*	1E-146
Contig05301	Fascin-like	XP_003443269.1	*Oreochromis niloticus*	0
lchead_c76077	Rho guanine nucleotide exchange factor 11-like	XP_003458910.1	*Oreochromis niloticus*	1E-57
Contig18720	ADP-ribosylation factor-like protein 3-like	XP_003441784.1	*Oreochromis niloticus*	3E-94
Contig09378	Neuronal migration protein doublecortin-like isoform 1	XP_003446904.1	*Oreochromis niloticus*	1E-171
Contig17353	Ras-related protein Rab-40C-like isoform 1	XP_003453881.1	*Oreochromis niloticus*	4E-40
lchead_c76634	Protein bassoon-like	XP_003973339.1	*Takifugu rubripes*	5E-49
Contig09653	Vascular endothelial growth factor receptor kdr-like	XP_003445218.1	*Oreochromis niloticus*	4E-58
Contig18146	Cytoplasmic phosphatidylinositol transfer protein 1-like isoform X1	XP_003458369.1	*Oreochromis niloticus*	1E-117

Additional file 2.15d. List of top most significantly upregulated genes between metamorphic climax stage 9B and premetamorphic stage 5 as determined by a linear model in Bayseq with a Benjamin-Hochberg adjustment for multiple testing analysis with a cut-off set at 0.05 (FDR<0.05). Contig name, Gene name, Accession number (no.), Organism and E-value are shown for each gene.

Up regulated in metamorphic climax stage 9B compared to premetamorphic stage 5				
Contig ID	***Gene name***	***Accession no.***	***Organism***	***E-value***
Contig06286	Serpin A3-5-like	XP_003445650.1	*Oreochromis niloticus*	1E-134
Contig03409	Hypothetical protein LOC100330916	XP_002660725.2	*Danio rerio*	1E-135
Contig12118	Elastase-like serine protease	ACG50688.1	*Paralichthys olivaceus*	1E-141
Contig1422	Fructose-bisphosphate aldolase A	NP_001167391.1	*Salmo salar*	2E-18
Contig708	Adenine nucleotide translocator s254	NP_001037840.1	*Takifugu rubripes*	1E-68
Contig05820	Fish-egg lectin	BAL61198.1	*Oplegnathus fasciatus*	2E-83
Contig05635	Alpha-2-HS-glycoprotein-like	XP_004078952.1	*Oryzias latipes*	2E-111
Contig02752	Cytosolic phospholipase A2 zeta-like	XP_003446488.1	*Oreochromis niloticus*	0
Contig1284	Keratin, type I cytoskeletal 13-like	XP_003442483.1	*Oreochromis niloticus*	1E-29
Contig00708	Von Willebrand factor A domain-containing protein 7-like isoform X1	XP_003448088.2	*Oreochromis niloticus*	0
Up regulated in premetamorphic stage 5 compared to metamorphic climax stage 9B				
Contig05607	Type I keratin isoform 2	BAF56914.1	*Solea senegalensis*	1E-145
Contig494	High choriolytic enzyme 1-like	XP_003456934.1	*Oreochromis niloticus*	4E-87

Additional file 2.15e. List of top most significantly upregulated genes between metamorphic climax stage 9C and premetamorphic stage 5 as determined by a linear model in Bayseq with a Benjamin-Hochberg adjustment for multiple testing analysis with a cut-off set at 0.05 (FDR<0.05). Contig name, Gene name, Accession number (no.), Organism and E-value are shown for each gene.

Up regulated in metamorphic climax stage 9C compared to premetamorphic stage 5

Contig ID	*Gene name*	*Accession no.*	*Organism*	*E-value*
Contig10225	Apolipoprotein A-IV4 precursor	NP_001027893.1	*Takifugu rubripes*	1E-109
Contig179	Lumican-like	XP_003444990.1	*Oreochromis niloticus*	1E-155
Contig28338	Parvalbumin I	1206380A	*Electrophorus sp.*	7E-12
Contig28441	Putative fast skeletal muscle troponin	AAP82940.1	*Paralichthys olivaceus*	4E-15
Contig00901	Immunoglobulin-like and fibronectin type III domain-containing protein 1-like	XP_003438838.1	*Oreochromis niloticus*	0
Contig16531	Gelsolin-like	XP_003437831.1	*Oreochromis niloticus*	5E-74
Contig06996	Inositol monophosphatase 1-like isoform X1	XP_003439317.1	*Oreochromis niloticus*	1E-135
Contig00664	Calpain-11	ACY78223.1	*Hippoglossus hippoglossus*	0
Contig06286	Serine protease inhibitor A3K-like	XP_003445650.1	*Oreochromis niloticus*	3E-164
Contig08272	Beta-2-glycoprotein 1	ADX97142.1	*Perca flavescens*	1E-174
Contig27668	Apolipoprotein C-I-like	XP_004550997.1	*Maylandia zebra*	3E-14
Contig00663	Fibronectin 1	CAQ13985.1	*Danio rerio*	0
Contig708	Adenine nucleotide translocator s254	NP_001037840.1	*Takifugu rubripes*	1E-68
Contig12118	Elastase-like serine protease	ACG50688.1	*Paralichthys olivaceus*	1E-141
Contig01049	Sushi domain-containing protein 2-like	XP_003453945.1	*Oreochromis niloticus*	0
Contig03409	Hypothetical protein LOC100330916	XP_002660725.2	*Danio rerio*	1E-135
Contig00274	Desmocollin-2-like	XP_003437940.1	*Oreochromis niloticus*	0
Contig28671	Trypsinogen Flou2	AAY23358.1	*Hippoglossus hippoglossus*	5E-43
Contig553	15-hydroxyprostaglandin dehydrogenase [NAD(+)]-like	XP_003451463.1	*Oreochromis niloticus*	3E-73
Contig03291	Hyaluronan-binding protein 2, partial	CBN81454.1	*Dicentrarchus labrax*	0
Contig03682	Heparin cofactor II	ACC86113.1	*Paralichthys olivaceus*	0
Contig06935	Inosine-uridine preferring nucleoside hydrolase-like	XP_003977955.1	*Takifugu rubripes*	0
Contig00037	Alpha-tectorin	CBN81411.1	*Dicentrarchus labrax*	0

Contig00708	Von Willebrand factor A domain-containing protein 7-like isoform X1	XP_003448088.2	*Oreochromis niloticus*	0
Contig05820	Fish-egg lectin	BAL61198.1	*Oplegnathus fasciatus*	2E-83
Contig1284	Keratin, type I cytoskeletal 13-like	XP_003442483.1	*Oreochromis niloticus*	1E-29
Contig07352	Dentin sialophosphoprotein-like	XP_003447913.1	*Oreochromis niloticus*	7E-12
Contig01673	Collagen alpha-1(IV) chain-like	XP_003961761.1	*Takifugu rubripes*	3E-159
Contig08806	Intermediate light meromyosin	ABR19833.1	*Ctenopharyngodon idella*	1E-137
Contig05635	Alpha-2-HS-glycoprotein-like	XP_004078952.1	*Oryzias latipes*	2E-111
Contig02752	Cytosolic phospholipase A2 zeta-like	XP_003446488.1	*Oreochromis niloticus*	0
Contig21676	Beta-microseminoprotein-like	XP_003452718.1	*Oreochromis niloticus*	7E-33
Contig05350	Uncharacterized protein LOC102080835	XP_005476593.1	*Oreochromis niloticus*	2E-71
Contig659	Epidermis-type lipoxygenase 3-like	XP_003449933.1	*Oreochromis niloticus*	0
Contig02069	Na/Pi cotransport system protein	AAB16821.1	*Pseudopleuronectes americanus*	0
Upregulated genes in premetamorphic stage 5 compared to metamorphic climax stage9C				
Contig05607	Type I keratin isoform 2	BAF56914.1	*Solea senegalensis*	1E-145
Contig494	High choriolytic enzyme 1-like	XP_003456934.1	*Oreochromis niloticus*	4E-87
Contig01773	Meprin A subunit beta-like	XP_003450581.1	*Oreochromis niloticus*	0
Contig00039	Fatty acid synthase isoform 2	XP_003454104.1	*Oreochromis niloticus*	0
Contig01282	Hypothetical protein LOC100691699	XP_003439216.1	*Oreochromis niloticus*	1E-166

Additional file 2.15f. List of significantly upregulated genes between metamorphic climax stage 9A and prometamorphic stage 7 as determined by a linear model in Bayseq with a Benjamin-Hochberg adjustment for multiple testing analysis with a cut-off set at 0.05 (FDR<0.05). Contig name, Gene name, Accession number (no.), Organism and E-value are shown for each gene.

Upregulated genes in metamorphic climax stage 9A compared to prometamorphic stage 7				
Contig ID	***Gene name***	***Accession no.***	***Organism***	***E-value***
Contig1159	Collagen alpha-1(I) chain-like	XP_003460741.1	*Cavia porcellus*	1E-62

Additional file 2.15g. List of significantly upregulated genes between metamorphic climax stage 9A and metamorphic proclimax stage 8 as determined by a linear model in Bayseq with a Benjamin-Hochberg adjustment for multiple testing analysis with a cut-off set at 0.05 (FDR<0.05). Contig name, Gene name, Accession number (no.), Organism and E-value are shown for each gene.

Upregulated genes in metamorphic climax stage 9A compared to metamorphic proclimax stage 8				
Contig ID	***Gene name***	***Accession no.***	***Organism***	***E-value***
Contig02895	Oreochromis niloticus UPF0661 TPR repeat-containing protein C16D10.05c-like	XM_005472393.1	*Oreochromis niloticus*	4E-177

Additional file 2.15h. List of significantly upregulated genes between metamorphic climax stage 9A and metamorphic climax stage 9C as determined by a linear model in Bayseq with a Benjamin-Hochberg adjustment for multiple testing analysis with a cut-off set at 0.05 (FDR<0.05). Contig name, Gene name, Accession number (no.), Organism and E-value are shown for each gene.

Upregulated genes in metamorphic climax stage 9A compared to metamorphic climax stage 9C				
Contig ID	***Gene name***	***Accession no.***	***Organism***	***E-value***
Contig00039	Fatty acid synthase isoform 2	XP_003454104.1	*Oreochromis niloticus*	0
Upregulated genes in metamorphic climax stage 9C compared to metamorphic climax stage 9A				
Contig02069	Na/Pi cotransport system protein	AAB16821.1	*Pseudopleuronectes americanus*	0
Contig24460	Estrogen-regulated protein	ACX94453.1	*Sparus aurata*	1E-28
lchead_c7171	Cytochrome c oxidase subunit 4 isoform 2, mitochondrial	P80971.2	*Thunnus obesus*	2E-32
Contig21525	Alpha-globin 1	ACI28515.1	*Hippoglossus hippoglossus*	6E-70
Contig07132	Betaine-homocysteine S-methyltransferase 1	ACQ58374.1	*Anoplopoma fimbria*	0
Contig02419	Epinephelus coioides hypoxia-inducible factor 4 alpha (HIF-4a) mrna	AY735011.1	*Epinephelus coioides*	0
Contig08214	Takifugu rubripes Krueppel-like factor 3-like (LOC101072211)	XM_003978083.1	*Takifugu rubripes*	4E-113
Contig02675	Dehydrogenase/reductase SDR family member 7C-A-like	XP_003438705.1	*Oreochromis niloticus*	1E-149

Additional file 2.15i. List of significantly upregulated genes between metamorphic climax stage 9B and metamorphic proclimax stage 8 as determined by a linear model in Bayseq with a Benjamin-Hochberg adjustment for multiple testing analysis with a cut-off set at 0.05 (FDR<0.05). Contig name, Gene name, Accession number (no.), Organism and E-value are shown for each gene.

Upregulated genes in metamorphic climax stage 9B compared to metamorphic proclimax stage 8				
Contig ID	***Gene name***	***Accession no.***	***Organism***	***E-value***
lcgut_c20403	Warm temperature acclimation-related 65 kda protein	ACU86959.1	*Paralichthys olivaceus*	5E-41

Additional file 2.15j. List of significantly upregulated genes between metamorphic climax stage 9C and prometamorphic stage 7 as determined by a linear model in Bayseq with a Benjamin-Hochberg adjustment for multiple testing analysis with a cut-off set at 0.05 (FDR<0.05). Contig name, Gene name, Accession number (no.), Organism and E-value are shown for each gene.

Upregulated genes in metamorphic climax stage 9C compared to prometamorphic stage 7				
Contig ID	***Gene name***	***Accession no.***	***Organism***	***E-value***
Contig02675	Dehydrogenase/reductase SDR family member 7C-A-like	XP_003438705.1	*Oreochromis niloticus*	1E-149
Contig02069	Na/Pi cotransport system protein	AAB16821.1	*Pseudopleuronectes americanus*	0
Contig07132	Betaine--homocysteine S-methyltransferase 1	ACQ58374.1	*Anoplopoma fimbria*	0
lcgut_c20403	Warm temperature acclimation-related 65 kda protein	ACU86959.1	*Paralichthys olivaceus*	5E-41
Contig21525	Alpha-globin 1	ACI28515.1	*Hippoglossus hippoglossus*	6E-70
Contig00708	Von Willebrand factor A domain-containing protein 7-like isoform X1	XP_003448088.2	*Oreochromis niloticus*	0
Contig02581	Ryanodine receptor 3	XP_001922113.2	*Danio rerio*	0

Additional file 2.15k. List of top most significantly upregulated genes between prometamorphic stage 7 and juvenile stage as determined by a linear model in Bayseq with a Benjamin-Hochberg adjustment for multiple testing analysis with a cut-off set at 0.05 (FDR<0.05). Contig name, Gene name, Accession number (no.), Organism and E-value are shown for each gene.

Upregulated genes in prometamorphic stage 7 compared to juvenile				
Contig ID	***Gene name***	***Accession no.***	***Organism***	***E-value***
Contig1085	DNA-directed RNA polymerase I subunit RPA43-like isoform X1	XP_003457324.1	*Oreochromis niloticus*	1E-119
Contig26841	Hypothetical protein	XP_002723892.1	*Oryctolagus cuniculus*	5E-26
Upregulated genes in juvenile compared to prometamorphic stage 7				
Contig1356	Beta actin	ACZ63697.1	*Hippoglossus hippoglossus*	4E-74
Contig899	40S ribosomal protein S3	AAT01919.1	*Pseudopleuronectes americanus*	8E-46
Contig14523	Chitinase1	BAD15059.1	*Paralichthys olivaceus*	1E-134
Contig04218	Acidic mammalian chitinase-like	XP_003459087.1	*Oreochromis niloticus*	0
Contig10095	AF156788_1 pepsinogen A form iib precursor	AAD56284.1	*Pseudopleuronectes americanus*	1E-178
Contig06093	Betain homocystein methyltransferase	CBA10400.1	*Platichthys flesus*	0

Contig32428	Hypothetical protein EGM_09444, partial	EHH59357.1	*Macaca fascicularis*	1E-11
Contig1703	Tubulin alpha-5 chain-like	XP_003641692.1	*Gallus gallus*	6E-67
Contig1301	Flocculation protein FLO11-like isoform X5	XP_004538412.1	*Maylandia zebra*	7E-50
Contig30057	40S ribosomal protein S15-like	XP_003437814.1	*Oreochromis niloticus*	7E-15
Contig21525	Alpha-globin 1	ACI28515.1	*Hippoglossus hippoglossus*	6E-70
Contig12585	Elastase 3 precursor	BAA82369.2	*Paralichthys olivaceus*	1E-150
Contig09675	Ubiquitin carboxyl-terminal hydrolase 28-like	XP_003453773.1	*Oreochromis niloticus*	1E-129
Contig00708	Von Willebrand factor A domain-containing protein 7-like isoform X1	XP_003448088.2	*Oreochromis niloticus*	0
Contig02265	Creatine kinase U-type, mitochondrial-like	XP_003455474.1	*Oreochromis niloticus*	0
Contig08947	Unnamed protein product	CAG06445.1	*Tetraodon nigroviridis*	1E-139
Contig16328	Actin, partial	AEM53400.1	*Pontoscolex corethrurus*	5E-24
Contig26844	Ras-related protein Rab-11B-like	XP_003461453.1	*Cavia porcellus*	4E-33
Contig05598	CCAAT/enhancer-binding protein delta-like	XP_003438154.1	*Oreochromis niloticus*	1E-111
Contig15968	Myosin-binding protein H-like	XP_003448314.1	*Oreochromis niloticus*	2E-39
Contig01329	Arrestin domain-containing protein 2-like isoformx2	XP_003449080.1	*Oreochromis niloticus*	0
Contig07184	Myelin basic protein-like	XP_003443685.1	*Oreochromis niloticus*	8E-29
Contig09813	Uncharacterized protein LOC100690208 isoform X1	XP_003450545.1	*Oreochromis niloticus*	1E-110
Contig20583	Cellular retinol-binding protein type II	AEM37665.1	*Epinephelus bruneus*	1E-65
Contig14695	Tenebrosin-C-like	XP_003448747.1	*Oreochromis niloticus*	1E-60
Contig23899	Tributyltin binding protein type 2	BAF56478.1	*Paralichthys olivaceus*	2E-56
Contig02070	Protein TFG-like	XP_003451650.1	*Oreochromis niloticus*	1E-106
Contig18680	Uncharacterized protein LOC101071481	XP_003977893.1	*Oryzias latipes*	2E-24
Contig04032	Argininosuccinate lyase-like	XP_003447016.1	*Oreochromis niloticus*	0
Contig07430	Claudin 31	AAT64077.1	*Takifugu rubripes*	4E-81
Contig19916	L-rhamnose-binding lectin CSL2-like	XP_003455367.1	*Oreochromis niloticus*	4E-68
Contig19678	Putative ferric-chelate reductase 1	AEH76583.1	*Epinephelus bruneus*	7E-37
Contig06206	Inhibitor of nuclear factor kappa B alpha	ABO40445.1	*Siniperca chuatsi*	1E-131

Additional file 2.15l. List of top most significantly upregulated genes between metamorphic proclimax stage 8 and Juvenile stage as determined by a linear model in Bayseq with a Benjamin-Hochberg adjustment for multiple testing analysis with a cut-off set at 0.05 (FDR<0.05). Contig name, Gene name, Accession number (no.), Organism and E-value are shown for each gene.

Upregulated genes in juvenile compared to metamorphic proclimax stage 8

Contig ID	*Gene name*	*Accession no.*	*Organism*	*E-value*
Contig1303	Cytochrome oxidase subunit I	CAO79645.1	*Hippoglossus hippoglossus*	2E-34
Contig1356	Beta actin	ACZ63697.1	*Hippoglossus hippoglossus*	4E-74
Contig00796	Kelch-like protein 31-like	XP_003441041.1	*Oreochromis niloticus*	0
Contig1808	Cytochrome c oxidase subunit III	YP_001403135.1	*Hippoglossus hippoglossus*	9E-51
Contig14523	Chitinase1	BAD15059.1	*Paralichthys olivaceus*	1E-134
Contig03270	S-adenosylmethionine synthase isoform type-1-like	XP_003448758.1	*Oreochromis niloticus*	0
Contig1525	Ubiquitin	XP_001664267.1	*Aedes aegypti*	5E-31
Contig26146	40S ribosomal protein S15	ACN10008.1	*Salmo salar*	2E-24
Contig01545	Aspartate aminotransferase, cytoplasmic-like	XP_003454182.1	*Oreochromis niloticus*	0
Contig06359	Actin, alpha, cardiac muscle 1a	NP_001001409.2	*Danio rerio*	0
Contig904	Eukaryotic translation initiation factor 1B	NP_955882.1	*Danio rerio*	8E-42
Contig27668	Unknown	AAT45249.1	*Sparus aurata*	3E-11
Contig1306	Sarcoplasmic/endoplasmic reticulum calcium atpase 1-like isoform X1	XP_004575013.1	*Maylandia zebra*	4E-37
Contig10095	Pepsinogen A form IIb precursor	AAD56284.1	*Pseudopleuronectes americanus*	1E-178
Contig1207	Chitinase 3	BAL14138.1	*Thunnus orientalis*	9E-76
Contig02050	5-aminolevulinate synthase, nonspecific, mitochondrial-like isoform X1	XP_003454600.1	*Oreochromis niloticus*	0
Contig968	Ribosomal protein S2-like isoform 3	XP_002727213.1	*Rattus norvegicus*	3E-27
Contig06606	60S ribosomal protein L3-like	XP_003456398.1	*Oreochromis niloticus*	0
Contig1651	Chymotrypsinogen 1	BAL14136.1	*Thunnus orientalis*	5E-52
Contig04737	Protein phosphatase 1 catalytic subunit beta isoform	ABC94584.1	*Scophthalmus maximus*	0
Contig08734	Muscle specific ring finger protein 1-like	NP_001133124.1	*Salmo salar*	1E-161
Contig08133	Induced myeloid leukemia cell differentiation protein Mcl-1 homolog	XP_003450317.1	*Oreochromis niloticus*	4E-64

Contig1494	Beta-actin	ABM92344.1	*Laternula elliptica*	2E-44
Contig477	Nascent polypeptide-associated complex subunit alpha, muscle-specific form isoform X4	XP_005448685.1	*Oreochromis niloticus*	4E-25
Contig1703	Tubulin alpha-5 chain-like	XP_003641692.1	*Gallus gallus*	6E-67
Contig30057	40S ribosomal protein S15-like	XP_003437814.1	*Oreochromis niloticus*	7E-15
Contig21525	Alpha-globin 1	ACI28515.1	*Hippoglossus hippoglossus*	6E-70
Contig21976	Rasgap-activating-like protein 1	XP_003445666.1	*Oreochromis niloticus*	7E-12
Contig12585	Elastase 3 precursor	BAA82369.2	*Paralichthys olivaceus*	1E-150
Contig09675	Ubiquitin carboxyl-terminal hydrolase 28-like	XP_003453773.1	*Oreochromis niloticus*	1E-129
Contig02265	Creatine kinase U-type, mitochondrial-like	XP_003455474.1	*Oreochromis niloticus*	0
Contig27523	40S ribosomal protein S3	AAT01919.1	*Pseudopleuronectes americanus*	2E-19
Contig16328	Actin, partial	AEM53400.1	*Pontoscolex corethrurus*	5E-24
Contig495	Actin, alpha 1, skeletal muscle	NP_001006709.1	*Xenopus (Silurana) tropicalis*	0
Contig09238	Homocysteine-responsive endoplasmic reticulum-resident ubiquitin-like domain member 2 protein-like	XP_003450304.1	*Oreochromis niloticus*	3E-50
Contig26844	Ras-related protein Rab-11B-like	XP_003461453.1	*Cavia porcellus*	4E-33
Contig09231	Hematological and neurological expressed 1 protein-like	XP_003452909.1	*Oreochromis niloticus*	1E-58
Contig30975	Cytochrome b	YP_001403141.1	*Hippoglossus hippoglossus*	2E-20
Contig09962	Fish-egg lectin	BAL61198.1	*Oplegnathus fasciatus*	2E-58
Contig23899	Tributyltin binding protein type 2	BAF56478.1	*Paralichthys olivaceus*	2E-56

Additional file 2.15m. List of top most significantly upregulated genes between metamorphic climax stage 9A and juvenile stage as determined by a linear model in Bayseq with a Benjamin-Hochberg adjustment for multiple testing analysis with a cut-off set at 0.05 (FDR<0.05). Contig name, Gene name, Accession number (no.), Organism and E-value are shown for each gene.

Upregulated genes in metamorphic climax stage 9A compared to juvenile				
Contig ID	***Gene name***	***Accession no.***	***Organism***	***E-value***
Contig26888	ATP synthase subunit beta	XP_003627732.1	*Medicago truncatula*	2E-38
Upregulated genes in juvenile compared to metamorphic climax stage 9A				
Contig1352	Actin alpha skeletal muscle	ACM41845.1	*Epinephelus coioides*	1E-114
Contig1500	Ribosomal protein, large, P0	NP_001080134.1	*Xenopus laevis*	6E-50
Contig1162	Cytochrome oxidase subunit I	CAO79645.1	*Hippoglossus hippoglossus*	1E-112
Contig20504	Type-4 ice-structuring protein	Q8JI37.1	*Paralichthys olivaceus*	3E-40
Contig28671	Trypsinogen Flou2	AAY23358.1	*Hippoglossus hippoglossus*	5E-43
Contig25330	Sarcoendoplasmic reticulum calcium atpase	ABG90496.1	*Silurus lanzhouensis*	2E-28
Contig1056	Sarcoplasmic/endoplasmic reticulum calcium atpase 1-like isoform X1	XP_003454037.1	*Oreochromis niloticus*	0
Contig24482	Actin, gamma-enteric smooth muscle-like isoform 1	XP_003201904.1	*Meleagris gallopavo*	2E-26
Contig05820	Fish-egg lectin	BAL61198.1	*Oplegnathus fasciatus*	2E-83
Contig25352	Alpha-cardiac actin	AAA37165.1	*Mus musculus*	1E-22
Contig1356	Beta actin	ACZ63697.1	*Hippoglossus hippoglossus*	4E-74
Contig500	Ferritin high chain	CAR66078.1	*Trematomus bernacchii*	4E-93
Contig899	40S ribosomal protein S3	AAT01919.1	*Pseudopleuronectes americanus*	8E-46
Contig1808	Cytochrome c oxidase subunit III	YP_001403135.1	*Hippoglossus hippoglossus*	9E-51
Contig14523	Chitinase1	BAD15059.1	*Paralichthys olivaceus*	1E-134
Contig00193	Kelch-like protein 31-like	XP_003458597.1	*Oreochromis niloticus*	0
Contig1525	Ubiquitin	XP_001664267.1	*Aedes aegypti*	5E-31
Contig26146	40S ribosomal protein S15	ACN10008.1	*Salmo salar*	2E-24
Contig01545	Aspartate aminotransferase, cytoplasmic-like	XP_003454182.1	*Oreochromis niloticus*	0
Contig06359	Actin, alpha, cardiac muscle 1a	NP_001001409.2	*Danio rerio*	0

Contig10095	AF156788_1 pepsinogen A form iib precursor	AAD56284.1	*Pseudopleuronectes americanus*	1E-178
Contig1062	Cytochrome b	YP_001403141.1	*Hippoglossus hippoglossus*	2E-62
Contig06093	Betain homocystein methyltransferase	CBA10400.1	*Platichthys flesus*	0
Contig06606	60S ribosomal protein L3-like	XP_003456398.1	*Oreochromis niloticus*	0
Contig08242	Leukocyte elastase inhibitor-like isoform X1	XP_003457347.1	*Oreochromis niloticus*	5E-77
Contig08734	Muscle specific ring finger protein 1-like	NP_001133124.1	*Salmo salar*	1E-161
Contig08657	Myosin-10-like	XP_003448012.1	*Oreochromis niloticus*	1E-145
Contig08133	Induced myeloid leukemia cell differentiation protein Mcl-1 homolog	XP_003450317.1	*Oreochromis niloticus*	4E-64
Contig05461	Nebulin-like	ACH85357.1	*Salmo salar*	7E-153
Contig477	Nascent polypeptide-associated complex subunit alpha, muscle-specific form isoform X4	XP_005448685.1	*Oreochromis niloticus*	4E-25
Contig1703	Tubulin alpha-5 chain-like	XP_003641692.1	*Gallus gallus*	6E-67
Contig03898	Cathepsin L	ABJ99858.1	*Hippoglossus hippoglossus*	0
Contig21525	Alpha-globin 1	ACI28515.1	*Hippoglossus hippoglossus*	6E-70
Contig12585	Elastase 3 precursor	BAA82369.2	*Paralichthys olivaceus*	1E-150
Contig495	Actin, alpha 1, skeletal muscle	NP_001006709.1	*Xenopus tropicalis*	0
Contig26844	Ras-related protein Rab-11B-like	XP_003461453.1	*Cavia porcellus*	4E-33
Contig07011	Ubiquitin carboxyl-terminal hydrolase 28-like	XP_003453773.1	*Oreochromis niloticus*	1E-124
Contig09813	Uncharacterized protein LOC100690208	XP_003450545.1	*Oreochromis niloticus*	6E-140

Additional file 2.15n. List of top most significantly upregulated genes between metamorphic climax stage 9B and Juvenile stage as determined by a linear model in Bayseq with a Benjamin-Hochberg adjustment for multiple testing analysis with a cut-off set at 0.05 (FDR<0.05). Contig name, Gene name, Accession number (no.), Organism and E-value are shown for each gene.

Upregulated genes in metamorphic climax stage 9B compared to juvenile				
Contig ID	***Gene name***	***Accession no.***	***Organism***	***E-value***
Contig00749	Cdh1-d	AAL31950.1	*Gallus gallus*	2E-27
Contig26841	Hypothetical protein	XP_002723892.1	*Oryctolagus cuniculus*	5E-26
Upregulated genes in juvenile compared to metamorphic climax stage 9B				
Contig1303	Cytochrome oxidase subunit I	CAO79645.1	*Hippoglossus hippoglossus*	2E-34
Contig1356	Beta actin	ACZ63697.1	*Hippoglossus hippoglossus*	4E-74
Contig1808	Cytochrome c oxidase subunit III	YP_001403135.1	*Hippoglossus hippoglossus*	9E-51
Contig434	WD repeat-containing protein 20-like	XP_003459593.1	*Oreochromis niloticus*	1E-173
Contig08734	Muscle specific ring finger protein 1-like	NP_001133124.1	*Salmo salar*	1E-161
Contig08133	Induced myeloid leukemia cell differentiation protein Mcl-1 homolog	XP_003450317.1	*Oreochromis niloticus*	4E-64
Contig32428	Hypothetical protein EGM_09444, partial	EHH59357.1	*Macaca fascicularis*	1E-11
Contig1703	Tubulin alpha-5 chain-like	XP_003641692.1	*Gallus gallus*	6E-67
Contig21976	Rasgap-activating-like protein 1	XP_003445666.1	*Oreochromis niloticus*	7E-12
Contig12585	Elastase 3 precursor	BAA82369.2	*Paralichthys olivaceus*	1E-150
Contig02012	Protein Tob1-like	XP_003452855.1	*Oreochromis niloticus*	1E-162
Contig09675	Ubiquitin carboxyl-terminal hydrolase 28-like	XP_003453773.1	*Oreochromis niloticus*	1E-129
Contig13939	Proteasome subunit beta type-6-like	XP_003456484.1	*Oreochromis niloticus*	1E-113
Contig22705	Ribosomal protein L29	CBN80862.1	*Dicentrarchus labrax*	8E-21
Contig14585	Heat shock protein beta-11-like	XP_003446493.1	*Oreochromis niloticus*	2E-71
Contig03419	Twinfilin-2-like	XP_003448434.1	*Oreochromis niloticus*	0
Contig27523	40S ribosomal protein S3	AAT01919.1	*Pseudopleuronectes americanus*	2E-19
Contig16328	Actin, partial	AEM53400.1	*Pontoscolex corethrurus*	5E-24
Contig07754	Membrane-spanning 4-domains subfamily A member 4A	ACO09823.1	*Osmerus mordax*	1E-38

Contig26844	Ras-related protein Rab-11B-like	XP_003461453.1	*Cavia porcellus*	4E-33
Contig01134	Transmembrane protease serine 9-like	XP_005469283.1	*Oreochromis niloticus*	0
Contig05598	CCAAT/enhancer-binding protein delta-like	XP_003438154.1	*Oreochromis niloticus*	1E-111
Contig21640	ATP synthase-coupling factor 6, mitochondrial precursor	ACQ58964.1	*Anoplopoma fimbria*	8E-48
Contig938	Ras-related protein Rab-10-like	XP_003446295.1	*Oreochromis niloticus*	1E-110
Contig02215	Galectin-3-like	XP_003445459.1	*Oreochromis niloticus*	1E-57
Contig27091	60S ribosomal protein L34	AEG78366.1	*Epinephelus coioides*	1E-25
Contig30975	Cytochrome b	YP_001403141.1	*Hippoglossus hippoglossus*	2E-20
Contig07880	Calumenin-A-like	XP_003448805.1	*Oreochromis niloticus*	1E-106
Contig08853	Uncharacterized protein	CBN82110.1	*Dicentrarchus labrax*	3E-54
Contig07526	Vesicle-associated membrane protein-associated protein A	ACQ58821.1	*Anoplopoma fimbria*	1E-107
Contig21841	CD59 glycoprotein-like	XP_004085111.1	*Oryzias latipes*	9E-28
Contig14695	Tenebrosin-C-like	XP_003448747.1	*Oreochromis niloticus*	1E-60
Contig01833	Signal transducer and activator of transcription 1	ABS19629.1	*Paralichthys olivaceus*	0

Additional file 2.15o. List of top most significantly upregulated genes between metamorphic climax stage 9C and Juvenile stage as determined by a linear model in Bayseq with a Benjamin-Hochberg adjustment for multiple testing analysis with a cut-off set at 0.05 (FDR<0.05). Contig name, Gene name, Accession number (no.), Organism and E-value are shown for each gene.

Upregulated genes in metamorphic climax stage 9C compared to juvenile				
Contig ID	***Gene name***	***Accession no.***	***Organism***	***E-value***
Contig1159	Collagen alpha-1(I) chain-like	XP_003460741.1	*Cavia porcellus*	1E-62
Contig14322	CD59 glycoprotein-like	XP_003460314.1	*Oreochromis niloticus*	2E-43
Contig1362	Rrna promoter binding protein-like	XP_002724111.1	*Oryctolagus cuniculus*	9E-27
Contig13553	1-acyl-sn-glycerol-3-phosphate acyltransferase epsilon-like	XP_003441167.1	*Oreochromis niloticus*	2E-93
Upregulated genes in juvenile compared to metamorphic climax stage 9C				
Contig08242	Leukocyte elastase inhibitor-like isoform X1	XP_003457347.1	*Oreochromis niloticus*	5E-77
Contig08657	Myosin-10-like	XP_003448012.1	*Oreochromis niloticus*	1E-145
Contig08133	Induced myeloid leukemia cell differentiation protein Mcl-1 homolog	XP_003450317.1	*Oreochromis niloticus*	4E-64
Contig32428	Hypothetical protein EGM_09444, partial	EHH59357.1	*Macaca fascicularis*	1E-11
Contig477	Nascent polypeptide-associated complex subunit alpha, muscle-specific form isoform X4	XP_005448685.1	*Oreochromis niloticus*	4E-25
Contig1703	Tubulin alpha-5 chain-like	XP_003641692.1	*Gallus gallus*	6E-67
Contig30057	40S ribosomal protein S15-like	XP_003437814.1	*Oreochromis niloticus*	7E-15
Contig08838	Carbonyl reductase-like 20beta-hydroxysteroid dehydrogenase	ACK99046.1	*Solea senegalensis*	1E-130
Contig13939	Proteasome subunit beta type-6-like	XP_003456484.1	*Oreochromis niloticus*	1E-113
Contig27523	40S ribosomal protein S3	AAT01919.1	*Pseudopleuronectes americanus*	2E-19
Contig16328	Actin, partial	AEM53400.1	*Pontoscolex corethrurus*	5E-24
Contig09238	Homocysteine-responsive endoplasmic reticulum-resident ubiquitin-like domain member 2 protein-like	XP_003450304.1	*Oreochromis niloticus*	3E-50
Contig26844	Ras-related protein Rab-11B-like	XP_003461453.1	*Cavia porcellus*	4E-33
Contig01134	Polyserase-2-like	XP_003442512.1	*Oreochromis niloticus*	1E-126
Contig07011	Ubiquitin carboxyl-terminal hydrolase 28-like	XP_003453773.1	*Oreochromis niloticus*	1E-124
Contig09231	Hematological and neurological expressed 1 protein-like	XP_003452909.1	*Oreochromis niloticus*	1E-58
lchead_c50924	Beta-crystallin A2-like isoform 1	XP_003443383.1	*Oreochromis niloticus*	1E-114

Contig01786	Tyrosine aminotransferase	XP_003439428.1	*Oreochromis niloticus*	0
Contig07880	Calumenin-A-like	XP_003448805.1	*Oreochromis niloticus*	1E-106
Contig01833	Signal transducer and activator of transcription 1	ABS19629.1	*Paralichthys olivaceus*	0
Contig875	Alpha tubulin	AAG15324.1	*Notothenia coriiceps*	7E-99
Contig07730	Translation initiation factor eif-2B precursor	AAF61750.1	*Sciaenops ocellatus*	0
Contig18680	Uncharacterized protein LOC101071481	XP_003977893.1	*Takifugu rubripes*	2E-24
Contig31578	Unnamed protein product	CAF90797.1	*Tetraodon nigroviridis*	9E-12
Contig01775	Cullin-associated NEDD8-dissociated protein 1-like isoform X1	XP_003451898.1	*Oreochromis niloticus*	0
Contig05847	14-3-3 protein beta/alpha-1	NP_001117940.1	*Oncorhynchus mykiss*	1E-108
Contig03424	Phenylalanine-4-hydroxylase	XP_003448110.1	*Oreochromis niloticus*	0
Contig19916	L-rhamnose-binding lectin CSL2-like	XP_003455367.1	*Oreochromis niloticus*	4E-68
Contig19678	Putative ferric-chelate reductase 1	AEH76583.1	*Epinephelus bruneus*	7E-37
Contig1780	40S ribosomal protein s5	ADX97209.1	*Perca flavescens*	4E-20
Contig22533	ATP synthase subunit alpha, mitochondrial-like	XP_003213404.1	*Meleagris gallopavo*	1E-20
Contig12770	NHP2-like protein 1	ACQ58311.1	*Anoplopoma fimbria*	3E-55
Contig04309	Purine nucleoside phosphorylase 5a	NP_998476.1	*Danio rerio*	1E-153

Additional file 2.16. Expression profile of putative TH-responsive transcripts that had a differential expression between Atlantic halibut metamorphic stages (7 – 9C) and the juvenile. Expression levels are represented as log2 of fold-change (juvenile/metamorphic stages expression levels).

		log2 fold change (juvenile versus metamorphic stage)				
Gene name	**Gene symbol**	**Stage7**	**Stage8**	**Stage9A**	**Stage9B**	**Stage9C**
Coronin, actin binding protein, 1C	*coro1c*	-4.8	-3.5	-2.3	-4.2	-5.2
Cyclin B1	*ccnb1*	-4.7	0	0	0	-4.3
Regulator of chromosome condensation 1	*rcc1*	-4	-3.5	0	0	-4.5
Olfactomedin 4	*olm4*	-4.5	-3.8	-1.6	0	-4.5
High mobility group protein-1	*hmg1*	-6.5	-3.1	-1.6	0	-4.6
Alkaline phosphatase	*alo*	-4.3	-3.7	0	-3.7	-3.7
Chromodomain helicase DNA binding protein 4	*chd4*	-4.9	-3.6	0	-3.3	-3.6
Mitogen-activated protein kinase kinase 1	*map2k1*	-3.7	-3.7	-2.3	-3.7	-3.7
Ubiquilin	*xdrp1*	-5	-3.8	-2.8	-3.6	0
C-Jun protein	*c-jun*	-4.4	-4.4	-1.6	-3.8	0
Protein kinase	*pkn*	-4	-3.9	-2	-2.3	-2
Histone deacetylase 1	*hdac1*	-4.2	-4.2	0	-3.6	-2.6
General transcription factor IIH	*gtf2h*	-4.2	-4.2	0	-2.6	0
Transcription factor AP-2	*tfap2*	-5.3	-4.3	-2.3	-3.7	-3.7
hnRNP I-related RNA transport protein (Polypyrimidine Tract Binding Protein 1)	*vgrbp60*	-5	-4.4	-1	-4.4	-3.1
Acetylcholine receptor subunit 1A	*chrna1*	-5.8	-5.4	-2	-5.2	-4
Biglycan	*bgn*	-5.2	-2.2	0	-3.6	0
RNA helicase II/Gu	*ddx21*	-4.7	-4.3	-1.6	-4.6	-4.2
Chaperonin subunit CCT	*cct*	-9.1	-4.7	-2.8	-6	-4.4
Proto-Oncogene Serine/Threonine-Protein Kinase Pim-1	*pim1*	-4.4	-4.4	-3.5	-4.4	-3.8
Aconitase	*aco*	-2	-3.3	0	0	0
NFI-X2 transcription factor	*nfix*	-3.9	-4.9	0	0	0

SRY (sex determining region Y)-box 4	*sox4*	-3.4	-4.4	-2.3	-2.8	-2.8
Putative alanine:glyoxylate aminotransferase	*agxt*	-4.2	-3.4	0	0	0
Methyl-CpG binding domain protein 3	*mbd3*	-5	-5	-1.6	0	0
Larval beta-globin	*hbb*	-5.8	-5.8	-2.6	0	0
Fibronectin	*fn*	-4.3	-3.7	-1	0	0
Alpha2 Collagen type 1	*col1a2*	-4.2	-3.1	-2.8	0	0
Secreted protein, acidic, cysteine-rich (osteonectin)	*sparc*	-6.4	-3	-1.6	0	0
Myelin proteolipid protein	*plp1*	-6.2	-5	-1.6	0	-4.4
Caveolin-3	*cav3*	-0.3	0	0	0	0
Nucleophosmin/nucleoplasmin	*npm*	-3.2	0	0	0	0
Minichromosome maintenance complex component 2	*mcm2*	-2.6	0	0	0	0
Minichromosome Maintenance Complex Component (MCM5/CDC46)	*cdc46*	-4.4	0	-2.3	0	0
Alpha1 Collagen type 1	*col1a1*	-5.2	0	-2	-4.5	-3.4
Cysteine-Rich, Angiogenic Inducer, 61	*cyr61*	-5.5	-3.9	-1.6	-4.9	-4.9
Aldolase	*aldo*	-7.3	-4.4	-1.6	-5.8	-4.9
BCL2-Associated Athanogene 6	*bag6*	-3.2	-3.2	-2	-4.2	-3.2
Heat shock 60 kDa protein (chaperonin)	*hspd1*	-4.7	-4	-1	-7	-5.6
Poly A-binding protein ABP-EF	*abp-ef*	-4.2	-3.8	-2	-5	-4.2
Cyclin-dependent kinase 7	*cdk7*	-3.6	-3.2	-1.6	-4.6	-3.6
Lactate dehydrogenase B	*ldhb*	-6.3	-4.7	-1.6	-7.3	-5.7
Arginase type II	*arg2*	-7.4	-3.9	-2	-7.4	-6.1
Tubulin beta	*tubb*	-4.2	-3.3	-1.6	-4.2	-4.2
Nucleolar and coiled-body phosphoprotein	*nolc*	-5	-3.6	-2.8	-5	-5
Glutamate-cysteine ligase , modifier subunit	*gclm*	-4.9	-3.3	-3.7	-4.3	0
Corticotropin releasing hormone binding protein	*crhbp*	-4.6	0	-1.6	-4.1	0
CCAAT/Enhancer Binding Protein (C/EBP),Delta	*cebpd*	-7.9	-6.1	-2.8	-8.3	-5.1

Minichromosome maintenance complex component 7	*mcm7*	-5.4	-3.3	0	-6.1	0
Defender against cell death 1	*dad1*	-4.8	0	0	-5.2	0
RNA polymerase I TF UBF	*ubf*	-2.8	0	0	-2.8	0
Enhancer of zeste homolog 2	*ezh2*	-2	0	-1.6	-3.2	-3.1
Kirsten rat sarcoma viral oncogene homolog	*kras*	0	0	-1	-3.6	-2.9
Collagenase 3	*mmp13*	0	0	-1	-4.8	-3.8
Sulfotransferase family, cytosolic, 2B, member 1	*sult2b1*	0	0	0	-4.5	-4
Eukaryotic peptide chain release factor subunit 1	*etf1*	0	0	0	-5.1	-3.6
V-Raf-1 Murine Leukemia Viral Oncogene Homolog 1	*craf*	0	0	0	-4.5	-4.5
COX assembly mitochondrial protein homolog	*kit*	0	0	0	-2.3	-3.3
Glycine dehydrogenase	*gldc*	-4.4	-4.5	-4.3	-4.8	-4.8
KDEL (Lys-Asp-Glu-Leu) endoplasmic reticulum proteinretention receptor 2	*kdelr2*	-4.5	-4.6	-4.6	-5.9	-5.9
Sodium/potassium-transporting ATPase subunit alpha-1 isoform a	*atp1a1*	-1.9	-2.8	-2.8	-6.1	-5.2
Ribose-phosphate pyrophosphokinase 2 isoform 2	*prps2*	-1.4	-3	-4.2	-5.2	-5.2
T-Complex Protein 1 Subunit Alpha	*tcp1*	0	-3.6	-2	-5.2	-4.8
Alpha-2-macroglobulin precursor	*a2m*	0	-3.1	-2.8	-4.9	-3.5
Aminolevulinate, Delta-, Synthase 1	*alas*	0	-3.9	-3.7	-6.1	-5.2
Fc fragment of IgG binding protein	*fcgbp*	0.1	-4.2	-2.6	-6.2	-5.3
Deoxyribonuclease I-like 3	*dnase1l3*	0	-3.6	-3.3	-4	-4
Histidine triad nucleotide-binding protein 2, mitochondrial precursor	*hint2*	-1	-3.8	-1.4	-4.2	-4.2
Lysophospholipase-like protein 1	*lyplal1*	0	2.7	0	-4	-3.8
Cytochrome c oxidase subunit 6B1	*cox6b1*	0	-3.6	-3.2	-5	-5.1
Ras-related C3 botulinum toxin substrate 2	*rac2*	-1	-3.5	-1.6	-4.5	-5.5
14-3-3 protein zeta/delta	*ywhaz*	0	-3.1	-2	-5	-6.6
Cathepsin S	*ctss*	0.3	-5.2	-3.6	-5.3	-6

2-amino-3-ketobutyrate coenzyme A ligase, mitochondrial isoform 2 precursor	*gcat*	0.2	-4.2	-3.5	-6.7	-7.7
Gastrula stage epidermal type I cytokeratin	*krt*	0	0	0	0	-3.5
Nucleoplasmin-like protein NO29	*no29*	0.3	0	0	0	-3.2
Minichromosome maintenance deficient 3	*mcm3*	0	0	0	-3	0
Secreted frizzled-related protein 2	*sfrp2*	0	0	0	-3.6	0
Phosphoglucomutase-2	*pgm2*	0	0	0	-4.2	0
Actin, aortic smooth muscle	*acta1*	-2.8	-3.3	-7.3	-6.8	-6.3
Aspartoacylase	*aspa*	0	-2.9	-3.9	-6.9	-2.8
Fragile X mental retardation protein 1	*fmr1*	0	-3.9	-4	-4.3	0
poly(U)-specific endoribonuclease isoform 2	*endou*	0	0	-1.6	-3.8	0
Replication protein A	*rpa1*	0	0	-1	-4.7	0
B-cell translocation gene 1, anti-proliferative	*btg*	0	-4.8	-1.6	-6.4	-4.3
Heat shock 70 kDa protein 5	*hspa5*	0	-3.9	-2	-5	-3.7
Beta-hexosaminidase subunit beta preproprotein	*hexb*	1.6	-5	-3.9	-6.9	-4.9
Stress-70 protein, mitochondrial precursor	*hspa9*	0	-4.3	-1.6	-5	-3.7
X-prolyl aminopeptidase (aminopeptidase P) 2, membrane-bound	*xpnpep2*	0	-5.2	-2	-5.2	-4.6
Nicotinamide riboside kinase 2 isoform 2	*nmrk2*	0	6	2	6	3.6
Calmodulin	*calm1*	0.2	-4.9	-2.3	-4.9	-4.5
T-box transcription factor 2	*tbx2*	0	-5	-1.4	-3.5	-3.5
Ras-related protein Rab-11A isoform 1	*rab11a*	0	-4.7	-1.6	-4.6	-4.6
Activator of 90 kDa heat shock protein ATPase homolog 1	*ahsa1*	0	0	-1.6	-3.6	-3.7
Protein phosphatase-2A B'epsilon subunit	*ppp2r5e*	0	-4.7	0	3	-3.1
Calcium/calmodulin-dependent protein kinase type II subunit beta isoform 3	*camk2b*	0	-3.5	0	-2.6	-2.6
Glutamine synthetase	*glul*	0	-5.7	-2.6	-5	-4.5
Epsin 3	*epn3*	0	-6.2	0	-3.8	-2.8

Nuclear receptor corepressor 1	*ncor1*	-3.2	-4.2	0	-3.6	0
Embryonic serine protease-2	*esp2*	0	-6.1	0	-5.2	0
Leucine rich repeat containing 20	*lrrc20*	0	-3.2	0	-2.6	0
COMM domain containing 7	*commd7*	0	-7.2	0	-2.3	0
3'-phosphoadenosine 5'-phosphosulfate synthase 2	*papss2*	-2	-2.7	0	-4.6	0
Monocarboxylate transporter 7	*slc16a6*	-2.6	-4.4	0	-6	0
MAPK MPK1	*mpk1*	-3.5	-4.1	-1	-4.5	-3.5
Thyroid hormone binding protein/pyruvate kinase type M2	*pkm*	0	-4	0	-5.8	0
High affinity copper uptake protein 1	*slc31a1*	-1	-3.5	-3.2	-3.9	-2.9
Serine/threonine-protein kinase Nek3	*nek3*	0	-5.2	-4.2	-6.5	0
Bubblegum-Related Protein (Acyl-CoA Synthetase Bubblegum Family Member 2 or Long-Chain-Fatty-Acid--CoA Ligase)	*brgl*	-0.3	-3.9	-1.5	-4.4	0
Ferritin heavy chain	*fth1*	0.3	-5.6	-3.5	-5.5	0
DnaJ homolog subfamily B member 6 isoform b	*dnajb6*	0	-5.3	-1.4	-3.3	0
Myosin regulatory light polypeptide 9 isoform a	*myl9*	0	-4.6	-3.5	-4	0
General transcription factor IIF	*gtf2f*	-2.3	-3.9	0	-2.3	-2.3
TGFB-induced factor homeodomain	*tgif1*	-2.8	-4.4	-1	-2.8	-2.8
Peptidyl-prolyl cis-trans isomerase FKBP2 precursor	*fkbp2*	-2.6	-4.5	0	-4.2	-4.2
FOS-like antigen 2	*fosl2*	-3	-4.6	-1.6	-3	-4
Actin-Like 6A	*actl6a*	0	-4.4	0	0	-3.2
Far upstream element (FUSE) binding protein 1	*fubp1*	0	-4	0	0	-3.6
RNA binding motif protein 14	*rbm14*	0	-3.9	0	0	-2.3
Phenylalanyl-tRNA synthetase, alpha subunit	*farsa*	0	-4.7	0	0	-3.8
Es1 protein isoform Ia precursor	*es1*	0	-4.4	0	0	-4.3
P450 (cytochrome) oxidoreductase	*por*	0.3	-4.3	-1	0	-4.2
Glutaredoxin-1	*glrx*	-0.3	-6.3	-1.6	0	-3.5

Casein kinase 1-& isoform	*csnk1a*	0	-5.2	-2.6	0	-4
phosphatidylethanolamine-binding protein 1 preproprotein	*pebp1*	0	-5.2	-1.6	0	-4.6
Thioredoxin domain-containing protein 2 isoform 1	*txndc2*	0	-5.2	-2.3	0	-4.5
High mobility group 20A	*hmg20a*	0.1	-3.7	-2.6	0	-3.6
Dystroglycan 1	*dag1*	0	-3.5	-2.3	0	-4.7
Histocompatibility (minor) 13	*hm13*	0	-2.8	0	0	-4.6
Protein Arginine Methyltransferase 1	*prmt1*	0	-2.3	0	0	0
Cu-Zn superoxide dismutase	*sodb*	0	-3.1	0	0	0
Kruppel-like factor 9	*klf9*	-4	-4.6	-4	-4	-4
Myosin-11 isoform SM2A	*myh11*	0.2	-3.7	-1.5	0	0
Transmembrane protein 79	*tmem79*	-1	-5.2	-4.7	-4.7	-4.7
Sarcoplasmic/endoplasmic reticulum calcium ATPase 2 isoform b	*atp2a2*	1.3	-7.3	0	0	0
Aldehyde dehydrogenase, mitochondrial isoform 1 precursor	*aldh2*	0	-4.9	-1	0	0
Solute carrier family 7 (cationic amino acid transporter, y+system), mem ber 3	*slc7a3*	0	-4.8	-1.3	0	0
Sodium- and chloride-dependent neutral and basic amino acid transporter B(0+)	*slc6a14*	0	4.1	-2.6	0	0
Nucleoside diphosphate kinase 7 isoform a	*nme7*	0	-3.4	-3.5	0	-3.3
Calbindin 1, 28 kDa	*calb1*	-5	-5.5	-6.2	-5	5
Collagenase 4	*mmp2*	-3.4	-2.8	-4.3	-2.8	-3.8
Cyclin-dependent kinase inhibitor 1B	*cdkn1b*	0	0	-1.6	0	-2.3
REV1, polymerase (DNA directed)	*rev1*	0	2.3	-3.7	0	0
Myosin regulatory light chain 2, atrial isoform	*myl7*	0	0	-1.3	0	0
EH domain-containing protein 4	*ehd4*	0	0	-1.3	0	0

Additional file 2.17. Heat map with the expression profile (log2 of fold-change) of putative thyroid hormones (TH) responsive transcripts with differential expression between juvenile and metamorphic stages of Atlantic halibut.
Please see the Additional file 12 in https://bmcgenomics.biomedcentral.com/articles/10.1186/s12864-016-2699-x#Bib1

Additional file 2.18. Reactome pathway analysis for the 145 differential expressed TH-responsive transcripts identified when Atlantic halibut metamorphic stages were compared with the juvenile. Reactome analysis was performed using INTREPROSCAN accession numbers obtained from the functional annotation of the Atlantic halibut transcriptome with Blast2GO.

Pathway	Species	IDs in pathway (%)	Enrichment (pval)	FDR
Circadian Clock	*Homo sapiens*	6 (16%)	5.00E-10	1.10E-08
Cellular responses to stress	*Homo sapiens*	52 (21%)	1.54E-06	1.69E-05
Cell Cycle	*Homo sapiens*	75 (15%)	1.00E-05	6.66E-05
DNA Repair	*Homo sapiens*	14 (13%)	2.69E-05	1.35E-04
Disease	*Homo sapiens*	176 (15%)	2.34E-04	9.08E-04
Membrane Trafficking	*Homo sapiens*	26 (19%)	3.03E-04	9.08E-04
DNA Replication	*Homo sapiens*	14 (14%)	3.86E-04	1.16E-03
Apoptosis	*Homo sapiens*	25 (16%)	1.86E-03	3.73E-03
Developmental Biology	*Homo sapiens*	135 (34%)	1.11E-02	2.22E-02
Metabolism	*Homo sapiens*	141 (9%)	1.27E-02	2.55E-02
Metabolism of proteins	*Homo sapiens*	89 (15%)	1.27E-02	2.55E-02
Signal Transduction	*Homo sapiens*	291 (16%)	1.73E-02	3.47E-02

Additional file 2.19. Relative gene expression analysis of transcripts involved in the TH cascade during Atlantic halibut development (stage 5 to juvenile; n = 5 per stage) using quantitative RT-PCR (qPCR). Thyroglobulin (*tg*), TH receptor alpha A (*trαa*), TH receptor alpha B (*trαb*), TH receptor beta (*trβ*), deiodinase 3 (*dio3*), deiodinase 2 (*dio2*), deiodinase 1 (*dio1*), monocarboxylate transporter 8 (*mct8*), and monocarboxylate transporter 10 (*mct10*) gene expression. Results are presented as mean ± SEM of the candidate gene expression, normalized using the geometric mean of the reference genes *rps4* and *ef1a1*. Significant difference ($p < 0.05$; one-way ANOVA) of normalized transcript expression between stages are indicated by different letters.

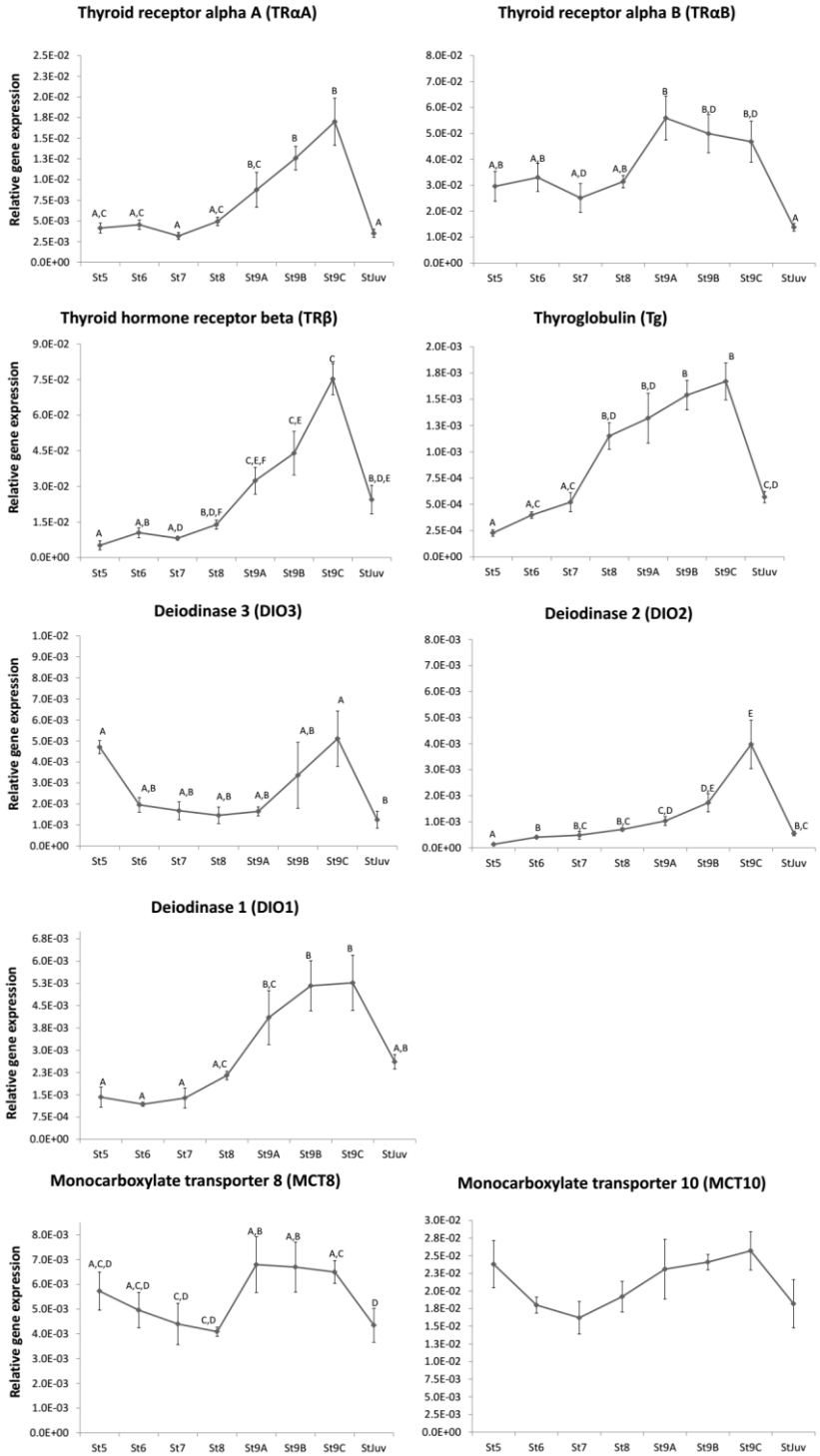

Additional file 2.20. Quantitative RT-PCR (qPCR) of the relative expression of ribosomal protein L7 (*rpl7*), 40S ribosomal protein S30 (*fau*); alpha-globin 1 (*gloα1*), carboxypeptidase A2 (*cpa2*), apolipoprotein A-I (*apoai*) and type I keratin isoform 2 (*krt1i2*). Analysis of the indicated transcripts was performed in whole Atlantic halibut larvae during development (stage 5 to juvenile; n=5). The results are presented as mean ± SEM of the normalized expression, using the geometric mean of the reference genes RPS4 and EFIAI. Different letters represent significantly different mean values ($p<0.05$; one-way ANOVA).

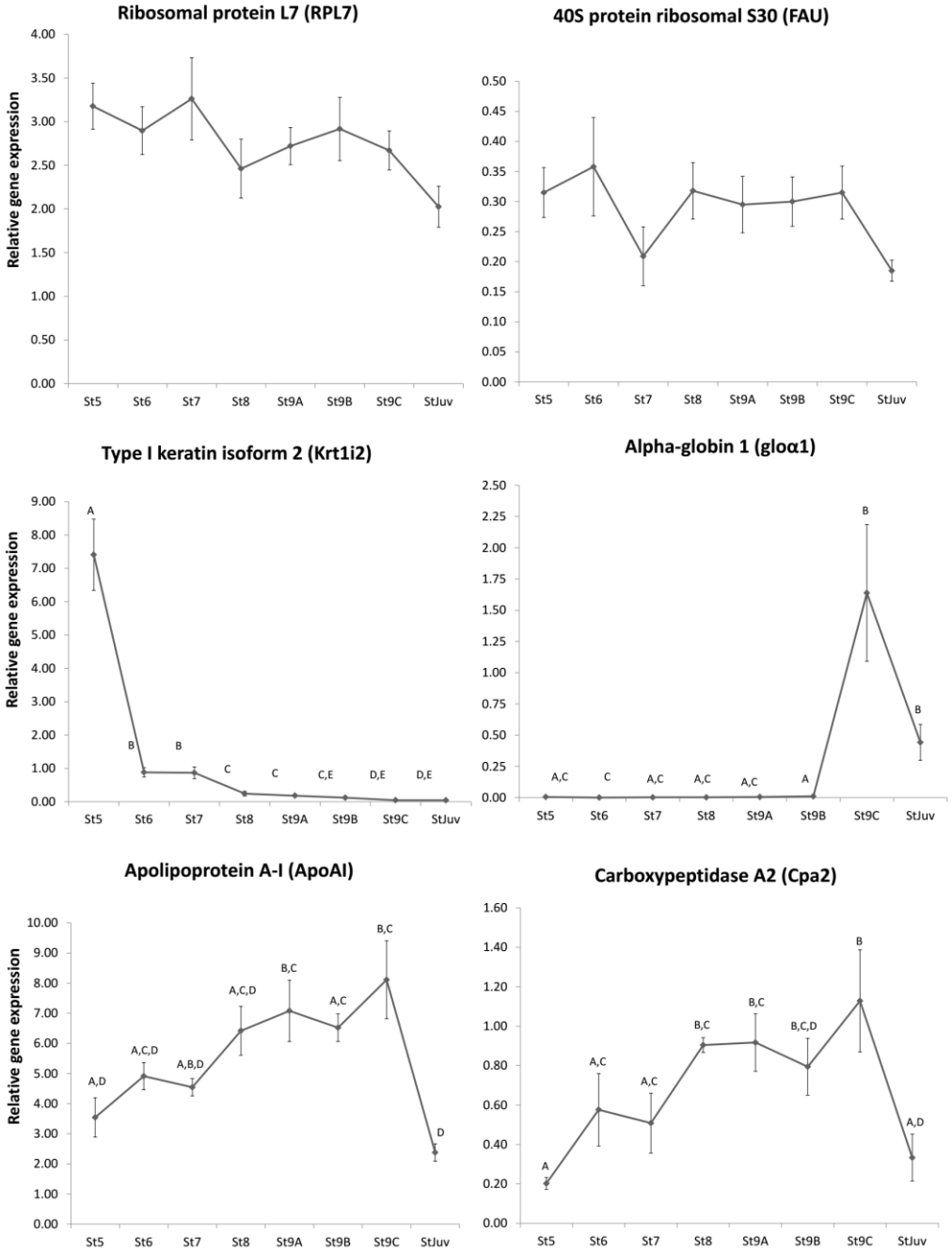

Chapter 3

Duplicate deiodinase 3 genes in teleost fish and their role during Atlantic halibut (*Hippoglossus hippoglossus*) metamorphosis

Chapter 3

Abstract

Deiodinase 3 (Dio3) plays an essential role during early development in vertebrates by controlling tissue thyroid hormone (TH) availability. The Atlantic halibut (*Hippoglossus hippoglossus*) possesses duplicate *dio3* genes (*dio3a* and *dio3b*). Expression analysis indicates that *dio3b* levels change in abocular skin during metamorphosis and this suggests that this enzyme is associated with the divergent maturation of larval skin to the juvenile phenotype. In larvae exposed to MMI, a chemical that inhibits TH production and blocks metamorphosis, expression of *dio3b* in ocular skin is significantly up-regulated indicating that THs normally repress this gene during this developmental event.

The molecular basis for divergent *dio3a* and *dio3b* expression and responsiveness to MMI treatment is explained by the multiple conserved TREs in the proximal promoter region of teleost *dio3b* and their absence from the promoter of *dio3a*. We propose that the divergent expression of *dio3* in ocular and abocular skin during halibut metamorphosis contributes to their asymmetric development in response to THs.

Keywords: deiodinase 3, flatfish, gene duplication, hormone-regulated gene expression, metamorphosis

Chapter 3

3.1. Introduction

The thyroid hormones (THs), thyroxin (T_4) and 3', 5, 3-triiodothyronine (T_3), are pleiotropic hormones that control development, growth and metabolic homeostasis in vertebrates (Brown and Cai, 2007, Buchholz, 2015, Darras et al., 2015, Laudet, 2011, Mullur et al., 2014, Power et al., 2001, Sinha et al., 2014 and Tata, 2006). These hormones are released from the thyroid follicles in vertebrates and in responsive tissue bind to nuclear TH receptors (TRs), which function as hormone-activated transcription factors and regulate gene expression (Buchholz, 2015 and Sachs et al., 2000). T_4 is the predominant hormone secreted by the thyrocytes and is converted to T_3, the biologically active hormone, by deiodination in the peripheral tissues. A unique family of selenoproteins in chordates, the iodothyronine deiodinases (DIO), are responsible for activation and inactivation of THs (Bianco et al., 2002).

The deiodinases are thioredoxin fold-containing selenoenzymes a group of transmembrane enzymes (DIO1-3) that tightly regulate the cellular availability of THs in peripheral tissues by intracellular activation or inactivation of T_4 and T_3 (Kohrle, 1999). Three deiodinase isoforms with a highly conserved function have been identified in most vertebrates. DIO1 and DIO2 are activating enzymes that convert the prohormone, T_4, into the active isoform, T_3, by removing an iodine from their outer-ring structure (outer-ring deiodination, ORD), (Bianco and Larsen, 2005, Gereben et al., 2008 and Schweizer and Steegborn, 2015). DIO3 is an inactivating enzyme that reduces TH levels by converting the prohormone T_4 into rT_3 (3,3',5'-triiodothyronine) by inner-ring deiodination (IRD) and T_3 into T_2 (3,3'-diiodothyronine), (Bianco and Larsen, 2005, Bianco and Kim, 2006, Bianco et al., 2002 and Gereben et al., 2008). An important difference between deiodinases in fish and terrestrial vertebrates is that in the former gene duplicates for *dio2* and *dio3* have been identified as a consequence of the teleost-specific whole genome duplication (Jaillon et al., 2004, Orozco et al. 2012, Ravi and Venkatesh, 2008 and Volff, 2005). Furthermore, the deiodinases from fish have specific functional characteristics including; i) their resistance to inhibition by 6-n-propyl-2-thyouracil (PTU), and ii) the variable effect of dithiothreitol (DTT) on ORD of different teleost deiodinases (Klaren et al., 2012, Klaren et al., 2005, Orozco et al., 2012, 2003 and Sanders et al., 1997).

In mammals, modifications in DIO3 abundance are associated with thyroid pathophysiological conditions (reviewed by Darras et al., 2015 and Dentice and Salvatore, 2011). In hypothyroidism *dio3* expression decreases whereas in hyperthyroidism it increases (Hernandez and Germain, 2002). High levels of *dio3* mRNA are associated with cardiac disorders (Pol et al., 2010 and Wassen et al., 2002). During development, DIO3 plays a major role in controlling the tissue availability of T_3 (Darras et al., 1992 and Debaveye et al., 2005) and high levels of T_3 in D3-deficient mice (D3KO) are linked to growth retardation, neonatal lethality and persistent congenital hypothyroidism (St Germain et al., 2009). DIO3 and DIO2 are essential for foetal and early neonatal brain development (Galton et al., 2014) and for brain cell maturation in mice (Friesema et al., 2012). DIO3 also plays an important role in the development of retinal and auditory function and skeletal myogenesis in mammals (Dentice et al., 2013). The conserved role of Dio3 in regulating TH availability through its role in T_3 degradation, especially during early development, has only recently been confirmed in teleost fish. In zebrafish the *dio3* paralogs (*dio3a* and *dio3b*) encode two highly similar enzymatically active proteins with high affinity for THs (Guo et al., 2014). Knock-down (KD) studies of the duplicate *dio3* genes in zebrafish provide indirect evidence of the importance of T_3 availability for successful embryonic development (Bohnsack and Kahana, 2013 and Heijlen et al., 2014). The similar phenotypes of *dio3a* and *dio3b* KDs (perturbed swim bladder development and muscle development/function) indicates that the genes have overlapping functions, although KD of *dio3b* produces a more severe phenotype (Heijlen et al., 2014 and Houbrechts et al., 2016). The role of Dio3 in other fish and during later stages of development has not been described.

Metamorphosis in fish is a late developmental event that is associated with changes in external phenotype as fish transition from the larval into the juvenile state. In flatfish (Pleuronectiformes), this process is particularly extreme as they undergo dramatic morphological reorganization as they change from a symmetric larva to an asymmetric juvenile (Power et al., 2008). As fish become asymmetric, the skin also acquires asymmetric characteristics and the upper side becomes pigmented (ocular side) and the bottom side (abocular or blind side) is devoid of pigmentation (Power et al., 2008). In several species of flatfish asymmetry in pigmentation is regulated by THs and

in the olive flounder (*Paralichthys olivaceus*) (Yoo et al., 2000) and the spotted halibut (*Verasper variegatus*) (Tagawa and Aritaki, 2005), administration of T_4 in early metamorphosis stops the formation of adult type melanophores on the blind side and disrupts the normal asymmetric pigment pattern. In the Senegalese sole (*Solea senegalensi*s), the whole body expression of *dio2* and *dio3* is regulated during metamorphosis, and the concentration of T_3 and T_4 is correlated to *dio3* expression (Isorna et al., 2009).

In the Atlantic halibut (*Hippoglossus hippoglossus*), changes in TH levels and the expression of thyroid receptors (TRs) are correlated with the transition from prometamorphosis to the metamorphic climax in larvae (Galay-Burgos et al., 2008). During these stages, *dio2* and *dio3* expression is linked to TH levels; however unlike the Senegalese sole no significant differences occur in the expression of *dio3* in skin during the establishment of pigmentation asymmetry (Campinho et al., 2012a). One of the possible explanations for the conflicting results obtained for *dio3* expression during flatfish metamorphosis may be related to the recent identification in fish of duplicate *dio3* genes and their possible divergent function. To test this hypothesis, we analysed *dio3* genes in the recently released transcriptome of the Atlantic halibut (Alves et al., 2016) and other flatfish, teleosts and terrestrial vertebrates to establish an evolutionary model for *dio3* genes. To elucidate how the same hormone can have divergent effects in the same tissue we took advantage of the divergent ocular and abocular skin phenotype of flatfish. The large size of the Atlantic halibut and their slow metamorphosis (occurring over approx. 58 days) permitted analysis of *dio3* gene duplicates for the first time in ocular and abocular skin of individuals at different stages of metamorphosis. *In silico* promoter analysis and manipulation of THs *in vivo* using methimazole (MMI) revealed that the *dio3* duplicates are differentially regulated by THs during metamorphosis. Overall the results suggest that *dio3b* gene expression in skin is repressed by THs during metamorphosis. Divergent expression levels and patterns of *dio3b* in ocular and abocular skin presumably modify TH availability, and context specific maturation program are triggered.

3.2. Materials and methods

3.2.1. Larvae and sampling for natural metamorphosis

Atlantic halibut larvae were supplied from a normal production cycle by the aquaculture company Fiskeldi Eyjafjarðar Ltd (Iceland). Samples were collected by a qualified member of staff from a standard commercial production cycle (Galay-Burgos et al., 2008) undergoing normal metamorphosis. The legislation and measures implemented by the commercial producer complied with Directive 98/58/EC (protection of animals kept for farming) and production and sampling by an experienced worker were optimised to avoid unnecessary pain, suffering or injury and to maximise larval survival.

Fish were euthanized using a lethal dose of MS222 (50 $mg.l^{-1}$, ethyl 3-aminobenzoate methanesulfonate salt, Sigma-Aldrich, USA) and individual larvae and juveniles were stored in RNA later (Life Technologies, Carlsbad, USA) at -20ºC until further analysis. Larval stages were classified by measuring the myotome height (MH) and standard length (SL), (Saele et al., 2004). Atlantic halibut samples from developmental stages: 5 (premetamorphosis); 6 and 7 (prometamorphosis); 8 (proclimax metamorphosis), 9 (climax metamorphosis) and post-metamorphic juveniles were used in the study. Larvae from stage 9 were further sub-divided into 9A, 9B and 9C to represent early, mid- and late climax stages as described in Alves et al. (2016).

To characterise the tissue distribution of *dio3a* and *dio3b* the gills, liver, brain, eye, heart, duodenum, pyloric ceca, intestine, rectum, operculum, ocular skin, abocular skin, fin, cranial bone and white muscle were dissected from post-metamorphic juveniles (n = 4 per stage) and stored in RNAlater (Life Technologies). For expression studies during metamorphosis, whole-larvae from stages 5 to 9C and post-metamorphic juveniles (n = 5 per stage) were used. For skin expression, ocular skin (top side, designated skin top - ST) and abocular skin (bottom side, designated skin bottom – SB) were used from metamorphic larval stages 7 to 9B (n = 5 per stage).

3.2.2. Methimazole treatment of Atlantic halibut larvae

The experiments with Atlantic halibut larvae were performed at the Institute of Marine Research (IMR) Austevoll, Norway. The experiments were covered by a Norwegian Food Safety Authority facility (licence n. 093; experiment approval n. 4395). The Food Safety Authority handles everything connected with animal welfare and experimental animals in Norway.

The experimental system contained 4 1000 l, PVC round tanks, with a circular water flow and a central standpipe outlet. The waterflow was kept at around 0.3 $l.min^{-1}$, the temperature at 10.5 °C and the oxygen level at full saturation. The tanks were cleaned with a siphon each day and mortalities were registered. Duplicate experimental tanks were used for the control and methimazole (MMI) treatments that was initiated 12 days post start feeding (dpsf) by incorporating it into the *Artemia*. In brief, a solution of MMI (0.1 mg ml^{-1}, Sigma M8506) was prepared in distilled water and 1 ml of the MMI stock was used per liter of *Artemia* (each liter containing 300,000 *Artemia* naupli). The MMI stock was added to the enrichment emulsion (lipid/vitamin mix) that was fed (0.2 g l^{-1}) to the naupli before they were fed to the larvae. It was not possible to confirm the concentration of MMI taken up by the Artemia, but in previous experiments with the structurally similar T_4 (3-4-hydroxy-3,5-diiodophenoxy-3,5-diiodophenyl-L-alanine, Sigma T2501, 1 mg ml^{-1}) enriched *Artemia* contained 2 μg T_4 g^{-1} wet weight.

Control or MMI enriched *Artemia* was fed daily to the larvae; in the morning the larvae were fed MMI enriched *Artemia* (2/3 of the total daily feed) and in the afternoon (1/3 of the total daily feed) with non-treated enriched *Artemia*. Larvae were treated with MMI up until 47 dpsf. Larvae were sampled prior to and during metamorphosis, sacrificed and either frozen at –80 ^{o}C or fixed in 4 % paraformaldehyde in phosphate buffered saline for subsequent molecular and histological analysis. Mortality rates as well as metamorphic success were quantified, and observations of metamorphic status were made.

To confirm the efficacy of the MMI treatment thyroid tissue activity was assessed by histology as previously reported (Pinto et al., 2013). In brief, the heads from fixed and staged larvae were micro-dissected and decalcified in EDTA (0.5M pH 8), washed in water, dehydrated and embedded in wax and serial sections (5 μm) prepared. Sections

were then dehydrated, dewaxed and stained using haematoxylin and eosin and mounted in DPX (Sigma-Aldrich, Spain). The stained sections were examined with a microscope (Leica DM2000), and digital images were obtained with a microscope coupled to a digital camera (Leica DFC480). The thyroid in all samples was examined in the same area and the total number of thyroid follicles was counted in alternating slides in six consecutive sections. Five randomly selected follicles per section were used to measure the internal follicle areas. The thyrocyte height (µm) was determined by measuring four cells per follicle, lying 90° from one another. All measurements were executed using Image J (http://rsbweb.nih.gov/ij/).

3.2.3. RNA extraction and cDNA synthesis

Total RNA was extracted from Atlantic halibut samples using a Maxwell®16 System (Promega, USA), following the manufacturer's instructions. To avoid contamination with genomic DNA, total RNA was treated with a Turbo DNA-Free kit (Ambion, USA) and 0.5 µg of DNase treated RNA was used to synthesize cDNA. The cDNA synthesis reaction was performed using 200 ng of random hexamers (GE Healthcare, UK), 0.5 mM dNTP's, 8 U of Ribolock RNase inhibitor (Fermentas, Germany), and 100 U of RevertAid M-MuLV Reverse Transcriptase (Fermentas, Germany) to give a final reaction volume of 20 µl. The reactions were carried out at 25 ºC for 10 min; 42ºC for 60 min with a final step at 72 ºC for 10 min in a MyCycler BioRad thermocycler (BioRad).

3.2.4. Isolation of Atlantic halibut deiodinase 3b

Atlantic halibut *dio* 1, 2 and 3 were identified during routine screening of a recently generated metamorphosing Atlantic halibut larval transcriptome (Alves et al., 2016, Gomes et al., 2014) using the European sea bass deiodinase genes as the bait (Http://seabass.mpipz.de, accession numbers: DLAgn_00150470, DLAgn_00018780, DLAgn_00023090 and DLAgn_00068090 for Dio1, Dio2, Dio3a and Dio3b, respectively). Preliminary analysis of the isolated transcripts revealed two putative *dio3* transcripts, the previously identified Atlantic halibut *dio3* (DQ856303.2) and a novel

isoform (referred to as *dio3b*) with a deduced amino acid sequence similarity for the 266 bp fragment of 80%. The sequences of the entire coding region and the 3'UTR for *dio3b* were obtained by 3'-rapid amplification of cDNA ends (RACE) using a SMARTer RACE cDNA Amplification Kit (Clontech, USA). Three µg of total RNA from whole larvae (stage 5) was reverse transcribed using SuperScript® III Reverse Transcriptase (Invitrogen, USA) and 3'RACE CDS primer (designated A), 5'-AAGCAGTGGTATCAACGCAGAGTAC$(T)_{30}$VN-3' (V = A, G, or C; N = A, C, G, or T), following the manufacturer's instructions. The target template was amplified using touch-down PCR (5 min at 95 ºC; 5 cycles: 30 sec at 95 ºC, 3 min at 72 ºC; 5 cycles: 30 sec at 95 ºC, 30 sec at 70ºC, 3 min at 72ºC; 25 cycles at 30 sec at 95 ºC, 30 sec at 68 ºC, 3 min at 72 ºC; 5 min at 72 ºC) and the 3'RACE CDS reverse primer A and a *dio3* specific forward primer (5'-GAGGCAGGACGGCCCGGAC-3'). The amplified fragment was isolated and a nested PCR was performed (5 min at 95 ºC followed by 40 cycles of: 30 sec at 95 ºC, 30 sec at 60 ºC, 90 sec at 72 ºC; and a final 5 min at 72 ºC). The PCR product was cloned into the pGEM®-T Easy Vector (Promega, USA) and subsequently sequenced to confirm its identity. The existence of a SECIS element in the 3'UTR was assessed using the software SECISearch 2.19 (http://genome.unl.edu/SECISearch.html, Kryukov et al. 2003).

3.2.5. Databases searches

Putative *dio3* transcripts and genes were retrieved from several fish species using the deduced amino acid sequence of the duplicate Atlantic halibut *dio3a* (DQ856303.2) and *dio3b* (under submission) as queries. Searches were performed by mining the non-redundant protein collection (nr) and available EST's at NCBI (http://www.ncbi.nlm.nih.gov/, accessed November 2013) for Teleostei (taxid:32443), cartilaginous fish (taxid:7777) and fish genomes (Agnatha, cartilaginous, ray-finned fish and lobe-finned fish). The identity of the teleost and cartilaginous fish *dio3* ESTs retrieved was confirmed by comparing them with the the orthologs in human and zebrafish.

Thirteen genomes from ray-finned fish were searched for putative *dio3* genes and included the two pufferfish (*Tetraodon nigroviridis*; *Takifugu rubripes*); stickleback

(*Gasterosteus aculeatus*); Nile tilapia (*Oreochromis niloticus*); medaka (*Oryzias latipes*); platyfish (*Xiphophorus maculatus*); Atlantic cod (*Gadus morhua*); cavefish (*Astyanax mexicanus*); zebrafish (*Danio rerio*) and the primitive freshwater ray-finned fish, the spotted gar (*Lepisosteus oculatus*) available from ENSEMBL (http://www.ensembl.org, accessed April 2016) and the genome of the European sea bass (*Dicentrarchus labrax*) (http://seabass.mpipz.de, accessed April 2016), and the genome of the flatfish half-smooth tongue sole (*Cynoglossus semilaevis*) available from NCBI (http://www.ncbi.nlm.nih.gov). Sequences from the Senegalese sole (*Solea senegalensis*) were retrieved from genome scaffolds (IFAPA, Spain). The sea lamprey (*Petromyzon marinus*) and the lobe-finned coelacanth (*Latimeria chalumnae*) genome assemblies were accessed in ENSEMBL (http://www.ensembl.org, accessed April 2016). The cartilaginous fish *dio3* was identified and retrieved from the elephant shark (*Callorhinchus milii)* genome (http://esharkgenome.imcb.a-star.edu.sg, accessed April 2016). The presence of the TGA codon that encodes a modified Selenocystein in the protein was evaluated *in silico*. The full-length *dio3* mRNA were extracted from genomes, EST's and the transcriptomes included in the analysis, the protein sequences were deduced using the Expasy translate tool (http://web.expasy.org) and used for evolutionary analysis. The homologues of the teleost *dio1* and *dio2* were also retrieved from the ascidians, *Halocynthia roretzi* and *Ciona intestinalis* and used for phylogenetic analysis.

3.2.6. Multiple sequence comparisons and phylogeny

The deduced mature protein sequence of Dio3 from vertebrates (Additional file 3.1.) were aligned using Clustal W (http://www.genome.jp/tools/clustalw/) and the percentages of similarity/identity between sequences were calculated using GeneDoc software (http://iubio.bio.indiana.edu/). For phylogenetic analysis of the Dio family members, alignments included sequences from several vertebrates and from tunicates. The aligned deiodinase sequences were manually edited and the selenocystein amino acid was removed. The edited sequence alignment (Additional file 3.2.) was analysed using ProtTest version 2.4 (http://darwin.uvigo.es/software/prottest2_server.html) to

select the best statistical model to study protein family evolution based on the Akaike Information Criterion (AIC) statistical model (Abascal et al., 2005).

Phylogenetic trees were constructed using both the Maximum Likelihood (ML) and Neighbor joining (NJ) methods with a Jones-Taylor-Thornton (JTT) model (Jones et al., 1992) and 4-gamma distributed categories (fixed gamma parameter, 1.459 and proportion of invariable sites, 0.075). The ML tree was constructed in PhyML 3.0 using 75 deiodinase sequences (http://www.atgc-montpellier.fr/phyml/), (Guindon et al., 2010). The accuracy of the phylogenetic clades was assessed using 100 bootstrap replicates (Felsenstein, 1985). Data was also analysed using the NJ method (Saitou and Nei, 1987) in the Phylogeny.fr (http://phylogeny.lirmm.fr) suite of programs and was performed with 4 gamma-distributed rate categories, and a fixed gamma parameter (1.5). The reliability of internal branches of the NJ tree was assessed using 1000 bootstrap replicates. ML and NJ trees were rooted with the ascidian deiodinases and produced trees with similar topologies.

3.2.7. Gene synteny analysis

The gene environment of teleost *dio3* genes was characterized and compared to the homologue *dio3* genome region in tetrapods and other vertebrates. Species included in the analysis were the *dio3* genes from the two pufferfish (*Takifugu rubripes*, *Tetraodon novirigidis*), medaka (*Oryzias latipes*), marine lamprey (*Petromyzon marinus*) and the primitive freshwater ray-finned fish the spotted gar (*Lepisosteus oculatus*), lobe-finned coelacanth (*Latimeria chalumnae*), frog (*Xenopus tropicalis*) and human (*Homo sapiens*). Genes flanking the *dio3* gene were identified using the annotation provided by Genomicus software (http://www.genomicus.biologie.ens.fr/). When gene annotation was not available orthologue genes were used to query the genome assembly.

3.2.8. *Dio3a* and *dio3b* promoter analysis

The 1.5 kb promoter flanking sequences of *dio3a* and *dio3b* were isolated from sea bass (http://seabass.mpipz.de *dio3a* DLAgn_00023090 LG12: 13527062-13528564

and *dio3b* DLAgn_00068090, LG17:7914104-7915735), half-smooth tongue sole (NCBI, *dio3a* LOC103380986 and *dio3b* LOC103378336), Senegalense sole (*dio3a* scaffold_6856 and dio3b scaffold_1344), *Takifugu rubripes* (Ensembl, *dio3a* ENSTRUG00000009227 and *dio3b* ENSTRUG00000012791) and zebrafish (Ensembl, *dio3a* Chr17: 1388795-1390297 and *dio3b* Chr.20: 54012674- 54014176). The thyroid response elements (TRE) were predicted using TF Bind software (Tsunoda and Takagi, 1999) and only the predicted TRE binding sites with a p value ≥ 0.80 were considered in the analysis.

3.2.9. Quantitative real-time PCR (qPCR)

Expression analysis of *dio3a* and *dio3b* were carried out using RT-qPCR. Specific primers for the target transcripts were designed using Beacon Design and Primer Premier 5.0 software (Premier Biosoft Int., Palo Alto, CA) (**Table 3.1**) to generate a product of between 100-200 bp in lenght. qPCR reactions were carried out in duplicate with a final reaction volume of 15 µl using SsoFast™ EvaGreen® Supermix (Bio-Rad, Marnes La Coquette, France) chemistry. The reaction was performed in a StepOnePlus™ Real-Time PCR System (Applied Biosystems, Foster City, USA) and cycling conditions were 30 sec at 95 ºC followed by 45 cycles of 5 sec at 95 ºC and 10 sec at the optimal annealing temperature for primer pairs (**Table 3.1**), followed by a final melt curve at 60 to 90 ºC. Melt curve analysis confirmed the amplification of a single gene product in each reaction. The PCR products were analyzed by electrophoresis (2% agarose gel /1x TBE) to confirm the size of the amplified target and were also sequenced to confirm qPCR specificity. For each gene analyzed, a standard curve relating initial template quantity to amplification cycle was generated using serial dilutions of the target gene cloned in the pGEM®-T Easy Vector (Promega, Madison, USA) (initial concentration, 10^8 copies amplicon/µl). The use of a standard curve for *dio3a* and *dio3b*, their similar PCR reaction efficiency (**Table 3.1**) and analysis of copy number permitted comparison of the relative abundance of each transcript.

The efficiency of the qPCR reactions varied between 85% and 100% with a $R^2 \geq 0.99$ (**Table 3.1**). Negative controls included absence of cDNA and an RT control (cDNA synthesis reaction without reverse transcriptase). Expression data was

normalized using three reference genes: Eukaryote elongation factor I alpha (*efa1*), 40S ribosomal protein S4 (*rps4*) and ribosomal protein L7 (*rpl7*) (**Table 3.1**). The geometric mean of the reference genes *rps4* and *ef1a1* was used to normalize *dio3a* and *b* expression in whole larvae and ocular/abocular skin during metamorphosis. The geometric mean of *rps4* and *rpl7* was used to normalize *dio3a* and *b* expression in juvenile Atlantic halibut tissues (**Table 3.1**).

Table 3.1. Specific primers used for qPCR gene expression analysis. Gene symbol, name and function are shown. The annealing temperature (TaºC), amplicon length (bp), R^2 and qPCR efficiency (%) are indicated for each primer pair.

Gene symbol	Gene name	Primer sequence(5'→3')	Annealing temperature (Ta)	Amplicon length (bp)	R^2	PCR efficiency
dio3a	Deiodinase 3a	F: ACTCCAGATAGATAGATTGTGTC R: TAAACAAACCTTTTTTTCCTGAA	60ºC	178	0.99	97%
dio3b	Deiodinase 3b	F: GCCGCTGCTCTGCCCATTC R: GGAGAGAGGCTTCAACCTGACTTC	62ºC	162	0.99	99%
ef1a1	Elongation factor 1 alpha	F: AAGAGGACCATCGAGAAGTT R: GTCTCAAACTTCCACAGAGC	60ºC	140	0.99	85%
rps4	40S ribosomal protein S4	F: CAAGTTTGATACTGCCAACCTGTG R: GGAGAGCCTGGTAGCGAAGC	60ºC	172	0.99	90%
rpl7	Ribosomal protein L7	F: TTCTCGGTGGACGCAATGG R: GCCAGCATCTTCTTTGACACG	60ºC	120	0.99	100%

3.2.10. Statistical analysis

Differences in thyrocyte height (μm) were detected using two-way ANOVA in SigmaPlot v10.0 (Systat Software, Inc., CA, USA) after checking for homogeneity. Tukey's post-hoc test was used for pair wise multiple comparisons to detect for statistical significance. Results are presented as mean ± standard error of the mean (SEM) unless otherwise stated. A value of $P < 0.05$ was taken as significant.

Statistical analysis of the relative gene expression between tissues was analyzed by one-way, ANOVA using SigmaPlot v10.0 (Systat Software, Inc., CA, USA) after checking for homogeneity. For the relative gene expression between metamorphic stages (whole larvae and ocular/abocular skin, MMI experiment) a two-way ANOVA was applied using SigmaPlot v10.0 (Systat Software, Inc., CA, USA) after checking for homogeneity. Tukey's post-hoc test was used for pair wise multiple comparisons. The expression of *dio3a* and *dio3b* is presented as the mean ± SEM.

When normality tests failed the data was log-transformed to achieve a normal distribution and analyzed using ANOVA by Ranks followed by Dunn's test for pairwise comparisons. Statistical significance was taken at $p < 0.05$. Gene expression is presented as the mean ± SEM.

3.3. Results

3.3.1. Deiodinase 3 (*dio3*) transcripts in Atlantic halibut

Two putative *dio3* transcripts were identified using blast to search the transcriptome of metamorphosing halibut (Alves et al., 2016 and Gomes et al., 2014). Sequence comparisons revealed that one of the *dio3* transcripts corresponded to the previously identified isoform in halibut (DQ856303, designated hereafter as *dio3a*, Campinho et al. 2012a) but the other transcript corresponded to an isoform not previously reported in halibut (that was designated *dio3b*, GenBank accession number, under submission). The full-length sequence of *dio3b* was amplified by RACE and generated a transcript of 1,389 bp in length, of which the first 780 bp corresponded to the open reading frame (ORF) and encoded a protein of 259 amino acids (Additional file 3.3). The deduced amino acid sequence of the two *dio3* paralogs shared 82%

similarity and the 3'UTRs of the transcripts were 47% identical. Sequence comparisons revealed that the Atlantic halibut *dio3b* transcript contained the deiodinase TGA codon that encodes a selenocystein (U) amino acid (aa) (**Figure 3.1,** Additional file 3.3.). The selenocystein insertion sequence (SECIS) in Atlantic halibut *dio3b* was type 2, which is also a characteristic of all other vertebrate *Dio3's* and it contained a canonical SECIS motif, with a conserved UGA_GA motif and two adenosines in the apical loop (Additional file 3.3.).

The Atlantic halibut Dio3b shared 51% and 50% amino acid sequence similarity with Dio1 and Dio2, respectively and 61% similarity with human DIO3 (Additional file 3.2., Additional file 3.4). Sequence alignment of the four Atlantic halibut Dio members (Dio1, Dio2, Dio3a and Dio3b) revealed that they all shared the four characteristics of a functional selenoprotein, namely: a transmembrane (TM) domain and a hinge (H) and linker (L) domain in the variable region and a globular (G) domain within the conserved region. The "signature string" was identified in the globular domain and contained the highly conserved Phe (F), Ser (S), Thr (T) and Sel (U) residues that are in the active catalytic centre of the enzyme, although in Atlantic halibut Dio3b, threonine (T) was substituted by serine (S) (**Figure 3.1**).

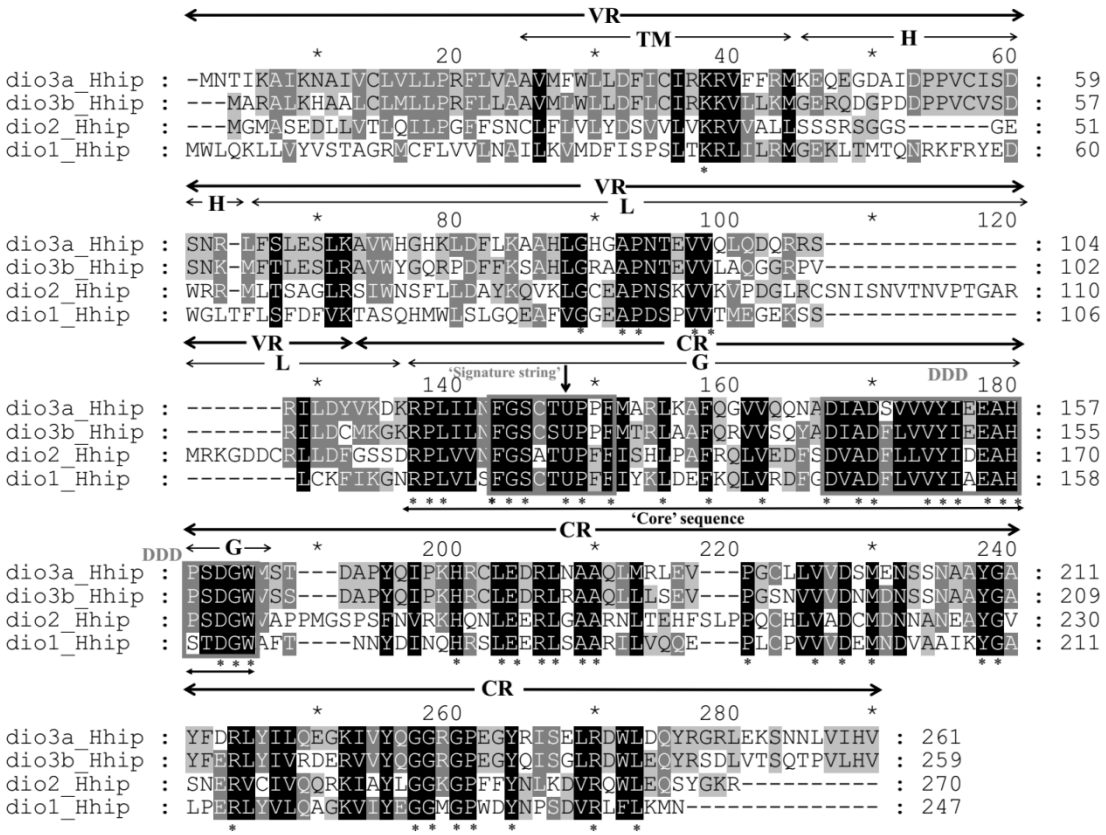

Figure 3.1. Sequence alignment of the Atlantic halibut Dio3 paralogues (Dio3a and Dio3b) with Dio1 and Dio2. Black bold arrows indicate the limits of the variable region (VR) and conserved region (CR). Black arrows demark the main protein domains characteristic of the vertebrate deiodinases: the transmembrane domain (TM), the hinge (H), the linker (L) and the globular or catalytic domain (G). Boxes in the "core sequence" of the globular domain indicate the two highly conserved residues in vertebrates: the 'signature string' and the deiodinase dimerization domain (DDD). The selenocysteine (SeCys - U) residue within the "core sequence" is indicated by an arrow. Shading denotes amino acid conservation and dark grey indicates 80% conservation and black 100% conservation. Dio1 NCBI accession number - ABI93488, 247 aa; Dio2 NCBI accession number - ABI93490, 270 aa; Dio3a NCBI accession number - ABI93489, 261 aa).

3.3.2. Deiodinase 3 genes and transcripts in other fishes

Putative *dio3* transcripts were identified in several fish species (Additional file 3.5 and 3.6). Searches in teleost fish genomes revealed that most of the species included in the analysis had two *dio3* genes. Indeed, *dio3* duplicates were found in the puffer fishes Tetraodon (*Tetraodon novirigidis*) and Takifugu (*Takifugu rubripes*), stickleback (*Gasterosteus aculeatus*), medaka (*Oryzias latipes*), Atlantic cod (*Gadus morhua*), cavefish (*Astyanax mexicanus*), platyfish (*Xiphophorus maculatus*), zebrafish (*Danio rerio*) and sea bass (*Dicentrarchus labrax*). Duplicate *dio3* genes were also retrieved from the half smooth tongue sole genome (*Cynoglossus semilaevis*), the only flatfish genome currently available. A single *dio3* gene was found in the genome of the primitive ray-finned fish, spotted gar (*Lepisosteus oculatus*), in the lobe-finned fish, coelacanth (*Latimeria chalumnae*), in the cartilaginous fish, Elephant shark (*Callorhinchus milii*) and in the genome of the jawless sea lamprey (*Petromyzon marinus*) (Additional file 3.5).

The deduced Atlantic halibut Dio3b shared 77 % aa sequence similarity with the previously described zebrafish Dio3b and 76 % with zebrafish Dio3a. Comparison of Atlantic halibut Dio3b with Dio3b in other flatfish, the flounder (*Paralichthys olivaceus*) and Senegalese sole (*Solea senegalensis*) revealed they are 97% and 91% similar, respectively (Additional file 3.4).

3.3.3. Phylogeny and sequence comparisons

Phylogenetic analysis of the vertebrate deiodinases revealed that the two *dio3*'s identified in the halibut and the *dio3* genes retrieved from other teleosts were the result of the whole genome duplication that occurred in the teleost lineage (**Figure 3.2**). The Atlantic

halibut Dio3b and Dio3a sequences and also the two paralogues identified in the smooth tongue sole and Senegalese sole clustered with the duplicate zebrafish homologues. Additionally, duplicate *dio3b* transcripts (*dio3b1* and *dio3b2*) and a single *dio3a* form were found in the salmon and the clustering in the phylogenetic tree revealed that the two salmon *dio3b's* identified emerged during the proposed Salmoniforme lineage specific genome duplication (Lorgen et al., 2015). In the flatfish, the *dio3's* previously isolated from the olive flounder and the Senegalese sole clustered with Atlantic halibut Dio3b and not with Dio3a confirming they were Dio3b isoforms (**Figure 3.2**); no Dio3a homologue was identified in the flounder.

The tree topology suggested that the vertebrate deiodinase proteins shared a common ancestral origin and that they descended via gene/genome duplications from a putative ancestral gene that was already present in early deuterostomes. The vertebrate *dio1* gene was the first to diverge from the common ancestral *dio* gene and *dio2* and *dio3* emerged subsequently as a result of a later duplication event and the presence of *dio3* as well as of *dio2* genes in the lamprey genome suggest that this event occurred prior to the divergence of the jawless fish. In ascidians such as *Ciona intestinalis* the tree topology suggests that the two *dio*'s identified arose from a species-specific gene duplication event.

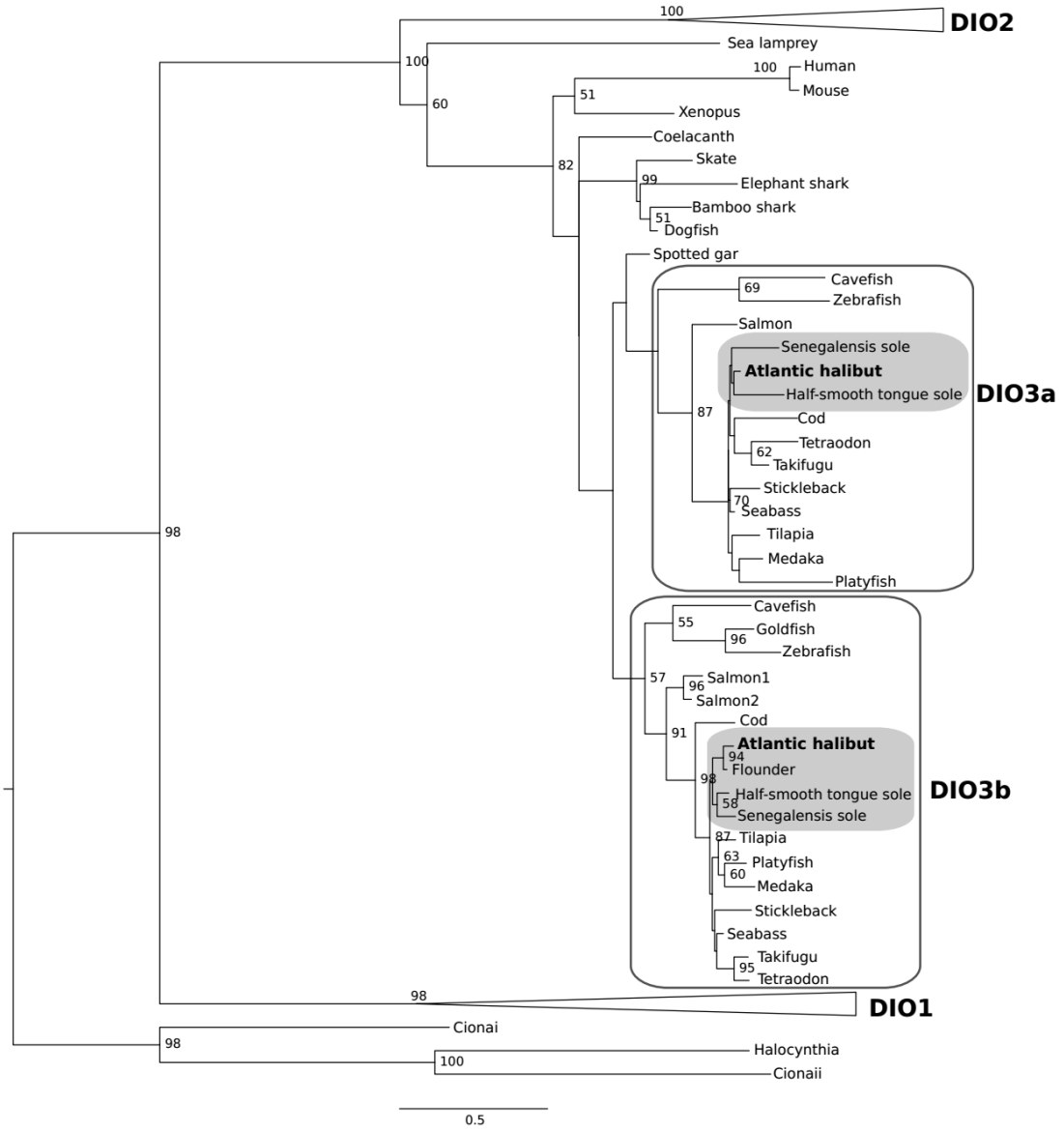

Figure 3.2. Phylogenetic analysis of the vertebrate deiodinases. The tree was constructed using the Maximum Likelihood (ML) method with a JTT substitution model and 100 bootstrap replicates. Only branches with bootstrap support higher than 50 are indicated and the vertebrate DIO1 and DIO2 clades have been condensed to facilitate interpretation. The duplicate teleost Dio3a (A) and Dio3b (B) clades are indicated. The deiodinase from the ascidians *Halocynthia roretzi* and *Ciona intestinalis* (Cionai and Cionaii) were used to root the tree. The DIO1 and DIO2 clades contain fish and tetrapod sequences retrieved from the NCBI database. The accession numbers of the Dio3 sequences used in the analysis are indicated in additional file 3.5.

Protein sequence comparisons revealed that *dio3* has been well conserved in vertebrates and the Dio3 deduced proteins shared a maximum of 45% aa sequence similarity with the ascidian deiodinases. The most highly conserved region of Dio3 in vertebrates was the globular region and in the teleost fish the Dio3a catalytic centre (FGSCTUPPF) was 100%

identical to those of the cartilaginous fish, spotted gar, coelacanth and tetrapods. Although in Atlantic halibut Dio3b the consensus threonine (T) prior to the selenocystein (U) was mutated to serine (S) (Additional file 3.2).

3.3.4. *Dio3* gene synteny analysis

The gene environment of the teleost *dio3* duplicates was compared with the homologue genome region in other vertebrates (**Figure 3.3**). Characterization of the Atlantic halibut *dio3a* and *dio3b* gene environment was not carried out, as the genome of this species was not available. However, the conserved gene synteny of the *dio3* genome region across the fishes indicated that this region was highly conserved in the teleosts.

At least six linked genes were conserved in the teleost gene environment of *dio3a* and five of these genes (*slc25a29*, *slc25a47*, *ppp2r5c* and *wdr20*) were also in linkage with teleost *dio3b*. This suggests that a segment of the chromosome bearing the ancestral *dio3* gene duplicated and that *dio3* and the flanking genes were retained in teleost genomes (**Figure 3.3**). However, the genes *wars*, *wdr25*, *begain* and *dlk1* that map near teleost *dio3b* were lost from the region flanking *dio3a*.

Orthologues of the genes in linkage with teleost *dio3* were also identified in the neighborhood of *dio3* in the spotted gar, coelacanth, amphibian and human. The conserved genes that flank *dio3a* and *dio3b* in *Tetraodon*, medaka and zebrafish, *slc25a29*, *slc25a47*, *ppp2r5c*, *hsp90aa1* and *wdr20* and *wars*, *wdr25*, *begain* and *dlk1*, respectively were identified in close proximity with the human *DIO3* gene on chromosome 14 and were also present in scaffold GL172858.1 of the amphibian homologue genome region (**Figure 3.3**). The orthologue of the human *DYNC1H1* gene that is also located in the neighborhood of the frog, coelacanth and spotted gar *dio3* genes was lost in teleosts. In the lamprey genome only a single gene (*ppp2r5c*) was in linkage with the *dio3* gene due most likely to the short genome scaffolds available. This gene was also found in close proximity with other vertebrate *dio3* genes, suggesting that the *dio3* genome environment has been conserved in vertebrates. Overall, the greater similarity between the linkage map for teleost *dio3b* and that of the spotted gar and terrestrial vertebrates suggests it is most like the ancestral chromosome that gave rise to the duplicates in teleosts.

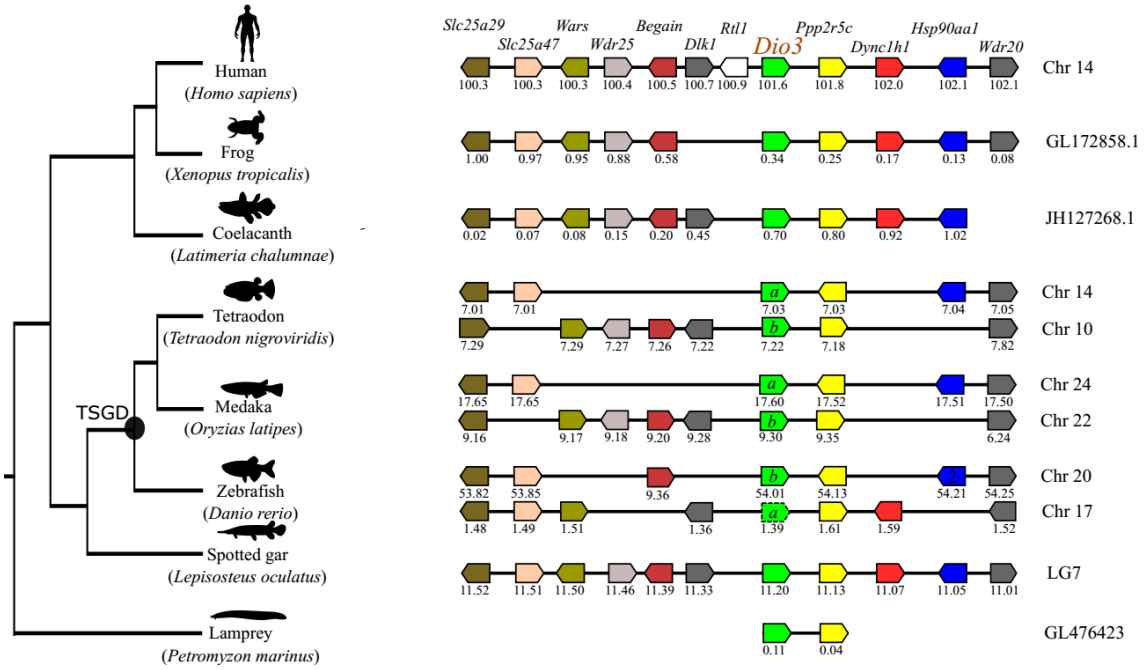

Figure 3.3. Comparison with other vertebrates of the homologous genome regions harboring the teleost deiodinase 3 (*dio3*) genes. The *dio3* gene environment was compared between several fish species (*Tetraodon*, medaka, zebrafish, spotted gar, coelacanth and lamprey) and the tetrapods, *Xenopus* and human. Gene names are indicated and are based on the human annotation. The colours represent gene homologues and their position in the chromosome is indicated below (Mb). The zebrafish dio3a gene is represented by a dashed arrow as it has not been predicted in the genome assembly. Horizontal lines represent chromosome/ genome fragments and the teleost specific genome duplication (TSGD) is indicated. Gene symbols and names: *slc25a29* solute carrier family 25 member 29, *slc25a47* - solute carrier family 25 member 47, *wars* - tryptophanyl-TRNA synthetase, *wdr25- WD repeat domain 25*, *begain* - brain-enriched guanylate kinase-associated, *dlk1* - delta-Like 1 homolog (Drosophila), *rtl* -retrotransposon-Like 1, *ppp2r5c* - protein phosphatase 2, regulatory subunit B', gamma, *dync1h1* - dynein, cytoplasmic 1, heavy chain 1, *hsp90aa1* - heat shock protein 90kDa 1 alpha (cytosolic), class A member 1, and *wdr20 - WD repeat domain 20*. The figure is not drawn to scale.

3.3.5. Deiodinases and metamorphosis

3.3.5.1. Tissue expression of Dio3

Dio3 ESTs were identified in several species of teleost (NCBI) and indicated that both gene transcripts have a widespread tissue distribution (Additional file 3.6). Likewise, characterization of the *dio3a* and *dio3b* gene expression in tissues of post-metamorphic Atlantic halibut juveniles (**Figure 3.4**) further confirmed the widespread distribution of these transcripts. Overall, *dio3b* was most abundant in the eye ($p < 0.05$) and liver of all the tissue analyzed while *dio3a* was most abundant in the brain and eye ($p < 0.05$) (**Figure 3.4A**).

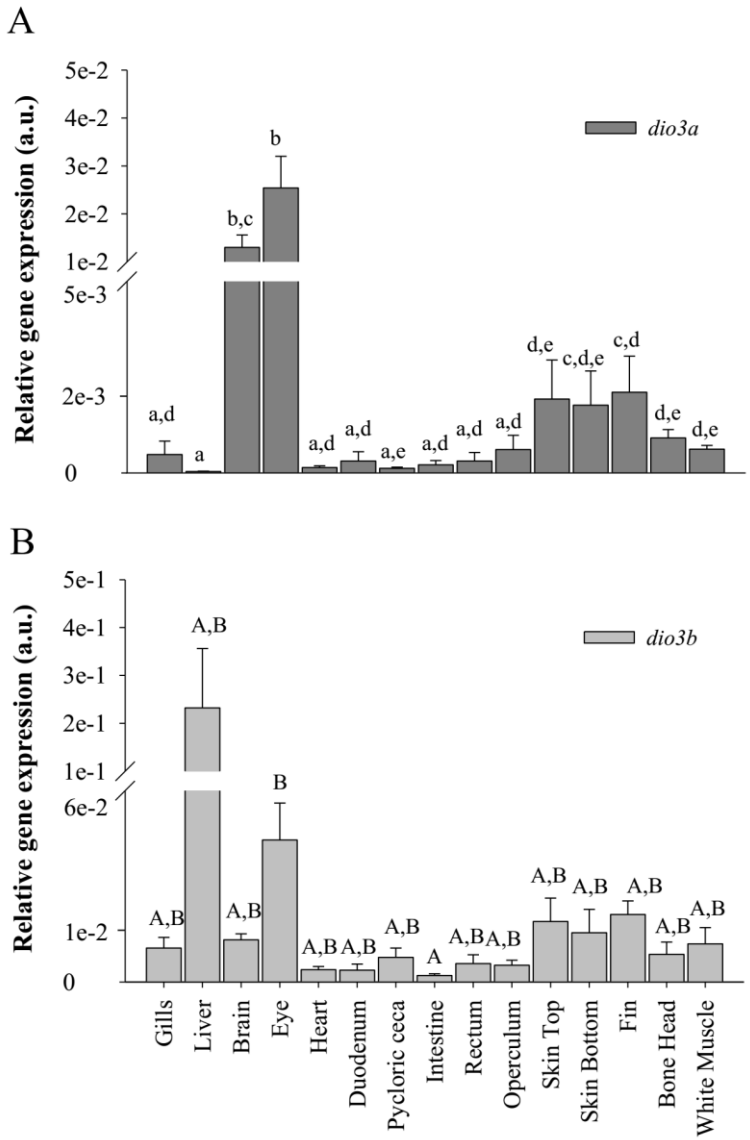

Figure 3.4. Relative tissue distribution of *dio3a* and *dio3b* in Atlantic halibut juveniles. Relative gene expression of *dio3a* (A) and *dio3b* (B) was determined by quantitative RT-PCR (qPCR) in tissues from juvenile Atlantic halibut. Gene expression was normalized using the geometric mean of the reference genes 40S ribosomal protein S4 (*rps4*) and ribosomal protein L7 (*rpl7*) and is represented as the mean ± standard error of the mean (n = 4, with the exception of liver for *dio3b* in which n = 3). Tissues that have a significantly ($p < 0.05$; one-way ANOVA) different abundance of *dio3a* or *dio3b* are represented by different lower case and upper case letters, respectively.

3.3.5.2. Expression of dio3 in whole larvae during metamorphosis

The duplicate *dio3* genes were expressed in all metamorphic stages of Atlantic halibut larvae, but *dio3b* was relatively more abundant than *dio3a* throughout metamorphosis ($p < 0.05$) (**Figure 3.5**). In stages 7 and 8 halibut larvae significant down-regulation ($p < 0.05$) of *dio3a*

transcripts occurred relative to stage 5 and significant up-regulation ($p < 0.05$) of *dio3a* to levels found in stage 5 larvae only occurred at stage 9C. Similarly, *dio3b* transcripts were significantly down-regulated ($p < 0.05$) in stages 6, 7, 8 and 9A halibut larvae relative to stage 5 larvae. Significant up-regulation ($p < 0.05$) of *dio3b* transcripts to levels found in stage 5 larvae only occurred in stage 9C. After metamorphosis *dio3b* expression was maintained relatively constant while *dio3a* was significantly down-regulated ($p < 0.05$) in the juveniles (**Figure 3.5**).

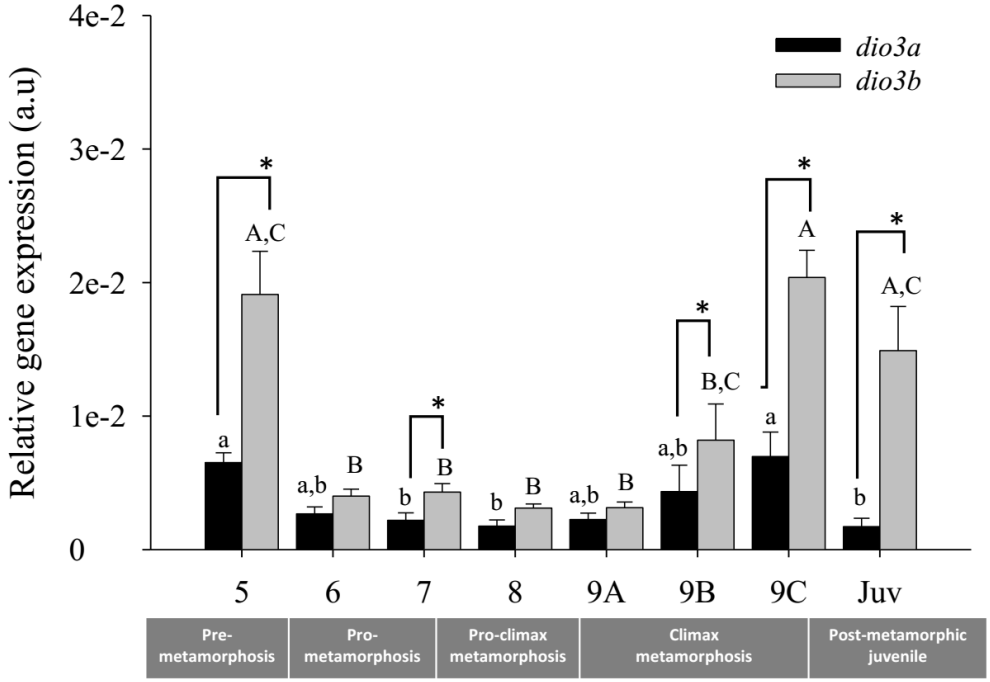

Figure 3.5. Ontogeny of *dio3a* and *dio3b* during Atlantic halibut metamorphosis. Relative gene expression of *dio3a* and *dio3b* was determined by quantitative RT-PCR (qPCR) during metamorphosis in whole larva extracts (stage 5 - premetamorphosis, stages 6 and 7 – prometamorphosis, stage 8 – proclimax metamorphosis, stages 9A to 9C – metamorphosis climax, and juvenile - postmetamorphosis). Gene expression was normalized using the geometric mean of the reference genes 40S ribosomal protein S4 (*rps4*) and elongation factor 1 alpha (*efa1*) and is represented as mean ± standard error of the mean (n = 5). Significant differences ($p < 0.05$; two-way ANOVA) in *dio3a* and *dio3b* expression are represented by different lower case and upper case letters, respectively. * indicates significant differences between *dio3a* and *dio3b*.

3.3.6. Regulation of halibut *dio3* genes in skin during metamorphosis

3.3.6.1. Effect of MMI in thyroid morphology and activity

The histomorphology of the thyroid in MMI treated Atlantic halibut confirmed the efficacy of the treatment in blocking TH production (**Figure 3.6A-C**). In stages 7 - 8 the control fish had the well characterized fish thyroid histomorphology and consisted of oval thyroid follicles surrounded by a uniform monolayer of thyrocytes. The thyrocytes were cuboidal and the follicle lumen was filled with dense pink-stained colloid. In MMI treated Atlantic halibut thyroid tissue histomorphology was similar to the control in the stage 7 and 8 halibut but a significant increase ($p < 0.05$) in the height of the thyrocytes indicated they were more active (**Figure 3.6A**).

The effect of MMI treatment on thyroid morphology was most evident in stages 9A - 9B (**Figure 3.6**). The thyroid tissue in stage 9A – 9B control Atlantic halibut was similar to the earlier larval stages. In the MMI treated Atlantic halibut, the thyroid morphology was dramatically changed and follicles were flattened and depleted of colloid (**Figure 3.6A**). The thyrocyte epithelium was columnar and the thyrocyte height was significantly increased ($p < 0.05$, **Figure 3.6B**) relative to the control and in some thyroid follicles a multilayer of thyrocytes was observed (**Figure 3.6A**). The histomorphology of the thyroid was typical of that associated with hypothyroidism in fish (eg. reduced TH production).

3.3.6.2. Effect of MMI on the expression of dio3 in ocular (ST) and abocular (SB) skin

No significant differences in *dio3a* transcript abundance were detected between ocular and abocular skin during metamorphosis or when only ocular or abocular expression was compared in different metamorphic stages of control Atlantic halibut (**Figure 3.6D and E**). No significant differences in *dio3b* transcript abundance were detected in ocular skin during metamorphosis of Atlantic halibut. A significant up-regulation ($p < 0.05$) of *dio3b* transcripts was detected in abocular skin of metamorphic stages 9A and 9B Atlantic halibut relative to stages 7 and 8 in the control fish (**Figure 3.6G and H**).

MMI treatment did not significantly modify *dio3a* transcript abundance in ocular or abocular skin during metamorphosis of Atlantic halibut (**Figure 3.6D and E**). The

ocular/abocular ratio of *dio3a* in control fish was characterized by a peak at stage 9A in control halibut. The ocular/abocular *dio3a* ratio in the skin from MMI treated fish was not significantly different from control fish although the peak was shifted to stage 8 halibut larvae (**Figure 3.6F**).

In MMI-treated Atlantic halibut, a significant up-regulation ($p < 0.05$) of *dio3b* transcript abundance occurred in stage 9A and 9B ocular skin relative to stages 7 and 8 (**Figure 3.6G**). Significant up-regulation of *dio3b* transcript abundance occurred in stage 9B abocular skin relative to stages 7, 8 and 9A in MMI treated Atlantic halibut (**Figure 3.6H**). Comparison of the skin from control and MMI treated Atlantic halibut revealed MMI caused a significant up-regulation of *dio3b* in ocular skin in stage 9A (**Figure 3.6G**). The ocular/abocular ratio of *dio3b* transcripts in skin was symmetric and constant throughout metamorphosis in control Atlantic halibut. In MMI treated Atlantic halibut skin relative to control skin significant ($p < 0.002$) asymmetry in *dio3b* transcript abundance occurred between ocular and abocular skin at the metamorphic climax (stage 9A, **Figure 3.6I**). The results from MMI treated larvae suggest the Atlantic halibut *dio3b* gene is responsive to TH levels during metamorphosis, while the *dio3a* gene is not (**Figure 3.6I**).

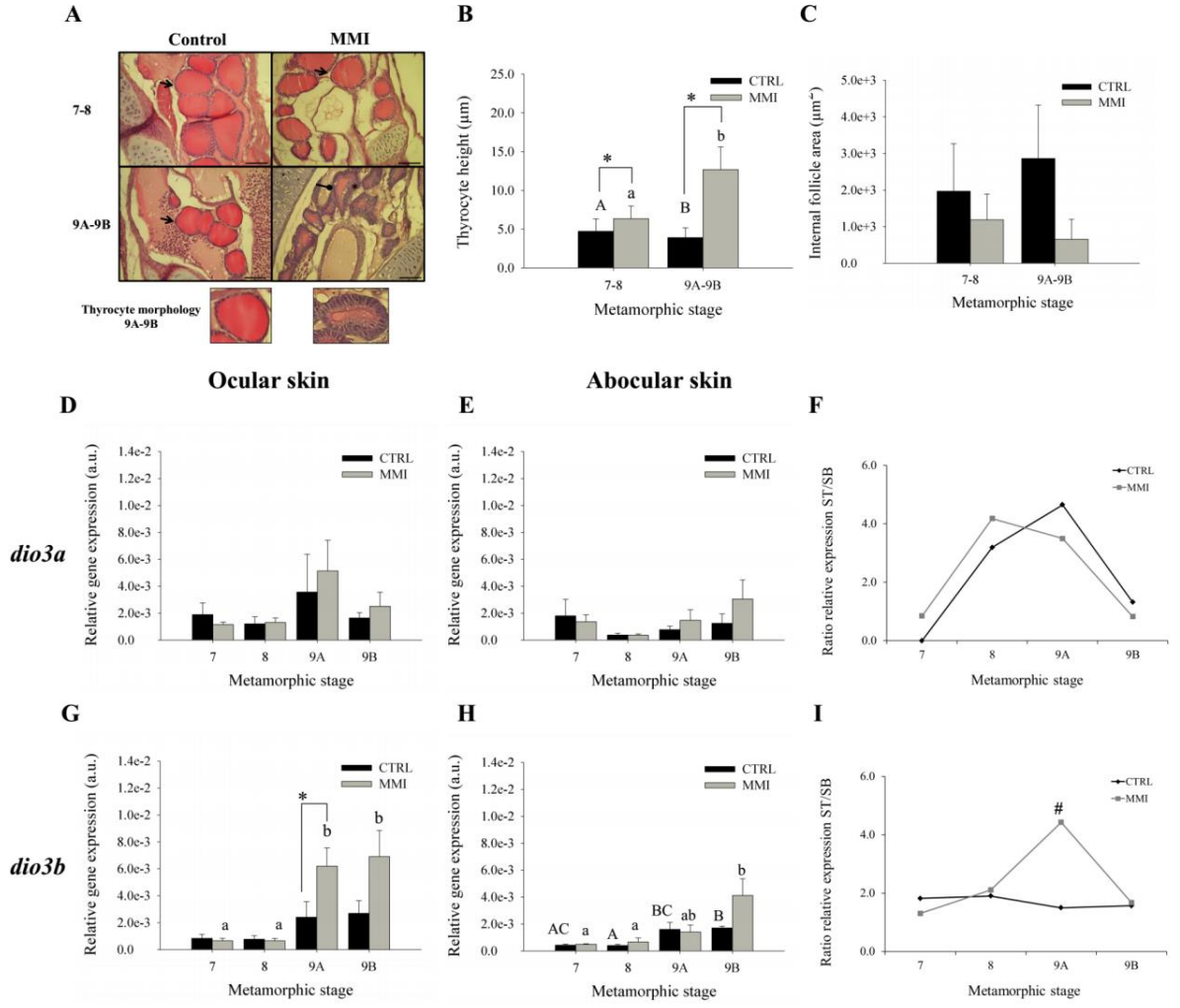

Figure 3.6. Effect of methimazole (MMI) on *dio3a* and *dio3b* in the ocular and abocular skin during Atlantic halibut metamorphosis. **A** - Histological characterization of thyroid follicles of control and MMI treated Atlantic halibut in metamorphic stages 7 - 8 (n = 3) and stages 9A-9B (n = 3). Characteristic thyroid follicles in control fish are indicated by an arrow; an example of an abnormal thyroid follicle is indicated with an arrow with a round tip. * indicates abnormal columnar thyrocytes. Scale bar – 50 µm. **B** and **C** – Analysis of thyroid activity by measurement of thyrocyte height (µm) and internal follicle area (µm^2). Results are presented as group mean ± SEM. Different letters in each sampling indicate significant differences between the treatments ($p < 0.05$). Different upper case letters represent significant differences in thyrocyte height between metamorphic stages in the control ($p < 0.05$; two-way ANOVA). Different lower case letters represent significant differences in thyrocyte height between metamorphic stages in MMI treated larvae ($p < 0.05$; two-way ANOVA). *Significant differences in thyrocyte height between control and MMI treated Atlantic halibut. **D-I** - Relative gene expression of *dio3a* (D and E) and *dio3b* (G and H) was determined by quantitative RT-PCR (qPCR) in ocular (ST) and abocular (SB) skin in several metamorphic stages of Atlantic halibut of control and MMI treated fish: 7 - prometamorphosis, 8 - proclimax metamorphosis, 9A and 9B – climax metamorphosis. Gene expression was normalized with the geometric mean of the reference genes 40S ribosomal protein S4 (*rps4*) and elongation factor 1 alpha (*efa1*). Relative gene expression is represented as mean ± standard error of the mean (n = 5). Different upper case letters represent significant differences in expression between metamorphic stages in ocular skin (p <0.05; two-way ANOVA). Different lower case letters represent significant differences in expression between metamorphic stages in abocular skin (p <0.05; two-way ANOVA). * Significant differences between CTRL and MMI. (F and I) The ratio of relative gene expression between ST and SB during halibut metamorphosis for *dio3* genes. # Significant differences between CTRL and MMI.

3.3.6.3 Presence of thyroid response elements (TREs) in dio3 gene promoters

The role of the promoter in the divergent response of *dio3* duplicates to changes in TH levels during metamorphosis was assessed. Analysis of the promoters of the *dio3* duplicate genes in several teleosts showed that most *dio3a* promoters lacked a TRE, (the exception was the gene in the half-smooth tongue sole). Conversely, all the *dio3b* promoters had multiple putative TRE binding sites (the exception was the gene in zebrafish). TRE binding sites were not identified in the single *dio3* gene from spotted gar (**Table 3.2**).

Table 3.2. Thyroid response elements (T_3R/TRE) predicted by TF Bind in teleost dio3 duplicates. The matrix consensus sequence for TRE is: (C/G) NNT (A/G) AGGTCACG (C/G) NN, where N can be any nucleotide. The consensus sequence, frame orientation, location relative to the transcription start site and the *P* value of the predicted binding sites are also indicated.

Species	Gene	Consensus sequence	Frame	Location	P value
Cynoglossus semilaevis	*dio3a*	GAGGGTGACGTCAAAGAC	(+)	-1430	0.87
		CAATGACGTCATAAGT	(+)	-789	0.86
	dio3b	AACTGGGGTCACAGTA	(+)	-1418	0.89
		CACTCAGGTGACACAC	(+)	-1133	0.82
		CCGGATGACCTGCATT	(+)	-1096	0.82
		TGTTTTTACCTCAGTC	(-)	-703	0.82
Solea senegalensis	*dio3a*	-	-	-	-
	dio3b	CATGTAGGTCACACGC	(+)	-1492	0.829
		GAGTGAGTTCAGCGGG	(-)	-502	0.81
Dicentrarchus labrax	*dio3a*	-	-	-	-
	dio3b	GGTTGAGGTGACAAGA	(+)	-1301	0.82
		GTTTCAGATCACACTC	(+)	-980	0.82
Takifugu rubripes	*dio3a*	-	-	-	-
	dio3b	GGGCGCGACGTCACTT	(-)	-1364	0.80
		GGGGGGGGTCACTATA	(+)	-1285	0.81
		CCTTATGACCTTCTCT	(-)	-987	0.80
		CTCTGAGGTCAGAGGA	(+)	-341	0.85
Danio rerio	*dio3a*	-	-	-	-
	dio3b	-	-	-	-
Lepisosteus oculatus	*dio3*	-	-	-	-

3.4. Discussion

Characterization of the diverse elements required for thyroid axis action during flatfish metamorphosis highlights the importance of the deiodinases that activate and inactivate THs (Galay-Burgos et al., 2008, Inui et al., 1995, Isorna et al., 2009, Marsh-Armstrong et al.,

1999, Tagawa and Aritaki, 2005, Van Herck et al., 2015, Yamano and Inui, 1995 and Yamano et al., 1994). In the Atlantic halibut, three deiodinases (*dio1*, *dio2* and *dio3*) have previously been identified and their ontogeny during metamorphosis reported (Campinho et al., 2012a). However, in the present study analysis of a comprehensive transcriptome of metamorphosing Atlantic halibut (Alves et al., 2016) revealed the existence of duplicate *dio3* genes.

3.4.1. Duplication of *dio3* genes occurred during the teleost specific whole genome duplication

Phylogenetic analysis confirmed that Atlantic halibut *dio3a* and *dio3b* were homologous of *dio3a* and *dio3b* in zebrafish (Guo et al., 2014 and Heijlen et al., 2014). In addition, analysis of available transcriptomes and genomes of other fishes revealed duplicate *dio3* genes in most other teleost fish, suggesting that they emerged during the teleost-specific whole genome duplication (Jaillon et al., 2004, Ravi and Venkatesh, 2008 and Volff, 2005), (**Figure 3.7**). It should be noted, that species-specific duplication events also occurred and this is the case of the Atlantic salmon (*Salmon salar*) that possesses duplicate *dio3b* genes (*dio3b1*, *dio3b2*) and a single copy of *dio3a*, probably as a result of the tetraploidization event in the salmoniform lineage (Lorgen et al., 2015), (**Figure 3.7**). Phylogenetic analysis of the deiodinase family in teleosts and other vertebrates and *dio* members in early deuterostomes suggests that the family members emerged early during deuterostome evolution. The *dio2* and *dio3* genes shared a common ancestral origin and both emerged prior to the divergence of the jawless fishes.

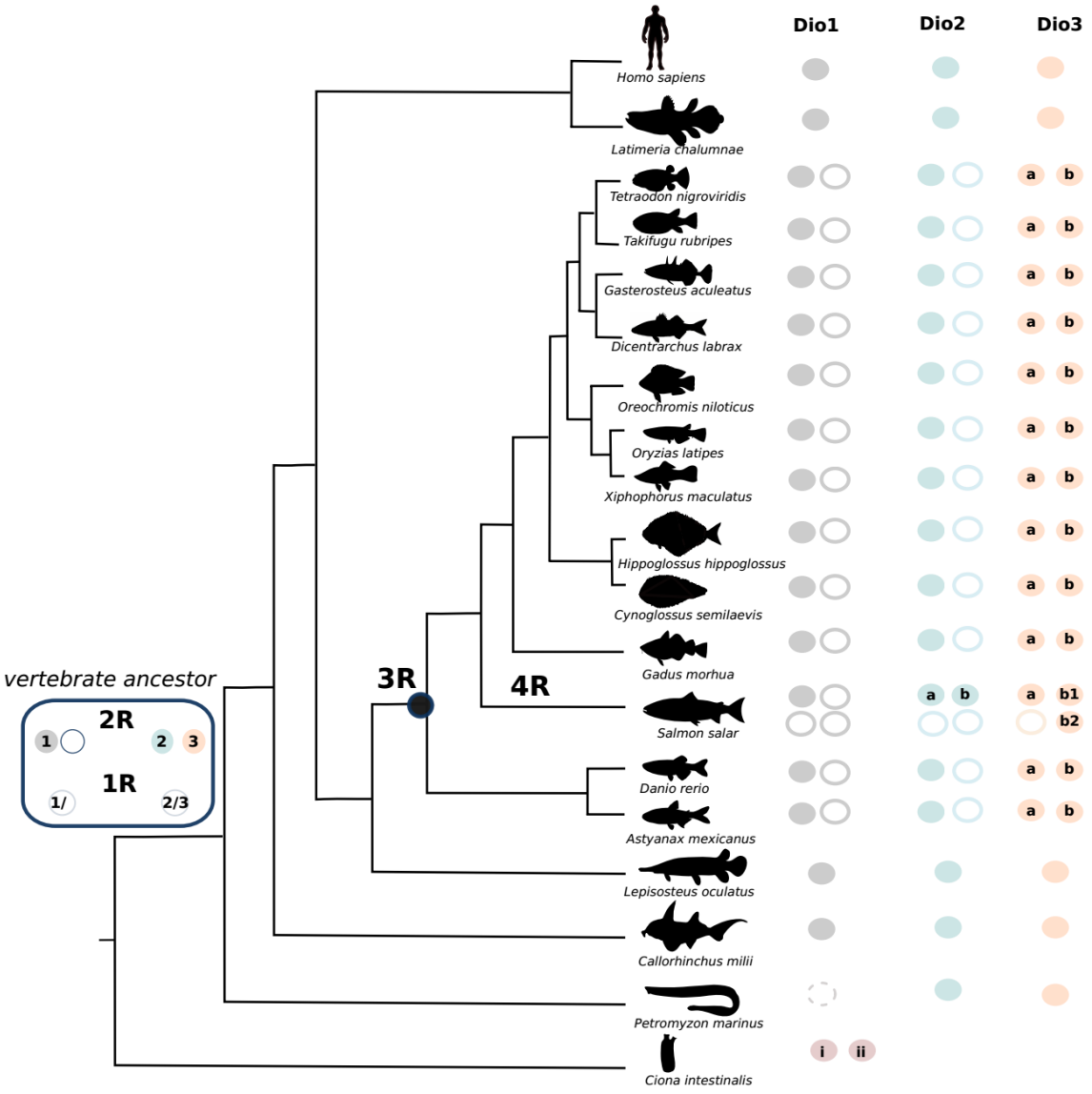

Figure 3.7. Proposed evolutionary scheme of the vertebrate DIO family members. Genes are represented by circles and DIO1 is grey, DIO2 is blue and DIO3 is pink. The tetraploidization events that occurred in the vertebrate ancestral genome are marked as 1R and 2R, the teleost specific genome duplication as 3R (indicated by a black circle) and the salmonid lineage specific duplication as 4R. Genes that were not found in the genomes analyzed and that were probably lost soon after each tetraploidization event are represented by white circles. The teleost paralogue genes that resulted from 3R are indicated as a and b and the ones that are likely to result from the specific tetraploidization in Salmonids (4R) are numbered b1 and b2. No putative dio1 gene was identified in lamprey (*Petromyzus marinus*) and this is most likely a result of its incomplete genome assembly and thus it is represented by a dashed circle. In the ascidian *Ciona intestinalis* the two putative *dio*-like genes resulted from a species-specific duplication.

The factors explaining the persistence of the duplicate *dio3* genes in teleost genomes have not been studied. However, the high amino acid sequence similarity of halibut *dio3a* and *dio3b* (82%) and the conservation of the main functional motifs; the SeCys-encoding TGA codon; the histidine residues in the catalytic center and Sec insertion sequence (SECIS) in the

3'UTR (Bianco et al., 2002 and Orozco et al., 2012) is intriguing and raises questions about why the duplicate genes have been maintained. To gain insight into contributing factors the tissue distribution and hormone responsiveness was assessed.

3.4.2. Divergent *dio3a* and *dio3b* expression during Atlantic halibut metamorphosis

The two *dio3* isoforms in Atlantic halibut had a similar widespread and overlapping tissue distribution, although *dio3a* was most highly expressed in the brain and eye, while *dio3b* was most expressed in the liver and eye. The distribution pattern observed for halibut *dio3b* is similar to that described for *dio3* in the immature fresh water fish, walleye (*Sander vitreus*) (Picard-Aitken et al., 2007), rainbow trout (*Oncorhynchus mykiss*) and the Australian lungfish (*Neoceratodus forsteri*) (Bres et al., 2006 and Sutija et al., 2004). In addition, *dio3b* expression in post-metamorphic halibut juvenile tissues is similar to *dio3* transcript localization in the flounder (*P. olivaceus*) after the metamorphic climax (Itoh et al., 2010). The high abundance of the *dio3* duplicates in the brain and eyes of juvenile Atlantic halibut is unsurprising taking into consideration the role of THs in brain development and neurogenesis in vertebrates (Dong et al., 2013, Friesema et al., 2012, Preau et al., 2015 and Van Herck et al., 2012, 2013). Indeed, during early development in vertebrates Dio3 regulates the levels of THs and is crucial for normal brain development (reviewed by Darras et al., 2015 and Preau et al., 2015). Elimination of *dio3* by knockout (KO) in mice causes growth retardation and abnormal brain development and knockdown (KD) of *dio3b* in zebrafish causes morphological and functional abnormalities of the cerebellum and eyes during development (Bagci et al., 2015, Heijlen et al., 2014, Houbrechts et al., 2016 and Peeters et al., 2013).

Characterization of the expression of *dio3a* and *dio3b* transcripts in whole-larvae of Atlantic halibut undergoing metamorphosis highlights that both are actively regulated during this process, which is similar to the results of previous studies that analyzed a single *dio3* isoform in other flatfish (Isorna et al., 2009 and Itoh et al., 2010). However, divergence in the pattern of *dio3* isoform expression in whole larvae occurred during Atlantic halibut metamorphosis and *dio3a* was significantly down-regulated during the transition of pro-metamorphosis to early pro-climax stages, and also in post-metamorphic juveniles. Conversely, *dio3b* was strongly down-regulated from pro-metamorphosis (stage 6) to

metamorphic climax (stage 9B) and was up-regulated post-metamorphosis (stage 9C) and in the juvenile. In summary, in the Atlantic halibut *dio3b* appears to be the predominant transcript during early development as previously reported for the zebrafish *dio3b* homologue (Heijlen et al., 2014), and also in post-metamorphic Atlantic halibut (Stage 9C and Juveniles). The results of the expression analysis suggest that the maintenance in teleost genomes of duplicate *dio3* genes may be the result of subfunctionalization and that *dio3* genes play different roles during development and metamorphosis.

A previous *in situ* hybridization study of Atlantic halibut skin suggested that TH-driven maturation is probably symmetric since *dio2* and *dio3a* expression is regulated in pre-metamorphic stages but not during asymmetric differentiation (Campinho et al., 2012a). However, in the present study both *dio3* paralogues were identified in ocular and abocular skin from stage 7 to stage 9B but only *dio3b* was differentially expressed between developmental stages. Due to technical issues we were unable to establish if the differential transcription of the *dio3a* and *dio3b* genes also reflects alterations in Dio3 enzyme activity. However, the similarity between the pattern of *dio3b* transcription and previously published whole animal levels of T_3 and T_4 during Atlantic halibut metamorphosis (Einarsdottir et al., 2006) suggests that *dio3b* expression is TH regulated. This notion is supported by the experiments in the present study with MMI and *in silico* analysis of the gene promoters of the *dio3a* and *dio3b* genes in teleosts including flatfish (with the exception of the half-smooth tongue sole).

MMI is a well-established inhibitor of the peroxidase enzyme in the thyroid follicle of vertebrates and interferes with the incorporation of iodine into tyrosyl residues of thyroglobulin thus blocking TH production (Fetter et al., 2015 and Roy and Mugesh, 2005). When MMI is administered to teleosts it decreases thyroid activity and TH levels (Campinho et al., 2012b, Crane et al., 2006, Fetter et al., 2015, Jomaa et al., 2014, Mol et al., 1998 and Van der Geyten et al., 1999) and in flatfish it blocks metamorphosis (Campinho et al., 2015, Schreiber and Specker, 2000, Schreiber et al., 2010). The observed histology of the thyroid in the Atlantic halibut treated with MMI in the present study was similar to that of hypothyroid sea bream (Campinho et al., 2012b). MMI treatment of Atlantic halibut caused up-regulation of *dio3b* transcription in ocular and abocular skin, although *dio3a* was unaltered and suggests that Atlantic halibut *dio3b* is TH responsive. Interestingly during amphibian metamorphosis, a

process analogous to flatfish metamorphosis, *dio3* is one of several TH responsive genes identified (Das et al., 2009, Helbing et al., 2003 and Suzuki et al., 2009). The divergent response of *dio3* isoforms in skin to THs may represent a mechanism to fine-tune specific cellular responses during metamorphosis as has previously been suggested to explain the differential regulation of TH receptors by THs in Senegalese sole (Manchado et al., 2009).

The divergent expression of *dio3b* in ocular and abocular skin during metamorphosis is intriguing and suggests the cellular context plays a determinant role in its expression and this may explain how the same hormone in an organism can simultaneously bring about a different outcome in the same tissue. A further caveat is that teleost skin is an important source of rT_3 due to its high IRD activity and during rainbow trout development whole animal rT_3 levels vary (Fenton et al., 1997). The results of previous studies indicate *Dio3* has a role in modulating TH availability but also the concentration of rT_3. The accumulation of rT_3 may have a secondary impact on TH availability since elevated concentrations are linked to reduced T_4 transport into the cell (Van der Geyten et al., 1999). In the present study the functional significance of the asymmetric expression of *dio3b* was not established nor was the cellular context in ocular and abocular skin and this will be an important target for future work. In frogs Dio3 is essential for acquisition of asymmetric growth of the retina and the regulation of cell proliferation in the ciliary marginal zone (CMZ) during metamorphosis (Marsh-Armstrong et al., 1999). The recent observation that T_4, T_2 and rT_3 are physiologically active (Moreno et al., 2008) also raises intriguing new possibilities for investigation.

Further support and an explanation for the divergent response of *dio3a* and *dio3b* to THs came from the study of the proximal promoter region of the genes in several teleosts including the flatfish, Senegalese sole. Most of the promoters analyzed revealed several putative thyroid response elements (TRE) in the *dio3b* gene but none in the *dio3a* gene and this most likely explains their different expression patterns during Atlantic halibut metamorphosis, a TH driven process. The *dio3b* gene in the half-smooth tongue sole is the exception but since the *dio3a* promoter contains several conserved TREs, nonetheless *dio3b* in this species contained the greatest number of TREs. In the case of *dio3b,* during Atlantic halibut metamorphosis it appears that elevated TH levels repress gene expression, since when TH production is blocked with MMI strong up-regulation of *dio3b* occurs. The repressive

action on gene expression of high levels of THs was not unexpected as in our recent large scale transcriptome study of Atlantic halibut metamorphosis a very high proportion of differentially expressed genes during metamorphosis were down-regulated rather than activated (Alves et al., 2016).

3.5. Conclusions

Teleost specific *dio3* gene duplicates (*dio3a* and *dio3b*) were identified in Atlantic halibut and their presence in other flatfish species and teleosts was confirmed. The duplication of *dio3* genes occurred during the teleost specific whole genome duplication and phylogenetic analysis revealed that the *dio3b* gene identified in the present study is the orthologue of the *dio3* reported in Senegalese sole (Isorna et al., 2009). The small size of fish larvae means that previous studies of flatfish metamorphosis analysed pools of whole larvae and the role of the thyroid system in the development of specific tissues has not been studied (Isorna et al., 2009 and Tagawa and Aritaki, 2005).

In the present study the large size of the Atlantic halibut larvae was exploited and the abundance of *dio3* duplicates in ocular and abocular skin from individual larvae during metamorphosis revealed that *dio3* gene duplicates had a divergent expression pattern and it was different from what was observed when whole larvae were analysed. The results indicate that *dio3b* levels change in Atlantic halibut abocular skin during metamorphosis and suggest that this enzyme is associated with the divergent maturation of larval skin to the juvenile phenotype. In Atlantic halibut larvae exposed to MMI, a chemical that inhibits thyroid function and blocks metamorphosis (by inhibiting TH production) the expression of *dio3b* in ocular skin was significantly up-regulated and this suggests that during metamorphosis this gene is repressed by THs. The molecular basis for divergent *dio3a* and *dio3b* expression during Atlantic halibut metamorphosis is most likely explained by the multiple TREs in the proximal promoter region of *dio3b* and this is a common feature of the gene in teleosts and also *DIO3* in mammals.

Based on our results we hypothesise that regulation of *dio3* and other deiodinases in fish tissues modulates the forms and abundance of THs locally and that this explains how a single hormone can be responsible for the myriad tissue specific transformations occurring during metamorphosis in flatfish.

Acknowledgements

This research study was funded by the European Community FP7 project LIFECYCLE (FP7 222719, http://www.lifecycle.gu.se/, 17.08.2012) and the Europen Regional Development Fund (ERDF) COMPETE – Operational Competitiveness Programme and Portuguese funds through the Foundation for Science and Technology (FCT), Portugal (project Pest-C/MAR/LA0015/2013). RNA, RSTM and JCRC were funded by FCT Portugal (SFRH/BD/69209/2010, SFRH/BPD/66742/2009 and Pest-C/MAR/LA0015/2013, respectively). We thank Velimir Nola & Ragnfrid Mangor-Jensen for halibut feeding and assistance during the MMI experiment at IMR; We thank Heiddis Smáradóttir of Samherji hf., Glerárgötu 30, 600 Akureyri, Iceland for providing Atlantic halibut samples from Industrial scale production.

References

Abascal, F., Zardoya, R., Posada, D., 2005. ProtTest: selection of best-fit models of protein evolution. Bioinformatics 21, 2104-5.

Alves, R.N., Gomes, A.S., Stueber, K., Tine, M., Thorne, M.A., Smaradottir, H., Reinhard, R., Clark, M.S., Ronnestad, I., Power, D.M., 2016. The transcriptome of metamorphosing flatfish. BMC Genomics 17, 413.

Bagci, E., Heijlen, M., Vergauwen, L., Hagenaars, A., Houbrechts, A.M., Esguerra, C.V., Blust, R., Darras, V.M., Knapen, D., 2015. Deiodinase Knockdown during Early Zebrafish Development Affects Growth, Development, Energy Metabolism, Motility and Phototransduction. Plos One 10.

Bianco, A.C., Larsen, P.R., 2005. Cellular and structural biology of the deiodinases. Thyroid 15, 777-86.

Bianco, A.C., Kim, B.W., 2006. Deiodinases: implications of the local control of thyroid hormone action. Journal of Clinical Investigation 116, 2571-2579.

Bianco, A.C., Salvatore, D., Gereben, B., Berry, M.J., Larsen, P.R., 2002. Biochemistry, cellular and molecular biology, and physiological roles of the iodothyronine selenodeiodinases. Endocrine Reviews 23, 38-89.

Bohnsack, B.L., Kahana, A., 2013. Thyroid hormone and retinoic acid interact to regulate zebrafish craniofacial neural crest development. Developmental Biology 373, 300-309.

Bres, O., Plohman, J.C., Eales, J.G., 2006. A cDNA for a putative type III deiodinase in the trout (*Oncorhynchus mykiss*): influence of holding conditions and thyroid hormone treatment on its hepatic expression. General and Comparative Endocrinology 145, 92-100.

Brown, D.D., Cai, L., 2007. Amphibian metamorphosis. Developmental Biology 306, 20-33.

Buchholz, D.R., 2015. More similar than you think: Frog metamorphosis as a model of human perinatal endocrinology. Developmental Biology 408, 188-195.

Campinho, M.A., Galay-Burgos, M., Silva, N., Costa, R.A., Alves, R.N., Sweeney, G.E., Power, D.M., 2012a. Molecular and cellular changes in skin and muscle during metamorphosis of Atlantic halibut (*Hippoglossus hippoglossus*) are accompanied by changes in deiodinases expression. Cell Tissue Research 350, 333-46.

Campinho, M.A., Morgado, I., Pinto, P.I.S., Silva, N., Power, D.M., 2012b. The goitrogenic efficiency of thioamides in a marine teleost, sea bream (*Sparus auratus*). General and Comparative Endocrinology 179, 369-375.

Campinho, M.A., Silva, N., Roman-Padilla, J., Ponce, M., Manchado, M. , Power, D.M., 2015. Flatfish metamorphosis: a hypothalamic independent process?. Molecular and Cellular Endocrinology 404, 16-25.

Crane, H.M., Pickford, D.B., Hutchinson, T.H., Brown, J.A., 2006. The effects of methimazole on development of the fathead minnow, *Pimephales promelas*, from embryo to adult. Toxicological Sciences 93, 278-85.

Darras, V.M., Houbrechts, A.M., Van Herck, S.L., 2015. Intracellular thyroid hormone metabolism as a local regulator of nuclear thyroid hormone receptor-mediated impact on vertebrate development. Biochimica et Biophysica Acta 1849, 130-41.

Darras, V.M., Visser, T.J., Berghman, L.R., Kuhn, E.R., 1992. Ontogeny of Type-I and Type-III Deiodinase Activities in Embryonic and Posthatch Chicks - Relationship with Changes in Plasma Triiodothyronine and Growth-Hormone Levels. Comparative Biochemistry & Physiology Part A: Molecular & Integrative Physiology 103, 131-136.

Das, B., Heimeier, R.A., Buchholz, D.R., Shi, Y.B., 2009. Identification of Direct Thyroid Hormone Response Genes Reveals the Earliest Gene Regulation Programs during Frog Metamorphosis. The Journal of Biological Chemistry 284, 34167-34178.

Debaveye, Y., Ellger, B., Mebis, L., Van Herck, E., Coopmans, W., Darras, V., Van den Berghe, G., 2005. Tissue deiodinase activity during prolonged critical illness: Effects of exogenous thyrotropin-releasing hormone and its combination with growth hormone releasing peptide-2. Endocrinology 146, 5604-5611.

Dentice, M., Salvatore, D., 2011. Local impact of thyroid hormone inactivation. Journal of Endocrinology 209, 273-282.

Dentice, M., Marsili, A., Zavacki, A., Larsen, P.R., Salvatore, D., 2013. The deiodinases and the control of intracellular thyroid hormone signaling during cellular differentiation. Biochimica et Biophysica Acta 1830, 3937-45.

Dong, W., Macaulay, L.J., Kwok, K.W., Hinton, D.E., Stapleton, H.M., 2013. Using whole mount in situ hybridization to examine thyroid hormone deiodinase expression in embryonic and larval zebrafish: a tool for examining OH-BDE toxicity to early life stages. Aquatic Toxicology 132-133, 190-9.

Einarsdottir, I.E., Silva, N., Power, D.M., Smaradottir, H., Bjornsson, B.T., 2006. Thyroid and pituitary gland development from hatching through metamorphosis of a teleost flatfish, the Atlantic halibut. Anatomy and Embryology 211, 47-60.

Felsenstein, J., 1985. Confidence-Limits on Phylogenies - an Approach Using the Bootstrap. Evolution 39, 783-791.

Fenton, B., Orozco, A., Valverde, C., 1997. Kinetic characterisation of skin inner-ring deiodinative pathway and its correlation with circulating levels of reverse tri-iodothyronine in developing rainbow trout. Journal of Endocrinology 154, 547-554.

Fetter, E., Baldauf, L., Da Fonte, D.F., Ortmann, J., Scholz, S., 2015. Comparative analysis of goitrogenic effects of phenylthiourea and methimazole in zebrafish embryos. Reproductive Toxicology 57, 10-20.

Friesema, E.C., Visser, T.J., Borgers, A.J., Kalsbeek, A., Swaab, D.F., Fliers, E., Alkemade, A., 2012. Thyroid hormone transporters and deiodinases in the developing human hypothalamus. European Journal of Endocrinology 167, 379-86.

Galay-Burgos, M., Power, D.M., Llewellyn, L., Sweeney, G.E., 2008. Thyroid hormone receptor expression during metamorphosis of Atlantic halibut (*Hippoglossus hippoglossus*). Molecular and Cellular Endocrinology 281, 56-63.

Galton, V.A., Hernandez, A., St Germain, D.L., 2014. The 5 '-Deiodinases Are Not Essential for the Fasting-Induced Decrease in Circulating Thyroid Hormone Levels in Male Mice: Possible Roles for the Type 3 Deiodinase and Tissue Sequestration of Hormone. Endocrinology 155, 3172-3181.

Gereben, B., Zavacki, A.M., Ribich, S., Kim, B.W., Huang, S.A., Simonides, W.S., Zeold, A., Bianco, A.C., 2008. Cellular and molecular basis of deiodinase-regulated thyroid hormone signaling. Endocruine Reviews 29, 898-938.

Gomes, A.S., Alves, R.N., Stueber, K., Thorne, M.A., Smaradottir, H., Reinhard, R., Clark, M.S., Ronnestad, I., Power, D.M., 2014. Transcriptome of the Atlantic halibut (*Hippoglossus hippoglossus*). Marine Genomics 18 Pt B, 101-103.

Guindon, S., Dufayard, J.F., Lefort, V., Anisimova, M., Hordijk, W. and Gascuel, O., 2010. New algorithms and methods to estimate maximum-likelihood phylogenies: assessing the performance of PhyML 3.0. Systematic Biology 59, 307-321.

Guo, C., Chen, X., Song, H., Maynard, M.A., Zhou, Y., Lobanov, A.V., Gladyshev, V.N., Ganis, J.J., Wiley, D., Jugo, R.H., Lee, N.Y., Castroneves, L.A., Zon, L.I., Scanlan, T.S., Feldman, H.A., Huang, S.A., 2014. Intrinsic expression of a multiexon type 3 deiodinase gene controls zebrafish embryo size. Endocrinology 155, 4069-80.

Heijlen, M., Houbrechts, A.M., Bagci, E., Van Herck, S.L.J., Kersseboom, S., Esguerra, C.V., Blust, R., Visser, T.J., Knapen, D., Darras, V.M., 2014. Knockdown of Type 3 Iodothyronine Deiodinase Severely Perturbs Both Embryonic and Early Larval Development in Zebrafish. Endocrinology 155, 1547-1559.

Helbing, C.C., Werry, K., Crump, D., Domanski, D., Veldhoen, N., Bailey, C.M., 2003. Expression profiles of novel thyroid hormone-responsive genes and proteins in the tail of *Xenopus laevis* tadpoles undergoing precocious metamorphosis. Molecular Endocrinology 17, 1395-409.

Hernandez, A., Germain, D.L.S., 2002. Dexamethasone inhibits growth factor-induced type 3 deiodinase activity and mRNA expression in a cultured cell line derived from rat neonatal brown fat vascular-stromal cells. Endocrinology 143, 2652-2658.

Houbrechts, A.M., Vergauwen, L., Bagci, E., Van Houcke, J., Heijlen, M., Kulemeka, B., Hyde, D.R., Knapen, D., Darras, V.M., 2016. Deiodinase knockdown affects zebrafish eye development at the level of gene expression, morphology and function. Molecular and Cellular Endocrinology 424, 81-93.

Inui, Y., Yamano, K., Miwa, S., 1995. The role of thyroid hormone in tissue development in metamorphosing flounder. Aquaculture 135, 87-98.

Isorna, E., Obregon, M.J., Calvo, R.M., Vazquez, R., Pendon, C., Falcon, J., Munoz-Cueto, J.A., 2009. Iodothyronine deiodinases and thyroid hormone receptors regulation during flatfish (*Solea senegalensis*) metamorphosis. Journal of experimental zoology. Part B, Molecular and Developmental Evolution 312B, 231-246.

Itoh, K., Watanabe, K., Wu, X., Suzuki, T., 2010. Three members of the iodothyronine deiodinase family, dio1, dio2 and dio3, are expressed in spatially and temporally specific patterns during metamorphosis of the flounder, *Paralichthys olivaceus*. Zoological Sciences 27, 574-80.

Jaillon, O., Aury, J.M., Brunet, F., Petit, J.L., Stange-Thomann, N., Mauceli, E., Bouneau, L., Fischer, C., Ozouf-Costaz, C., Bernot, A., Nicaud, S., Jaffe, D., Fisher, S., Lutfalla, G., Dossat, C., Segurens, B., Dasilva, C., Salanoubat, M., Levy, M., Boudet, N., Castellano, S., Anthouard, R., Jubin, C., Castelli, V., Katinka, M., Vacherie, B., Biemont, C., Skalli, Z., Cattolico, L., Poulain, J., de Berardinis, V., Cruaud, C., Duprat, S., Brottier, P., Coutanceau, J.P., Gouzy, J., Parra, G., Lardier, G., Chapple, C., McKernan, K.J., McEwan, P., Bosak, S., Kellis, M., Volff, J.N., Guigo, R., Zody,

M.C., Mesirov, J., Lindblad-Toh, K., Birren, B., Nusbaum, C., Kahn, D., Robinson-Rechavi, M., Laudet, V., Schachter, V., Quetier, F., Saurin, W., Scarpelli, C., Wincker, P., Lander, E.S., Weissenbach, J., Crollius, H.R., 2004. Genome duplication in the teleost fish *Tetraodon nigroviridis* reveals the early vertebrate proto-karyotype. Nature 431, 946-957.

Jomaa, B., Hermsen, S.A.B., Kessels, M.Y., van den Berg, J.H.J., Peijnenburg, A.A.C.M., Aarts, J.M.M.J.G., Piersma, A.H., Rietjens, I.M.C.M., 2014. Developmental Toxicity of Thyroid-Active Compounds in a Zebrafish Embryotoxicity Test. Alternatives to Animal Experimentation 31, 303-317.

Jones, D.T., Taylor, W.R., Thornton, J.M., 1992. The Rapid Generation of Mutation Data Matrices from Protein Sequences. Computer Applications in the Biosciences 8, 275-282.

Klaren, P.H.M., Geven, E.J.W., Nagelkerke, A., Flik, G., 2012. Kinetics and thiol requirements of iodothyronine 5 '-deiodination are tissue-specific in common carp (*Cyprinus carpi* L.). Comparative Biochemistry and Physiology Part B: Biochemistry and Molecular Biology 161, 275-282.

Klaren, P.H.M., Haasdijk, R., Metz, J.R., Nitsch, L.M.C., Darras, V.M., Van der Geyten, S., Flik, G., 2005. Characterization of an iodothyronine 5 '-deiodinase in gilthead seabream (*Sparus auratus*) that is inhibited by dithiothreitol. Endocrinology 146, 5621-5630.

Kohrle, J., 1999. Local activation and inactivation of thyroid hormones: the deiodinase family. Molecular and Cellular Endocrinology. 151, 103-119.

Laudet, V., 2011. The Origins and Evolution of Vertebrate Metamorphosis. Current Biology 21, R726-R737.

Lorgen, M., Casadei, E., Krol, E., Douglas, A., Birnie, M.J., Ebbesson, L.O.E., Nilsen, T.O., Jordan, W.C., Jorgensen, E.H., Dardente, H., Hazlerigg, D.G., Martin, S.A.M., 2015. Functional Divergence of Type 2 Deiodinase Paralogs in the Atlantic Salmon. Current Biology 25, 936-941.

Manchado, M., Infante, C., Rebordinos, L., Cañavate, J.P., 2009. Molecular characterization, gene expression and transcriptional regulation of thyroid hormone receptors in Senegalese sole. General and Comparative Endocrinology 160, 139–147.

Marsh-Armstrong, N., Huang, H.C., Remo, B.F., Liu, T.T., Brown, D.D., 1999. Asymmetric growth and development of the *Xenopus laevis* retina during metamorphosis is controlled by type III deiodinase. Neuron 24, 871-878.

Mol, K.A., Van der Geyten, S., Burel, C., Kuhn, E.R., Boujard, T., Darras, V.M., 1998. Comparative study of iodothyronine outer ring and inner ring deiodinase activities in five teleostean fishes. Fish Physiology and Biochemistry 18, 253-266.

Moreno, M., de Lange, P., Lombardi, A., Silvestri, E., Lanni, A., Goglia, F., 2008. Metabolic effects of thyroid hormone derivatives. Thyroid 18, 239-253.

Mullur, R., Liu, Y.Y., Brent, G.A., 2014. Thyroid Hormone Regulation of Metabolism. Physioll Rev. 94, 355-382.

Orozco, A., Villalobos, P., Jeziorski, M.C., Valverde, R.C., 2003. The liver of *Fundulus heteroclitus* expresses deiodinase type 1 mRNA. General and Comparative Endocrinology 130, 84-91.

Orozco, A., Valverde, C., Olvera, A. and Garcia, C., 2012. Iodothyronine deiodinases: a functional and evolutionary perspective. Journal of Endocrinology 215, 207-219.

Peeters, R.P., Hernandez, A., Ng, L., Ma, M., Sharlin, D.S., Pandey, M., Simonds, W.F., St Germain, D.L., Forrest, D., 2013. Cerebellar Abnormalities in Mice Lacking Type 3 Deiodinase and Partial Reversal of Phenotype by Deletion of Thyroid Hormone Receptor alpha 1. Endocrinology 154, 550-561.

Picard-Aitken, M., Fournier, H., Pariseau, R., Marcogliese, D.J., Cyr, D.G., 2007. Thyroid disruption in walleye (*Sander vitreus*) exposed to environmental contaminants: Cloning and use of iodothyronine deiodinases as molecular biomarkers. Aquatic Toxicology 83, 200-211.

Pinto, P.I.S., Guerreiro, E.M., Power, D.M., 2013. Triclosan interferes with the thyroid axis in the zebrafish (*Danio rerio*). Toxicology Research 2, 60-69.

Pol, C.J., Muller, A., Simonides, W.S., 2010. Cardiomyocyte-specific inactivation of thyroid hormone in pathologic ventricular hypertrophy: an adaptative response or part of the problem?. Heart Failure Reviews 15, 133-142.

Power, D.M., Llewellyn, L., Faustino, M., Nowell, M.A., Bjornsson, B.T., Einarsdottir, I.E., Canario, A.V., Sweeney, G.E., 2001. Thyroid hormones in growth and development of fish. Comparative Biochemistry and Physiology Part C: Toxicology & Pharmacology 130, 447-59.

Power, D.M., Einarsdottir, I.E., Pittman, K., Sweeney, G.E., Hildahl, J., Campinho, M.A., Silva, N., Saele, O., Galay-Burgos, M., Smaradottir, H., Bjornsson, B.T., 2008. The Molecular and Endocrine Basis of Flatfish Metamorphosis. Reviews in Fisheries Science 16, 95-111.

Preau, L., Fini, J.B., Morvan-Dubois, G., Demeneix, B., 2015. Thyroid hormone signaling during early neurogenesis and its significance as a vulnerable window for endocrine disruption. Biochimica et Biophysica Acta (BBA) - Gene Structure and Expression 1849, 112-121.

Ravi, V., Venkatesh, B., 2008. Rapidly evolving fish genomes and teleost diversity. Current Opinion in Genetics & Development 18, 544-50.

Roy, G., Mugesh, G., 2005. Anti-thyroid drugs and thyroid hormone synthesis: Effect of methimazole derivatives on peroxidase-catalyzed reactions. Journal of the American Chemical Society 127, 15207-15217.

Sachs, L.M., Damjanovski, S., Jones, P.L., Li, Q., Amano, T., Ueda, S., Shi, Y.B., Ishizuya-Oka, A., 2000. Dual functions of thyroid hormone receptors during Xenopus development. Comparative Biochemistry and Physiology Part B: Biochemistry and Molecular Biology 126, 199-211.

Saele, O., Solbakken, J.S., Watanabe, K., Hamre, K., Power, D., Pittman, K., 2004. Staging of Atlantic halibut (*Hippoglossus hippoglossus* L.) from first feeding through metamorphosis, including cranial ossification independent of eye migration. Aquaculture 239, 445-465.

Saitou, N., Nei, M., 1987. The neighbor-joining method: a new method for reconstructing phylogenetic trees. Molecular Biology and Evolution 4, 406-25.

Sanders, J.P., VanderGeyten, S., Kaptein, E., Darras, V.M., Kuhn, E.R., Leonard, J.L., Visser, T.J., 1997. Characterization of a propylthiouracil-insensitive type I iodothyronine deiodinase. Endocrinology 138, 5153-5160.

Schreiber, A.M., Specker, J.L., 2000. Metamorphosis in the summer flounder, *Paralichthys dentatus*: Thyroidal status influences gill mitochondria-rich cells. General and Comparative Endocrinology 117, 238-250.

Schreiber, A.M., Wang, X., Tan, Y., Sievers, Q., Sievers, B., Lee, M., Burrall, K., 2010. Thyroid hormone mediates otolith growth and development during flatfish metamorphosis. General and Comparative Endocrinology 169, 130-137.

Schweizer, U., Steegborn, C., 2015. New insights into the structure and mechanism of iodothyronine deiodinases. Journal of Molecular Endocrinology 55, R37-R52.

Sinha, R.A., Singh, B.K., Yen, P.M., 2014. Thyroid hormone regulation of hepatic lipid and carbohydrate metabolism. Trends in Endocrinology and Metabolism 25, 538-45.

St Germain, D.L., Galton, V.A., Hernandez, A., 2009. Minireview: Defining the roles of the iodothyronine deiodinases: current concepts and challenges. Endocrinology 150, 1097-107.

Sutija, M., Longhurst, T.J., Joss, J.M., 2004. Deiodinase type III in the Australian lungfish, *Neoceratodus forsteri*, General and Comparative Endocrinology 136, 152-61.

Suzuki, K., Machiyama, F., Nishino, S., Watanabe, Y., Kashiwagi, K., Kashiwagi, A., Yoshizato, K., 2009. Molecular features of thyroid hormone-regulated skin remodelling in *Xenopus laevis* during metamorphosis. Development, Growth & Differentiation 51, 411-427.

Tagawa, M., Aritaki, M., 2005. Production of symmetrical flatfish by controlling the timing of thyroid hormone treatment in spotted halibut *Verasper variegatus*. General and Comparative Endocrinolgy 141, 184-189.

Tata, J.R., 2006. Amphibian metamorphosis as a model for the developmental actions of thyroid hormone. Molecular and Cellular Endocrinology 246, 10-20.

Van der Geyten, S., Buys, N., Sanders, J.P., Decuypere, E., Visser, T.J., Kuhn, E.R., Darras, V.M., 1999. Acute pretranslational regulation of type III iodothyronine deiodinase by growth hormone and dexamethasone in chicken embryos. Molecular and Cellular Endocrinology 147, 49-56.

Van Herck, S.L., Geysens, S., Delbaere, J., Tylzanowski, P., Darras, V.M., 2012. Expression profile and thyroid hormone responsiveness of transporters and deiodinases in early embryonic chicken brain development. Molecular and Cellular Endocrinology 349, 289-97.

Van Herck, S.L., Geysens, S., Bald, E., Chwatko, G., Delezie, E., Dianati, E., Ahmed, R.G., Darras, V.M., 2013. Maternal transfer of methimazole and effects on thyroid hormone availability in embryonic tissues. Journal of Endocrinology 218, 105-15.

Van Herck, S.L.J., Delbaere, J., Bourgeois, N.M.A., McAllan, B.M., Richardson, S.J. Darras, V.M., 2015. Expression of thyroid hormone transporters and deiodinases at the brain barriers in the embryonic chicken: Insights into the regulation of thyroid hormone availability during neurodevelopment. Gen Comp Endocr. 214, 30-39.

Volff, J.N., 2005. Genome evolution and biodiversity in teleost fish. Heredity (Edinb). 94, 280-94.

Wassen, F.W.J.S., Schiel, A.E., Kuiper, G.G.J.M., Kaptein, E., Bakker, O., Visser, T.J., Simonides, W.S., 2002. Induction of thyroid hormone-degrading deiodinase in cardiac hypertrophy and failure. Endocrinology 143, 2812-2815.

Yamano, K. Inui, Y., 1995. cDNA Cloning of Thyroid-Hormone Receptor-Beta for the Japanese Flounder. General and Comparative Endocrinology 99, 197-203.

Yamano, K., Araki, K., Sekikawa, K., Inui, Y., 1994. Cloning of thyroid hormone receptor genes expressed in metamorphosing flounder. Developmental Genetics 15, 378-82.

Yoo, J.H., Takeuchi, T., Tagawa, M., Seikai, T., 2000. Effect of Thyroid Hormones on the Stage-specific Pigmentation of the Japanese Flounder *Paralichthys olivaceus*. Zoological Sciences 17, 1101-6.

Additional Files

Additional file 3.1. Specific primers used to isolate the complete CDS including the 3'UTR region of *dio3a* and *dio3b*. Gene symbol, gene name, annealing temperature (TaºC) and amplicon length (bp) are shown.

Gene symbol	Gene name	Primer sequence(5'→3')	Annealing temperature (Ta)	Amplicon length (bp)
Hhip_dio3a	Deiodinase 3a	F: ATGAATACTATCAAAGCTATTAA R: TGAAAAATATATCCATAAAACGTAAC	58-60ºC	1,310
Hhip_dio3b	Deiodinase 3b	F: ATGGCGAGGGCGCTGAAGC R: AAAATTTCAGTTACACAATGTTGTC	60ºC	1,351

Additional file 3.2. Multiple sequence alignment (MSA) of vertebrate deiodinase 3 used for phylogenetic analysis. The accession numbers of the Dio3 sequences used are indicated in additional file 3.5. Deiodinase homologues from *Halocynthia roretzi* and *Ciona intestinalis* are also presented in the alignment.

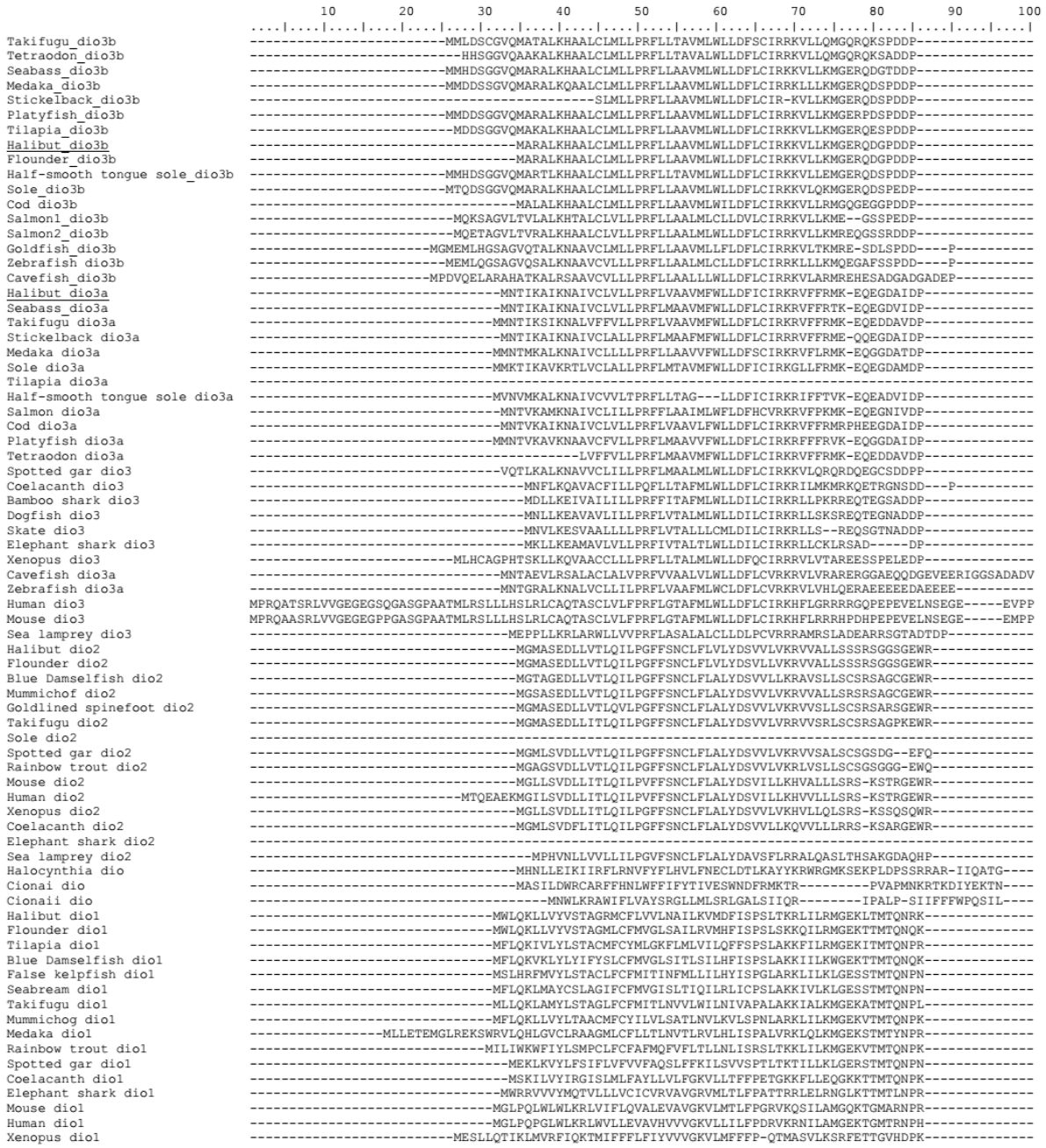

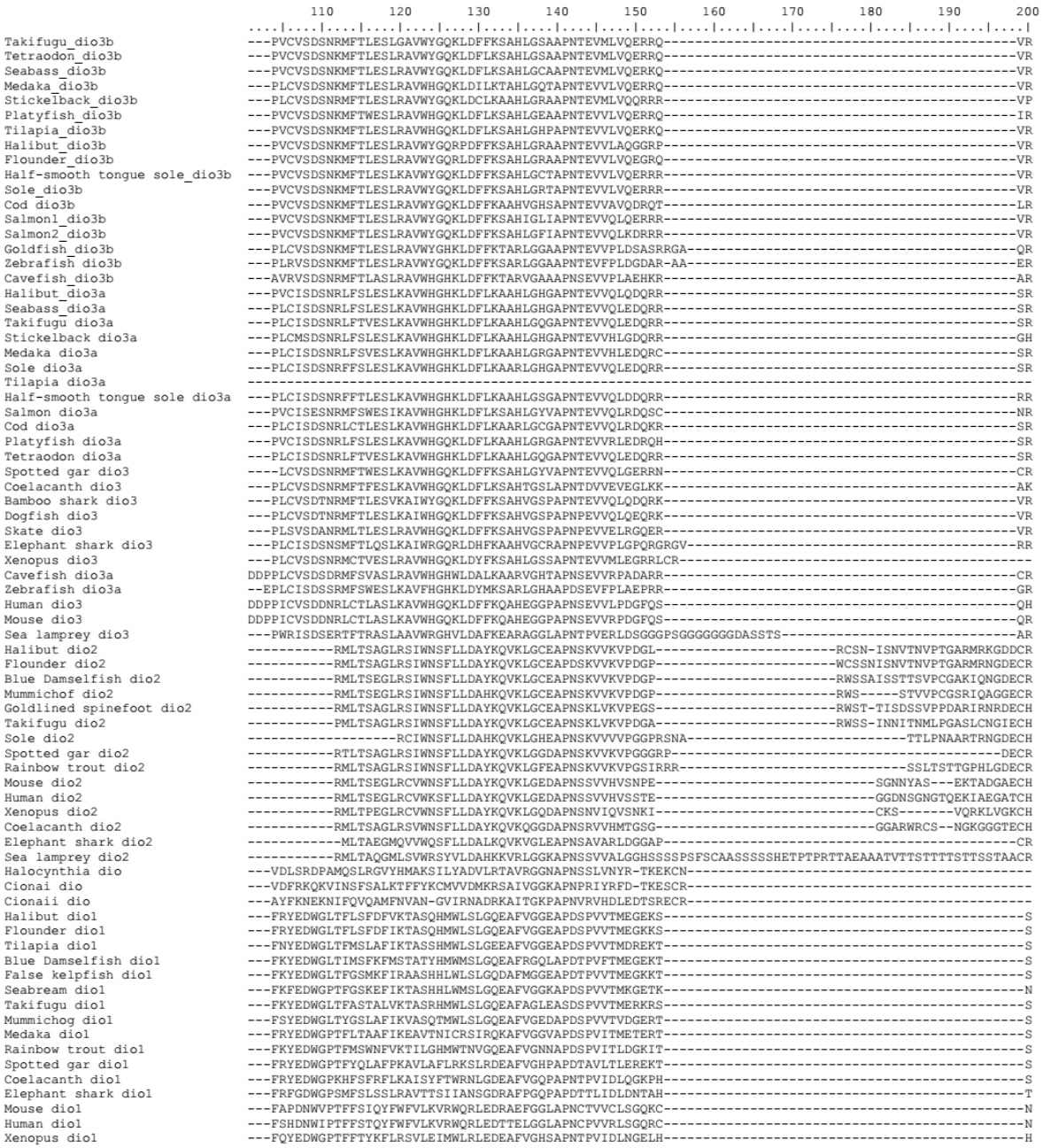
110 120 130 140 150 160 170 180 190 200
Takifugu_dio3b
Tetraodon_dio3b
Seabass_dio3b
Medaka_dio3b
Stickelback_dio3b
Platyfish_dio3b
Tilapia_dio3b
Halibut_dio3b
Flounder_dio3b
Half-smooth tongue sole_dio3b
Sole_dio3b
Cod dio3b
Salmon1_dio3b
Salmon2_dio3b
Goldfish_dio3b
Zebrafish dio3b
Cavefish_dio3b
Halibut_dio3a
Seabass_dio3a
Takifugu dio3a
Stickelback dio3a
Medaka dio3a
Sole dio3a
Tilapia dio3a
Half-smooth tongue sole dio3a
Salmon dio3a
Cod dio3a
Platyfish dio3a
Tetraodon dio3a
Spotted gar dio3
Coelacanth dio3
Bamboo shark dio3
Dogfish dio3
Skate dio3
Elephant shark dio3
Xenopus dio3
Cavefish dio3a
Zebrafish dio3a
Human dio3
Mouse dio3
Sea lamprey dio3
Halibut dio2
Flounder dio2
Blue Damselfish dio2
Mummichof dio2
Goldlined spinefoot dio2
Takifugu dio2
Sole dio2
Spotted gar dio2
Rainbow trout dio2
Mouse dio2
Human dio2
Xenopus dio2
Coelacanth dio2
Elephant shark dio2
Sea lamprey dio2
Halocynthia dio
Cionai dio
Cionaii dio
Halibut dio1
Flounder dio1
Tilapia dio1
Blue Damselfish dio1
False kelpfish dio1
Seabream dio1
Takifugu dio1
Mummichog dio1
Medaka dio1
Rainbow trout dio1
Spotted gar dio1
Coelacanth dio1
Elephant shark dio1
Mouse dio1
Human dio1
Xenopus dio1

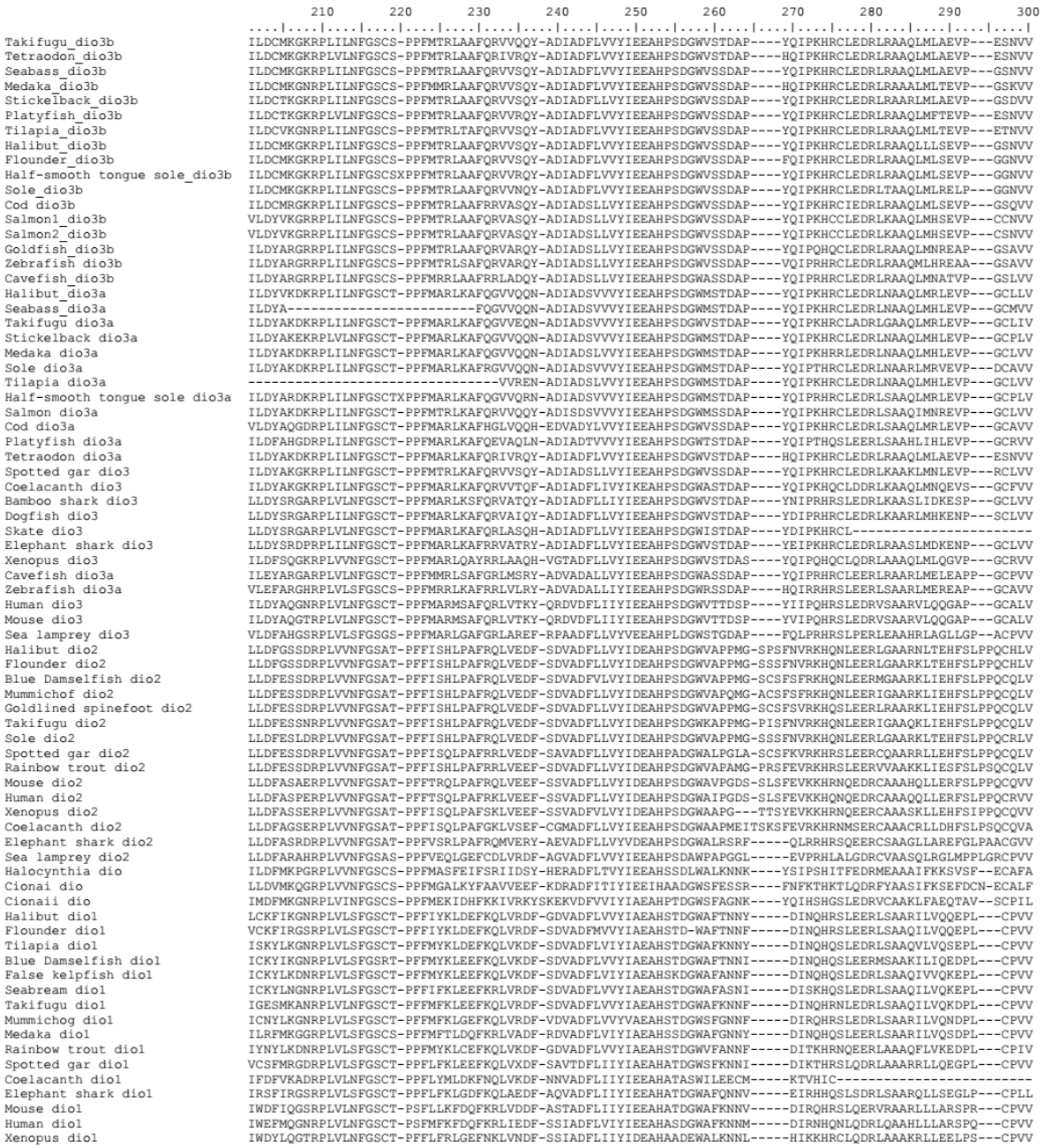
210 220 230 240 250 260 270 280 290 300
Takifugu_dio3b ILDCMKGKRPLILNFGSCS-PPFMTRLAAFQRVVQQY-ADIADFLVVYIEEAHPSDGWVSTDAP----YQIPKHRCLEDRLRAAQLMLAEVP---ESNVV
Tetraodon_dio3b ILDCMKGKRPLVLNFGSCS-PPFMTRLAAFQRIVRQY-ADIADFLVVYIEEAHPSDGWVSTDAP----HQIPKHRCLEDRLRAAQLMLAEVP---ESNVV
Seabass_dio3b ILDCMKGKRPLILNFGSCS-PPFMTRLAAFQRVVSQY-ADIADFLVVYIEEAHPSDGWVSSDAP----YQIPKHRCLEDRLRAAQLMLAEVP---GSNVV
Medaka_dio3b ILDCMKGNRPLILNFGSCS-PPFMMRLAAFQRVVSQY-ADIADFLVVYIEEAHPSDGWVSSDAP----HQIPKHRCLEDRLRAAALMLTEVP---GSKVV
Stickelback_dio3b ILDCTKGKRPLILNFGSCS-PPFMTRLAAFQRVVSQY-ADIADFLLVYIEEAHPSDGWVSSDAP----YQIPKHRCLEDRLRAARLMLAEVP---GSDVV
Platyfish_dio3b ILDCTKGKRPLVLNFGSCS-PPFMTRLAAFQRVVRQY-ADIADFLVVYIEEAHPSDGWVSSDAP----YQIPKHRCLEDRLRAAQLMFTEVP---ESNVV
Tilapia_dio3b ILDCVKGNRPLILNFGSCS-PPFMTRLTAFQRVVSQY-ADIADFLVVYIEEAHPSDGWVSSDAP----YQIPKHRCLEDRLRAAQLMLTEVP---ETNVV
Halibut_dio3b ILDCMKGKRPLILNFGSCS-PPFMTRLAAFQRVVSQY-ADIADFLVVYIEEAHPSDGWVSSDAP----YQIPKHRCLEDRLRAAQLLLSEVP---GSNVV
Flounder_dio3b ILDCMKGKRPLILNFGSCS-PPFMTRLAAFQRVVSQY-ADIADFLVVYIEEAHPSDGWVSSDAP----FQIPKHRCLEDRLRAAQLMLSEVP---GGNVV
Half-smooth_tongue_sole_dio3b ILDCMKGKRPLILNFGSCSXPPFMTRLAAFQRVVRQY-ADIADFLVVYIEEAHPSDGWVSSDAP----YQIPKHRCLEDRLRAAQLMLSEVP---GGNVV
Sole_dio3b ILDCMKGKRPLILNFGSCS-PPFMTRLAAFQRVVNQY-ADIADFLVVYIEEAHPSDGWVSSDAP----YQIPKHRCLEDRLTAAQLMLRELP---GGNVV
Cod_dio3b ILDCMRGKRPLILNFGSCS-PPFMTRLAAFRRVASQY-ADIADSLLVYIEEAHPSDGWVSSDAP----YQIPKHRCIEDRLRAAQLMLSEVP---GSQVV
Salmon1_dio3b VLDYVKGRRPLILNFGSCS-PPFMTRLAAFQRVASQY-ADIADSLLVYIEEAHPSDGWVSSDAP----YQIPKHCCLEDRLKAAQLMHSEVP---CCNVV
Salmon2_dio3b VLDYVKGRRPLILNFGSCS-PPFMTRLAAFQRVASQY-ADIADSLLVYIEEAHPSDGWVSSDAP----YQIPKHCCLEDRLKAAQLMHSEVP---CSNVV
Goldfish_dio3b ILDYARGRRPLILNFGSCS-PPFMTRLAAFQRVARQY-ADIADSLLVYIEEAHPSDGWVSSDAP----YQIPQHQCLEDRLRAAQLMNREAP---GSAVV
Zebrafish_dio3b ILDYARGRRPLILNFGSCS-PPFMTRLSAFQRVARQY-ADIADSLLVYIEEAHPSDGWVSSDAP----VQIPRHRCLEDRLRAAQMLHREAA---GSAVV
Cavefish_dio3b ILDYARGRRPLILNFGSCS-PPFMRRLAAFRRLADQY-ADIADSLLVYIEEAHPSDGWASSDAP----YQIPRHRCLEDRLRAAQLMNATVP---GSLVV
Halibut_dio3a ILDYVKDKRPLILNFGSCT-PPFMARLKAFQGVVQQN-ADIADSVVVYIEEAHPSDGWMSTDAP----YQIPKHRCLEDRLNAAQLMRLEVP---GCLLV
Seabass_dio3a ILDYA----------FQGVVQQN-ADIADSVVVYIEEAHPSDGWMSTDAP----YQIPKHRCLEDRLNAAQLMHLEVP---GCMVV
Takifugu_dio3a ILDYAKDKRPLILNFGSCT-PPFMARLKAFQGVVEQN-ADIADSVVVYIEEAHPSDGWVSTDAP----YQIPKHRCLADRLGAAQLMRLEVP---GCLIV
Stickelback_dio3a ILDYAKERRPLVLNFGSCT-PPFMARLKAFQGVVQQN-ADIADSVVVYIEEAHPSDGWMSTDAP----YQIPKHRCLEDRLNAAQLMHLEVP---GCPLV
Medaka_dio3a ILDYAKDRRPLILNFGSCT-PPFMARLKAFQGVVQQN-ADIADSLVVYIEEAHPSDGWMSTDAP----YQIPKHRRLEDRLNAAQLMHLEVP---GCLVV
Sole_dio3a ILDYAKDKRPLILNFGSCT-PPFMARLKAFRGVVQQN-ADIADSVVVYIEEAHPSDGWMSTDAP----YQIPTHRCLEDRLNAARLMRVEVP---DCAVV
Tilapia_dio3a ----------VVREN-ADIADSLVVYIEEAHPSDGWMSTDAP----YQIPKHRCLEDRLNAAQLMHLEVP---GCLVV
Half-smooth_tongue_sole_dio3a ILDYARDKRPLILNFGSCTXPPFMARLKAFQGVVQRN-ADIADSVVVYIEEAHPSDGWMSTDAP----YQIPRHRCLEDRLSAAQLMRLEVP---GCPLV
Salmon_dio3a ILDYAKDRRPLILNFGSCT-PPFMTRLKAFQRVVQQY-ADISDSVVVYIEEAHPSDGWMSSDAP----YQIPKHRCLEDRLSAAQIMNREVP---GCLVV
Cod_dio3a VLDYAQGDRPLILNFGSCT-PPFMARLKAFHGLVQQH-EDVADYLVVYIEEAHPSDGWVSSDAP----YQIPKHRCLEDRLSAAQLMRLEVP---GCAVV
Platyfish_dio3a ILDFAHGDRPLILNFGSCT-PPFMARLKAFQEVAQLN-ADIADTVVVYIEEAHPSDGWTSTDAP----YQIPTHQSLEERLSAAHLIHLEVP---GCRVV
Tetraodon_dio3a ILDYAKDRRPLILNFGSCT-PPFMARLKAFQRIVRQY-ADIADFLVVYIEEAHPSDGWVSTDAP----HQIPKHRCLEDRLRAAQLMLAEVP---ESNVV
Spotted_gar_dio3 ILDYAKGKRPLILNFGSCT-PPFMTRLKAFQRVVSQY-ADIADSLLVYIEEAHPSDGWVSSDAP----YQIPKHRCLEDRLKAAKLMNLEVP---RCLVV
Coelacanth_dio3 ILDYAKGKRPLILNFGSCT-PPFMARLKAFQRVVTQF-ADIADFLIVYIKEAHPSDGWASTDAP----YQIPKHQCLDDRLKAAQLMNQEVS---GCFVV
Bamboo_shark_dio3 LLDYSRGARPLVLNFGSCT-PPFMARLKSFQRVATQY-ADIADFLLIYIEEAHPSDGWVSTDAP----YNIPRHRSLEDRLKAASLIDKESP---GCLVV
Dogfish_dio3 LLDYSRGARPLILNFGSCT-PPFMARLKAFQRVAIQY-ADIADFLLVYIEEAHPSDGWVSTDAP----YDIPRHRCLEDRLKAARLMHKENP---SCLVV
Skate_dio3 LLDYSRGARPLVLNFGSCT-PPFMARLKAFQRLASQH-ADIADFLLVYIEEAHPSDGWISTDAP----YDIPKHRCL----------
Elephant_shark_dio3 LLDYSRDPRPLILNFGSCT-PPFMARLKAFRRVATRY-ADIADFLLVYIEEAHPSDGWVSTDAP----YEIPKHRCLEDRLRAASLMDKENP---GCLVV
Xenopus_dio3 ILDFSQGKRPLVVNFGSCT-PPFMARLQAYRRLAAQH-VGTADFLLVYIEEAHPSDGWVSTDAS----YQIPQHQCLQDRLAAAQLMLQGVP---GCRVV
Cavefish_dio3a ILEYARGARPLVLNFGSCT-PPFMMRLSAFGRLMSRY-ADVADALLVYIEEAHPSDGWASSDAP----YQIPRHRCLEERLRAARLMELEAPP---GCPVV
Zebrafish_dio3a VLEFARGHRPLVLSFGSCS-PPFMRRLKAFRRLVLRY-ADVADALLIYIEEAHPSDGWRSSDAP----HQIRHRHSLEERLSAARLMEREAP---GCAVV
Human_dio3 ILDYAQGNRPLVLNFGSCT-PPFMARMSAFQRLVTKY-QRDVDFLIIYIEEAHPSDGWVTTDSP----YIIPQHRSLEDRVSAARVLQQGAP---GCALV
Mouse_dio3 ILDYAQGTRPLVLNFGSCT-PPFMARMSAFQRLVTKY-QRDVDFLIIYIEEAHPSDGWVTTDSP----YVIPQHRSLEDRVSAARVLQQGAP---GCALV
Sea_lamprey_dio3 VLDFAHGSRPLVLSFGSGS-PPFMARLGAFGRLAREF-RPAADFLLVYVEEAHPLDGWSTGDAP----FQLPRHRSLPERLEAAHRLAGLLGP--ACPVV
Halibut_dio2 LLDFGSSDRPLVVNFGSAT-PFFISHLPAFRQLVEDF-SDVADFLLVYIDEAHPSDGWVAPPMG-SPSFNVRKHQNLEERLGAARNLTEHFSLPPQCHLV
Flounder_dio2 LLDFGSSDRPLVVNFGSAT-PFFISHLPAFRQLVEDF-SDVADFLLVYIDEAHPSDGWVAPPMG-SSSFNVRKHQNLEERLGAARKLTEHFSLPPQCHLV
Blue_Damselfish_dio2 LLDFESSDRPLVVNFGSAT-PFFISHLPAFRQLVEDF-SDVADFVLVYIDEAHPSDGWVAPPMG-SCSFSFRKHQNLEERMGAARKLIEHFSLPPQCQLV
Mummichof_dio2 LLDFESSDRPLVVNFGSAT-PFFISHLPAFRQLVEDF-SDVADFLLVYIDEAHPSDGWVAPQMG-ACSFSFRKHQNLEERIGAARKLIEHFSLPPQCQLV
Goldlined_spinefoot_dio2 LLDFESSDRPLVVNFGSAT-PFFISHLPAFRQLVEDF-SDVADFLLVYIDEAHPSDGWVAPPMG-SCSFSVRKHQSLEERLRAARKLIEHFSLPPQCQLV
Takifugu_dio2 LLDFESSNRPLVVNFGSAT-PFFISHLPAFRQLVEDF-SDVADFLLVYIDEAHPSDGWKAPPMG-PISFNVRKHQNLEERIGAAQKLIEHFSLPPQCQLV
Sole_dio2 LLDFESLDRPLVVNFGSAT-PFFISHLPAFRQLVEDF-SDVADFLLVYIDEAHPSDGWVAPPMG-SSSFNVRKHQNLEERLGAARKLTEHFSLPPQCRLV
Spotted_gar_dio2 LLDFESSDRPLVVNFGSAT-PPFISQLPAFRRLVEDF-SAVADFLLVYIDEAHPADGWALPGLA-SCSFKVRKHRSLEERCQAARRLLEHFSLPPQCQLV
Rainbow_trout_dio2 LLDFESSDRPLVVNFGSAT-PFFISHLPAFRRLVEEF-SDVADFLLVYIDEAHPSDGWVAPAMG-PRSFEVRKHRSLEERVVAAKKLIESFSLPSQCQLV
Mouse_dio2 LLDFASAERPLVVNFGSAT-PFFTRQLPAFRQLVEEF-SSVADFLLVYIDEAHPSDGWAVPGDS-SLSFEVKKHRNQEDRCAAAHQLLERFSLPPQCQVV
Human_dio2 LLDFASPERPLVVNFGSAT-PFFTSQLPAFRKLVEEF-SSVADFLLVYIDEAHPSDGWAIPGDS-SLSFEVKKHQNQEDRCAAAQQLLERFSLPPQCRVV
Xenopus_dio2 LLDFASSERPLVVNFGSAT-PFFISQLPAFSKLVEEF-SSVADFVLVYIDEAHPSDGWAAPG---TTSYEVKKHRNQEERCAAASKLLEHFSIPPQCQVV
Coelacanth_dio2 LLDFAGSERPLVVNFGSAT-PPFISQLPAFGKLVSEF-CGMADFLLVYIEEAHPSDGWAAPMEITSKSFEVRKHRNMSERCAAACRLLDHFSLPSQCQVA
Elephant_shark_dio2 LLDFASRDRPLVVNFGSAT-PPFVSRLPAFRQMVERY-AEVADFLLVYVDEAHPSDGWALRSRF-----QLRHRSQEERCSAAGLLAREFGLPAACGVV
Sea_lamprey_dio2 LLDFARAHRPLVVNFGSAS-PPFVEQLGEFCDLVRDF-AGVADFLVVYIEEAHPSDAWPAPGGL-----EVPRHLALGDRCVAASQLRGLMPPLGRCPVV
Halocynthia_dio LLDFMKPGRPLVVNFGSCS-PPFMASFEIFSRIIDSY-HERADFLTVYIEEAHSSDLWALKNNK----YSIPSHITFEDRMEAAAIFKKSVSF--ECAFA
Cionai_dio LLDVMKQGRPLVVNFGSCS-PPFMGALKYFAAVVEEF-KDRADFITIYIEEIHAADGWSFESSR----FNFKTHKTLQDRFYAASIFKSEFDCN-ECALF
Cionaii_dio IMDFMKGNRPLVINFGSCS-PPFMEKIDHFKKIVRKYSKEKVDFVVIYIAEAHPTDGWSFAGNK----YQIHSHGSLEDRVCAAKLFAEQTAV--SCPIL
Halibut_dio1 LCKFIKGNRPLVLSFGSCT-PPFIYKLDEFKQLVRDF-GDVADFLVVYIAEAHSTDGWAFTNNY-----DINQHRSLEERLSAARILVQQEPL---CPVV
Flounder_dio1 VCKFIRGSRPLVLSFGSCT-PPFIYKLDEFKQLVRDF-SDVADFMVVYIAEAHSTD-WAFTNNF-----DINQHRSLEERLSAAQILVQQEPL---CPVV
Tilapia_dio1 ISKYLKGNRPLVLSFGSCT-PFFMYKLDEFKQLVKDF-SDVADFLVIYIAEAHSTDGWAFKNNY-----DINQHQSLEDRLSAAQVLVQSEPL---CPVV
Blue_Damselfish_dio1 ICKYIKGNRPLVLSFGSRT-PFFMYKLEEFKQLVKDF-SDVADFLVVYIAEAHSTDGWAFTNNI-----DINQHQSLEERMSAAKILIQEDPL---CPVV
False_kelpfish_dio1 ICKYLKDNRPLVLSFGSCT-PFFMYKLEEFKQLVKDF-SDVADFLVIYIAEAHSKDGWAFANNF-----DINQHQSLEDRLSAAQIVVQKEPL---CPVV
Seabream_dio1 ICKYLNGNRPLVLSFGSCT-PFFIFKLEEFKRLVRDF-SDVADFLVVYIAEAHSTDGWAFASNI-----DISKHQSLEDRLSAAQILVQKEPL---CPVV
Takifugu_dio1 IGESMKANRPLVLNFGSCT-PFFMFKLEEFKQLVRDF-SDVADFLVVYIAEAHSTDGWAFKNNF-----DINQHRNLEDRLSAAQILVQKDPL---CPVV
Mummichog_dio1 ICNYLKGNRPLVLSFGSCT-PFFMFKLGEFKQLVRDF-VDVADFLVVYVAEAHSTDGWSFGNNF-----DIRQHRSLEDRLSAARILVQNDPL---CPVV
Medaka_dio1 ILRFMKGGRPLVLSFGSCS-PFFMFTLDQFKRLVADF-RDVADFLVIYIAEAHSSDGWAFGNNY-----DINQHQSLEERLSAARILVQSDPL---CPVV
Rainbow_trout_dio1 IYNYLKDNRPLVLSFGSCT-PPFMYKLCEFKQLVKDF-GDVADFLVVYIAEAHSTDGWVFANNF-----DITKHRNQEERLAAAQFLVKEDPL---CPIV
Spotted_gar_dio1 VCSFMRGDRPLVLSFGSCT-PPFLFKLEEFKQLVXDF-SAVTDFLIIYIAEAHATDGWSFKNNI-----DIKTHRSLQDRLAAARRLLQEGPL---CPVV
Coelacanth_dio1 IFDFVKADRPLVLNFGSCT-PPFLYMLDKFNQLVKDF-NNVADFLIIYIEEAHATASWILEECM-----KTVHIC----------
Elephant_shark_dio1 IRSFIRGSRPLVLSFGSCT-PPFLFKLGDFKQLAEDF-AQVADFLIIYIEEAHATDGWAFQNNV-----EIRHHQSLSDRLSAARQLLSEGLP---CPLL
Mouse_dio1 IWDFIQGSRPLVLNFGSCT-PSFLLKFDQFKRLVDDF-ASTADFLIIYIEEAHATDGWAFKNNV-----DIRQHRSLQERVRAARLLLARSPR---CPVV
Human_dio1 IWEFMQGNRPLVLNFGSCT-PSFMFKFDQFKRLIEDF-SSIADFLVIYIEEAHASDGWAFKNNM-----DIRNHQNLQDRLQAAHLLLARSPQ---CPVV
Xenopus_dio1 IWDYLQGTRPLVLNFGSCT-PPFLFRLGEFNKLVNDF-SSIADFLIIYIDEAHAADEWALKNNL-----HIKKHRCLQDRLAAAKRLLEELPS---CPVV

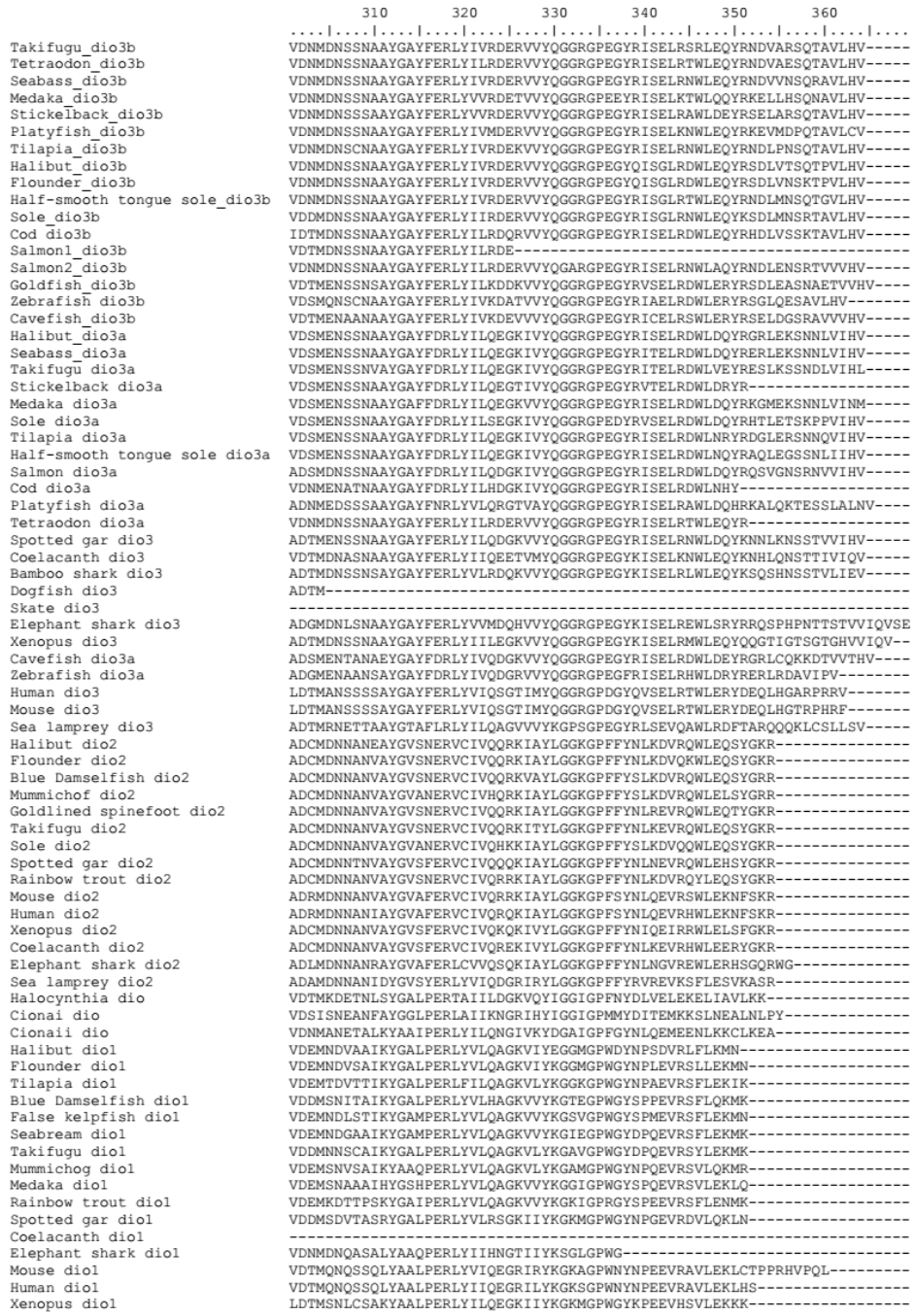
310 320 330 340 350 360
Takifugu_dio3b VDNMDNSSNAAYGAYFERLYIVRDERVVYQGGRGPEGYRISELRSRLEQYRNDVARSQTAVLHV-----
Tetraodon_dio3b VDNMDNSSNAAYGAYFERLYILRDERVVYQGGRGPEGYRISELRTWLEQYRNDVAESQTAVLHV-----
Seabass_dio3b VDNMDNSSNAAYGAYFERLYIVRDERVVYQGGRGPEGYRISELRNWLEQYRNDVVNSQRAVLHV-----
Medaka_dio3b VDNMDNSSNAAYGAYFERLYVVRDETVVYQGGRGPEEYRISELKTWLQQYRKELLHSQNAVLHV-----
Stickelback_dio3b VDNMDNSSSAAYGAYFERLYVVRDERVVYQGGRGPEGYRISELRAWLDEYRSELARSQTAVLHV-----
Platyfish_dio3b VDNMDNSSNAAYGAYFERLYIVMDERVVYQGGRGPEGYRISELKNWLEQYRKEVMDPQTAVLCV-----
Tilapia_dio3b VDNMDNSCNAAYGAYFERLYIVRDEKVVYQGGRGPEGYRISELRNWLEQYRNDLPNSQTAVLHV-----
Halibut_dio3b VDNMDNSSNAAYGAYFERLYIVRDERVVYQGGRGPEGYQISGLRDWLEQYRSDLVTSQTPVLHV-----
Flounder_dio3b VDNMDNSSNAAYGAYFERLYIVRDERVVYQGGRGPEGYQISGLRDWLEQYRSDLVNSKTPVLHV-----
Half-smooth tongue sole_dio3b VDNMDNSSNAAYGAYFERLYIVRDERVVYQGGRGPEGYRISGLRTWLEQYRNDLMNSQTGVLHV-----
Sole_dio3b VDDMDNSSNAAYGAYFERLYIIRDERVVYQGGRGPEGYRISGLRNWLEQYKSDLMNSRTAVLHV-----
Cod_dio3b IDTMDNSSNAAYGAYFERLYILRDQRVVYQGGRGPEGYRISELRDWLEQYRHDLVSSKTAVLHV-----
Salmon1_dio3b VDTMDNSSNAAYGAYFERLYILRDE----------
Salmon2_dio3b VDNMDNSSNAAYGAYFERLYILRDERVVYQGARGPEGYRISELRNWLAQYRNDLENSRTVVVHV-----
Goldfish_dio3b VDTMENSSNSAYGAYFERLYILKDDKVVYQGGRGPEGYRVSELRDWLERYRSDLEASNAETVVHV----
Zebrafish_dio3b VDSMQNSCNAAYGAYFERLYIVKDATVVYQGGRGPEGYRIAELRDWLERYRSGLQESAVLHV-------
Cavefish_dio3b VDTMENAANAAYGAYFERLYIVKDEVVVYQGGRGPEGYRICELRSWLERYRSELDGSRAVVVHV-----
Halibut_dio3a VDSMENSSNAAYGAYFDRLYILQEGKIVYQGGRGPEGYRISELRDWLDQYRGRLEKSNNLVIHV-----
Seabass_dio3a VDSMENSSNAAYGAYFDRLYILQEGKIVYQGGRGPEGYRITELRDWLDQYRERLEKSNNLVIHV-----
Takifugu_dio3a VDSMENSSNVAYGAYFDRLYILQEGKIVYQGGRGPEGYRITELRDWLVEYRESLKSSNDLVIHL-----
Stickelback_dio3a VDSMENSSNAAYGAYFDRLYILQEGTIVYQGGRGPEGYRVTELRDWLDRYR----------
Medaka_dio3a VDSMENSSNAAYGAFFDRLYILQEGKVVYQGGRGPEGYRISELRDWLDQYRKGMEKSNNLVINM-----
Sole_dio3a VDSMENSSNAAYGAYFDRLYILSEGKIVYQGGRGPEDYRVSELRDWLDQYRHTLETSKPPVIHV-----
Tilapia_dio3a VDSMENSSNAAYGAYFDRLYILQEGKIVYQGGRGPEGYRISELRDWLNRYRDGLERSNNQVIHV-----
Half-smooth tongue sole_dio3a VDSMENSSNAAYGAYFDRLYILQEGKIVYQGGRGPEGYRISELRDWLNQYRAQLEGSSNLIIHV-----
Salmon_dio3a ADSMDNSSNAAYGAYFDRLYILQDGKIVYQGGRGPEGYRISELRDWLDQYRQSVGNSRNVVIHV-----
Cod_dio3a VDNMENATNAAYGAYFDRLYILHDGKIVYQGGRGPEGYRISELRDWLNHY----------
Platyfish_dio3a ADNMEDSSSAAYGAYFNRLYVLQRGTVAYQGGRGPEGYRISELRAWLDQHRKALQKTESSLALNV----
Tetraodon_dio3a VDNMDNSSNAAYGAYFERLYILRDERVVYQGGRGPEGYRISELRTWLEQYR----------
Spotted_gar_dio3 ADTMENSSNAAYGAYFERLYILQDGKVVYQGGRGPEGYRISELRNWLDQYKNNLKNSSTVVIHV-----
Coelacanth_dio3 VDTMDNASNAAYGAYFERLYIIQEETVMYQGGRGPEGYKISELKNWLEQYKNHLQNSTTIVIQV-----
Bamboo_shark_dio3 ADTMDNSSNSAYGAYFERLYVLRDQKVVYQGGRGPEGYKISELRLWLEQYKSQSHNSSTVLIEV-----
Dogfish_dio3 ADTM----------
Skate_dio3 ----------
Elephant_shark_dio3 ADGMDNLSNAAYGAYFERLYVVMDQHVVYQGGRGPEGYKISELREWLSRYRRQSPHPNTTSTVVIQVSE
Xenopus_dio3 ADTMDNSSNAAYGAYFERLYIILEGKVVYQGGRGPEGYKISELRMWLEQYQQGTIGTSGTGHVVIQV--
Cavefish_dio3a ADSMENTANAEYGAYFDRLYIVQDGKVVYQGGRGPEGYRISELRDWLDEYRGRLCQKKDTVVTHV----
Zebrafish_dio3a ADGMENAANSAYGAYFDRLYIVQDGRVVYQGGRGPEGFRISELRHWLDRYRERLRDAVIPV--------
Human_dio3 LDTMANSSSSAYGAYFERLYVIQSGTIMYQGGRGPDGYQVSELRTWLERYDEQLHGARPRRV--------
Mouse_dio3 LDTMANSSSSAYGAYFERLYVIQSGTIMYQGGRGPDGYQVSELRTWLERYDEQLHGTRPHRF-------
Sea_lamprey_dio3 ADTMRNETTAAYGTAFLRLYILQAGVVVYKGPSGPEGYRLSEVQAWLRDFTARQQQKLCSLLSV-----
Halibut_dio2 ADCMDNNANEAYGVSNERVCIVQQRKIAYLGGKGPFFYNLKDVRQWLEQSYGKR----------
Flounder_dio2 ADCMDNNANVAYGVSNERVCIVQQRKIAYLGGKGPFFYNLKDVQKWLEQSYGKR----------
Blue_Damselfish_dio2 ADCMDNNANVAYGVSNERVCIVQQRKVAYLGGKGPFFYSLKDVRQWLEQSYGRR----------
Mummichof_dio2 ADCMDNNANVAYGVANERVCIVHQRKIAYLGGKGPFFYSLKDVRQWLELSYGRR----------
Goldlined_spinefoot_dio2 ADCMDNNANVAYGVSNERVCIVQQRKIAYLGGKGPFFYNLREVRQWLEQTYGKR----------
Takifugu_dio2 ADCMDNNANVAYGVSNERVCIVQQRKITYLGGKGPFFYNLKEVRQWLEQSYGKR----------
Sole_dio2 ADCMDNNANVAYGVANERVCIVQHKKIAYLGGKGPFFYSLKDVQQWLEQSYGKR----------
Spotted_gar_dio2 ADCMDNNTNVAYGVSFERVCIVQQQKIAYLGGKGPFFYNLNEVRQWLEHSYGKR----------
Rainbow_trout_dio2 ADCMDNNANVAYGVSNERVCIVQRRKIAYLGGKGPFFYNLKDVRQYLEQSYGKR----------
Mouse_dio2 ADRMDNNANVAYGVAFERVCIVQRRKIAYLGGKGPFSYNLQEVRSWLEKNFSKR----------
Human_dio2 ADRMDNNANIAYGVAFERVCIVQRQKIAYLGGKGPFSYNLQEVRHWLEKNFSKR----------
Xenopus_dio2 ADCMDNNANVAYGVSFERVCIVQKQKIVYLGGKGPFFYNIQEIRRWLELSFGKR----------
Coelacanth_dio2 ADCMDNNANVAYGVSFERVCIVQREKIVYLGGKGPFFYNLKEVRHWLEERYGKR----------
Elephant_shark_dio2 ADLMDNNANRAYGVAFERLCVVQSQKIAYLGGKGPFFYNLNGVREWLERHSGQRWG----------
Sea_lamprey_dio2 ADAMDNNANIDYGVSYERLYVIQDGRIRYLGGKGPFFYRVREVKSFLESVKASR----------
Halocynthia_dio VDTMKDETNLSYGALPERTAIILDGKVQYIGGIGPFNYDLVELEKELIAVLKK----------
Cionai_dio VDSISNEANFAYGGLPERLAIIKNGRIHYIGGIGPMMYDITEMKKSLNEALNLPY----------
Cionaii_dio VDNMANETALKYAAIPERLYILQNGIVKYDGAIGPFGYNLQEMEENLKKCLKEA----------
Halibut_dio1 VDEMNDVAAIKYGALPERLYVLQAGKVIYEGGMGPWDYNPSDVRLFLKMN----------
Flounder_dio1 VDEMNDVSAIKYGALPERLYVLQAGKVIYKGGMGPWGYNPLEVRSLLEKMN----------
Tilapia_dio1 VDEMTDVTTIKYGALPERLFILQAGKVLYKGGKGPWGYNPAEVRSFLEKIK----------
Blue_Damselfish_dio1 VDDMSNITAIKYGALPERLYVLHAGKVVYKGTEGPWGYSPPEVRSFLQKMK----------
False_kelpfish_dio1 VDEMNDLSTIKYGAMPERLYVLQAGKVVYKGSVGPWGYSPMEVRSFLEKMN----------
Seabream_dio1 VDEMNDGAAIKYGAMPERLYVLQAGKVVYKGIEGPWGYDPQEVRSFLEKMK----------
Takifugu_dio1 VDDMNNSCAIKYGALPERLYVLQAGKVLYKGAVGPWGYDPQEVRSYLEKMK----------
Mummichog_dio1 VDEMSNVSAIKYAAQPERLYVLQAGKVLYKGAMGPWGYNPQEVRSVLQKMR----------
Medaka_dio1 VDEMSNAAAIHYGSHPERLYVLQAGKVVYKGGIGPWGYSPQEVRSVLEKLQ----------
Rainbow_trout_dio1 VDEMKDTTPSKYGAIPERLYVLQAGKVVYKGKIGPRGYSPEEVRSFLENMK----------
Spotted_gar_dio1 VDDMSDVTASRYGALPERLYVLRSGKIIYKGKMGPWGYNPGEVRDVLQKLN----------
Coelacanth_dio1 ----------
Elephant_shark_dio1 VDNMDNQASALYAAQPERLYIIHNGTIIYKSGLGPWG----------
Mouse_dio1 VDTMQNQSSQLYAALPERLYVIQEGRIRYKGKAGPWNYNPEEVRAVLEKLCTPPRHVPQL---------
Human_dio1 VDTMQNQSSQLYAALPERLYIIQEGRILYKGKSGPWNYNPEEVRAVLEKLHS----------
Xenopus_dio1 LDTMSNLCSAKYAALPERLYILQEGKIIYKGKMGPWGYKPEEVHSVLEKKK----------

Additional file 3.3. Predicted amino acid and SECIS element sequence in Atlantic halibut *dio3a* (A, A') and *dio3b* (B, B') transcripts. A, B - * Termination codon. Single underlined nucleotides correspond to the predicted SECIS element. Double underlined nucleotides correspond to the TGA selenocystein (Sec) insertion codon. A', B' –SECIS element structure predicted by the software SECISearch 2.19 (http://genome.unl.edu/SECISearch.html). Conserved nucleotides associated with the SECIS element are indicated in bold and the SECIS core is boxed.

dio3a

```
1     ATG AAT ACT ATC AAA GCT ATT AAA AAT GCC ATA GTC TGC CTG GTG
1      M   N   T   I   K   A   I   K   N   A   I   V   C   L   V

46    CTG CTG CCC CGG TTC CTG GTG GCA GCG GTC ATG TTC TGG CTG CTT
16     L   L   P   R   F   L   V   A   A   V   M   F   W   L   L

91    GAC TTT ATC TGC ATT AGG AAA AGG GTC TTC TTC AGG ATG AAG GAG
31     D   F   I   C   I   R   K   R   V   F   F   R   M   K   E

136   CAG GAG GGC GAT GCC ATT GAT CCT CCT GTC TGC ATA TCC GAC TCC
46     Q   E   G   D   A   I   D   P   P   V   C   I   S   D   S

181   AAT CGC CTG TTC AGC CTG GAG TCC CTC AAA GCT GTG TGG CAC GGC
61     N   R   L   F   S   L   E   S   L   K   A   V   W   H   G

226   CAC AAG CTG GAC TTT CTG AAG GCG GCG CAC CTC GGA CAC GGA GCG
76     H   K   L   D   F   L   K   A   A   H   L   G   H   G   A

271   CCC AAC ACC GAA GTA GTT CAG CTG CAG GAT CAG CGG CGC AGC CGG
91     P   N   T   E   V   V   Q   L   Q   D   Q   R   R   S   R

316   ATC CTC GAT TAC GTG AAG GAC AAG AGA CCG CTC ATC CTC AAC TTT
106    I   L   D   Y   V   K   D   K   R   P   L   I   L   N   F

361   GGC AGC TGC ACC TGA CCA CCG TTC ATG GCG CGT CTC AAG GCT TTC
121    G   S   C   T   U   P   P   F   M   A   R   L   K   A   F

406   CAG GGA GTT GTG CAG CAG AAC GCA GAC ATC GCA GAC TCT GTA GTT
136    Q   G   V   V   Q   Q   N   A   D   I   A   D   S   V   V

451   GTG TAC ATT GAG GAA GCG CAC CCC TCC GAC GGC TGG ATG AGC ACA
151    V   Y   I   E   E   A   H   P   S   D   G   W   M   S   T

496   GAC GCG CCC TAT CAG ATC CCC AAG CAC CGG TGT CTG GAG GAC CGG
166    D   A   P   Y   Q   I   P   K   H   R   C   L   E   D   R

541   CTG AAC GCG GCG CAG CTG ATG CGC CTG GAG GTG CCC GGC TGT CTG
181    L   N   A   A   Q   L   M   R   L   E   V   P   G   C   L

586   CTG GTC GTC GAC AGC ATG GAG AAC TCT TCC AAC GCC GCG TAC GGA
196    L   V   V   D   S   M   E   N   S   S   N   A   A   Y   G

631   GCT TAT TTC GAC AGA CTT TAT ATT CTA CAG GAG GGA AAG ATA GTT
211    A   Y   F   D   R   L   Y   I   L   Q   E   G   K   I   V

676   TAC CAG GGC GGC AGA GGA CCC GAG GGC TAC CGG ATC TCA GAG CTC
226    Y   Q   G   G   R   G   P   E   G   Y   R   I   S   E   L

721   AGA GAC TGG CTG GAT CAA TAC AGA GGG AGG CTG GAG AAA TCC AAT
241    R   D   W   L   D   Q   Y   R   G   R   L   E   K   S   N

766   AAT CTA GTT ATC CAT GTG TAG ATT CAT TTC CAT CTT TCC ACA GAT
256    N   L   V   I   H   V   *

811   GCT GTG GCG AAA ACA GCA AGA AAC AAT GCT GCA GAT TTT TCA GTA
856   TTA TAA CTC CAG ATA GAT AGA TTG TGT CCC TCA TTA ATG GTT TAT
901   TAC GTG TAT TTA TTT TTT ATA TGA TTG GAT CAA AGT AAT TTG GTT
946   CAA CAT TGT CGG ATG TGC TAA GGT AGG CTC CTT CAT TTC CTA TTG
991   GAC ATA TGC ATC CTG TTA GGA TCC ATT CAG GAA AAA AAG GTT TGT
1036  TTA GGC AAA TTG TTT GTC TAC GAA CAA AAG TAT TTG TGT GTC AAA
1081  AGT TCT GTT TTT ATT TCT TCT CCG TGT GTA AAT GCG CCT TCA TTG
1126  AAT CCG TCA GGA GGA TGG TGA GTT TTG CGC ATC ACT GTG CTC CTC
1171  AGT ACT GTT GTG AAG TTC GGT TTT TAA ACG GGC TGA GTC CAG AGA
1216  ACC GAT ACT GAT GTT TTT CAT ACT GCA GAT CAC AGT GAG GCT GCT
1261  GCT CTC AAC TGT TTT GTA AAT ATT GTT ACG TTT TAT GGA TAT ATT
1306  TTT CAT ACA ATA AAA TGT TTT GAT CTA AAA AAA AAA AAA AAA AA
```

A

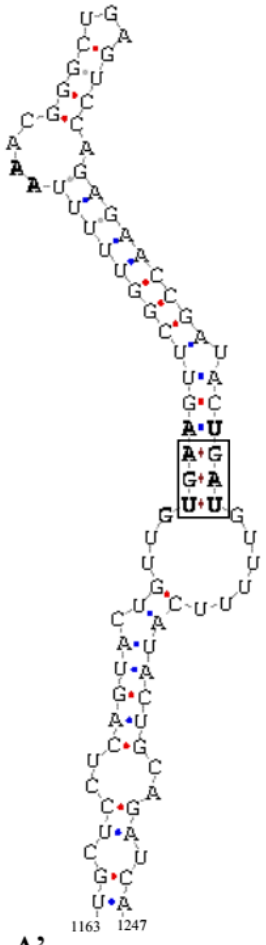

A'

dio3b

```
1     ATG GCG AGG GCG CTG AAG CAT GCG GCG CTG TGC CTG ATG CTG CTG
1      M   A   R   A   L   K   H   A   A   L   C   L   M   L   L

46    CCC CGG TTC CTC CTG GCC GCC GTC ATG CTG TGG CTC CTG GAT TTC
16     P   R   F   L   L   A   A   V   M   L   W   L   L   D   F

91    TTG TGC ATC AGG AAA AAA GTG CTG CTG AAG ATG GGG GAG AGG CAG
31     L   C   I   R   K   K   V   L   L   K   M   G   E   R   Q

136   GAC GGC CCG GAC GAC CCG CCG GTG TGC GTC TCC GAC TCC AAC AAG
46     D   G   P   D   D   P   P   V   C   V   S   D   S   N   K

181   ATG TTC ACC TTG GAG TCC CTC AGG GCC GTG TGG TAC GGC CAG AGG
61     M   F   T   L   E   S   L   R   A   V   W   Y   G   Q   R

226   CCG GAC TTT TTC AAA TCC GCG CAC CTC GGA CGC GCG GCG CCC AAC
76     P   D   F   F   K   S   A   H   L   G   R   A   A   P   N

271   ACC GAG GTG GTG CTG GCG CAG GGG GGG CGG CCG GTC CGG ATC CTG
91     T   E   V   V   L   A   Q   G   G   R   P   V   R   I   L

316   GAC TGC ATG AAA GGG AAG AGA CCG CTC ATC CTC AAC TTT GGC AGC
106    D   C   M   K   G   K   R   P   L   I   L   N   F   G   S

361   TGC TCC TGA CCG CCG TTC ATG ACG CGC CTG GCC GCG TTT CAG CGC
121    C   S   U   P   P   F   M   T   R   L   A   A   F   Q   R

406   GTC GTG AGC CAG TAC GCG GAC ATT GCG GAC TTT TTA GTT GTA TAT
136    V   V   S   Q   Y   A   D   I   A   D   F   L   V   V   Y

451   ATC GAG GAG GCG CAT CCG TCG GAC GGC TGG GTG AGC TCG GAC GCG
151    I   E   E   A   H   P   S   D   G   W   V   S   S   D   A

496   CCG TAC CAG ATC CCC AAG CAC CGC TGC CTG GAG GAC CGG CTC CGA
166    P   Y   Q   I   P   K   H   R   C   L   E   D   R   L   R

541   GCC GCG CAG CTG CTG CTC AGC GAG GTG CCC GGC AGC AAC GTG GTG
181    A   A   Q   L   L   L   S   E   V   P   G   S   N   V   V

586   GTG GAC AAC ATG GAC AAC TCG TCC AAC GCC GCG TAC GGA GCC TAC
196    V   D   N   M   D   N   S   S   N   A   A   Y   G   A   Y

631   TTT GAG AGA CTT TAC ATC GTG AGG GAC GAG CGG GTG GTG TAC CAG
211    F   E   R   L   Y   I   V   R   D   E   R   V   V   Y   Q

676   GGG GGC AGG GGT CCC GAG GGA TAC CAA ATA TCG GGG CTC CGG GAC
226    G   G   R   G   P   E   G   Y   Q   I   S   G   L   R   D

721   TGG CTG GAG CAG TAC AGG AGC GAC CTG GTG ACT TCC CAG ACG CCG
241    W   L   E   Q   Y   R   S   D   L   V   T   S   Q   T   P

766   GTG CTC CAT GTG TAG CTG AGG ATG CTG AAC CAG CCG CTG CTC TGC
256    V   L   H   V   *

811   CCA TTC GGC CTC AGT GTC CAG CCC AAC AGT GCG AAC TAC CAG ATG
856   CTG CTA TCA AGT GTT CAC ACA GGA CAC TTG TTT ATT TTC CAC GCG
901   TAA AGA CAT AAA GAC AGA AAC CGG ACT CAT AGC CTG AAG TCA GGT
946   TGA AGC CTC TCT CCA GGC TGT AGG CTG ATC TAT TGA TAC ATT GAT
991   AAA TTG ACT CAT GTG CGC TTG TCT CGA CGT TAA TTG ATT AAT TGC
1036  TTA TAG CGA TTT TAT TTT TTG TTT TTT TTT TTT GTA TGG AAA AGT
1081  CTT GGA TCA GTT GAA ACT GGA TTC AAT AAG TAA TCA CTC TAT TTT
1126  TTT ACA GTG TGT GTG TGT GTG TGT GTG CGC GCG CGC TCA TGT TAA
1171  TATCTCGCTCCTCTCACGGTGTTTTTATGAAGGTCGGTTTTAAA
1216  AGGCGCAGCCAGAAGACCGACACTGATTTTTCCCTGACACCGGG
1261  AGCGGGTCCATATTAACGGGAAGTACTTCCTCCTCATGCGCCA
1306  ACCCCATGTGTGTAACATGTTGACAACATTGTGTAACTGAAATTT
1351  TTTTTTTTAATAAATGTCCAGATCACTCATAAAAAAAAA
```

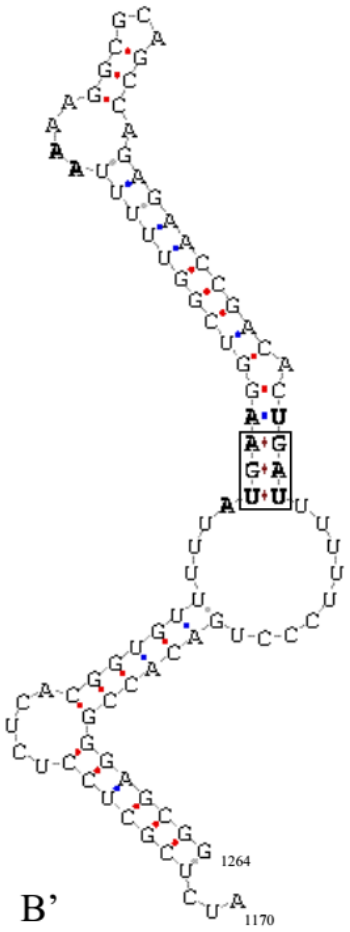

B’

B

Additional file 3.4. Amino acid sequences similarity of the Atlantic halibut, flounder, sole, zebrafish and human deiodinase 3 (DIO3).

	Halibut_dio3a	Halibut_dio3b	Flounder_dio3b	Sole_dio3b	Zebrafish_dio3a	Zebrafish_dio3b	Human_dio3
Halibut_dio3a	0	83%	84%	82%	80%	77%	63%
Halibut_dio3b	-	0	97%	91%	83%	77%	61%
Flounder_dio3b	-	-	0	94%	78%	78%	61%
Sole_dio3b	-	-	-	0	76%	78%	63%
Zebrafish_dio3a	-	-	-	-	0	76%	63%
Zebrafish_dio3b	-	-	-	-	-	0	62%
Human_dio3	-	-	-	-	-	-	0

Additional file 3.5. Accession numbers of the vertebrate deiodinase 3 sequences used in the phylogenetic analysis. Sequence accession numbers were retrieved from NCBI (http://www.ncbi.nlm.nih.gov, September 2015), ENSEMBL (www.ensembl.org, September 2015) and from the elephant shark genome project (http://esharkgenome.imcb.a-star.edu.sg).

			Acession number			
Species	**Name in the tree**	**Gene**	**Database**	**EST**	**protein**	**genome**
Hippoglossus hippoglossus	Halibut	*dio3b*	-	-	-	-
		dio3a	NCBI	-	ABI93489.2	-
		dio2	NCBI	-	ABI93490.2	-
		dio1	NCBI	-	ABI93488.2	-
Solea senegalensis	Sole	*dio3a*	NCBI			to fill
		dio3b	NCBI	-	CAP16956.1	to fill
		dio2	NCBI	-	CAP16957.1	-
Cynoglossus semilaevis	Half-smooth tongue sole	*dio3a*	NCBI	-	-	LOC103380986
		dio3b	NCBI	-	-	LOC103378336
Paralichthys olivaceus	Flounder	*dio3b*	NCBI	-	BAG15908.1	-
		dio2	NCBI	-	BAG15907.1	-
		dio1	NCBI	-	BAG15906.1	-
Takifugu rubripes	Takifugu	*dio3a*	NCBI	-	NP_001129619.1	-
		dio3b	NCBI	-	NP_001129618.1	-
		dio2	NCBI	-	NP_001129617.1	-
		dio1	NCBI	-	NP_001129616.1	-
Tetraodon novirigidis	Tetraodon	*dio3a*	Ensembl	-	-	ENSTNIG00000010973
		dio3b	Ensembl	-	-	ENSTNIG00000017283
Gasterosteus aculeatus	Stickleback	*dio3a*	Ensembl	-	-	Chr_groupXV (7200451-7201194)
		dio3b	Ensembl	-	-	ENSGACG00000012922

Oryzias latipes	Medaka	*dio3a*	Ensembl	-	-	ENSORLG00000017559
		dio3b	Ensembl	-	-	ENSORLG00000014548
		dio1	NCBI	-	XP_011488600.1	-
Gadus morhua	Cod	*dio3a*	Ensembl	-	-	ENSGMOG00000019990
		diob	Ensembl	-	-	ENSGMOG00000020296
Oreochromis niloticus	Tilapia	*dio3a*	Ensembl	-	-	ENSONIG00000020627
		dio3b	NCBI	-	CAA71997.1	-
		dio1	NCBI	-	CAA71995.1	-
Xiphophorus maculatus	Platyfish	*dio3a*	NCBI	FK038549, FK036328, FK037916, FK037917,FK038550	-	-
		dio3b	NCBI	-	XP_014331224.1	-
Dicentrarchus labrax	Seabass	*dio3a*	European seabass Genome Project			DLAgn_00023090
		dio3b	European seabass Genome Project			DLAgn_00068090
Salmon salar	Salmon	*dio3b1*	NCBI	-	AKJ23338.1	-
		dio3b2	NCBI	-	XP_014061348	-
		dio3a	NCBI	-	AKJ23340.1	-
Danio rerio	Zebrafish	*dio3a*	NCBI	-	NP_001242932.1	-
		dio3b	NCBI	-	NP_001171406.2	-
Astyanax mexicanus	Cavefish	*dio3a*	Ensembl	-	-	ENSAMXG00000025003
		dio3b	Ensembl	-	-	ENSAMXG00000025292
Carassius auratus	Goldfish	*dio3b*	NCBI	-	ABP64747.1	-
Chrysiptera cyanea	Blue Damselfish	*dio2*	NCBI	-	ADD82413.1	-
		dio1	NCBI	-	ADD82414.1	-

Sebastiscus marmoratus	False kelpfish	*dio1*	NCBI	-	AFP99133.1	-
Sparus aurata	Seabream	*dio1*	NCBI	-	DQ888894.1	-
Fundulus heteroclitus	Mummichog	*dio2*	NCBI	-	AAB39651.2	-
		dio1	NCBI	-	NM_001309995.1	-
Oncorhynchus mykiss	Rainbow trout	*dio2*	NCBI	-	NP_001117740.1	-
Siganus guttatus	Goldlined spinefoot	*dio2*	NCBI	-	ADB46158.1	-
Lepisosteus oculatus	Spotted gar	*dio3*	Ensembl	-	-	ENSLOCG00000017707
		dio2	Ensembl	-	-	ENSLOCG00000008880
		dio1	Ensembl	-	-	ENSLOCG00000003136
Leucoraja erinacea	Skate	*dio3*	NCBI	GE617280.1	-	-
Callorhinchus milii	Elephant shark	*dio3*	Elephant shark Genome Project	-	-	KI635863.1
		dio2	Elephant shark Genome Project	-	-	KI636007.1
		dio1	NCBI	-	-	XP_007907162.1
Chiloscyllium punctatum	Bamboo shark	*dio3*	NCBI	-	ABX60542.1	-
Squalus acanthias	Dogfish	*dio3*	NCBI	ES788294.1	-	-
Petromyzon marinus	Sea lamprey	*dio3*	Ensembl	-	-	ENSPMAG00000009904
		dio2	NCBI	-	KC306946.1	-
Latimeria chalumnae	Coelacanth	*dio3*	NCBI	-	XP_006014666	-
		dio2	NCBI	-	XM_005992719.2	-
		dio1	NCBI	-	XM_014492371.1	-
Xenopus laevis	Xenopus	*dio3*	Ensembl	-	-	ENSXETG00000024414
		dio2	NCBI	-	NP_001184161.2	-
		dio1	NCBI	-	NP_001243226.1	-
Mus musculus	Mouse	*dio3*	Ensembl	-	ENSMUSG00000075707	-

		dio2	NCBI	-	NP_034180.1	-
		dio1	NCBI	-	AAH19786.1	-
Homo sapiens	Human	*dio3*	NCBI	-	NP_001116120.1	-
		dio2	NCBI	-	AAC95470.1	-
		dio1	NBCI	-	NP_000783.2	-
Halocynthia roretzi	Halocynthia	*dio*	NCBI	-	AY377937.1	-
Ciona intestinalis	Cionai	*dio*	NCBI	-	XM_004225520.2	-
	Cionaii	*dio*	NCBI	-	XM_002130972.2	-

Additional file 3.6. Deiodinase 3 expression sequence tags (ESTs) identified in teleosts.

Species	Gene	EST accession number	Tissue/Condition
Paralichthys lethostigma	*dio3b*	EB740696.1	whole body larvae
Xiphophorus maculatus	*dio3b*	FK038549.1, FK036328.1, FK037916.1, FK037917.1, FK038550.1	melanoma
Lates calcarifer	*dio3b*	EX469694.1	brain
Dicentrarchus labrax	*dio3b*	FM010053.1	mixture (brain, pituitary)
Ictalurus furcatus	*dio3b*	CK407668.1, CK407507.1, CK408137.1, CF971886.1	liver
Osmerus mordax	*dio3b*	EL527680.1	mixture (brain, kidney, spleen)
Salmo salar	*dio3a*	DW562425.1	mixture (brain, kidney, spleen)
Cyprinus carpio	*dio3a*	JZ198390.1	mixture (brain, gill, heart, blood, head kidney, kidney, liver, gonad)

Chapter 4

Structural and functional maturation of skin during metamorphosis in the Atlantic halibut (*Hippoglossus hippoglossus*

Chapter 4

Abstract

The present study targets the development of the primary barrier and osmoregulatory capacity of Atlantic halibut skin (*Hippoglossus hippoglossus*) during metamorphosis by combining histological, histochemical and electrophysiological measurements. The ontogeny of goblet cells (secreting mucins) and ionocytes (presence of Na^+,K^+-ATPase) in ocular and abocular (blind) skin during metamorphosis was evaluated. Epithelial integrity and electrical properties of ocular skin were assessed using electrophysiology. Atlantic halibut skin changes from a simple epithelium to a highly stratified tissue during the transition from pre-metamorphosis to post-metamorphosis. The morphology of the ocular and abocular skin started to diverge during the metamorphic climax and ocular skin appeared thicker and more stratified. Differences in the abundance of the extracellular matrix protein, osteonectin (OSN), were detected by immunohistochemistry between ocular and abocular skin at the metamorphic climax. Neutral mucins were the main glycoproteins produced by the goblet skin cells in Atlantic halibut skin during metamorphosis. Moreover, the number of goblet cells producing neutral mucins increased during metamorphosis and in stages 8 up to 9B, were more abundant in ocular skin compared to abocular skin. The increase in goblet cell number and their asymmetric abundance in skin was concomitant with the increase in THs and suggests they may be under the control of the hormones. Na^+,K^+-ATPase positive cells (NKA) were observed in all metamorphic stages but the NKA cell number in the skin significantly decreased with the onset of metamorphosis. No asymmetry was observed between ocular and abocular skin in NKA cells. The morphological changes observed had a demonstrated effect on the barrier function of the skin as reflected by the electrophysiological properties of the epithelia (transepithelial resistance/potential and short circuit current). However, maturation of functional characteristics occurred at stage 8 prior to the full maturation of the skin and metamorphosis climax. The study indicates that there is asymmetric development of skin and that this is associated with metamorphosis although establishment of its functional properties occurs early and is independent of metamorphosis.

Keywords: metamorphosis, skin development, asymmetry, THs, mucins, Na+,K+-ATPase

Chapter 4

4.1. Introduction

The body fluids of fish are in contact with the external environment across the primary barriers, *i.e.* gills, skin and gastro-intestinal tract, and this means that changes in the external environment constitute a major physiological challenge. The maturation state of the primary barriers varies with ontogeny and determines their capacity to respond especially during early life stage transitions (reviewed by Esteban, 2000). For flatfish, the early life stages undergo a particularly dramatic transformation in external morphology during metamorphosis, when there is a shift from a symmetric pelagic larva to an asymmetric benthic juvenile with both eyes on the ocular side of the head (Power et al., 2008). Metamorphosis is a thyroid hormone (TH) driven process that prepares the larval fish for subsequent lifecycle stages (Miwa et al., 1992; Schreiber et al., 2010). Substantial remodelling of larval organs and tissues during metamorphosis underpin the functional maturation of juveniles. One example of skin maturation is the modifications that occur in the Atlantic halibut (*Hippoglossus hippoglossus*) when the skin changes from a thin epithelium in pre-metamorphic larvae to a highly stratified epidermis in the juvenile (Campinho et al., 2007).

The availability of THs in tissue during flatfish metamorphosis is modulated by the coordinated action of the deiodinases (Campinho et al., 2012). In fish, as in other vertebrates, the skin constitutes a primary barrier composed of two main physical structures. The outer, extrinsic barrier that consists of a mucous layer containing antibacterial compounds such as lysozymes, complement and antibodies (Aranishi, 1999; Cole et al., 1997; Esteban and Cerezuela, 2015; Subramanian et al., 2007; Tsutsui et al., 2011). The epithelial cells and the tight junctions, underlying the mucous constitute the intrinsic component of the physical barrier (Elliott, 2000; Henrikson and Matoltsy, 1968; Rakers et al., 2010). The production of a mucous layer by the skin is the first line of defense against infection by microorganisms in the surrounding water (Alvarez-Pellitero, 2008; Gomez et al., 2013; van del Marel et al., 2010; Esteban and Cerezuela, 2015).

The epidermal mucous is mainly produced by the goblet cells (Harris and Hunt, 1975), unicellular exocrine glands located in the middle to outer layer of the epidermis (Elliott, 2000). The predominant components of the mucous layer are high molecular weight, large, filamentous glycoproteins, called mucins. Mucins are composed of long peptide chains repeated in tandem with sites of extensive O-glycosylation (Cone, 1999; Perez-Vilar and Hill,

1999). Around 50% of the dry weight of most mucins is attributed to the carbohydrate moiety that is associated with the amino acids, serine, threonine and proline that are highly abundant in the protein (Gendler and Spicer, 1995; Padra et al., 2014).

The composition and localization of mucous cells in the epidermis of fish has recently been studied using conventional histochemical techniques (Adamek et al., 2013; Arellano et al., 2004; Garg et al., 2010; Ledy et al., 2003; Padra et al., 2014; Park et al., 2003; Rai et al., 2012; Sadovy et al., 2004; van del Marel, 2010). These histochemical procedures detect neutral and acidic mucins and are based on their reactivity with periodic acid/Schiff's reagent (PAS), and on the affinity of the anionic groups for the cationic dye Alcian blue (AB), respectively. Such approaches have revealed that the mucus cells in the epidermis of early life stages of plaice (*Pleuronectes platessa*) only contain neutral mucins (Roberts et al., 1973) and that the scarce mucous cells in the epidermis of yolk-sac larvae of Atlantic halibut only react with PAS (Ottesen and Olafsen 1997). In the finfish *Cyprinus carpio*, the number of mucous cells, in the buccal cavity, containing acidic mucins increases during larval development (El-Gamal, 2009). A similar phenomenon has also been reported for the Atlantic halibut (Ottesen and Olafsen, 1997). In the latter species, a shift from predominantly neutral to a mixture of neutral and acidic mucins occurs during ontogeny, suggesting that these changes are related to the transition from a pelagic to a benthic habitat. A similar situation has also been observed in tissues such as oesophagus, gills, and intestine of the flatfish, brill *Scophthalmus rhombus* (Hachero-Cruzado et al., 2009), and during development of the Senegalese sole (*Solea senegalensis*) in both the epidermis and gills. (Sarasquete et al., 1998). Surprisingly little, and partly contradictory, information exists about the ontogeny of mucous cells during the profound structural and functional modifications of the epidermis during flatfish metamorphosis.

Teleost skin has an important osmoregulatory role particularly during early life stages (eg. from hatching to juvenile). Apart from being a major barrier for passive ion exchange, the presence and importance of ionocytes, mitochondria-rich cells (MRC) responsible for ionic exchange (Pisam and Rambourg, 1991; Wilson and Laurent, 2002) has been shown in larvae of several fish species: *Pagrus major* (Yamashita, 1978), *Anguilla japonica* (Sasai et al., 1998), *Fundulus heteroliticus* (Kataho et al., 2000), *Dicentrarchus labrax* (Varsamos, 2002), *Saratherodon galilaeus* (Fishelson and Bresler, 2002). At the basolateral membrane of the ionocytes from sea water (SW) adapted fish, Na^+,K^+-ATPases are highly abundant and drive

the excretion of monovalent ions against an electrochemical gradient (Marshall, 2002). In most teleost species, during ontogeny there is a shift in the localization of ionocytes and ion regulation from a predominantly extra-branchial to a branchial site (reviewed by Varsamos et al., 2005). For example, in Mozambique tilapia (*Oreochromis mossambicus*) the number of skin ionocytes decreases after hatching concomitant with a progressive increase in the gill ionocytes (Yanagie et al., 2009). In the late larval stage and juveniles of sea bass the highest number of ionocytes is associated with the fins and the lateral line (Diaz et al., 2003; Varsamos et al., 2002). A similar situation is suggested to occur in the flatfish where the number of positive immunoreactive ionocytes containing Na^+,K^+-ATPases in the skin gradually decreases from early larval stages to the juvenile and this change is associated with the development of the gills (Hiroi et al., 1998; Einarsdóttir et al., 2011). The Na^+/K^+ ATPaseα1a (*atp1a1a*) transcripts decreased in the gastrointestinal tract (GI-tract) and increased in the gills and skin between 1 and 3 days post hatch (dph) in larva maintained in 36 ppt (parts per thousand) seawater but this shift was delayed when the larvae were maintained at lower salinity (20 ppt) (Armesto et al., 2014). However, to our knowledge, no functional studies exist on the physiological effects of the ontogenetic changes in the skin of goblet cells and ionocytes during flatfish metamorphosis.

The main aim of the present study was to examine the detailed development of the primary barrier and osmoregulatory capacity of Atlantic halibut skin by combining detailed histological and histochemical techniques to determine skin morphology and structure with electrophysiological measurements of barrier and osmoregulatory functions. The relative importance of the extrinsic and intrinsic components of the barrier as well as the potential structural and functional divergence of the ocular and abocular skin during flatfish metamorphosis were targeted.

4.2. Material and methods

4.2.1. Animals and tissue collection

Atlantic halibut larvae 530 – 800 D^o (stages 7, 8, 9A, 9B; Einarsdottir et al., 2006) were reared at the Institute of Marine Research (IMR, Austevoll, Norway) following standard procedures (Harboe et al., 1998). In brief, larvae were reared with a continuous flow of seawater (1 $L.min^{-1}$ at the start of the experiment increasing gradually to 5 $L.min^{-1}$) in conical

cylindrical tanks (diameter: 1.5 m; height: 1 m; water depth: 87 cm) with a central standpipe. Continuous daylight was used throughout the experiment and the water temperature was maintained at 12.2 ± 0.7 °C (mean ± SD). The fish were fed live artemia twice daily (Olsen et al., 1999). Dead larvae were siphoned from the tanks each day and the mortality in each tank registered. The larvae were sampled with a dip-net at regular intervals from the age of 530 D^o through to the end of metamorphosis. Sampled larvae were photographed (Ixus 115 HS, Canon), and staging was performed using mytome height (MH) and standard length (SL), (Sæle et al., 2004). The following stages were used in this study: 7 - prometamorphic; 8 – proclimax metamorphosis; and 9 - climax metamorphosis. Stage 9 was further subdivided into 9A, 9B and 9C to capture the changes occurring in early, mid- and late climax (Alves et al., 2016).

For histology and immunohistochemistry, fish were euthanized with a lethal dose, 0.1% in seawater, of ethyl 3-aminobenzoate methanesulfonate salt (MS-222, Sigma-Aldrich, Spain) followed by fixation in 4% paraformaldehyde at 4ºC overnight with gentle agitation. After fixation, the samples were washed in phosphate-buffered saline containing Triton X-100 (PBS-T) and stored in 100% methanol at -20°C. The larvae for the electrophysiology were placed in petri dishes containing chilled seawater (4 ^oC), killed by decapitation, and the skin removed using fine forceps. To maintain tissue viability a custom made temperature control dissection table was used and the surgery was performed under fibre optic cold light. The experiments were covered by a Norwegian Food Safety Authority facility (licence n. 093; experiment approval n. 4395). The Food Safety Authority handles everything connected with animal welfare and experimental animals in Norway.

4.2.2. Histological, histochemical and immunohistochemical procedures

The fixed Atlantic halibut, of different development stages (stages 7-9A, n = 4; 9B n = 2), were decalcified in EDTA 0.5M pH 8, washed in water, dehydrated through a graded ethanol series (0, 50%, 70%, 90% and 100%), followed by xylene and then embedded in low melting point paraffin using a Histosec tissue processor (Merk, Darmstadt, Germany). No stage 9C specimens were available for histological and immunohistochemical procedures. Sagittal serial sections of the head (5 µm) were cut using a rotary microtome (Leica RM 2135, Germany) and the skin of the head (designated skin head, SH in figures), epithelia of the

mouth, gill cavity, oesophagus, stomach and intestine, and gill cavity were analyzed. Transverse serial sections (5 µm) of the trunk were used to examine the ocular skin (top side, designated skin top – ST in figures) and abocular skin (bottom side, designated skin bottom – SB in figures) sections. Serial sections were mounted on 3-aminopropyltriethoxysilane (2% v/v in acetone) coated slides.

Histology was carried out on serial sections (5 µm) of Atlantic halibut using conventional staining approaches. In brief, consecutive slides were dewaxed in xylene, rehydrated (through a graded ethanol series, 100% to water) and stained using haematoxylin and eosin, Masson's trichrome (Witten and Hall, 2003) and Picro-sirius red (to detect the birefringence of collagen fibers in polarized light, Pearse, 1985). To distinguish different types of goblet cells in the ocular/abocular skin of Atlantic halibut during metamorphosis several staining procedures were used. Neutral mucins were detected using periodic acid-Schiff (PAS) stain (modified McManus, 1946), acidic carboxylated and/or weakly sulphated mucins were detected using Alcian Blue at pH 2.5 (AB-pH 2.5, AB2.5) (modified Mowry, 1956); and (AB-pH 1, AB1) and acidic sulphated mucins were detected using Alcian Blue at pH 1 (Lev and Spicer, 1964). The goblet cells were stained purple to magenta with PAS and blue with AB-pH 2.5 and AB-pH 1. After staining, slides were dehydrated in ethanol (0% - 100%), cleared in xylene and mounted in DPX (Fluka, Germany).

Immunohistochemistry was performed to determine the expression pattern of ionocytes in Atlantic halibut ocular and abocular body skin, head skin (SH) and gills during metamorphosis. A monoclonal antibody against the alfa-subunit of avian Na+, K+-ATPase (α5) was purchased from the Developmental Studies Hybridoma Bank (University of Iowa, USA) and was used at a concentration of 1:350. The specificity of the antisera for Atlantic halibut Na+, K+-ATPases has previously been characterised (Einarsdóttir et al., 2011). Matricellular components of the skin were assessed using a polyclonal antisera (1/3000) against the matricellular glycoprotein osteonectin (OSN, rabbit anti-seabream OSN), the specificity of which has been previously characterized.

For staining, serial sections of Atlantic halibut were dewaxed and rehydrated (as described above), washed in phosphate-buffered saline – Triton X100 (PBST, pH 7), and endogenous peroxidase activity was inactivated with 3% H_2O_2 in 20% methanol in PBST, for 20 min. Sections were washed in PBST, blocked with 4% sheep serum in TCT (0.7 % Tris-λ-carrageenan and 0.5 % Triton X100) for 30 min at room temperature and then incubated with

the antisera (α5, 1/300 or anti-OSN, 1/3000) overnight at 4ºC. Sections were washed in PBST and incubated for 1 hr at room temperature with a secondary antibody for α5 (1:200 of sheep anti-mouse Ig, biotinylated species-specific whole antibody, GE Healthcare UK Limited) or anti-OSN (1/200 of donkey anti-rabbit Ig, biotinylated species-specific whole antibody, GE Healthcare UK Limited), followed by streptavidin-peroxidase conjugated complex (1:400, Streptavidin Peroxidase conjugate, GE Healthcare UK Limited) for 45 min at room temperature. Sections were washed in PBS (0.15M, pH 7.2) and developed using the chromagen diaminobenzidine tetrahydrochloride (DAB) 0.05 %, H_2O_2 0.015 % in 0.15 M PBS (0.15M, pH 7.2) for 15 minutes in the dark. Sections were dehydrated by immersion through a graded ethanol series (0 to 100%), cleared in xylene and mounted in DPX. Negative controls included omission of the primary or secondary antisera and in the case of the anti-OSN primary antisera pre-absorption with recombinant OSN. All the negative controls failed to give a reaction and confirmed the specificity of the staining detected.

Slides stained with H&E, Masson's trichrome, PAS and immunohistochemistry were examined with a Leica DM2000 microscope. The slides stained with Picro-sirius red were examined in polarized light with an Olympus BH2 microscope. Digital images were obtained using a digital camera (Leica DFC480) and were used to evaluate the organization and ontogeny of halibut skin during metamorphosis.

4.2.3. Skin epithelial integrity and electrical properties

The permeability of skin was assessed in Atlantic halibut larvae in metamorphic stages 7 (n = 9), 8 (n = 10), 9A (n = 13), 9B (n = 8) and 9C (n = 10) using a custom made Ussing chamber system (UCC-401, UCC-Labs ltd; Sundell and Sundh, 2012). Using this *in vitro* technique, the electrical parameters, transepithelial resistance (TER), transepithelial potential (TEP) and short circuit current (SCC) was measured. Analysis of TER gave information on the tightness of the junctional complexes and of the epithelial cell layer. Assessment of SCC reflects the active transporting events taking place within the epithelia and TEP gives an indirect measure of gradients of charged molecules that are created across the epithelia.

The skin segments were mounted into modified Ussing chambers (Grass and Sweetana, 1988) specifically made for small sized biopsies like the halibut larvae skin (aperture: 4 x 2 mm, 8 mm2). After dissection and mounting, the chambers were filled (half

chamber volume: 2 ml) with halibut Ringer solution and the temperature was kept at 10°C by a cooling mantle. Mixing and oxygenation was obtained by gas-lift with pressurized air. The chambers were equipped with four electrodes each: one pair of Pt-electrodes for voltage passage and one pair of Ag/AgCl-electrodes (Radiometer, Copenhagen) bathing in 3 M KCl solution for measurement of the current obtained and the potential obtained at different currents.

Electrical connections between the half-chambers and the voltage recording Ag/AgCl-electrodes were made first by 0.9 % NaCl agar bridges from the half-chambers to a container with a 0.9 % NaCl solution, and then by 3.0 M KCl agar bridges to the container with the recording electrodes. The tip of the 0.9 % NaCl agar bridges were positioned as close as possible to the tissue surface. The voltage application and current as well as the transepithelial voltage were controlled through an Ussing chamber control unit, UCC-401 (UCCLabs ltd, see Sundell and Sundh 2012). The background potential differences between the Ag/AgCl electrodes and the background electrical resistance, originating from the electrode/agar-salt-bridge system and the Ringer solution, were corrected for by determining these parameters in the chambers in the absence of skin biopsies. TEP values were referenced to the apical, i.e. the out-facing side of the skin. The electrical parameters were measured from the start of the experiment, directly after mounting the skins in the Ussing chambers, until t = 150 min. All tissues were allowed a 60 min equilibration period before calculations of electrical parameters was made.

4.2.4. Statistical analysis

All results are shown as mean ± standard error of the mean (SEM). The goblet cell number was counted in three consecutive sections for each larva (stages 7-9A, n = 4; 9B n = 2) using the same epithelia area in both ocular and abocular skin sides. The goblet cells containing acidic or neutral mucins were quantified in both ocular and abocular skin of the trunk (post cranial region) of the larvae present in each section. In the skin of the head, the number of goblet cells was measured between the mouth and the most posterior part of the skull (the suprascapula) using the entire area of the skin present in the sections. The number of NKA cells was counted in two consecutive sections using the same methodology as for the goblet cells (stages 7-9A, n = 4; 9B n = 2).

The number of goblet cells containing neutral mucins (PAS) for the three skin regions was analyzed by Two-way ANOVA with the significance level set as 5 %, and Tukey's HSD test was applied for pair-wise multiple comparisons. In the case of acidic mucins (AB1 and AB2.5) and NKA cell number, a Two-way ANOVA on Ranks was performed to detect statistical significance. A Tukey's HSD test was applied for pair-wise multiple comparisons. A difference in $P < 0.05$ between means was considered to be significant. For TER and SCC electrical skin parameters, One-way ANOVA was performed to detect statistical significance between metamorphic stages. In the case of TEP, the statistical analysis was carried out using One-way ANOVA on Ranks. A Tukey's HSD test was applied for pair-wise multiple comparisons. For the three skin electrical parameters, statistical significance was considered at $p < 0.05$.

4.3. Results

4.3.1. Morphology and cellular changes of ocular and abocular skin during Atlantic halibut metamorphosis

The structure, morphology and cellular changes in both ocular (ST) and abocular (SB) skin during metamorphosis were stage specific with conventional histochemical procedures (**Figure 4.1**). The overall ontogeny of the skin in metamorphosing Atlantic halibut was characterised by increasing stratification so that by climax it was composed of an epidermis with several strata, a basement membrane and a thick dermis containing numerous fibroblast-like cells (**Figure 4.1a-h**).

In prometamorphosis stage 7 Atlantic halibut larvae, the skin had a simple organisation and consisted of a thin epidermis composed of few epithelial cell (ec) layers above a monolayer of pyramidal larval basal cells (lbc) (**Figure 4.1a, a', e, e'**). Infrequent goblet/mucous cells were evident in the epidermis (**Figure 4.1a, a', e, e'**), and a thin acellular collagen lamella was visible below the larval basal cell layer (**Figure 4.1 a', e', a'', e''**). Osteonectin (OSN) immunoreactivity was localised in the outermost epithelial cells and in the myotomes but the signal was very weak (**Figure 4.1a''',e'''**). No differences in morphology were observed in the skin between the ocular and abocular sides of stage 7 larvae.

In stage 8 Atlantic halibut larvae entering metamorphosis the thickness of the supra-basal cell layer increased (**Figure 4.1b', f'**) and the collagen lamella (cl) of the dermis was thicker relative to stage 7 larvae (**Figure 4.1b'', f''**). The distribution of immunoreactive OSN was similar to stage 7 larvae but it was more intense and a positive signal was also detected in the supra-basal cells (**Figure 4.1b''', f''''**).

At metamorphic climax (stages 9A and 9B), the skin was highly stratified and the cells had acquired the cuboidal shape characteristic of adult cells. The epidermis was composed of several cell layers and included the outermost epithelial cells (ec), adult supra-basal cells (asbc) and adult basal cells (abc), which contacted a thicker and more complex collagen lamella than in earlier stages (**Figure 4.1c', d', g', h'**). Bluish/green collagen fibres characteristic of reticular collagen type I fibres or thin fibers of the minor collagen type V or type II were observed in all metamorphic stages (**Figure 4.1a'' to h''**). However, in stages 9A and 9B a greater number of collagen layers with a different pattern of colouration including orange fibres associated with larger collagen type I fibres were observed (**Figure 4.1c'', d'', g'', h''**). At metamorphic climax OSN reacted strongly not only with epithelial cells but also with the adult basal and supra-basal cells (**Figure 4.1a''' to h'''**). During the metamorphic climax, a reduction in the immunoreactivity signal was observed in ocular skin (stage9A) and in abocular skin (stage 9B). During stages 9A and 9B the morphology of the ocular and abocular skin started to diverge and the former appeared thicker and more stratified. At metamorphic climax numerous dark coloured melanocytes were evident in the dermis and were far more numerous in the ocular skin relative to the abocular skin.

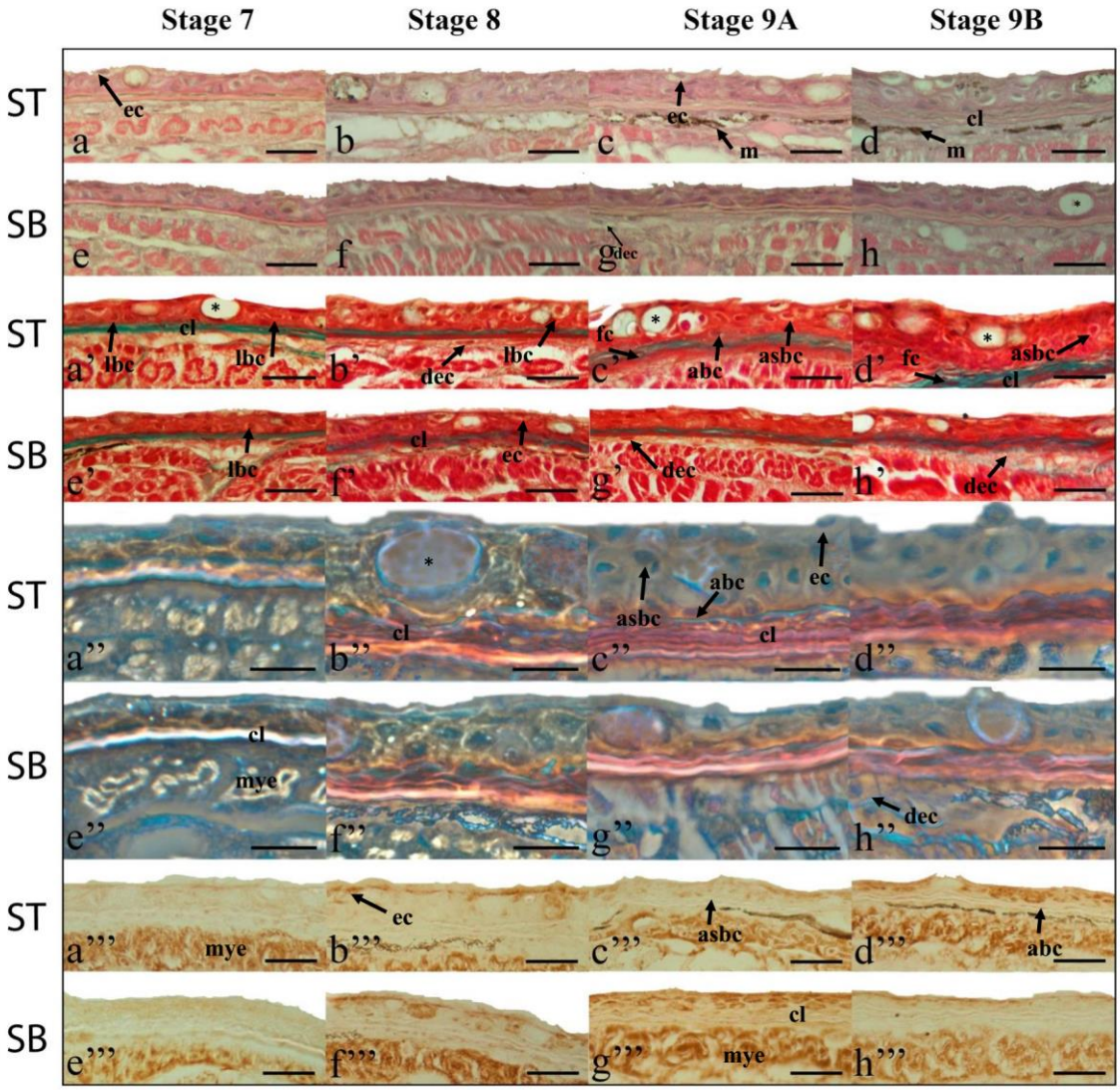

Figure 4.1. Histological characterization of both ocular (ST) and abocular (SB) skin during several *Hippoglossus hippoglossus* metamorphic stages: 7 - prometamorphosis, 8 - proclimax metamorphosis, 9A and 9B – climax metamorphosis. Skin changes during development were evaluated using several procedures: (a to h) - Haematoxylin and Eosin, (a' to h') – Masson's Trichrome, (a'' to h'') - Picro-sirius red, (a''' to h''') – immunohistochemistry for osteonectin (OSN). ec, epithelial cell; m, melanocyte; cl, collagen lamella; dec, dermal endothelial cells; *, mucous cells; lbc, larval basal cells; fc, fibroblast-like cells; abc, adult basal cells; asbc, adult supra-basal cells; mye, myotome. Scale bar – 20 μm (a to h; a' to h'; a''' to h''') and 10 μm (a'' to h'').

4.3.2. Histochemical characterization of mucous containing cells (goblet cells) of the halibut skin during metamorphosis

The histochemical properties of neutral and acidic mucins in skin of the Atlantic halibut during different metamorphic stages are summarised in table I. The number of goblet cells increased as metamorphosis advanced (**Figure 4.1c, d, g, h, c', d', g', h'**). A detailed analysis of neutral and acidic mucins is showed in figures 2 and 3 - 4, respectively. Both types of mucins were found in goblet cells in the epidermis of the skin and also in other tissues rich in goblet cells such as (eg. mouth cavity, oesophagus and the intestine). The distribution and staining intensity of mucins in the goblet cells diverged between the diverse tissues analysed (**Table 4.1**).

Neutral mucins were the predominant mucins present in the goblet cells of the ocular, abocular and head skin in the Atlantic halibut skin during metamorphosis, indicating that glycoproteins with oxidizable vicinal diols were most abundant (**Table 4.1, Figure 4.2**). The goblet cells containing neutral mucins were randomly distributed in the epidermis and were abundant in all metamorphic stages but increased in staining intensity at the start of metamorphosis, stage 8 (**Figure 4.2**). A decrease in the number of empty/non-reactive goblet cells and an increase in the number of goblet cells secreting mucous from prometamorphosis to metamorphic climax was observed (**Figure 4.2A**). The goblet cells of the intestine and the mouth cavity had a moderate to strong abundance of neutral mucins (based on PAS staining), whereas the goblet cells in the oesophagus had only a low to moderate abundance of neutral mucins (**Table 4.1, Figure 4.2B**).

No significant differences in goblet cell number existed between the ocular (ST), abocular (SB) and head (SH) skin in prometamorphosis Atlantic halibut (**Figure 4.2C**). The number of neutral mucous producing goblet cells increased significantly ($p < 0.05$) at the start of metamorphosis (stage 8) in the ocular (ST), abocular (SB) and head (SH) skin. For example, the number of goblet cells in ocular skin increased more than 50 % from stage 7 (9.96 ± 1.51 goblet cells/1.5 mm epithelia) to stage 8 (23.01 ± 1.06 goblet cells/1.5 mm epithelia) (**Figure 4.2C**). Between stages 8 to 9B asymmetry in the distribution of goblet cells developed and the number of goblet cells with PAS positive staining in the ocular skin (ST) was significantly higher ($p < 0.05$) than the abocular (SB) and head skin (SH) in metamorphic stages 8 to 9B. Abocular (13.86 ± 2.90 goblet cells/1.5 mm epithelia) and head (17.61 ± 1.54

goblet cells/1.5 mm epithelia) skin had significantly ($p < 0.05$) fewer PAS positive goblet cells relative to the ocular skin (23.01 ± 1.06 goblet cells/1.5 mm epithelia) (**Figure 4.2C**).

The intensity and amount of carboxylated and sulphated acidic glycoproteins (AB-pH 1 and AB-pH 2.5) was lower in the skin (faint to moderate), compared to the oesophagus and mouth cavity (moderate to very strong), (**Table 4.1**). Figures 3 and 4 show the number of goblet cells stained with Alcian blue at different pH's in all skin regions analysed during metamorphosis. The number of goblet cells staining for acidic glycoproteins (AB-pH 2.5) in ocular (ST) and abocular (SB) skin did not change significantly ($p > 0.05$) during metamorphosis (**Figure 4.3A, C**). The number of goblet cells in the skin of the head increased at metamorphic climax ($p < 0.05$). In almost all stages, the quantity of AB-pH 2.5 reactive goblet cells in ocular and head skin was significantly ($p < 0.05$) different. For example, in stage 9A the SH (3.45 cells/1.5 mm epithelia) had more AB-pH 2.5 positive goblet cells than the ocular skin (ST, 0.48 cells/1.5 mm epithelia) (**Figure 4.3C**).

The positive stain for AB-pH 1 revealed sulphated mucins were produced in the epidermis during development, although in much lower abundance than the neutral and carboxylated mucins (**Table 4.1, Figure 4.4**). The abundance of sulphated mucins in the goblet cells of the skin (faint to weak – AB-pH 1, weak to moderate – AB-pH 2.5) was lower than in the intestine and mouth cavity (**Figure 4.4B**). The number of goblet cells containing sulphated and carboxylated mucins was highly variable in ocular and abocular skin (**Figure 4.4C**). The number of stained goblet cells in the ocular skin was higher than those in the abocular skin in stages 7 ($p = 0.004$) and 8 ($p = 0.001$) of the Atlantic halibut. At the start of metamorphosis, the number of goblet cells containing sulphated mucous was not significantly different between the ocular (5.53 ± 2.63 cells/1.5 mm) and abocular 4.39 ± 0.72 cells/1.5 mm) skin (**Figure 4.4C**). In general, no sulphated acidic mucins were produced by the goblet cells of the head skin (**Figure 4.4A, C**).

Table 4.1. Summary of histochemical procedures to identify the nature of the mucous producing cells in *Hippoglossus hippoglossus* during metamorphosis

				Tissue					
Histochemical procedure	**Reaction result**	**Type of reaction**	**Reference**	**Ocular skin (ST)**	**Abocular skin (SB)**	**Head skin (SH)**	**Intestine**	**Oesophagus**	**Mouth cavity**
Periodic acid-Schiff (PAS)	Purple-magenta	neutral mucosubstances by presence of GPs with oxidizable vicinal diols and/or glycogen	modified from McManus (1946)	Moderate to very strong	Moderate to very strong	Moderate to very strong	Weak to moderate	Moderate	Moderate to very strong
Alcian blue pH 2.5 (AB2.5)	Blue	acidic carboxylated and sulphated mucosubstances by presence of GPs with carboxyl groups and/or GPs with O-sulphate esters	modified from Mowry (1967)	Weak to moderate	Weak to moderate	Faint to weak	Weak to moderate	Strong to very strong	Weak to strong
Alcian blue pH 1 (AB1)	Blue	acidic sulphated mucosubstances by presence of GPs with O-sulphate esters	modified from Lev and Spicer (1964)	Faint to moderate	Faint to moderate	No to faint	Weak	Strong to very strong	Weak to strong

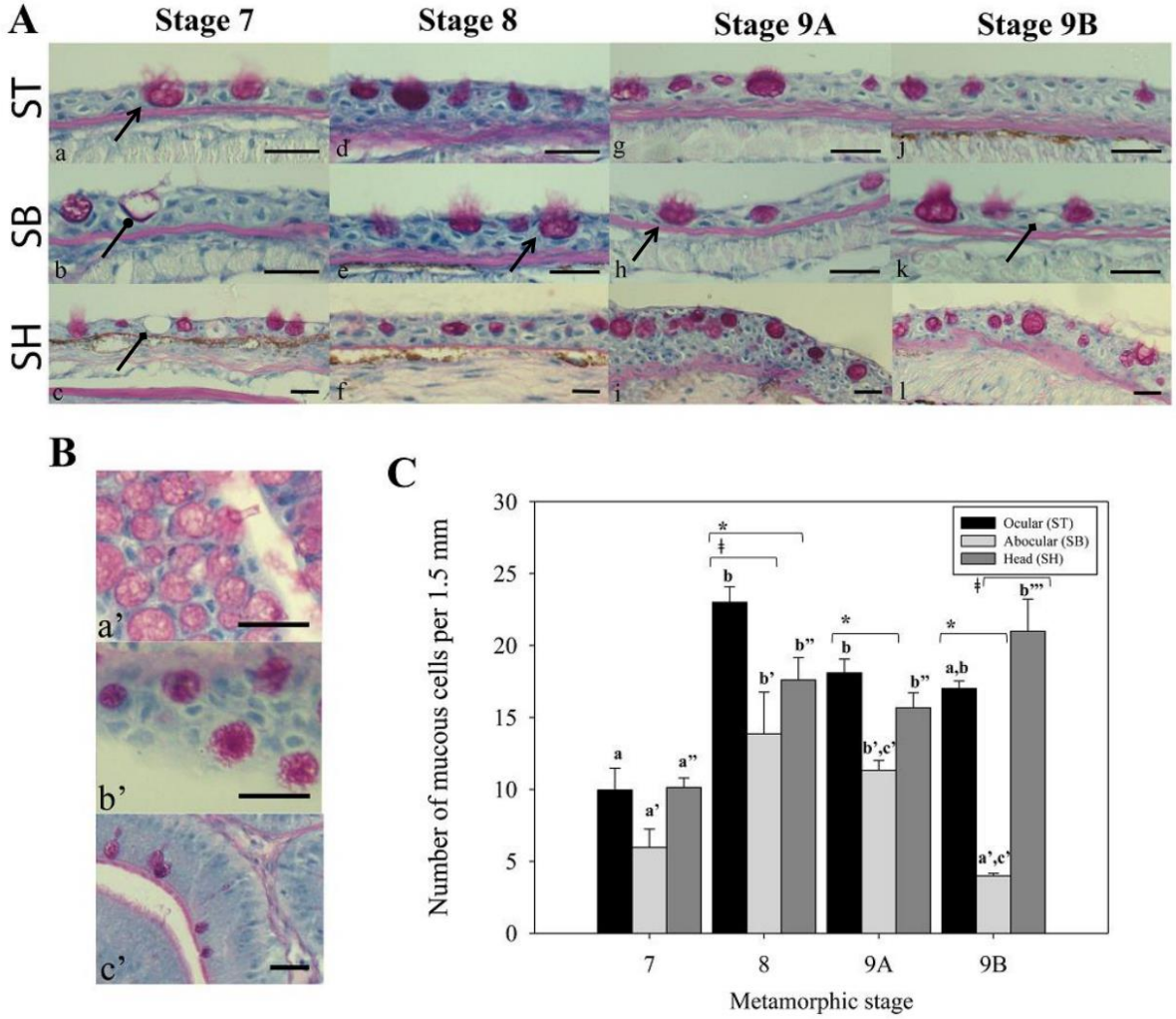

Figure 4.2. Histological characterization of neutral mucosubstances (PAS) in mucous cells of *Hippoglossus hippoglosus* during the metamorphic stages: 7 – prometamorphosis (n = 4), 8 - proclimax metamorphosis (n = 4), 9A (n = 4) and 9B (n = 2) – climax metamorphosis. A – distribution of mucous cells in the epidermis of transversal (skin ocular, ST – a, d, g, j ; skin abocular, SB – b, e, h, k) and sagittal (skin from head region, SH – c,f, i, l) sections. Most mucous cells present a purple color result. Examples of mucous cells secreting/releasing mucous are shown with an arrow; examples of empty mucous cells are represented by an arrow with round tip and the example of non reactive mucous cells was represented by an arrow with square tip. Scale bar – 20 μm. **B** – Identification of neutral glycoproteins in other Atlantic halibut tissues: a' - oesophagus, b' – mouth cavity and c' – intestine. Scale bar – 20 μm. **C** – Number of mucous cells with neutral glycoproteins by 1.5 mm of skin length in ST, SB and SH regions. Results are presented as mean ± SEM (standard error of mean). Two-way ANOVA was performed with the significance level set as 5% and Tukey's post-hoc test applied for pair-wise multiple comparisons. Different letters represent significant differences between stages in each skin region (lowercase letters, ST; lowercase letters', SB; lowercase letters'', SH). * different number of mucous cells between skin regions for a certain metamorphic stage ($p < 0.05$). ǂ different number of mucous cells between skin regions for a certain metamorphic stage ($p < 0.01$).

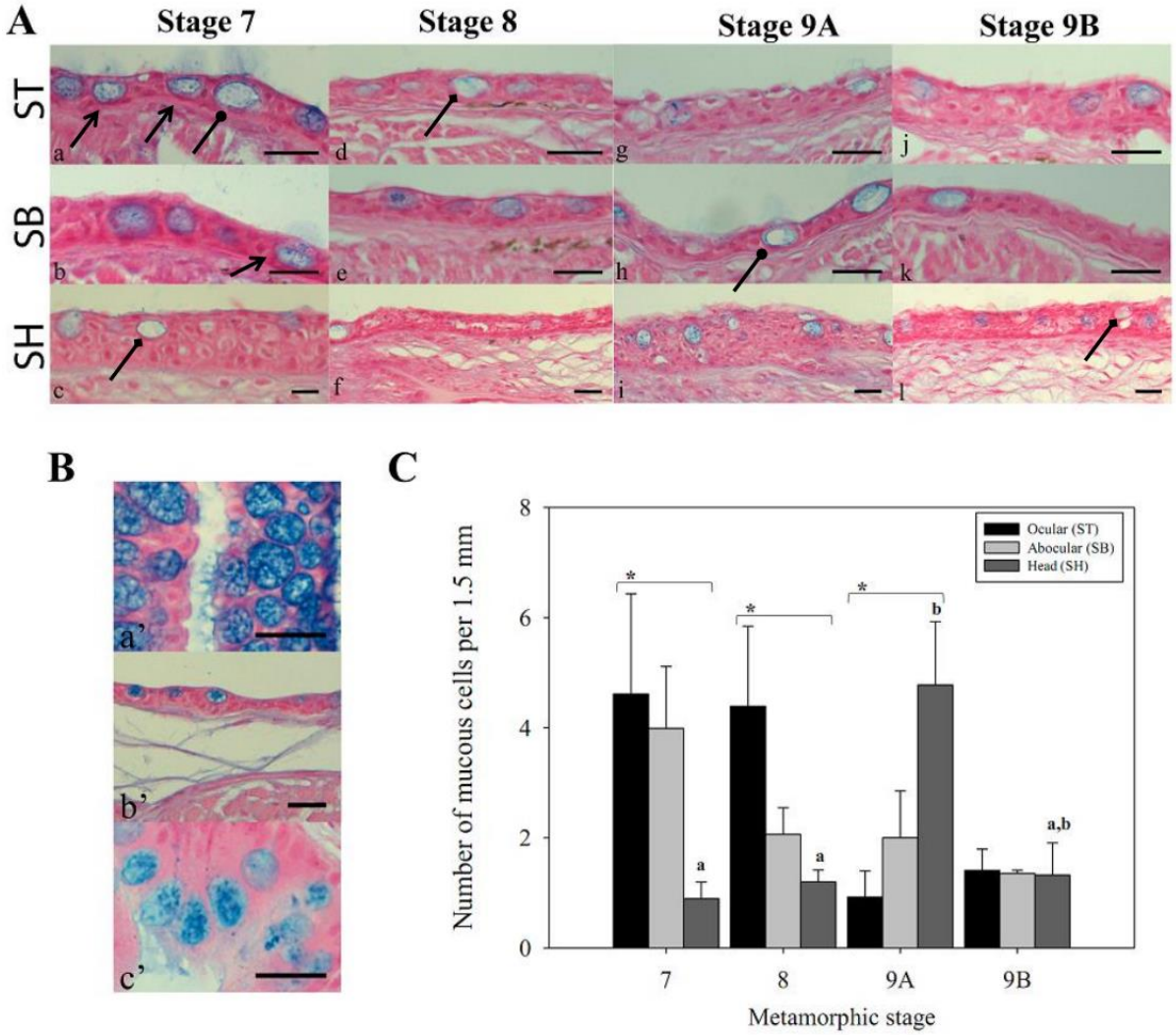

Figure 4.3. Histological characterization of acidic carboxylated and sulphated mucosubstances (AB2.5) in mucous cells of *Hippoglossus hippoglosus* during the metamorphic stages: 7 – prometamorphosis (n = 3), 8 - proclimax metamorphosis (n = 3), 9A (n = 3) and 9B (n = 2) – climax metamorphosis. A – distribution of mucous cells in the epidermis of transversal (skin ocular, ST – a, d, g, j ; skin abocular, SB – b, e, h, k) and sagittal (skin from head region, SH – c, f, i, l) sections. Mucous cells present a blue color result. Examples of mucous cells secreting/releasing mucous are shown with an arrow; examples of empty mucous cells are represented by an arrow with round tip and the example of non-reactive mucous cells was represented by an arrow with square tip. Scale bar – 20 µm. **B** – Identification of acidic glycoproteins in other Atlantic halibut tissues: a' - oesophagus, b' – mouth cavity and c' – intestine. Scale bar – 20 µm. **C** – Number of mucous cells with acidic glycoproteins by 1.5 mm of skin length in ST, SB and SH regions. Results are presented as mean ± SEM (standard error of mean). Non parametric Two-way ANOVA on Ranks was performed with the significance level set as 5% and Tukey's post-hoc test applied for pair-wise multiple comparisons. Different letters represent significant differences between stages in SH skin region. No differences were observed between stages in both ocular and abocular skin regions. * different number of mucous cells between skin regions for a certain metamorphic stage ($p < 0.05$). ǂ different number of mucous cells between skin regions for a certain metamorphic stage ($p < 0.01$).

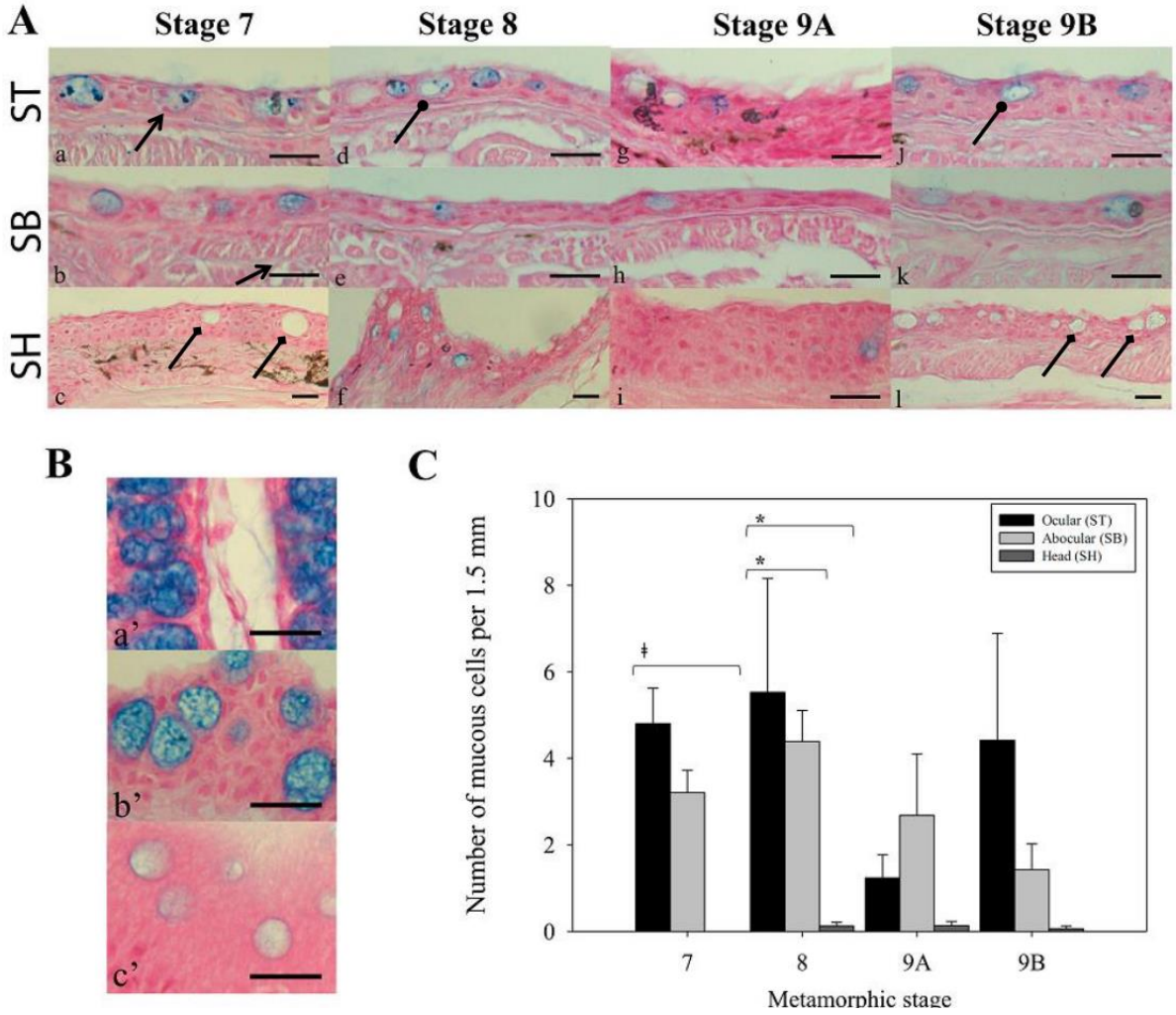

Figure 4.4. Histological characterization of acidic mucosubstances (AB1) in mucous cells of *Hippoglossus hippoglosus* during the metamorphic stages: 7 – prometamorphosis (n = 3), 8 - proclimax metamorphosis (n = 3), 9A (n = 3) and 9B (n = 2) – climax metamorphosis. A – distribution of mucous cells in the epidermis of transversal (skin ocular, ST – a, d, g, j; skin abocular, SB – b, e, h, k) and sagittal (skin from head region, SH – c, f, i, l) sections. Mucous cells present a blue color result. Examples of mucous cells secreting/releasing mucous are shown with an arrow; examples of empty mucous cells are represented by an arrow with round tip and the example of non-reactive mucous cells was represented by an arrow with square tip. Scale bar – 20 μm. **B** – Identification of acidic glycoproteins in other Atlantic halibut tissues: a' - oesophagus, b' – mouth cavity and c' – intestine. Scale bar – 20 μm. **C** – Number of mucous cells with acidic glycoproteins by 1.5 mm of skin length in ST, SB and SH regions. Results are presented as mean ± SEM (standard error of mean). Non parametric Two-way ANOVA on Ranks was performed with the significance level set as 5% and Tukey's post-hoc test applied for pair-wise multiple comparisons. No differences were observed between stages in all skin regions. * different number of mucous cells between skin regions for a certain metamorphic stage ($p < 0.05$). ǂ different number of mucous cells between skin regions for a certain metamorphic stage ($p < 0.01$).

4.3.3. Characterization of Na^+, K^+-ATPase in NKA cells in halibut skin during metamorphosis

The distribution of Na^+, K^+-ATPase immunoreactivity in the skin of Atlantic halibut undergoing metamorphosis is shown in figure 5. Na^+,K^+-ATPase positive cells were observed in all metamorphic stages in the ocular, abocular and head skin and in the gill, intestine and kidney (**Figure 4.5A, B**). In the skin, the NKA cells had a widespread distribution and the intensity of the signal and the size of the ionocytes decreased during metamorphosis, particularly in the head (**Figure 4.5A**). No significant differences in NKA cell number existed between ocular, abocular and head skin (**Figure 4.6A**).

The NKA cell number in the skin significantly decreased with the onset of metamorphosis ($p < 0.05$) in ocular and abocular skin. The number of ionocytes decreased from 6.12 ± 0.79 and 8.11 ± 1.40 cells/1.5 mm in ocular and abocular skin in stage 7, respectively to 3.01 ± 0.62 ($p = 0.029$) and 2.12 ± 0.29 ($p < 0.001$) cells/1.5 mm epithelia in stage 9A. In the head region, the number of ionocytes decreased more than 65 % from prometamorphosis (stage 7) to metamorphic climax (stage 9A), (ANOVA on Ranks, $p < 0.001$), (**Figure 4.6A**). Strong Na^+, K^+-ATPase immunoreactivity was detected in the operculum, gill filaments and kidney of the metamorphosed stage 8 and 9A Atlantic halibut (**Figure 4.5B**).

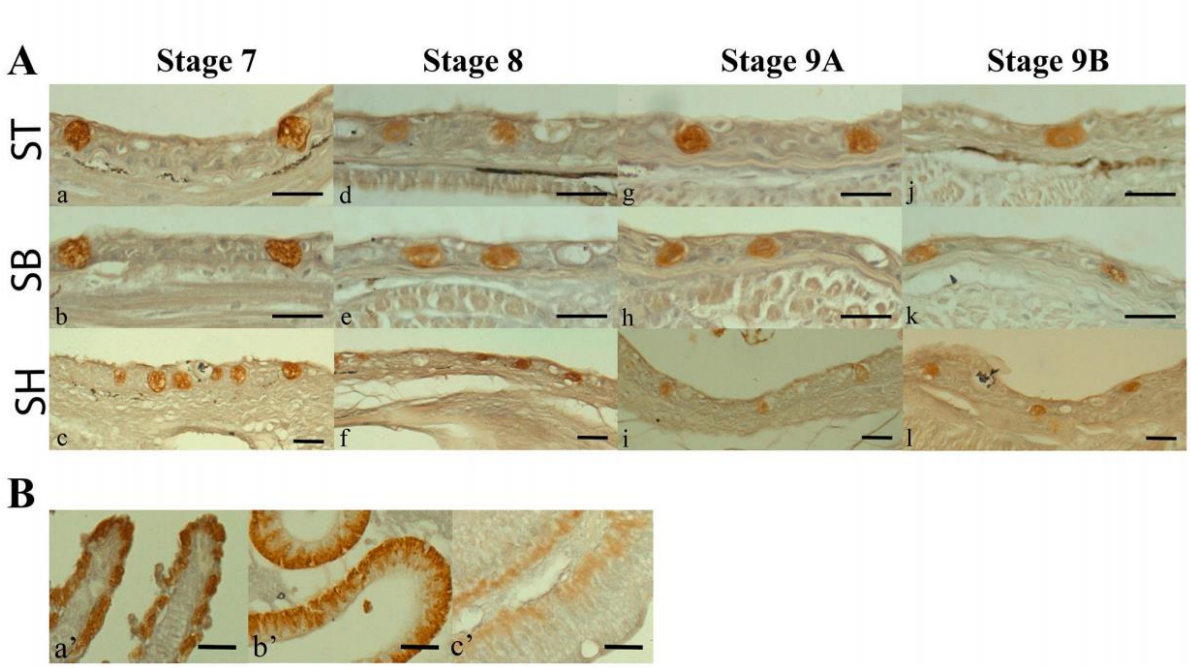

Figure 4.5. Na^+,K^+-ATPase (NKA) imunoreactivity in *Hippoglossus hippoglosus* cells during the metamorphic stages: 7 – prometamorphosis (n = 3), 8 - proclimax metamorphosis (n = 3), 9A (n = 3) and 9B (n = 2) – climax metamorphosis. A – distribution of NKA cells in the epidermis of transversal (skin ocular, ST – a, d, g, j ; skin abocular, SB – b, e, h, i) and sagittal (skin from head region, SH – c, f, k, l) sections. Scale bar – 20 μm. **B** – Identification of ionocytes in other Atlantic halibut tissues: a' - gills, b' – kidney and c' – intestine. Scale bar – 20 μm.

4.3.4. Characterization of the electrical, transporting and permeability properties of skin epithelia during metamorphosis

The electrical parameters transepithelial resistence (TER), transepithelial potential (TEP) and short circuit current (SCC) were measured in the skin epithelia using in vitro Ussing chambers and the results are summarized in **Figure 4.6**.

The TER indicates the tightness of the epithelium and stage 7 Atlantic halibut had the lowest TER, ~ 20 Ω.cm2 ($p < 0.05$, n = 9). The TER increased at the onset of metamorphosis, however, no significant differences occurred between the proclimax stage 8 (n = 11) and the metamorphic climax stages 9A and 9B ($p > 0.05$, n = 13 and n = 8), indicating the skin had a low paracellular permeability. Stage 9B had the highest TER, but it was not significantly higher than the other stages (**Figure 4.6C**). The scales started to develop after stage 9C and were only visible in the ocular skin. A high number of scale pockets initially appeared in the mid-line region and a lesser number were evident in the rest of the body (**Figure 4.6B**). The SSC value was not changed between the stages 7 to 9A ($p > 0.05$), however, significant differences ($p < 0.05$) were observed between the pro metamorphic stage 7 and the metamorphic climax stage 9B (**Figure 4.6E**). The potential difference (TEP) was lower, i.e. closer to zero, in stage 7 compared to the other stages which may reflect a higher permeability of the epithelium with a larger leakiness (**Figure 4.6D**).

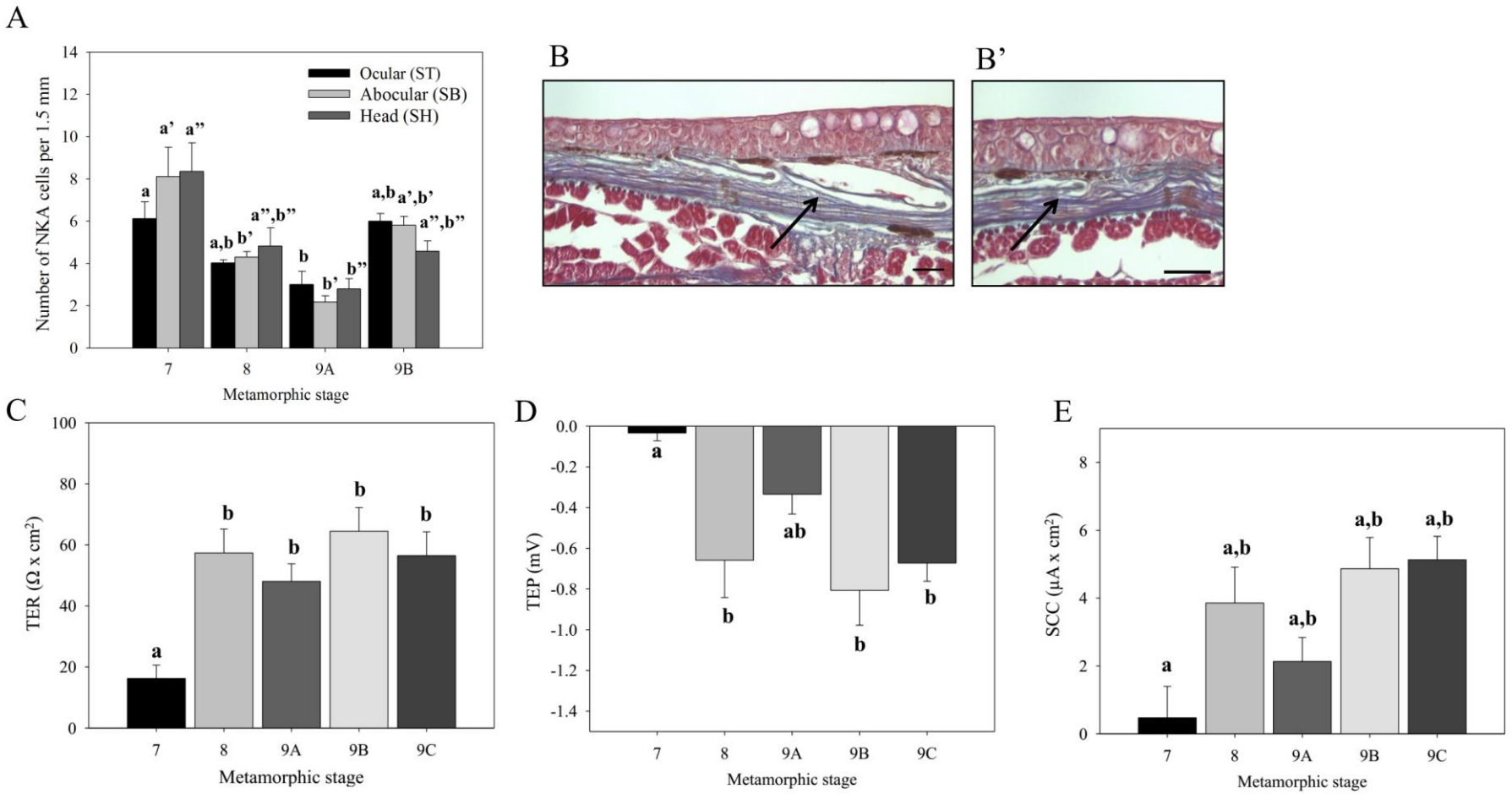
A
Number of NKA cells per 1.5 mm
Ocular (ST)
Abocular (SB)
Head (SH)
Metamorphic stage
B
B'
C
TER (Ω x cm²)
Metamorphic stage
D
TEP (mV)
Metamorphic stage
E
SCC (µA x cm²)
Metamorphic stage

Figure 4.6. NKA cells in Atlantic halibut and electrical, transporting and permeability properties of skin epithelia during metamorphosis. A – Number of NKA cells by 1.5 mm of skin length in skin ocular (ST), abocular skin (SB) and skin from head (SH) regions. Results are presented as mean ± SEM (standard error of mean). Non parametric Two-way ANOVA on Ranks was performed with the significance level set as 5% and Tukey's post-hoc test applied for pair-wise multiple comparisons. Different letters represent significant differences between stages in each skin region (lowercase letters, ST; lowercase letters', SB; lowercase letters'', SH. No differences were observed between skin regions for a certain metamorphic stage. **B**/**B'** – Histological characterization of post-metamorphic juvenile Atlantic halibut ocular skin (ST) using Masson trichome staining. Scales start to appear in the mid-line region (**B**) and are extended for the rest of the body (**B'**); Examples of scale-pocket are shown with an arrow Scale bar – 20 μm. Transepithelial resistence (TER; **C**) - Ωcm^2, transepithelial potential (TEP; **D**) – mV, and short circuit current (SCC, **E**) - μAcm^2 in ocular skin (ST) during Atlantic halibut metamorphosis measured in Ussing chambers. Results are presented as mean ± SEM (standard error of mean). One-way ANOVA was performed for TER and SCC with the significance level set as 5% and Tukey's post-hoc test applied for pair-wise multiple comparisons. Different letters represent significant differences between stages. In the case of TEP, One-way ANOVA on Ranks was performed with the significance level set as 5% and Tukey's post-hoc test applied for pair-wise multiple comparisons. Different letters represent significant differences between metamorphic stages.

4.4. Discussion

This study is the first to describe and characterize the role of the skin as a primary barrier and in osmoregulation during Atlantic halibut metamorphosis. The modification in the structure of the skin was reflected by its change in function from a largely leaky, permeable barrier to a tight membrane. Although it was not possible to characterize the functional properties of both ocular and abocular skin the asymmetry of mucous producing cells (goblet cells) and mitochondria-rich NKA cells (ionocytes) at climax and thereafter support the idea of functional asymmetry.

4.4.1. Ocular (ST) and abocular (SB) skin sides differs in morphology during metamorphosis

During Atlantic halibut metamorphosis, the skin undergoes TH-dependent remodelling and differentiation, and changes from a simple epithelium to a highly stratified skin with epidermis, dermis and hypodermis during the transition from pre-metamorphosis (stage 5) to post-metamorphosis (stage 9) (Campinho et al., 2012; reviewed Power et al., 2008). The results of the present study revealing a thicker and more complex collagen lamella in stage 7 and 8 Atlantic halibut and an increased number of goblet cells consistent with the

development of a new stratum as described in another study of the developing Atlantic halibut skin (Campinho et al., 2007). Our results suggest asymmetry develops in the structure of skin and that during metamorphosis in addition to development of asymmetric pigmentation other skin properties are asymmetric (Bolker and Hill, 2000; Hamre et al., 2007; Matsumoto and Seikai, 1992; McMenamin and Parichy, 2013).

The highly stratified skin at the metamorphic climax with an epidermis composed of several layers and cell types in contact with a complex collagen lamella, was also observed in winter flounder (*Pseudopleuronectes americanus*) and plaice (*Pleuronectes platessa*) (Murray et al., 2003; Roberts et al., 1973). The increasing molecular complexity of the skin during metamorphosis was supported by the increase during metamorphosis of immunoreactive OSN, a matricellular protein important for structural integrity and tissue development (Damjanovski et al., 1998; Delany et al., 2000, 2003; Renn et al., 200; Rotllant et al., 2008, Termine et al., 1981). A faint signal in the epithelial cells at stage 7 was substituted by a strong signal in the majority of the cells including the supra- and basal layers in the epidermis at stage 9. Previous studies have demonstrated that OSN is highly expressed in the skin of the perciforme, sea bream (*Sparus aurata*) during development (Estevão et al., 2005). Ishida and co-authors (2003) reported that OSN is up-regulated in amphibian skin during metamorphosis and suppresses rana adult keratin (rak) during epidermal differentiation. The change in expression on OSN in Atlantic halibut ocular skin (a reduction in 9A) and abocular skin (a reduction in stage 9B) suggest skin development is asynchronous at this stage. Furthermore, the timing of the change in OSN expression is coincident with the change in keratin expression previously reported and suggest that like amphibians it may have a role in epidermal differentiation (Campinho et al., 2007).

4.4.2. Atlantic halibut skin acts as a primary barrier during metamorphosis: changes in mucins composition and localization

The fish epidermis is in direct contact with the environment and mucous forms an important protective barrier (Shephard, 1994). High diversity and qualitative differences in the skin mucins have been reported in the last decade from studies on several fish species: sea bream (*Sparus aurata*) and sea bass (*Dicentrarchus labrax*) (Kalogianni et al., 2011); *Agrammus agrammus, Inimicus japonicas, Erosa erosa, Liparis tessellatus, Scombrops boops*

(Jeong, 2008); Senegalese sole (*Solea senegalensis*) and sturgeon (*Acipenser baeri*) (Sarasquete et al., 2001); dogfish (*Seriola quinqueradiata*), *Oplegnathus fasciatus*, *Epinephelus chlorostigma*, *Ditrema temmincki*, and *Halichoeres poecilopter* (Jeong and Jo, 2007). For example, the majority of goblet cells in plaice (*Pleuronectes platessa*) contain sulphomucins, whereas these are less frequent in the flounder (*Platichthys flesus*), (Fletcher et al., 1976). The ontogeny and role of mucins during larval development, particularly during flatfish metamorphosis is still relatively unstudied.

In the flatfish, turbot (*Scophthalmus rhombus*), an increase in acidic mucins in goblet cells occurs in a wide range of tissues during larval organogenesis (Hachero-Cruzado et al., 2009). In Atlantic halibut, the mucous in goblet cells in the epidermis is composed of predominantly neutral mucins in the early larval stages and becomes a mixture of neutral and acidic glycoproteins in the juvenile epidermis (Ottesen and Olafsen, 1997). Neutral mucins have frequently been associated with pelagic early life stages (Varsamos et al., 2005). In the present study, in which goblet cells were quantified, neutral mucins (average number – 13.92 ± 0.63 number of mucous cells per 1.5 mm), were most abundant in all metamorphic stages and acidic carboxylated and sulphated mucins (average number 2.60 ± 0.33 number of mucous cells per 1.5 mm) were only a minor component. This is similar to the situation in the turbot (*Psetta maxima*) in which skin goblet cells have a strong PAS positive reaction but no reaction with alcian blue in the dorsal and ventral skin (Failde et al., 2014). The neutral mucins are suggested to be reduce abrasive lesions when the larvae are in contact with the sediment/bottom of the tanks (Failde et al., 2014), to control the acidity of the acidic glycoproteins of the mucous secretions and maintain the skin barrier under stress conditions (Rai et al., 2012). The increase in goblet cells producing neutral mucins from prometamorphosis (stage 7) to metamorphic climax (stage 9A) accompanies the change in the THs that drive metamorphosis (Power et al., 2008) and skin maturation (Campinho et al., 2007, 2012) and suggests a role for these hormones in goblet cell and mucin differentiation during the transition from a symmetric pelagic larva to an asymmetric benthic juvenile. In the Atlantic halibut mucins with sulphated groups (AB1) were also absent from the skin near the cranial area and since the divergent localization of mucins has been associated with their functional role understanding this divergent expression is relevant for understanding primary barrier function and maturation (Failde et al., 2014; Pérez-Sánchez et al., 2013; Rai et al., 2012; Varsamos et al., 2005).

Chapter 4

Asymmetry in the distribution of goblet cells and the mucins they produce between ocular and abocular skin during flatfish metamorphosis has not previously been reported (Alves, unpublished observations). The factors causing the asymmetry detected during Atlantic halibut metamorphosis was not established directly. Nonetheless, the importance of THs for skin development may suggest these results from differences in the TH responsiveness of ocular (ST) and abocular skin (SB). The responsiveness of mucous differentiation to THs has previously been reported in human tracheobronchial epithelial cells in which triiodothyronine (T_3) through supressing retinoic acid receptor (RAR) signalling regulates the transcription of *MUC5AC* (Gray et al., 2001). A more detailed analysis of skin asymmetry including measurement of TH availability, the thyroid signalling pathway (TH receptors, deiodinases and TH cellular transporters) and mucins in both ocular and abocular skin during metamorphosis, would contribute to understanding the mechanisms underlying the maturation of skin during metamorphosis.

In a previous study on sea bream skin variability in mucin types was associated with location in the body and neutral mucins were detected in the cranial epidermis (Kalogianni et al., 2011) and acidic mucins with carboxylated and sulphated mucins were weakly reactive in the tail and fins (Sarasquete et al., 1998). In Atlantic halibut the production of acidic mucins was higher in the oesophagus and mouth cavity than in the skin, although mucins containing both carboxylated and sulphated mucins were higher in ocular skin of Atlantic halibut at stages 7 and 8. High amounts of acidic mucins have previously been reported in the buccal epithelium in catfish (*Rita rita*, Yashpal et al., 2007), in the gills of tench (*Tinca tinca*, Senol, 2014), in the oesophagus of the loach (*Misgurnus mizolepis*, Park and Kim, 2001), and in the intestine of sturgeon (*Acipenser baeri*, Sarasquete et al., 2001). Acidic mucins (e.g with O-sulphate esters) have an important role in lubrication and increase mucous viscosity (Yashpal et al., 2007,Yashpal and Mittal, 2014) and this explains their high abundance in the gastrointestinal tract where they facilitate the passage of food (Arellano et al., 2001; Diaz et al., 2006) and trap bacteria and other pathogens (Domeneghini et al., 2005). If the acidic mucin content is of functional significance or is related to differentiation of the goblet cells remains to be established as does the impact of mucins on the protection function of the skin.

4.4.3. Atlantic halibut skin acts as an osmoregulation tissue during metamorphosis

The skin during larval development is essential for osmoregulation and the ion movements are carried out by several enzymes, including Na^+, K^+-ATPases, ion channels, and ion transporters. These are transmembrane proteins located in the basolateral and apical membrane of the ionocytes (Marshall and Singer, 2002; Wilson and Laurent, 2002). Na^+, K^+-ATPase have commonly been used to assess ionocyte distribution during larval development (Fishelson and Bresler, 2002; Hiroi et al., 1998; Hwang, 1989; Kaneko et al., 2002; van der Heijden et al., 1999; Varsamos et al., 2002). In agreement with findings in other teleost fish, the ionocytes with Na^+, K^+-ATPase immunoreactivity were detected in the skin, gills, and kidney of Atlantic halibut.

The abundance of ionocytes in the skin during Atlantic halibut metamorphosis was in agreement with a previous study on ionocyte distribution (Einársdottir et al., 2011). A direct role for THs in the down-regulation the Na^+, K^+-ATPase in the skin is suggested by studies in summer flounder that reveal treatment with thiourea (TU) in premetamorphic larvae reduce Na^+, K^+-ATPase immunoreactivity and modify ionocyte ultrastructure (Schreiber and Specker, 2000). In contrast, to goblet cells and mucins no asymmetry in the Na^+, K^+-ATPase in skin occurred during metamorphosis of the Atlantic halibut, suggesting that the cellular context of THs probably explains why the goblet cells and ionocyte have a different responsiveness.

Interestingly, in the early developmental stages of Atlantic halibut there is a leaky physical barrier as shown by the results of electrophysiology of the ocular skin and this is when skin is a thinner and less stratified epithelia and has lower number of mucous producing goblet cells relative to later stages of Atlantic halibut. This is the first time that the electrophysiological properties of larval skin have been reported and the results were generally concordant with the results of the skin morphology. Skin in early larvae had a low resistance (Ω) and transepithelial potential (mV) suggesting that the early larval stages are exposed to large passive, diffusional forces due to a poorly developed extrinsic and intrinsic barrier. This suggestion is supported by the high number of Na^+, K^+-ATPase positive cells in skin from stage 7 Atlantic halibut but shows low short circuit current. This indicates that although there is a high number of Na^+, K^+-ATPase positive cells they are not the only route for ion movement. As the skin developed it acquired the electrophysiological characteristics

of post-metamorphic skin (stage 9C) before metamorphosis (at stage 8). This suggests that the functional characteristics of skin are established before metamorphosis and may be TH-independent, presumably due to the importance of the primary barrier function of the skin for survival (Proksch et al., 2008; Rakers et al., 2010). An interesting feature in the electrophysiology was the significant reduction in TEP and SSC in skin of stage 9A Atlantic halibut. An explanation for this event may be linked to the maturation of the epithelia and it coincided with a notable reduction in OSN immunoreactivity and may correspond approximately to the transition from larval epithelial cells to adult epithelial cells reported in a previous study (Campinho et al., 2007).

The development of the morphology of the skin barrier diverged between the ocular and abocular side of the metamorphosing halibut larvae. The increased complexity and thickness of both epithelial cells and connective tissue were more pronounced on the ocular side, which was also the case for the specific cell types, melanophores (only present on the ocular side) and goblet cells, more numerous on the ocular side. This suggests that diffusional and invasive forces from the surrounding water needs larger degree of protection than the more mechanical effects from the underlying substrate. Technical limitations meant it was not possible to establish if the electrophysiological properties of skin diverged between ocular and abocular skin and this will be the objective of future work.

4.5. Conclusions

In conclusion, this study contributes to our understanding of how asymmetry development occurs in the structure of Atlantic halibut skin during metamorphosis. The morphology of the ocular and abocular skin diverges during the metamorphic climax, with the ocular side developing a greater thickness and stratification. During metamorphosis, the skin goblet cells produce mainly neutral mucins but acidic carboxylated and sulphated mucins are also secreted but at much lower amounts. The neutral mucins increased during metamorphosis and this increase was concomitant with the reported peak of THs. Furthermore, we demonstrated for the first time that the distribution of goblet cells and mucins are asymmetric during metamorphosis, and the explanation for the highest cell/mucin number in the ocular side may be related to possible differences in the TH responsiveness of ocular and abocular skin. In contrast to goblet cells and mucins no asymmetry occurred between ocular and

abocular skin in the Na^+, K^+-ATPas immunoreactivity during metamorphosis of the Atlantic halibut.

The morphological changes observed had a demonstrated effect on the barrier function of the skin as reflected by the electrophysiological properties of the epithelia. Stage 7 Atlantic halibut had a leaky epithelia, with low transepithelial resistance (TER) and in stage 8 and 9 TER more than doubled. The maturation of the barrier is also reflected in its ability to maintain a transepithelial potential (TEP) which increased with ontogeny. Nonetheless the skins primary barrier function matures before metamorphosis suggesting it is a TH independent process.

The factors causing the asymmetry between ocular and abocular skin functions detected during Atlantic halibut metamorphosis was not established directly, but we hypothesize that the responsiveness of skin to THs is asymmetric. Further research is required to validate our hypothesis including how thyroid signalling pathways (TH receptors, deiodinases and TH cellular transporters) in both ocular and abocular skin influence the change in skin during metamorphosis. Experiments with manipulation of THs in vivo using for example methimazol (MMI) will contribute to establish at a molecular level how THs influence mucin production and the development of Na+, K+-ATPase during metamorphosis.

Acknowledgements

This research study was funded by the European Community FP7 project LIFECYCLE (FP7 222719, http://www.lifecycle.gu.se/, 17.08.2012) and the European Regional Development Fund (ERDF) COMPETE – Operational Competitiveness Programme and Portuguese funds through the Foundation for Science and Technology (FCT), Portugal (project Pest-C/MAR/LA0015/2013). RNA and LA were funded by FCT Portugal (SFRH/BD/69209/2010 and SFRH/BPD/79105/2011, respectively).

References

Adamek, M., Syakuri, H., Harris, S., Rakus, K.L., Brogden, G., Matras, M., Irnazarow, I., Steinhagen, D., 2013. Cyprinid herpesvirus 3 infection disrupts the skin barrier of common carp (*Cyprinus carpio* L.), Veterinary Microbiology 162, 456-70.

Alvarez-Pellitero, P., 2008. Fish immunity and parasite infections: from innate immunity to immunoprophylactic prospects. Veterinary immunology and immunopathology 126, 171-198.

Alves, R.N., Gomes, A.S., Stueber, K., Tine, M., Thorne, M.A., Smaradottir, H., Reinhard, R., Clark, M.S., Ronnestad, I., Power, D.M., 2016. The transcriptome of metamorphosing flatfish. BMC Genomics 17, 413.

Aranishi, F., 1999. Purification and Characterization of Serum Serpin from Carp (*Cyprinus carpio*). Marine biotechnology 1, 81-88.

Arellano, J.M., Storch, V., Sarasquete, C., 2001. Histological and histochemical observations in the stomach of the Senegal sole, *Solea senegalensis*, Histology and Histopathology 16, 511-21.

Armesto, P., Campinho, M.A., Rodriguez-Rua, A., Cousin, X., Power, D.M., Manchado, M., Infante, C., 2014. Molecular characterization and transcriptional regulation of the Na +/K+ ATPase alpha subunit isoforms during development and salinity challenge in a teleost fish, the Senegalese sole (*Solea senegalensis*). Comparative biochemistry and physiology. Part B, Biochemistry & Molecular biology 175, 23-38.

Bolker, J.A., Hill, C.L., 2000. Pigmentation development in hatchery-reared flatfishes. Journal of Fish Biology 56.

Campinho, M.A., Silva, N., Sweeney, G.E., Power, D.M., 2007. Molecular, cellular and histological changes in skin from a larval to an adult phenotype during bony fish metamorphosis, Cell and Tissue Research 327, 267-84.

Campinho, M.A., Galay-Burgos, M., Silva, N., Costa, R.A., Alves, R.N., Sweeney, G.E., Power, D.M., 2012. Molecular and cellular changes in skin and muscle during metamorphosis of Atlantic halibut (*Hippoglossus hippoglossus*) are accompanied by changes in deiodinases expression, Cell and Tissue Research 350, 333-46.

Cole, A.M., Weis, P., Diamond, G., 1997. Isolation and characterization of pleurocidin, an antimicrobial peptide in the skin secretions of winter flounder. The Journal of Biological Chemistry 272, 12008-12013.

Cone, R., 1999. Mucus, in: P.L. Ogra, Mestecky, L., Lamm, M. E., Strober, W., Bienestock, J., McGhee, J. R. Eds (Ed.), Mucosal Immunology. Academic Press, London, UK, 43-64.

Damjanovski, S., Huynh, M.H., Motamed, K., Sage, E.H., Ringuette, M., 1998. Regulation of SPARC expression during early Xenopus development: evolutionary divergence and conservation of DNA regulatory elements between amphibians and mammals, Development Genes and Evolution 207, 453-61.

Delany, A.M., Kalajzic, I., Bradshaw, A.D., Sage, E.H., Canalis, E., 2003. Osteonectin-null mutation compromises osteoblast formation, maturation, and survival, Endocrinology. 144, 2588-96.

Delany, A.M., Amling, M., Priemel, M., Howe, C., Baron, R., Canalis, E., 2000. Osteopenia and decreased bone formation in osteonectin-deficient mice, The Journal of Clinical Investigation 105, 915-23.

Diaz, J.P., Prié-Granié, M., Kentouri, M., Varsamos, S., Connes, R., 2003. Development of the lateral line system in the sea bass. Journal of Fish Biology 62, 24-40.

Diaz, A.O., Escalante, A.H., Garcia, A.M., Goldemberg, A.L., 2006. Histology and histochemistry of the pharyngeal cavity and oesophagus of the silverside *Odontesthes bonariensis* (Cuvier and Valenciennes), Anatomia, Histologia, Embryologia 35, 42-6.

Domeneghini, C., Arrighi, S., Radaelli, G., Bosi, G., Veggetti, A., 2005. Histochemical analysis of glycoconjugate secretion in the alimentary canal of *Anguilla anguilla* L, Acta Histochemica 106, 477-87.

El-Gamal, A.E.E., 2009. Effect of Temperature on Hatching and Larval Development and Mucin Secretion in Common Carp, *Cyprinus carpio* (Linnaeus, 1758) Global Veterinaria 3, 80-90.

Elliott, D.G., 2011. Functional Morphology of the Integumentary System in Fishes, in: A.P. Farrell (Ed.), Encyclopedia of Fish Physiology: From Gene to Environment. Academic Press, 476-488.

Einarsdóttir, I.E., Power, D.M., Jonsson, E., Bjornsson, B.T., 2011. Occurrence of ghrelin-producing cells, the ghrelin receptor and Na^+,K^+-ATPase in tissues of Atlantic halibut (*Hippoglossus hippoglossus*) during early development, Cell and Tissue Research 344, 481-98.

Esteben, M.A., 2012. An Overview of the Immunological Defenses in Fish Skin. International Scholarly Research Network Immunology, 1-29

Esteban, M.A., Cerezuela, R., 2015. Fish mucosal immunity: skin, in: B.H. Beck and E. Peatman Eds (Ed.), Mucosal Health in Aquaculture. Academic Press, 67-92

Estevão, M.D., Redruello, B., Canario, A.V., Power, D.M., 2005. Ontogeny of osteonectin expression in embryos and larvae of sea bream (*Sparus auratus*), General and Comparative Endocrinology 142, 155-62.

Failde, L.D., Bermudez, R., Vigliano, F., Coscelli, G.A., Quiroga, M.I., 2014. Morphological, immunohistochemical and ultrastructural characterization of the skin of turbot (*Psetta maxima* L.), Tissue Cell 46, 334-42.

Fishelson, L. Bresler, V., 2002. Comparative studies of the development and differentiation of chloride cells in tilapine fish with different reproductive styles, Journal of Morphology 253, 118-31.

Fletcher, T.C., Jones, R., Reid, L., 1976. Identification of glycoproteins in goblet cells of epidermis and gill of plaice (*Pleuronectes platessa* L.), flounder (*Platichthys flesus* (L.)) and rainbow trout (*Salmo gairdneri* Richardson), The Histochemical Journal 8, 597-608.

Gendler, S.J., Spicer, A.P., 1995. Epithelial Mucin Genes, Annual Review of Physiology 57, 607-634

Gomez, D., Sunyer, J.O., Salinas, I., 2013. The mucosal immune system of fish: the evolution of tolerating commensals while fighting pathogens. Fish and shellfish immunology 35, 1729-1739.

Grass, G.M., Sweetana, S.A., 1988. *In vitro* measurement of gastrointestinal tissue permeability using a new diffusion cell. Pharmaceutical Research 5, 372–376.

Gray, T., Koo, J.S., Nettesheim, P., 2001. Regulation of mucous differentiation and mucin gene expression in the tracheobronchial epithelium, Toxicology 160, 35-46.

Hachero-Cruzado, I., Ortiz-Delgado, J.B., Borrega, B., Herrera, M., Navas, J.I., Sarasquete, C., 2009. Larval organogenesis of flatfish brill *Scophthalmus rhombus* L: Histological and histochemical aspects. Aquaculture 286, 138-149.

Hamre, K., Holen, E., Moren, M., 2007. Pigmentation and eye migration in Atlantic halibut (*Hippoglossus hippoglossus* L.) larvae: new findings and hypotheses. Aquaculture Nutrition 13, 65-80.

Harboe, T., Mangor-Jensen, A., Naas, K.E, Næss, T., 1998. A tank design for first feeding of Atlantic halibut, *Hippoglossus hippoglossus* L., larvae. Aquaculture Research 29, 919–923.

Henrikson, R.C., Matoltsy, A.G., 1968. The fine structure of teleost epidermis. II. Mucous cells. Journal of Ultrastructure Research 21, 222–232.

Harris, J.E., Hunt, S., 1975. The fine structure of the epidermis of two species of salmonid fish, the Atlantic salmon (*Salmo salar* L.). and the brown trout (*Salmo trutta* L.). Cell and Tissue Research 163, 535-543.

Hiroi, J., Kaneko, T., Seikai, T., Tanaka, M., 1998. Developmental Sequence of Chloride Cells in the Body Skin and Gills of Japanese Flounder (*Paralichthys olivaceus*) Larvae, Zoological Sciwnces 15, 455-60.

Hwang, P.P., 1989. Distribution of chloride cells in teleost larvae, Journal of Morphology 200, 1-8.

Ishida, Y., Suzuki, K., Utoh, R., Obara, M., Yoshizato, K., 2003. Molecular identification of the skin transformation center of anuran larval skin using genes of Rana adult keratin (RAK) and SPARC as probes, Development Growth and Differentiation 45, 515-26.

Jeong, G.M., 2008. A study on the epidermal structure and mucosubstance histochemistry of spotty belly, devil stinger, stone fish, cubed Snailfish, and Japanese bluefish, Animal Cells and Systems 85-91.

Jeong, G.M., Jo, U.B., 2007. Mucosubstance histochemistry of the epidermis in Yellowtail, Striped Beakperch, Brown Spotted Grouper, Sea Chub, and Multicolorfin Rainbowfish, Integrative Biosciences 11, 183-189.

Kalogianni, E., Alexis, M., Tsangaris, C., Abraham, M., Wendelaar Bonga, S.E., Iger, Y., van Ham, E.H., Stoumboudi, M.T., 2011. Cellular responses in the skin of the gilthead sea bream Sparus aurata L. and the sea bass *Dicentrarchus labrax* (L.) exposed to high ammonia, Journal of Fish Biology. 78, 1152-69.

Kaneko, T., Shiraishi, K., Katoh, F., Hasegawa, S., Hiroi, J., 2002. Chloride cells during early life stages of fish and their functional differentiation, Fisheries Science 68, 1-9.

Katoh, F., Shimizu, A., Uchida, K., Kaneko, T., 2000. Shift of chloride cell distribution during early life stages in seawater-adapted killifish (*Fundulus heteroclitus*). Zoological Science 17, 11–18.

Ledy, K., Giamberini, L., Pihan, J.C., 2003. Mucous cell responses in gill and skin of brown trout *Salmo trutta* fario in acidic, aluminium-containing stream water, Diseases of Aquatic Organisms 56, 235-40.

Lev, R., Spieer, S.S., 1964. Specific staining of sulphate groups with alcian blue at low pH. Journal of Histochemistry and Cytochemistry 12, 309.

Marshall, W.S., Singer, T.D., 2002. Cystic fibrosis transmembrane conductance regulator in teleost fish, Biochimica et Biophysica Acta 1566, 16-27.

Matsumoto, J., Seikai, T., 1992. Asymmetric pigmentation and pigment disorders in pleuronectiformes (flounders). Pigment cell research / sponsored by the European Society for Pigment Cell Research and the International Pigment Cell Society Suppl 2, 275-282.

McManus, J.F.A., 1946. Histological demonstration of mucin after periodic acid. Nature 158, 202

McMenamin, S.K., Parichy, D.M., 2013. Chapter Five – Metamorphosis in Teleosts, in: S. Yun-Bo (Ed.), Current Topics in Developmental Biology. Academic Press, 127-165.

Miwa, S., Yamano, K., Inui, Y., 1992. Thyroid hormone stimulates gastric development in flounder larvae during metamorphosis. Journal of Experimental Zoology 261, 424-430.

Mowry, R.W., 1956. Alcian blue techniques for histochemical study and acid carbohydrates. Journal of Histochemistry and Cytochemistry 4, 407.

Murray, H.M., Hew, C.L., Fletcher, G.L., 2003. Spatial expression patterns of skin-type antifreeze protein in winter flounder (*Pseudopleuronectes americanus*) epidermis following metamorphosis, Journal of Morphology 257, 78-86.

Olsen, Y., Evjemo, J.O., Olsen, A., 1999. Status of the cultivation technology for production of Atlantic halibut (*Hippoglossus hippoglossus*) juveniles in Norway/Europe, Aquaculture 176, 3-13

Ottensen, O.H., Olafsen, J.A., 1997. Ontogenetic development and composition of the mucous cells and the occurrence of saccular cells in the epidermis of Atlantic halibut, Journal of Fish Biology 50, 620–633.

Padra, J.T., Sundh, H., Jin, C., Karlsson, N.G., Sundell, K., Lindén, S.K., 2014. Aeromonas salmonicida binds differentially to mucins isolated from skin and intestinal regions of Atlantic salmon in an N-acetylneuraminic acid-dependent manner. Infection and Immunity 82, 5235-45

Park, J., Kim, S., 2001. Histology and mucin histochemistry of the gastrointestinal tract of the mud loach, in relation to respiration, Journal of Fish Biology 58, 861-872.

Park, J.Y., Lee, Y.J., Kim, I.S. and Kim, S.Y., 2003. A comparative study of the regional epidermis of an amphibious mudskipper fish, *Boleophthalmus pectinirostris* (Gobiidae, Pisces), Folia Zoologica 52, 431-440.

Pearse, A. G. E., 1985. Histochemistry - Theoretical and Applied, Churchill Livingstone.

Perez-Vilar, J., Hill, R.L., 1999. The structure and assembly of secreted mucins. The Journal of Biological Chemistry 274, 31751-31754.

Pérez-Sánchez, J., Estensoro, I., Redondo, M.J., Calduch-Giner, J.A., Kaushik, S., Sitja-Bobadilla, A., 2013. Mucins as diagnostic and prognostic biomarkers in a fish-parasite model: transcriptional and functional analysis, PLoS One 8, e65457.

Pisam, M., Rambourg, A., 1991. Mitochondria-rich cells in the gill epithelium of teleost fishes: an ultrastructural approach. International Review of Cytology 130, 191-232.

Power, D.M., Einsarsdóttir, I. E., Pittman, K., Sweeney, G. E., Hildahl, J., Campinho, M. A., Silva, N., Saele, O., Galay-Burgos, M., Sráradóttir, H., Bjornsson, B. T., 2008. The Molecular and Endocrine Basis of Flatfish Metamorphosis, Reviews in Fisheries Science 16, 95-111.

Proksch, E., Brandner, J.M., Jensen, J.M., 2008. The skin: an indispensable barrier. Experimental Dermatology 17, 1063-1072.

Rai, A.K., Srivastava, N., Kumari, U., Mittal, S., Mittal, A.K., 2012. Histochemical analysis of glycoproteins in the secretory cells in the epidermis of the head skin of Indian Major Carp, *Labeo rohita*, Tissue and Cell 44, 409-17.

Rakers, S., Gebert, M., Uppalapati, S., Meyer, W., Maderson, P., Sell, A.F., Kruse, C., Paus, R., 2010. 'Fish matters': the relevance of fish skin biology to investigative dermatology. Experimental Dermatology 19, 313-324.

Renn, J., Winkler, C., Schartl, M., Fischer, R., Goerlich, R., 2006. Zebrafish and medaka as models for bone research including implications regarding space-related issues, Protoplasma 229, 209-14.

Roberts, R.J., Bell, M., Young, H., 1973. Studies on the skin of plaice (*Pleuronectes platessa* L.). II. The development of larval plaice skin, Journal of Fish Biology 5, 103-108.

Rotllant, J., Liu, D., Yan, Y.L., Postlethwait, J.H., Westerfield, M., Du, S.J., 2008. Sparc (Osteonectin) functions in morphogenesis of the pharyngeal skeleton and inner ear, Matrix Biololgy 27, 561-72.

Sadovy, Y., Randall, J.E., Rasotto, M.B., 2005. Skin structure in six dragonet species (Gobiesociformes; Callionymidae): interspecific differences in glandular cell types and mucus secretion, Journal of Fish Biology 66, 1411-1418.

Sæle, Ø., Solbakken, J.S., Watanabe, K., Hamre, K., Power, D., Pittman, K., 2004. Staging of Atlantic halibut (*Hippoglossus hippoglossus* L.) from first feeding through metamorphosis, including cranial ossification independent of eye migration. Aquaculture 239, 445-465.

Sarasquete, C., Gisbert, E., Ribeiro, L., Vieira, L., Dinis, M.T., 2001. Glyconjugates in epidermal, branchial and digestive mucous cells and gastric glands of gilthead sea bream, *Sparus aurata*, Senegal sole, *Solea senegalensis* and Siberian sturgeon, *Acipenser baeri* development, European Journal of Histochemistry. 45, 267-78.

Sarasquete, C., Gonzalez de Canales, M.L., Arellano, J., Munoz Cueto, J.A., Ribeiro, L., Dinis, M.T., 1998. Histochemical study of skin and gills of Senegal sole, *Solea senegalensis* larvae and adults, Histology Histopathology 13, 727-35.

Sasai, S., Kaneko, T., Tsukamoto, K., 1998. Extrabranchial chloride cells in early life stages of the Japanese eel, *Anguilla japonica*, Ichthyology Research 45, 95– 98.

Schreiber, A.M., Specker, J.L., 2000. Metamorphosis in the summer flounder, *Paralichthys dentatus*: thyroidal status influences gill mitochondria-rich cells, General and Comparative Endocrinology 117, 238-50.

Schreiber, A.M., Wang, X., Tan, Y., Sievers, Q., Sievers, B., Lee, M., Burrall, K., 2010. Thyroid hormone mediates otolith growth and development during flatfish metamorphosis. General and Comparative Endocrinology 169, 130-137.

Senol, N., 2014. Identification of Glycoproteins in Mucous Cells of Epidermis and Gill of *Tinca tinca* Linnaeus, 1758 (Cypriniformes: Cyprinidae), YYU Veteriner Fakultesi Dergisi 25, 47-49.

Shephard, K.L., 1994. Functions for fish mucus, Rev. Fish Biol. Fish. . 4, 401-429.

Subramanian, S., MacKinnon, S.L., Ross, N.W., 2007. A comparative study on innate immune parameters in the epidermal mucus of various fish species. Comparative Biochemistry and Physiology. Part B, Biochemistry and Molecular Biology 148, 256-263.

Sundell, K., Sundh, H., 2012. Intestinal fluid absorption in anadromous salmonids: importance of tight junctions and aquaporins. Frontiers in Physiology 3, 1-13.

Termine, J.D., Belcourt, A.B., Conn, K.M. and Kleinman, H.K., 1981. Mineral and collagen-binding proteins of fetal calf bone, The Journal of Biological Chemistry 256, 10403-8.

Tsutsui, S., Komatsu, Y., Sugiura, T., Araki, K., Nakamura, O., 2011. A unique epidermal mucus lectin identified from catfish (*Silurus asotus*): first evidence of intelectin in fish skin slime. Journal of Biochemistry 150, 501-514.

van der Heijden, A.J., van der Meij, J.C., Flik, G., Wendelaar Bonga, S.E., 1999. Ultrastructure and distribution dynamics of chloride cells in tilapia larvae in fresh water and sea water, Cell and Tissue Research 297, 119-30.

van der Marel M., Caspari, N., Neuhaus, H., Meyer, W., Enss, M.L., Steinhagen, D., 2010. Changes in skin mucus of common carp, *Cyprinus carpio* L., after exposure to water with a high bacterial load. Journal of Fish Diseases 33, 431–439.

Varsamos, S., Diaz, J.P., Charmantier, G., Blasco, C., Connes, R. and Flik, G., 2002. Location and morphology of chloride cells during the post-embryonic development of the european sea bass, *Dicentrarchus labrax*, Anatomy and embryology 205, 203-13.

Varsamos, S., Nebel, C., Charmantier, G., 2005. Ontogeny of osmoregulation in postembryonic fish: a review. Comparative Biochemistry and Physiology. Part A, Molecular and Integrative Physiology 141, 401-429.

Wilson, J.M., Laurent, P., 2002. Fish gill morphology: inside out, Journal of Experimental Zoology 293, 192-213.

Witten, P.E., Hall, B.K., 2003. Seasonal changes in the lower jaw skeleton in male Atlantic salmon (*Salmo salar* L.): remodelling and regression of the kype after spawning. Journal of Anatomy 203, 435–450.

Yamashita, K., 1978. Chloride cells in the skin of the larval red seabream *Pagrus major*, Japanese Journal of Ichthyology 25, 211-215

Yanagie, R., Lee, K.M., Watanabe, S., Kaneko, T., 2009. Ontogenic change in tissue osmolality and developmental sequence of mitochondria-rich cells in Mozambique tilapia developing in freshwater. Comparative Biochemistry and Physiology. Part A, Molecular and Integrative Physiology 154, 263-269.

Yashpal, M., Kumari, U., Mittal, S., Mittal, A.K., 2007. Histochemical characterization of glycoproteins in the buccal epithelium of the catfish, *Rita rita*, Acta Histochemica 109, 285-303.

Yashpal, M., Mittal, A.K., 2014. Serous goblet cells: the protein secreting cells in the oral cavity of a catfish, *Rita rita* (Hamilton, 1822) (Bagridae, Siluriformes), Tissue Cell. 46, 9-14.

Chapter 5

Asymmetric thyroid hormone responsiveness of ocular and abocular skin associated with changing pigmentation during flatfish metamorphosis

Chapter 5

Abstract

Metamorphosis in flatfish is a post-embryonic event driven by thyroid hormones (THs) and their involvement in skin development has been recently described. The present study focused on the mechanisms underlying the TH responsiveness of skin and the asymmetry in pigmentation arising during metamorphosis in ocular and abocular skin during Atlantic halibut metamorphosis. Genes involved in TH metabolism (deiodinases), transport (monocarboxylate transporters) and action (THs receptors), and genes involved in melanogenesis (tyrosinase related protein 1, *tyrp1* and dopachrome tautomerase, *dct*) and regulation of skin pigmentation, agouti signalling protein (*asip*), proopiomelanocortin beta (*pomcβ*) and SRY (sex determining region Y)-box 10 (*sox10*) were targeted. We also investigated the potential cross-talk during skin maturation and pigmentation of the thyroid and stress axis and their role in abnormal pigmentation using respectively, methimazole (MMI) and RU486. The selected genes involved in TH signalling and pigmentation were expressed in ocular and abocular skin during metamorphosis and *dio3b*, *trβ*, *mct8*, *mct10*, *dct*, *tyrp1* and *sox10* were differentially expressed during the prometamorphosis and the metamorphic climax. The expression of TH receptors and deiodinases (*dio1*, *dio2*, *dio3a*, *dio3b*, *trαa* and *trβ*) in skin was symmetric during metamorphosis, but expression of the TH transporters (*mct8*, *mct10*) was asymmetric during metamorphosis. Genes involved in melanogenesis (*tyrp1*, *dct*) and regulation of pigmentation (*sox10*) had an asymmetric expression in skin during metamorphosis. MMI and RU486 had a similar effect on metamorphosis and both modified the thyroid signalling pathway and during the metamorphic climax caused significant up-regulation of *trβ* in the ocular skin and *mct8*, *mct10*, *tyrp1*, *dct* and *sox10* in the abocular skin relative to untreated fish. This study contributes to a better understanding of the molecular basis of the asymmetric pigmentation observed during metamorphosis in Atlantic halibut and reveals a central role for the thyroid axis. We also hypothesize that cross-talk between the thyroid and cortisol axis occurs during metamorphosis and that both THs and cortisol act synergistically in modulating the changes in skin during halibut metamorphosis.

Keywords: metamorphosis, skin development, THs, cortisol, asymmetry, pigmentation

Chapter 5

5.1. Introduction

Metamorphosis in vertebrates is a post-embryonic event driven by thyroid hormones (THs; thyroxin - T_4 and 3,5,3'-triiodothyronine - T_3) and is accompanied by modifications in morphology, physiology, behaviour, habitat and feeding mode (Laudet, 2011). In flatfish, the transformation of the pelagic symmetric larva into a benthic asymmetric juvenile is accompanied by a dramatic change in external morphology that leads to asymmetry in the head and body pigmentation and resorption of the elongated dorsal fin ray (reviewed by Power et al., 2008).

A characteristic feature of flatfish metamorphosis is the peak in THs that accompanies the climax of metamorphosis (Campinho et al., 2012a; Einarsdóttir et al., 2006; Iziga et al., 2010; Sun et al., 2015). The THs are obligatory for metamorphosis since inhibition of their production using thiourea (TU) or methimazole (MMI) blocks metamorphosis (Campinho et al., 2015; Inui and Miwa, 1985, Schreiber and Specker, 2000; Schreiber et al., 2010). THs bring about their action after they enter the cell via specific membrane transporters, monocarboxylate transporters MCT8 and MCT10 (Visser et al., 2011) and bind to nuclear thyroid hormone receptors (TRs) that trigger gene transcription and a plethora of changes in the structure, maturation and function of tissues and organs (reviewed by Power et al., 2008). The biologically active form of the hormone T_3 is generated in the periphery from T_4 through the action of a family of iodothyronine deiodinases (DIO), that also inactivate THs (Bianco et al., 2002).

The TH axis is not the only endocrine system active during metamorphosis and other endocrine axis such as the hypothalamus-pituitary–interrenal axis (HPI) that produces cortisol in teleost fish is also active and may have a role during flatfish metamorphosis (Einarsdóttir et al., 2006; de Jesus et al., 1990). Evidence supporting a direct role of cortisol in fish metamorphosis is inconclusive, but cortisol levels peak at climax during metamorphosis of the Japanese flounder (*Paralichthys olivaceus*) (de Jesus et al., 1991) and cortisol enhances the effect of THs on dorsal fin ray resorption *in vitro* in the Japanese flounder (de Jesus et al., 1990). In the threadfin, cortisol treatment causes early maturation of gut and somatic pigmentation (Brown and Kim, 1995) and corticotropin injections produce partial metamorphosis in ammocoetes (larval lamprey, Youson, 1988). The importance of peripheral thyroid/corticoid interactions are well established in the regulation of amphibian

metamorphosis (reviewed by Denver, 2013). In anurans, reptiles and birds the cross-talk between the HPT and HPA axis is well established and corticotropin releasing hormone (CRH) rather than thyrotropin releasing hormone (TRH) regulates thyrotropin (TSHβ) secretion and T_4 serum levels (Denver, 2013; de Groef et al., 2006). The cross-talk between the thyroid axis and the HPI axis is relatively poorly studied during flatfish metamorphosis but observations about its possible role make it a relevant target.

A fascinating metamorphic remodelling process in flatfish that involves asymmetry is the development and pigmentation of the skin (reviewed in Power et al., 2008). In flatfish metamorphosis the skin changes from a very thin epithelium to a highly stratified, pigmented epidermis in the fully metamorphosed juvenile. The availability of THs in the skin during metamorphosis is modulated by the coordinated action of deiodinases (Campinho et al., 2007, 2012). The pigmentation pattern of skin in fish arises from the maturation of neural crest-derived chromatophores, the melanophores, xantophores, leucophores and iridophores (Burton, 2010). Large sized larval type melanophores appear sporadically and bilaterally on both sides of the skin around hatching and small sized adult type melanophores, appear numerously only on the ocular side at the latest stage of metamorphosis (Burton, 2010; Nakamura et al., 2010). Recently the pivotal role of THs in the formation of the adult pigment cell lineages and pigment pattern phenotype in teleosts was revealed (McMenamin et al., 2014). However, the molecular basis of skin pigmentation during flatfish metamorphosis has been poorly described.

Melanogenesis in fish is similar to what has been described in mammals and occurs in the melanophores inside the melanosomes, by the action of melanogenic enzymes (reviewed by Lin and Fisher, 2007; Yamaguchi et al., 2007). Several genes have been described that are involved in the direct or indirect regulation of pigmentation such as microphtalmia-associated transcription factor (Mitf), agouti signaling protein (Asip), SRY-related HMG-box 10 (Sox10) and paired box protein 3 (Pax3), (Cerdá-Reverter et al., 2005; Ebanks et al., 2009; Hunt and Thody, 1995; Wegner, 2006). Recently, Darias et al., (2013a) associated the morphological ontogeny of skin pigmentation with the expression profile of genes involved in pigmentation in Senegalese sole (*Solea senegalensis*) during metamorphosis. They observed that the melanophore, xanthophore and iridophore populations only changed in the post-metamorphic stage (Darias et al., 2013a). Three different biological processes were found to act cooperatively during pigmentation development: tissue remodeling (involving apoptosis),

differentiation of chromatophores and pigment production. During metamorphosis genes involved in these biological processes are highly expressed, but their expression levels decreased after metamorphosis (Darias et al., 2013a). However, the molecular basis of the asymmetric pigmentation pattern in skin that is characteristic of metamorphosis was not established.

Moreover, abnormal pigmentation is an important issue for flatfish aquaculture and the hypomelanosis (pseudoalbinism) and hypermelanosis (ambicoloration) are considered the main pigmentation related problems, (reviewed in Power et al., 2008). In the present study we took advantage of the large size of Atlantic halibut larvae (*Hippoglossus hippoglossus*) to collect samples of ocular and abocular (blind) skin from individual larvae and analyze the molecular players behind the asymmetric pigmentation that develops during metamorphosis. The expression profile of genes involved in TH transport (monocarboxylate transporter 8 – *mct8*, monocarboxylate transporter 10 – *mct10*), action (thyroid hormone receptor alpha A – *trαa* and thyroid hormone receptor beta – *trβ*) and metabolism (deiodinase 1 - *dio1*, deiodinase 2 - *dio2*, deiodinase 3A - *dio3a*, deiodinase 3B *dio3b*), as well as pigmentation related genes (melanogenic enzymes: tyrosinase related protein 1 - *tyrp1*, dopachrome tautomerase – *dct*; regulation of pigmentation: agouti signalling protein - *asip*, proopiomelanocortin beta – *pomcβ*, SRY (sex determining region Y)-box 10 - *sox10*) were analysed in both ocular and abocular skin of Atlantic halibut (*Hippoglossus hippoglossus*) during normal larval development. Furthermore, the involvement of the HPT and HPI axis in skin maturation and pigmentation was further verified by blocking TH production with methimazol (MMI, a thyroid peroxidase inhibitor, Campinho et al., 2015; Schreiber et al., 2010) or mifepristone (RU486), an antagonist of cortisol (Alderman et al., 2012).

5.2. Material and methods

5.2.1. Animals, experimental design and sampling

The experiments with Atlantic halibut larvae were performed at the Institute of Marine Research (IMR) Austevoll, Norway. The experiments were covered by a Norwegian Food Safety Authority facility (licence n. 093; experiment approval n. 4395). The Food Safety

Authority handles everything connected with animal welfare and experimental animals in Norway.

Atlantic halibut larvae, 10 days post first feeding (dpff), were reared at the Institute of Marine Research (IMR, Austevoll, Norway) using standard procedures (Harboe et al., 1998). Thereafter, larvae were transferred to the experimental system that consisted of 6, 1000 l, PVC conical cylindrical tanks (diameter: 1.5 m; height: 1 m; water depth: 87 cm) with a circular water flow and a central standpipe, and maintained with a continuous flow of seawater kept at around 0.3 $l.min^{-1}$ and the oxygen level at full saturation. Water temperature was maintained at 12.2 ± 0.7 ºC (mean ± SD) and continuous daylight was used throughout the experiment. Larvae were fed live *Artemia* twice daily (Olsen et al., 1999). The tanks were cleaned with a siphon each day and mortalities were registered. After two days of acclimation, fish larvae were exposed to MMI (3 mM; Sigma-Aldrich, Ref. M8506) or RU486 (0.15 µM; Sigma-Aldrich, Ref., M8046). Duplicate experimental tanks were used and treatments were initiated 12 days post start feeding (dpsf) by incorporating the chemicals (MMI or RU486) into the *Artemia*. In brief, MMI and RU486 were dissolved in DMSO and introduced into the lipid/vitamin mix used to enrich the artemia for 60 minutes prior to larval feeding. The *Artemia* administrated to the control groups contained an equivalent volume of DMSO to that used in the treatments previously described (chapter 3). It was not possible to confirm the concentration of MMI and RU486 taken up by the artemia, but in previous experiments with T_4 (3-4-hydroxy-3,5-diiodophenoxy-3,5-diiodophenyl-L-alanine, Sigma T2501, 1 mg ml^{-1}) enriched *Artemia* contained 2 µg T_4 g^{-1} wet weight.

Regular sampling was performed to obtain larvae at several different development stages. For sampling, fish larvae were euthanized with a lethal dose of ethyl 3-aminobenzoate methanesulfonate salt (MS-222, Sigma-Aldrich, Spain). Sampled larvae were photographed (Ixus 115 HS, Canon), and staging was performed using mytome height (MH) and standard length (SL) (Alves et al., 2016; Sæle et al., 2004). Individual larvae were collected into RNAlater (Life Technologies, Carlsbad, USA), gently agitated for 24h at 4 °C and then transferred to −20ºC for long term storage or fixed in formaldehyde (5%).

5.2.2. RNA extraction and cDNA synthesis

The following metamorphic stages of Atlantic halibut were used in this experiment: prometamorphosis (stage 7), proclimax metamorphosis (stage 8) and metamorphic climax (stages 9A and 9B). The ocular (top side, designated skin top - ST) and abocular (bottom side, designated skin bottom – SB) skin were dissected from five larvae per stage. Total RNA was extracted using a Maxwell® 16 Total RNA Purification Kit system (Promega, Madison, USA) following the manufacturer's instructions. To avoid genomic DNA contamination, 5 µg of total RNA was treated with a DNA-free Turbo DNase Treatment and Removal kit (Ambion, Life Technologies, Carlsbad, USA), according to the manufacturer's guidelines.

The cDNA synthesis was performed using 500 ng DNAse treated total RNA, 200 ng of random hexamers (GE Healthcare, Amersham, UK), 100 U of RevertAid M-MuLV Reverse Transcriptase (Fermentas, St Leon-Rot, Germany), 8 U of Ribolock RNase inhibitor (Fermentas, St Leon-Rot, Germany), and 0.5 mM dNTP's in the Mycler thermocycler (Bio-Rad, Marnes La Coquette, France). A cDNA negative control reaction without reverse transcriptase was also performed.

5.2.3. Real-time quantitative PCR (qPCR)

Thirteen genes involved in the TH cascade (metabolism, transport and action), stress axis and pigmentation (melanogenesis and pigmentation regulation) were selected (Alves et al. 2016). Genes involved in the TH axis include: thyroid hormone receptor alpha A (*trαa*), thyroid hormone receptor beta (*trβ*), monocarboxylate transporter 10 (*mct10*), monocarboxylate transporter 8 (*mct8*), deiodinase 1 (*dio1*), deiodinase 2 (*dio2*), deiodinase 3A (*dio3a*) and deiodinase 3B (*dio3b*). Genes involved in the pigmentation axis used in this study include: tyrosinase related protein 1 (*tyrp1*), dopachrome tautomerase (*dct*), agouti signaling protein (*asip*) and SRY (sex determining region Y)-box 10 (*sox10*). A single gene proopiomelanocortin beta (*pomcβ*) was used to monitor the stress axis. 40S ribosomal protein S4 (*rps4*) and elongation factor I alpha (*ef1a1*) were used as reference genes. Specific primers were designed using Beacon Design and Primer Premier 5.0 software (Premier Biosoft Int.,

Palo Alto, CA). Primers sequences and the biological role of all analyzed genes are shown in **Table 5.1**.

qPCR reactions were performed in duplicate using SsoFast™ EvaGreen® Supermix (Bio-Rad, Marnes La Coquette, France) chemistry in a StepOnePlus™ Real-Time PCR System (Applied Biosystems, Foster City, USA). The qPCR conditions were 30 sec at 95 ºC; 45 cycles of 5 sec at 95 ºC and 10 sec at the optimal temperature for each primer pair (**Table 5.1**). A final melting curve ranging from 60-95 ºC was performed for all reactions, and for each qPCR assay, a no-template control was included. PCR products were quantified relative to a standard curve constructed using a 10-fold stepwise dilution series (initial concentration of 108 copies amplicon/µl) of the target gene plasmid (cloned into pGEM®-T Easy, Promega, Madison, USA). The qPCR efficiency for primer pairs ranged between 89 % and 100 % with a $R^2 \geq 0.992$ (**Table 5.1**). PCR products were analyzed by agarose gel electrophoresis to confirm that single reaction products were obtained and sequenced to confirm primer specificity. The geometric mean of the reference genes *rps4* and *ef1a1* was used to normalize the qPCR data.

Table 5.1: Sequences of the specific primers used for qPCR gene expression analysis. Gene symbol, name and function are shown. The annealing temperature (Ta; ºC), amplicon length (bp), R^2 and qPCR efficiency (%) are indicated for each primer pair.

Gene symbol	Gene name	Biological role	Primer sequence(5'→3')	Annealing temperature (Ta)	Amplicon length	R^2	PCR efficiency
trαa	Thyroid receptor alpha A	THs receptor activity	F: GAATCGGGAGAAGAGGAAGCG R: GACCCTGACCGATATCATCCGA	62	179	0.995	90%
trβ	Thyroid receptor beta		F: CAAGCGTCCATGGCAAATACAC R: CAAAGTCCACCACTCGGGTT	62	106	0.993	100%
mct8	Monocarboxylate transporter 8	Transport of iodo-thyronines (T_3 and T_4)	F: TTCGGCTGGCTGGTGGTGCTC R: CGTCTGGGTCTGCGTGCTCCTTC	60	115	0.994	90%
mct10	Monocarboxylate transporter 10	Aromatic amino acid transporter. Can transport THs	F: GCTCCGAGAACGATGACGAC R: GTGAAGACGCTGACGATGG	60	100	0.994	96%
dio1	Deiodinase 1	Activation and inactivation of THs by deiodination	F: CCAAAAACTCCTCGTCTATGTCT R: CTTGGTGAGGCTTGGTGAAATAA	60	108	0.997	89%
dio2	Deiodinase 2	Major role in activation of THs by deiodination	F: TGGACGCATACAAGCAGGTG R: TGGCACATTGGTCACATTACTG	60	106	0.994	95%
dio3a	Deiodinase 3a		F: ACTCCAGATAGATAGATTGTGTC R: TAAACAAACCTTTTTTTCCTGAA	60	178	0.992	100%
dio3b	Deiodinase 3b	Major role in inactivation of THs by deiodination	F: GCCGCTGCTCTGCCCATTC R: GGAGAGAGGCTTCAACCTGACTTC	62	162	0.995	96%
tyrp1	Tyrosinase related protein 1	Melanin synthesis	F: GCACCGACGACCTGATGG R: CATAGTCCTCCACGCTCTCGC	62	108	0.996	100%
dct	Dopachrome tautomerase		F: GCCCAGTTTCCACGAGTATG R: GACAGAGAGCCGCACACG	62	101	0.996	99%
asip	Agouti signaling protein	Antagonist of melanocortin receptors	F: TTTCTGTGCCTTCTGCCAGTG R:CAGCGAGGGTTGCCCATT	62	69	0.994	89%
pomcβ	Proopiomelanocortin beta	Precursor of melanocyte stimulating hormones	F: GCCTCCAGCGAAGACAAG R: CCTCCAGAGATGACATGAAGAC	62	138	0.994	100%
sox10	SRY (sex determining region Y)-box 10	Survival and differentiation of the melanocytes	F: CTTCCTCACTACAGTTCTGCTTT R: GGCGGGTCGCTGATGGG	60	183	0.994	89%
rps4	40S ribosomal protein S4	Structural component of the small 40S ribosomal subunit	F: CAAGTTTGATACTGCCAACCTGTG R: GGAGAGCCTGGTAGCGAAGC	60	172	0.997	98%
ef1a1	Elongation factor 1 alpha	Protein synthesis	F: AAGAGGACCATCGAGAAGTT R:GTCTCAAACTTCCACAGAGC	60	140	0.994	99%

5.2.4. Statistical analysis

Statistical significance of the relative gene expression between metamorphic stages and treatments (CTRL, MMI, RU486) for each skin side (ocular (ST) and abocular (SB) were conducted using SigmaStat v3.5 (Systat Software, Inc., CA, USA). Two-way ANOVA was performed after checking for normality (Shapiro-Wilk W-test) and homogeneity of variance (Levene's F-test) for the following comparisons: metamorphic stages and experimental treatments (for ST and SB); metamorphic stages and ST and SB (for each experimental treatment). Tukey's post-hoc test was used for pair wise multiple comparisons. Data was log-transformed to achieve normal distribution. When the normality test failed, ANOVA by Ranks followed by Dunn's test for pairwise comparisons was performed. Statistical significance was established at $p < 0.05$. Gene expression levels are presented as the mean ± standard error of the mean (SEM). Pearson correlation analysis was used to compare the selected genes in both ST and SB using the qPCR relative gene expression levels. For correlation analysis, 13 genes were selected and statistical significance was established at $p < 0.05$.

5.3. Results

5.3.1. Molecular characterization of TH related and pigmentation genes in Atlantic halibut skin during metamorphosis

5.3.1.1. TH related genes: metabolism, transport and action in control Atlantic halibut

The expression profile of genes involved in TH metabolism (*dio1*, *dio2*, duplicate *dio3a* and *dio3b*), action (*trαa*, *trβ*) and transport (*mct8, mct10*), (**Figure 5.1**, Additional file 5.1) was evaluated in both ocular (ST) and abocular (SB) skin during normal Atlantic halibut metamorphosis using qPCR.

The four deiodinases were expressed in halibut skin during metamorphosis (stages 7-9B) and had a symmetric expression between ST and SB (**Figure 5.1**, Additional file 1). *Dio3b* expression increased significantly during metamorphosis in both skin sides, and the

highest expression was observed in the metamorphic climax stage 9B ($p < 0.05$), (**Figure 5.1A-B**). The relative abundance of deiodinase genes in skin at the metamorphic climax was *dio3b* > *dio1* > *dio3a* > *dio2*. *Dio1*, *dio2* and *dio3a* expression did not change significantly during metamorphosis in ocular and abocular skin ($p > 0.05$), (Additional file 5.1).

Trαa was more abundant than *trβ* in ST and SB (Additional file 5.1). However, only *trβ* expression significantly ($p < 0.05$) increased during the climax of metamorphosis at stage 9B in ST and SB (**Figure 5.1A-B**). *Trβ* had a symmetric expression pattern during metamorphosis and no significant differences ($p > 0.05$) were observed between ocular and abocular skin in any metamorphic stages (**Figure 5.1C**).

The two TH transporters, *mct8* and *mct10* were expressed in the skin of all metamorphic stages, but significant differences were only observed in abocular skin (SB, **Figure 5.1**). *Mct8* and *mct10* expression significantly ($p < 0.05$) decreased from stage 7 to the metamorphic climax stage 9A (**Figure 5.1B**). For both TH transporters, asymmetric gene expression occurred in ocular and abocular skin. *Mct8* was up-regulated in the ocular skin relative to the abocular skin ($p < 0.01$) in stage 9A. *Mct10* was highly expressed in ocular skin in all metamorphic stages ($p < 0.05$) and the highest level of expression was observed in the stage 9A ($p < 0.001$), (**Figure 5.1C**).

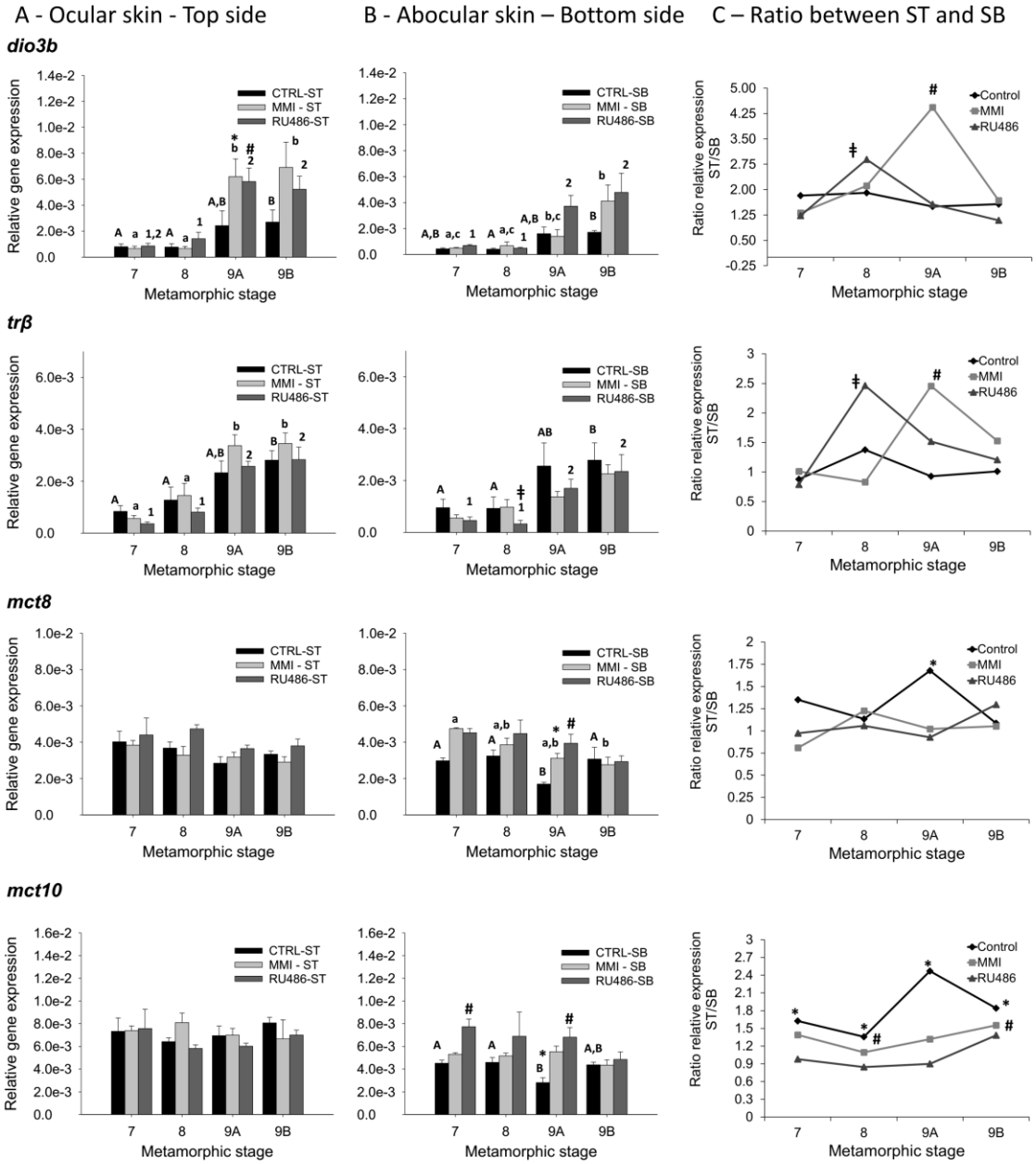

Figure 5.1. Relative gene expression analysis by qPCR of TH related genes during Atlantic halibut metamorphosis (stage 7 to 9B, n = 5 per stages) in ocular (ST) (A) and abocular (SB) (B) skin in control, MMI and RU486 exposed fish. The ratio of the relative gene expression between ocular and abocular skin (C). Deiodinase 3b (*dio3b*), TH receptor beta (*trβ*), monocarboxylate transporter 8 (*mct8*), and monocarboxylate transporter 10 (*mct10*) gene expression. Results are presented as mean ± SEM of the candidate gene expression, normalized using the geometric mean of the reference genes *rps4* and *ef1a1*. Significant differences ($p < 0.05$; two-way ANOVA) of normalized transcript expression between stages, skin sides and treatments are indicated by different letters. (**A**) and (**B**) Different upper case letters represent significant differences in gene expression between metamorphic stages in control; different lower case letters represent significant differences in gene expression between metamorphic stages in MMI; different numbers represent significant differences in gene expression between metamorphic stages in RU486. * Significant differences between control and methimazole; # significant differences between control and RU486; ǂ significant differences between MMI and RU486. (C) * significant up-regulation in control, # significant up-regulation in MMI; ǂ significant up-regulation in RU486.

5.3.1.2. Melanogenesis and regulation of pigmentation

The levels of expression of pigmentation related genes, involved in melanin synthesis (*tyrp1*, *dct*), melanocyte differentiation and melanogenesis regulation (*sox10*, *pomcβ*) and an antagonist of the melanocortin receptor involved in melanogenesis regulation (*asip*) were analysed in ocular (ST) and abocular (SB) skin of Atlantic halibut larvae (**Figure 5.2** and Additional file 5.2).

Melanogenic enzymes (*tyrp1*, *dct*) had a similar expression pattern during metamorphosis although it differed in ST and SB. In ST, the expression of these two genes increased significantly ($p < 0.05$) during metamorphosis and peaked at the metamorphic climax stage 9B. In contrast, both genes were down-regulated ($p < 0.05$) during the metamorphic climax in SB (**Figure 5.2A-B**). During the metamorphic climax (stages 9A-9B), significant ($p < 0.001$) asymmetric expression was observed between ST and SB (**Figure 5.2C**). The highest expression levels of s*ox10* in ST were also observed during the metamorphic climax, stage 9B (**Figure 5.2A-B**). The transcript expression of *sox10* between ST and SB was asymmetric. A significant ($p < 0.001$) up-regulation of s*ox10* occurred between stages 8 to 9B in ST relative to SB (Figure 5.2C). No significant differences in transcript abundance of *sox10* in SB were observed during metamorphosis (**Figure 5.2B**). *Pomcβ* and *asip* were expressed symmetrically in both ocular and abocular skin and no significant ($p > 0.05$) differences in abundance were observed at any metamorphic stages (Additional file 5.2).

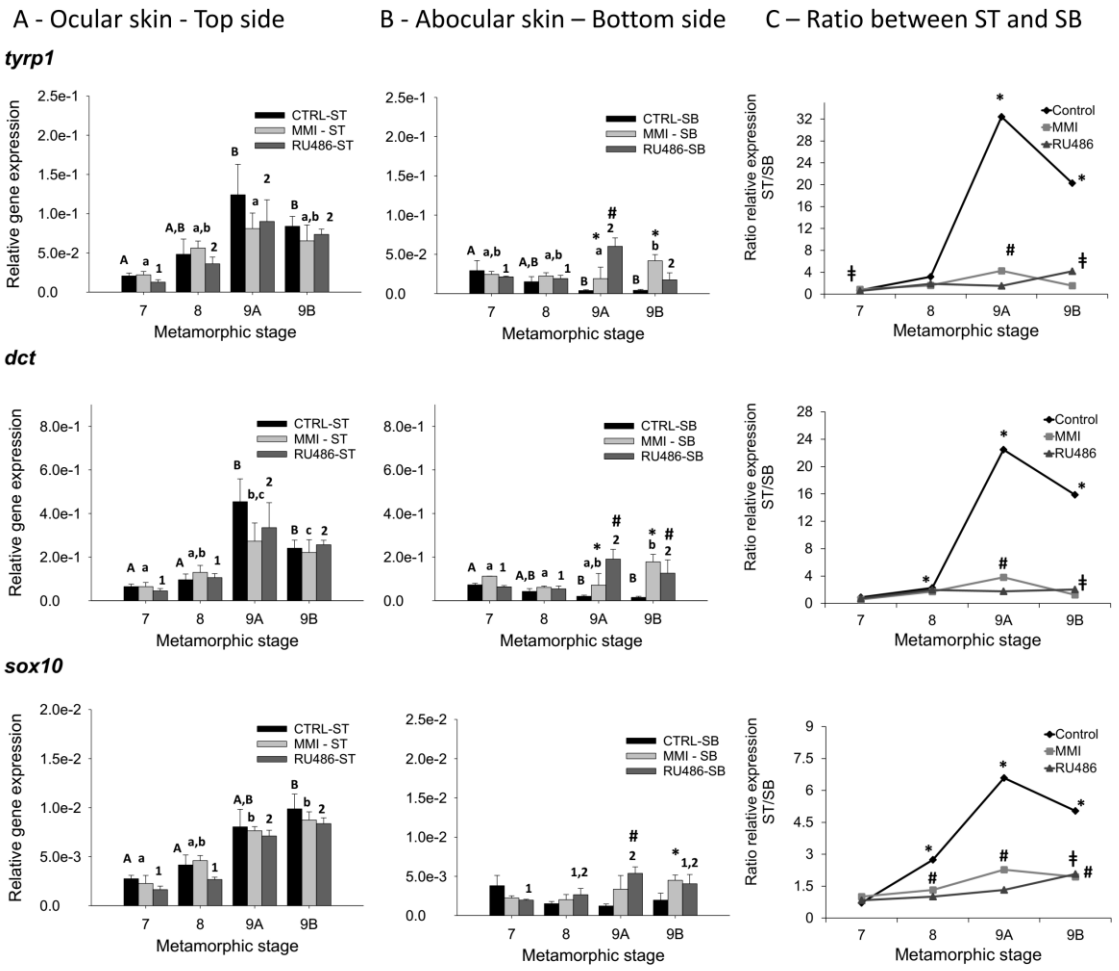

Figure 5.2. Relative gene expression analysis (qPCR) of pigmentation related genes during Atlantic halibut ocular - ST (A) and abocular – SB (B) skin metamorphosis (stage 7 to 9B, n = 5 per stages) in control, MMI and RU486 exposed fish. Ratio of the relative gene expression between ocular and abocular skin sides (C). Tyrosinase related protein 1 (*tyrp1*), dopachrome tautomerase (*dct*) and SRY (sex determining region Y)-box 10 (*sox10*). Results are presented as mean ± SEM of the candidate gene expression, normalized using the geometric mean of the reference genes *rps4* and *ef1a1*. Significant differences ($p < 0.05$; two-way ANOVA) of normalized transcript expression between stages, skin sides and treatments are indicated by different letters. (**A**) and (**B**) Different upper case letters represent significant differences in gene expression between metamorphic stages in control; different lower case letters represent significant differences in gene expression between metamorphic stages in MMI; different numbers represent significant differences in gene expression between metamorphic stages in RU486. * significant differences between control and methimazole; # significant differences between control and RU486; ǂ significant differences between MMI and RU486. (C) * significant up-regulation in control, # significant up-regulation in MMI; ǂ significant up-regulation in RU486.

5.3.1.3. The relationship between thyroid axis and pigmentation related genes

The correlation between thyroid and pigmentation related genes in ocular and abocular skin are shown in **Table 5.2** and **5.3**, respectively.

In the ocular skin TH related genes were positively correlated. For example, *dio1* was correlated with *dio2* (p = 0.005), *trα* (p = 0.012), *trβ* (p = 0.001). Deiodinase 3b was correlated with both thyroid hormone transporters, *mct8* and *mct10* (*trα*, r = 0.617; *trβ*, r = 0.616). No correlation was observed between other deiodinases or TRs or *mct8* and *mct10* (p > 0.05). In relation to pigmentation genes, only *sox1*0 was correlated with *asip* (r = 0.711, p < 0.01). *Tyrp1* and *dio3a* were correlated. Additionally, *sox10* mRNA expression increased when *dio1*, *dio3b* and *trαa* increased (p < 0.05).

In the abocular skin, *dio2* was positively correlated with *dio3b* and negatively correlated with *mct10*. A correlation was observed between *sox10* and *tyrp1* (r = 0.871, p < 0.001). Deiodinases were positively correlated with melanogenic enzymes and *sox10* (p < 0.05). No correlation was observed between the TH transporters (*mct8* and *mct10*) and pigmentation related genes (p > 0.05), (**Tables 5.2** and **5.3**).

Table 5.2. Correlation coefficient analysis between TH and pigmentation related genes in control ocular skin. Statistical significance, $p < 0.05$

Ocular skin	*dio1*	*dio2*	*dio3a*	*dio3b*	*trαa*	*trβ*	*mct8*	*mct10*	*tyrp1*	*dct*	*sox10*	*asip*	*pomcβ*
dio1	-	0.611	-0.174	0.135	0.564	0.699	-0.12	0.104	0.133	0.421	0.744	0.65	0.399
dio2	-	-	-0.352	0.193	0.37	0.421	0.272	0.147	-0.108	0.205	0.476	0.273	0.497
dio3a	-	-	-	-0.0657	-0.32	-0.266	0.0277	0.358	0.733	0.473	-0.224	-0.0191	0.306
dio3b	-	-	-	-	0.617	0.616	-0.462	-0.114	0.276	0.466	0.555	0.217	0.103
trαa	-	-	-	-	-	0.764	-0.304	-0.223	0.19	0.186	0.686	0.458	0.226
trβ	-	-	-	-	-	-	-0.419	-0.0389	0.208	0.506	0.91	0.507	0.205
mct8	-	-	-	-	-	-	-	0.489	-0.297	-0.43	-0.425	-0.258	0.491
mct10	-	-	-	-	-	-	-	-	0.0987	-0.00392	0.0718	0.222	0.415
tyrp1	-	-	-	-	-	-	-	-	-	0.548	0.366	0.392	0.352
dct	-	-	-	-	-	-	-	-	-	-	0.464	0.329	0.362
sox10	-	-	-	-	-	-	-	-	-	-	-	0.711	0.284
asip	-	-	-	-	-	-	-	-	-	-	-	-	0.308
pomcβ	-	-	-	-	-	-	-	-	-	-	-	-	-

Table 5.3. Correlation coefficient analysis between TH and pigmentation related genes in control abocular skin. Statistical significance, $p < 0.05$

Abocular skin	*dio1*	*dio2*	*dio3a*	*dio3b*	*trαa*	*trβ*	*mct8*	*mct10*	*tyrp1*	*dct*	*sox10*	*asip*	*pomcβ*
dio1	-	0.0533	0.449	-0.172	0.73	0.143	-0.38	0.203	0.52	0.506	0.636	0.415	0.00342
dio2	-	-	-0.0136	0.728	-0.264	0.371	-0.222	-0.498	-0.116	-0.214	-0.0946	-0.216	0.199
dio3a	-	-	-	0.0663	0.441	0.131	-0.158	-0.0376	0.71	0.094	0.841	0.325	0.0963
dio3b	-	-	-	-	-0.16	0.472	-0.223	-0.403	-0.343	-0.242	-0.185	-0.263	-0.00856
trαa	-	-	-	-	-	0.29	-0.196	0.305	0.225	0.417	0.538	0.358	-0.0329
trβ	-	-	-	-	-	-	-0.26	-0.42	-0.247	-0.25	-0.021	-0.0769	0.589
mct8	-	-	-	-	-	-	-	-0.329	-0.107	-0.115	-0.118	-0.242	-0.394
mct10	-	-	-	-	-	-	-	-	0.0682	0.152	0.0529	0.286	-0.314
tyrp1	-	-	-	-	-	-	-	-	-	0.27	0.871	0.0312	0.0361
dct	-	-	-	-	-	-	-	-	-	-	0.412	0.253	-0.0555
sox10	-	-	-	-	-	-	-	-	-	-	-	0.184	0.0216
asip	-	-	-	-	-	-	-	-	-	-	-	-	-0.029
pomcβ	-	-	-	-	-	-	-	-	-	-	-	-	-

5.3.2. Effects of MMI and RU486 in TH related and pigmentation genes expression in the halibut larvae skin

5.3.2.1. MMI

The exposure of Atlantic halibut larvae to MMI induced transcriptional changes in thyroid and pigmentation related genes (**Figures 5.1-2**). *Dio3b* was significantly ($p < 0.05$) up-regulated in MMI exposed larvae during the metamorphic climax stage 9A in relation to the control group, in the ocular skin (**Figure 5.1A**). In MMI treated larvae *dio3b* expression was asymmetric between ocular and abocular skin at the climax of metamorphic (stage 9A) and significant up-regulation occurred in the ocular skin ($p = 0.002$). Similar results were obtained for the ratio of *trβ* between ocular and abocular skin ($p < 0.001$), although no differences were observed between control and MMI (**Figure 5.1C**). In contrast to the control, *trαa* expression in MMI exposed fish increased during metamorphosis in ocular skin (Additional file 5.1). In abocular skin, the TH transporters (*mct8*, *mct10*) were up-regulated during metamorphic climax (stage 9A) in the MMI treated larvae (**Figure 5.1B**). MMI treatment did not affect the *mct8* and *mct10* expression levels in the ocular skin (**Figure 5.1A**). The asymmetric gene expression of *mct8* and *mct10* in MMI and in the control larvae undergoing metamorphosis was symmetric in the MMI exposed halibut (**Figure 5.1C**). Expression of *dio1*, *dio2* and d*io3a* genes was not affected by MMI exposure (Additional file 5.1).

The expression of melanogenic enzymes in halibut larvae exposed to MMI was significantly ($p < 0.001$) changed in abocular skin. Both *dct* and *tyrp1*were up-regulated in the abocular skin during the metamorphic climax (stages 9A-9B) compared to the control larvae group (**Figure 5.2B**). Therefore, asymmetry of *dct* and *tyrp1* did not occur in MMI treated larvae (**Figure 5.2C**). In the case of *sox10*, as verified for the melanogenic enzymes, this gene was significantly ($p = 0.028$) up-regulated in the abocular skin during metamorphic climax in the MMI exposed group. Asymmetric expression of *sox10* was only marginally maintained between ocular and abocular skin after MMI exposure relative to control fish. In the ocular skin side, no significant changes in *dct*, *tyrp1* and *sox10* gene abundance relative to the

controls were observed after exposure to MMI (**Figure 5.2A**). Expression of *asip* and *pomcβ* in control and MMI exposed fish were not significantly different (Additional file 5.2).

5.3.2.2. RU486

As verified for the MMI exposed Atlantic halibut larvae, the expression of genes involved in the thyroid axis and pigmentation were significantly ($p < 0.05$) changed after exposure to RU486. The main transcriptional changes were similar to those observed in the MMI treatment group, although they frequently occurred at different metamorphic stages (**Figures 5.1-2**). For example, in RU486 treated Atlantic halibut up-regulation of *dio3b* occurred in the ocular skin relative to the abocular skin at stage 8 rather than at stage 9A as recorded for the MMI group, ($p < 0.05$). During stage 8 of RU486 treated Atlantic halibut *trβ* was significantly ($p < 0.01$) up-regulated in the ocular skin relative to the abocular skin (**Figure 5.1C**). In the RU486 treatment group in common with the control, *trβ* expression increased significantly in the abocular skin at climax (stages 9A, $p < 0.01$) and 9B, $p < 0.001$). In the abocular skin, significant ($p = 0.032$) differences in *trβ* were observed between MMI and RU486 treatment groups during stage 8 (**Figure 5.1B**). No significant ($p > 0.05$) differences were found for the TH transporters *mct8* and *mct10* expression levels in ocular and abocular skin of RU486 exposed larvae during the time corresponding to metamorphosis in the control. In stages 7 and 9B of RU486 group, *mct10* was more abundant than in the control. In RU486 treated Atlantic halibut *mct8* and *mct10* had a symmetric expression pattern like in the MMI exposed larval (**Figure 5.1C**). For mct10, the asymmetric expression between ocular and abocular skin during stages 7 – 9B was lost in RU486 treatment.

In the RU486 treated group, *tyrp1* and *dct* were up-regulated in the abocular skin (stages 9A and 9B) in relation to the control group. Expression of both transcripts was symmetric in stage 9A ($p < 0.05$, **Figure 5.1C**). No significant differences between the control and RU486 groups were observed during metamorphosis for *sox10* transcripts in the ocular skin. In contrast, *sox10* was up-regulated ($p = 0.019$) in abocular skin at the metamorphic climax stage 9A (**Figure 2B**). Expression levels of *pomcβ* were not affected by RU486 exposure (Additional file 5.2). During the stages 7 and 9A, *asip* transcripts were less

abundant in the RU486 treated group, compared to MMI exposed larvae ($p < 0.05$, Additional file 5.2).

The effects of MMI and RU486 treatments had a similar effect on gene transcription in ocular and abocular skin (**Figure 5.3**). The up-regulation of pigmentation related genes in the abocular skin side occurred earlier in the RU486 exposed metamorphic larvae (**Figure 5.3**). MMI and RU486 treatments both affected thyroid signalling and during the metamorphic climax resulted in a significant ($p < 0.05$) up-regulation of *trβ* in the ocular skin and *mct8*, *mct10*, *tyrp1*, *dct a*nd *sox10* in the abocular skin. The deiodinases and TRs were down-regulated in the ocular skin from stage 7 and up-regulated in abocular skin from stages 9A and 9B in both treatments.

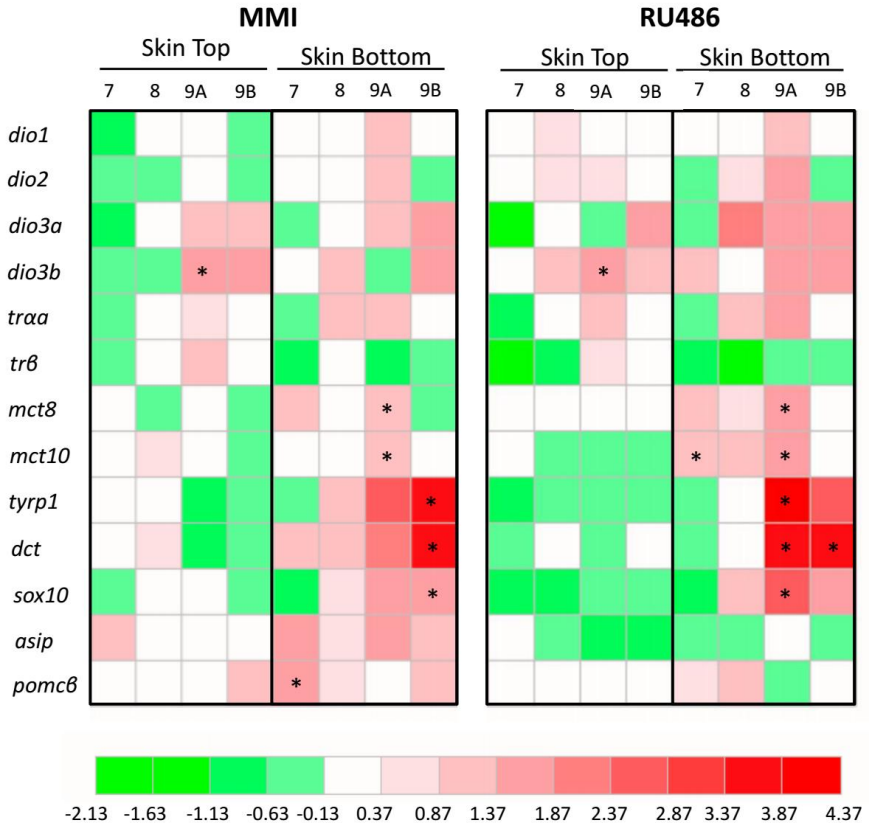

Figure 5.3. Heat map with the expression profile (log2 of fold-change between MMI or RU486 and control) of TH cascade and pigmentation related genes between metamorphic stages (7 to 9B) in ocular and abocular skin sides. *dio1* (deiodinase 1), *dio2* (deiodinase 2), *dio3a* (deiodinase 3A), *dio3b* (deiodinase 3B), *trαa* (thyroid hormone receptor α A), *trβ* (thyroid hormone receptor β), *mct8* (monocarboxylate transporter 8), *mct10* (monocarboxylate transporter 10), *tyrp1* (tyrosinase related protein 1), *dct* (dopachrome tautomerase), *sox10* (SRY (sex determining region Y)-box 10), *asip* (agouti signaling protein) and *pomcβ* (proopiomelanocortin beta). * represents significant differences between MMI /RU486 and control.

5.4. Discussion

The involvement of thyroid hormones in skin development in relation to changes in keratin expression during metamorphosis has been described (Campinho et al. 2012a), but the possible asymmetric responsiveness of ocular and abocular skin and the role of THs as a driver of asymmetric pigmentation is unstudied. Moreover, questions about the relationship between the skin TH responsiveness and the development of skin complexity and its possible asymmetry during metamorphosis is still largely unexplored. To the best of our knowledge, we reported for the first time how genes involved in THs cascade and pigmentation are expressed in the two skin sides during the flatfish metamorphosis. MMI and RU486 treatment is used to infer about the role of THs and cortisol and their possible cross-talk during skin morphogenetic development.

5.4.1. Genes involved in the TH cascade are differentially expressed between development stages and between ST and SB during metamorphosis

Molecular data in relation to TRs, TH transporters and deiodinases during metamorphosis have been exploited in several flatfish species, including the Atlantic halibut (Alves et al., 2016; Campinho et al. 2012a; Galay-Burgos et al. 2008; Isorna et al. 2009; Yamano et al., 1998; Zhang et al., 2016). The presence of the deiodinases (*dio1*, *dio2*, *dio3a* and *dio3b*), TRs (*trαa*, *trβ*) and THs transporters (*mct8, mct10*) in both ocular and abocular skin (stages 7 - 9B) in the present study confirmed the importance of the TH cascade in the metamorphosing halibut skin.

Deiodinases act to regulate the circulating and tissue levels of THs during flatfish metamorphosis through their coordinated action (Atlantic halibut, Alves et al. 2016, Campinho et al. 2012a; Senegalese sole, Isorna et al., 2009; Japanese flounder, Itoh et al., 2010). The expression of both activating and inactivating deiodinases in Atlantic halibut skin during metamorphosis in the present study is in agreement with results of earlier studies in which *dio2* and *dio3* was detected by *in situ* hybridisation (ISH) in skin dermal endothelial cells, basal and supra-basal cells in metamorphosing Atlantic halibut (Campinho et al. 2012a). The *dio* transcripts were correlated with the down-regulation of halibut larval collagen1α1 and keratin 1 during differentiation of larval to adult type cells at the metamorphic climax

(Campinho et al. 2012a). This contrasts with previous results obtained in *Paralichthys olivaceus* (Itoh et al. 2010) in which ISH failed to reveal *dio* transcripts in the skin of *P. olivaceus* during metamorphosis (Itoh et al. 2010). Using microdissected skin samples all 3 *dios* were identified in skin, although only of the recently identified *dio3* duplicate genes (chapter 3), *dio3b*, was up-regulated at metamorphic climax in ocular and abocular skin and this is in general agreement with previous studies based on expression of *dio3* whole flatfish larvae (Alves et al., 2016; Isorna et al., 2009). Deiodinase 3 is an important gene during vertebrates metamorphosis (Brown, 2005; Dentice et al. 2010), and we demonstrate the *dio3b* but not -*3a* (chapter 3) in teleosts is TH responsive. In *Xenopus laevis* skin, administration of THs induced an up-regulation of deiodinase 3 gene during the first 24 h after treatment (Suzuki et al., 2009). The constant expression of *dio1* and *dio2* in the Atlantic halibut skin during metamorphosis suggests the former enzymes maintain a constant supply of T_3 at a tissue level throughout development. However, at the metamorphic climax the up-regulation of these enzymes at a whole larval level presumably increases availability of THs and regulation of THs at the level of the skin is controlled by the strong up-regulation in *dio3b* during the metamorphic climax (Alves et al., 2016).

TRs play an essential role during vertebrates metamorphosis (Grimaldi et al. 2013), and both *trαa* and *trβ* expression generally increases in whole flatfish larvae throughout metamorphosis (Alves et al., 2016; Galay-Burgos et al. 2008; Yamano & Miwa, 1998). In our study, the *trαa* expression was unchanged in skin during metamorphosis, but *trβ* was up-regulated at the metamorphic climax (stage 9B) in both ocular and abocular skin, suggesting that *trβ* is the main TR isoform mediating the morphogenetic changes in skin during metamorphosis. As observed for *dio3, trβ* was also up-regulated in *X. laevis* skin after treatment with THs (Suzuki et al., 2009). In amphibians TRα is the main expressed unliganded TR and is responsible for the repression of the TH-inducible genes, preventing premature metamorphosis. The role of repression by unliganded TRs was not investigated in skin during Atlantic halibut metamorphosis and further research is needed to establish if this is important during flatfish metamorphosis. Ocular and abocular halibut skin is an interesting target to address this question. To better understand the role of TRs in skin during flatfish metamorphosis, more efforts are needed such as the study of TR splice forms as well other factor including potential heterodimerization with the retinoic acid receptors (RXR).

The transport of THs across the plasma membrane is a rate-limiting step in TH metabolism and two of the known THs transporters, *mct8* and *mct10* were expressed in ocular and abocular skin in all Atlantic halibut metamorphic stages. This is unsurprising taking into consideration the role of these monocarboxylate transporter family members in teleosts (Campinho et al. 2014; Vatine et al. 2013). We previously evaluated the expression of *mct8* and *mct10* in whole-larvae during metamorphosis (Alves et al. 2016), but as far we know, this is the first study exploring the TH transporters in individual tissues during flatfish metamorphosis. We hypothesize that TH transporters play a role in skin asymmetry as the expression of *mct8* and *mct10* was constant in ocular skin but decreased in obocular skin during entry into metamorphic climax (stage 9A). Furthermore, the ocular/abocular ratio for *mct8* (stage 9A) and *mct10* (stages 7-9B) transcripts in the skin was asymmetric, suggesting that in the ocular skin, the cellular uptake and efflux of thyroid hormones has a greater influence on tissue morphogenesis particularly since it is associated with the timing of the highest T_4 and T_3 levels during the metamorphic climax (Galay-Burgos et al. 2008). In amphibians, the temporal expression pattern of THs transporters varied between the major resorbing, growing and remodelling tissues and is correlated with the timing of their metamorphic changes (Connors et al. 2010). Little is known about these transporters in skin, but in humans with *mct8* mutations the skin fibroblasts have a lower uptake of T_3 and T_4 and the skin has modified properties (Visser et al., 2009).

5.4.2. Genes involved in the pigmentation are differentially expressed between development stages and between ST and SB during metamorphosis

In flatfish, distinct populations of chromatophores contribute to the characteristic pigmentation pattern before and after metamorphosis (Matsumoto & Seikai, 1992; Nakamura et al. 2010). Even though the morphological changes in the melanophores only occurs post-metamorphosis and promotes the shift to the adult pigmentation pattern, the molecular signalling essential for skin pigmentation (e.g. melanogenesis, regulation of melanophores differentiation) is triggered during metamorphosis (Daris et al. 2013a).

Tyrosine is the main precursor of melanin and tyrosinase (*try*) is the rate limiting enzyme of melanogenesis and catalyzes hydroxylation of L-tyrosine to DOPA and the oxidation of DOPA to DOPAquinone, (reviewed by Slominski et al. 2004; Wang et al. 2007).

Tyrosinase related protein 1 (*tyrp1*) and the L-dopachrome tautomerase (*dct*) are two other enzymes involved in melanogenesis. *Dct* catalyzes the tautomerization step of DOPAchrome to 5,6-dihydroxyindole-2-carboxylic acid (5,6-DHI-2-CA) and, in the last step of the melanogenic pathway 5,6-DHI-2-CA is oxidized to melanin by *tyrp1* (reviewed by Slominski et al. 2004). In the present study, *tyrp1* and *dct* were up-regulated in ocular skin during metamorphosis but decreased in abocular skin. These observations are in accordance with ocular/abocular skin phenotypes observed in post-metamorphic juvenile, where only the ocular skin becomes pigmented after metamorphosis. In *P. olivaceus* larvae, *dct* was expressed mainly on melanized melanophores (Yamada et al. 2010) and has been used as a marker gene for melanin-producing cells and melanocytes differentiation (Kumasaka et al. 2003; Quigley et al., 2004). TYRP1 is also associated with the production of black melanin. In zebrafish, the knockdown (KO) of both *tyrp1* duplicates resulted in severe melanosome defects including the formation of brown instead of black eumelanin (Braasch et al., 2009). Moreover, in mammals, the absence or dysfunction of these melanogenic enzymes results in oculocutaneous albinism, which presents with intact melanocytes but inability to produce pigment (reviewed by Slominski et al. 2004). Nevertheless, the *tyrp1* expression pattern observed in the ocular skin of Atlantic halibut diverged from the general reduction in whole larvae *tyrp1* expression in Senegalese sole during metamorphosis. This highlights the importance of analysing tissue specific changes in gene expression as whole body gene expression gives a very general overview when genes are expressed in multiple tissues.

The transcription factor, *sox10,* had a similar expression pattern to *tyrp1* and *dct* and is up-regulated in ocular skin from stage 8 to 9B. SOX10 is one of the transcription factors which regulates microphtalmia-associated transcription factor (*mitf*) expression and in mammals is involved in melanocyte specification (Elworthy et al., 2003). MITF is considered to be the main regulator of melagonesis as it activates several melanocyte specific genes especially the melanogenic enzymes (Ebanks et al., 2009) and when up-regulated by *sox10* activates the melanogenic pathway. In mammals, *sox10* also directly regulates *dct* (Wegner, 2006). Therefore, the machinery that activates melanogenesis and melanophore differentiation is present in ocular skin during halibut metamorphosis. This explains why after metamorphosis the main chromatophores on the abocular side of flatfish are the iridophores, whereas on the ocular side both melanophores and iridophores are present (Burton, 2010). It

will be interesting in the future to evaluate in skin the maturation of other chromatophores and also the involvement of other regulatory systems (eg. melanocortin).

Two other key genes involved in regulation of pigmentation (*asip, pomcβ*) were expressed in ocular and abocular skin of Atlantic halibut, but no asymmetry or changes were observed during metamorphosis. POMCβ (also called POMC-C) is the precursor of α-MSH and is the widespread POMC in dorsal and ventral skin of barfin flounder (Takahashi et al. 2005). The POMCs are exressed in the pituitary and skin of the Atlantic halibut but are not modified during metamorphosis and we hypothesize that during metamorphosis before the establishment of pigmentation the POMC system is unimportant but that after metamorphosis, as occurs in the barfin flounder (Takahashi et al. 2009), α-MSH regulates skin pigmentation via endocrine and paracrine regulation.

ASIP is generally associated with the absence of pigmentation as ASIP blocks melanin dispersion induced by α-MSH scale melanophores by acting as a competitive antagonist at MC1R (Cerdá-Reverter et al., 2005). Transgenic zebrafish which overexpressed *asip* have a marked reduction in the number of melanophores within the dark stripes and an increased number of iridophores, leading to a severe disruption of the stripe pattern characteristic in this species (Cerdá-Reverter et al. 2011). Moreover, ASIP1 has been implicated in turbot pseudoalbinism, where its level of expression in unpigmented patches of the dorsal skin of pseudoalbino fish was similar to levels in ventral skin (Guillot et al 2012). It will be of interest to study TH signalling and pigmentation pathways in Atlantic halibut with normal and abnormal pigmentation to determine the factors underlying this abnormality.

5.4.3. MMI and RU486 disrupt the thyroid cascade and induce changes in THs metabolism, transport and action in ST and SB

In flatfish, the negative feedback loop between the thyroid and the pituitary gland is evident before metamorphosis, and MMI inhibits metamorphosis by blocking TH production (Campinho et al., 2015, Schreiber et al., 2010). Levels of THs were not determined , in the present study but the thyroid histology of Atlantic halibut treated with MMI was indicative of a hypothyroid state during the metamorphic climax (please see Chapter 3), suggesting lower THs in MMI exposed fish, as previously reported in seabream (Campinho et al. 2012b). During metamorphosis, mainly at the beginning of the metamorphic climax, the effect of

MMI on THs was reflected by a shift in gene expression with symmetric (*dio3b*, *trβ*) and asymmetric (*mct8*, *mct10*) patterns in ocular and abocular skin unlike the situation in control skin. MMI treatment caused an up-regulation of *dio3b* in ocular skin, leading to an asymmetric expression in ocular and abocular skin. During amphibian metamorphosis, a process analogous to flatfish metamorphosis, *dio3* is one of several TH responsive genes identified (Das et al., 2009, Helbing et al., 2003, Suzuki et al., 2009). The up-regulation of *dio3b* caused by MMI treatment in Atlantic halibut is reminiscent of its up-regulation in kidney, liver and gills from *P. olivaceus* and *Oreochromis niloticus* exposed to the endocrine disruptor Aroclor 1254 (Coimbra et al., 2005; Dong et al. 2014). Similar findings were observed in zebrafish exposed to the endocrine disruptor 6-OH-BDE 47 (Dong et al., 2013). As discussed in chapter 3, MMI treatment of Atlantic halibut caused up-regulation of *dio3b* transcription in ocular skin, although *dio3a* was unaltered and this plus promoter analysis suggests that Atlantic halibut *dio3b* is TH responsive. Interestingly the divergent response of *dio3* isoforms to THs may represent a mechanism to fine-tune specific cellular responses during metamorphosis as has previously been suggested to explain the differential regulation of TH receptors by THs in Senegalese sole (Manchado et al., 2009). The up-regulation of *trαa* observed in MMI-treated ocular skin during Atlantic halibut metamorphosis (unchanged in control) is in agreement with previous observations in the half-smooth tongue sole (*Cynoglossus semilaevis*) (Zhang et al., 2016). In the case of *trβ*, expression remained unchanged during Atlantic halibut metamorphosis in the abocular skin from MMI-treated fish, and the asymmetry in expression of *tr*s between ocular and abocular skin may indicate they have a different role during metamorphosis.

MMI induced up-regulation of *mct8* and *mct10* in abocular skin during stage 9A when compared with the control fish, and expression between ST and SB becomes symmetric. We suggest that THs are important in abocular skin during the metamorphic climax, and the up-regulation of both transporters can be part of a compensatory response to the low circulating THs, by increasing the uptake of THs by the skin cells. This hypothesis was also proposed for adult male minnows fed T_3 and MMI for 14 days and up-regulation of *mct8* and *mct10* was observed in the brain of MMI-treated fish compared to T_3-treated fish (Muzzio et al., 2014). Noyes et al (2013) also verified up-regulation of *mct8* in brain and liver after exposure to the endocrine disruptor decabromodiphenyl ether BDE-209. No transcriptional changes were observed in the main deiodinases (*dio1*, *dio2*, *dio3a*) after the MMI treatment to block Atlantc

halibut metamorphosis, suggesting that these deiodinases are not major contributors for TH availability in the skin after perturbations of circulating hormone levels. The results from adult minnows with hypothyroidism caused by BDE-209 exposure in which several genes of thyroid signalling (*dio1*, *dio2*, *trα*, *trβ*, *mct8*, and *oatp1c1*) were up-regulated, supports the observed up-regulation of transcripts in ocular (*dio3b*, *trαa*) and abocular (*mct8*, *mct10*) skin responsible for the change in TH responsiveness of halibut skin during metamorphosis.

RU486 is a selective glucocorticoid receptor (GC) blocker and in teleosts increases the levels of circulating cortisol (reviewed by Mommsen et al., 1999) by inhibition of the negative feedback effects of cortisol on the pituitary (Marshall et al. 2005; McCormick et al., 2008; Scott et al., 2005). Exposure of fish to cortisol reduces TH levels in plasma (Brown et al. 1991; Walpita et al. 2007). Previous studies of flatfish metamorphosis revealed an interaction between cortisol and THs (de Jesus et al., 1990; 1991) but the mechanism is unclear (Geven et al., 2009). In the present study RU486 had a similar effect on metamorphosis to MMI in the skin of halibut. We hypothesize that one mechanisms of action of RU486 on metamorphosis may result from high cortisol levels that affect TH levels during halibut metamorphosis. In teleosts, several studies have been described the occurrence of changes in the expression and activity of deiodinases in response to the cortisol exposure (Arjona et al. 2011; Todd & Eales, 2002). For example, in Nile tilapia injection of dexamethasone (DEX) and handling stress caused a decreased in T_3 circulating levels by changing deiodinases expression, especially by up-regulation of *dio3* in liver and gills. (Walpita et al. 2007). Our results indicated that *dio3b* was up-regulated in RU486 exposed fish compared to control fish, suggesting TH inactivating pathways (T_4 to rT_3 and T_3 to T_2) were activated and teleost skin has previously been shown to be an important source of rT_3 due to its high IRD activity (Fenton et al., 1997).

Recently, it was demonstrated in teleosts that both TREs (thyroid response elements) and GREs (glucocorticoid response elements) are present in *trβ* and that THs and cortisol cross-modulate the expression of this receptor. T_2 and T_3 down-regulate the expression of long and short *trβ*, but cortisol up-regulates the expression of *trβ* (Hernandez-Puga et al., 2016; Orozco et al. 2014). In addition, T_2 represses *trβ* expression and impairs its up-regulation by cortisol possibly through a trans-repression mechanism (Hernandez-Puga et al., 2016). The down-regulation of *trβ* in Atlantic halibut abocular skin at stage 8 relative to MMI

treated larvae during metamorphosis suggests the skin model will be a good target to elucidate *in vivo* the cross-talk between the two axes and to study the action of T_2. Furthermore, expression of the thyroid hormone transporters (*mct8, mct10*) was modified after exposure to RU486 providing further evidence of potential regulation of thyroid signalling by cortisol during metamorphosis.

5.4.4. MMI and RU486 induced changes in molecular ontogeny of skin pigmentation

The involvement of THs in pigmentation during development has previously been shown (Huang et al. 1998; Jegstrup & Rosenkilde, 2003) as the involvement of THs in pigmentation asymmetry in flatfish (Okada et al., 2005; Tagawa & Aritaki, 2005; Yoo et al. 2000). However, the molecular mechanisms involved in pigmentation asymmetry are still unknown. In early development, the absence of T_3 in zebrafish embryos by knock-down (KD) of *dio2* has a negative effect on pigmentation. In *dio2* KD down-regulation of tyrosinase occurs suggesting THs have a direct effect on pigment formation in addition to their effects on development (Walpita et al., 2009).

To the best of our knowledge, this is the first study focusing on the effect of THs endocrine disruption on the molecular ontogeny of pigmentation related genes in ocular/abocular flatfish skin. The expected low THs resulted from the MMI treatment affected pigmentation related genes mainly in the abocular skin. Both melanogenic enzymes were up-regulated in this skin during the metamorphic climax. This suggests that THs have a critical role in the regulation of asymmetric expression of *tyrp1* and *dct*, and the up-regulation of both THs transporters observed in this skin side supports this hypothesis. Tagawa & Aritaki (2005) suggested that THs is expected to induce abocular side characteristics, and timely differential responsiveness to THs between right and left (abocular side in normal juvenile) sides is strongly suggested as the central mechanism for the expression of metamorphic asymmetry. In fact, T_4 administration to *P. olivaceus* at the early stages of metamorphosis led to the development of pseudoalbinism in juveniles (Yoo et al., 2000). We propose the following mechanism for THs in pigmentation: (1) during normal conditions, THs are more abundant in ocular rather than abocular skin due to the down-regulation of *mct8* and *mct10* at stage 9A; (2) under MMI exposure, *mct8* and *mct10* are up-regulated and ensure adequate THs are available for skin maturation but not for pigmentation; (3) the uptake of T_3 is required to up-

regulate the melanogenic enzymes in the abocular skin. Analysis of the progress of pigmentation in ocular and abocular skin after metamorphosis will be essential to test this hypothesis. An important role of THs in pigmentation is also supported from results from fish exposed at different developmental stages to endocrine disruptors of the thyroid system that have reduced pigmentation (Huang et al., 1998; Jegstrup & Rosenkilde, 2001, Karlsson et al., 2001; Lam et al., 2005; Trijuno et al., 2002).

As observed for genes involved in THs cascade, the effect of RU486 on expression of pigmentation related genes was similar to that observed in fish exposed to MMI, indicating again the possible cross-talk between the two axes. Interestingly, the asymmetric *sox10* expression observed between ST and SB was suppressed in the RU486 treated larvae, due to an up-regulation of this gene at the stage 9A in SB. The up-regulation of *sox10* may be associated with the higher expression of *dct* detected in RU486 (stage 9A) and MMI (stage 9B). Another explanation could be related to the known role in vertebrates of *sox10* in the melanocyte/phore differentiation (Elworthy et al., 2003). This up-regulation may compromise the pigmentation pattern in the abocular side after metamorphosis. Unfortunately, it was not possible to analyse the pigmentation pattern in the post-metamorphosed juvenile in ocular/abocular skin. That cortisol influences pigmentation is evident from the increase in dark skin coloration in *Salvelinus alpinus* and *Solea senegalensis* larvae with high levels of cortisol are associated to as observed in (Höglund et al., 2000; Ruane et al., 2005).

Overall, the present data indicates ocular and abocular skin has different TH responsiveness during metamorphosis and provides insight into the molecular basis of this difference. Synergy between cortisol and thyroid hormone occurred during Atlantic halibut metamorphosis as has previously been described in amphibians (Bonett et al., 2010; Denver, 2009). At the end of the experiment, the standard length of larvae exposed to MMI was significantly higher than in control fish, although no significant differences in standard length existed between the control and RU486 treated Atlantic halibut (data not shown). Similar results were obtained for *Pimephales promelas* exposed to MMI during development. Between the 28 and 56 dpf, fish exposed to MMI 32 µg L^{-1} had a significantly greater standard length than control fish (Crane et al. 2006). Another important observation during the experiment was the most accentuated pigmentation in the ocular side in fish exposed to both MMI and RU586 (data not shown). Clearly, more research will be required to evaluate if

the cross-talk between THs and cortisol occurs at a central or peripheral level during flatfish metamorphosis. Determination of both THs and cortisol and the expression of genes of the HPT/HPI axes will be crucial to address this question. It will be of interest to establish if the other factors associated with abnormal pigmentation in flatfish, such as, the rearing environment, larval nutrition, effects of lighting and substratum type (reviewed by Bolker & Hill, 2000) also act via THs and cortisol.

5.5. Conclusions

In summary, the involvement of TH and cortisol in the asymmetric development of ocular and abocular (blind) skin during Atlantic halibut metamorphosis was confirmed. The large size and slow development of Atlantic halibut larvae allowed us to successfully study the expression of genes involved in THs metabolism, transport and action and in pigmentation in skin. The results indicated a symmetric expression of TRs and deiodinases (*dio1*, *dio2*, *dio3a*, *dio3b*, *trαa a*nd *trβ*), but an asymmetric expression of THs transporters (*mct8, mct10*) in ocular and abocular skin existed during metamorphosis. Genes involved in melanogenesis (*tyrp1, dct*) and regulation of pigmentation (*sox10*) were also asymmetric in skin. The use of MMI revealed in Atlantic halibut that THs have a direct role in flatfish skin development.

In Atlantic halibut exposed to MMI (inhibition of THs production) and RU486 (increase of cortisol levels), had similar transcriptional changes in genes of thyroid signalling and pigmentation related genes. Thus, we hypothesized that cross-talk occurs between the thyroid and interrenal axes and that THs and cortisol may act synergistically in the skin and change Atlantic halibut metamorphosis. A better understanding of the molecular basis that pigmentation asymmetry during metamorphosis in Atlantic halibut will contribute to understanding the factors underling the genesis in aquaculture of flatfish with abnormal pigmentation. This study contributes with new insights about the molecular mechanisms involved in skin THs responsiveness.

Acknowledgments

We thank Velimir Nola & Ragnfrid Mangor-Jensen for halibut feeding and assistance during the experiment at IMR.

References

Alderman, S.L., McGuire, A., Bernier, N.J., Vijayan, M.M., 2012. Central and peripheral glucocorticoid receptors are involved in the plasma cortisol response to an acute stressor in rainbow trout. General and comparative endocrinology 176, 79-85.

Alves, R.N., Gomes, A.S., Stueber, K., Tine, M., Thorne, M.A., Smaradottir, H., Reinhard, R., Clark, M.S., Ronnestad, I., Power, D.M., 2016. The transcriptome of metamorphosing flatfish. BMC Genomics. 17, 413.

Arjona, F.J., de Vrieze, E., Visser, T.J., Flik, G., Klaren, P.H.M., 2011. Identification and Functional Characterization of Zebrafish Solute Carrier Slc16a2 (Mct8) as a Thyroid Hormone Membrane Transporter. Endocrinology 152, 5065-5073.

Bianco, A.C., Salvatore, D., Gereben, B., Berry, M.J., Larsen, P.R., 2002. Biochemistry, cellular and molecular biology, and physiological roles of the iodothyronine selenodeiodinases. Endocrine Reviews 23, 38-89.

Bolker, J.A., Hill, C.L., 2000. Pigmentation development in hatchery-reared flatfishes. Journal of Fish Biology 56.

Bonett, R.M., Hoopfer, E.D., Denver, R.J., 2010. Molecular mechanisms of corticosteroid synergy with thyroid hormone during tadpole metamorphosis. General and Comparative Endocrinology 168, 209-219.

Braasch, I., Schartl, M., Volff, J.N., 2007. Evolution of pigment synthesis pathways by gene and genome duplication in fish. BMC Evolutionary Biology 7, 74.

Braasch, I., Brunet, F., Volff, J.N., Schartl, M., 2009. Pigmentation pathway evolution after whole-genome duplication in fish. Genome Biology and Evolution 1, 479-493.

Brown, D.D., 2005. The role of deiodinases in amphibian metamorphosis. Thyroid: official journal of the American Thyroid Association 15, 815-821.

Brown, L., Kim, B.Q., 1995. Combined application of cortisol and triiodothyronine in the culture of larval marine finfish. Aquaculture 135, 79-86.

Brown, S.B., MacLatchy, D.L., Hara, T.J., Eales, J.G., 1991. Effects of cortisol on aspects of 3,5,3′-triiodo-L-thyronine metabolism in rainbow trout (*Oncorhynchus mykiss*), General and Comparative Endocrinology 81, 207–216.

Burton, D., 2010. Flatfish (Pleuronectiformes) chromatic biology. Rev Fish Biol Fisheries 20, 31-46.

Campinho, M.A., Silva, N., Sweeney, G.E., Power, D.M., 2007. Molecular, cellular and histological changes in skin from a larval to an adult phenotype during bony fish metamorphosis. Cell and Tissue Research 327, 267-284.

Campinho, M.A., Galay-Burgos, M., Silva, N., Costa, R.A., Alves, R.N., Sweeney, G.E., Power, D.M., 2012a. Molecular and cellular changes in skin and muscle during metamorphosis of Atlantic halibut (*Hippoglossus hippoglossus*) are accompanied by changes in deiodinases expression. Cell and Tissue Research 350, 333-346.

Campinho, M.A., Morgado, I., Pinto, P.I., Silva, N., Power, D.M., 2012b. The goitrogenic efficiency of thioamides in a marine teleost, sea bream (*Sparus auratus*). General and Comparative Endocrinology 179, 369-375.

Campinho, M.A., Saraiva, J., Florindo, C., Power, D.M., 2014. Maternal thyroid hormones are essential for neural development in zebrafish. Molecular Endocrinology 28, 1136-1149.

Campinho, M.A., Silva, N., Roman-Padilla, J., Ponce, M., Manchado, M., Power, D.M., 2015. Flatfish metamorphosis: a hypothalamic independent process? Molecular and Cellular Endocrinology 404, 16-25.

Cerda-Reverter, J.M., Haitina, T., Schioth, H.B., Peter, R.E., 2005. Gene structure of the goldfish agouti-signaling protein: a putative role in the dorsal-ventral pigment pattern of fish. Endocrinology 146, 1597-1610.

Cerda-Reverter, J.M., Agulleiro, M.J., Guillot, R., Sanchez, E., Ceinos, R., Rotllant, J., 2011. Fish melanocortin system. European Journal of Pharmacology 660, 53-60.

Coimbra, A.M., Reis-Henriques, M.A., Darras, V.A., 2005. Circulating thyroid hormone levels and iodothyronine deiodinase activities in Nile tilapia (*Oreochromis niloticus*) following dietary exposure to Endosulfan and Aroclor 1254, Comparative Biochemistry and Physiology C-Toxicology & Pharmacology 141, 8-14.

Connors, K.A., Korte, J.J., Anderson, G.W., Degitz, S.J., 2010. Characterization of thyroid hormone transporter expression during tissue-specific metamorphic events in *Xenopus tropicalis*. General and Comparative Endocrinology 168, 149-159.

Crane, H.M., Pickford, D.B., Hutchinson, T.H., Brown, J.A., 2006. The Effects of Methimazole on Development of the Fathead Minnow, *Pimephales promelas*, from Embryo to Adult. Toxicology Science 93, 278-285.

Darias, M.J., Andree, K.B., Boglino, A., Fernandez, I., Estevez, A., Gisbert, E., 2013. Coordinated regulation of chromatophore differentiation and melanogenesis during the ontogeny of skin pigmentation of *Solea senegalensis* (Kaup, 1858). PloS one 8, e63005.

Das, B., Heimeier, R.A., Buchholz, D.R., Shi, Y.B., 2009. Identification of direct thyroid hormone response genes reveals the earliest gene regulation programs during frog metamorphosis. Journal of Biological Chemistry 284, 34167-34178.

De Groef, B., Van der Geyten, S., Darras, V.M., Kühn, E.R., 2006. Role of corticotropin-releasing hormone as a thyrotropin-releasing factor in non-mammalian vertebrates. General and Comparative Endocrinology 146, 62-68.

De Jesus, E.G., Hirano, T., Inui, Y., 1991. Changes in cortisol and thyroid hormone concentrations during early development and metamorphosis in the Japanese flounder, *Paralichthys olivaceus*. General and Comparative Endocrinology 82, 369-376.

De Jesus, E.G., Inui, Y., Hirano, T., 1990. Cortisol enhances the stimulating action of thyroid hormones on dorsal fin-ray resorption of flounder larvae in vitro. General and Comparative Endocrinology 79, 167-173.

Dentice, M., Marsili, A., Ambrosio, R., Guardiola, O., Sibilio, A., Paik, J.H., Minchiotti, G., DePinho, R.A., Fenzi, G., Larsen, P.R., Salvatore, D., 2010. The FoxO3/type 2 deiodinase pathway is required for normal mouse myogenesis and muscle regeneration. The Journal of Clinical Investigation 120, 4021-4030.

Denver, R.J., 2009. Stress hormones mediate environment-genotype interactions during amphibian development. General and Comparative Endocrinology 164, 20-31.

Denver, R.J., 2013. Neuroendocrinology of amphibian metamorphosis. Current topics in developmental biology 103, 195-227.

Dong, W., Macaulay, L.J., Kwok, K.W., Hinton, D.E., Stapleton, H.M., 2013. Using whole mount in situ hybridization to examine thyroid hormone deiodinase expression in embryonic and larval zebrafish: a tool for examining OH-BDE toxicity to early life stages. Aquatic toxicology 132-133, 190-199.

Dong, Y., Tian, H., Wang, W., Zhang, X., Liu, J., Ru, S., 2014. Disruption of the thyroid system by the thyroid-disrupting compound Aroclor 1254 in juvenile Japanese flounder (*Paralichthys olivaceus*), PLoS One 9, e104196.

Ebanks, J.P., Wickett, R.R., Boissy, R.E., 2009. Mechanisms regulating skin pigmentation: the rise and fall of complexion coloration. International journal of molecular sciences 10, 4066-4087.

Einarsdóttir, I.E., Silva, N., Power, D.M., Smaradottir, H., Bjornsson, B.T., 2006. Thyroid and pituitary gland development from hatching through metamorphosis of a teleost flatfish, the Atlantic halibut. Anat Embryol (Berl). 211, 47-60.

Elworthy, S., Lister, J.A., Carney, T.J., Raible, D.W., Kelsh, R.N., 2003. Transcriptional regulation of mitfa accounts for the sox10 requirement in zebrafish melanophore development, Development 130, 2809-2818.

Fenton, B., Orozco, A., Valverde, C., 1997. Kinetic characterization of skin inner-ring deiodinative pathway and its correlation with circulating levels of reverse tri-iodothyronine in developing rainbow trout. J Endocrinol. 154, 547-554.

Galay-Burgos, M., Power, D.M., Llewellyn, L., Sweeney, G.E., 2008. Thyroid hormone receptor expression during metamorphosis of Atlantic halibut (*Hippoglossus hippoglossus*). Molecular and Cellular Endocrinology 281, 56-63.

Geven, E.J., Flik, G., Klaren, P.H., 2009. Central and peripheral integration of interrenal and thyroid axes signals in common carp (*Cyprinus carpio* L.). The Journal of Endocrinology 200, 117-123.

Grimaldi, A.G., Buisine, N., Bilesimo, P., Sachs, L.M., 2013. High-throughput sequencing will metamorphose the analysis of thyroid hormone receptor function during amphibian development. Current Topic Development Biology 103, 277-303.

Guillot, R., Ceinos, R.M., Cal, R., Rotllant, J., Cerda-Reverter, J.M., 2012. Transient ectopic overexpression of agouti-signalling protein 1 (asip1) induces pigment anomalies in flatfish. PloS One 7, e48526.

Harboe, T., Mangor-Jensen, A., Naas, K.E, Næss, T., 1998. A tank design for first feeding of Atlantic halibut, *Hippoglossus hippoglossus* L., larvae. Aquaculture Research 29, 919–923.

Helbing, C.C., Werry, K., Crump, D., Domanski, D., Veldhoen, N., Bailey, C.M., 2003. Expression Profiles of Novel Thyroid Hormone-Responsive Genes and Proteins in the Tail of *Xenopus laevis* Tadpoles Undergoing Precocious Metamorphosis. Molecular Endocrinology 17, 1395-1409.

Hernandez-Puga, G., Navarrete-Ramirez, P., Mendoza, A., Olvera, A., Villalobos, P., Orozco, A., 2016. 3,5-Diiodothyronine-mediated transrepression of the thyroid hormone receptor beta gene in tilapia. Insights on cross-talk between the thyroid hormone and cortisol signaling pathways. Molecular and Cellular Endocrinology 425, 103-110.

Höglund, E., Balm, P.H.M., Winberg, S., 2000. Skin darkening, a potential social signal in subordinate Arctic charr (*Salvelinus alpinus*): The regulatory role of brain monoamines and pro-opiomelanocortin-derived peptides, Journal of Experimental Biology 203, 1711-1721.

Huang, L., Schreiber, A.M., Soffientino, B., Bengtson, D.A., Specker, J.L., 1998. Metamorphosis of summer flounder (*Paralichthys dentatus*): thyroid status and the timing of gastric gland formation. The Journal of Experimental Zoology A 280, 413-420.

Hunt, G., Thody, A.J., 1995. Agouti protein can act independently of melanocyte-stimulating hormone to inhibit melanogenesis. The Journal of endocrinology 147, R1-4.

Inui, Y., Miwa, S., 1985. Thyroid hormone induces metamorphosis of flounder larvae. General and Comparative Endocrinology 60, 450-454.

Isorna, E., Obregon, M.J., Calvo, R.M., Vazquez, R., Pendon, C., Falcon, J., Munoz-Cueto, J.A., 2009. Iodothyronine deiodinases and thyroid hormone receptors regulation during flatfish (*Solea senegalensis*) metamorphosis. Journal of experimental zoology. Part B, Molecular and Developmental Evolution 312B, 231-246.

Itoh, K., Watanabe, K., Wu, X., Suzuki, T., 2010. Three members of the iodothyronine deiodinase family, dio1, dio2 and dio3, are expressed in spatially and temporally specific patterns during metamorphosis of the flounder, *Paralichthys olivaceus*. Zoology Sciences 27, 574-580.

Iziga, R., Ponce, M., Infante, C., Rebordinos, L., Canavate, J.P., Manchado, M., 2010. Molecular characterization and gene expression of thyrotropin-releasing hormone in Senegalese sole (*Solea senegalensis*). Comparative biochemistry and physiology. Part B, Biochemistry & molecular biology 157, 167-174.

Jegstrup, I.M., Rosenkilde, P., 2003. Regulation of post-larval development in the European eel: thyroid hormone level, progress of pigmentation and changes in behaviour, Journal of Fish Biology 63, 168-175.

Karlsson, J., von Hofsten, J., Olsson, P.E., 2001. Generating transparent zebrafish: A refined method to improve detection of gene expression during embryonic development, Marine Biotechnology 3, 522-527.

Kumasaka, M., Sato, S., Yajima, I., Yamamoto, H., 2003. Isolation and developmental expression of tyrosinase family genes in *Xenopus laevis*, Pigment and Cell Research 16, 455–462.

Lam, S.H., Sin, Y.M., Gong, Z., Lam, T.J., 2005. Effects of thyroid hormone on the development of immune system in zebrafish, General and Comparative Endocrinology 142, 325-335.

Lamason, R.L., Mohideen, M.A.P.K., Mest, J.R., Wong, A.C., Norton, H.L., Aros, M.C., Jurynec, M.J., Mao, X.Y., Humphreville, V.R., Humbert, J.E., Sinha, S., Moore, J.L., Jagadeeswaran, P., Zhao, W., Ning, G., Makalowska, I., McKeigue, P.M., O'Donnell, D., Kittles, R., Parra, E.J., Mangini, N.J., Grunwald, D.J., Shriver, M.D., Canfield, V.A., Cheng, K.C., 2005. SLC24A5, a putative cation exchanger, affects pigmentation in zebrafish and humans, Science 310, 1782-1786.

Laudet, V., 2011. The Origins and Evolution of Vertebrate Metamorphosis. Curr Biol. 21, R726-R737.

Lin, J.Y., Fisher, D.E., 2007. Melanocyte biology and skin pigmentation. Nature 445, 843-850.

Manchado, M., Infante, C., Rebordinos, L., Cañavate, J.P., 2009. Molecular characterization, gene expression and transcriptional regulation of thyroid hormone receptors in Senegalese sole. General and Comparative Endocrinology 160, 139-147.

Marshall, W.S., Cozzi, R.R., Pelis, R.M., McCormick, S.D., 2005. Cortisol receptor blockade and seawater adaptation in the euryhaline teleost *Fundulus heteroclitus*. Journal of experimental zoology. Part A, Comparative experimental biology 303, 132-142.

Matsumoto, J., Seikai, T., 1992. Asymmetric pigmentation and pigment disorders in pleuronectiformes (flounders). Pigment cell research / sponsored by the European Society for Pigment Cell Research and the International Pigment Cell Society Suppl 2, 275-282.

McCormick, S.D., Regish, A., O'Dea, M.F., Shrimpton, J.M., 2008. Are we missing a mineralocorticoid in teleost fish? Effects of cortisol, deoxycorticosterone and aldosterone on osmoregulation, gill Na^+,K^+-ATPase activity and isoform mRNA levels in Atlantic salmon. General and Comparative Endocrinology 157, 35-40.

McMenamin, S.K., Bain, E.J., McCann, A.E., Patterson, L.B., Eom, D.S., Waller, Z.P., Hamill, J.C., Kuhlman, J.A., Eisen, J.S., Parichy, D.M., 2014. Thyroid hormone-dependent adult pigment cell lineage and pattern in zebrafish. Science 345, 1358-1361.

Mommsen, T.P., Vijayan, M.M., Moon, T.W., 1999. Cortisol in teleosts: dynamics, mechanism of action, and metabolic regulation. Reviews in Fish Biology and Fisheries 9.

Muzzio, A.M., Noyes, P.D., Stapleton, H.M., Lema, S.C., 2014. Tissue distribution and thyroid hormone effects on mRNA abundance for membrane transporters Mct8, Mct10, and organic anion-transporting polypeptides (Oatps) in a teleost fish. Comparative Biochemistry and Physiology. Part A, Molecular & Integrative Physiology 167, 77-89.

Nakamura, M., Seikai, T., Aritaki, M., Masuda, R., Tanaka, M., Tagawa, M., 2010. Dual appearance of xanthophores, and ontogenetic changes in other pigment cells during early development of Japanese flounder *Paralichthys olivaceus*. Fish Sciences 76.

Noyes, P.D., Lema, S.C., Macaulay, L.J., Douglas, N.K., Stapleton, H.M., 2013. Low level exposure to the flame retardant BDE-209 reduces thyroid hormone levels and disrupts thyroid signaling in fathead minnows. Environmental Science and Technology 47, 10012-10021.

Okada, N., Morita, T., Tanaka, M., Tagawa, M., 2005. Thyroid hormone deficiency in abnormal larvae of the Japanese flounder *Paralichthys olivaceus*, Fisheries Science 71, 107-114.

Olsen, Y., Evjemo, J.O., Olsen, A., 1999. Status of the cultivation technology for production of Atlantic halibut (*Hippoglossus hippoglossus*) juveniles in Norway/Europe, Aquaculture 176, 3-13

Orozco, A., Navarrete-Ramirez, P., Olvera, A., Garcia, G.C., 2014. 3,5-Diiodothyronine (T2) is on a role. A new hormone in search of recognition. General and Comparative Endocrinology 203, 174-180.

Power, D.M., Einarsdóttir, I.E., Pittman, K., Sweeney, G.E., Hildahl, J., Campinho, M.A., Silva, N., Sæle, Ø., Galay-Burgos, M., Sráradóttir, H., Björnsson, B.T., 2008. The Molecular and Endocrine Basis of Flatfish Metamorphosis. Reviews in Fisheries Science 16, 95-111.

Ruane, N.M., Makridis, P., Balm, P.H.M., Dinis, M.T., 2005. Skin darkness is related to cortisol, but not MSH, content in post-larval *Solea senegalensis*, Journal of Fish Biology 67, 577-581.

Saele, O., Solbakken, J.S., Watanabe, K., Hamre, K., Power, D., Pittman, K., 2004. Staging of Atlantic halibut (*Hippoglossus hippoglossus* L.) from first feeding through metamorphosis, including cranial ossification independent of eye migration. Aquaculture. 239, 445-465.

Schreiber, A.M., Specker, J.L., 2000. Metamorphosis in the Summer Flounder, *Paralichthys dentatus*: Thyroidal Status Influences Gill Mitochondria-Rich Cells. General and Comparative Endocrinology 117, 238-250.

Schreiber, A.M., Wang, X., Tan, Y., Sievers, Q., Sievers, B., Lee, M., Burrall, K., 2010. Thyroid hormone mediates otolith growth and development during flatfish metamorphosis. General and Comparative Endocrinology 169, 130-137.

Scott, G.R., Keir, K.R., Schulte, P.M., 2005. Effects of spironolactone and RU486 on gene expression and cell proliferation after freshwater transfer in the euryhaline killifish. Journal of Comparative Physiology. B, Biochemical, Systemic, and Environmental Physiology 175, 499-510.

Slominski, A., Tobin, D.J., Shibahara, S., Wortsman, J., 2004. Melanin pigmentation in mammalian skin and its hormonal regulation. Physiological Reviews 84, 1155-1228.

Sun, M., Wei, F., Li, H., Xu, J., Chen, X., Gong, X., Tian, Y., Chen, S., Bao, B., 2015. Distortion of frontal bones results from cell apoptosis by the mechanical force from the up-migrating eye during metamorphosis in *Paralichthys olivaceus*. Mechanisms of development 136, 87-98.

Suzuki, K.-i., Machiyama, F., Nishino, S., Watanabe, Y., Kashiwagi, K., Kashiwagi, A., Yoshizato, K., 2009. Molecular features of thyroid hormone-regulated skin remodeling in *Xenopus laevis* during metamorphosis. Development, Growth and Differentiation 51, 411-427.

Tagawa, M., Aritaki, M., 2005. Production of symmetrical flatfish by controlling the timing of thyroid hormone treatment in spotted halibut *Verasper variegatus*. General and Comparative Endocrinology 141, 184-189.

Takahashi, A., Kobayashi, Y., Amano, M., Yamanome, T., 2009. Structural and functional diversity of proopiomelanocortin in fish with special reference to barfin flounder, Peptides 30, 1374-1382.

Todd, K.J., Eales, J.G., 2002. The effect of handling and blood removal on plasma levels and hepatic deiodination of thyroid hormones in adult male and female rainbow trout, *Oncorhynchus mykiss*. Canadian Journal of Zoology 80, 372-375.

Trijuno, D.D., Yoseda, K., Hirokawa, J., Tagawa, M., Tanaka, M., 2002. Effects of thyroxine and thiourea on the metamorphosis of coral trout grouper *Plectropomus leopardus*, Fisheries Science 68, 282-289.

Vatine, G.D., Zada, D., Lerer-Goldshtein, T., Tovin, A., Malkinson, G., Yaniv, K., Appelbaum, L., 2013. Zebrafish as a model for monocarboxyl transporter 8-deficiency. The Journal of Biological Chemistry 288, 169-180.

Quigley, A.K., Turner, J.M., Nuckels, R.J., Manuel, J.L., Budi, E.H., MacDonald, E.L., Parichy, D.M., 2004. Pigment pattern evolution by differential deployment of neural crest and post-embryonic melanophore lineages in Danio fishes, Development 131, 6053-6069.

Visser, W.E., Philp, N.J., van Dijk, T.B., Klootwijk, W., Friesema, E.C., Jansen, J., Beesley, P.W., Ianculescu, A.G., Visser, T.J., 2009. Evidence for a homodimeric structure of human monocarboxylate transporter 8, Endocrinology 150, 5163-70.

Visser, W.E., Friesema, E.C., Visser, T.J., 2011. Minireview: thyroid hormone transporters: the knowns and the unknowns. Molecular Endocrinology 25, 1-14.

Walpita, C.N., Van der Geyten, S., Rurangwa, E., Darras, V.M., 2007. The effect of 3,5,3'-triiodothyronine supplementation on zebrafish (*Danio rerio*) embryonic development and expression of iodothyronine deiodinases and thyroid hormone receptors. General and Comparative Endocrinology 152, 206-214.

Walpita, C.N., Crawford, A.D., Janssens, E.D., Van der Geyten, S., Darras, V.M., 2009. Type 2 iodothyronine deiodinase is essential for thyroid hormone-dependent embryonic development and pigmentation in zebrafish. Endocrinology 150, 530-539.

Wang, J., Hou, L., Zhang, R., Zhao, X., Jiang, L., Sun, W., An, J., Li, X., 2007. The tyrosinase gene family and albinism in fish, Chinese Journal of Oceanology and Limnology 25, 191-198.

Wegner, M., 2006. Melanocytes and the Transcription Factor Sox10 in: V. J. Hearing, S. P. L. Leong. EDs, From Melanocytes to Melanoma: The Progression to Malignancy. Humana Press Inc., Totowa, NJ, 71-80.

Yamada, T., Okauchi, M., Araki, K., 2010. Origin of adult-type pigment cells forming the asymmetric pigment pattern, in Japanese flounder (*Paralichthys olivaceus*). Developmental dynamics: an official publication of the American Association of Anatomists 239, 3147-3162.

Yamaguchi, Y., Brenner, M., Hearing, V.J., 2007. The regulation of skin pigmentation. The Journal of biological chemistry 282, 27557-27561.

Yamano, K., Miwa, S., 1998. Differential gene expression of thyroid hormone receptor alpha and beta in fish development. General and Comparative Endocrinology 109, 75-85.

Yoo, J.H., Takeuchi, T., Tagawa, M., Seikai, T., 2000. Effect of Thyroid Hormones on the Stage-specific Pigmentation of the Japanese Flounder *Paralichthys olivaceus*. Zoological Science 17, 1101-1106.

Youson, J. H., 1988. First metamorphosis. In "Fish Physiology". W. S. Hoar and D. J. Randall, Eds., 135-196. Academic Press, San Diego.

Zhang, W.T., Liu, K., Xiang, J.S., Zhang, L.Y., Liu, W.J., Dong, Z.D., Li, Y.Z., Li, H.L., Chen, S.L., Wang, N., 2016. Molecular cloning, expression of, and regulation by thyroid-hormone receptor alpha A in the half-smooth tongue sole *Cynoglossus semilaevis* during metamorphosis. Journal Fish Biology 88, 1693-1707.

Additional Files

Additional file 5.1. Relative gene expression analysis (qPCR) of TH related genes during Atlantic halibut ocular - ST (**A**) and abocular – SB (**B**) skin metamorphosis (stage 7 to 9B, n = 5 per stages) in control, MMI and RU486 exposed fish. *Dio1* (deiodinase 1), *dio2* (deiodinase 2), *dio3a* (deiodinase 3A), *trαa* (thyroid hormone receptor α A) gene expression. Results are presented as mean ± SEM of the candidate gene expression, normalized using the geometric mean of the reference genes *rps4* and *ef1a1*. Significant difference ($p < 0.05$; three-way ANOVA) of normalized transcript expression between stages, skin sides and treatments are indicated by different letters. Different lower case letters represent significant differences in gene expression between metamorphic stages in MMI; different numbers represent significant differences in gene expression between metamorphic stages in RU486.

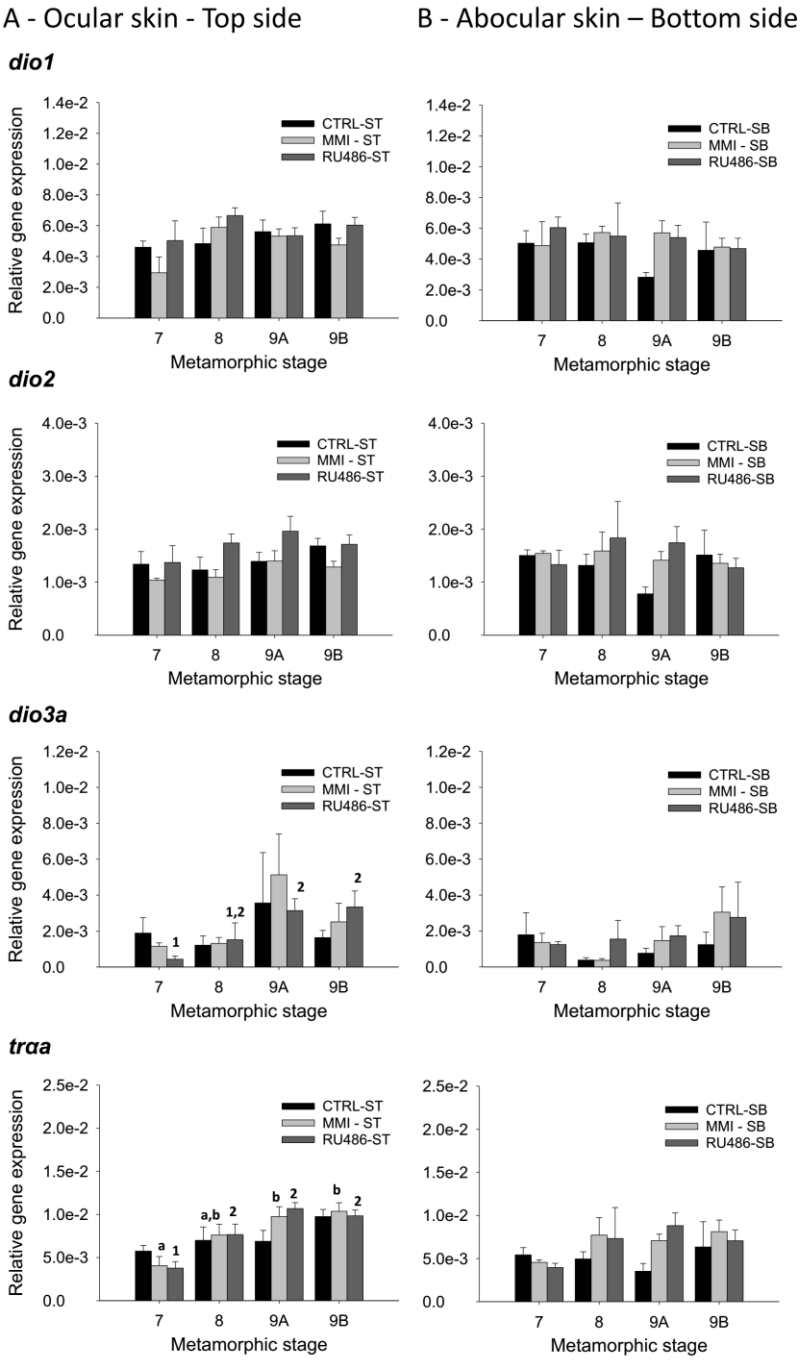

Additional file 5.2. Relative gene expression analysis (qPCR) of pigmentation related genes during Atlantic halibut ocular - ST (**A**) and abocular – SB (**B**) skin metamorphosis (stage 7 to 9B, n = 5 per stages) in control, MMI and RU486 exposed fish. *Asip* (agouti signaling protein) and *pomcβ* (proopiomelanocortin beta) gene expression. Results are presented as mean ± SEM of the candidate gene expression, normalized using the geometric mean of the reference genes *rps4* and *ef1a1*. Significant difference ($p < 0.05$; three-way ANOVA) of normalized transcript expression between stages, skin sides and treatments are indicated by different letters. Different lower case letters represent significant differences in gene expression between metamorphic stages in MMI; different numbers represent significant differences in gene expression between metamorphic stages in RU486. * significant differences between control and methimazole; ǂ significant differences between MMI and RU486.

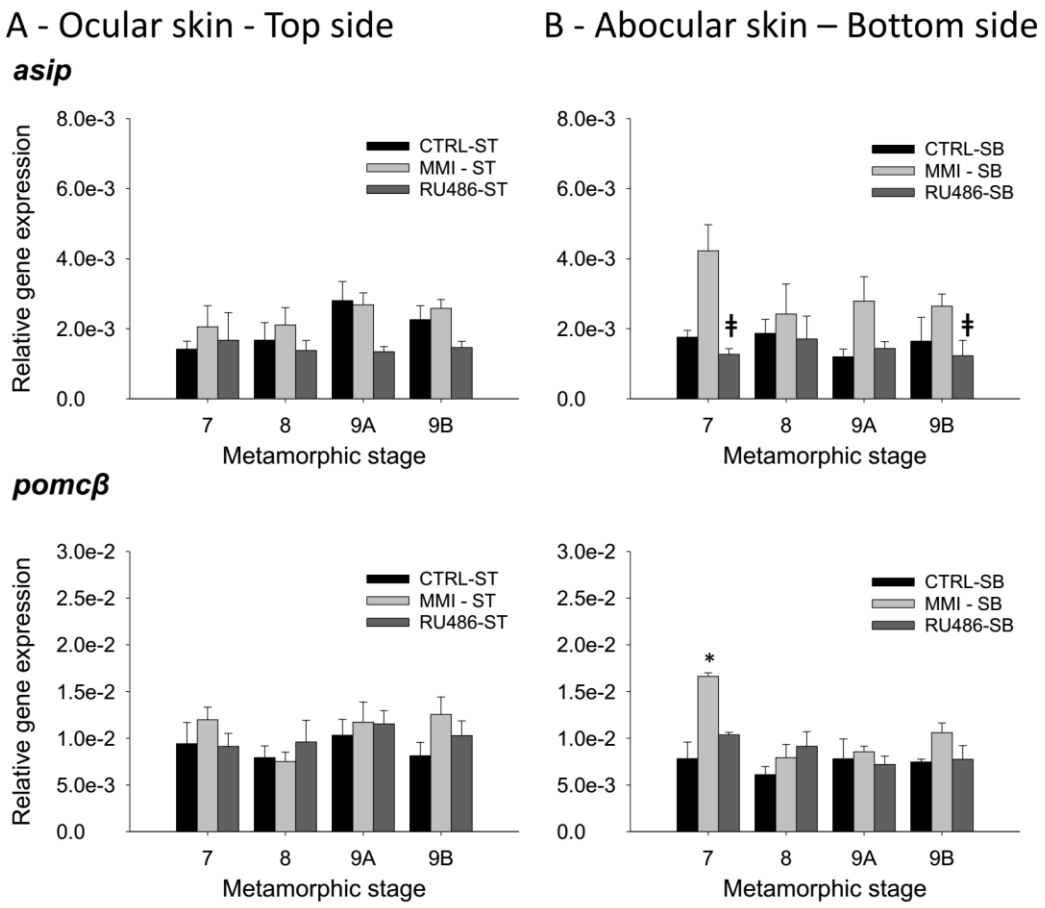

Chapter 5

Chapter 6
General discussion and future perspectives

Chapter 6

6.1 General discussion

The importance of THs in the development of flatfish particularly during metamorphosis has been recognised for at least twenty years. THs drive the dramatic morphologic transformations occurring when flatfish transform from a pelagic symmetric larva to a benthic asymmetric juvenile (Inui et al., 1995; Miwa et al., 1998, 1992; Einarsdóttir et al., 2006; Power et al., 2008; Schreiber & Specker, 1998). In addition to the readily observed external transformation in flatfish morphology, THs promote a plethora of changes during the growth and differentiation of tissues and organs, such as the skin. The involvement of THs in these changes has previously been described (Campinho et al., 2007a, 2007b, 2012a, Gomes et al., 2014a; Schreiber and Specker, 1998; Schreiber et al., 2010; Sun et al., 2013; Yamano et al., 1991; Yamano et al., 1994; Yoo et al., 2000; Zambonino et al., 2008; Zhang et al., 2016). However, little is known about the molecular basis of flatfish metamorphosis, specifically the tissue specific changes, and how they are coordinated by THs. Characterising the molecular basis of metamorphosis was the first challenge of the present thesis and it has contributed new insights into the tissue-specific molecular modifications associated with metamorphosis in flatfish, by exploring the transcriptome of three major tissues, the skin, head and GI-tract in the Atlantic halibut (chapter 2). The second major challenge was focused on the skin, in order to establish how THs are involved in its differentiation and maturation during metamorphosis. A further challenge was to identify factors that may explain the asymmetric pigmentation and if this was a consequence of asymmetric responsiveness of the ocular and abocular skin to THs. In the thesis evidence is presented showing that not only is the pigmentation of skin asymmetric but also structural asymmetry of this primary barrier also exists between ocular and abocular skin. Furthermore, both thyroid responsive and non-responsive changes were identified and characterisation of ocular and abocular skin provided insight into the role of THs in the skin in the context of its role as a barrier, in osmoregulation and pigmentation during development (Chapters 3-5). Manipulation of THs and cortisol were used to determine if cross-talk occurs between THs (HPT) and cortisol (HPI) and how this is involved in the maturation of skin during Atlantic halibut metamorphosis (Chapter 5).

Chapter 6

We used NGS 454 technology to determine for the first time the transcriptome of three major developing and remodelling tissues (skin, GI-tract and head) during Atlantic halibut metamorphosis (Chapter 2). NGS techniques are increasingly being used to generate transcriptome resources to study complex biological processes, there are relatively few studies of flatfish and none that focus on flatfish metamorphosis and a further limitation is that the small size of eggs and larvae mean that studies have focussed on pools of whole larvae rather than tissue from individuals (Ferraresso et al., 2013). Studies on individual tissue have been on juveniles or adults (Benzekri et al., 2014; Ferraresso et al., 2013; Pereiro et al., 2012; Wang et al., 2014). In the present study taking advantage of the large size of Atlantic halibut larvae and their slow metamorphosis, it was possible to identify tissue specific molecular changes during skin, GI-tract and head development and morphogenesis. These Atlantic halibut transcriptomes were successfully annotated as similar sequencing outputs and annotation results were achieved to previous 454 experiments on fish (Coppe et al., 2010; Fu and He, 2012; Pereiro et al., 2012; Yúfera et al., 2012). The 454 sequencing significantly increased flatfish transcripts in public databases as thousands of new sequences were generated that will benefit studies of development and morphogenesis. The generated halibut transcriptome will be an important tool to investigate new potential markers for solving problems related to flatfish production mainly during metamorphosis (Hamre et al., 2007; Harboe et al., 2009).

The SOLiD analysis of several individuals by stage and core TH-responsive genes responsible for the timing of stage specific responses of individual tissues were identified (Chapter 2). Analysis if DEG genes detected during metamorphosis revealed the majority were not directly TH-responsive, indicating that many of the TH effects may be indirect and that THs act as a trigger. In addition, cross-referencing of putative TH-responsive genes in whole larvae with the tissue specific transcriptomes revealed the core tissue changes occurring during metamorphosis. In summary, genes involved in signalling pathways and also transcription factors represent targets for future studies, and it seems probable that in common with amphibian metamorphosis play a crucial role in regulating flatfish metamorphosis (Buccolz et al., 2006, 2007; Das et al., 2006, 2009; Helbing et al., 2003). The robustness of the results of DGE from SOLiD analysis of Atlantic halibut metamorphosis was assessed in two ways: (1) validation by qPCR of several DGEs identified by SOLiD analysis and confirmation that they were significantly correlated ($p<0.05$). For example, alpha-globin 1

and type I keratin isoform 2 mRNA expression displayed a strongly differential expression pattern during metamorphosis, as has previously been demonstrated in candidate gene studies in Atlantic halibut (Campinho et al. 2007, Power et al. 2008); (2) The SOLiD DEG analysis was also in agreement with the results of previous candidate gene studies in fish and amphibians. For example, osteonectin (Sparc) that plays an essential role in tissue morphogenesis in mammals (Brekken and Sage, 2001; Tremble et al., 1993; Yan et al., 2003) was strongly down-regulated at stages 7 and significantly increased in stage 9A Atlantic halibut. This is reminiscent of what occurs in the flatfish *Scophthalmus maximus* (Torres-Nunez et al., 2015) and in the present thesis additional immunohistochemical (IHC) studies of osteonectin in the ocular skin confirmed that the protein also accumulates during metamorphosis (Chapter 4).

The skin, which has largely been neglected in studies of metamorphosis was the main target of the present thesis, the skin transcriptome was enriched in transcripts related to the epidermis and connective tissue development, appendage morphogenesis and pigmentation (Roosterman et al., 2006; Zouboulis, 2000). In addition, genes involved in vertebrate skin development and morphogenesis were also enriched and included components of the extracellular matrix structure, remodelling and break-down, which are generally associated with metamorphosis, several of which are described as responsive to THs (Ishizuya-Oka, 2011; Le Guellec et al., 2004; Olaso et al., 2011; Vogel et al., 2006; Page et al., 2009; Page et al., 2008; Suzuki et al., 2009). Some of the TH-responsive proteins together with the detected TH-independent growth factors, chemokines, adhesion molecules and proteoglycans have previously been identified in relation to tissue differentiation, development and morphogenesis of vertebrate skin (Le Guellec et al., 2004; Page et al., 2008; Suzuki et al., 2009; Watt and Fujiwara, 2011). Genes related to the ECM should be future targets as they will provide insight into the mechanisms underlying skin maturation and differentiation and their potential relationship with THs and other endocrine factors that may co-regulate this processes. The enrichment of the skin transcriptome with ECM related genes and their differential expression between metamorphic stages in SOLiD analysis highlights the importance of these genes. Potential ECM candidates include *mmp13*, *col1a2* and fibronectin that are reported to be modified during amphibian metamorphosis (Helbing et al., 2003; Suzuki et al. 2009). Another interesting feature of skin transcriptome was the enrichment of

GO terms involved in immune response. The results are unsurprising when the importance of the skin as an innate immune barrier is considered and it is a point of direct interaction between organisms and their environment. Barrier function has mainly been considered in skin, gill and GI-tract of adults (Cain and Swan, 2010) and next generation sequencing has been used to explore the transcriptome of such tissue in mud loach (*Misgurnus anguillicaudatus*; Long et al., 2013), yellow croaker (*Pseudosciaena crocea*; Mu et al., 2010) and turbot (Pereiro et al., 2012). The assembly and interpretation of the Atlantic halibut skin transcriptome was a long process but it established an essential tool that underpinned the other chapters of this thesis (Chapters 3 to 5) and is a rich source of data for hypothesis generation.

In Atlantic halibut, the GI-tract undergoes extensive remodeling to prepare it for the shift in habitat and diet in the juvenile (Gomes et al., 2014a; Gomes et al., 2015). In fact, the sequenced GI-tract during metamorphosis was enriched in biological processes such as, digestion, proteolysis and lipid metabolism including the cholesterol metabolic process and triglyceride mobilization. These results are similar to that reported during amphibian metamorphosis, in which GO terms related to digestion were "shut down" at metamorphic climax, but increased again at the end of metamorphosis (Heimeier et al., 2010). In addition, SOLiD analysis revealed DE of digestive enzymes, such as trypsin, chymotrypsin and phospholipase A2 during Atlantic halibut metamorphosis, as previously reported in other fish species (Ozkizilcik et al., 1996; Zambonino Infante and Cahu, 1999; Zambonino et al., 2008). We further generated a list of candidate genes involved in the development and morphogenesis of the Atlantic halibut GI-tract. For example, important signal transduction pathways involved in intestinal development in other vertebrates, including, Shh, Wnt and BMP (Ishizuya-Oka et al., 2006; Kim et al., 2011; van der Flier and Clevers, 2009) were identified in the GI-tract transcriptome (Chapter 2).

The head transcriptome was unsurprisingly the NGS dataset with the highest number of unique transcripts (8,359) and GO terms (1,170) due to the complexity of the sample, which contains several different tissues (brain, nervous tissue, skin, brain, bone, muscle. This transcriptome was enriched in genes related to the development of the nervous system, spinal cord and otoliths, cartilage and endochondral bone and also pituitary gland development and thyroid hormone metabolic processes. Essential signalling pathways that trigger tissue

development and cell proliferation and differentiation (e.g. Notch, Sonic hedgehog, Wnt, BMP) (Botchkarev and Sharov, 2004; Ingham and McMahon, 2001; Janicke et al., 2007; Logan and Nusse, 2004; Paridaen and Huttner, 2014; Pascual and Aranda, 2013), were well represented in all three tissue transcriptomes, but especially in the head transcriptome. Several of the signalling pathways are regulated by THs and specific studies will be required to establish their precise mode of action and the tissue specific consequences of their up-regulation. Another highlight of the head transcriptome was the identification of TFs specific for thyroid gland development, such as homeobox protein NK2.1, hematopoietically expressed homeobox (*hhex*) and *pax8* (Fernandez et al., 2015), and this suggests that the modification of thyroid tissue is essential for successful metamorphosis (Klaren et al., 2008) and disruption of this process may explain failed metamorphosis in some cases (Chapter 2).

In Atlantic halibut, the initiation of metamorphosis is associated with a surge in T_4 and T_3, which increases up until the metamorphic climax and decreases in post-climax stages (Einarsdóttir et al., 2006; Galay-Burgos et al., 2008). The activation of the thyroid gland occurs in early premetamorphic larvae and this supports the notion that THs play a significant role in the metamorphic process of flatfish (Einarsdóttir et al., 2006). Thyroid follicle activity increases significantly before the metamorphic climax and it is strongly correlated to the appearance of abundant thyrotrophs in the pituitary gland (Einarsdóttir et al., 2006). The results of thyroid activity based upon morphological and RIA studies were confirmed by the molecular data, which was enriched in genes involved in thyroid gland development in the head transcriptome. We also confirmed that the TH cascade is activated in the three metamorphosing transcriptomes since we identified genes involved in THs production, transport, metabolism and action (Chapter 2). Our results are in agreement with previous candidate gene studies that targeted thyroglobulin, thyroid hormone receptors and deiodinases in the Atlantic halibut and Senegalese sole (Campinho et al., 2012; Galay-Burgos et al., 2008; Manchado et al., 2008, 2009). A novel observation resulting from the work reported in this thesis was the identification and mapping of two thyroid hormones transporters in the metamorphosing Atlantic halibut transcriptome. To our knowledge, no other studies have reported or demonstrated the expression of *mct8* and *mct10* during flatfish metamorphosis. These two THs transporters have been considered to be essential for fish development (Vatine et al., 2013) and KD of *mct8* in zebrafish affected the spinal cord and brain development and

mct8 morphants has impaired eye development. Both transporters are expressed in whole larvae during metamorphosis, but only *mct8* was significantly up-regulated during the metamorphic climax. These results suggest that changes in cellular TH uptake and efflux are essential for local regulation of nuclear TR-mediated signalling in flatfish metamorphosis, as observed in amphibians (Connors et al., 2010). Nevertheless, these expression results should be interpreted with caution, as the gene expression was performed with whole-larvae, and as observed for amphibians, temporal expression pattern of THs transporters can vary between tissues and is correlated with the timing of their metamorphic changes (Connors et al., 2010).

Another exciting finding from the halibut transcriptome analysis was the existence of two different deiodinase 3 transcripts. In fact, the existence of duplicate dio3 genes was recently described and characterized in zebrafish and shown to have divergent biological roles during development (Guo et al., 2014; Heijlen et al., 2014). We confirmed by phylogenetic analysis the existence of duplicated *dio3* in Atlantic halibut (Chapter 3) and in other teleosts, results that suggest that they emerged during the teleost specific-specific whole genome duplication (Jaillon et al., 2004). The Atlantic halibut *dio3a* and *dio3b* were homologous of *dio3a* and *dio3b* in zebrafish, described previously by Guo et al. (2014). Subsequently, we tried to resolve the intriguing question about why these duplicate *dio3* genes have been maintained. The results obtained for tissue distribution and ontogeny in whole larvae suggested that subfunctionalization of these two genes occurred so that they have different roles during metamorphosis (Chapter 3). Sub-functionalization is supported by the finding that *Dio3b* seems to be the predominant transcript and is responsive to THs during flatfish metamorphosis. The sub-functionalization hypothesis is supported by the observation in zebrafish development that *Dio3a* and *b* have some overlapping but other divergent functions (Guo et al., 2014; Heijlen et al., 2014).

In the Chapter 3 the potential asymmetric TH responsiveness of the ocular and abocular skin was explored to understand the molecular basis of its characteristic phenotype observed after metamorphosis. Our results suggested that *dio3* gene duplicates had a divergent expression pattern in skin and these results were very different from those of whole larvae and this highlights the limitations of using whole larvae to establish the role of THs in the non-synchronous developmental events during metamorphosis. Of the Atlantic halibut *dio* duplicates only *dio3b* was differential expressed between metamorphic stages in skin, and

the experiment with MMI and "*in silico*" analysis of the fish *dio3a* and *dio3b* promoters suggest that Atlantic halibut *dio3b* is TH responsive and is repressed by THs during metamorphosis (Chapter 3). In fact, *dio3* has previously been identified as TH-responsive in amphibians (Das et al., 2009; Suzuki et al., 2009). Overall, the results indicated that *dio3b* is one of the genes important for the divergent maturation of ocular and abocular larval skin to the juvenile phenotype. However, the functional significance, in relation to TH levels, of the asymmetric expression of *dio3b* was not established nor was the cellular context that explains the divergent expression of *dio3* in ocular and abocular skin and this will be an important target for future work. Moreover, the recent reports showing that T_4, T_2 and rT_3 are physiologically active (Moreno et al., 2008) also raises intriguing new possibilities for investigation.

The skin constitutes a very interesting model to study the mechanisms underlying teleost development. First, skin is the major barrier between the animal and its external environment (Madison, 2003; Proksch et al., 2008). Second, the fish epidermis is composed of different functional cell types and is under endocrine control of several hormones and neuropeptides (reviewed by Rakers et al., 2010). Third, the involvement of THs in skin development during metamorphosis has previously been described (Campinho et al. 2012), but the possible asymmetric responsiveness to THs of ocular and abocular skin is unclear. The study of this asymmetric characteristic of flatfish, with special attention in pigmentation has increased the knowledge about the mechanisms that underlying normal pigmentation but also give insight into malpigmentation problems during production of flatfish.

The evidence of potential asymmetric responsiveness of ocular and abocular skin to THs during metamorphosis revealed for the first time in a flatfish in chapter 3 led us to investigate if the other genes involved in THs metabolism (deiodinases, *dio1*, *dio2*), transport (*mct8*, *mct10*) and action (TRs, *trαa* and *trβ*) have a similar or opposite expression patterns (Chapter 5). In relation to deiodinases, the constant *dio1* and *dio2* expression in the skin and their symmetric expression between ocular and abocular skin is presumably essential for maintenance of basal levels of T_3. In whole larvae, both *dio1* and *dio2* were up-regulated during metamorphic climax in whole larvae (Chapter 2), suggesting that morphogenetic events at metamorphic climax can be synchronized by T_3 coming from other peripheral tissues, such as the liver (Isorna et al., 2009). Both TRs were expressed in ocular and abocular

skin, but only *trβ* was up-regulated suggesting that *trβ* is the main TR isoform acting in the morphogenetic changes induced by THs that occur during skin metamorphosis, as previously observed in *X. laevis* skin after treatment with THs (Suzuki et al., 2009). However, an important aspect about the TRs is their dual role resulting from the presence or absence of a ligand and the failure to measure the tissue specific concentration of THs meant the functional mode could not be established. Further research is required in relation to the TRs to determine their role in the presence or absence of a ligand in the skin during metamorphosis. In addition, to the TRs and deiodinases, the TH transporters seem to be the most important genes in the regulation of cellular availability of THs in ocular and abocular skin during metamorphosis (Chapter 5). We hypothesized that *mct8* and *mct10* may have different roles in the ocular (ST) and abocular skin (SB), as their expression was constant in ST but decreased in SB during the early metamorphic climax (stage 9A) and the ocular/abocular ratio for both transporters was asymmetric, suggesting that in the ocular skin side, the cellular uptake and efflux of THs is more pronounced during metamorphosis. The up-regulation of *mct8* and *mct10* in ocular skin in the stage 9A may be associated with the time that levels of T_4 and T_3 are highest during the metamorphic climax of the Atlantic halibut (Galay-Burgos et al. 2008). Overall, the results for *dio's* and *mct's* suggest that the ocular skin has a higher uptake of the THs during metamorphosis. In amphibians, the temporal expression pattern of TH transporters varied between the major resorbing, growing and remodeling tissues and is correlated with the timing of their metamorphic changes (Connors et al. 2010), and that seems to be also the case of flatfish metamorphosis.

In chapter 4 we investigated the structural and functional maturation of skin during metamorphosis in the Atlantic halibut. Using a histochemical approach the functional asymmetry of primary barrier and osmoregulation functions in skin was established. The mucous producing cells and mitochondria-rich NKA cells were the main focus. We observed that skin morphology in the ocular side appears to be more complex with, more cells in the epidermis and a thicker collagen lamella when compared to abocular skin raising interesting questions in relation to the role of THs in this process. These observations are consistent with the previous results obtained by Campinho et al. (2007) that showed that in the skin of the stage 7 and 8 Atlantic halibut a new stratum starts to develop in the epidermis, due to an increased number of supra-basal and goblet cells and a thicker collagen lamella. However,

this stratum developed prior to metamorphosis and the peak of THs and detailed cellular studies will be required to establish if they trigger this maturation. The high stratified skin observed in the metamorphic climax had an epidermis composed of several layers and cell types in contact with a complex collagen lamella and this maturation was coincident with the peak of THs. Moreover, as highlighted above a number of elements of the matrix and its remodelling were enriched in the transcriptome and are also reported to be involved in amphibian metamorphosis. More specifically we also hypothesized that osteonectin is important in epidermis remodelling during halibut metamorphosis.

The early appearance of mucous producing cells during development of the skin establishes the role of mucous as first line of defence (Hachero-Cruzado et al., 2009). Both neutral and acidic mucins were presented in ocular, abocular and head region skin, but varied between skin regions and metamorphic stages, suggesting for potential different roles of neutral and acidic mucins during halibut development. Furthermore, the early appearance in skin of goblet cells raises questions about the role of THs in their differentiation, although mucin differentiation has been proposed to be TH responsive in other vertebrates. In the present thesis, we reported for the first time several salient aspects in relation to the mucins during flatfish development: (1) neutral mucins predominated during metamorphosis in ocular and abocular skin; (2) the number of neutral mucins increased from stage 7 to metamorphic climax stage 9A and (3) higher number of mucins in ocular skin compared to the abocular side was observed during the metamorphic stages 8, 9A, and 9B. These results revealed that THs influence goblet cells in skin and mucous production. Moreover, the asymmetry observed in the number of mucous positive PAS producing (neutral mucins) cells may be a consequence of divergent TH tissue responsiveness possibly as a result of asymmetric *mct's* and TR's in stage 9A Atlantic halibut ocular and abocular skin (Chapter 5) that leads to down-regulation of mucin genes in the abocular skin. In mammals, THs promote mucous differentiation by regulating the mucin genes (Gray et al., 2011), (Chapter 4). Overall, the mucous and other cell composition and permeability properties of the skin suggests that diffusional and invasive forces on ocular skin from the surrounding water needs a larger degree of protection than the more mechanical effects from the underlying substrate on abocular skin.

The role of skin as an osmoregulatory tissue was confirmed by the presence of ionocytes (Na^+, K^+-ATPase enriched cells) in the skin of the head and body during the

metamorphosis, and in contrast to mucous producing cells, no asymmetry was observed between skin sides (Chapter 4). The decreasing in the number of Na^+, K^+-ATPase enriched cells in the skin during the metamorphosis was related with gill development (Einarsdottir et al., 2011). In addtion, THs to the Na^+, K^+-ATPase were down-regulated in the skin during the metamorphosis. The responsiveness of ionocytes to THs was previously shown by the treatment of premetamorphic larvae with thiorea (TU) which inhibits the Na^+, K^+-ATPase immunoreactivity (Schreiber and Specker, 2000). Nonetheless, the timing of the appearance of Na^+, K^+-ATP in skin was not co-incident with the main peak of THs associated with metamorphosis and clearly further work will be required to resolve this puzzle.

The development of the morphology of the skin barrier diverged between the ocular and abocular side of the metamorphosing halibut larvae. The increased complexity and thickness of both epithelial cells and connective tissue were more pronounced on the ocular side, which was also the case for the specific cell types, melanophores (only present on the ocular side) and goblet cells, more numerous on the ocular side. This suggests that diffusional and invasive forces from the surrounding water needs larger degree of protection than the more mechanical effects from the underlying substrate.

The asymmetric pigmentation observed in the body of post-metamorphic flatfish is a characteristic of these organisms. Until the onset of metamorphosis, flatfish larvae are bilaterally symmetric, but in contrast to other teleosts, only the ocular skin side of the body becomes pigmented, whereas the abocular side that rests on the sea bottom lacks pigment (reviewed in Power et al., 2008). In flatfish, the molecular signalling of skin pigmentation and melanogenesis occurs during metamorphosis (Darias et al. 2013), and we revealed for the first time, how this molecular signalling differs between ocular and abocular skin sides, by showing a clear asymmetric expression pattern of genes that regulate this process (Chapter 5). By searching the skin transcriptome (Chapter 2), genes were identified that have a well-recognised role in pigmentation and by qPCR we observed that the melanogenic enzymes *tyrp1* and *dct* were up-regulated in ocular skin, and expression of both enzymes increased during metamorphosis in this skin side, but decreased in abocular skin. The increase only in the ocular skin of melanogenic enzymes was concomitant with the expression of the transcription factor *sox10*, which contributes to activate several melanocyte specific genes especially the melanogenic enzymes and is also responsible for melanophore differentiation

(Ebanks et al., 2009; Wegned, 2000). We proposed that activation of the machinery responsible for melanogenesis and melanophore differentiation occurs in the ocular skin during halibut metamorphosis (Chapter 5). This may explain why after metamorphosis the main chromatophores on the abocular side of flatfish are the iridophores, whereas on the ocular side both melanophores and iridophores are present (Burton, 2010). These molecular changes in the pigmentation related genes are in accordance with the changes observed in the genes involved in THs cascade, suggesting for a potential direct involvement of THs in the pigmentation of flatfish, as evidenced by previous authors (Okada et al., 2005; Tagawa & Aritaki, 2005; Yoo et al., 2000).

The involvement of THs and the possible cross-talk with the HPI axis on the molecular ontogeny of pigmentation during Atlantic halibut metamorphosis was investigated in chapter 5 of this thesis. The thyroid peroxidase inhibitor, MMI, induced transcriptional changes in the TH elements (*dio3b*, *trαa*, *trβ*, *mct8* and *mct10*) affecting both ocular and abocular skin sides. This confirmed the importance of THs in the skin development during the Atlantic halibut metamorphosis. Such transcriptional changes were in accordance with previous TH disruption studies (Dong et al., 2013; Muzzio et al., 2014; Noyes et al., 2013. In addition, MMI also affected the expression of genes involved in melanogenesis. The histology of the thyroid gland revealed reduced thyroid activity indicative of low circulating THs resulted from MMI treatment and affected pigmentation related genes mainly in the abocular skin. Both melanogenic enzymes were up-regulated in the skin during the metamorphic climax. The results of MMI treatment suggests a critical role for THs in the regulation of asymmetric expression of *tyrp1* and *dct*, and the up-regulation of both THs transporters observed in the abocular skin supports this hypothesis. Unfortunately, the phenotype of abocular skin after metamorphosis was not evaluated. Moreover, the effect of RU486 (GR antagonist) on expression of TH-responsive pigmentation related genes was similar to that observed in fish exposed to MMI, evidencing again the possible cross-talk between the two axes. We suggest that THs and cortisol can be linked and act together during flatfish metamorphosis. Such evidence of synergy between cortisol and thyroid hormone during metamorphosis has been described in amphibians (Bonett et al., 2010; Denver, 2009). Clearly, more research will be required to evaluate if this cross-talk between THs and cortisol occurs at central or peripheral level during flatfish metamorphosis, and determination of both THs

and cortisol as well evaluate the expression of genes involved from HPT/HPI will be crucial to address this question.

6.2. Future perspectives

The findings presented in this thesis indicate that halibut is an interesting model to study the cellular TH effects in development, as revealed by the study of the skin, GI-tract and head transcriptomes during metamorphosis. In addition, we contribute to a better understanding about the asymmetric development of ocular and abocular skin and how THs drive this process. Further studies are now required to determine the tissue and cell specific localization and function of candidate genes and to provide experimental evidence for the key networks/pathways involved in Atlantic halibut larvae-to-juvenile transition. Other NGS analysis approaches including the transcriptome analysis of metamorphosing halibut after THs axis disruption and at different metamorphic stages will be interesting to explore in the future. In addition, further analysis will be carried out to explore the tissues transcriptomes including analysis of splice variants, duplicate genes, and transcription factors.

The data presented in the chapter 3 about two duplicate deiodinase 3 genes in the skin during the Atlantic halibut metamorphosis gave insight into the putative divergent functions of both genes in ocular and abocular skin. To confirm our findings, functional assays should be performed, and cells transfected with Atlantic halibut *dio3a* and 3b and deiodinases activity (deiodination) assessed.

Chapter 4 studies and analysis the asymmetric development of skin structure and barrier and osmoregulation functions in Atlantic halibut during metamorphosis and a possible link to THs responsiveness was established. In addition, analysis of mucins and NKA cells and electrical, transporting and permeability properties of skin epithelia in ocular and abocular skin after HPT and HPI axis disruption will be conducted. In chapter 5, we hypothesize that asymmetric responsiveness to THs of ocular and abocular skin determines their fate during metamorphosis and it will be interesting to evaluate the proteome of both skin sides during halibut metamorphosis.

References

Benzekri, H., Armesto, P., Cousin, X., Rovira, M., Crespo, D., Merlo, M., Mazurais, D., Bautista, R., Guerrero-Fernandez, D., Fernandez-Pozo, N., Ponce, M., Infante, C., Zambonino, J., Nidelet, S., Gut, M., Rebordinos, L., Planas, J., Begout, M.-L., Claros, M., Manchado, M., 2014. De novo assembly, characterization and functional annotation of Senegalese sole (*Solea senegalensis*) and common sole (*Solea solea*) transcriptomes: integration in a database and design of a microarray. BMC Genomics 15, 952.

Bonett, R.M., Hoopfer, E.D., Denver, R.J., 2010. Molecular mechanisms of corticosteroid synergy with thyroid hormone during tadpole metamorphosis. General and Comparative Endocrinology 168, 209-219.

Botchkarev, V.A., Sharov, A.A., 2004. BMP signaling in the control of skin development and hair follicle growth. Differentiation 72, 512-526.

Brekken, R.A., Sage, E.H., 2001. SPARC, a matricellular protein: at the crossroads of cell-matrix communication. Matrix Biology 19, 816-827.

Buchholz, D.R., Paul, B.D., Fu, L., Shi, Y.-B., 2006. Molecular and developmental analyses of thyroid hormone receptor function in *Xenopus laevis*, the African clawed frog. General and Comparative Endocrinology 145, 1-19.

Buchholz, D.R., Heimeier, R.A., Das, B., Washington, T., Shi, Y.-B., 2007. Pairing morphology with gene expression in thyroid hormone-induced intestinal remodelling and identification of a core set of TH-induced genes across tadpole tissues. Development Biology 303, 576-590.

Campinho, M.A., Silva, N., Sweeney, G.E., Power, D.M., 2007. Molecular, cellular and histological changes in skin from a larval to an adult phenotype during bony fish metamorphosis. Cell Tissue Research 327, 267-284.

Campinho, M.A., Galay-Burgos, M., Silva, N., Costa, R.A., Alves, R.N., Sweeney, G.E., Power, D.M., 2012. Molecular and cellular changes in skin and muscle during metamorphosis of Atlantic halibut (*Hippoglossus hippoglossus*) are accompanied by changes in deiodinases expression. Cell Tissue Research 350, 333-46.

Connors, K.A., Korte, J.J., Anderson, G.W., Degitz, S.J., 2010. Characterization of thyroid hormone transporter expression during tissue-specific metamorphic events in *Xenopus tropicalis*. General and Comparative Endocrinology 168, 149-159.

Coppe, A., Pujolar, J.M., Maes, G.E., Larsen, P.F., Hansen, M.M., Bernatchez, L., Zane, L., Bortoluzzi, S., 2010. Sequencing, de novo annotation and analysis of the first *Anguilla anguilla* transcriptome: EeelBase opens new perspectives for the study of the critically endangered European eel. BMC Genomics 11, 63.

Darias, M.J., Andree, K.B., Boglino, A., Fernandez, I., Estevez, A., Gisbert, E., 2013. Coordinated regulation of chromatophore differentiation and melanogenesis during the ontogeny of skin pigmentation of *Solea senegalensis* (Kaup, 1858). PloS one 8, e63005.

Das, B., Cai, L., Carter, M.G., Piao, Y.L., Sharov, A.A., Ko, M.S., Brown, D.D., 2006. Gene expression changes at metamorphosis induced by thyroid hormone in *Xenopus laevis* tadpoles. Devevelopment Biology 291, 342-355.

Das, B., Heimeier, R.A., Buchholz, D.R., Shi, Y.B., 2009. Identification of direct thyroid hormone response genes reveals the earliest gene regulation programs during frog metamorphosis. The Journal of Biological Chemistry 284, 34167-34178.

Denver, R.J., 2009. Stress hormones mediate environment-genotype interactions during amphibian development. General and Comparative Endocrinology 164, 20-31.

Dong, W., Macaulay, L.J., Kwok, K.W., Hinton, D.E., Stapleton, H.M., 2013. Using whole mount in situ hybridization to examine thyroid hormone deiodinase expression in embryonic and larval zebrafish: a tool for examining OH-BDE toxicity to early life stages. Aquatic toxicology 132-133, 190-199.

Ebanks, J.P., Wickett, R.R., Boissy, R.E., 2009. Mechanisms regulating skin pigmentation: the rise and fall of complexion coloration. International journal of molecular sciences 10, 4066-4087.

Einarsdóttir, I., Silva, N., Power, D., Sámaradóttir, H., Björnsson, B., 2006. Thyroid and pituitary gland development from hatching through metamorphosis of a teleost flatfish, the Atlantic halibut. Anatomy and embryology 211, 47-60.

Einarsdóttir, I.E., Power, D.M., Jonsson, E., Bjornsson, B.T., 2011. Occurrence of ghrelin-producing cells, the ghrelin receptor and Na^+,K^+-ATPase in tissues of Atlantic halibut (*Hippoglossus hippoglossus*) during early development, Cell and Tissue Research 344, 481-98.

Fernandez, L.P., Lopez-Marquez, A., Santisteban, P., 2015. Thyroid transcription factors in development, differentiation and disease. Nature Reviews Endocrinology 11, 29-42.

Ferraresso, S., Bonaldo, A., Parma, L., Cinotti, S., Massi, P., Bargelloni, L., Gatta, P.P., 2013. Exploring the larval transcriptome of the common sole (*Solea solea* L.). BMC Genomics 14, 315.

Fu, B., He, S., 2012. Transcriptome Analysis of Silver Carp (*Hypophthalmichthys molitrix*) by Paired-End RNA Sequencing. DNA Research 19, 131-142.

Galay-Burgos, M., Power, D.M., Llewellyn, L., Sweeney, G.E., 2008. Thyroid hormone receptor expression during metamorphosis of Atlantic halibut (*Hippoglossus hippoglossus*). Molecular and Cellular Endocrinology 281, 56-63.

Gomes, A., Kamisaka, Y., Harboe, T., Power, D., Ronnestad, I., 2014a. Functional modifications associated with gastrointestinal tract organogenesis during metamorphosis in Atlantic halibut (*Hippoglossus hippoglossus*). BMC Development Biology 14, 11.

Gomes, A.S., Alves, R.N., Stueber, K., Thorne, M.A., Smaradottir, H., Reinhard, R., Clark, M.S., Ronnestad, I., Power, D.M., 2014b. Transcriptome of the Atlantic halibut (*Hippoglossus hippoglossus*). Marine Genomics 18 Pt B, 101-103.

Gomes, A.S., Alves, R.N., Rønnestad, I., Power, D.M., 2015. Orchestrating change: The thyroid hormones and GI-tract development in flatfish metamorphosis. General and Comparative Endocrinology 220, 2-12.

Gray, T., Koo, J.S., Nettesheim, P., 2001. Regulation of mucous differentiation and mucin gene expression in the tracheobronchial epithelium, Toxicology 160, 35-46.

Guo, C., Chen, X., Song, H., Maynard, M.A., Zhou, Y., Lobanov, A.V., Gladyshev, V.N., Ganis, J.J., Wiley, D., Jugo, R.H., Lee, N.Y., Castroneves, L.A., Zon, L.I., Scanlan, T.S., Feldman, H.A., Huang, S.A., 2014. Intrinsic expression of a multiexon type 3 deiodinase gene controls zebrafish embryo size. Endocrinology 155, 4069-4080.

Hachero-Cruzado, I., Ortiz-Delgado, J.B., Borrega, B., Herrera, M., Navas, J.I., Sarasquete, C., 2009. Larval organogenesis of flatfish brill *Scophthalmus rhombus* L: Histological and histochemical aspects. Aquaculture 286, 138-149.

Hamre, K., Holen, E., Moren, M., 2007. Pigmentation and eye migration in Atlantic halibut (*Hippoglossus hippoglossus* L.) larvae: new findings and hypotheses. Aquaculture Nutrition 13, 65-80.

Harboe, T., Mangor-Jensen, A., Naas, K.E, Næss, T., 1998. A tank design for first feeding of Atlantic halibut, *Hippoglossus hippoglossus* L., larvae. Aquaculture Research 29, 919–923.

Heijlen, M., Houbrechts, A.M., Bagci, E., Van Herck, S.L., Kersseboom, S., Esguerra, C.V., Blust, R., Visser, T.J., Knapen, D., Darras, V.M., 2014. Knockdown of type 3 iodothyronine deiodinase severely perturbs both embryonic and early larval development in zebrafish. Endocrinology 155, 1547-1559.

Heimeier, R., Das, B., Buchholz, D., Fiorentino, M., Shi, Y.-B., 2010. Studies on *Xenopus laevis* intestine reveal biological pathways underlying vertebrate gut adaptation from embryo to adult. Genome Biology 11, R55.

Helbing, C.C., Werry, K., Crump, D., Domanski, D., Veldhoen, N., Bailey, C.M., 2003. Expression Profiles of Novel Thyroid Hormone-Responsive Genes and Proteins in the Tail of *Xenopus laevis* Tadpoles Undergoing Precocious Metamorphosis. Molecular Endocrinology 17, 1395-1409.

Ingham, P.W., McMahon, A.P., 2001. Hedgehog signaling in animal development: paradigms and principles. Genes and Development 15, 3059-3087.

Inui, Y., Yamano, K., Miwa, S., 1995. The role of thyroid hormone in tissue development in metamorphosing flounder. Aquaculture 135, 87-98.

Ishizuya-Oka, A., 2011. Amphibian organ remodelling during metamorphosis: insight into thyroid hormone-induced apoptosis. Development Growth Differentiation 53, 202-212.

Ishizuya-Oka, A., Hasebe, T., Buchholz, D.R., Kajita, M., Fu, L., Shi, Y.B., 2009. Origin of the adult intestinal stem cells induced by thyroid hormone in *Xenopus laevis*. The Federation of American Societies for Experimental Biology Journal. 23, 2568-2575.

Isorna, E., Obregon, M.J., Calvo, R.M., Vazquez, R., Pendon, C., Falcon, J., Munoz-Cueto, J.A., 2009. Iodothyronine deiodinases and thyroid hormone receptors regulation during flatfish (*Solea senegalensis*) metamorphosis. Journal of experimental zoology. Part B, Molecular and Developmental Evolution 312B, 231-246.

Itoh, K., Watanabe, K., Wu, X., Suzuki, T., 2010. Three members of the iodothyronine deiodinase family, dio1, dio2 and dio3, are expressed in spatially and temporally specific patterns during metamorphosis of the flounder, *Paralichthys olivaceus*. Zoology Sciences 27, 574-580.

Jaillon, O., Aury, J.M., Brunet, F., Petit, J.L., Stange-Thomann, N., Mauceli, E., Bouneau, L., Fischer, C., Ozouf-Costaz, C., Bernot, A., Nicaud, S., Jaffe, D., Fisher, S., Lutfalla, G., Dossat, C., Segurens, B., Dasilva, C., Salanoubat, M., Levy, M., Boudet, N., Castellano, S., Anthouard, R., Jubin, C., Castelli, V., Katinka, M., Vacherie, B., Biemont, C., Skalli, Z., Cattolico, L., Poulain, J., de Berardinis, V., Cruaud, C., Duprat, S., Brottier, P., Coutanceau, J.P., Gouzy, J., Parra, G., Lardier, G., Chapple, C., McKernan, K.J., McEwan, P., Bosak, S., Kellis, M., Volff, J.N., Guigo, R., Zody, M.C., Mesirov, J., Lindblad-Toh, K., Birren, B., Nusbaum, C., Kahn, D., Robinson-Rechavi, M., Laudet, V., Schachter, V., Quetier, F., Saurin, W., Scarpelli, C., Wincker, P., Lander, E.S., Weissenbach, J., Crollius, H.R., 2004. Genome duplication in the teleost fish *Tetraodon nigroviridis* reveals the early vertebrate proto-karyotype. Nature 431, 946-957.

Janicke, M., Carney, T.J., Hammerschmidt, M., 2007. Foxi3 transcription factors and Notch signaling control the formation of skin ionocytes from epidermal precursors of the zebrafish embryo. Development Biology 307, 258-271.

Klaren, P.H.M., Wunderink, Y.S., Yúfera, M., Mancera, J.M., Flik, G., 2008. The thyroid gland and thyroid hormones in Senegalese sole (*Solea senegalensis*) during early development and metamorphosis. General and Comparative Endocrinology 155, 686-694.

Kim, T.H., Kim, B.M., Mao, J., Rowan, S. and Shivdasani, R.A. 2011. Endodermal Hedgehog signals modulate Notch pathway activity in the developing digestive tract mesenchyme. Development 138, 3225-3233.

Le Guellec, D., Morvan-Dubois, G., Sire, J.Y., 2004. Skin development in bony fish with particular emphasis on collagen deposition in the dermis of the zebrafish (*Danio rerio*). The International Journal of Developmental Biology 48, 217-231.

Logan, C.Y., Nusse, R., 2004. The Wnt signaling pathway in development and disease. Annual Review of Cell and Developmental Biology 20, 781-810.

Madison, K.C., 2003. Barrier function of the skin: "la raison d'etre" of the epidermis. The Journal of Investigative Dermatology 121, 231-241.

Manchado, M., Infante, C., Asensio, E., Planas, J.V., Cañavate, J.P., 2008. Thyroid hormones down-regulate thyrotropin β subunit and thyroglobulin during metamorphosis in the flatfish Senegalese sole (*Solea senegalensis* Kaup). General and Comparative Endocrinology 155, 447-455.

Manchado, M., Infante, C., Rebordinos, L., Cañavate, J.P., 2009. Molecular characterization, gene expression and transcriptional regulation of thyroid hormone receptors in Senegalese sole. General and Comparative Endocrinology 160, 139-147.

Miwa, S., Tagawa, M., Inui, Y., Hirano, T., 1988. Thyroxine surge in metamorphosing flounder larvae. General and Comparative Endocrinology 70, 158-163.

Miwa, S., Yamano, K., Inui, Y., 1992. Thyroid hormone stimulates gastric development in flounder larvae during metamorphosis. Journal of Experimental Zoology 261, 424-430.

Moreno, M., de Lange, P., Lombardi, A., Silvestri, E., Lanni, A., Goglia, F., 2008. Metabolic effects of thyroid hormone derivatives. Thyroid 18, 239-253.

Muzzio, A.M., Noyes, P.D., Stapleton, H.M., Lema, S.C., 2014. Tissue distribution and thyroid hormone effects on mRNA abundance for membrane transporters Mct8, Mct10, and organic anion-transporting polypeptides (Oatps) in a teleost fish. Comparative Biochemistry and Physiology. Part A, Molecular & Integrative Physiology 167, 77-89.

Noyes, P.D., Lema, S.C., Macaulay, L.J., Douglas, N.K., Stapleton, H.M., 2013. Low level exposure to the flame retardant BDE-209 reduces thyroid hormone levels and disrupts thyroid signaling in fathead minnows. Environmental Science and Technology 47, 10012-10021.

Okada, N., Morita, T., Tanaka, M., Tagawa, M., 2005. Thyroid hormone deficiency in abnormal larvae of the Japanese flounder *Paralichthys olivaceus*, Fisheries Science 71, 107-114.

Olaso, E., Lin, H.C., Wang, L.H., Friedman, S.L., 2011. Impaired dermal wound healing in discoidin domain receptor 2-deficient mice associated with defective extracellular matrix remodelling. Fibrogenesis and Tissue Repair 4, 5.

Ozkizilcik, S., Chu, F.-L.E., Place, A.R., 1996. Ontogenetic changes of lipolytic enzymes in striped bass (*Morone saxatilis*). Comparative Biochemistry and Physiology Part B: Biochemistry and Molecular Biology113, 631-637.

Page, R.B., Monaghan, J.R., Walker, J.A., Voss, S.R., 2009. A model of transcriptional and morphological changes during thyroid hormone-induced metamorphosis of the axolotl. General and Comparative Endocrinology 162, 219-232.

Page, R.B., Voss, S.R., Samuels, A.K., Smith, J.J., Putta, S., Beachy, C.K., 2008. Effect of thyroid hormone concentration on the transcriptional response underlying induced metamorphosis in the Mexican axolotl (*Ambystoma*). BMC Genomics 9, 78.

Paridaen, J.T., Huttner, W.B., 2014. Neurogenesis during development of the vertebrate central nervous system. EMBO Report 15, 351-364.

Pascual, A., Aranda, A., 2013. Thyroid hormone receptors, cell growth and differentiation. Biochimica et Biophysica Acta 1830, 3908-3916.

Pereiro, P., Balseiro, P., Romero, A., Dios, S., Forn-Cuni, G., Fuste, B., Planas, J.V., Beltran, S., Novoa, B., Figueras, A., 2012. High-Throughput Sequence Analysis of Turbot (*Scophthalmus maximus*) Transcriptome Using 454-Pyrosequencing for the Discovery of Antiviral Immune Genes. PLoS One 7, e35369.

Power, D.M., Einarsdóttir, I.E., Pittman, K., Sweeney, G.E., Hildahl, J., Campinho, M.A., Silva, N., Sæle, Ø., Galay-Burgos, M., Sráradóttir, H., Björnsson, B.T., 2008. The Molecular and Endocrine Basis of Flatfish Metamorphosis. Reviews in Fisheries Science 16, 95-111.

Proksch, E., Brandner, J.M., Jensen, J.M., 2008. The skin: an indispensable barrier. Experimental Dermatology 17, 1063-1072.

Rakers, S., Gebert, M., Uppalapati, S., Meyer, W., Maderson, P., Sell, A.F., Kruse, C., Paus, R., 2010. 'Fish matters': the relevance of fish skin biology to investigative dermatology. Experimental Dermatology 19, 313-324.

Roosterman, D., Goerge, T., Schneider, S.W., Bunnett, N.W., Steinhoff, M., 2006. Neuronal control of skin function: the skin as a neuroimmunoendocrine organ. Physiolgy Reviews 86, 1309-1379.

Schreiber, A.M., Specker, J.L., 1998. Metamorphosis in the summer flounder (*Paralichthys dentatus*): stage-specific developmental response to altered thyroid status. General and Comparative Endocrinology 111, 156-166.

Schreiber, A.M., Specker, J.L., 2000. Metamorphosis in the Summer Flounder, *Paralichthys dentatus*: Thyroidal Status Influences Gill Mitochondria-Rich Cells. General and Comparative Endocrinology 117, 238-250.

Schreiber, A.M., Wang, X., Tan, Y., Sievers, Q., Sievers, B., Lee, M., Burrall, K., 2010. Thyroid hormone mediates otolith growth and development during flatfish metamorphosis. General and Comparative Endocrinology 169, 130-137.

Suzuki, K., Machiyama, F., Nishino, S., Watanabe, Y., Kashiwagi, K., Kashiwagi, A., Yoshizato, K., 2009. Molecular features of thyroid hormone-regulated skin remodelling in *Xenopus laevis* during metamorphosis. Development, Growth & Differentiation 51, 411-427.

Tagawa, M., Aritaki, M., 2005. Production of symmetrical flatfish by controlling the timing of thyroid hormone treatment in spotted halibut *Verasper variegatus*. General and Comparative Endocrinology 141, 184-189.

Torres-Nunez, E., Suarez-Bregua, P., Cal, L., Cal, R., Cerda-Reverter, J.M., Rotllant, J., 2015. Molecular cloning and characterization of the matricellular protein Sparc/osteonectin in flatfish, *Scophthalmus maximus*, and its developmental stage-dependent transcriptional regulation during metamorphosis. Gene 568, 129-139.

Tremble, P.M., Lane, T.F., Sage, E.H., Werb, Z., 1993. SPARC, a secreted protein associated with morphogenesis and tissue remodelling, induces expression of metalloproteinases in fibroblasts through a novel extracellular matrix-dependent pathway. Journal of Cell Biology 121, 1433-1444.

van der Flier, L.G. and Clevers, H. 2009. Stem cells, self-renewal, and differentiation in the intestinal epithelium. Annual Review of Physiology 71, 241-260

Vatine, G.D., Zada, D., Lerer-Goldshtein, T., Tovin, A., Malkinson, G., Yaniv, K., Appelbaum, L., 2013. Zebrafish as a model for monocarboxyl transporter 8-deficiency. The Journal of Biological Chemistry 288, 169-180.

Vogel, W.F., Abdulhussein, R., Ford, C.E., 2006. Sensing extracellular matrix: An update on discoidin domain receptor function. Cellular Signalling 18, 1108-1116.

Wang, X., Tan, Y., Sievers, Q., Sievers, B., Lee, M., Burrall, K., Schreiber, A.M., 2011. Thyroid hormone-responsive genes mediate otolith growth and development during flatfish metamorphosis. Comparative Biochemistry and Physiology Part A: Molecular & Integrative Physiology 158, 163-168.

Watt, F.M., Fujiwara, H., 2011. Cell-extracellular matrix interactions in normal and diseased skin. Cold Spring Harbor Perspectives in Biology 3.

Wegner, M., 2006. Melanocytes and the Transcription Factor Sox10 in: V. J. Hearing, S. P. L. Leong. EDs, From Melanocytes to Melanoma: The Progression to Malignancy. Humana Press Inc., Totowa, NJ, 71-80.

Yamano, K., Miwa, S., Obinata, T., Inui, Y., 1991. Thyroid hormone regulates developmental changes in muscle during flounder metamorphosis. General and Comparative Endocrinology 81, 464-472.

Yamano, K., Takano-Ohmuro, H., Obinata, T., Inui, Y., 1994. Effect of Thyroid Hormone on Developmental Transition of Myosin Light Chains during Flounder Metamorphosis. General and Comparative Endocrinology 93, 321-326.

Yan, Q., Blake, D., Clark, J.I., Sage, E.H., 2003. Expression of the matricellular protein SPARC in murine lens: SPARC is necessary for the structural integrity of the capsular basement membraneJournal of Histochemistry and Cytochemistry 51, 503-511.

Yoo, J.H., Takeuchi, T., Tagawa, M., Seikai, T., 2000. Effect of Thyroid Hormones on the Stage-specific Pigmentation of the Japanese Flounder *Paralichthys olivaceus*. Zoological Sciences 17, 1101-6.

Yoo, J.H., Takeuchi, T., Tagawa, M., Seikai, T., 2000. Effect of Thyroid Hormones on the Stage-specific Pigmentation of the Japanese Flounder *Paralichthys olivaceus*. Zoological Science 17, 1101-1106.

Yúfera, M., Halm, S., Beltran, S., Fuste, B., Planas, J.V., Martinez-Rodriguez, G., 2012a. Transcriptomic characterization of the larval stage in gilthead seabream (*Sparus aurata*) by 454 pyrosequencing. Marine Biotechnology 14, 423-435.

Zambonino Infante, J.L., Cahu, C.L., 1999. High dietary lipid levels enhance digestive tract maturation and improve *Dicentrarchus labrax* larval development. Journal of Nutrition 129, 1195-1200.

Zambonino, J.-L., Gisbert, E., Sarasquete, C., Navarro, I., Gutiérrez, J., Cahu, C., 2008. Ontogeny and physiology of the digestive system of marine fish larvae, in: J. Cyrino, D. Bureau, B. Kapoor (Eds.), Feeding and Digestive Functions of Fishes. Oxford & IBH Publishing Co. Pvt. Ltd, Enfield, NH, 281-348.

Zhang, W.T., Liu, K., Xiang, J.S., Zhang, L.Y., Liu, W.J., Dong, Z.D., Li, Y.Z., Li, H.L., Chen, S.L., Wang, N., 2016. Molecular cloning, expression of, and regulation by thyroid-hormone receptor alpha A in the half-smooth tongue sole *Cynoglossus semilaevis* during metamorphosis. Journal Fish Biology 88, 1693-1707.

Zouboulis, C.C., 2000. Human skin: an independent peripheral endocrine organ. Hormone Research 54, 230-242.